Lasers in Endodontics

Scientific Background and Clinical Applications

Giovanni Olivi
Roeland De Moor
Enrico DiVito
Editors

Springer

HIGH DENT

PRODUCTS SERVICES TRAINING

همیار دندانسازان و دندانپزشکان در پروتز

مرکز تخصصی پروتزهای دندانی

های دنت

طراحی و ساخت انواع پروتزهای دندانی بویژه ایمپلنت

برگزار کننده دوره های آموزشی تخصصی و جامع دندانسازی و...

با ما همراه باشید...

WWW.HIGHDENT.IR

@highdent

@highdent

Lasers in Endodontics

Giovanni Olivi • Roeland De Moor
Enrico DiVito
Editors

Lasers in Endodontics

Scientific Background and Clinical Applications

Springer

Editors
Giovanni Olivi
InLaser Rome
Advanced Center for Esthetic
and Laser Dentistry
Rome
Italy

Enrico DiVito
Arizona School of Dentistry and Oral
Health
Mesa
Arizona
USA

Roeland De Moor
Restorative Dentistry and
Endodontology
Ghent University
Ghent
Belgium

ISBN 978-3-319-19326-7 ISBN 978-3-319-19327-4 (eBook)
DOI 10.1007/978-3-319-19327-4

Library of Congress Control Number: 2016930668

Springer Cham Heidelberg New York Dordrecht London

Printed on acid-free paper

Springer International Publishing AG Switzerland is part of Springer Science+Business Media (www.springer.com)

Foreword I

There has been a volcanic eruption of endodontic technology over the past 30 years. This renaissance began in the early 1980s with the introduction of the dental operating microscope, continued with the development of NiTi shaping files, and was followed by the debut of a remarkable biocompatible material, MTA. More recently, the transformation has continued with the advent of CBCT for improved diagnostics, minimally invasive technologies that promote the maximum preservation of tooth structure, and breakthrough methods for 3D disinfecting *root canal systems*, a term first coined by Professor Herbert Schilder. In conjunction with better-trained general dentists and specialists alike, these unprecedented advancements have sparked an endodontic awakening that predictably successful endodontics is not only possible, but, with desire, is readily attainable, and the naturally retained root is the ultimate dental implant.

To this end, it is a pleasure and honor for me to write the Foreword for this textbook, *Laser Applications in Endodontics*. The authors, Drs. Giovanni Olivi, Enrico DiVito, and Roeland De Moor, as well as their impressive contributors, are recognized experts in this subject matter. This book begins by emphasizing endodontic morphology and anatomy, shaping the root canal, and the role of irrigation in 3D disinfection. The authors go on to clearly describe the basic science and physics of lasers and, specifically, identify the different lasers used in endodontics. Various clinical applications of lasers in endodontics are completely discussed, as well as leading-edge advancements in laser-activated irrigation. The book's organization and thoroughness, as well as the sheer volume of knowledge contained within, makes this effort unmatched. Each chapter brilliantly balances intelligent scholarly text with outstanding visual content.

In every instance, the contributors worked diligently in spite of many other heavy professional responsibilities. All are teachers and authors of considerable note, and many also devote substantial time to clinical practice. They have contributed with enthusiasm, and their efforts will undoubtedly be appreciated by any dentist who is committed to exquisitely cleaning root canal systems. I recommend this book to all dentists who aspire to move ever closer toward their full potential. Laser applications in endodontics will have

a profound impact in the coming years; specifically, laser-activated irrigation is creating a genuine opportunity for the field of regenerative endodontics to accelerate forward. What once seemed the basis of science fiction is now clinical reality; the future is now! "*Whatever you can do or dream you can, begin it. Boldness has genius, power and magic in it*!" – Scottish Himalayan Expedition.

Santa Barbara, CA-USA Clifford J. Ruddle, DDS

Foreword II

In the most recent years, notable progress has been made in all facets of dentistry and even more so in endodontics. The laser has opened new horizons and improved the possibilities of long-term success for our therapies. In the field of endodontics, lasers have numerous applications ranging from access preparation to disinfection, activated irrigation, and even surgical. All these applications, together with numerous others, are magnificently described in this book authored by doctors Giovanni Olivi, Enrico DiVito, and Roeland De Moor to which I have the pleasure to recommend to all my colleagues that wish to learn more about this fascinating branch of endodontics. Also discussed in this book are the details of various lasers and the principles of physics that governs them, helping the reader to determine which type is best suited for their use. I congratulate all the authors of this book for their accuracy in writing the chapters and for the clarity in their description of the laws of physics that form the fundamentals of knowledge for all laser types and for making this subject easy to read and comprehend. The endodontic literature was lacking a book of this caliber. I want again to congratulate the authors and all the collaborators for completing this difficult task and sharing with the readers all their knowledge and clinical experience in this fascinating field of endodontics.

Florence, Italy — Arnaldo Castellucci MD, DDS

Contents

Contents

Part I

Endodontic Background

1 Endodontic Morphology and Anatomy of Human Teeth

Vasilios Kaitsas and Giovanni Olivi

Abstract

The aim of root canal therapy is to remove the content of the endodontic space and subsequently to fill it. A correct treatment requires the knowledge of both the external and internal anatomies of the tooth in order to reduce the risk of failure and the possibility of iatrogenic biological damage.

This chapter describes the basic microscopic and macroscopic morphological features of human teeth.

Understanding the crown morphology guides us to the access of the endodontic space of the roots in the most conservative way; the design of the access cavity is described for all the teeth. The study of the morphology of the root canal system with its several variations makes it understandably obvious why there are operative difficulties during instrumentation, as shown by the iconographic part. The morphological and histological tables by Hess demonstrated the radicular and apical complexity of the roots, confirming the difficulty of removing the entire pulp tissue from the endodontic space and encouraging the search for new endodontic techniques and technologies.

The part on microscopic anatomy summarizes the composition of root dentin walls that are the target of the interaction of mechanical (files, ultrasound), chemical (irrigants) and physical (lasers) instrumentation during the therapy. In particular, in order to understand the different laser interactions on tissue using different wavelengths, it is very important to closely examine the ultrastructure and histology of the dentin in the canal.

V. Kaitsas, DDS, PhD
University of Thessaloniki-Greece,
via Tronto 32 00198, Roma, Italy
e-mail: v.kaitsas@tiscali.it

G. Olivi, MD, DDS (✉)
InLaser Rome – Advanced Center for Esthetic and Laser Dentistry, Rome, Italy
e-mail: olivilaser@gmail.com

G. Olivi et al. (eds.), *Lasers in Endodontics: Scientific Background and Clinical Applications*,
DOI 10.1007/978-3-319-19327-4_1

1.1 Deciduous Teeth Anatomy

The macroscopic anatomy of deciduous teeth is very similar to that of permanent teeth with just a few differences between them that are summarized in this section.

Ernst Zurcher (1922), from Walter Hess's school in Zurich, carried out the first scientific work on pulp morphology in deciduous teeth [1, 2].

The endodontic morphology of deciduous teeth is very similar to that of permanent but smaller in size. Deciduous teeth are generally shorter and smaller than permanent teeth; the roots are narrow while permanent teeth roots are wider especially in the cervical one-third. However, on the contrary, the anterior deciduous coronal aspect is larger in comparison to their length. The roots of deciduous molars, in addition to being thinner than permanent ones, are spatially wider opened in order to allow eruption of the permanent premolar teeth, first during their formation and later during the eruption.

The primary upper and lower molars often have a fourth canal in the mesial-buccal root of the upper molar and in the distal root of the lower molar.

During child growth, the primary teeth show a decrease in radicular length due to physiological reabsorption (exfoliation) (Figs. 1.1 and 1.2). Sometimes reabsorption of the floor of the pulp chamber in the area of furcation precedes the apical root reabsorption (Fig. 1.3a–d).

Contrary to permanent teeth, the exfoliation of deciduous teeth explains why the filling of the radicular space at the end of endodontic treatment of primary teeth requires the use of resorbable materials which permit the gradual reabsorption of the root.

Fig. 1.1 Primary upper molar: radicular reabsorption starting in the apical area (*arrows*)

Fig. 1.2 Primary lower molar: radicular reabsorption involving all the radicular portions from apical to coronal

1.2 Permanent Teeth

1.2.1 Macroscopic Anatomy

Permanent human teeth have a crown and one or more roots. The endodontic space, defined by radicular and chamber dentin, is very complex, and it is differently classified depending on crown-root relationship and morphology of the canals.

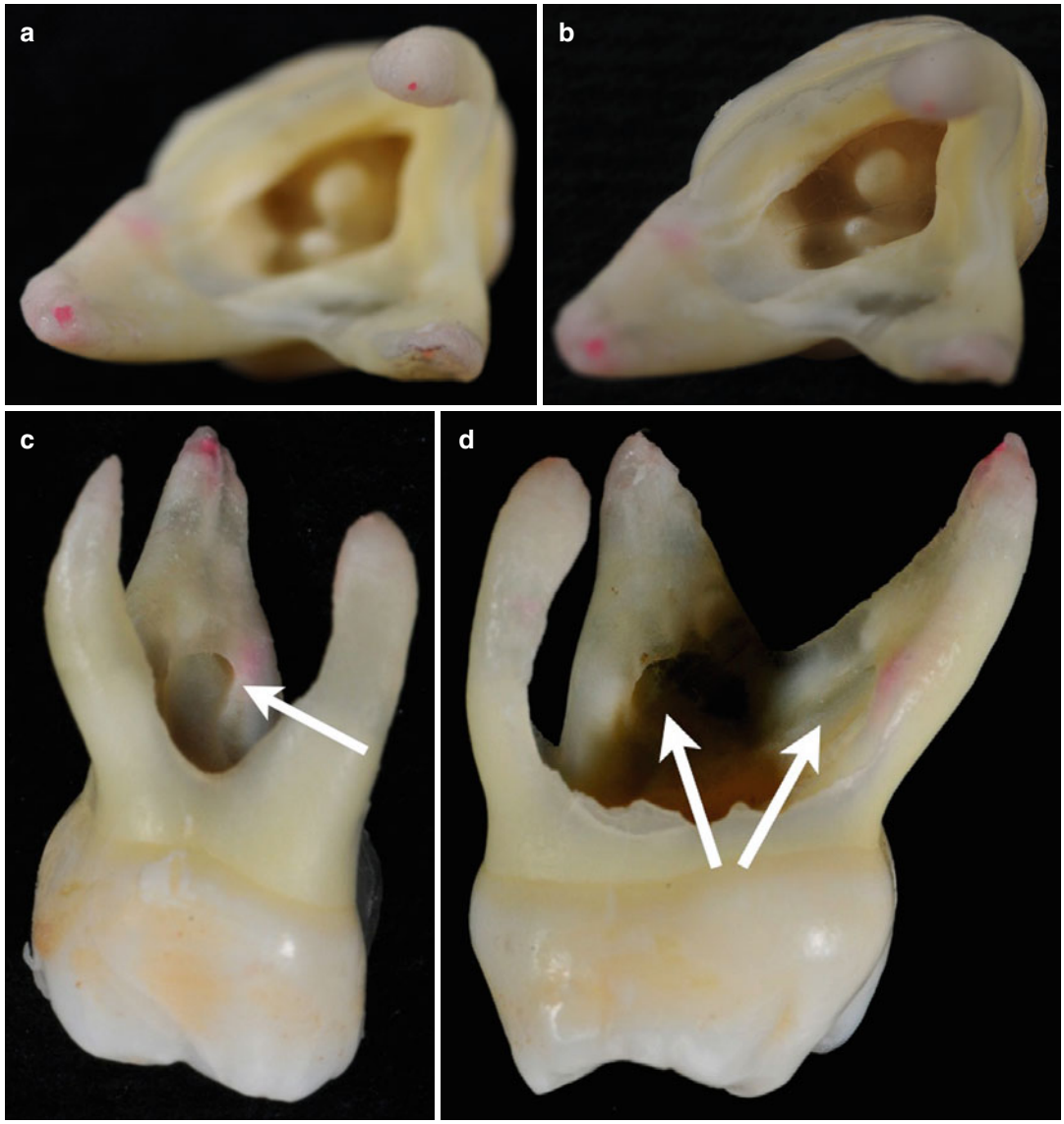

Fig. 1.3 Primary upper molar: the radicular reabsorption is more evident at the floor of the pulp chamber in the area of furcation that in this case precedes the apical reabsorption; (**a**) radicular apices are intact; (**b**) reabsorption in the area of furcation of the floor of the pulp chamber; (**c**) buccal view of the furcation of palatine tooth (*arrows*); (**d**) mesial view of furcation reabsorption (*arrows*)

Weine (1996) classified the complexity of the endodontic system in four typologies while considering the relationships between pulp chamber, radicular canals and their apical termination [3] (Fig. 1.4).

Vertucci (1984) defined instead eight basic typologies [4]. Later on, Vertucci's classification was expanded to include other morphological classifications by Gulabivala et al. (2001 and 2002) [5, 6] and by Sert and Bayirili (2004) [7] (Figs. 1.5, 1.6 and 1.7).

Schneider [1971] analysed single-radicular human teeth and classified them depending on the degree of curvature in the root, as straight, with curvature less than or equal to 5°, with a moderate curvature between 10° and 20° and

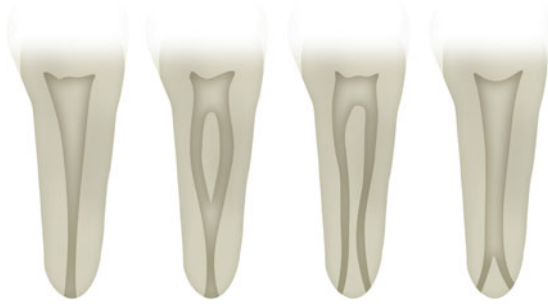

Fig. 1.4 Weine's classification of the endodontic system takes into account the relationships between pulp chamber, root canals and their apical termination [3] (Graphic drafts courtesy of Giovanni Olivi, Rome, Italy)

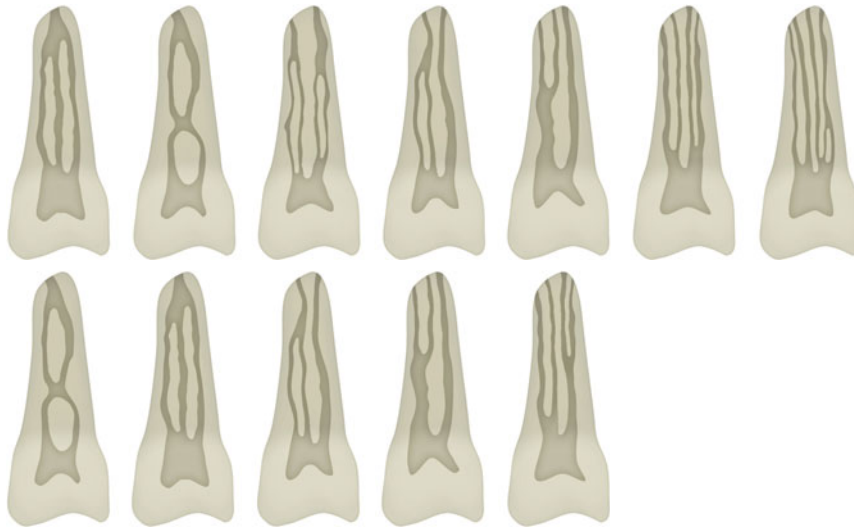

Figs. 1.5 and 1.6 Graphic representation of Gulabivala's morphological classification of the endodontic system [5, 6] (Graphic drafts courtesy of Giovanni Olivi, Rome, Italy)

with a severe curvature between 25° and 70° [8]. Lautrou [1987] also described and classified the various morphologies of transverse sections of roots [9] (Fig. 1.8).

Zidell (1985) and Ingle and Taintor (1985), in addition to the degree of root and apical curvature, also considered the anatomical complexity, including the presence of bifurcations, the presence of additional channels and the presence of lateral and accessory channels [10, 11].

Various studies and texts later described the anatomy and morphology of permanent human teeth and their countless possible shapes [12–16].

In the paragraphs related to a single type of tooth, the age of eruption considered is that of Logan and Kronfeld, slightly modified by Schour and included in Ash's text [13, 14]. The dimensions of human teeth reported in this textbook are instead taken from different texts [11, 17, 18].

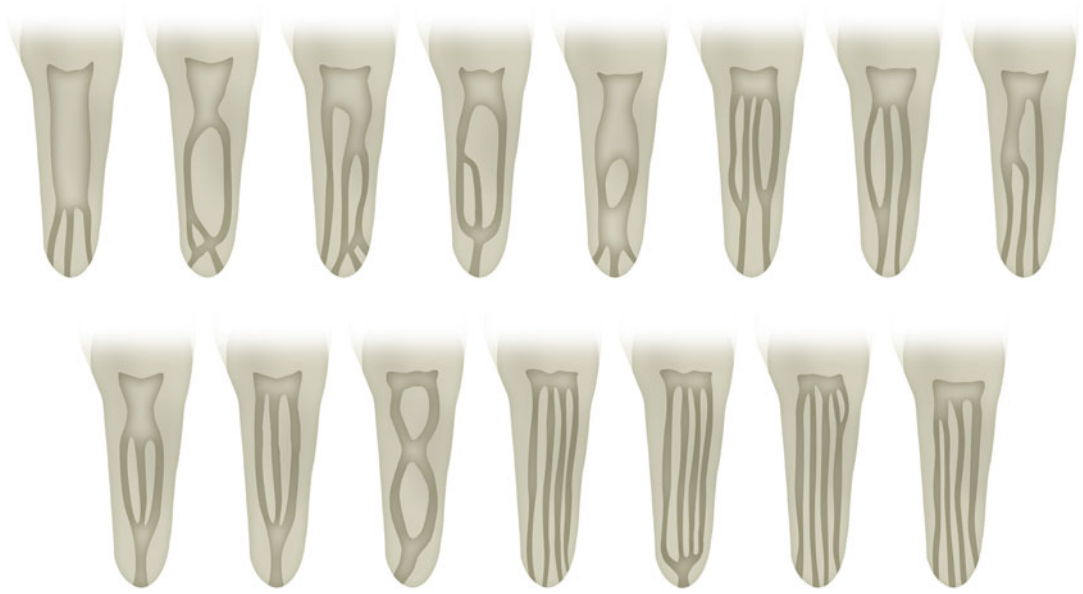

Fig. 1.7 Graphic representation of Sert and Bayirili's morphological classification of endodontic system [7] (Graphic drafts courtesy of Giovanni Olivi, Rome, Italy)

Fig. 1.8 Graphic representation of Lautrou's classification of morphologies of transverse sections of roots [9] (Graphic drafts courtesy of Giovanni Olivi, Rome, Italy)

1.3 Upper Incisors

1.3.1 Central Upper Incisor

The central upper incisor erupts (one per hemiarch) at the age of six to seven, and the complete formation of the apical third is defined 2 or 3 years later. It has an average length of 22–23 mm.

The crown, with its triangular base, is about 10.5 mm long, and its base extends in a mesial-distal direction, corresponding to the tooth's front edge, to about 9 mm, and its buccal-palatal dimension is 7 mm (Fig. 1.9).

The root is usually straight (75 %) but according to Ingle could present small curvatures in a small percentage. The root exhibits a radicular canal with side canals in more than 20 % of cases and frequently apical delta (35 %) [11].

The endodontic coronal space has also a triangular shape, especially in the area of the cervical radicular one-third, with the base towards the chamber wall and the narrower part palatally

Fig. 1.9 Upper central incisors: palatal view of the crown

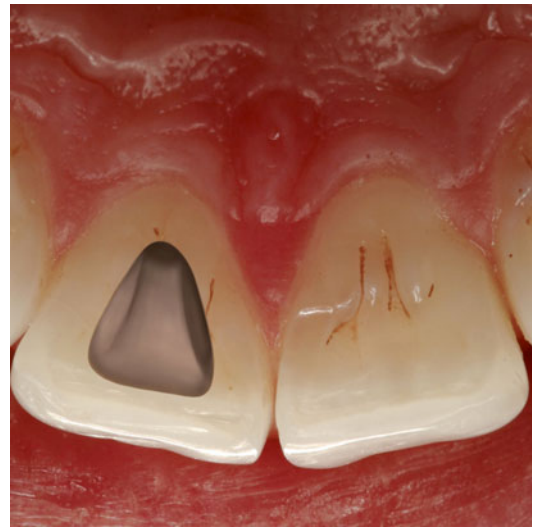

Fig. 1.10 Upper central incisor: graphic representation of the access cavity (Courtesy of Giovanni Olivi, Rome, Italy)

Fig. 1.11 Upper lateral incisor: palatal view of the crown

Fig. 1.12 Upper lateral incisor: graphic representation of the access cavity (Courtesy of Giovanni Olivi, Rome, Italy)

after which it gradually ends with a round canal until the apex.

The access cavity is triangular and reproduces the shape of the endodontic space (Fig. 1.10).

1.3.2 Lateral Upper Incisor

The upper lateral eruption (one per hemi-arch) occurs 1 year after the central incisor, and its complete formation takes approximately 3 years.

It is about 1 or 2 mm shorter than the central incisor and its mesial-distal dimension is smaller: about 7 mm and just 5.5–6 mm in the chamber-palatal side (Fig. 1.11).

Normally it presents only one radicular canal, straight in 30 % of cases, and frequently there is a distal curvature (53 %) with a small percentage of variation in other directions. It has an egg shape in the cervical area, with the tendency to become more round in the apical area, and the access cavity is consequently configured (Fig. 1.12).

Fig. 1.13 Lower incisors: lingual view of the crowns

Fig. 1.14 Lower central incisor: graphic representation of the access cavity (Courtesy of Giovanni Olivi, Rome, Italy)

1.4 Lower Incisors

The lower incisors, two per hemi-arch, are very similar to each other keeping some peculiarity.

1.4.1 Lower Central Incisors

The lower central incisors are the first permanent teeth to erupt in the mouths of the children, usually between 6 and 7 years of age, and they generally complete their radicular and apical formation at 9 or 10 years old. The lower central incisor is about 21.5 mm long. The apical third of the root is straight in 60 % of cases and bends towards the distal in 23 % of the cases.

The crown has a trapezoidal shape with the major base corresponding to the incisal edge and the minor base that continues with the cervical third of the root. Its half distal dimension is 5.5 mm in the area of the incisor, in correspondence to the next contact point, and gradually decreases to 3 mm at cervical level (Fig. 1.13).

The lower central incisor presents a buccal inclination. The root has a second canal positioned lingually to the principal canal in 18–23 % of cases [12, 13] (Fig. 1.14).

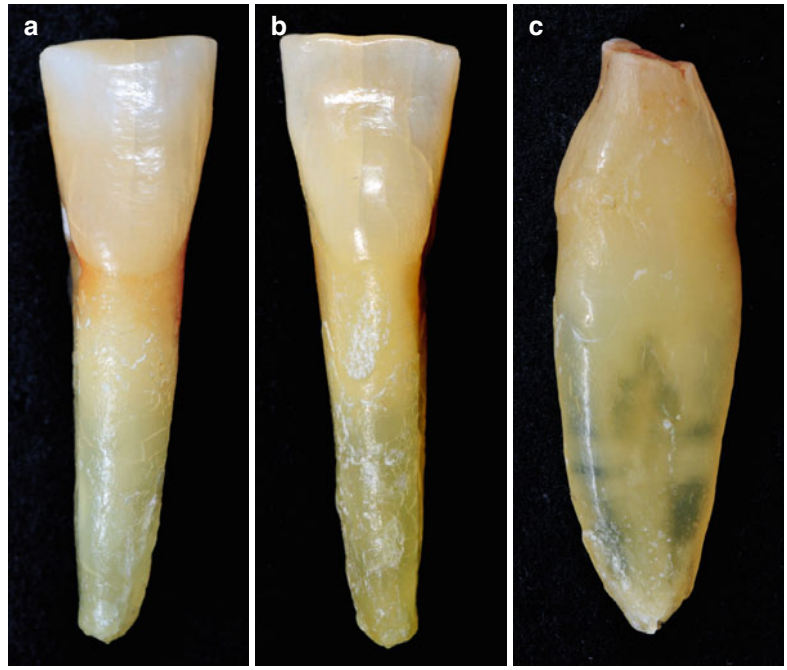

Fig. 1.15 (**a**–**c**) Lower central incisor: buccal, lingual and proximal view

1.4.2 Lower Lateral Incisor

Lower lateral incisor is similar to the central one, but a bit bigger by about 1 mm, and it normally comes out 1 year after the lower central incisor and completes its formation in 3 years.

The study of the root confirms the presence of two canals in 15 % of cases.

The access cavity of lower incisors is designed in a buccal-lingual direction in order to search for the second canal, positioned lingually (Fig. 1.15a–c).

1.5 Cuspids

1.5.1 Upper Canine (Cuspid)

Upper canine, one per hemi-arch, comes out at the age of approximately 11–12 and completes its radicular formation 3–4 years later.

It is the longest tooth in human arch (about 27 mm or more).

The crown has a rhomboidal shape with a peculiar sharp cusp which on the vestibular side divides the mesial and distal sides of the crown. The crown is 10 mm high (long) and has a maximum mesial-distal diameter of 7.5 mm at the proximal contact point, and it undergoes cervical reduction to 5.5 mm. The buccal-palatal diameter is wider (8 mm), and it maintains itself at 7 mm at the cervical level because of the presence of a noticeable cingulum (Fig. 1.16).

The long root, like the crown, is narrow in the mesial-distal dimension and more pronounced in the buccal-palatal dimension. There is almost always just one radicular canal, with localized side canals at various heights in about 24 % of cases. The apical third is straight in 40 % of cases, and it is often bent towards the distal (32 %) and/or towards the chamber (13 %) (Fig. 1.17).

The endodontic space, at the level of the cervical one-third and the radicular middle one-third, has an oval shape in the buccal-palatal dimension; frequently two canals are present with the tendency to become one common round canal in the apical one-third (Fig. 1.18a, b).

The access cavity of the pulp chamber has an oval shape, going from the cusp to the cingulum of the coronal cervical one-third in order to access the radicular space without dental interference which could force the instruments creating ledges or transposition of the apical foramen (Fig. 1.19).

Fig. 1.16 Upper cuspid: palatal view

Fig. 1.17 Upper cuspid: graphic representation of the access cavity (Courtesy of Giovanni Olivi, Rome, Italy)

Fig. 1.18 (**a**, **b**) Upper cuspid: buccal and proximal view

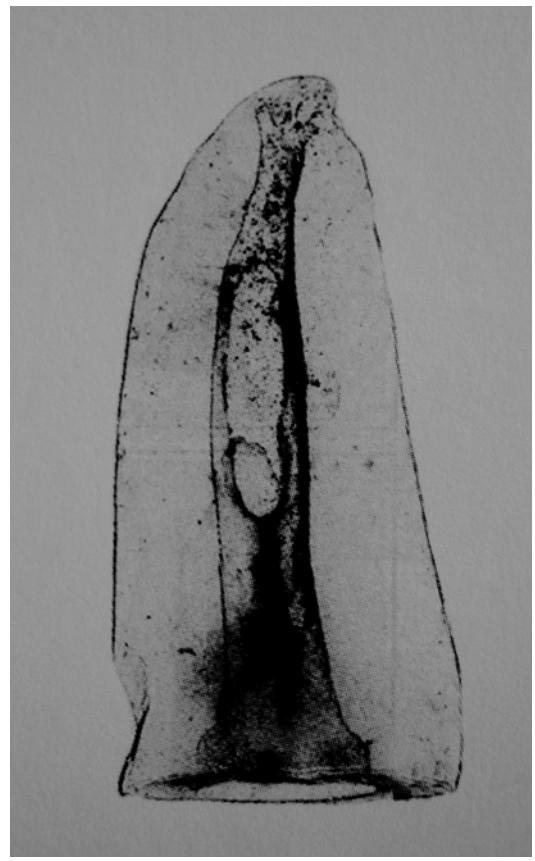

Fig. 1.19 Anatomical tables from Hess and Keller: the endodontic space of upper cuspid at the level of the cervical one-third of the canal shows a unique oval-shaped canal, while at the middle one-third, it is divided into two different canals and frequently becomes a single round canal at the apical one-third [2] (Image reprint with permission from Perrini [1])

Fig. 1.20 Lower cuspid: lingual view of the crown

Fig. 1.21 Lower cuspid: graphic representation of the access cavity (Courtesy of Giovanni Olivi, Rome, Italy)

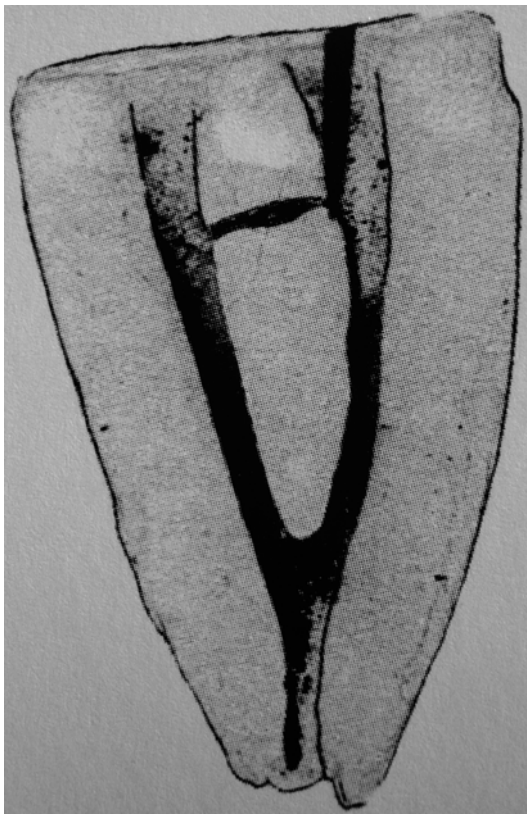

Fig. 1.22 Anatomical tables from Hess and Keller: the endodontic space of lower cuspid shows two different canals connected by an isthmus at the coronal one-third; the canals end in the same unique foramen at the apical one-third [2] (Image reprint with permission from Perrini [1])

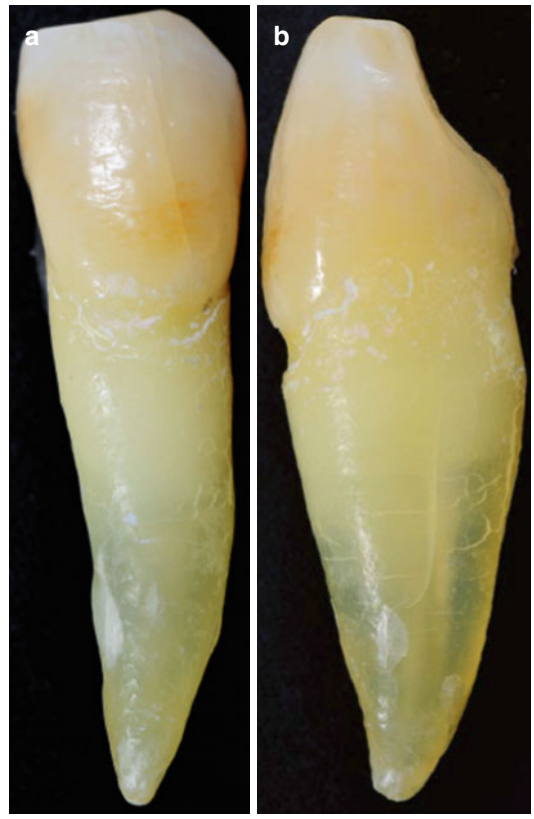

Fig. 1.23 (**a**, **b**) Lower cuspid: buccal and proximal view

1.5.2 Lower Canine (Cuspid)

The lower canine, one per hemi-arch, erupts approximately 8–10 months before the upper and completes its formation in 3–4 years.

The crown is 11 mm long and its half distal diameter is narrower than the upper (7 mm), and it reduces itself to 5.5 mm at cervical level. The maximum buccal-lingual diameter is 7.5 mm wide and it reduces itself minimally at cervical level. The cervical lingual cingulum is less pronounced than the upper one (Fig. 1.20).

The lower canine is about 27 mm long, and it presents two separate roots in 6 % of cases or two canals in just one root, split by an isthmus, with a common or two separate apices (Fig. 1.21). In 20 % of cases the apical one-third has a distal inclination (Fig. 1.22).

The endodontic space is oval shaped in buccal-lingual direction for two one-thirds of the radicular length, and then gradually it assumes a round shape.

The access cavity of the pulp chamber must have an oval shape in the buccal-lingual direction, from the cusp to the cingulum (Fig. 1.23a, b).

1.6 Upper Premolars (or Bicuspid)

They are two per every half (hemi-)arch, they erupt at the age between 10 and 12 years and their radicular formation is complete after 3 years. They replace the primary molars.

The first and the second premolars have a similar crown but a different morphology.

1.6.1 Upper First Premolar

The first upper premolar erupts when the child is about 10–11 years old. It is about 21–22 mm long and its buccal-palatal dimension is 9 mm, while the mesial-distal one is 7 mm. It has two cusps, a buccal and a palatal one, which is a bit shorter (about 1 mm). The endodontic space is determined by the shape and the dimension of the external crown (Fig. 1.24).

In about 72 % of cases, two roots with two different apical foramina are present (Fig. 1.25). Premolars may also have just one root with two canals (13 %) (Fig. 1.26a, b) and also some cases with three roots (6 %) (Figs. 1.27). In addition, in 37 % of cases we found a distal curvature of the root in the apical third.

Fig. 1.24 First upper premolar: occlusal view

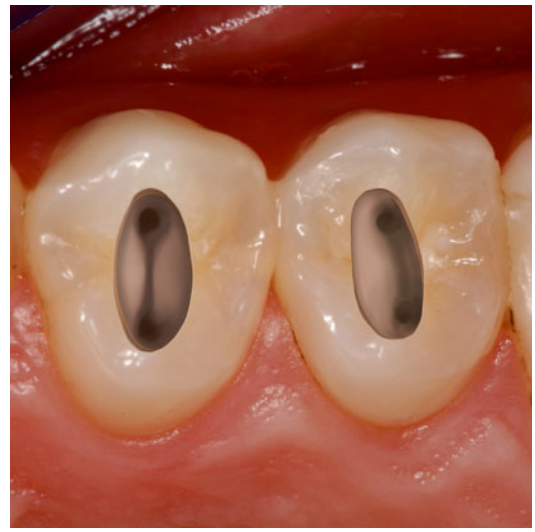

Fig. 1.25 Upper premolars: graphic representation of the access cavity; note the mesial position of the access cavity of the second premolar (on the right of the picture), to facilitate the negotiation of distally curved canals (Courtesy of Giovanni Olivi, Rome, Italy)

Fig. 1.26 (**a**, **b**) Upper single-root premolar: buccal and proximal view

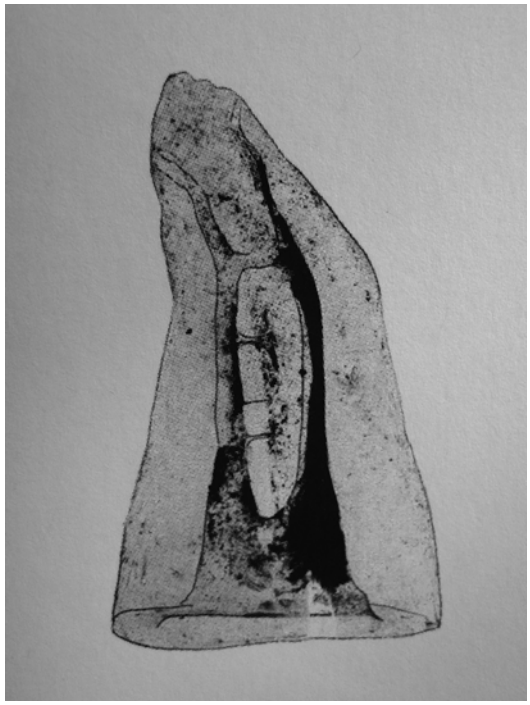

Fig. 1.27 Anatomical tables from Hess and Keller: complex endodontic space of upper single-root premolar; two different canals presenting several communications along the root and two different ports of exit [2] (Image reprint with permission from Perrini [1])

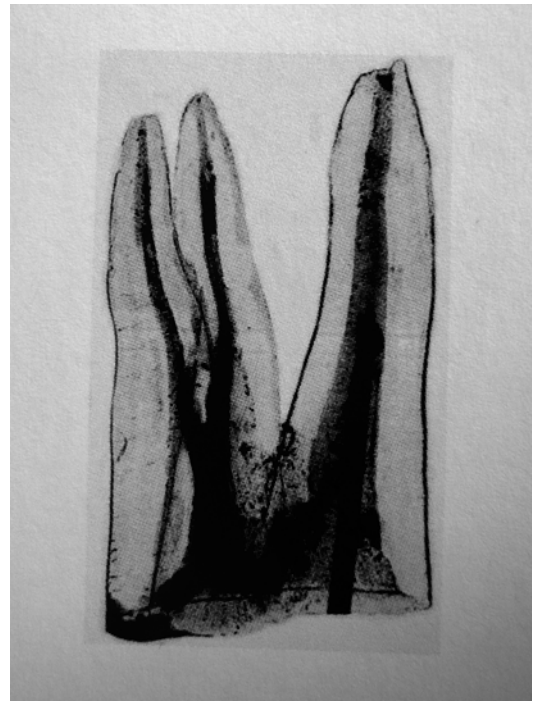

Fig. 1.28 Anatomical tables from Hess and Keller: upper premolar with three roots, two buccal and one longer palatal [2] (Image reprint with permission from Perrini [1])

Fig. 1.29 (**a**, **b**) First upper premolar: mesial and distal view

The crown access cavity to the pulp chamber must have an oval shape in the buccal-palatal direction, extending from one cusp to the other Fig. 1.28.

1.6.2 Upper Second Premolar

The second upper premolar erupts at the age between 10 and 12 years. It is very similar to the upper first premolar, both in dimension and in the shape of the crown. But there are some main radicular differences, presented in three variations:

- One root with one canal in 75 % of cases (Fig. 1.29a, b)
- One root with two canals with one or two separate foramina (12 %) (Figs. 1.30 and 1.31)
- Two separate roots and canals (12 %)
- Three separate roots (usually two of them are buccal) with three canals (1 %)

From the buccal side the roots have a distal direction inclined in 27 % of cases and a vestibular curvature in 12 % of cases, and in 20 % of cases they present a double bayonetted curvature.

The opening of the access cavity to the pulp chamber is oval shaped in the buccal-palatal direction. In the presence of a notable distal apical curvature, access must be kept close to the mesial marginal ridge keeping the oval-shaped form (Fig. 1.28).

Fig. 1.30 Anatomical tables from Hess and Keller: upper single-root premolar presenting two canals with same confluent terminus; also lateral canals are present in the apical and middle one-third of the canal [2] (Image reprint with permission from Perrini [1])

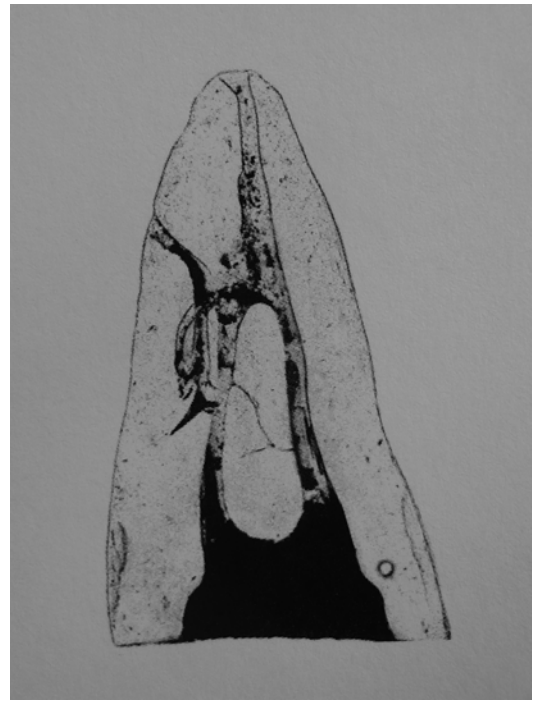

Fig. 1.31 Anatomical tables from Hess and Keller: upper single-root premolars presenting two canals with separated termini, one apically and the other lateral [2] (Image reprint with permission from Perrini [1])

1.7 Lower Premolars (or Bicuspid)

There are two per every hemi-arch and they come out between the age of 10 and 12 and complete their own radicular formation in about 3 years. They substitute the primary molars. Unlike the upper premolars, they are different to each other (Fig. 1.32).

1.7.1 Lower First Premolar

The lower first premolar erupts sometimes months before and at times after the lower canine and is the smallest of all the premolars. The crown has two cusps, one very big and similar to that of the canine. The other is shorter by about 2 mm in correspondence with the canine's lingual cingulum (Fig. 1.33).

About 21–22 mm in length, it generally has one root with one canal (73–74 %). Sometimes it has one root with two canals (19 %) (Fig. 1.34a, b), two roots with two canals (6 %) (Fig. 1.35a, b) or three canals (1–2 %).

The root often has a distal curvature in 35 % of cases and a bayonet curvature in 7 % of cases. The shape of the access cavity of the pulp chamber is oval shaped, extending from the main cusp to the top of the small lingual cusp (Fig. 1.36).

Fig. 1.32 Lower premolars: occlusal view

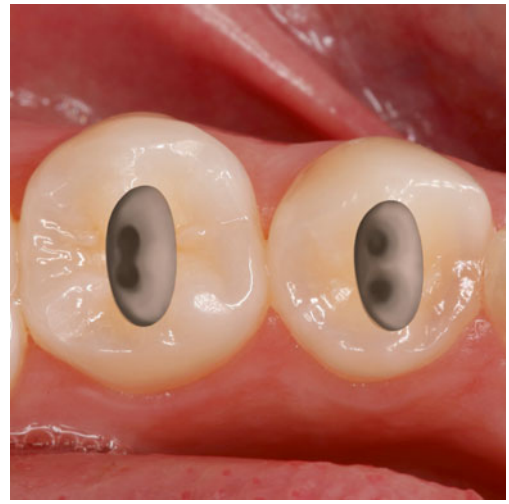

Fig. 1.33 Lower premolars: graphic representation of the access cavity (Courtesy of Giovanni Olivi, Rome, Italy)

1.7.2 Lower Second Premolar

The second lower premolar erupts at the age of 11–12 and is bigger than the first by 1 or 2 mm. The crown has two cusps (a bigger buccal and a smaller lingual), but the lingual cusp is often divided in two (Fig. 1.37).

It has just one root with one canal in 85 % of cases, but we could also find two different canals in one root (11.5 %) or two canals which merge into just one apical foramen (1.5 %) (Fig. 1.37). Rarely are there three canals (0.5–1 %). In about 40 % cases the root is straight while in about 40 % the apical third is distally inclined. It is possible to find a bayonetted curvature (7 %) and a vestibular curvature (10 %).

The access cavity to the pulp chamber is oval shaped also in this tooth with a buccal-lingual direction centred on the occlusal surface (Fig. 1.36).

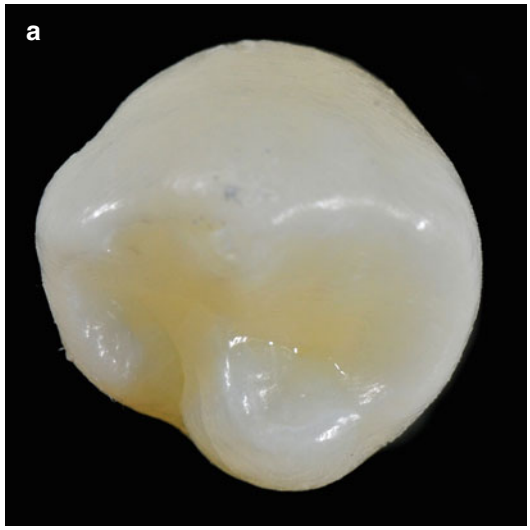

Fig. 1.34 (**a**, **b**) First lower premolar: occlusal and proximal view

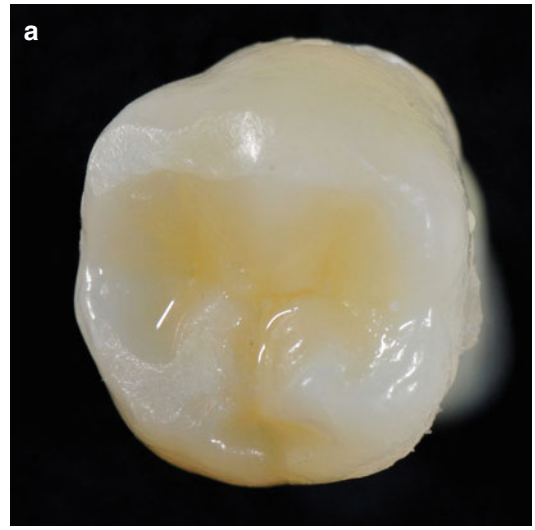

Fig. 1.35 (**a**, **b**) Second lower premolar: (**a**) coronal view; (**b**) proximal view shows the presence of one root

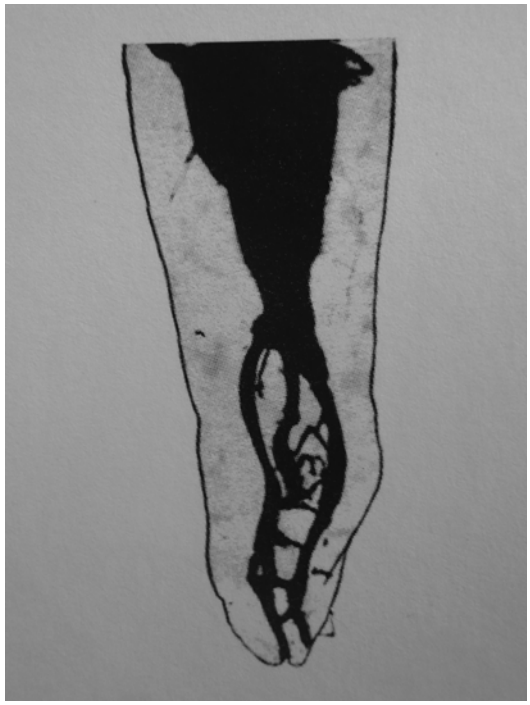

Fig. 1.36 Anatomical tables from Hess and Keller: lower single-rooted premolar with complex canal system that includes two main canals connected by several fins and two different apices [2] (Image reprint with permission from Perrini [1])

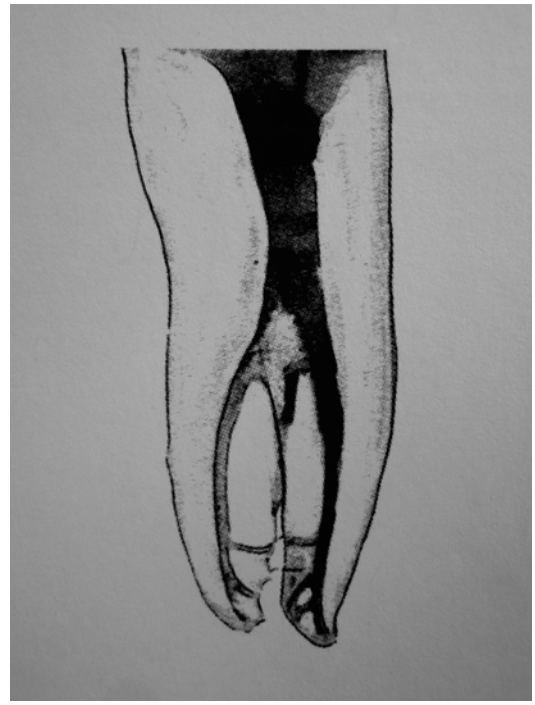

Fig. 1.37 Anatomical tables from Hess and Keller: lower premolar with two roots and two canals; several fine lateral canals are present in the apical one-third [2] (Image reprint with permission from Perrini [1])

1.8 Upper Molars

There are three molars per hemi-arch, and they don't have a corresponding primary tooth.

1.8.1 First Upper Molar

It erupts between the age of 6 and 7 behind the second primary molar. It completes its apical formation between the age of 9 and 10 years.

The crown has four cusps on the occlusal side and three roots, one palatal and two vestibular (Fig. 1.38).

It is about 21–22 mm long and has a canal in the palatal root and another one in the distal-buccal root.

The mesial-buccal root presents two different canals in 60–70 % of cases (MB1 and MB2). A second canal in the distal-buccal roots (DB2) is infrequent (2–3 %) (Figs. 1.39, 1.40 and 1.41).

The access cavity to the pulp chamber is triangular with its base turned towards the buccal side and the top towards the mesial-palatal cusp; the cavity is always located mesial (anterior) to the oblique enamel ridge that unifies the mesial-palatal cusp with the distal-buccal cusp. The orifices of the canals are located at the top of the triangle that forms the access cavity (Fig. 1.42); if we unify the orifice of the MB1 canal with the palatal orifice, we can find the second canal of the mesial-buccal root (MB2), often covered by calcification (Fig. 1.43).

Fig. 1.38 First upper molar: occlusal view

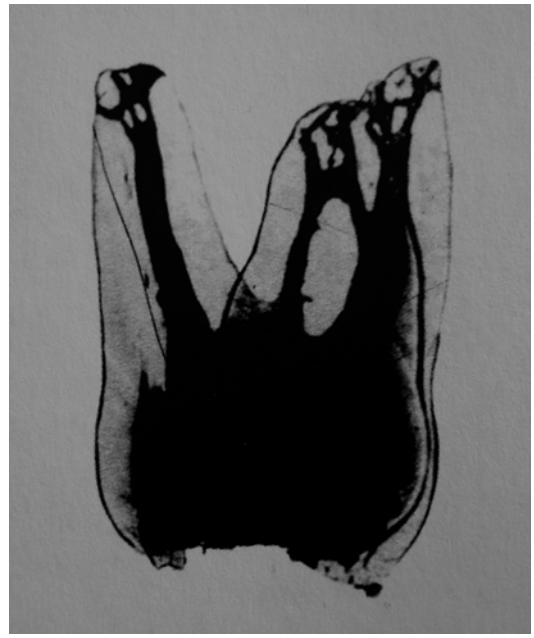

Fig. 1.40 Anatomical tables from Hess and Keller: upper molar with very complex pulp anatomy; MB1 and MB2 are visible in the mesial-buccal root [2] (Image reprint with permission from Perrini [1])

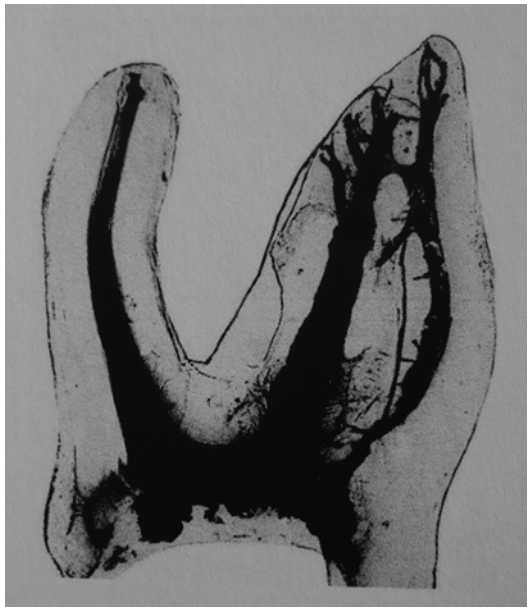

Fig. 1.39 Anatomical tables from Hess and Keller: upper molar with very complex pulp anatomy [2] (Image reprint with permission from Perrini [1])

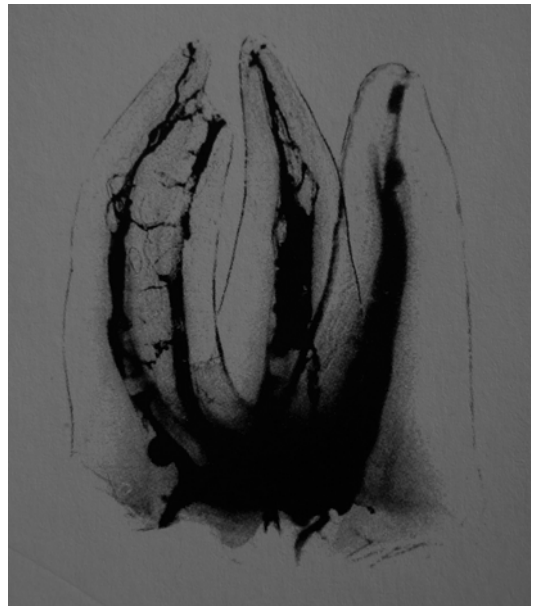

Fig. 1.41 Anatomical tables from Hess and Keller: upper molar with very complex pulp anatomy; MB1 and MB2 are visible in the mesial-buccal root [2] (Image reprint with permission from Perrini [1])

1.8.2 Second Upper Molar

Eruption occurs at the age of 12 years and the formation of the apical one-third is completed at about 14 years.

It is smaller and shorter than the first molar by about 1–2 mm, it is about 19–20 mm long and it has four occlusal cusps. It has three roots and three canals, like the first molar, and there is a second canal in the root MB as well (37–42 %). The shape of the pulp chamber is more rhomboidal than triangular (see Figs. 1.42 and 1.43).

Fig. 1.42 First upper molar: three angular access cavities with three canals (Courtesy of Giovanni Olivi, Rome, Italy)

Fig. 1.43 First upper molar: access cavity is enlarged towards the mesial ridge in order to find the MB2 canal, on the line that converges mesial-buccal and palatal canal (Courtesy of Giovanni Olivi, Rome, Italy)

1.8.3 Third Upper Molar

This tooth erupts in the mouth after the age of 17. It has a very peculiar anatomical morphology and the crown presents three or five cusps (Fig. 1.44). The average length of the third molar is about 18 mm. The root could be one or frequently more than one, such as three or four roots, usually distally curved (Figs. 1.45, 1.46, 1.47 and 1.48).

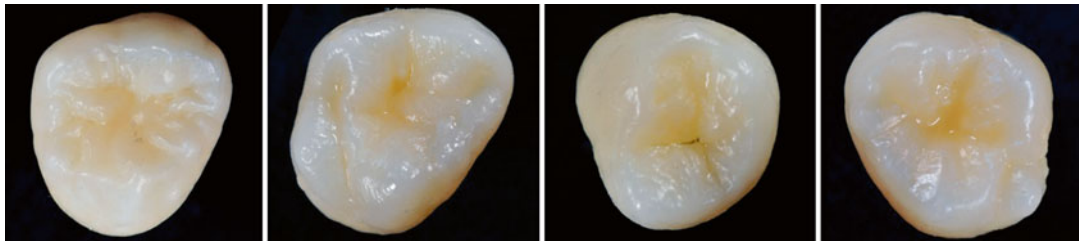

Fig. 1.44 Upper third molars showing very peculiar occlusal morphology with three or four cusps

Fig. 1.45 Upper single-root third molar

Fig. 1.46 Upper third molar with four distally curved canals

Fig. 1.47 Upper third molar with atypical anatomy

Fig. 1.48 Upper third molar with severe 3D root curvature

1.9 Lower Molars

There are three molars per hemi-arch and they don't have a corresponding primary tooth.

1.9.1 First Lower Molar

It is the first permanent tooth to erupt at the age of 6 years; it completes its formation when the child is around 9–10 years old. The crown has five cusps, two lingual and three buccal (Fig. 1.49). It is 22–23 mm long. Roots are usually two, one mesial and one distal (97 %), and we can rarely find a third disto-lingual root (3 %). In the mesial root we find two canals in 65 % of cases: they can have just one apical foramen (40 %) or two separate foramina (60 %). In the distal root there is one canal (70 %) or two canals (30 %); here there can also be two different apical foramina (38 %) or just one (62 %) (Figs. 1.50, 1.51 and 1.52) (Figs. 1.53 and 1.54).

All the roots, on the buccal side, present a moderate distal inclination. The pulp chamber is triangular or square, depending on the number of canals (3 or 4), and it is located in the centre of the crown, in the mesial-lingual area. Because of this peculiarity, during the opening of the access cavity of the pulp chamber, it is important to be careful not to remove precious dental tissue in the distal area.

The design of the access cavity must be triangular or trapezoidal with the larger base towards the mesial ridge of the occlusal surface and the smaller base (or the apex of the triangle if the distal canal is just one) slightly distal of the central occlusal fossa (Figs. 1.55 and 1.56).

In the case of a third root, its orifice can be found looking along the floor of the pulp chamber in the corners of the base of the trapezoid.

Fig. 1.49 First lower molar: occlusal view

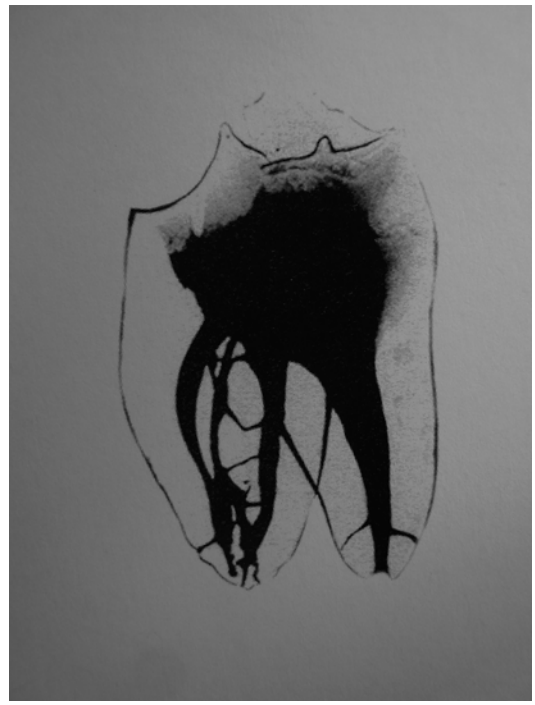

Fig. 1.51 Anatomical tables from Hess and Keller: lower molar with very complex pulp anatomy [2] (Image reprint with permission from Perrini [1])

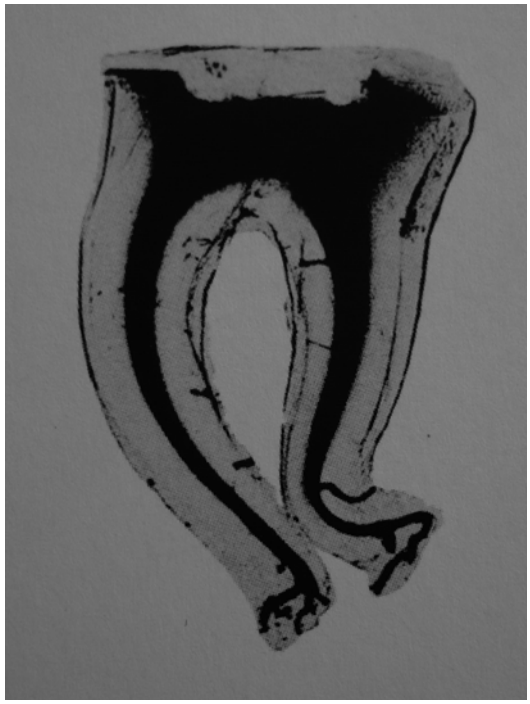

Fig. 1.50 Anatomical tables from Hess and Keller: lower molar with very complex pulp anatomy [2] (Image reprint with permission from Perrini [1])

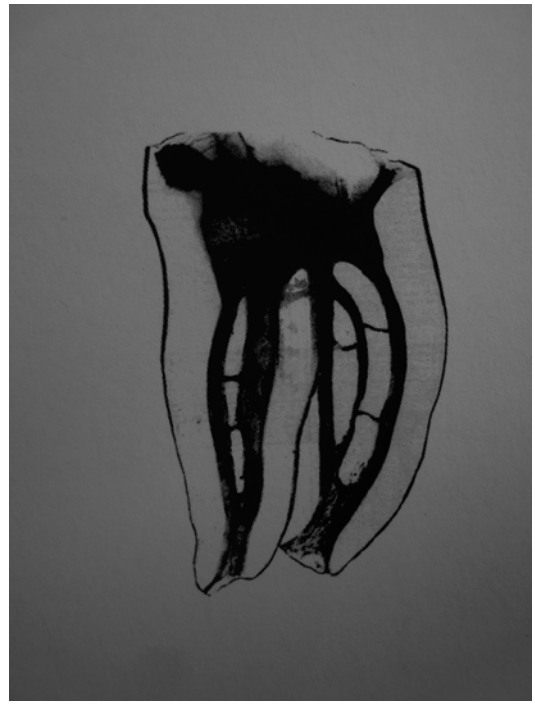

Fig. 1.52 Anatomical tables from Hess and Keller: lower molar with very complex pulp anatomy [2] (Image reprint with permission from Perrini [1])

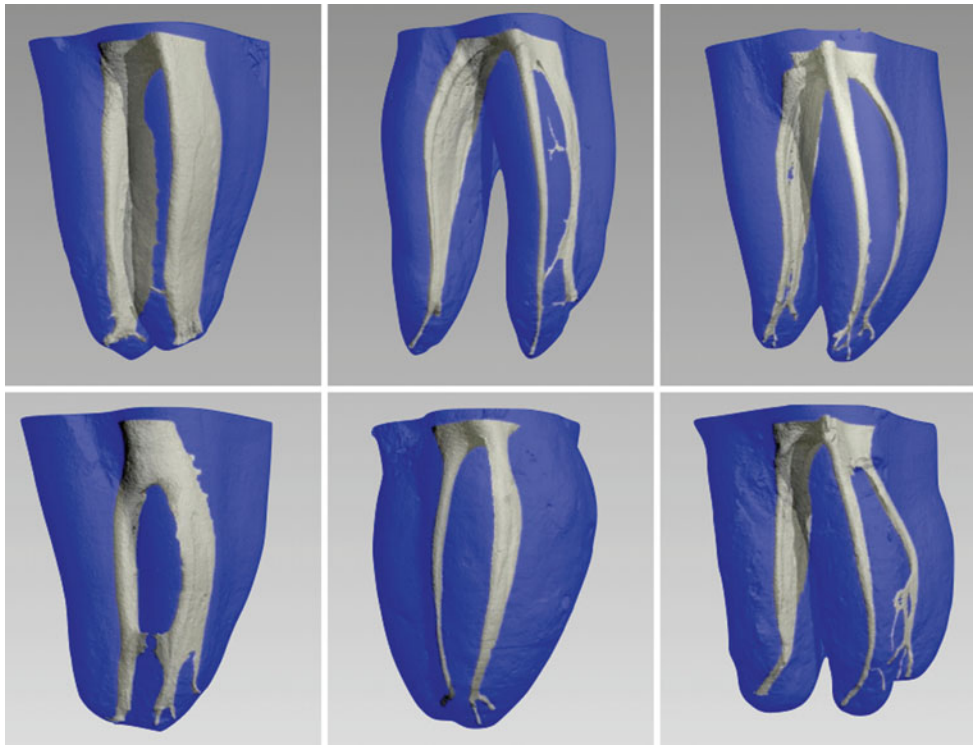

Fig. 1.53 CT scan of roots of lower molars: note the complex morphology of the pulp space

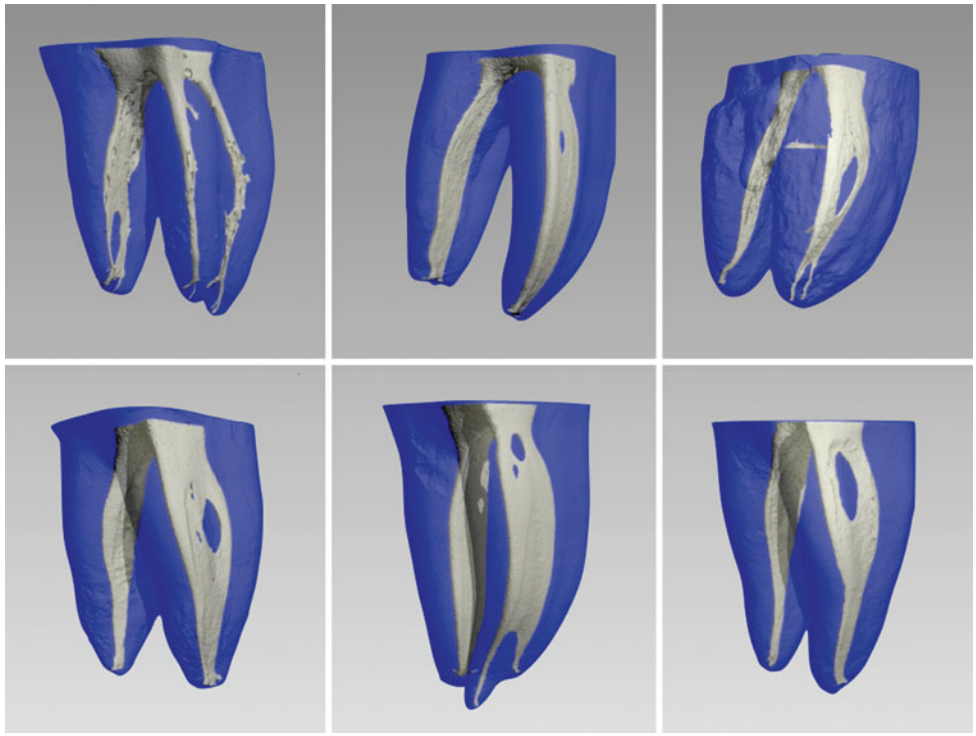

Fig. 1.54 CT scan of roots of lower molars: modern digital instruments reproduce the fine and complex morphology of the pulp space previously illustrated by the histological tables of Hess (CT scan courtesy of Dr. Frank Paqué, University of Zürich, Switzerland and Dr. Enrico DiVito, Scottsdale, Arizona, USA.)

1.9.2 Second Lower Molar

It erupts at the age of 11 years and it is very similar to the first lower molar with some differences.

It is smaller than the first by 1–2 mm in every direction. It presents four cusps on the occlusal surface and it usually has two roots, one mesial and one distal. The mesial root has just one canal in 13 % of cases; more frequently there are two canals which end in just one foramen (49 %), or there are two canals with two independent foramina (38 %). The distal root presents just one canal in 92 % of cases. Rarely are there two canals with one apical foramen (5 %) or two separate foramina (3 %).

The access cavity to the pulp chamber is located in the middle of the mesial-lingual area, and it has a trapezoidal design. Because of the dimensions of the pulp chamber and its proximity to the mesial-lingual wall, we advise attention during the opening of the chamber in order to avoid unnecessary destruction of dental substance (see Figs. 1.55 and 1.56).

1.9.3 Third Lower Molar

It erupts after the age of 17 years and usually at the age of 25 years. Also called "wisdom tooth,"

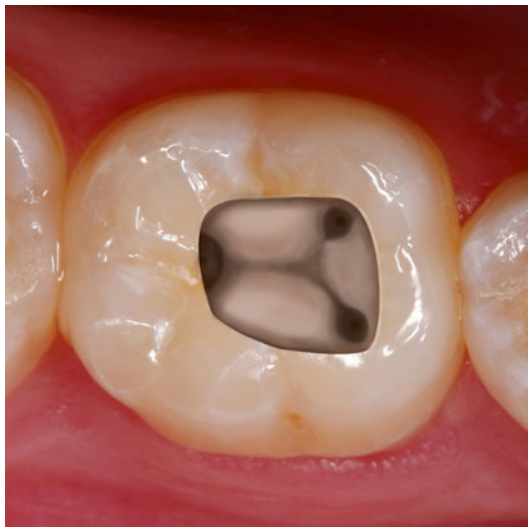

Fig. 1.55 Lower molar: access cavity to three canals (Courtesy of Giovanni Olivi, Rome, Italy)

Fig. 1.56 Lower molar: trapezoidal access cavity to four canals (Courtesy of Giovanni Olivi, Rome, Italy)

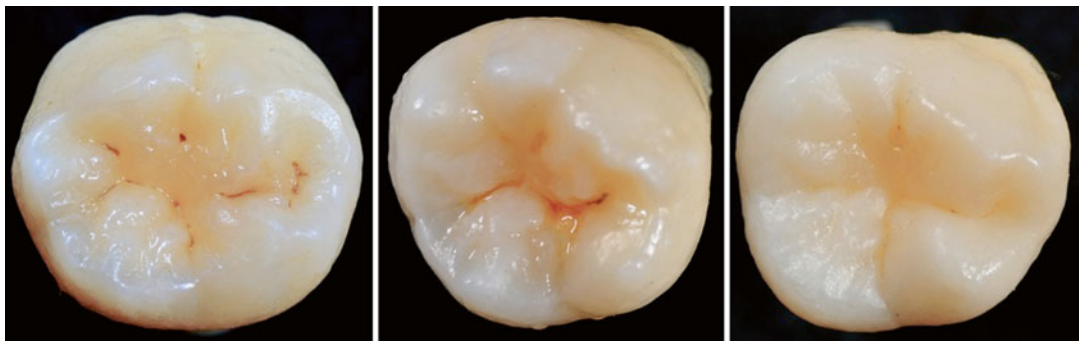

Fig. 1.57 Variegated occlusal morphology of third lower molars can have four to five cusps

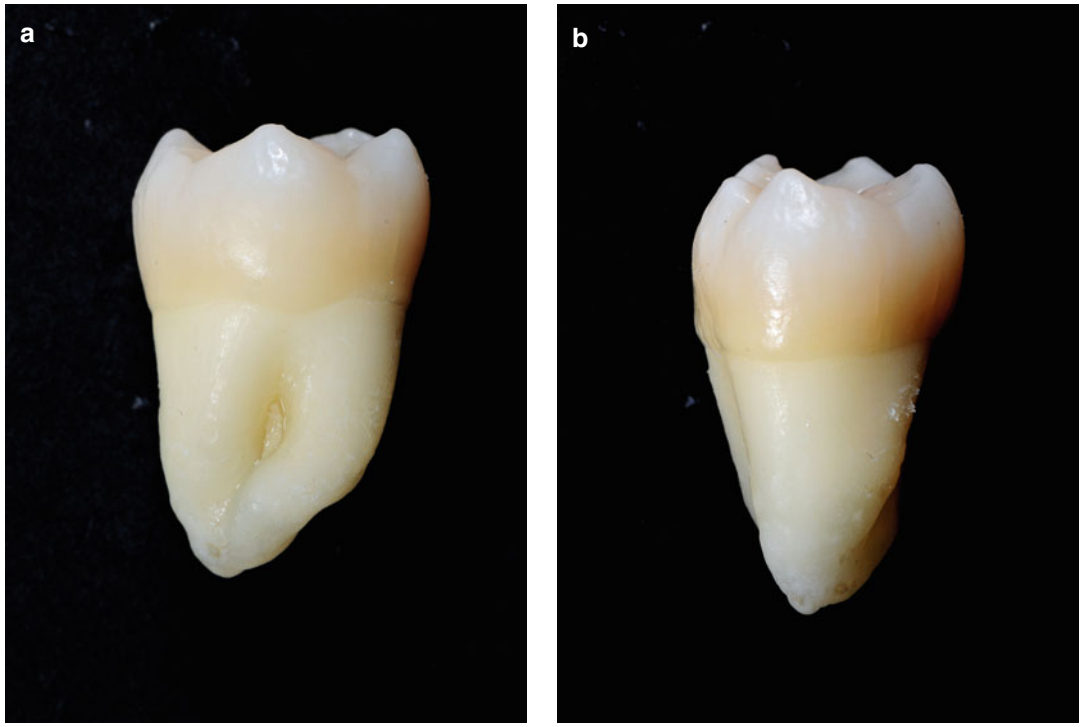

Fig. 1.58 (**a**) Lower third molar with curved mesial root fused to the distal. (**b**) Lower third molar: distal root

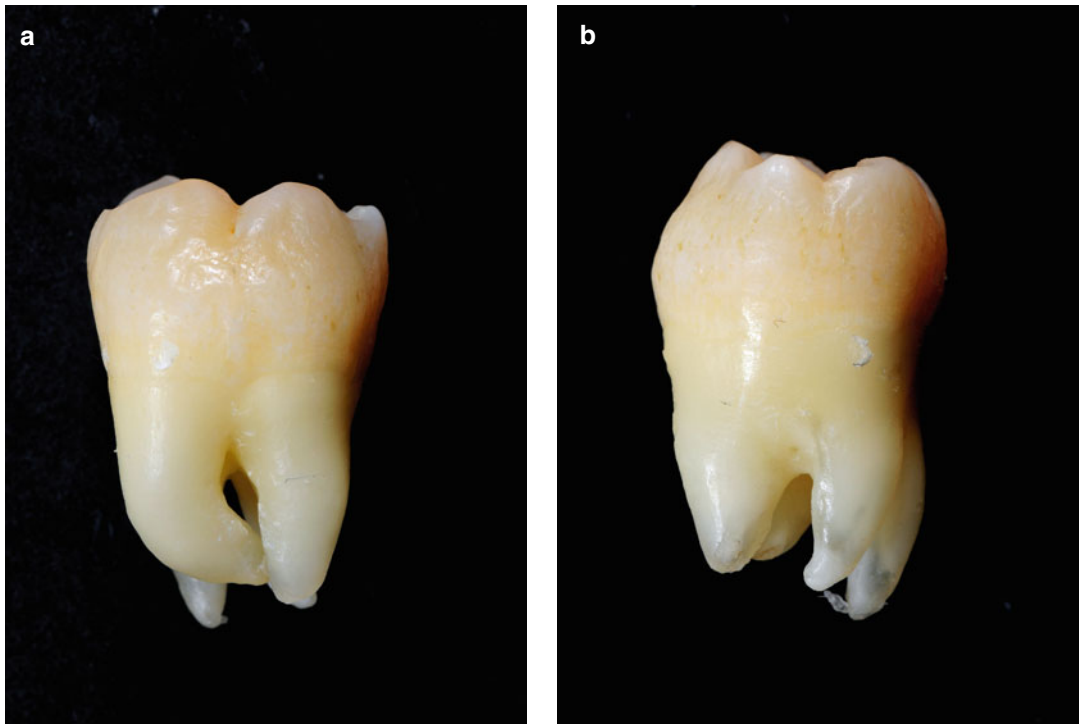

Fig. 1.59 (**a**) Lower third molar showing four roots, two mesial and two distal: the mesial-buccal root presents a very curved canal at the middle one-third. (**b**) Lower third molar: the distal view shows the delicate curvature of the disto-lingual root

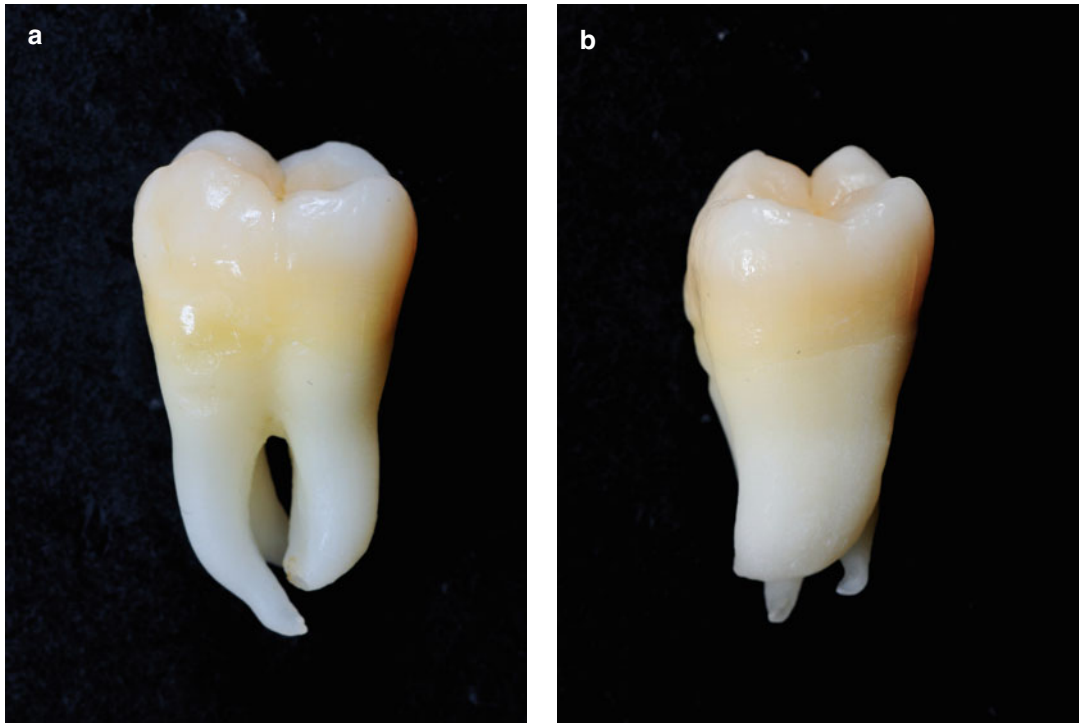

Fig. 1.60 (**a**) Lower third molar: the buccal view shows two separated mesial roots with quite severe-grade curvature, according to Schneider. The distal presents a moderate 3D curvature towards mesial and lingual. (**b**) Lower third molar: the distal view shows the 3D curvature of the distal root in lingual direction and also towards mesial

it has an atypical and variegated morphology. It can have from three to five cusps (Fig. 1.57). Often there is a melding of the roots into two or three roots. As a consequence its endodontic anatomy cannot be schematized, as with the upper molar. Experience in dental operation will lead the operator to the correct negotiation with the endodontic procedure (Figs. 1.58, 1.59 and 1.60).

1.10 Apical Anatomy

The radicular and apical anatomy of the teeth is very complex and summarily assessed preoperatively. The conventional X-ray diagnosis produces a two-dimensional image of the existence of multiple roots and possible curvatures in the mesial-distal direction. The cone-beam computed tomography (CBCT) or 3DCB led dental diagnostic radiology to a three-dimensional level, allowing the study of root curvature on the three planes of space and improving pre- and post-operative diagnosis.

Also the anatomy of the apices in their bizarre variations remains difficult to assess and also not treatable operatively. Hess's tables explain the impossibility of pre-operative correct interpretation of the tooth anatomy and of complete instrumentation of the apical one-third often cause of endodontic failure (Figs. 1.61, 1.62, 1.63, 1.64, 1.65 and 1.66). Delta terminus, fine ramifications and multiple apices are only a summary of several anatomy variations in the apical one-third of the root.

The different irrigation or laser irradiation techniques used for root canal cleaning and decontamination have their greater limit in the macroscopic and microscopic anatomy of the apical third, whose unpredictable variability affects the prognosis of endodontic therapy.

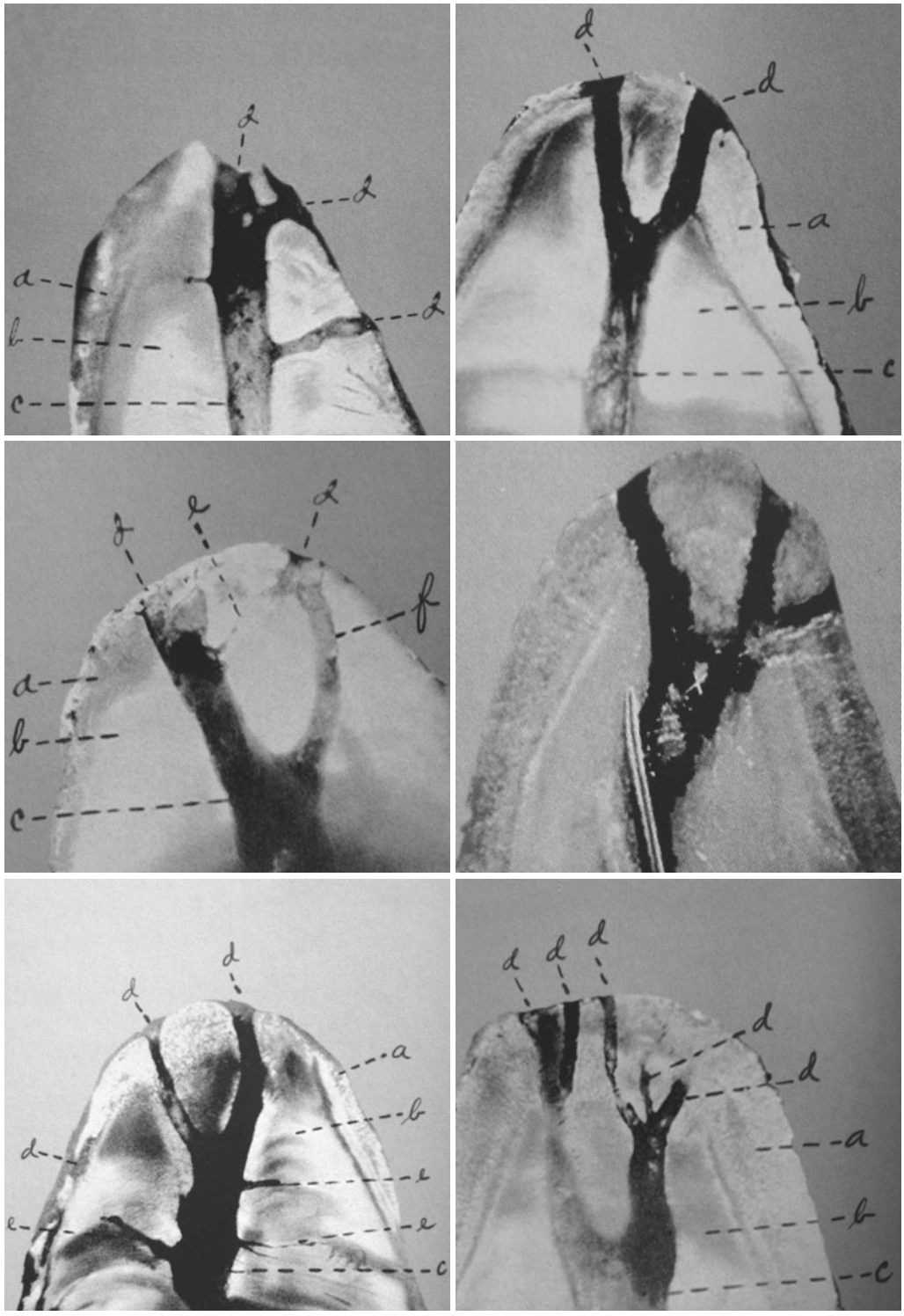

Figs. 1.61, 1.62, 1.63, 1.64, 1.65 and 1.66 Images showing the complex anatomy of the apical one-third. A single canal can finish with a single port of exit or a delta; many times three or more termini are present. Davis emphasized the impossibility to remove all the pulp tissue from the apical part of the root, also investigating the fate of the organic content remained in the apical ramifications after a root canal therapy (From "Essential of Operative dentistry, W. Clyde Davis" [1], reprinted in [2]) (Image reprint with permission from Perrini [1])

1.11 Microscopical Anatomy of Permanent Teeth

The dental crown is made by an external layer of very hard and highly mineralized tissue, the *enamel*, and by an internal part of less hard and less mineralized tissue, the *dentin*, composed by an organic part rich in collagen fibrils and of inorganic component, the hydroxyapatite.

The root is composed of an external part called *cementum*, which covers it entirely, and by an inner part, the dentin, which defines the endodontic space of the canal containing the pulp tissue.

In case of chronic or acute pathology, the pulp shows the histological signs of irreversible and degenerative inflammation until necrosis occurs. Later on the dentin becomes the guest tissue for bacterial flora responsible of the endodontic pathology. Bacteria colonize the dentin surface of the main and lateral canals as free cell form (planktonic) or as organized conglomerate, highly adherent to the surface (biofilm); both these bacterial forms penetrate the surface of the canal towards the dentin tubules, point of passage from the endodontic space to the apical and radicular or periradicular space (periodontium).

During root canal therapy, dentin tubules represent a critical anatomic area to decontaminate. Due to the difficulty and limitations of the common irrigation techniques, of medicaments and/or of laser irradiation to penetrate deeply the dentin walls and to reach and kill bacteria deeply hosted, the radicular dentin microanatomy and the effective disinfection represent the potential causes of endodontic failure.

This concept must be kept in mind when considering specific laser irradiation and its interaction with the targets, the radicular dentin or the bacteria hosted in it.

1.12 Dentin

Dentin has a various composition (proportions are 70 % of inorganic material, 18 % of organic matrix and 12 % of water, in weight). It is characterized by a structure of mineralized collagen fibrils which define the architecture of dentinal tubules that extend from the pulp to the enamel or to the radicular cement.

Dentin is formed from mineralization of the organic matrix with inorganic elements gradually secreted by the odontoblasts of the dental pulp (Figs. 1.67 and 1.68).

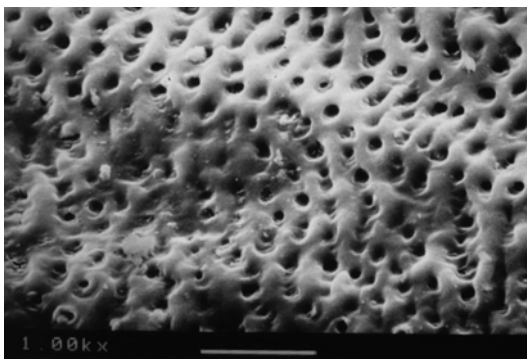

Fig. 1.67 SEM image at 1000× magnification: orifices of dentinal tubules of the radicular cervical one-third; the presence of the collagen architecture is evident

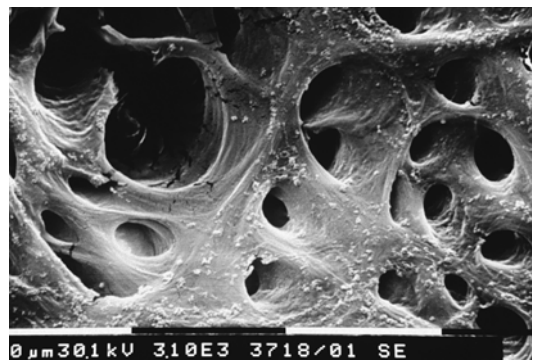

Fig. 1.68 SEM image at 3100× magnification: orifices of dentinal tubules of the apical one-third of the root

1.12.1 Predentin and Calcospherules

Dentin is separated from the dental pulp by a thin non-mineralized tissue (15–40 μm thickness or width), the predentin. The predentin is composed of twine of fibres and fundamental substance. The mineralization front of predentin is formed of calcospherules and calcoglobulin (Figs. 1.69, 1.70, 1.71 and 1.72).

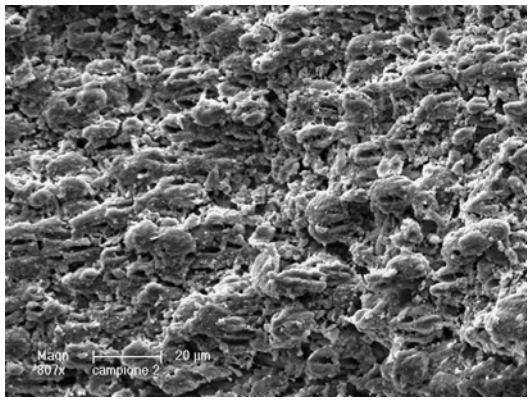

Fig. 1.69 SEM image at 807× magnification: predentin with calcospherules in the middle one-third of the root

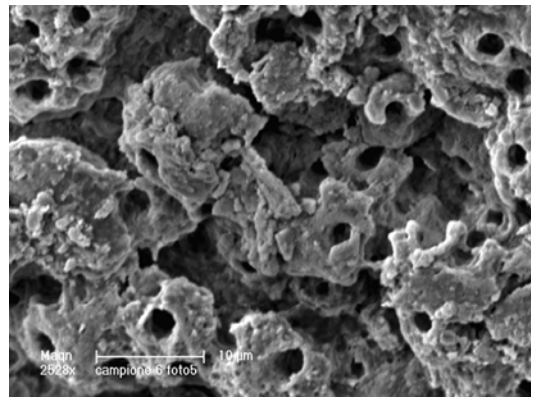

Fig. 1.70 SEM image at 2528× magnification: predentin with calcospherules in the middle one-third of the root

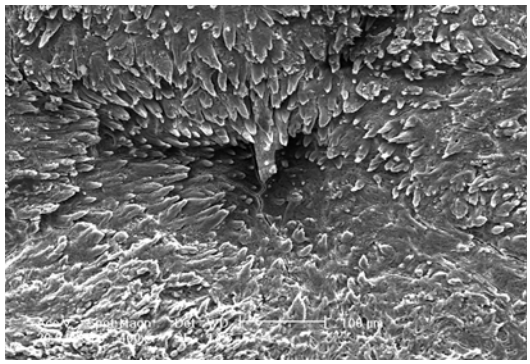

Fig. 1.71 SEM image at 400× magnification: predentin with irregular calcospherules in the middle one-third of the root

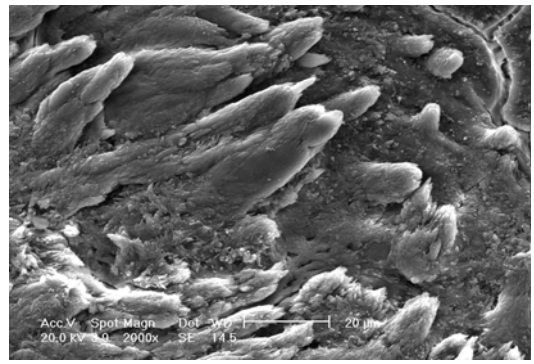

Fig. 1.72 SEM image at 2000× magnification: predentin with irregular calcospherules in the middle one-third of the root; this irregular aspect depends on immature mineralization of the predentin caused by a sudden and violent but not carious insults

1.12.2 Dentinal Tubules

Dentin tubules have an "S" pattern in the crown and mainly straight in the root. They connect the pulp tissue with the cement and enamel. The number of tubules and their diameter depends on their radicular or coronal position and on their proximity to the pulp. An increased number and diameter of dentin tubules are present from the periphery of the dentin to the pulp (from 45,000 to 19,000 for mm^2 and from 0.9 μm to 2–3 μm) (Fig. 1.73).

1.12.3 Peritubular and Intertubular Dentin

Dentin tubules are delimitated by peritubular dentin, a tissue with a high level of mineralization produced by the odontoblasts during the dentinogenesis. The intertubular dentin constitutes most part of the dentin, richer in organic material and water (Figs. 1.74 and 1.75). As a consequence of the dentin ultrastructural composition, peritubular dentin is the more exposed part to the acid of bacterial metabolism and the less ablated by the erbium laser irradiation (2780 and 2940 nm) because of the less water content than the intertubular dentin. The dentin ultrastructural composition explains the peculiar microscopic morphology after erbium laser irradiation (Figs. 1.76 and 1.77).

Following external irritative stimulus, odontoblasts start again the deposition of the peritubular dentin, producing a reduction of the tubules diameter, in the attempt to protect the tooth by interrupting the communication between pulp and dentin in a process called *dentin sclerosis* (Figs. 1.78, 1.79 and 1.80).

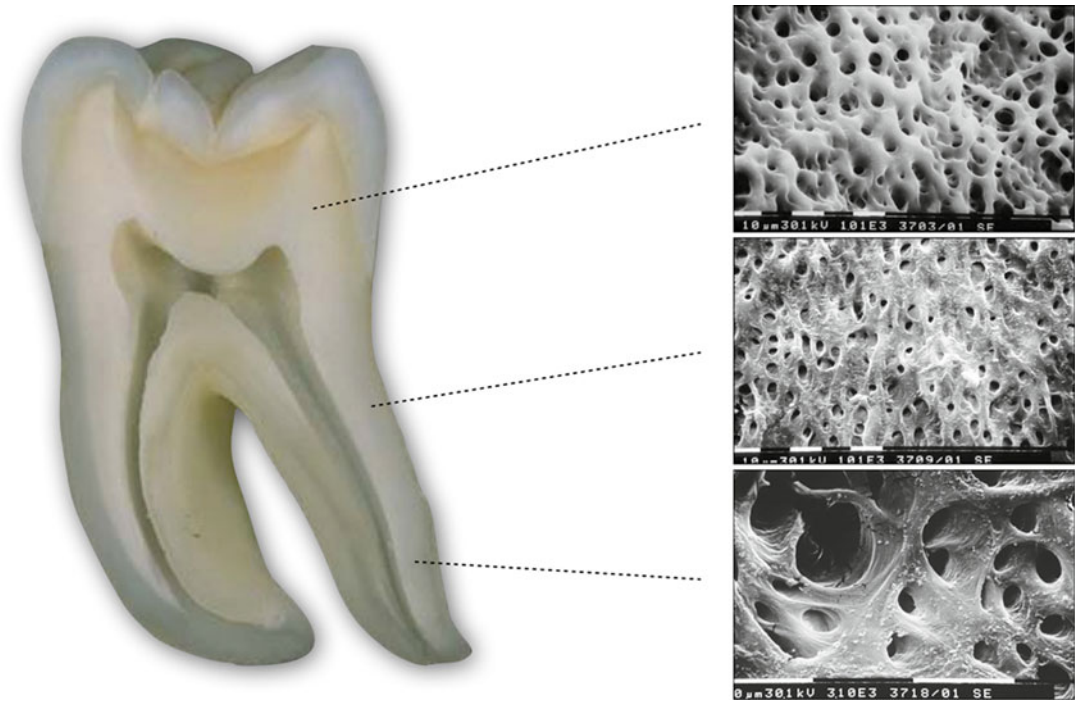

Fig. 1.73 Coronal, middle root and apical dentin (total width). The number and diameter of dentin tubules vary from the coronal to the apical part, decreasing from coronal to apical

Fig. 1.74 SEM image at 4620× magnification: coronal dentin with visible odontoblastic filaments

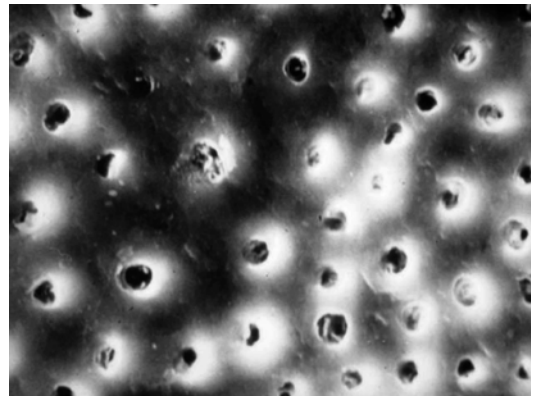

Fig. 1.75 SEM image at 2500× magnification shows intertubular and peritubular dentin: the higher dentin mineralization in the peritubular area appears whiter because of more electron reflection

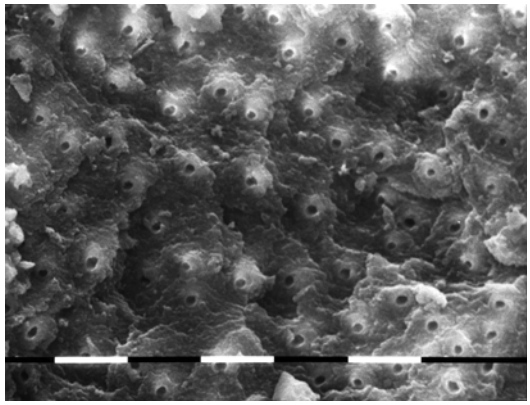

Fig. 1.76 SEM image at 2000× magnification of dentin irradiated with Er,Cr:YSGG laser at 75 mJ, 20 Hz with a 200 μm fibre. More mineralized peritubular dentin presents less ablation compared to the intertubular, showing the typical erbium-lased pattern termed "chimney" effect

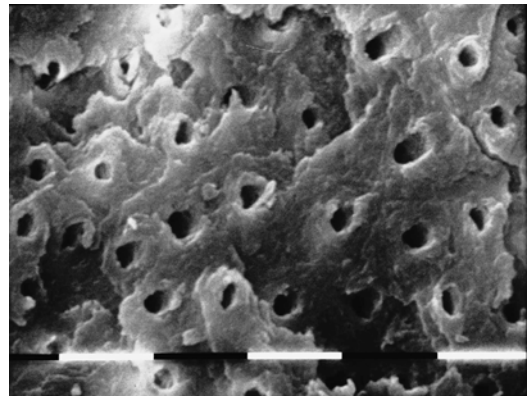

Fig. 1.77 SEM image at 2500× magnification shows dentin irradiated with Er,Cr:YSGG laser at 125 mJ, 20 Hz with a 200 μm fibre. Higher power setting produces a wider dentin ablation which involves both intertubular and peritubular dentins; superficial thermal effect is also present with vaporization of the organic matrix

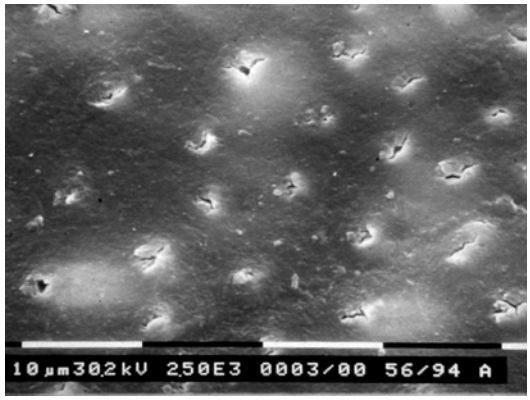

Fig. 1.78 Image at 2500× magnification shows sclerotic dentin. In correspondence to dental caries, inside the dentinal tubules, the acids, produced by the bacterial dentin destruction, cause a precipitation of calcium salts with saturation of dentin fluid and consequently a precipitation of calcium crystals and formation of hydroxyapatite crystals that form calcified moulds of dentinal tubules

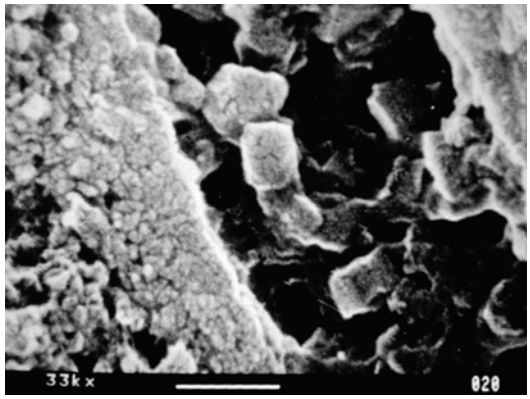

Fig. 1.79 SEM image at 33,000× magnification shows the presence of calcification (*whitlockite*) inside a dentinal tubule, occluding it (Reprinted with permission from PICCIN)

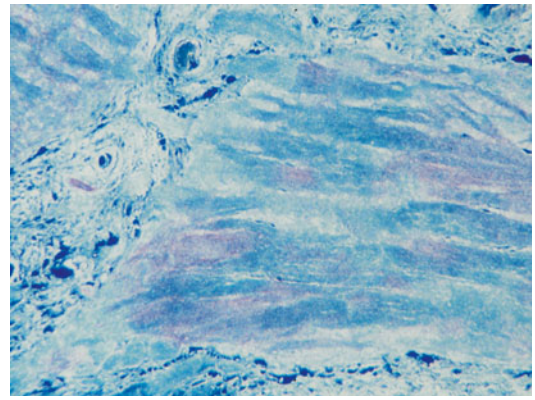

Fig. 1.80 Thready calcification spread along pulp capillaries (image at OM) (Reprinted with permission from EDRA)

1.13 Types of Dentin

During the lifetime of a tooth through the years, a progressive mineralization of the dentin's organic part happens to define different morphologic types of dentin. *Primary* dentin is that produced during the odontogenesis before the dental eruption.

After the eruption, the dentinogenesis produces the *secondary* dentin, starting from the *predentin* at the level of the pulp horns (cornets) and at the floor of the pulp chamber, leading to the maturation and completion of the root.

Tertiary dentin is a *reactive* dentin, formed as a pulp reaction to external acute irritative

stimulation, physical (hot, cold, bruxism, abrasions), chemical (erosions) or bacterial (cavities) especially in the crown. *Tertiary* dentin is formed from pre-existing odontoblasts and from the undifferentiated cells of the pulp, which differentiate into odontoblasts deprived of peripheral extension. *Tertiary* or *reactive* dentin doesn't have tubules or have just some incomplete traces.

Over the *tertiary* dentin, another defence mechanism of the dental pulp is the *sclerotic* dentin (see Figs. 1.78, 1.79 and 1.80).

For a more accurate analysis of the histology of the human dental tissues, the reader is invited to explore other texts, including *Laser in Restorative Dentistry*, also published by Springer [19].

References

1. Perrini N. Storia anatomica del sistema dei canali radicolari. Milano: Edizioni SIE; 2010. p. 195–6.
2. Hess W, Golding P, Castagnola L, Perrini P, Keller O. Le tavole anatomiche di W. Hess ed O. Keller: ricerche sull'anatomia dei canali radicolari della dentatura umana mediante il metodo di diafanizzazione (1928). Saronno: Edizioni Scientifiche Oral B; 1988. Fondazione Luigi Castagnola; edizione bilingue italiano-inglese.
3. Weine FS. Access cavity preparation and initiating treatment. In: Weine FS, editor. Endodontic therapy. St.Louis: CV Mosby Co; 1996. p. 243.
4. Vertucci FJ. Root canal anatomy of the human permanent teeth. Oral Surg Oral Med Oral Pathol. 1984;58(5):589–99.
5. Gulabivala K, Aung TH, Alavi A, Ng Y-L. Root canal morphology of Burmese mandibular molars. Int Endod J. 2001;34:359–70.
6. Gulabivala K, Opasanon A, Ng Y-L, Alavi A. Root canal morphology of Thai mandibular molars. Int Endod J. 2002;35:56–62.
7. Sert S, Bayirli GS. Evaluation of the root canal configurations of the mandibular and maxillary permanent teeth by gender in the Turkish population. J Endod. 2004;30:391–8.
8. Schneider SW. A comparison of canal preparations in straight and curved root canals. Oral Surg Oral Med Oral Pathol. 1971;32:271–5.
9. Lautrou A. Anatomia dentaria. IIth ed. Milano: Masson; 1987.
10. Zidell J. Classification of root canal system. In: Ingle JI, Taintor JF, editors. Endodontics. 3rd ed. Philadelphia: Lea & Febiger; 1985. p. 246.
11. Ingle JI. Endodontics. 3rd ed. Philadelphia: Lea & Febiger; 1985.
12. Gagliani M, Fornara R. Testo atlante di anatomia endodontica. Milano: Tecniche Nuove; 2011. p. 15–8.
13. Ash MM, Nelson SJ. Wheeler's dental anatomy, physiology and occlusion. 9th ed. Philadelphia: WB Saunders; 2009.
14. Ash MM. L'Anatomia funzionale del dente e l'occlusione di Wheeler. Milano: Edi Ermes edizione italiana; 1986.
15. Berutti E, Gagliani M. SIE-Manuale di Endodonzia. Milano: Edra Masson; 2013.
16. Ricucci D. Patologia e Clinica Endodontica. Bologna: Edizioni Martina; 2009.
17. Cohen S, Burns RC. Pathways of the pulp. 4th ed. St. Louis: CV Mosby; 1987. Piccin edizione italiana.
18. Berkovitz BKB, Boyde A, Frank RM, Hohling HJ, Moxham BJ, Nalbandian J, Tonge CH. Handbook of microscopic anatomy, Teeth, vol. V/6. Berlin: Springer; 1989. p. 175.
19. Olivi G, Olivi M. Laser in restorative dentistry. Chapter 1. Cham: Springer International Publishing; 2015. Title to be defined.

Root Canal Catheterization

2

Mohammed Alshahrani, Roberto DiVito, and Enrico E. DiVito

Abstract

The ultimate goal of endodontic treatment is the eradication of microorganisms, which lead to endodontic disease. Ultimately a triad approach to treating dental pathology in endodontics results. They are shaping, cleaning, and disinfection via irrigation and finally obturation.

The complete sterilization of the root canal system is a daunting task and frequently unattainable due to the complex anatomy of the root canal system. However, a more reasonable and achievable goal is to bring the microorganism count down to a level where the body can heal itself. Current techniques encompass the use of chemo-mechanical debridement followed by a three-dimensional obturation of the root canal system.

The cleaning and shaping are an integral part that must be carried out in a smooth, dynamic way and reproducible way. A prior comprehensive knowledge of tooth anatomy helped the clinician to perform the endodontic treatment safely and efficiently.

In this chapter, a thorough description of the routine orthograde endodontic treatment will be addressed. It includes a comprehensive explanation of biological and technical objectives as well as the strategies of shaping the root canals. The armamentarium required to complete the non-surgical endodontic treatment will be discussed including the use of nickel-titanium rotary instruments in contemporary endodontics. Objectives, requirements, and techniques available for optimal results will be explained.

M. Alshahrani, BDS, DScD, CAGS
Department of Endodontics, Boston University, Henry M. Goldman School of Dental Medicine, 100 East Newton Street, G 705, Boston, MA 02118, USA
e-mail: shahrani@bu.edu

R. DiVito, DDS
General Residency Program, Arizona Center for Laser Dentistry, Arizona School of Dentistry and Oral Health, 7900 East Thompson Peak Parkway #101, Scottsdale, AZ 85255, USA
e-mail: rdivito@azcld.com

E.E. DiVito, DDS, PC (✉)
General Residency Program, Arizona Center for Laser Dentistry, 7900 East Thompson Peak Parkway #101, Scottsdale, AZ 85255, USA
e-mail: edivito@azcld.com; http://www.drdivito.com

G. Olivi et al. (eds.), *Lasers in Endodontics: Scientific Background and Clinical Applications*,
DOI 10.1007/978-3-319-19327-4_2

Early in root canal treatment history, procedures were focused on exposing the root canals to receive a medicament because technology had not progressed to a point where doing so was even feasible. However, according to Schilder (1974), the goal of modern endodontics is to clean the canal's contents as well as possible and then shape it to receive a three-dimensional biocompatible filling material [1]. By doing so, harmful contents are removed to a degree that enables the body to heal itself.

The "cleaning and shaping" process can be divided into several stages. First, access cavity preparation is required to locate all root canals; then each canal is debrided and shaped to receive the inert filling material.

2.1 Access Cavity Preparation

The access cavity is considered by many to be the most difficult part of root canal therapy. It is the process which opens the tooth's occlusal surface to expose the coronal aspect of the root canal system. If done well, it greatly facilitates cleaning, shaping, and obturation. If done poorly, it makes proper root canal treatment much more difficult and can lead to incidences of unnecessary iatrogenic events. Proper access cavity preparation should meet the following objectives:

- Caries removal
- Conservation of crown tooth structure while creating a straight-line path to each canal's midpoint
- Complete de-roofing of pulp chamber
- Coronal pulp tissue removal
- Locating all canal orifices
- Establishing restorative margin to minimize the leakage and ultimate reinfection
- Eliminating the chance of lateral strip perforations during the cleaning and shaping process

Proper access cavity preparation must include the careful examination of both the pulp chamber and root canal anatomy. Radiographs reveal valuable information but one must consider that radiographs reveal only two dimensions of a three-dimensional object. Therefore, much interpretation and assumption still remain, and accurate treatment is left up to the skill and experience of the clinician.

Recently the use of 3D CT cone beam has been introduced and gives the clinician more accurate and comprehensive information of both external and internal root morphologies. Krasner and Rankow (2004) found that the pulp chamber of every tooth is located at the middle of the tooth in relation to the level of CEJ [2]. They referred to this as the law of centrality. They also described that the wall of the pulp chamber is always concentric to the external surface of the crown at the CEJ level. As such, teeth should be probed to locate the CEJ. Once the CEJ is located, the point of entry can be then determined. Clinicians should avoid using the angulation of clinical crowns only to access preparations as this can lead to mishaps. Tables 2.1 and 2.2 demonstrate this occurrence.

After locating the point of the entry, the access preparation should be initiated using the appropriate bur. Bur selection depends on clinician preferences and the type of material (natural or man-made) that you are cutting. Usually #2 round bur will be used with small teeth and #4 round bur used with larger teeth. There are also other burs such as a tapered fissure bur which cuts efficiently through prosthetic restorations. Tapered diamond, Endo Z bur, and 245 burs can be used also. The drilling should be carried on until a "drop" is felt. Caution must be taken since this drop is not applicable in teeth with shallow pulp chamber as defined by pre-treatment radiographs. De-roofing should be attempted until the

Table 2.1 Krasner and Rankow's proposed laws [2]

Relationships of the pulp chamber to the clinical crown
Law of centrality: the floor of the pulp chamber is always located in the center of the tooth at the level of the CEJ
Law of concentricity: the walls of the pulp chamber are always concentric to the external surface of the tooth at the level of the CEJ
Law of the CEJ: the CEJ is the most consistent, repeatable landmark for locating the position of the pulp chamber

Table 2.2 Krasner and Rankow's proposed laws [2]

Law relationships of the pulp-chamber floor
Law of symmetry 1: except for maxillary molars, the orifices of the canals are equidistant from a line drawn in a mesial-distal direction through the pulp-chamber floor
Law of symmetry 2: except for the maxillary molars, the orifices of the canals lie on a line perpendicular to a line drawn in a mesial-distal direction across the center of the floor of the pulp chamber
Law of color change: the color of the pulp-chamber floor is always darker than the walls
Law of orifice location 1: the orifices of the root canals are always located at the junction of the walls and the floor
Law of orifice location 2: the orifices of the root canals are located at the angles in the floor-wall junction
Law of orifice location 3: the orifices of the root canals are located at the terminus of the root developmental fusion lines

pulp chamber is completely uncovered. No attempts should be made to locate the orifices until de-roofing is completely finished. Then the canals can be observed. Any unsupported tooth structure should be removed for restorative assessment.

2.2 The Shaping Concept

After adequate access opening has been prepared, a sharp endodontic explorer is typically used to locate the orifices and to assess for straight-line access. Pre-flaring the coronal third should be carried out with the goal of creating a "funnel" at each canal orifice so that instruments easily "drop into" the canal without the clinician having to "search and find" canals. Gates Glidden burs and many other "orifice opener" instruments are available for creating such funnels without gouging the pulpal floor. All dentin triangles in anterior teeth and dentinal overhangs in posterior teeth are removed to reveal orifices and establish straight-line access to the middle third of each root canal. Preparation in this manner makes the subsequent steps easier and faster while eliminating any unnecessary bending of instruments which can later lead to broken instruments and ledged canals.

Schilder (1974) described the cleaning and shaping process, often called "instrumentation," in great detail. He emphasized the importance of achieving certain objectives that result in successful endodontic treatment [1]:

- A continuous funneled and tapered preparation from apical to coronal third.
- As a result of this continuous taper, the smallest diameter should be kept apically and largest diameter coronally.
- The apical foramen should be kept as small as practical.
- The apical foramen should be kept in its original geographic location.
- When the canal is shaped, it should be shaped in three dimensions and the preparation should be a continuous funnel to the apical area.

A continuous funneled and tapered preparation ensures adequate delivery of irrigants close enough to the working length, and it exposes lateral canals by shortening its length. Tapered preparations increase the contact between the file and dentinal walls, whereas in parallel preparation it is less likely to have such contact. Obturation also will be enhanced with funneled preparations, and compaction forces are distributed evenly resulting in a better seal.

The diameter of the root canal should be as small as the canal preparation apically. This kind of preparation will transmit the compaction forces to the smallest area including lateral canals, fins, and isthmus. This results in denser compaction of gutta-percha. Caution must be taken not to weaken the coronal structure by creating too large of a taper. This is particularly true in teeth that have internal resorption.

Clinicians, during root canal therapy, frequently deviate from the canal's original path thereby creating a new artificial path, commonly called "transportation" of the canal. This is most often caused by the rigidity of the instruments and their inability to accurately follow the curves of the canals. One objective of proper root canal instrumentation is to minimize transportation because it can result in unnecessarily removing of healthy dentin and incomplete debridement of

the harmful contents within the main canal. However, conservative straightening of the canal's coronal third is often desirable in order to achieve better access to the apical third. Transportation of the foramen is one of the most common reasons for wet or bleeding canals, which can result in chronic persistent inflammation and failure of root canal therapy. The rigidity of the metals creates a lever effect when the instrument goes around a curve. This exerts a lateral force, which can lead to transporting the foramen. In severe cases, a lateral perforation through the side of the root is the result. Creating straight-line access to at least the mid-root of the canal helps to reduce this level effect and reduces the lateral force of the instrument leaning against the side wall of the canal. The use of copious amounts of irrigation during instrumentation also helps prevent accumulation of dentinal shavings and canal blockage that also cause instruments to deviate away from the canal's original path.

The following biological objectives are necessary for adequate root canal preparation:

(a) Confine the instrument to the root canal space without preparing the surrounding bone.
(b) Care should be taken not to force or push the root canal content to the periradicular area.
(c) Removing and debriding the root canal content meticulously.
(d) Completing vital and non-vital cases in one visit if the chance of successful treatment is not compromised by doing so.
(e) Creating sufficient space for effective irrigation and intracanal medicaments to accommodate the periradicular discharges as a result of inflammation caused by instrumentation.

2.2.1 Hand Instrumentation

There are essentially two primary techniques to shape the root canal system using hand files. They are step-back and crown-down technique.

- Step-back technique [3]
  This technique involves completing instrumentation of the apical third first and then debriding the remainder of the canal by "stepping back" coronally from the working length with successively larger instruments, in 0.5–1 mm increments.

- Crown-down technique [4]
  In this technique the coronal third is flared first, using Gates Glidden drills or similar instruments to remove the obstructions from coronal and middle third. The apical third is negotiated and completed last. Pre-curved files are advocated during this technique.

In many instances, clinicians use a combination of both crown-down and step-back techniques as they are not mutually exclusive of each other.

2.2.2 Rotary Instrumentation

Endodontic instruments typically have design features as described in Table 2.3.

2.2.2.1 File Design Features and Functions

Nickel-titanium rotary instruments were first introduced to the market in 1993. Nickel-titanium, also known as nitinol, is a metal alloy made of

Table 2.3 Rotary endodontic instrument components

File components	Definition	Role
Flutes	The groove in the working surface used to collect debris	Debris collection depends on the depth, design, and finish
Land	The non-cutting part of the file, which is a metal projection away from the center of the file	Reduces file engagement and keeps the file centered
Rake angle	The angle formed by the leading edge and radius of the file	The more obtuse the angle is, the more cutting the file is
Pitch	The distance between two adjacent leading edges	The more pitches the file has, the greater the helix angle
Helix angle	The angle formed by the cutting edge and long axis	It is important to determine the filing technique

nickel and titanium in generally equal proportions. It was developed initially in the 1960s for military purposes, but its potential in the dental field was recognized and has been used for hand files, rotary files, and even orthodontics.

The discovery of NiTi changed the way the root canal instruments were made and how canals were prepared. It allowed files to be placed into air-driven and electric handpieces, rotating them at high speeds thus making root canal preparation easier and faster for clinicians. Curved canals were more easily negotiated, and shaping errors were minimized due to NiTi's superior flexibility and its ability to return back to its original shape [5].

Many endodontic rotary systems exist in the industry today, with many more being introduced yearly. This chapter will discuss two of the most popular systems.

2.2.2.2 ProTaper Universal

The design of the ProTaper rotary files by Dentsply Maillefer differs from other designed instruments. It incorporates a progressive taper along the length of the instrument, whereas most other instruments have just one taper from one end of the cutting blade to the other. It has two shaping and five finishing files to choose from. It includes also an SX file, which is used in opening the orifice. S1 and S2 files are used to flare the coronal and middle third of the canal system. The finisher files F1, F2, F3, F4, or F5 are used for preparing the apical third.

Once the access opening is established, #10 and 15 k-type hand files are used to explore the coronal and middle third. S1 and S2 are taken to resistance not more than two thirds of the canal depth in brushing motion. Then #10 and 15 k-files are used to explore the apical third and to determine the working length. S1 and S2 are taken to working length followed by F1 as well. The apical foramen is then gauged with hand files passively. F2, F3, F4, and F5 are used as needed for refinement and completion of apical shaping.

2.2.2.3 Twisted Files (TF)

SybronEndo introduced the Twisted File rotary system to the market in 2008. These were the first files made using a proprietary heat treatment method to form the spiral-shaped cutting blades. Whereas files are typically ground into their final configuration by a grinding machine, TF's flutes are created by twisting a metal alloy blank, lengthwise, instead of grinding it. This process eliminates microfractures caused by grinding the surface of the metal which in turn reduces the chance of instrument separations and more flexible files. TF comes in two lengths, 23 and 27 mm, and also in different sizes and tapers. TF follows the typical crown-down instrumentation sequence described above.

2.3 Root Canal Obturation

The ultimate goal of root canal treatment is either to prevent the development of apical periodontitis or to create an adequate environment for the healing to occur. Thereafter, the root canal space is filled, or obturated, in three dimensions to seal and avoid reinfection of the cleaned root canal system. Obturation encompasses two key components: (1) the core filling material and (2) sealer. The core material occupies the canal space, whereas sealer fills the gaps between and the core material and canal walls. Some obturation techniques warm the filling material to allow it to better adapt (flow) to the root canal system. Yet, because sealer is liquid before it cures and becomes solid, it flows better into the areas of the root canal system than the solid or semisolid core filling material.

The filling material should meet most of the requirements listed in Table 2.4.

Table 2.4 Properties of an ideal obturation material

Ideal root canal filling Grossman [6]
Should be easily introduced in the canal system
Seal the canal apically and laterally
Should not shrink
Be radiopaque
Be bacteriostatic or at least prevents bacterial growth
Not stain the tooth structure
Not irritate the periradicular tissues
Sterilizable
Easily removed if necessary

2.3.1 Lateral Compaction

Lateral compaction is one of the oldest and more widely used methods to obturate the root canal. In this method a "master" gutta-percha (or similar material) cone is selected corresponding to the same size and shape as the final canal preparation size. The cone should exhibit resistance to removal (tug back) when placed to full working length. If the cone is too loose or goes passed the working length, then 1 mm cuts from the master cone tip should be made until good tug back is established. Conversely, if the cone cannot reach full working length, additional cones should be tried or a cone of the next smaller size might be required. To laterally compact the gutta-percha, a hand instrument called a spreader is used. Also available is a finger spreader. The advantages of using finger spreader over the hand instrument spreader are the tactile sensation and precise control of the applied force. Spreaders are available in different sizes and made from both nickel-titanium and stainless steel. Nickel-titanium finger spreader allows for more penetration, and it adapts better to the root canal especially in curved canals. The disadvantages of this technique are:

1. Lateral canals are not filled, with gutta-percha, because in its solid form gutta-percha is not able to flow laterally.
2. Lateral forces might cause root fracture or set up micro cracks that later can lead to root fracture.
3. It is typically slow and labor-intensive compared to some of the more modern techniques.
4. It often leaves large gaps which are easily penetrated by micro-sized organisms.

Table 2.5 shows the detailed procedure of lateral condensation.

Despite a well-shaped, cleaned, and obturated root canal, failure can occur if there is insufficient coronal seal. Therefore, one must not underestimate the importance of the coronal restoration.

Table 2.5 Lateral compaction

Lateral compaction technique
Cone fit to the working length
Canal then irrigated and dried
Sealer application using lentulo spiral or paper points
Spreader selection should match the accessory cone size
Spreader should be fit, 1–2 mm shorter of working length
Accessory cones fit immediately after spreader removal and repeated till the canal is completely filled
Accessory cones then are seared off and condensed well at coronal part

2.3.2 Warm Vertical Compaction

In an effort to improve upon then current obturation methods, Schilder (1977) advocated filling the root canal system "in three dimensions" as the primary goal of root canal obturation [7]. He understood that inadequate obturation is a likely cause of subsequent treatment failure and sought improvement by heating gutta-percha so that it would flow laterally.

Warm vertical compaction involves a number of devices such as heat sources (System B, Touch'n Heat, Elements Obturation Unit) and pluggers, which carry the heat down into the root canal. Like lateral compaction, this technique also requires a master cone to be precisely fit. A larger taper master cone helps to prevent the cone from buckling while applying the vertical force. Also the cone should fit tightly just short of working length to help prevent the cone from being pushed past the end of the root when the vertical force is applied. One concern of warm vertical compaction is heat damage to the periodontal ligament. Thus, care must be taken to avoid applying heat for extended periods of time. Manufacturer instructions should be followed strictly; most suggest removing the heat after no more than 5 s of application. Selected pluggers should be engaged against gutta-percha and not against the canal walls as root fracture might occur (Table 2.6).

2.3.3 Carrier-Based Obturation

Carrier-based obturation involves forming a thin layer of gutta-percha over a taper-shaped solid core of material. The rigidity of the carrier allows clinician to insert the gutta-percha easily into prepared root canal system. The gutta-percha is warmed in an oven just before use, and the

Table 2.6 Warm vertical compaction

1. Cone fit should be done in wet canal with tug back
2. The cone is cut 0.5 mm to compensate compaction forces
3. Pre-fitted pluggers should be selected for apical, middle, and coronal third
4. Canal then should receive the final rinse and dried appropriately
5. Sealer is applied to the canal using paper point or lentulo spiral
6. With caution, the cone is placed to working length
7. System B or Touch'n Heat tip is activated to sear off the gutta-percha cone at orifice level, and then coronal plugger is used to compact the heated portion. This process is repeated till desired apical 5 mm of gutta-percha is reached
8. If post space is needed, then the obturation is complete
9. If not the rest of the canal is filled with multiple segments of warmed gutta-percha

Table 2.7 Carrier-Based Gutta-Percha

Carrier-based gutta-percha technique
1. Canal should be dried and appropriate sealer is applied
2. The obturator selected should correspond to the apical size preparation
3. The obturator is then placed in the oven and heated according to manufacturer instructions
4. The heated carrier should be removed from the oven and immediately placed into the prepared root canal
5. The placement of the carrier should be smooth, and it should not require any serious force during placement
6. The carrier should be left in the canal to cool
7. Using a high-speed handpiece, the carrier is severed at the orifice level

hydraulic force of pushing the carrier into the canal causes the gutta-percha to flow vertically and laterally. This technique was adopted by many general dentists as it was both quick and easy. However, the disadvantage is that the carrier can be difficult to remove if retreatment is required in the future. Recently, manufacturers have helped alleviate this problem by making the carrier from materials more easily removed (Table 2.7).

2.4 Endodontic Instruments

Endodontic instruments for root canal debridement can be divided into several categories:

(a) Manually operated instruments
- K-type instruments
  - K-type instruments include both files and reamers. They are made in a grinding machine from tapered stainless steel or nickel-titanium wire having a square or triangular cross section. The difference between the file and reamer is the number of spirals around the file shaft. Reamers typically have fewer spirals and thus are slightly more flexible.
- H-file
  - Hedstrom files are very similar to K-type files except for their cross-section shape and the way they are used. Its sharp cutting edges cut when pulled in a coronal motion. Care must be taken not to twist or prebend these instruments as they are fragile and subject to fracture when using in a rotating motion.
- Barbed broaches
  - This is one of the earliest instruments used in root canal therapy to extirpate the pulp. These instruments are designed with small sharp projections along its working length to engage and remove soft tissue from the canal.

(b) Low-speed instrument with latch type

Gates Glidden drills and Peeso reamers are two low-speed instruments made mostly from stainless steel. They come in different sizes 1–6 (corresponding to 0.50, 0.70, 0.90, 1.10, 1.30, and 1.50 mm diameter) and lengths (28 and 32 mm). They have a non-cutting tip and are mainly used for the preparation of the coronal portion of the root canal to establish a straight-line access. Peeso reamers are mostly used for post space preparation.

(c) Engine-driven nickel-titanium rotary instrument, e.g., ProTaper and TF

(d) Adaptive files

The self-adjusting files are made from a hollow tube of NiTi with an abrasive mesh-like surface. This design allows the files cross-sectional to change its shape to closely match the root canal's cross-section anatomy. Its design allows continuous irrigant flow through the hollow portion of the file during

the instrumentation process. The concept is to remove a thin layer of dentin from all parts of the canal wall regardless of canal shape (oval or round) as opposed to always creating a round shape which tends to remove more or less dentin than necessary.

(e) Reciprocating file

The first introduction of this kind of handpiece was the Giromatic handpiece in 1969. It delivers 3000 quarter-turn reciprocating movements per minute. Stainless steel-barbed broaches and k-files are typically used with this handpiece.

Recently, several manufacturers have reintroduced reciprocating files made of nickel-titanium. Those include WaveOne, RECIPROC, and Twisted File Adaptive, and the goal is to reduce the number of instruments required to prepare canals to an absolute minimum.

(f) Sonic and ultrasonic

The sonic and ultrasonic have been used in cleaning and shaping the root canal. Ultrasonic is used in conjunction with files to instrument the root canal system, whereas the sonic needs special tips like Rispi-Sonic, Shaper-Sonic, TrioSonic, or Heli-Sonic files. The difference between both sonic and ultrasonic is the operating frequency. Ultrasonic frequencies range from 20 to 30 kHz. Sonic frequencies typically operate in the 2–3 kHz range.

References

1. Schilder H. Cleaning and shaping the root canal. Dent Clin North Am. 1974;18(2):269–96.
2. Krasner P, Rankow HJ. Anatomy of the pulp-chamber floor. J Endod. 2004;30(1):5–16.
3. Mullaney TP. Instrumentation of finely curved canals. Dent Clin North Am. 1979;23(4):575–92.
4. Marshall FJ, Pappin J. A crown-down pressureless preparation root canal enlargement technique. Technique Manual, Oregon Health Sciences University, 1980.
5. Thompson SA. An overview of nickel-titanium alloys used in dentistry. Int Endod J. 2000;33(4):297–310.
6. Grossman LI. An improved root canal cement. J Am Dent Assoc. 1958;56(3):381–5.
7. Schilder H. Filling root canals in three dimensions. Dent Clin North Am. 1967;1:723–44.

3 The Role of Irrigation in Endodontics

Luc W.M. van der Sluis, Bram Verhaagen, Ricardo Macedo, and Michel Versluis

Abstract

During root canal irrigation, we aim for the chemical dissolution or disruption and the mechanical detachment and removal of pulp tissue, dentin debris and smear layer (instrumentation products), microorganisms (planktonic or biofilm), and their products out of the root canal system. The different endodontic irrigation systems have their own irrigant flow characteristics, which should fulfill these aims. Flow (convection) promotes the distribution of irrigants through the root canal system. However without flow, the irrigant has to be distributed through diffusion which is slow and depends on temperature and concentration gradients. During the flow of irrigants, frictional forces will occur between the irrigant and the root canal wall (wall shear stress). These frictional forces participate in the mechanical cleaning of the root canal walls. This chapter describes the typical flow of irrigants produced by different irrigation systems including their related wall shear stress. Furthermore, the influence of flow on the chemical effect of the irrigants, including the effect on the biofilm (disinfection), will be discussed.

L.W.M. van der Sluis (✉)
Department of Conservative Dentistry, University of Groningen, Groningen, The Netherlands

Department of Dentistry and Oral Hygiene, University Medical Center Groningen, Groningen, The Netherlands
e-mail: l.w.m.van.der.sluis@umcg.nl

B. Verhaagen, MSc
BuBclean and University of Twente, Enschede, The Netherlands
e-mail: bram@bubclean.nl

R. Macedo, DMD, PhD
Department of Conservative Dentistry, Center for Dentistry and Oral Health, University of Groningen, Groningen, The Netherlands
e-mail: rgdmacedo@gmail.com

M. Versluis
Physical and Medical Acoustics Physics of Fluids group MIRA, Institute for Biomedical Technology and Technical Medicine, MESA+ Institute for Nanotechnology, University of Twente, Enschede, The Netherlands
e-mail: m.versluis@utwente.nl

G. Olivi et al. (eds.), *Lasers in Endodontics: Scientific Background and Clinical Applications*,
DOI 10.1007/978-3-319-19327-4_3

3.1 Introduction

Apical periodontitis (AP) is defined as an oral inflammatory disease caused by a reaction of the host immune system to the presence of microorganisms (planktonic state or biofilm) or their products. The microorganisms are close to or in the root canal system or at the outside around the root apex [1]. The goal of a root canal treatment is to prevent or to heal AP. Therefore microorganisms that have invaded the root canal system should be removed, in order to facilitate healing. Unfortunately, due to the complexity of the root canal system containing isthmuses, oval extensions, and lateral canals, a complete removal of biofilm from the root canal system is not feasible during a root canal treatment [1]. Furthermore, the tooth and root structure consist of dentin which is a porous material containing tubules with a typical diameter of 0.6–3.2 μm and length of 1–2 mm and which provide a shelter for microorganisms [1]. Nevertheless, minimization of the number of microorganisms after treatment should be attempted, using instrumentation complemented by irrigation.

Instrumentation of the root canal is associated with several disadvantages such as smear layer and dentin debris production, iatrogenic errors such as stripping and apical transportation, weakening of the root structure, and apical crack formation [2–6]. Furthermore, the instruments do not touch the whole surface of the root canal wall [7] impeding complete mechanical biofilm disruption. This problem was recognized by Lussi and coworkers [8] who introduced an irrigation device for root canal cleaning that did not require prior instrumentation. Promising results (in vitro and in vivo) were published; however, further improvements were needed, and the system is currently not commercially available [9]. Establishing an alternating negative and positive pressure that would enable an effective irrigation procedure without instrumentation and extrusion of the irrigant seems, for the moment, not to be possible. Therefore, it is still necessary to create space in the root canal system with instruments to be able to effectively apply and disperse antimicrobial disinfection solutions or medicaments throughout the root canal system.

When the root canal system is infected, so will the dentin debris and smear layer requiring its removal. The smear layer can be defined as a mixture of dentine debris, remnants of pulp tissue, odontoblastic processes, and microorganisms (if present). The smear layer is strongly attached to the root canal wall and can penetrate up to 40 μm into the dentinal tubules [2, 10]. Dentin debris may be defined as dentin chips, tissue remnants, and particles attached to the root canal wall or present in the root canal. Both dentin debris and smear layer will inactivate the root canal medicaments and irrigants and block their access to the biofilm [11]. Recently, it was shown that the production of dentin debris and the subsequent blockage of isthmuses may be a larger problem than anticipated [3]. After the first instrument is used in the root canal, the wall will be covered with an infected smear layer at the sites where the file touches the canal wall. At these sites, the biofilm is mechanically disrupted, but remnants of the biofilm will have been merged with the smear layer. At the sites where the files did not touch the walls, biofilm will remain as a thin film attached to the root canal wall, possibly covered with or blocked by dentin debris. This situation typically encountered will hinder disinfection procedures. Consequently the removal of dentin debris and smear layer plays a crucial role in the disinfection process.

Smear layer, dentin debris, and biofilm can only be removed by irrigation. An effective irrigation, involves both the *mechanical* detachment of pulp tissue, dentin debris and smear layer (instrumentation byproducts), microorganisms (planktonic or biofilm) and their byproducts (further on referred to as *substrate*) from the root canal wall and the *chemical* dissolution or disruption of these components. Both the mechanical and chemical aspects of irrigation are related to the flow of the irrigant.

Furthermore, irrigants are chemically inactivated after their reaction with the biofilm and dentin and therefore constantly need to be replenished or mixed with fresh irrigant to maintain an effective concentration. Consequently, insight in the flow of the irrigant during a root canal treatment is crucial in understanding the importance of the disinfection of the root canal system.

The objective for the flow of irrigants used during irrigation is to create fluid dynamics that exhibit the following characteristics:

- Movement throughout the full extent of the root canal system, allowing close contact with the substrate, with removal of the substrate while providing lubrication for instrumentation
- Ensuring an adequate delivery replenishment and mixing of the irrigant throughout the root canal system in order to retain an effective concentration of the active chemical component(s) and compensate for its rapid inactivation
- Ensuring a force on the root canal wall (wall shear stress) that promotes detachment and disruption the substrate
- Maintains the irrigant within the confines of the root canal system thus avoiding irrigant extrusion towards the periapical tissues

During the irrigation procedure, two phases can be distinguished: a flow phase, during which the irrigant is delivered and flows in and out of the root canal, and a resting phase, where the irrigant is at rest in the root canal. Since syringe irrigation alone has limitations concerning the flow produced [12], agitation/activation of the irrigant could help to improve irrigant delivery throughout the root canal system as well as enhancing the mixing, refreshment, and the chemical properties of the irrigant. Irrigant agitation/activation systems introduce an additional activation phase which enhances the streaming of the irrigant by an energy source. This chapter will discuss the operational characteristics, fluid dynamics, and mechanical and chemical interactions involved with syringe- (positive and negative pressure), sonic-, ultrasonic-, and laser-activated irrigation.

Research evaluating the smear layer of the root canal wall is not discussed in this chapter because the reliability of the methodology is not fully developed [13].

3.2 Irrigation Systems

Syringe irrigation is still the conventional method for root canal irrigation [14]; however, its efficacy and safety have been questioned [1]. To improve the efficacy of syringe irrigation or prevent extrusion of the irrigant, other irrigation systems have been developed that use various energy sources to activate or agitate the irrigant [15, 16]. The mechanism of energy transmission to the irrigant determines the specific flow characteristics of the irrigation systems and consequently their efficacy and safety. Combinations of syringe irrigation to deliver the irrigant in the root canal and different ways to agitate the irrigant have established a variety of irrigation techniques. In this chapter, we will focus on the most important irrigation systems available: syringe (negative pressure), (ultra)sonic, and laser-activated irrigation. Figure 3.1 provides a sketch of each of these irrigation techniques.

3.3 Operational Characteristics of the Irrigation Systems

3.3.1 Syringe Irrigation

As mentioned earlier, syringe irrigation is the most commonly used root canal irrigation procedure either as the sole irrigation technique or intermittent with other activation techniques [17]. During syringe irrigation, the irrigant is typically delivered by a needle connected to a syringe, with the needle tip preferably positioned as close to working length as possible [18]. There are various needle types available on the market, which can be categorized as open-ended (sharp or blunt end) or closed-ended (one or more side outlets) designs [12]. Various needle sizes are available, but most commonly used are the 27 and 30 gauge needles (respectively 0.4 and 0.3 mm outer diameter). Needles are made from stainless steel, NiTi, or flexible material like polyimide. The flow through the needle is generated by applying a pressure on the attached syringe [19]. Syringes are available at sizes ranging from 1 mL to 50 mL, with the smaller ones being more popular and easier to achieve high flow rates.

3.3.2 Negative Pressure Irrigation

Negative pressure irrigation systems make use of a microcannula that is placed in the middle

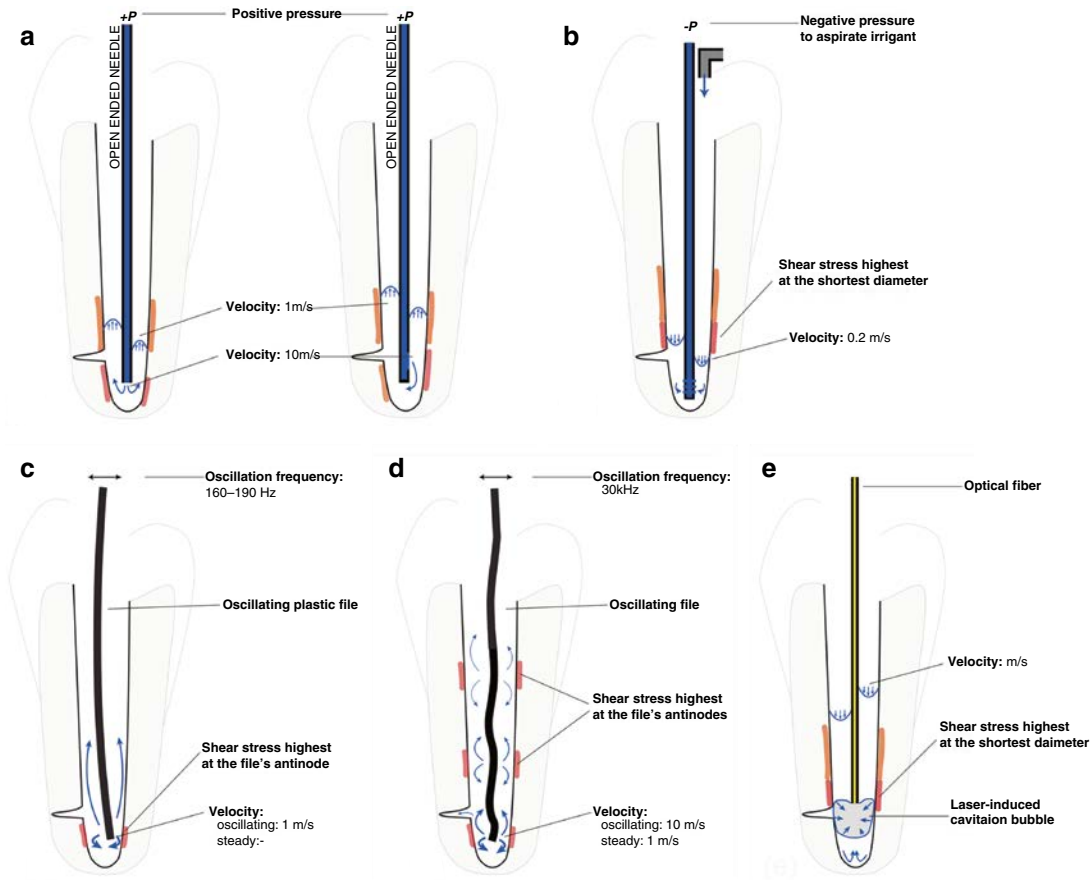

Fig. 3.1 Schematic representation of the discussed irrigation techniques. Sketches of the various manual (**a**, **b**) and automated (**c**–**e**) irrigation techniques. For positive pressure irrigation, (**a**) both the open-ended (*left*) and closed-ended (*right*) needles are shown; negative pressure irrigation is shown in (**b**). Sonic (**c**) and ultrasonic activation (**d**) involves oscillating instruments (*black-bended shapes*) with one or more nodes and antinodes. For laser-activation irrigation, (**e**) the optical fiber is drawn. The typical flow velocities and patterns for all irrigation techniques are indicated as well

part of the root canal or close to the working length [15]. Irrigant is aspirated through the cannula, while fresh irrigant is provided in the pulp chamber using a larger needle. Thus, the flow is directed from the pulp chamber to the aspirating cannula. The negative pressure systems involve less risk on irrigant extrusion through the apical foramen than positive pressure techniques due to the absence of a flow directed towards the foramen [20–22]. This technique is therefore considered safer than positive pressure syringe irrigation.

3.3.3 Laser Activation

One of the more recent techniques available for automated agitation/activation of irrigant in the root canal is laser-activated irrigation (LAI). This application uses laser energy to agitate and activate the irrigant. The lasers typically used for LAI are the erbium laser family such as ErCrYSGG and Er:YAG. These lasers have wavelengths in the medium-infrared region (2780–2940 nm) which is highly absorbed in water and NaOCl [23]. These laser devices cycle

and pulse at frequencies anywhere 1–100 Hz with energy's ranging from 5 to 1000 mJ per pulse. The laser light is delivered through an optical fiber or an articulated arm to a handpiece with a terminal flat or conical tip, suitable for insertion into the root canal close to the root apex. To be effective in the whole root canal, different LAI protocols are used to apply the laser tip in the different segments of the root canal. In a variation on this technique, the fiber tip is placed just above the root canal entrance, in the pulp chamber which is filled with irrigant [24, 25]. This leads to agitation/activation and streaming of the irrigant throughout the entire root canal system. This specific LAI technique, referred to as photon-induced photoacoustic streaming (PIPS), uses specially developed tapered and stripped laser fiber tips in combination with low energy (20 mJ) and short pulse duration (50 microseconds). These fibers allow lateral emission of the laser light *at* from the tip [25].

Pulse frequency and power do not appear to heat the root canal wall more the 5 C during laser activation [26]. Using the low pulse duration and energy as is recommended for PIPS protocol, the radicular apical third only increased 1.2 or 1.5 °C after 20–40 s of activation respectively [27]. This laser-activated irrigation is an indirect technique that utilizes photoacoustics for activation and agitation and not direct ablation of the biomaterial as seen in other applications [28].

3.3.4 Sonic Activation

Sonic activation employs instruments that are driven into vibration at one end (at the handpiece). The other (free) end of the instrument is inserted to near the working length of the root canal. The oscillations of the instruments agitate the irrigant inside the root canal in order to enhance mixing and cleaning of the irrigant by fluid flow.

Sonic devices operate at audible frequencies (below 20 kHz, typically 100 Hz for the current devices) [29]. The sonically driven instruments exhibit a simple bending pattern, consisting of a large amplitude at the tip (antinode) and a small amplitude at the driven end (node) [30]. The amplitude at the antinode may be as large as 1 mm, which is larger than the diameter of a root canal. Therefore, frequent wall contact is likely to occur, which reduces the effectiveness of the technique [29].

3.3.5 Ultrasonic Activation

Like sonic activation, the instruments used during ultrasonic activation have an enforced vibration at one end (at the handpiece) and are allowed to vibrate freely at the other end. The instruments are typically either cutting or non-cutting files. Recently, hollow instruments have been introduced, which allow for simultaneous ultrasonic oscillation and positive pressure irrigation [15].

Ultrasonic devices operate at higher frequencies (typically 20–200 kHz) and have amplitudes less than 100 μm [31–33]. The higher frequency employed by ultrasonic activation leads to a more complex pattern of several nodes and antinodes than those of sonic devices. The currently available ultrasonic devices operate at 30 kHz leading to an oscillation pattern of approximately three wavelengths, or six nodes, and antinodes spaced approximately 5 mm apart on the file [33]. The geometry and material properties of the instrument determine the exact oscillation pattern. The oscillation amplitude of the tip of current ultrasonic devices and instruments is on the order of 10–100 μm in the direction of oscillation. There is also a small oscillation perpendicular to the main oscillation direction [32, 33].

The cross-section of instruments available for ultrasonic activation is circular (non-cutting) or square (cutting). The cutting action of the instruments is not needed for this application; however, these files are used for ultrasonic activation for historical reasons. In 1980, Weller [34] proposed intentional wall contact during ultrasonic activation; however, later it was shown that the irrigant streaming is better in the absence of intentional

contact [35]. Nevertheless, it was recently demonstrated that unintentional contact with a root canal wall nearly always takes place [36]. The amount of contact depends not only on the power setting used but also on the instrument stiffness and on the force with which the instrument is pushed against the root canal wall. Light contact does not appear to affect its cleaning mechanisms of streaming and cavitation as the file oscillation is not damped out. Instead it builds up a secondary oscillation at audible frequencies during which the file displaces away from the wall and keeps on oscillating at the driving ultrasonic frequency [36].

Heating of the irrigant inside the root canal by the ultrasound is limited to at most 15 °C in 60 min [37].

3.4 Clinical Procedures of Irrigant Activation Techniques

3.4.1 Irrigation Activation Protocols

An easily application of irrigation protocol for sonic, ultrasonic, or laser-activated irrigation is the "intermittent flush technique" first described by Cameron [150]. The irrigant is first delivered into the root canal by syringe irrigation. Then the irrigant can be activated inside the root canal allowing the disruption of the substrate from the root canal wall. After activation, the root canal needs to be rinsed using syringe irrigation in order to remove the substrate loosened from the root canal wall by the irrigant activation.

Another protocol comprises a continuous flow of irrigant through or alongside the handpiece or fiber into the pulp chamber. The irrigant then has to flow from the pulp chamber or coronal root canal to the apical root canal by the activation of the instrument thereby enhancing irrigant delivery into the (apical) root canal.

There are also needles (23–30 gauge) on the market which allow a continuous flow of irrigant through the needle into the root canal during ultrasonic activation of the needle. These needles allow irrigant delivery refreshment and activation at the same time.

For the moment, it seems that irrigation protocols are most effective when the root canal has been shaped with a final apical file because there is more space in the root canal for fluid dynamic effects [45, 55]. However, this does not to imply that other protocols cannot be used or will not be effective during the root canal treatment.

3.4.2 Sonic Activation

Sonic-activated irrigation can be performed using sonic handpieces that can drive instruments at sonic frequencies (Fig. 3.2). Traditionally only cutting files were available. Today, there are also several new sonic activation systems available on the market like the EndoActivator system or the Vibringe. The EndoActivator system allows a variation in driving power, frequency, and the size of polymer tips that do not cut into the root canal wall. The suggested manufacturer use advises delivery of the irrigant into the root canal by syringe irrigation after creating a "fully tapered shape." The irrigant is activated for 30–60 s using a pumping action in short 2–3 mm strokes.

Vibringe system uses a sonically oscillating needle to deliver the irrigant into the root canal. The Vibringe can be used throughout the complete root canal treatment procedure.

3.4.3 Ultrasonic Activation

For ultrasonic activation, most of the devices already present in the clinic can be used in combination with a variety of instruments (Fig. 3.3). Occasionally special chucks or irrigation systems are needed. Instruments for all of the mentioned activation protocols are available. The instruments can be applied up to 1–2 mm from working length (with the exception of some of the ultrasonically activated needles) or at the beginning of a strong curvature in order to

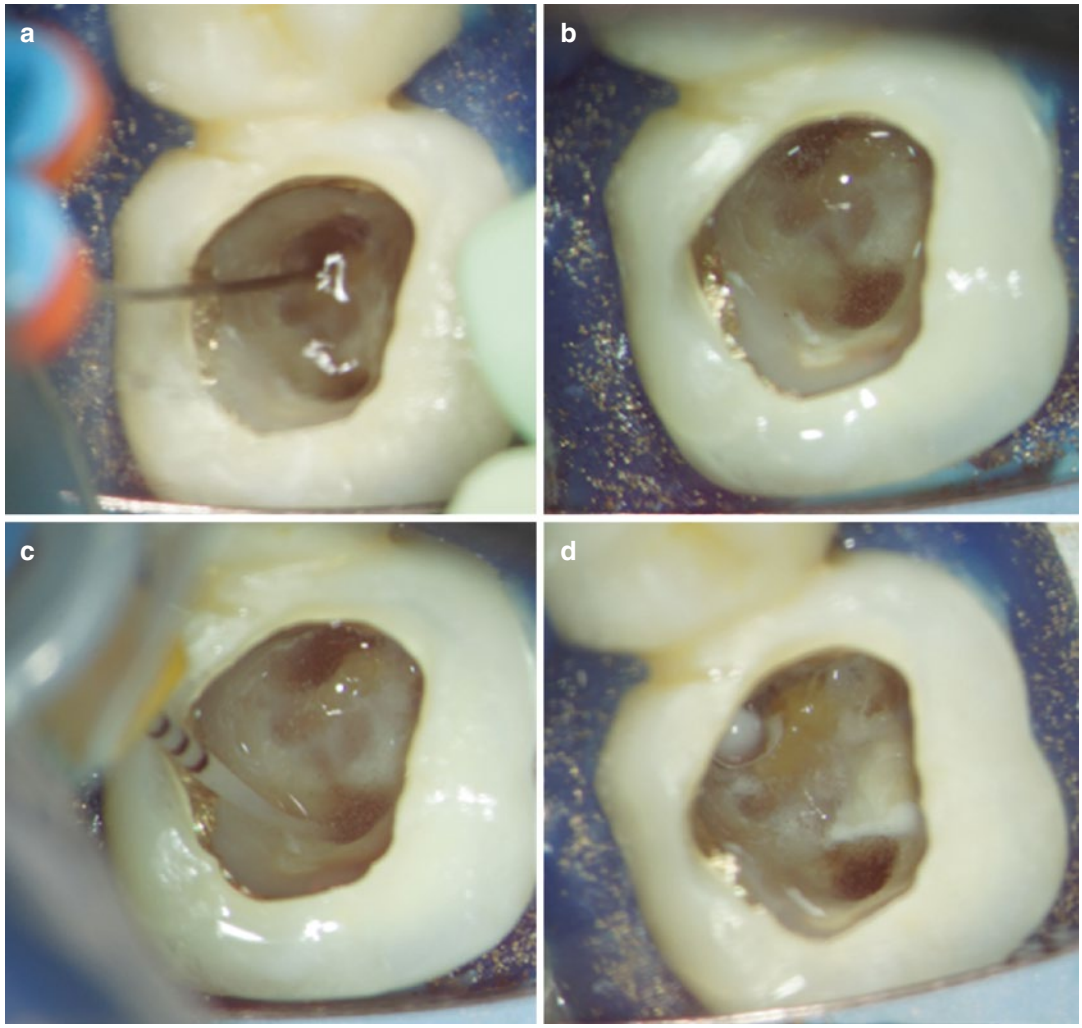

Fig. 3.2 (**a**–**d**) Sonic activation, effect on NaOCl in the pulp chamber

prevent heavy wall contact [80]. For the "intermittent flush technique," a sequence of three times 10 s seems to be favorable for dentin debris removal [17]. For a continuous flush, 1 min is advised. For optimal cleaning efficacy of oval extensions, isthmuses, and lateral canals of which the position is known, the instrument should be directed to oscillate towards these areas if possible [76].

At the moment, low-intensity settings of the ultrasonic energy are advised to prevent fracture of the instruments. Normally fractured instruments will easily flow out of the root canal. Non-cutting instruments are available which can safely be used in the root canal. Heavy contact of the file with the root canal walls should be avoided [36].

3.4.4 Laser Activation

For laser-activated irrigation, Er:YAG or ErCrYSGG laser systems are available on the market. The "intermittent flush technique" or a continuous flow into the pulp chamber can be used. The laser fiber can be inserted 1–2 mm

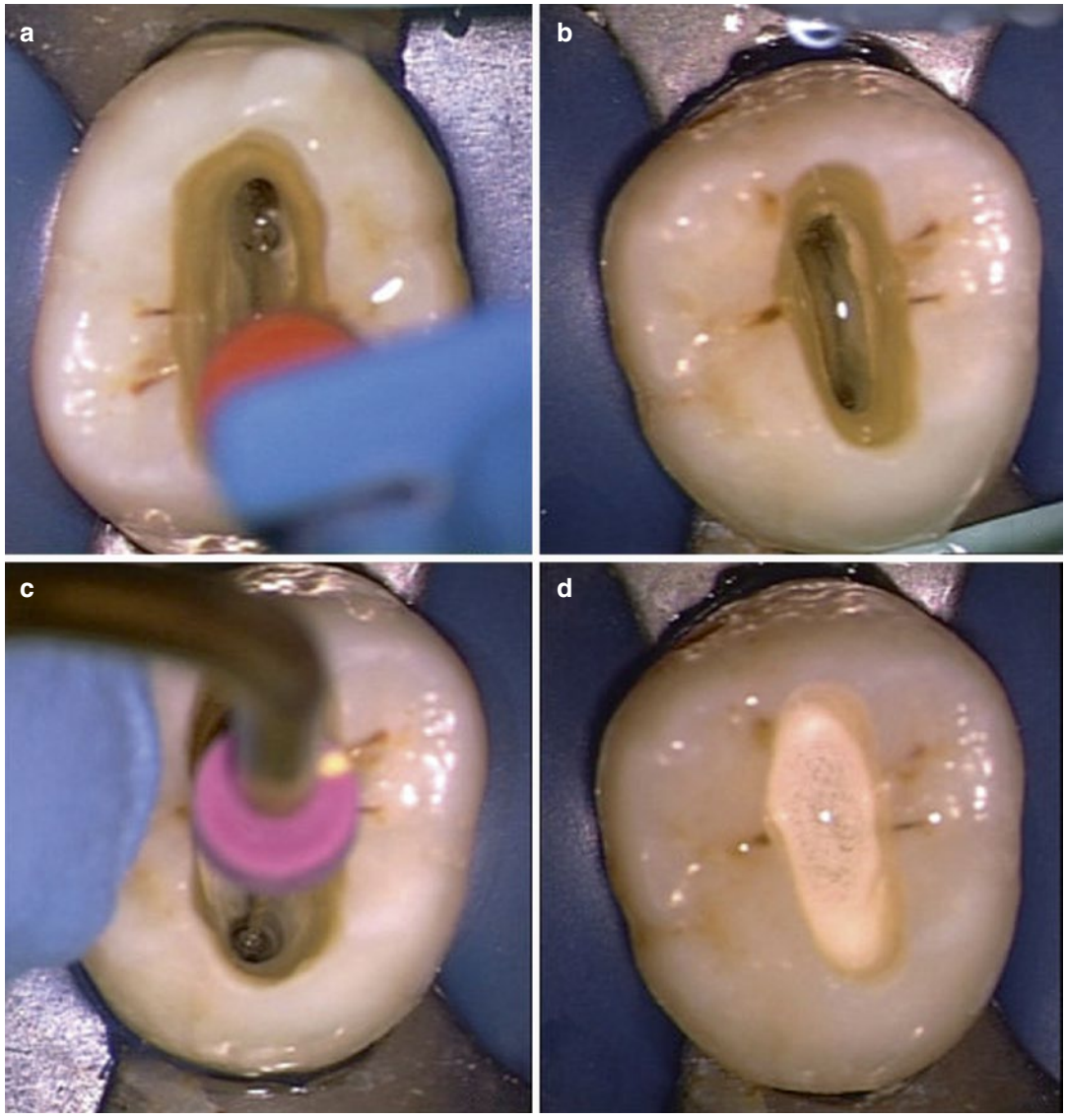

Fig. 3.3 (**a**–**d**) Ultrasonic activation, effect on NaOCl in the pulp chamber

short of working length and vertically moved up and down within the apical third [115]. It can also be placed in the pulp chamber just above the root canal orifice. The latter has been described for conventional fibers [24] and for specially designed fibers (PIPS: photon- induced photo-acoustic streaming) (Fig. 3.4) [25, 27].

Commercially available laser devices allow for a variation of the size and type of optical fibers, pulse repetition frequency (PRF), applied energy, and pulse length. De Groot et al. [115] reported as optimal settings a combination of low power (80 mJ) per pulse and a PRF of 15 Hz. Significant loss of irrigant from the pulp chamber was reported for energy settings higher than 120 mJ per pulse reducing the efficacy of the irrigation procedure.

For the PIPS technique, the recommended energy setting is even lower: 20 mJ. The PIPS fiber is placed at the coronal opening of the root canal after filling the root canal system and pulp chamber with irrigant. There is noticeable irrigant

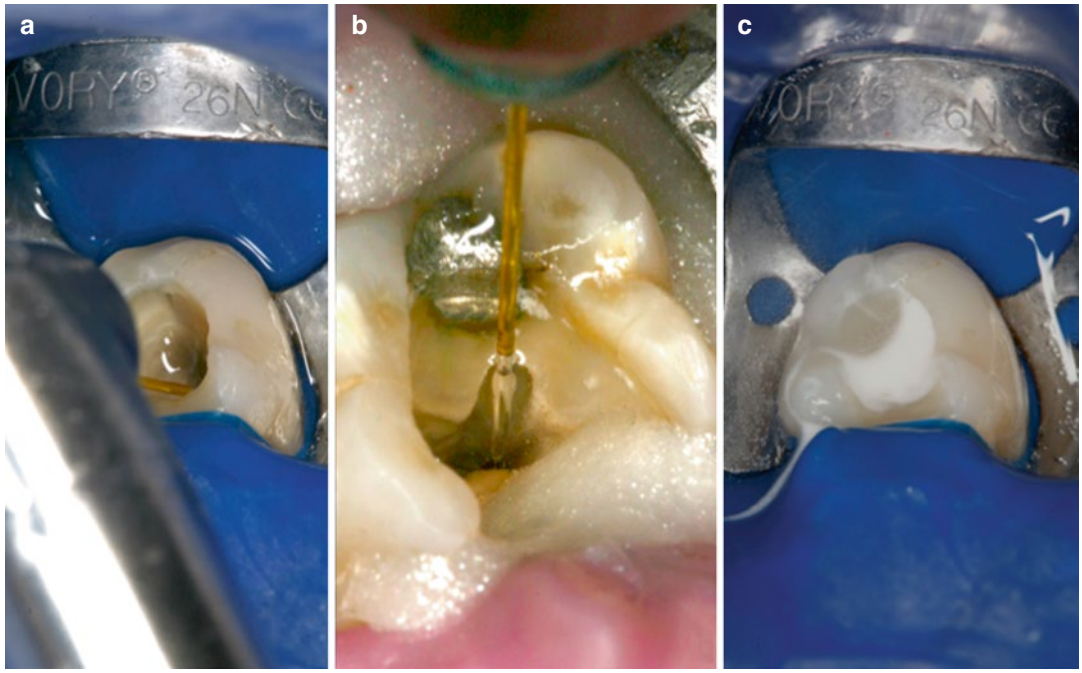

Fig. 3.4 (**a**–**c**) Laser activation, effect on NaOCl in the pulp chamber

loss during activation therefore a continuous flow of irrigant is required in the pulp chamber during activation. The laser-activated irrigation part will be also treated in depth in Chaps. 9 and 10.

3.5 Flow Characteristics for Different Irrigation Systems

3.5.1 Syringe Irrigation

The characteristics of the flow in the root canal during syringe irrigation depend primarily on the type of needle used [12, 38, 39] (Fig. 3.5). Two needle groups can be distinguished namely closed-ended and open-ended needles. The differentiation is based on the needle outlet type and the resulting flow. Open-ended needles, such as those with a flat, beveled, or notched outlets, generate a jet that extends along the longitudinal axis of the root canal apically to their tip. The irrigant then returns to the coronal opening along the outside of the needle as the apex is considered closed [40, 41]. As the jet is directed at the apical foramen, pressure is developed there with an associated risk on irrigant extrusion [42, 43]. The jet may become unstable and break-up at high flow rates or large distances from the apex [38] leading to unsteady (not turbulent) flow with enhanced mixing and reduced pressure at the apex.

In the case of the closed-ended needles (side-vented, double-side-vented), the irrigant leaves the needle from the side outlets and is directed towards the apex under an angle of approximately 30°. The flow then curves around the tip of the needle before it returns to the coronal opening [12, 39, 44]. A series of counter-rotating vortices (flow structures where the fluid is rotating) is formed apically from the tip up to the apex. The size, position, and number of vortices are determined by the needle insertion depth, root canal size, taper, and flow rate. The irrigant velocity inside each consecutive vortex drops rapidly towards the apex resulting in a very low irrigant replacement near the apex. The irrigant exchange of the closed-ended needles is therefore limited to 1 mm beyond the needle tip [12, 38, 39, 44–47] at clinically realistic timescales. A low velocity at the apex is associated with a small pressure,

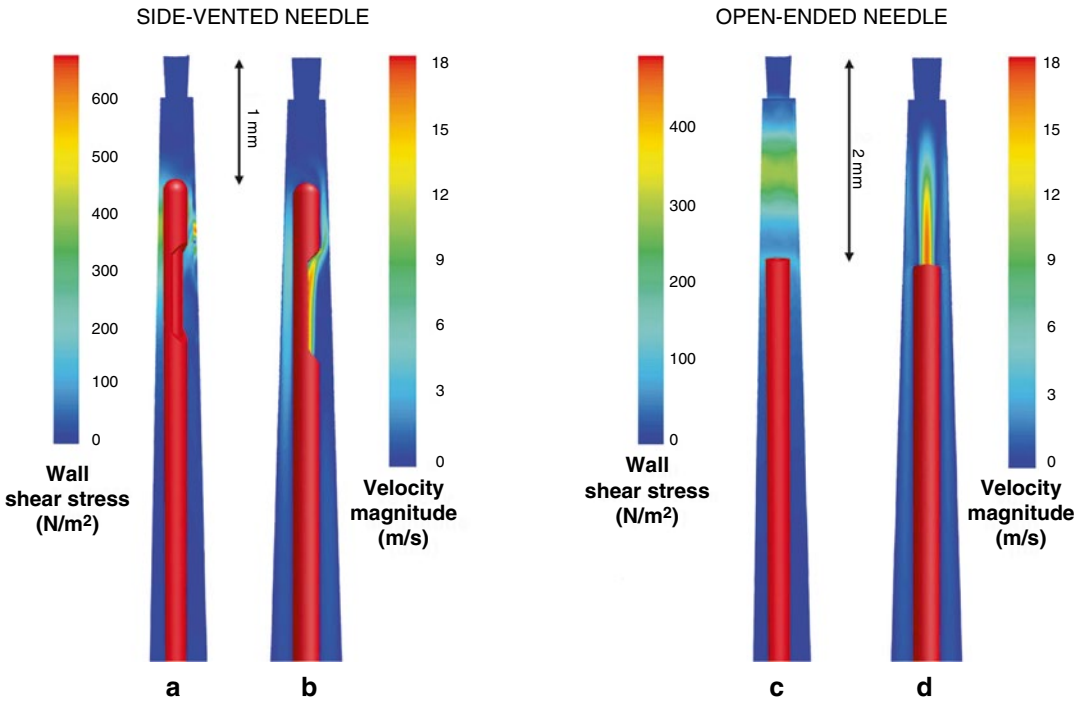

Fig. 3.5 Needle flow. Computational fluid dynamics results for the shear stress (**a**, **c**) and flow velocities (**b**, **d**) from a side-vented (**a**, **b**) or open-ended (**c**, **d**) needle inside a root canal (Boutsioukis et al. [47])

making closed-ended needles safer in terms of risk on irrigant extrusion [42, 43].

For both types of needles, the flow that is created contributes to the cleaning efficacy by replacing and mixing fresh irrigant with irrigant that has been consumed during its reaction with biomaterials in the root canal system. Concurrently with the flow, a shear stress up to 500 N/m [12] is exerted on (the material on) the wall, which is directly proportional to the flow velocity. As the flow from both needle types only dominates a limited area beyond the needle tip, it is important to place the needles close to working length. Closed-ended needles may be placed around 1 mm from WL. For open-ended needles, a larger distance is recommended due to the higher pressure developed apically.

A curved root canal limits the placement of stiff needles near the apex. However, small size (30G or 0.32 mm) flexible irrigation needles are currently available and can facilitate injection near the working length even in severely curved canals provided that the canal is enlarged at least to size 30 or 35. The influence of canal curvature on the flow and the apical pressure is limited [43, 48] except for severely curved canals (Schneider angle 24–28°).

Near the apex, the irrigant flow can be very slow, depending on needle placement and flow rate [12, 38, 45–47], and has even been dubbed as "dead-water" zone or stagnation zone [49, 50]. The flow doesn't actually stand still there but is too slow to contribute to mixing or to be observed on the time scale of seconds. In addition, the occurrence of a "vapor lock" (bubble entrapment) in the apical part of the root canal has been reported during syringe irrigation of root canals, ex vivo [40, 51] and in vivo [52]. The presence of such a bubble would prevent irrigant from reaching the apical area. A recent study dedicated to this phenomenon has shown that such bubbles could indeed be formed, depending on irrigant flow rate, needle type, insertion depth, and size of the root canal [53]. However, it was also shown (in vitro) that it can easily be removed or prevented by positioning the needle within 1 mm

away from working length or by using high flow rates in the order of 0.2 mL/s [53].

The flow pattern of both needles is influenced by the needle size, flow rate, needle insertion depth, horizontal positioning, root canal size, and taper [12, 36, 38, 44–47]. Small-diameter needles seem to be more effective even when positioned at the same depth [54]. Namely, a smaller needle results in an increase of the annulus area available for the reverse flow between the needle and the root canal wall and also increases the possibility for irrigants to mix apically at the tip for closed-ended needles [45, 46].

Several studies have shown that an increase in the preparation size or taper of the root canal results in a more efficient flow in the apical section of the root canal [45, 46, 54–58]. An apical size 30 .06 taper or larger allows irrigant to disperse and mix 2 mm apically to an open-ended needle, although still only 1 mm apically to the tip of a closed-ended needle [46]. The space that is created by preparation in the apical area appears to be important as a minimally tapered root canal preparation (size 60, .02 taper) appears to give a significant advantage over the tapered ones in terms of irrigant dispersion and mixing [46].

The amount of irrigant delivered is determined by the flow rate and duration of irrigation. An increase in the volume of irrigant allows for improved irrigant dispersion, mixing, and chemical effect and has been shown to improve canal cleanliness [59] and irrigant mixing [60–62].

3.5.2 Negative Pressure Irrigation

The aspiration of irrigant induced by the apically placed microcannula of the negative pressure systems creates a flow that resembles the inverse of the flow pattern described above for positive pressure systems. The irrigant is sucked along the cannula towards the apex, meanwhile creating shear stresses on the walls of the root canal [39]. As the microcannula can be placed up to the apex, irrigant mixing at the apex can be achieved [39, 63].

Various negative pressure irrigation systems are available [15]. Since a lot of data on this system is available, we use the EndoVac system for an estimation of the flow velocities and shear stresses. The maximum possible flow rate through the EndoVac microcannula (30G) is determined by the negative pressure and is, under ideal conditions, 0.05 mL/s for an aspiration pressure of 25.4 kPa [64]. The efficacy of the system depends on the magnitude of this pressure which is difficult to assess on the dental unit. The results of various studies are therefore sometimes difficult to relate to clinical practice.

Assuming a root canal of size 40, .04 taper (this is recommended for an optimal flow rate under clinical conditions) [64], an average irrigant velocity of 1.1 m/s can be calculated for the root canal near the tip of the microcannula [65]. At such flow rates, the flow will remain laminar [65]. As the flow velocities produced during positive pressure irrigation (syringe irrigation) are typically higher than this in areas near the needle outlets, negative pressure systems are expected to have a lower shear stress on the root canal walls [39] and therefore be less effective than syringe irrigation regarding cleaning efficacy of the root canal wall. On the other hand, the generation of a two-phase flow (irrigant and bubbles) has been suggested as a mechanism of enhanced cleaning [66]. In vitro tests are as of yet inconclusive on the cleaning efficacy of this technique compared to other techniques [16, 39, 66, 67].

The absence of high apical pressures could make the negative pressure technique safer than positive pressure systems [22, 68]. However, it is difficult to fully control the flow near the apex [16].

3.5.3 Intermezzo: Flow into Lateral Canals and Tubules

The flow generated by positive and negative pressure techniques is predominantly along the wall axis of the main root canal lumen. However, the lateral canals and isthmuses that are part of the root canal system can also harbor biofilm and dentin debris and should be cleaned as well [69]. The absence of a strong lateral flow component in the direction of these root canal extensions leaves many areas of the root canal uncleansed and consequently biofilm could remain. The clinical

relevance of this was highlighted by two recently published case reports [69, 70], where a direct correlation between persistent apical periodontitis and a biofilm remaining in a lateral canal or other ramifications was suggested.

The tubules that are present in the dentinal walls of the root canal can be considered an extreme case of these lateral canals. The tubules range from 0.5 to 3.2 μm in diameter but can nevertheless harbor bacteria [71]. Although there is no consensus on the possible clinical effect of these microorganisms on root canal treatment outcome, it seems reasonable to take efforts against them.

When irrigant flows only over the entrance of the lateral canal or tubule, only very limited irrigant enter the lateral canal/tubule [72]. Such a so-called cavity-driven flow is well known for its limited flow in this cavity [73]. It was recently shown that the flow is limited by two times the diameter of the cavity which is a few hundred micrometers for lateral canals but only a few micrometers for tubules [72]. Beyond this distance, irrigant will have to be transported by diffusion which is typically very slow [72, 74].

Irrigant activation/agitation techniques that create a flow in the lateral direction could improve the flow into lateral canals and tubules.

3.5.4 Sonic and Ultrasonic Activation

The sonically or ultrasonically oscillating instruments act as a mixing device when they are agitating the irrigant. The oscillations induce a streaming of the fluid around it, leading to alternating pressures and shear stresses on biological material on the root canal wall [75].

The flow along the file in the axial direction is determined by the pattern of nodes and antinodes that are set up along the instrument. Sonic instruments typically have a single antinode at the tip and a node at the driven end which leads to streaming from the tip to the driven end. The multitude of antinodes and nodes on an ultrasonically driven instrument leads to a more complex pattern of microstreaming along the instrument. In both cases, there is a strong component of the flow in the lateral direction, which is advantageous for cleaning extensions of the root canal (lateral canals, isthmuses, webs, fins, and oval extensions) [51, 76, 77]. Increasing the oscillation amplitude (e.g., a higher intensity of the ultrasound) leads to more effective cleaning [78].

The flow directed towards the apex is weak for both sonic and ultrasonic activations [79]. Mixing and replenishment of irrigant facilitates debris removal beyond the file tip when the ultrasonically activated instrument is inserted 3 mm from the working length [80]. The risk on irrigant extrusion is minor due to the absence of a strong flow towards the apical foramen.

Although sonic or ultrasonic instruments should be placed near working length, the curvature of a root canal may limit the access to the apex for the instrument. Nevertheless, when an instrument is inserted to or near the working length, its oscillation may be affected by heavy contact or binding of the instrument with the root canal wall [81]. Therefore, it is advised to insert the ultrasonically driven instrument just in the beginning of the curvature without bending of the instrument. The flow itself should not be affected by the curvature because the radius of curvature is typically much larger than the scale on which the streaming takes place [80].

3.5.4.1 Acoustic Streaming

Ultrasonic activation leads to a special kind of flow called *acoustic streaming*. Acoustic streaming is a phenomenon already introduced in 1884 by Lord Rayleigh [82] and extended later to the case of a cylinder oscillating with high amplitude [83] inside another cylinder [84, 85]. The application of acoustic streaming induced by an oscillating cylinder to clean biomaterial off a surface was first described by Williams and Nyborg in 1970 [86, 87].

Acoustic streaming consists of two flows superimposed on each other (Fig. 3.6). One part of the streaming is oscillatory and the other is steady. The strengths of both components depend on the oscillation amplitude of the file. Ahmad and coworkers [88] used the theory of acoustic streaming to describe

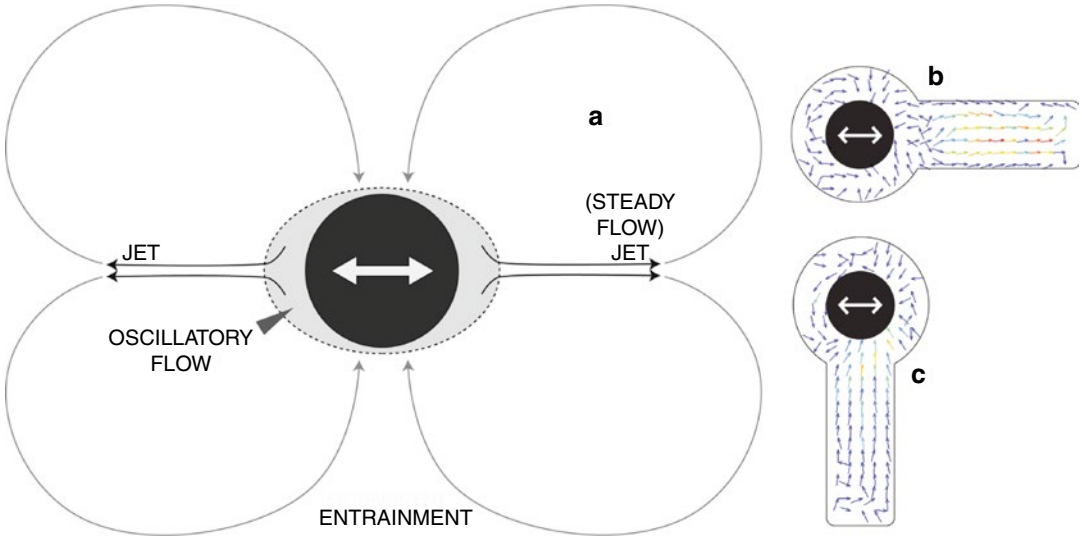

Fig. 3.6 Acoustic streaming. Sketch of the acoustic streaming induced by an ultrasonically oscillating file (*black circle* in (**a**)) (Verhaagen et al. [75]). Near the file, there is an area with oscillatory flow; further away and in the direction of oscillation, there is a steady flow in the shape of a jet. This jet is important for cleaning extensions of the root canal. When oscillating the file towards an extension (**b**), the jet will clean the extension, whereas when oscillating perpendicular to the extension, (**c**) there is much less flow in the extension (Jiang et al. [76])

ultrasonic activation in endodontics; however, only the steady part of the flow was considered. It was shown recently that the oscillatory component can also contribute significantly to the overall streaming [75].

The oscillatory part of the acoustic streaming makes the flow oscillate forward and backward together with the file, with a velocity equal to that of the file $u_0 = A\omega$. However, the velocity decreases quadratically with the distance from the file, and the oscillatory flow component is therefore only important near the file. Due to its oscillatory nature, the fluid exerts an alternating pressure and shear stress on the material on the root canal wall with magnitudes of 100 and 1 kPa, respectively [75]. The values for the pressure and the shear stress are similar to those reported for syringe irrigation at a very high flow rate (0.26 mL/s) near the outlet [44]. For ultrasonic activation, these forces are present around every antinode of the instrument; therefore, more sections of the wall can be cleaned simultaneously. The oscillatory nature of the pressure and the shear stress may furthermore induce fatigue in the substrate material [89].

Nonlinear effects of the fluid lead to steady (i.e., non-oscillatory) streaming in the direction of oscillation [76]. These "jets" have a velocity *us* given by:

$$u_s = 3$$

where ω is the oscillation frequency, y is the oscillation amplitude, and R is the radius of the file. The jet velocity is typically 1 m/s and increases with increasing amplitude or power setting [78]. Because jets specifically form in the direction of oscillation, the oscillation direction of the file should be taken into account in particular when cleaning oval canals, isthmuses, and lateral canals [76].

Whereas the oscillatory component only made the fluid oscillate back and forth, this steady part of the flow is doing the actual transport and mixing of the fluid. The jets also exert a pressure (1 kPa) and shear stress (10 Pa) onto the wall [75] and even at relatively large distances from the instrument, whereas the velocity of the jet only slowly decreases with increasing distance from the file. Near the file, the steady pressure and shear stress values can be one or

two orders of magnitude lower than the oscillatory components. That is to say that further away the components may become similar in strength. The pressure is highest in the center of the jet, while the shear stress is highest off-center at a distance of 0.1 times the distance between the oscillating file and the wall [90, 91]. Although the details of the streaming may change [92], especially near sharp corners, acoustic streaming is induced for all of the cross-sectional designs of the current instruments. A nearby wall or the confinement of a root canal significantly affects the streaming as well.

Oscillation of instruments at sonic frequencies does not lead to acoustic streaming because its frequency and associated oscillatory velocity are too low to lead to these nonlinear effects [29].

3.5.4.2 Cavitation

When an instrument oscillates ultrasonically with high amplitude, *transient cavitation* may be induced. Cavitation is defined as the growth and fast collapse of a bubble [93, 94] and is associated with surface cleaning [95–97], medical therapy, surface erosion [98, 99], and other mechanical effects [96]. This surface cleaning potential makes cavitation interesting for root canal cleaning. In non-pure water (tap water, distilled water), there are often tiny pockets of entrapped gas (*cavitation nuclei*) on surfaces of walls or particles from which bubbles can grow followed by a fast collapse (a process called *heterogeneous cavitation*).

The life cycle of a bubble is determined by the oscillating pressure of the ultrasound. The bubbles can grow when the pressure drops from ambient pressure to below the vapor pressure of the liquid (10^3 Pa for water) [93]. The typical velocity u necessary to generate this negative pressure ΔP in a liquid of density ρ can be estimated from the Bernoulli relation:

$$\Delta P = 1$$

In water, the velocity threshold is around 15 m/s which can be achieved with the current endodontic ultrasonic devices but not with sonic devices [29, 37, 100]. The bubble will collapse when the pressure becomes positive during the ultrasonic cycle. Small bubbles always collapse towards a nearby solid hard wall. Alternatively, during bubble collapse next to a soft wall (like a biofilm covering a wall), the soft material might be pulled from the wall towards the bubble [101]. High-velocity jets (hundreds of meters per second) and shock waves [93, 102] have been reported in the literature during the bubble collapse, and these jets lead locally to pressures on the order of 1 GPa and shear stresses of 1 MPa [98]. These small bubbles may therefore further enhance cleaning of the root canal walls.

Several studies have demonstrated the occurrence of cavitation on or very close to endodontic instruments [78, 103–105]. The bubbles prefer to form near the sharp edges of files with a square cross-section (cutting files) where the velocity and pressure gradients are highest. However, there is still a debate whether cavitation can contribution to cleaning the root canal walls or not [103]. Cavitation is well known for its cleaning ability [95, 96, 106]; however, earlier studies have ruled out cavitation as a significant contribution to root canal cleaning [103, 104]. On the other hand, recent articles with newer ultrasound systems show otherwise [37, 107] even at the lowest power settings [100]. High-speed imaging has revealed that a cloud of cavitation bubbles is generated around the tip of the instrument, and this bubble cloud grows and collapses two times per oscillation cycle. However, the bubble cloud was observed to collapse only onto the file itself and not onto a neighboring wall. Besides the bubble cloud, small single bubbles occur around other antinodes on the instrument which have been demonstrated to be sonochemically active. The amount of generated cavitation is different for each file type. However, in general, non-tapered instruments generate more of the small bubbles than tapered instruments [37] (Fig. 3.7). Irrigants with surface-active properties, such as NaOCl, may affect the bubble formation and collapse and therefore lead to a larger bubble cloud consisting of much smaller bubbles [37]. Finally, a smaller confinement (i.e., a narrower root canal) increases the amount of cavitation

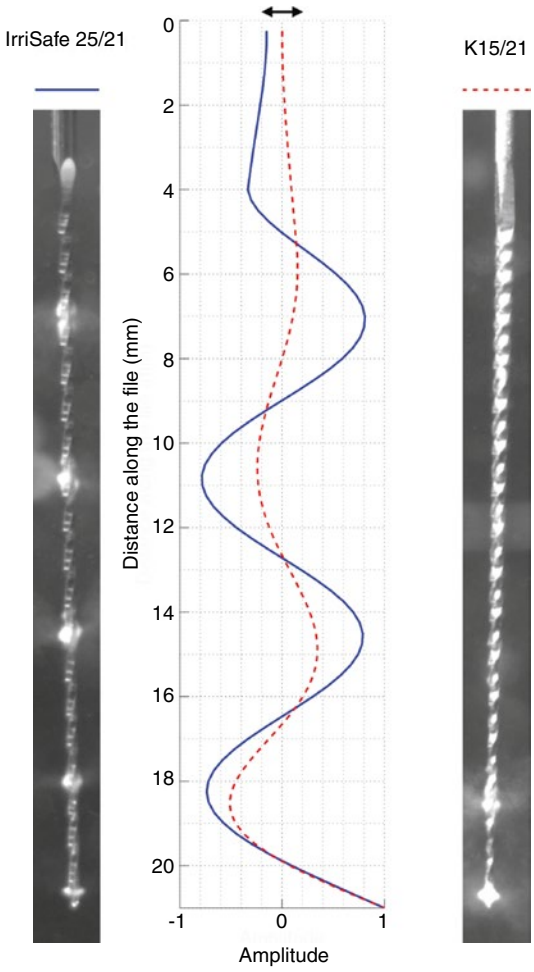

Fig. 3.7 Cavitation along file. Cavitation occurring on an IrriSafe 25/21 and a K15/21 during ultrasonic activation. The cavitation is visible as white clouds as they are reflecting light from the side. The location of the cavitation coincides well with antinodes on the files that have large amplitudes, as determined with a numerical model (Verhaagen et al. [33]). On the K15/21 file, there is only a large amplitude at the two nodes near the tip, whereas the antinodes on the IrriSafe 25/21 file all have the same amplitude, leading to cavitation at all antinodes on the file

even beyond the file towards the apex into lateral canals, isthmuses, and around a curvature [100]. Nevertheless, no proof of their added benefit for root canal cleaning has been presented as of today. Meanwhile, the bubbles (clouds) on the file may affect the generated acoustic streaming [75] and therefore may have a negative impact on cleaning.

Bubbles don't necessarily need to collapse. Gas-filled bubbles (such as in beer) may be stable for a relatively long time (seconds to minutes). The oscillating pressure field induced by the oscillating file can make these stable bubbles oscillate with large amplitude and thereby enhance the streaming, and consequently, the cleaning can be locally significantly [93, 106, 108]. This effect is especially useful when bubbles are located in an otherwise difficult to access area such as lateral canals and isthmuses. This mechanism (*stable cavitation*) was recently observed near an ultrasonically oscillating endodontic file where a stable cavitation was very effective in removing a layer of viscoelastic hydrogel [109]. In another study, a synergistic effect of a microbubble emulsion and ultrasonic agitation was observed to improve biofilm removal [110].

The largest oscillation of these bubbles can be achieved when they are driven at resonance with the ultrasound, which in water may be approximated with: [93].

$$R_{\text{bubble}} = 3.3$$

For ultrasound with a frequency of $f = 30$ kHz, bubbles are driven optimally when they have a radius of $R = 100$ μm.

There are three ways for introducing these stable bubbles into the root canal during ultrasonic activation. First, these bubbles may be introduced through entrapment which occurs when file-induced instabilities at the irrigant–air interface lead to gas being entrapped into the irrigant [37]. Secondly, these bubbles may grow during rectified diffusion [111] which is a process where during each ultrasound-induced oscillation of the bubble leads to a little bit of gas diffusion into the bubble. After several seconds (or hundreds of thousands of oscillations), the bubble can grow up to the resonance size of 100 μm in radius. A third mechanism for stable bubble formation is by the generation of gas during the reaction of the irrigant with organic material [109, 112].

As stable bubbles dissolve slowly over time their behavior is time-sensitive, which is why the resting time between ultrasonic activations (or pulsations) may be important [113].

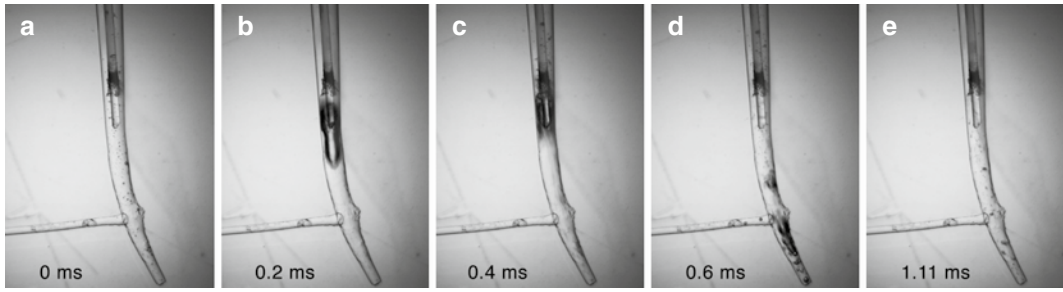

Fig. 3.8 Laser visualization. High-speed recording (9000 fps) of the vapor bubble generated by an Er:YAG laser with a flat-tip fiber inside a curved root canal model (size 35/0.06) with a lateral canal of 250 μm in diameter (**a**). The bubble grows for a few hundred microseconds (**b**) then collapses (**c**). During the final stage of its collapse, it creates (the growth of) bubbles at the apex and inside the lateral canal (**d**) before coming to rest again (**e**) until the next laser pulse

3.5.5 Laser-Activated Irrigation

Cavitation also plays a large role in LAI because it induces streaming of the irrigant at several locations and length scales. The dynamics of LAI have been studied using high-speed imaging [114–116] showing the initial generation and implosion of a large vapor bubble at the tip of the fiber (Fig. 3.8) generated by the absorption of laser energy and fast heating of the irrigant [28]. The size of the laser-generated bubble depends on the output energy, pulse duration, and the absorption by the irrigant for the wavelength of the laser. The following collapse of the laser-induced bubble pulls fluid from the coronal and the apical part, including the lateral canals, towards the bubble center and thereby induces fluid velocities of several meters per second that can loosen debris from the canal irregularities. The last stage of the bubble collapse was observed to induce a shock wave that causes (secondary) small cavitation bubbles throughout the root canal.

The pulsatile nature of the flow may also be beneficial due to transient effects induced in the flow by each pulse and also due to the interaction with the growing or dissolving bubbles.

Stable bubbles that were already present in the root canal, such as vapor lock at the apex, can be driven by the pressure changes from the growth and collapse of the laser-induced bubble and may thereby enhance locally the streaming and associated cleaning.

Plasma may also be induced by the laser through ionization of the vapor in the induced bubble [28]. The highly reactive ions of which the plasma is made of may provide an additional way of cleaning the root canal walls nearby the fiber tip [117].

At high laser power settings, the generated vapor bubble grows so large that it pushes irrigant out of the root canal to the coronal opening [115] thereby causing loss of irrigant inside the root canal. The irrigant may be replenished with an external supply. However, the activation mechanism of LAI does not necessarily create mixing of fresh and consumed irrigant; therefore, LAI should be used intermittently with syringe irrigation.

Irrigant extrusion has been reported in the literature [118]. However, during recent years, the LAI devices have been improved to optimize the laser absorption (e.g., by using conical laser fiber tips [119]) and to reduce the risk of irrigant extrusion [118]. Recent studies have also started to look at other types of lasers operating at different wavelengths but still with the purpose of inducing a cavitation bubble [120].

The bubble growth and collapse may be affected by surface-active irrigants such as NaOCl which has been demonstrated to lead to greater number and smaller bubbles as compared to water [115].

The flow produced by the collapse of the laser-induced bubble will produce a shear stress on the root canal wall. This shear stress results in a cleaning effect. The observed flow is similar to negative pressure systems except that for LAI the magnitude of the shear stress is of higher magnitude (1000 N/m^2) (Fig. 3.9).

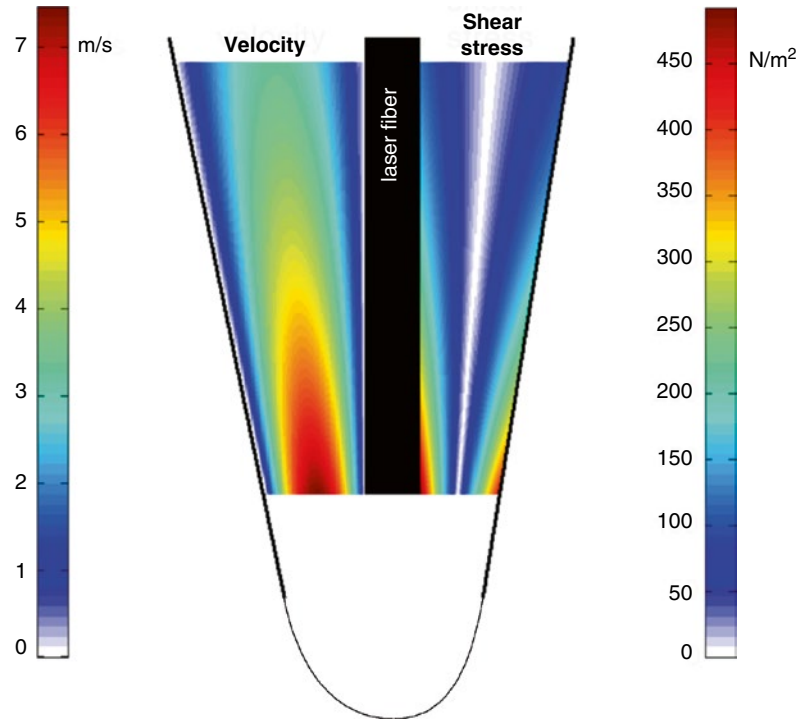

Fig. 3.9 Laser estimates. Measured fluid velocities and derived shear stresses during the collapse of a laser-generated vapor bubble inside a root canal. Because of the root canal taper, there is an increase in fluid velocity and shear stress closer to the fiber tip. More details can be found in De Groot et al. [115]

Laser-activated irrigation and PIPS have been shown in vitro to be more efficient in removing dentin debris or smear layer than positive pressure irrigation or ultrasonic activation [24, 27, 115, 121]. Nevertheless, despite the insight into the flow characteristics of LAI, the exact cleaning mechanisms during LAI or PIPS are to date not fully clarified (see Chaps. 9 and 10).

3.6 Chemical Effects Enhanced by the Irrigation Systems

When root canal irrigants are introduced in the root canal, they will chemically react with dentin, microorganisms, biofilm, tissue remnants [122, 123], or other irrigants [124]. This reduces the chemical concentration and cleaning efficacy. To maintain an active chemical process, the irrigant needs to be mixed frequently with fresh irrigant. Mixing of the irrigant involves transport of the irrigant which can take place by diffusion or convection (flow). Diffusion is the result of the random movement of individual particles (molecules/ions) in the fluid. This process is slow and depends on the temperature and concentration gradients present. Convection, on the other hand, is a faster and more efficient transport mechanism in which molecules are transported by the motion of the fluid [125]. Convection contributes to effective delivery, replenishment, and mixing of the irrigant. The flow and activation phase of irrigant agitation/activation techniques therefore assists with the chemical activity through convection and diffusion of the molecules/ions of the irrigant. During the resting phase, diffusion is dominant.

To obtain the optimal chemical effect of irrigants, they should be delivered throughout the root canal system and be refreshed and mixed as effectively as possible with respect to the chemical reaction time. This process can be characterized with the second Damköhler number, which is defined as the ratio of the typical irrigant transport time to the reaction time.[1]

[1] The second Damköhler number is defined as

$Da = \frac{\text{irrigant transport time}}{\text{reaction time}}$

in which U is the velocity and Ω the vorticity (rotation) of the irrigant and D is the diffusion coefficient. The length

It was shown recently that the Damköhler number during syringe irrigation with a side-vented needle was higher than 1 in the apical area suggesting that the fluid transport was too slow to ensure adequate refreshment of irrigant [38]. Irrigant activation systems can improve the delivery throughout the root canal system (irrigant transportation time) and the replenishment/mixing of the irrigant by inducing additional convection.

To determine the optimal flow rate of the irrigant, it is important to know its reaction rate with biofilm, pulp tissue, or the root canal wall (dentin and smear layer). Unfortunately, only the reaction rate of NaOCl with dentin is known. This reaction rate is enhanced with higher concentration or laser or ultrasonic activation [126]. Sonic activation has never been reported to affect this reaction rate. The increase of reaction rate with ultrasonic or laser activation was even observed in the resting phase [126] but reduced over time during the reaction. A similar synergistic effect of NaOCl and ultrasound in the dissolution of tissue [122] or the removal of dentin debris from root canals has been reported in the literature [16]. The influence of irrigant activation can be attributed to a sonochemical effect and/or refreshment/mixing of the irrigant [107] or due to the formation of small bubbles when NaOCl comes into contact with organic tissue. However, the exact mechanisms are not yet known.

The pH of the irrigant can also contribute to the reaction rate [127], although the buffering effect of dentin may compensate this effect [126].

With EDTA, an improved penetration into dentinal tubules in the pulp chamber after ultrasonic activation has been reported [128], but the cause has not yet been explained. Sonochemical reactions can be ruled out because they are not easily achieved as high-energy input is needed to drive sonochemical reactions in EDTA [129].

scale L is a typical length over which the reaction takes place near the surface.

Heating of the irrigant by ultrasonic and laser activation is a secondary effect that may enhance the chemical activity of NaOCl [130, 131]. Both activation mechanisms slowly heat up the irrigant by several degrees Celsius [26, 37, 132].

3.7 Effect of Irrigation on Root Canal Disinfection

Before we can discuss the impact of irrigation systems on the disinfection of the root canal system, it is important to understand the biological situation of the infected root canal system. When the root canal system is infected, biofilm will cover the root canal walls including those of the tubules, lateral canals, and apical deltas [1]. Furthermore, biofilm formation outside the root canal covering the outer root apex has been reported [1]. This external biofilm can never be removed by root canal irrigation.

Biofilm can be defined as microbial aggregates that usually accumulate at a solid–liquid interface and that are encased in a matrix of highly hydrated extracellular polymeric substances (EPS) [133]. The EPS mainly consists of water, proteins, and polysaccharides that effectively protect the microorganisms from attacks by antimicrobials [133]. Consequently, the antimicrobial irrigants need to diffuse or break through the matrix to kill the microorganisms. The EPS can make up more than 80 % of the biofilm content, and this makes the biofilm a viscoelastic fluid [134] causing the biofilm to exhibit elastic behavior at low stress and viscous flow behavior at high stress [135]. This viscoelastic behavior provides an excellent protection mechanism against mechanical attacks. Therefore, in order to obtain an effective disinfection, disintegration of the matrix structure is essential.

The specific constitution of biofilms strongly depends on the type of microbial species (e.g., in one root canal, around 600 bacterial species have been indentified [136]) and on environmental conditions during growth such as the presence of oxygen, nutrition, and typical substances present [137]. For example, metal ions like Ca^{++} can be incorporated in

the matrix, causing cross-links of the negative binding sides of polysaccharides thus reinforcing the matrix [138]. It is important to realize that in most of the research on disinfection in endodontics, planktonic (unbound) microorganisms have been used that are not protected by the EPS and are therefore less resistant [1]. Consequently, the effect of our disinfection strategies will be underestimated. Biofilm models that allow for effectively screening the efficacy of irrigation systems are not available yet; therefore, it is difficult to determine the real impact of irrigation procedures on biofilms.

Forces on the biofilm exerted by irrigant flow could cause absorption of energy into the biofilm leading to volumetric expansion [139]. Deformation beyond the yield point could disrupt the top layers of biofilm, or its EPS matrix (cohesive failure), or could completely remove the biofilm (adhesive failure). If deformation is in the plastic range but below the yield point, biofilm is expanded but not removed [139]. However, disruption of the top layers or EPS matrix or expansion of the biofilm facilitates irrigant penetration in the biofilm and could therefore already enhance the chemical effect of irrigants [140]. Furthermore, a disruption of the biofilm matrix could leave "footprints" in the remaining biofilm, which may facilitate or impede adhesion of microorganisms thereby influencing reorganization of the biofilm [139]. However, not much information is available in the literature on the effect of fluid flow on a biofilm mainly because of a large variety in biofilm constituents and associated physical properties, which makes it a difficult multidisciplinary subject. In addition, measurement of the mechanical properties should take place in a short time scale (within minutes) because the biofilm is a living organism and will adapt to its environment [89]. Also the time scale of irrigant activation systems should be considered, as the behavior of a biofilm under 30 kHz ultrasonic oscillations or laser pulsations may be different than when deforming it slowly. Critical loads necessary to disrupt biofilms by a variety of different techniques have recently been reviewed [141]. It was found that the sensitivity to certain loading modes, such as normal or shear stresses, varies extensively among biofilms. Furthermore, the reported values of adhesion strength depend greatly on the testing technique, which range from coarse macro-scale measurements down to atomic force microscopy (AFM) operating on a nanoscale [141]. Typical values found in the literature give an elastic modulus on the order of 10^{-1} – 10^{2} Pa and a cohesive shear strength of 10^{1} – 10^{3} Pa [89, 141, 142]. Pressures and shear stresses produced by different irrigation techniques show that some techniques should be able to remove biofilm. Unfortunately, the mechanical properties of an endodontic biofilm are not known therefore a prediction of the effect of fluidic stresses on biofilm removal in the root canal is not yet possible. Recently, a 3D numerical study on the effect of fluid flow on biofilm has shown that for high EPS matrix stability, only exposed structures at the surface of the biofilm are detached. Low EPS matrix stabilities may lead to the detachment of large portions from the top of the biofilm. Interestingly, it has been observed that a smooth basal biofilm surface structure remains after detachment [143]. This is confirmed by another study where smooth base biofilms remain after the biofilm had been subjected to high shear stresses using the fluid dynamic gauging (FDG) technique [144]. These observations can be explained by the stratification of biofilms, which leaves older, stronger layers at the base of the biofilm, typically adhering strongly to the substrate [144, 145]. Therefore, complete removal of biofilm from the root canal wall could be a difficult task, and a combination of mechanical *and* chemical stress on the biofilm remains crucial. Figure 3.10 shows the possible biofilm removal mechanisms related to irrigant flow and activation.

3.7.1 Interaction Between a Biofilm and the Flow Created by Sonic, Ultrasonic, or Laser Activation

Weak forces (low pressures and shear stresses) or a high EPS matrix stability cause only an elastic deformation of the biofilm that reverses as soon as the stress is removed. Repeated loading of the biofilm structure with a periodic stress, as is the case

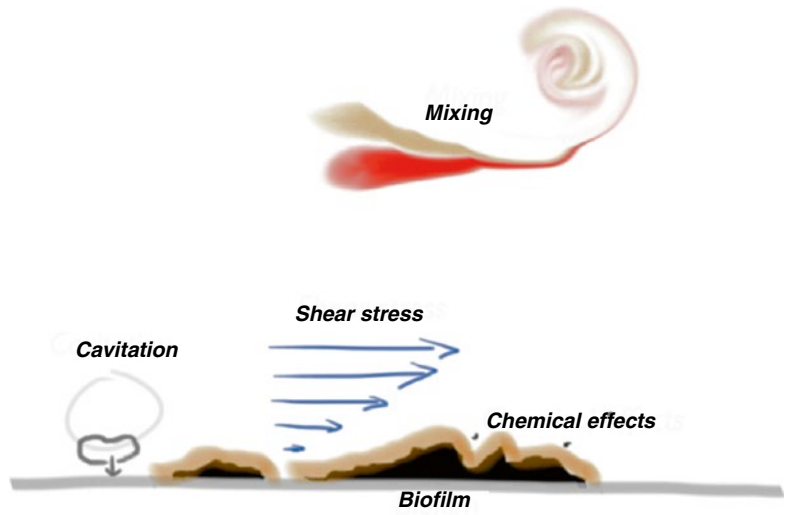

Fig. 3.10 Biofilm removal mechanisms

with sonic, ultrasonic, and laser activation, may result in cohesive failure or fatigue of the biofilm [89]; however, the threshold (force and number of loading cycles) for damage due to fatigue is unknown. At increased force (or lower EPS matrix stability), viscous deformation of the biofilm may occur. The biofilm deforms and displaces in order to distribute and minimize the applied stresses [146]. When a steady force is applied, for example, in the case of a steady flow, the biofilm will attain a steady state, and no further deformation or removal will take place. Therefore, it may be advantageous to generate a non-steady flow, for example, by unsteady oscillations of the ultrasonic file or by generating pulsations with ultrasound [113] or laser [115]. At stresses exceeding the cohesive or adhesive strength of the biofilm, parts of the biofilm may detach from the bulk biofilm (mechanical failure of the biofilm, a process called *sloughing* [142, 147, 148]) or from the substrate, respectively. Detached biofilm parts may reattach at a different location where the mechanical and chemical conditions are more favorable [142].

3.7.2 Interaction with Cavitation Bubbles Created by Ultrasonic or Laser Activation

The gradients associated with the time scales and length scales of the exerted stress are important with regard to the behavior of a viscoelastic material. Cavitation bubbles, such as those created by fast irrigant vaporization with a laser device, typically exhibit large velocities and accelerations on a small time scale, making them efficient in plastic deformation of the biofilm [93, 109]. For transient cavitation, velocities of 100 m/s are feasible at micron scales [101]. To clean larger areas such as the entire root canal system, many cycles (laser pulses) may be required.

3.8 Effect of Irrigation on Endodontic Outcome

From the activation systems discussed in this chapter, ultrasonic and laser activation contribute positively to both the mechanical and the chemical aspects of the irrigation procedure. However, it is not exactly known to what extent this will contribute to the disinfection procedure and if this eventually will improve the outcome of the treatment. Both systems have the potential to disrupt or remove biofilm, but to what extent they can remove biofilm from the root canal wall and from more remote regions such as oval extensions, lateral canals, and tubules is not known. No reliable endodontic biofilm models are currently available for research. Apical periodontitis is a multifactorial disease, and therefore, also its healing depends on a range of variables and not only on the irrigation during the endodontic treatment. From the

clinical research, it is clear that the length and the quality of the root canal filling are two of the few risk factors that are obvious. However, the influence of the irrigation procedure, complex canal anatomy (apical delta and dentinal tubules) structure of the biofilm, and external biofilm around the root apex on the endodontic outcome is not known because data from randomized controlled trials (RCT) are lacking. Recently, it was demonstrated in an RCT that an ultrasonic-assisted irrigation protocol did not significantly improve the endodontic outcome from syringe irrigation alone [149]. This could indicate that we need to improve the mechanical and chemical aspects of the irrigation procedures or that other factors such as the presence of an external biofilm or the biofilm structure itself is more important in determining the endodontic outcome. More RCTs are necessary to answer these questions.

References

1. Haapasalo M, Shen Y, Ricucci D. Reasons for persistent and emerging post-treatment endodontic disease. Endod Top. 2011;18:31–50.
2. Sen BH, Wesselink PR, Türkün M. The smear layer: a phenomenon in root canal therapy. Int Endod J. 1995;28:141–8.
3. Paqué F, Laib A, Gautschi H, Zehnder M. Hard-tissue debris accumulation analysis by high-resolution computed tomography scans. J Endod. 2009;35:1044–7.
4. Gorni FG, Gagliani MM. The outcome of endodontic retreatment: a 2-yr follow-up. J Endod. 2004;30:1–4.
5. Wu MK, van der Sluis LW, Wesselink PR. Comparison of mandibular premolars and canines with respect to their resistance to vertical root fracture. J Dent. 2004;32:265–8.
6. Liu R, Kaiwar A, Shemesh H, Wesselink PR, Hou BX, Wu MK. Incidence of apical root cracks and apical dentinal detachments after canal preparation with hand and rotary files at different instrumentation lengths. J Endod. 2013;39:129–32.
7. Peters OA. Current challenges and concepts in the preparation of root canal systems: a review. J Endod. 2004;30:559–67.
8. Lussi A, Nussbächer U, Grosrey J. A novel noninstrumented technique for cleansing the root canal system. J Endod. 1993;19:549–53.
9. Attin T, Buchalla W, Zirkel C, Lussi A. Clinical evaluation of the cleansing properties of the noninstrumental technique for cleaning root canals. Int Endod J. 2002;35:929–33.
10. Mader C, Baumgartner J, Peters D. Scanning electron microscopic investigation of the smeared layer on root canal walls. J Endod. 1984;10:477–83.
11. Haapasalo M, Qian W, Portenier I, Waltimo T. Effects of dentin on the antimicrobial properties of endodontic medicaments. J Endod. 2007;33:917–25.
12. Boutsioukis C, Verhaagen B, Versluis M, Kastrinakis E, Wesselink PR, Van der Sluis LWM. Evaluation of irrigant flow in the root canal using different needle types by an unsteady Computational Fluid Dynamics model. J Endod. 2010;36:875–9.
13. Zehnder M. Research that matters – irrigants and disinfectants. Int Endod J. 2012;45:961–2.
14. Dutner J, Mines P, Anderson A. Irrigation trends among American association of endodontists members: a web-based survey. J Endod. 2012;38:37–40.
15. Gu LS, Kim JR, Ling J, Choi KK, Pashley DH, Tay FR. Review of contemporary irrigant agitation techniques and devices. J Endod. 2009;35:791–804.
16. Jiang L-M, Lak B, Eijsvogel E, Wesselink PR, van der Sluis LWM. Comparison of the cleaning efficacy of different final irrigation techniques. J Endod. 2012;38:838–41.
17. Van der Sluis LWM, Vogels MPJM, Verhaagen B, Macedo R, Wesselink PR. Study on the influence of refreshment/activations cycles and irrigants on mechanical cleaning efficiency during ultrasonic activation of the irrigant. J Endod. 2010;36:737–40.
18. Moser JB, Heuer MA. Forces and efficacy in endodontic irrigation systems. Oral Surg Oral Med Oral Pathol. 1982;53:425–8.
19. Boutsioukis C, Lambrianidis T, Kastrinakis E, Bekiaroglou P. Measurement of pressure and flow rates during irrigation of a root canal *ex vivo* with three endodontic needles. Int Endod J. 2007;40:504–13.
20. Mitchell RP, Yang SE, Baumgartner JC. Comparison of apical extrusion of NaOCl using the EndoVac or needle irrigation of root canals. J Endod. 2010;36:338–41.
21. Mitchell RP, Baumgartner JC, Sedgley CM. Apical extrusion of sodium hypochlorite using different root canal irrigation systems. J Endod. 2011;37:1677–81.
22. Desai P, Himel V. Comparative safety of various intracanal irrigation systems. J Endod. 2009;35:545–9.
23. Meire MA, Poelman D, De Moor RJ. Optical properties of root canal irrigants in the 300–3,000-nm wavelength region. Lasers Med Sci. 2014;29(5):1557–62.
24. Peeters HH, Suardita K. Efficacy of smear layer removal at the root tip by using ethylenediaminetetraacetic acid and erbium, chromium: yttrium, scandium, gallium garnet laser. J Endod. 2011;37:1585–9.
25. Peters OA, Bardsley S, Fong J, Pandher G, Divito E. Disinfection of root canals with photon-initiated photoacoustic streaming. J Endod. 2011;37:1008–12.
26. Peeters HH, Mooduto L. Measurement of temperature changes during cavitation generated by an erbium, chromium: Yttrium, scandium, gallium garnet laser. Open J Stomatol. 2012;2:286–91.

27. DiVito E, Colonna M, Olivi G. Effectiveness of the Erbium:YAG laser and new design radial and stripped tips in removing the smear layer after root canal instrumentation. Lasers Med Sci. 2012;27: 273–80.
28. Song WD, Hong MH, Lukyanchuk B, Chong TC. Laser-induced cavitation bubbles for cleaning of solid surfaces. J Appl Phys. 2004;95:2952–6.
29. Jiang L-M, Verhaagen B, Versluis M, Van der Sluis LWM. Evaluation of a sonic device designed to activate irrigant in the root canal. J Endod. 2010;36:143–6.
30. Lumley PJ, Walmsley AD, Laird WRE. Streaming patterns produced around endosonic files. Int Endod J. 1991;24:290–7.
31. Lea SC, Walmsley AD, Lumley PJ, Landini G. A new insight into the oscillation characteristics of endosonic files used in dentistry. Phys Med Biol. 2004;49:2095–102.
32. Lea SC, Walmsley D, Lumley PJ. Analyzing endosonic root canal file oscillations: an *in vitro* evaluation. J Endod. 2010;36:880–3.
33. Verhaagen B, Lea SC, Van der Sluis LWM, Walmsley AD, Versluis M. Oscillation characteristics of endodontic files: numerical model and its validation. IEEE Trans Ultrason Ferroelect Freq Control. 2012;59:2448–59.
34. Weller RN, Brady JM, Bernier WE. Efficacy of ultrasonic cleaning. J Endod. 1980;6:740–3.
35. Van der Sluis LWM, Versluis M, Wu M-K, Wesselink PR. Passive ultrasonic irrigation of the root canal: a review of the literature. Int Endod J. 2007;40:415–26.
36. Boutsioukis C, Verhaagen B, Walmsley AD, Versluis M, Van der Sluis LWM. Measurement and visualization of file-wall contact during Passive Ultrasonic Irrigation in vitro. Int Endod J. 2013;46(11):1046–55.
37. Macedo RG, Verhaagen B, Fernandez Rivas D, Gardeniers JGE, Van der Sluis LWM, Wesselink PR, Versluis M. Sonochemical and high-speed optical characterization of cavitation generated by an ultrasonically oscillating dental file in root canal models. Ultrason Sonochem. 2014;21(1):324–35.
38. Verhaagen B, Boutsioukis C, Heijnen GL, Van der Sluis LWM, Versluis M. Role of the confinement of a root canal on jet impingement during endodontic irrigation. Exp Fluids. 2012;53:1841–53.
39. Chen JE, Nurbakhsh B, Layton G, Bussmann M, Kishen A. Irrigation dynamics associated with positive pressure, apical negative pressure and passive ultrasonic irrigations: a computational fluid dynamics analysis. Aust Endod J. 2014;40(2):54–60.
40. Tay FR, Gu L-s, Schoeffel GJ, Wimmer C, Susin L, Zhang K, Arun SN, Kim J, Looney WS, Pashley DH. Effect of vapor lock on root canal debridement by using a side-vented needle for positive-pressure irrigant delivery. J Endod. 2010;36:745–50.
41. Parente JM, Loushine RJ, Susin L, Gu L, Looney SW, Weller RN, Pashley DH, Tay FR. Root canal debridement using manual dynamic agitation or the EndoVac for final irrigation in a closed system and an open system. Int Endod J. 2010;43:1001–12.
42. Psimma Z, Boutsioukis C, Vasiliadis L, Kastrinakis E. A new method for real-time quantification of irrigant extrusion during root canal irrigation *ex vivo*. Int Endod J. 2013;46(7):619–31.
43. Psimma Z, Boutsioukis C, Kastrinakis E, Vasiliadis L. Effect of needle insertion depth and root canal curvature on irrigant extrusion *ex vivo*. J Endod. 2013;39:521–4.
44. Boutsioukis C, Lambrianidis T, Kastrinakis E. Irrigant flow within a prepared root canal using different flow rates: a Computational Fluid Dynamics study. Int Endod J. 2009;42:144–55.
45. Boutsioukis C, Gogos C, Verhaagen B, Versluis M, Kastrinakis E, Van der Sluis LWM. The effect of apical preparation size on the irrigant flow in root canals using an unsteady Computational Fluid Dynamics model. Int Endod J. 2010;43:874–81.
46. Boutsioukis C, Gogos C, Verhaagen B, Versluis M, Kastrinakis E, Van der Sluis LWM. The effect of root canal taper on the irrigant flow: evaluation by an unsteady Computational Fluid Dynamics model. Int Endod J. 2010;43:909–16.
47. Boutsioukis C, Lambrianidis T, Verhaagen B, Versluis M, Kastrinakis E, Wesselink PR, Van der Sluis LWM. The effect of needle insertion depth on the irrigant flow in the root canal: evaluation by an unsteady Computational Fluid Dynamics model. J Endod. 2010;36:1664–8.
48. Amato M, Vanoni-Heineken I, Hecker H, Weiger R. Curved versus straight root canals: the benefit of activated irrigation techniques on dentin debris removal. Oral Surg Oral Med Oral Pathol Oral Radiol Endod. 2011;111:529–34.
49. Gao Y, Haapasalo M, Shen Y, Wu H, Li B, Ruse ND, Zhou X. Development and validation of a three-dimensional computational fluid dynamics model of root canal irrigation. J Endod. 2009;35:1282–7.
50. Shen Y, Gao Y, Qian W, Ruse ND, Zhou X, Wu H, Haapasalo M. Three-dimensional numerical simulation of root canal irrigant flow with different irrigation needles. J Endod. 2010;36:884–9.
51. De Gregorio C, Estevez R, Cisneros R, Heilborn C, Cohenca N. Effect of EDTA, sonic, and ultrasonic activation on the penetration of sodium hypochlorite into simulated lateral canals: an in vitro study. J Endod. 2009;35:891–5.
52. Vera J, Arias A, Romero M. Dynamic movement of intracanal gas bubbles during cleaning and shaping procedures: the effect of maintaining apical patency on their presence in the middle and cervical thirds of human root canals-an in vivo study. J Endod. 2012;38:200–3.
53. Boutsioukis C, Kastrinakis E, Lambriandinis T, Verhaagen B, Versluis M, van der Sluis LWM. Formation and removal of apical vapor lock during syringe irrigation: a combined experimental and Computational Fluid Dynamics approach. Int Endod J. 2014;47(2):191–201.
54. Chow TW. Mechanical effectiveness of root canal irrigation. J Endod. 1983;9:475–9.

55. Falk KW, Sedgley CM. The influence of preparation size on the mechanical efficacy of root canal irrigation in vitro. J Endod. 2005;31:742–5.
56. Hsieh YD, Gau CH, Kung Wu SF, Shen EC, Hsu PW, Fu E. Dynamic recording of irrigating fluid distribution in root canals using thermal image analysis. Int Endod J. 2007;40:11–7.
57. Huang TY, Gulabivala K, Ng YL. A bio-molecular film ex-vivo model to evaluate the influence of canal dimensions and irrigation variables on the efficacy of irrigation. Int Endod J. 2008;41:60–71.
58. Bronnec F, Bouillaguet S, Machtou P. Ex vivo assessment of irrigant penetration and renewal during the cleaning and shaping of root canals: a digital subtraction radiographic study. Int Endod J. 2010; 43:275–82.
59. Baker NA, Eleazer PD, Averbach RE, Seltzer S. Scanning electron microscopic study of the efficacy of various irrigating solutions. J Endod. 1975;1:127–35.
60. Sedgley C, Applegate B, Nagel A, Hall D. Real-time imaging and quantification of bioluminescent bacteria in root canals in vitro. J Endod. 2004;30:893–8.
61. Sedgley CM, Nagel AC, Hall D, Applegate B. Influence of irrigant needle depth in removing bacteria inoculated into instrumented root canals using realtime imaging in vitro. Int Endod J. 2005; 38:97–104.
62. Bronnec F, Bouillaguet S, Machtou P. Ex vivo assessment of irrigant penetration and renewal during the final irrigation regimen. Int Endod J. 2010;43: 663–72.
63. Spoorthy E, Velmurugan N, Ballal S, Nandini S. Comparison of irrigant penetration up to working length and into simulated lateral canals using various irrigating techniques. Int Endod J. 2013;46(9):815–22.
64. Brunson M, Heilborn C, Johnson JD, Cohenca N. Effect of apical preparation size and preparation taper on irrigant volume delivered by using negative pressure irrigation system. J Endod. 2010;36:721–4.
65. Rothfus RR, Monrad CC, Senecal VE. Velocity distribution and fluid friction in smooth concentric annuli. Ind Eng Chem. 1950;42:2511–20.
66. Goode N, Khan S, Eid AA, Niu L-n, Gosier J, Susin LF, Pashley DH, Tay FR. Wall shear stress effects of different endodontic irrigation techniques and systems. J Dent. 2013;41(7):636–41.
67. De Gregorio C, Estevez R, Cisneros R, Paranjpe A, Cohenca N. Efficacy of different irrigation and activation systems on penetration of sodium hypochlorite into simulated lateral canals and up to working length: an *in vitro* study. J Endod. 2010;36:1216–21.
68. Khan S, Niu L-n, Eid AA, Looney SW, Didato A, Roberts S, Pashley DH, Tay FR. Periapical pressures developed by non-binding irrigation needles at various irrigation delivery rates. J Endod. 2013;39: 529–33.
69. Ricucci D, Loghin S, Sigueira Jr JF. Exuberant biofilm infection in a lateral canal as the cause of short-term endodontic treatment failure: report of a case. J Endod. 2013;39:712–8.
70. Arnold M, Ricucci D, Sigueira Jr JF. Infection in a complex network of apical ramifications as the cause of persistent apical periodontitis: a case report. J Endod. 2013;39(9):1179–84.
71. Vieira AR, Siqueira Jr JF, Ricucci D, Lopes WSP. Dentinal tubule infection as the cause of recurrent disease and late endodontic treatment failure: a case report. J Endod. 2012;38:250–4.
72. Verhaagen B, Boutsioukis C, Sleutel CP, Kastrinakis E, Van der Sluis LWM, Versluis M. Irrigant transport into dental microchannels. Microfluid Nanofluid. 2014;16(6):1165–77.
73. Shankar PN, Deshpande MD. Fluid mechanics in the driven cavity. Annu Rev Fluid Mech. 2000;32:93–136.
74. Zou L, Shen Y, Li W, Haapasalo M. Penetration of sodium hypochlorite into dentin. J Endod. 2010;36: 793–6.
75. Verhaagen B, Boutsioukis C, Van der Sluis LWM, Versluis M. Acoustic streaming induced by an ultrasonically oscillating endodontic file. J Acoust Soc Am. 2014;135(4):1717.
76. Jiang L-M, Verhaagen B, Versluis M, Van der Sluis LWM. The influence of the oscillation direction of an ultrasonic file on the cleaning efficacy of passive ultrasonic irrigation. J Endod. 2010;36:1372–6.
77. Al-Jadaa A, Paque F, Attin T, Zehnder M. Necrotic pulp tissue dissolution by passive ultrasonic irrigation in simulated accessory canals: impact of canal location and angulation. Int Endod J. 2009;42:59–65.
78. Jiang L-M, Verhaagen B, Versluis M, Langedijk J, Wesselink PR, Van der Sluis LWM. The influence of the ultrasonic intensity on the cleaning efficacy of passive ultrasonic irrigation. J Endod. 2011;37:688–92.
79. Nanzer J, Langlois S, Coeuret F. Electrochemical engineering approach to the irrigation of tooth canals under the influence of a vibrating file. J Biomed Eng. 1989;11:157–63.
80. Malki M, Verhaagen B, Jiang L-M, Nehme W, Naaman A, Versluis M, Wesselink PR, Van der Sluis LWM. Irrigant flow beyond the insertion depth of an ultrasonically oscillating file in straight and curved root canals: visualization and cleaning efficacy. J Endod. 2012;38:657–61.
81. Walmsley AD, Williams AR. Effects of constraints on the oscillatory pattern of endosonic files. J Endod. 1999;15:189–94.
82. Rayleigh L. On the circulation of air observed in Kundt's tubes and on some allied acoustical problems. Phil Trans R Soc Lond. 1884;175:1–21.
83. Stuart JT. Double boundary layers in oscillatory viscous flow. J Fluid Mech. 1966;24:673–87.
84. Duck PW, Smith FT. Steady streaming induced between oscillating cylinders. J Fluid Mech. 1979;91: 93–110.
85. Haddon EW, Riley N. The steady streaming induced between oscillating circular cylinders. Q J Mech Appl Math. 1979;32:265–82.
86. Williams AR, Nyborg WL. Microsonation using a transversely oscillating capillary. Ultrasonics. 1970;8:36–8.

87. Williams AR, Slade JS. Ultrasonic dispersal of aggregates of sarcina lutea. Ultrasonics. 1971;8:85–7.
88. Ahmad M, Pitt Ford TR, Crum LA. Ultrasonic debridement of root canals: acoustic streaming and its possible role. J Endod. 1987;13:490–9.
89. Flemming H-C, Wingender J, Szewzyk U. Biofilm highlights. Springer series on biofilms. 1st ed. Berlin/Heidelberg: Springer; 2011.
90. Deshpande MD, Vaishnav RN. Submerged laminar jet impingement on a plane. J Fluid Mech. 1982;114: 213–36.
91. Phares DJ, Smedley GT, Flagan RC. The wall shear stress produced by the normal impingement of a jet on a flat surface. J Fluid Mech. 2000;418:351–75.
92. Kim SK, Troesch AW. Streaming flows generated by high-frequency small-amplitude oscillations of arbitrary cylinders. Phys Fluid A. 1989;6:975–85.
93. Brennen CE. Cavitation and bubble dynamics. New York: Oxford University Press; 1995.
94. Prosperetti A. Bubbles. Phys Fluid. 2004;16: 1852–65.
95. Fernandez Rivas D, Verhaagen B, Seddon RT, Zijlstra AG, Jiang L-M, Van der Sluis LWM, Versluis M, Lohse D, Gardeniers JGE. Localized removal of layers of metal, polymer, or biomaterial by ultrasound cavitation bubbles. Biomicrofluidics. 2012;6: 034114.
96. Mason TJ, Peters D. Practical sonochemistry: power ultrasound uses and applications, Chemical science series. Chichester: Horwood; 2002.
97. Junge L, Ohl C-D, Wolfrum B, Arora M, Ikink R. Cell detachment method using shockwave-induced cavitation. Ultrason Med Biol. 2003;29: 1769–76.
98. Fernandez Rivas D, Betjes J, Verhaagen B, Bouwhuis W, Bor TC, Lohse D, Gardeniers JGE. Erosion evolution in mono-crystalline silicon surfaces caused by acoustic cavitation bubbles. Appl Phys Lett. 2013;113:064902.
99. Terwisga WJC, Fitzsimmons PA, Ziru L, Foeth EJ. Cavitation erosion – a review of physical mechanisms and erosion risk models. In: Proceedings of the 7th international symposium on cavitation CAV2009. Ann Arbor; 2009.
100. Macedo RG, Verhaagen B, Fernandez Rivas D, Versluis M, Wesselink PR, Van der Sluis LWM. Cavitation measurement during sonic and ultrasonic activated irrigation. J Endod. 2014;40(4):580–3.
101. Brujan E-A, Nahen K, Schmidt P, Vogel A. Dynamics of laser-induced cavitation bubbles near an elastic boundary. J Fluid Mech. 2001;433:251–81.
102. Versluis M, Schmitz B, Von der Heydt A, Lohse D. How snapping shrimp snap: through cavitating bubbles. Science. 2000;289:2114–7.
103. Ahmad M, Pitt Ford TR, Crum LA, Walton AJ. Ultrasonic debridement of root canals: acoustic cavitation and its relevance. J Endod. 1988;14:486–93.
104. Lumley PJ, Walmsley AD, Laird WRE. An investigation into cavitational activity occurring in endosonic instrumentation. J Dent. 1988;16:120–2.
105. Felver B, King DV, Lea SC, Price GJ, Walmsley AD. Cavitation occurrence around ultrasonic dental scalers. Ultrason Sonochem. 2009;16:692–7.
106. Jackson FJ, Nyborg WL. Small scale acoustic streaming near a locally excited membrane. J Acoust Soc Am. 1958;30:614–9.
107. Tiong J, Price GJ. Ultrasound promoted reaction of rhodamine B with sodium hypochlorite using sonochemical and dental ultrasonic instruments. Ultrason Sonochem. 2012;19:358–64.
108. Marmottant P, Versluis M, De Jong N, Hilgenfeldt S, Lohse D. High-speed imaging of an ultrasound-driven bubble in contact with a wall: “Narcissus” effect and resolved acoustic streaming. Exp Fluid. 2006;41:147–53.
109. Verhaagen B. Root canal cleaning through cavitation and microstreaming. PhD thesis, University of Twente, Enschede; 2012.
110. Haldford A, Ohl C-D, Azarpazhooh A, Basrani B, Friedman S, Kishen A. Synergistic effect of microbubble emulsion and sonic or ultrasonic agitation on endodontic biofilm in vitro. J Endod. 2012;38:1530–4.
111. Crum LA. Measurements of the growth of air bubbles by rectified diffusion. J Acoust Soc Am. 1980; 68:203–11.
112. Gmelin L. Handbuch der anorganische chemie, chapter Chlor. 8th ed. Leipzig: German Chemical Society, Verlag Chemie Gmbh; 1969.
113. Jiang L-M, Verhaagen B, Versluis M, Zangrillo C, Cuckovic D, Van der Sluis LWM. An evaluation of the effect of pulsed ultrasound on the cleaning efficacy of passive ultrasonic irrigation. J Endod. 2010;36:1887–91.
114. Blanken JW, Verdaasdonk RM. Cavitation as a working mechanism of the Er, Cr:YSGG laser in endodontics: a visualization study. J Oral Laser App. 2007;7:97–106.
115. De Groot SD, Verhaagen B, Versluis M, Wu M-K, Wesselink PR, Van der Sluis LWM. Laser activated irrigation within root canals: cleaning efficacy and flow visualization. Int Endod J. 2009;42:1077–83.
116. Matsumoto H, Yoshimine Y, Akamine A. Visualization of irrigant flow and cavitation induced by Er:YAG laser within a root canal model. J Endod. 2011;37:839–43.
117. Jiang C, Chen M-T, Gorur A, Schaudinn C, Jaramillo DE, Costerton JW, Sedghizadeh PP, Vernier PT, Gundersen MA. Nanosecond pulsed plasma dental probe. Plasma Process Polym. 2009;6:479–83.
118. George R, Walsh LJ. Apical extrusion of root canal irrigants when using Er:YAG and Er, Cr:YSGG lasers with optical fibers: an in vitro dye study. J Endod. 2008;34:706–8.
119. George R, Meyers IA, Walsh LJ. Laser activation of endodontic irrigants with improved conical laser fiber tips for removing smear layer in the apical third of the root canal. J Endod. 2008;34:1524–7.
120. Hmud R, Kahler WA, George R, Walsh LJ. Cavitation effects in aqueous endodontic irrigants generated by near-infrared lasers. J Endod. 2010;36:275–8.

121. de Moor RJ, Meire M, Goharkhay K, Moritz A, Vanobbergen J. Efficacy of ultrasonic versus laser-activated irrigation to remove artificially placed dentin debris plugs. J Endod. 2010;36:1580–3.
122. Moorer WR, Wesselink PR. Factors promoting the tissue dissolving capability of sodium hypochlorite. Int Endod J. 1982;15:187–96.
123. Haapasalo M, Endal U, Zandi H, Coil JM. Eradication of endodontic infection by instrumentation and irrigation solutions. Endod Top. 2005;10:77–102.
124. Rossi-Fedele G, Doğramaci EJ, Guastalli AR, Steier L, Poli de Figueiredo JA. Antagonistic interactions between sodium hypochlorite, chlorhexidine, EDTA, and citric acid. J Endod. 2012;38:426–31.
125. Incropera FP, de Witt DP. Fundamentals of heat and mass transfer. 3rd ed. New York: Wiley; 1990.
126. Macedo RG, Wesselink PR, Zaccheo F, Fanali D, Van Der Sluis LW. Reaction rate of NaOCl in contact with bovine dentine: effect of activation, exposure time, concentration and pH. Int Endod J. 2010;43:1108–15.
127. Jungbluth H, Marending M, De-Deus G, Sener B, Zehnder M. Stabilizing sodium hypochlorite at high pH: effects on soft tissue and dentin. J Endod. 2011;37:693–6.
128. Carrasco LD, Pécora JD, Fröner IC. In vitro assessment of dentinal permeability after the use of ultrasonic-activated irrigants in the pulp chamber before internal dental bleaching. Dent Traumatol. 2004;20:164–8.
129. Wang J, Wang X, Li G, Guo P, Luo Z. Degradation of EDTA in aqueous solution by using ozonolysis and ozonolysis combined with sonolysis. J Hazard Mater. 2010;176:333–8.
130. Cunningham WT, Balekjian AY. Effect of temperature on collagen-dissolving ability of sodium hypochlorite endodontic irrigant. Oral Surg Oral Med Oral Path. 1980;49:175–7.
131. Sirtes G, Waltimo T, Schaetzle M, Zehnder M. The effects of temperature on sodium hypochlorite short-term stability, pulp dissolution capacity, and antimicrobial efficacy. J Endod. 2005;31:669–71.
132. Zeltner M, Peters OA, Paqué F. Temperature changes during ultrasonic irrigation with different inserts and modes of activation. J Endod. 2009;35:573–7.
133. Flemming H-C, Neu TR, Wozniak DJ. The EPS matrix: the "house of biofilm cells". J Bacteriol. 2007;189:7945–7.
134. Wilking JN, Angelini TE, Seminara A, Brenner MP, Weitz DA. Biofilms as complex fluids. Mater Res Soc Bull. 2011;36:385–91.
135. Körstgens V, Flemming H-C, Wingender J, Borchard W. Uniaxial compression measurement device for investigation of the mechanical stability of biofilms. J Microbiol Methods. 2001;46:9–17.
136. Ozok AR, Persoon IF, Huse SM, Keijser BJ, Wesselink PR, Crielaard W, Zaura E. Ecology of the microbiome of the infected root canal system: a comparison between apical and coronal root segments. Int Endod J. 2012;45:530–41.
137. Marty N, Dournes JL, Chabanon G, Montrozier H. Influence of nutrient media on the chemical composition of the exopolysaccharide from mucoid and non-mucoid Pseudomonas aeruginosa. FEMS Microbiol Lett. 1992;98:35–44.
138. van der Waal SV, van der Sluis LWM. Potential of calcium to scaffold an endodontic biofilm, thus protecting the micro-organisms from disinfection. Med Hypotheses. 2012;79:1–4.
139. Busscher HJ, Rustema-Abbink M, Bruinsma GM, de Jager M, Gottenbos B, van der Mei HC. Non-contact removal of coadhering and non-coadhering bacterial pairs from pellicle surfaces by sonic brushing and *de novo* adhesion. Eur J Oral Sci. 2003;111:459–64.
140. He Y, Peterson BW, Ren Y, van der Mei HC, Busscher HJ. Visco-elasticity of oral biofilm and the penetration of chlorhexidine-an in vitro study. PLoS One. 2013;8, e63750.
141. Böl M, Ehret AE, Albero AB, Hellriegel J, Krull R. Recent advances in mechanical characterization of biofilm and their significance for material modeling. Crit Rev Biotechnol. 2013;33(2):145–71.
142. Picioreanu C, Van Loosdrecht M, Heijnen J. Two-dimensional model of biofilm detachment caused by internal stress from liquid flow. Biotechnol Bioeng. 2001;72:205–18.
143. Böl M, Möhle RB, Haesner M, Neu TR, Horn H, Krull R. 3D finite element model of biofilm detachment using real biofilm structures from CLSM data. Biotechnol Bioeng. 2009;103:177–86.
144. Möhle RB, Langemann T, Haesner M, Augustin W, Scholl S, Neu TR, Hempel DC, Horn H. Structure and shear strength of microbial biofilms as determined with confocal laser scanning microscopy and fluid dynamic gauging using a novel rotating disc biofilm reactor. Biotechnol Bioeng. 2007;98:747–55.
145. Derlon N, Massè A, Escudié R, Bernet N, Paul E. Stratification in the cohesion of biofilms grown under various environmental conditions. Water Res. 2008;42:2102–10.
146. Klapper I, Rupp CJ, Cargo R, Purvedorj B, Stoodley P. Viscoelastic fluid description of bacterial biofilm material properties. Biotechnol Bioeng. 2002;80:289–96.
147. Stoodley P, Lewandowski Z, Boyle JD, Lappin-Scott HM. Structural deformation of bacterial biofilms caused by short-term fluctuations in fluid shear: an in situ investigation of biofilm rheology. Biotechnol Bioeng. 1999;65:83–92.
148. Stoodley P, Wilson S, Cargo R, Piscitteli C, Rupp CJ. Detachment and other dynamic processes in bacterial biofilms. In: Surfaces in biomaterials 2001 symposium proceedings. Surfaces in Biomaterials Foundation, Minneapolis; 2001. p. 189–92.
149. Liang Y-H, Jiang L-M, Jiang L, Chen X-B, Liu Y-Y, Tian F-C, Bao X-D, Gao X-J, Versluis M, Wu M-K, van der Sluis LWM. Radiographic healing following root canal treatments performed in single-rooted teeth with and without ultrasonic activation of the irrigant: a randomized controlled trial. J Endod. 2013;39(10): 1218–25.
150. Cameron JA. The effect of ultrasonic endodontics on the temperature of the root canal wall. J Endod. 1988;14:554–8.

Part II

Basic Science of Laser Dentistry

The Physics of Lasers

4

Matteo Olivi and Giovanni Olivi

Abstract

The Bohr's atomic model and the Einstein's theory of stimulated emission of radiation were a prelude to the invention and realization of the first ruby laser.

The characteristics of laser light are described as well as the difference between laser and ordinary light. Most of the laser wavelength used in dentistry fall in the visible and infrared spectrum of the light. The visible and near- and far-infrared lasers are mainly used for soft tissue applications; some of them have applications in caries detection and biostimulation (LLLT). The medium infrared lasers, the Er,Cr:YSGG and Er:YAG lasers, represent all tissue lasers, for application on both the mucosa and gingiva, and the tooth and the bone. The basic components that constitute a dental laser unit are described as well as the parameters of use of the lasers.

4.1 History of Lasers

The word "laser" is an acronym of light amplification by stimulated emission of radiation.

If we take into consideration the theory of the atomic model (Neil Bohr, 1913), the description of stimulated emission (Albert Einstein, 1916), and the theory of the stimulated emission of radiation (Albert Einstein, 1917), laser technology already has a century of scientific history behind it.

M. Olivi (✉) • G. Olivi, MD, DDS
InLaser Rome - Advanced Center for Esthetic and Laser Dentistry, Rome, Italy
e-mail: olivimatt@gmail.com; olivilaser@gmail.com

In 1958 Charles Townes and Arthur Schawlow coined the word "maser," acronym of microwave amplification by stimulated emission of radiation, precondition for the realization of the first laser in 1960.

The word laser was first coined in 1957 by Gordon Gould, without patenting it, so that it was later used by Theodore Maiman, who introduced the acronym "laser," realizing the first ruby laser in 1960 [1].

In 1965 the physicist Leon Goldman was the first to use a ruby laser in vivo on dental tissues of his brother Bernard, who was a dentist, without any success due to excessive thermal damage [2].

G. Olivi et al. (eds.), *Lasers in Endodontics: Scientific Background and Clinical Applications*,
DOI 10.1007/978-3-319-19327-4_4

4.2 Electromagnetic Spectrum of Light

In nature, the electromagnetic spectrum of light is composed by visible and not visible radiations. The radioactivity produced from the cosmos generates cosmic radiations. From underground, telluric radiations are also emitted. The solar system emits a wide spectrum of radiations including ultraviolet, visible, and infrared radiations. The laser radiation, a human invention, belongs to the electromagnetic spectrum in different zones, depending on the specific wavelength produced.

4.2.1 Visible Spectrum of Light

The optical perception of human eyes does not recognize electromagnetic radiation beyond the violet zone of the spectrum (0.4 μm) or farther the red zone (0.7 μm). Accordingly, the spectrum of visible light covers a range approximately between 0.4 and 0.7 μm (400–700 nm); however, the border between visible and invisible spectrum is not precisely defined, depending on different factors, and is between 380 and 400 nm on one side and 700 and 800 nm on the other side.

4.2.2 Invisible Spectrum of Light

Beyond the violet zone, with a wavelength of less than 0.4 μm (400 nm), there is a zone called ultraviolet, between 0.4 and 0.01 μm. On the left side of this zone, with a decreasing wavelength, there are the X-rays extended to a wavelength of about 0006 μm. In the more external part, there are the gamma rays.

Beyond the red spectrum of light, with a wavelength superior to 0.7 μm (700 nm), the infrared spectrum is located between 0.7 and 400 μm.

On the right side of this zone, there are the microwaves and farther the radio waves (short 1–100 m; medium 200–600 m; far >600 m). Figure 4.1 illustrates the electromagnetic spectrum of radiations.

In the visible and invisible infrared spectrum of light, we find the majority of the wavelengths used in dentistry (Fig. 4.2).

4.3 Classification of Dental Lasers in the Electromagnetic Spectrum of Light [3]

A classification of lasers considers their position on the electromagnetic spectrum of light according to the wavelength :

- Laser in the ultraviolet spectrum
- Laser in the visible spectrum
- Laser in the near-infrared spectrum
- Laser in the mid-wavelength infrared spectrum
- Laser in the far-infrared spectrum (Table 4.1)

Another classification identifies the main applications of specific lasers in:

Laser for soft tissue applications, laser for hard and soft tissue applications (also called all-tissue laser), laser for low-level therapy, and laser for diagnosis (Table 4.2).

Another distinction considers the low-power lasers and the high-power lasers.

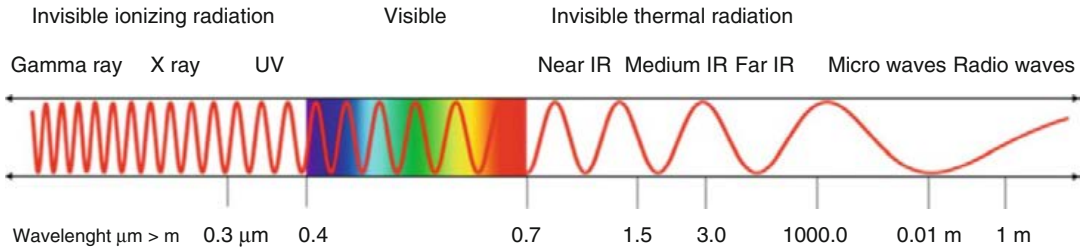

Fig. 4.1 Electromagnetic spectrum of radiations

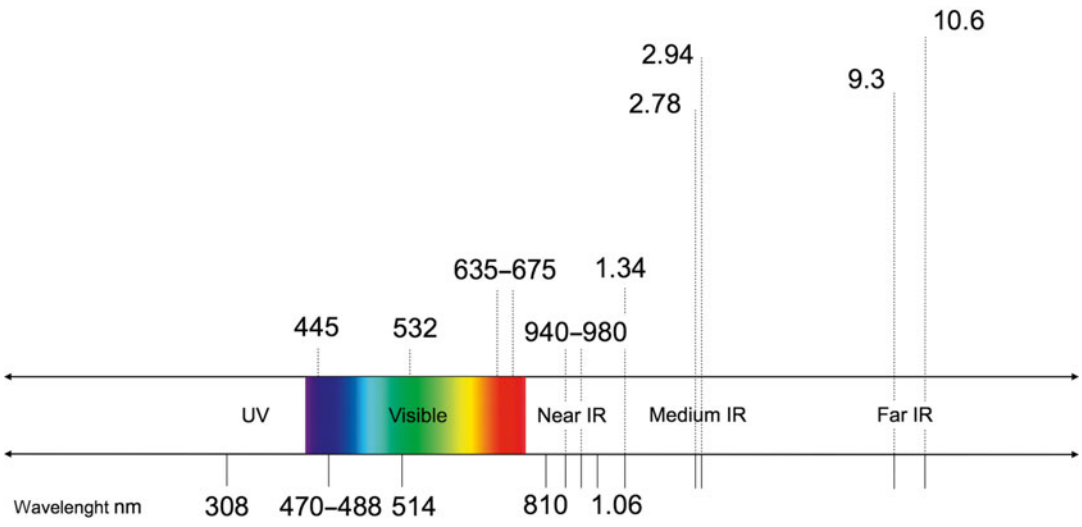

Fig. 4.2 Lasers in the electromagnetic spectrum of the light

Table 4.1 Classification of lasers according to their wavelength position on the electromagnetic spectrum of light

Ultraviolet	Visible	Near infrared	Medium infrared	Far infrared
Excimer 308 nm	Blue diode 445 nm	Diode 810 nm	Er,Cr:YSGG 2780 nm	CO_2 9300 nm
	Argon Blu 470-488 nm Green 514 nm	Diode 940 nm		CO_2 9600 nm
				CO_2 10,600 nm
	Green KTP 532 nm	Diode 970 nm		
	Red diode 635–675 nm	Diode 1064 nm Nd:YAG 1064 nm	Er:YAG 2940 nm	
		Nd:YAP 1340 nm		

Table 4.2 Classification of dental lasers according to clinical applications

Soft tissue lasers	Hard and soft tissue lasers	LLLT	Diagnosis
Diodes 445 > 1064 nm	Er,Cr:YSGG Er:YAG	Diodes 445 > 1064 nm	405 nm 655 nm
Nd:YAG, Nd:YAP	CO_2 9300 nm		
CO_2 10,600 nm			

4.4 Properties of Laser Light [3]

Light is an electromagnetic radiation which, besides its wave characteristic, has a photonic corpuscular characteristic that transports a defined amount of energy (quantum). A laser device is able to deliver (aim) an elevated quantity of energy in a limited space in the form of light radiation, visible or invisible, generating the laser light.

Laser light is different from ordinary light due to a number of characteristics:

- It is collimated, that is to say, it has a "one way" direction, thanks to the spatial coherence of emitted photons.

Table 4.3 Reports the active medium of lasers most used in dentistry

Laser	Abbreviation	Active medium	Hosting medium	Doping atom	Wavelength (nm)
Argon	Ar	Gas	–	–	488 and 514
Carbon dioxide	CO_2	Gas	–	–	9300; 9600 and 10,600
Diode	–	Semiconductor	–	–	445, 635–810 940–980–1064
Potassium titanyl phosphate	KTP	Solid	YAG crystal	Neodymium frequency doubled	532
Neodymium-doped yttrium aluminum garnet	Nd:YAG	Solid	YAG crystal	Neodymium	1064
Neodymium-doped yttrium aluminum perovskite	Nd:YAP	Solid	YAP crystal	Neodymium	1340
Erbium-doped yttrium scandium gallium garnet	Er,Cr:YSGG	Solid	YSGG crystal	Erbium and chromium	2780
Erbium-doped yttrium aluminum garnet	Er:YAG	Solid	YAG crystal	Erbium	2940

- It is coherent, that is to say, every photon has the photon phase which determines the emission kept in time and space.
- It is monochromatic, that is to say, there is just one visible color and just one wavelength.

4.5 Basic Components of Lasers [3]

A laser is composed of several basic elements for the generation and emission of the laser beam. The principal elements of a laser are:

- Optical resonator (or optical cavity)
- Active medium
- Source of energy (or pumping source)
- Controller (or microprocessor)
- Cooling system
- Delivery system
- Handpiece and tips

4.5.1 Optical Cavity

It is a cavity which contains the active medium and two mirrors located at its extremities, one completely reflective and the other partially reflective and permeable. Photons, emitted by the excitement of the active medium (stimulation), are reflected inside the optical cavity and pass through the active medium many times, amplifying their energy via a waterfall phenomenon (amplification), before exiting (coming out from) the partially permeable mirror.

4.5.2 Active Medium

It is the heart of a laser. The active medium can be solid, liquid, gas, or a semiconductor (diode) and determines the specific wavelength of different lasers; its name identifies different lasers. The atomic population of the active medium, excited by an external source of energy, supplies the electrons for energetic transition from one orbit to another, which produces the emission of laser photons (Table 4.3).

4.5.3 Energy Source (or Pumping Source)

The pumping source excites the atoms of the active medium, producing the inversion of the population of electrons. This source of energy is usually represented by an electric coil or a diode laser or a flash lamp. The characteristics of the energy source are important for the generation of the laser pulse, especially for short-duration pulses (high peak power).

4.5.4 Controller Subsystem and Cooler

The controller is a microprocessor that verifies the characteristics of the production of laser energy, the laser emission mode (continuous wave, mechanically interrupted or pulsed), the pulse frequency of repetition (pulses per second or pulse repetition rate, also improperly called Hz), and the length of the emission of the single pulse. The cooling system is necessary to dissipate the heat produced for the pumping process.

4.5.5 Delivery System

Once generated, laser light must be conducted to the point of use. There are various systems of delivery, depending on the difference of the wavelength carried: optic fiber, hollow fiber, and the articulated arm (Figs. 4.3, 4.4, 4.5, 4.6, 4.7, and 4.8).

4.5.6 Handpieces and Tips

All the delivery systems use angular or straight-ended handpieces. The ideal handpiece should be small, lightweight, and handy. Some handpiece does not have any terminal tip, but a reflecting mirror which works at a distance from the tissue (tipless or noncontact or far-contact handpiece). Some other has a terminal tip which works almost in contact with the tissue and/or within a root canal (close-contact handpiece) (Figs. 4.9 and 4.10). Others are hollow handpieces which permit the passage of the fiber up to the extremity (typically for the near-infrared laser) (Fig. 4.11).

Fig. 4.3 Erbium, chromium:YSGG laser equipped with flexible optic fiber

Fig. 4.4 Erbium:YAG laser equipped with flexible optic fiber

Fig. 4.5 Erbium:YAG laser equipped with articulated arm

4.6 Laser Parameters [3]

The laser energy is emitted with different modality and parameters, depending on the peculiarity of construction of different laser devices. Laser emission and parameters strongly influence (condition) the final effects of the procedure.

4.6.1 Laser Energy

The amount of energy emitted is calculated in Joule (J); normally each pulse energy ranges from few mJ (minimum 5 mJ) up to hundred mJ (maximum 1000 mJ or 1 J).

When considering the energy emitted, it is important to know the irradiated surface area and

Fig. 4.6 Erbium:YAG laser equipped with articulated arm

$$\text{Density of energy}\left(\text{fluence} = \text{J}/\text{cm}^2\right)$$

Fig. 4.7 Multi-wavelength diode laser with optic fiber and terminal handpiece with disposable tip

Fig. 4.8 940 nm diode laser with optic fiber and terminal handpiece with disposable tip

the diameter of the delivering laser fiber/tip that conditions the density of energy applied to the target tissue.

This is fundamental in endodontics, considering how the diameter of the canal and the irradiated surface vary from the apical one-third to the cervical one-third.

The minimum quantity of energy necessary to generate a clinical effect of ablation or vaporization is called "threshold of ablation." For every (each) target chromophore exists a threshold of ablation/vaporization under which no effect is produced. For example, if we consider the erbium laser and its target chromophore, the water contained in the enamel and dentin or in the irrigating solution, the threshold of ablation is about 12–20 J/cm^2 for the enamel and 8–14 J/cm^2 for the dentin, respectively, for erbium:YAG and erbium,chromium:YSGG lasers [4] and less for water. Apel et al. (2002) calculated enamel threshold values slightly inferior to previous ones [5, 6]. Lin et al. (2010) calculated a similar

Fig. 4.9 Noncontact tipless handpiece for erbium:YAG laser; the focus is at distance from the target

Fig. 4.10 Close-contact handpiece with tip for erbium:YAG laser, the focus is 1–1.5 mm close to the target. In this case the PIPS tip works directly onto the irrigant in liquid solution-filled canal

Fig. 4.11 Hallow handpiece for thin optic fibers (200–300 μm) that permits the passage of the fiber up to the extremity (typically for the near-infrared laser)

threshold of ablation: 2.97–3.56 J/cm^2 for Er:YAG and 2.69–3.66 J/cm^2 for Er,Cr:YSGG lasers [7]. Therefore, when using an erbium laser in endodontics, energy higher than 20 mJ with a 200 μm fiber produces ablation on the dentin surface; the ablation is much more with higher energy and less or none using lower energy and larger-diameter fiber/tip. Table 4.4 reports the parameters of laser emission.

Table 4.4 Parameters of laser light emission

Average power (P): expressed in Watt = E (J) × F (Hz or pps)
Energy (E): expressed in J
Frequency of pulsation (F): expressed in Hz or pps
Power density (Pd): expressed in W/cm^2
Fluence (Fl): expressed in J/cm^2
Peak power (PP): $W = E$ (J) ÷ duration of the single impulse (s)

4.6.2 Laser Emission Mode

The modality of emission of the energy (continuous or pulsed), the frequency of pulses in the time unit, and duration of each single pulse are important and condition the average power and the peak power of laser emission.

4.6.2.1 Continuous Wave and Gated Mode

A laser can emit energy in a continuous mode (cw), without interruption. A continuous emission of energy is not always advisable because of the excessive thermal effect released.

Alternatively, the emission can be mechanically interrupted (also called "chopped" or "gated" mode) in order to have a better control of the thermal emission. Short time of emission (t^{on}), of about 10–20 milliseconds (ms), is more correctly and effectively used in endodontics with KTP and diode lasers than continuous wave emission; shorter time, in the unit of microseconds, permits the use of higher power. Newest cutting-edge diode laser technology has frequency of emission of thousand hertz (10,000–20,000 Hz). Diode lasers typically emit laser energy in such a mode.

4.6.2.2 Free-Running Pulsed Mode

Nd:YAG lasers and erbium family lasers emit laser energy in "free-running pulsed mode" (defined also a pulsed mode); each pulse has a beginning, a peak, and an end, with a progressive increment and end in the unity of time. Between one impulse and the other, the tissue has the time to cool down, allowing a better control of the

thermal effect. This emission mode is much more efficient than the continuous wave or gated mode.

4.6.3 Pulse Duration and Pulse Repetition Rate

In pulsed laser, the duration of the single impulse influences the pick power (PP) of the laser emission (W = energy ÷ duration of the single impulse). The concentration of energy in a short time (high peak power) permits a better ablation, reducing the dispersion of thermal energy. In endodontics an elevated peak power allows an efficient activation effect on the irrigants, improving the effectiveness of cleaning and decontamination.

The number of pulses emitted in the unit of time (1 s) is defined as pulse repetition rate or pulse per second or pulse frequency (pps or Hz); the range varies from few pulses (2–3 Hz) up to many (100 Hz) in the free-running pulsed lasers.

In endodontics a pulse repetition of 10–20 pulses per second (Hz or pps) is currently used.

4.6.4 Laser Power

The power emitted by a laser is determined by the energy of each single pulse (expressed in J) multiplied by the number of pulse repetition in the time unit (pps or Hz). As previously reported for the energy, the power density is determined by power used per unit of surface of the irradiated area (expressed in W/cm^2).

Power (W) = Energy (J) × Frequency of repetition (pps or Hz).
Power density (W/cm^2).
Peak power (PP) = $W = E$ (J) ÷ duration of the single impulse (s).

The more power is applied, the faster the speed of the effect on the tissue.

The more energy is applied, the greater the effect on the tissue.

4.6.5 Operator Modality

Moreover, many other parameters, related to the operator, influence the result of irradiation. Operator modality of the clinician includes distance from the target, angulation of the irradiation, speed of the movement, and time of irradiation. The distance from the target influences energy density and power: when the distance between fiber and tip of the laser increases, the density of emitted energy decreases, enlarging the size of the spot due to the effect of a certain grade of emission divergence and increasing the necessary amount of energy for the interaction.

Conclusion

The knowledge of what has been addressed in this chapter and will be analyzed in successive chapters represents an essential basic theory for optimizing clinical results. Learning the variations of the parameters and operative modalities, it is possible to control and condition the quantity and quality of irradiation on the tissue, foreseeing the biological effects and reducing the collateral risks in the use of laser technology.

Bibliography

1. Maiman TH. Stimulated optical radiation in ruby masers. Nature. 1960;187:493.
2. Goldman L, Gray JA, Goldman J, Goldman B, Meyer R. Effects of laser beam impact on teeth. J Am Dent Assoc. 1965;70:601–6.
3. Olivi G, Margolis FS, Genovese MD. Pediatric laser dentistry: a user's guide. Chicago: Quintessence Publishing Co. Inc.; 2011.
4. Harris DM, White JM, Goodis H, et al. Selective ablation of surface enamel caries with a pulsed Nd:YAG dental laser. Lasers Surg Med. 2002;30:342–50.
5. Apel C, Meister J, Ioana RS, Franzen R, Hering P, Gutknecht N. The ablation threshold of Er:YAG and Er:YSGG laser radiation in dental enamel. Lasers Med Sci. 2002;17:246–52.
6. Apel C, Franzen R, Meister J, Sarrafzadegan H, Thelen S, Gutknecht N. Influence of the pulse duration of an Er:YAG laser system on the ablation threshold of dental enamel. Lasers Med Sci. 2002;17:253–7.
7. Lin S, Liu Q, Peng Q, Lin M, Zhan Z, Zhang X. The ablation threshold of Er:YAG laser and Er, Cr:YSGG laser in dental dentin. Sci Res Essays. 2010;5(16):2128–35.

Suggested Texts

Coluzzi DJ, Convissar RA. Atlas of laser applications in dentistry. Chicago: Quintessence Publishing Co. Inc.; 2007.

Miserendino LJ, Pick RM. Lasers in dentistry. Chicago: Quintessence Publishing Co. Inc.; 1995.

Moritz A. Oral laser application. Berlin: Quintessence Verlags-GmbH; 2006.

Olivi G, Margolis FS, Genovese MD. Chicago: Quintessence Publishing Co. Inc.; 2011.

5 Different Lasers Used in Endodontics

Giovanni Olivi and Matteo Olivi

Abstract

Lasers have been used in endodontics with different techniques to improve the percentage of success of pulp capping or apical surgery procedures in permanent teeth and of pulpotomy and/or pulpectomy in primary teeth. However, the main objective of laser in endodontics is to improve the decontamination and cleaning of the root canal system in permanent teeth. Accordingly, the lasers can be used to directly irradiate the dentin walls (conventional laser endodontics, CLE) or to irradiate/activate photoactive substances (photoactivated disinfection, PAD) or irrigants (laser-activated irrigation, LAI and PIPS), so performing the clinical action on the endodontic system, indirectly. The use of different wavelengths with different techniques is presented, exploring the effects of different techniques on dentin walls and discussing the several advantages and disadvantages related to the use of a fiber inserted into the canal or a tip positioned in the pulp chamber only.

5.1 History of Laser in Endodontics

Studies of the use of laser in endodontics began in the early seventies with Weichman and Johnson and Lenz (1971, 1972, 1974) [1–3] but were mainly developed from the early 1990s (nineties) onward.

G. Olivi, MD, DDS (✉) • M. Olivi
InLaser Rome - Advanced Center for Esthetic and Laser Dentistry, Rome, Italy
e-mail: olivilaser@gmail.com; olivimatt@gmail.com

The aim was to improve the results obtained with traditional procedures using laser light to:

- Increase the percentage of success in the procedures of pulp capping in permanent teeth and of pulpotomy and/or pulpectomy in primary teeth
- Improve decontamination of the endodontic system in permanent teeth
- Improve the capacity for cleaning and removal of pulp remnants and smear layer from the root canals
- Improve cutting procedures, decontamination, and sealing of the apex in endodontic surgery

G. Olivi et al. (eds.), *Lasers in Endodontics: Scientific Background and Clinical Applications*,
DOI 10.1007/978-3-319-19327-4_5

The first researches investigated the wavelengths available in those days in dentistry: the CO_2 laser (10,600 nm) first and excimer XeCl laser (308 nm) later, for periapical surgery and for vital and not vital pulp therapy.

Hooks et al. (1980) initiated investigations on CO_2 lasers as a new method for the sterilization of dental instruments [4]. Shoji et al. (1985) studied the histopathological changes induced on dental pulp after a CO_2 laser pulpotomy procedure [5]. Paschoud and Holz (1988) investigated the effects of low-energy therapy (LLLT) on the formation of the dentin bridge after direct pulp capping with calcium hydroxide [6]. Miserendino (1988) published the results of his studies on the use of CO_2 in periapical surgery [7], as also did Neiburger (1989 and 1992) who used the CO_2 laser to seal the not obturated, instrumented teeth using a procedure of dentin fusion (welting) [8, 9].

At the end of the 1980s (eighties), with the introduction of optical fibers with reduced diameters, studies on root canal application of the excimer laser light (308 nm) began. Pini et al. (1989) and Liesenhoff et al. (1989) investigated, ex vivo and with positive results, the application of excimer laser (308 nm) in endodontics for the removal of debris and organic remnants and for the preparation of the root canals [10, 11]. Studies of Frentzen et al. (1991) instead showed opposite results [12].

At the beginning of the 1990s (nineties), with the introduction of pulsed technology for Nd:YAG lasers with optical fibers [13], the research was aimed to the decontamination and the cleansing of the smear layer and organic remnants of root canals [13–21].

In the later years, all the available wavelengths were studied for different applications in endodontics, and in particular, many studies in vitro and in vivo confirmed the efficacy of different laser wavelengths in reducing the bacteria load of infected canals. This part will be extensively analyzed in Chaps. 6, 7, 10, and 11.

5.2 Laser Wavelengths Used in Endodontics

In the spectrum of electromagnetic radiation, many wavelengths are used in endodontics.

5.2.1 Laser in the Ultraviolet Spectrum of Light: Excimer Laser

In the left side of the visible spectrum in the ultraviolet spectrum of light (between 0.3 and 0.4 μm), there are the excimer lasers. The excimer lasers use a gas as active medium. In endodontics, the XeCl at 308 nm was among the first lasers to be experimented [10] and is mentioned here simply for historical reasons, since it is no longer used in endodontics, because of its large and bulky size, the cost, and the controversial results of the investigations [10–12, 22, 23].

5.2.2 Lasers in the Visible Spectrum of the Light

In the visible spectrum of light, there are many wavelengths that can be used in dentistry. Some of them are still in use nowadays for endodontic applications, such us the KTP laser (532 nm) and some diode laser (from 635 to 675 nm) for antibacterial photodynamic therapy (aPDT or PAD), while the argon lasers are partially abandoned and not in use anymore in dentistry Fig. 5.1.

5.2.2.1 Argon Laser

Argon is a noble and inert gas and extremely stable chemical element. Argon gas is used as active medium inside the optical cavity; when it is bombed by the pumping system, its ionized molecules produce different kinds of wavelengths, among them two in the blue spectrum (470–488 nm) and one in the green spectrum (514 nm).

The possibility of using the blue argon laser (470 nm) in dentistry has been extensively studied by a Japanese group at Showa University School of Dentistry, Tokyo, Department of Endodontics, in 1998 and 1999 [24–26]. The investigations verified the ability of argon laser for smear layer and debris removal from the root canals, prepared in a conventional way and irradiated at 1 W, with 0.05 s pulse duration and 5 Hz pulse frequency [24, 25] and at 0.3 W in continuous wave [26]. However, as of today, the use of the argon lasers remains limited only to ophthalmology in retinal pathology for superficial photocoagulation (see Fig. 5.1).

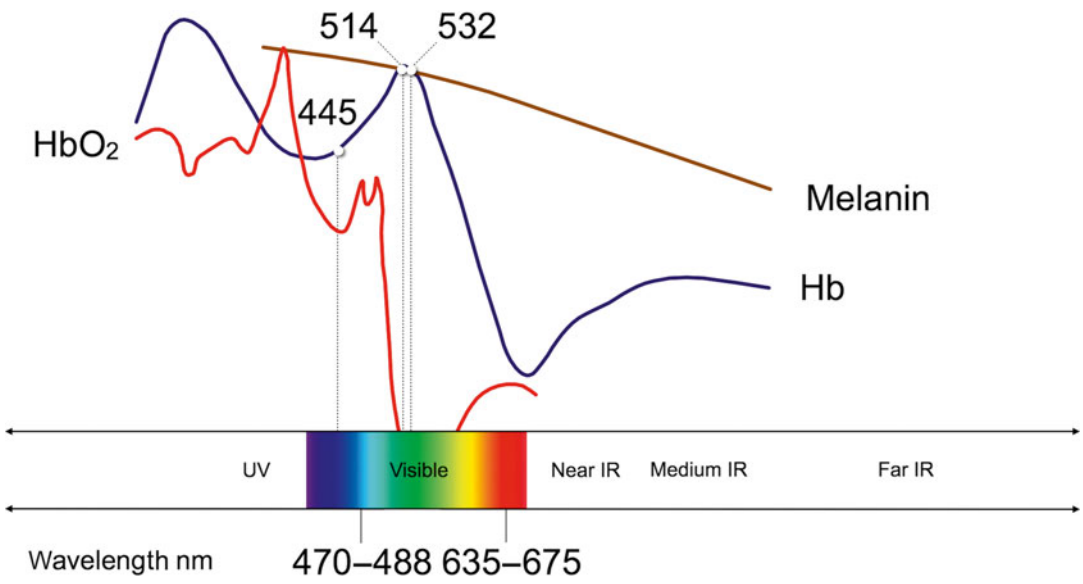

Fig. 5.1 Relative absorption in the visible electromagnetic spectrum of hemoglobin (Hb), oxyhemoglobin (HbO_2), and melanin (Image courtesy of Giovanni Olivi, Rome, Italy)

5.2.2.2 KTP Laser

In the spectrum of visible light, in the green band, the wavelength 532 nm was chosen for the construction of the KTP laser (a duplicate neodymium of 532 nm), with high affinity with hemoglobin (see Fig. 5.1). This laser in fact was introduced to dentistry in the 1990s (nineties), due to its elevated capacity for soft tissue cutting and coagulation [27, 28], and it is used mainly in oral surgery and periodontics. Nowadays however, its diffusion remains limited because of its cost.

Effectively its system of construction is complex. The active medium is a solid: a crystal of Nd:YAG is excited by a diode laser pumping system; a crystal of $KTiOPO_4$ is located between the active medium and the semi-reflecting mirror and duplicates the vibration frequency of photons, splitting the wavelength of the Nd:YAG (1,064 nm) and emitting a radiation of 532 nm in the green visible spectrum.

KTP laser emits energy continuously. Alternatively, a mechanically interrupted mode (chopped or gated) can be used to control the thermal rise in tissue during the irradiation. The delivery system is a flexible optic fiber that exits through a terminal handpiece. Fibers of different diameters (200, 300, and 600 μm) permit different uses in dentistry including endodontics.

The effective use in endodontics was reported by several studies [28–33], at power ranging from 2.25 to 3 W, at 5 Hz, per 2–5 s, and repeated for 4–5 cycles, depending on the study; no damaging thermal rise for the periodontal tissue was observed at these parameters [28, 29]. Also the root canal decontamination ability after conventional endodontic instrumentation was studied, at different power output (at 1 and 1.5 W), in dry mode or wet model [30–34].

5.2.2.3 Semiconductor Laser: Diode Lasers

Some diode lasers are built with wavelengths in the range of visible light. Lasers at 635–675 nm are used for antibacterial photodynamic therapy (aPDT or photoactivated disinfection, PAD) [35–40] because the light of these lasers, emitted in the red spectrum of light, is absorbed by particular photoactive colored substances, which when activated release singlet oxygen with elevated lytic capacity on many species of bacteria. For this reason, LED lights or diode lasers in this spectrum of light have been used in recent years with success in root canal, periodontal, and implant decontamination. This laser application in endodontics will be analyzed in Chap. 7. Recently, a new diode emitting laser radiations in both visible and

near-infrared spectrum of light is promisingly introduced at 445, 660, and 970 nm for several application in dentistry, including endodontics; the optical characteristics of the blue wavelength are similar to those of blue argon laser (see Fig. 5.1).

5.2.3 Near-Infrared Lasers

Following the first studies with excimer lasers, near-infrared lasers were the first to be studied and then largely used for root canal decontamination, in particular the Nd:YAG (1,064 nm) and then diode lasers (from 810 to 1,064 nm), thanks to the optic fiber technology, introduced at the end of the 1980s (eighties) [13] that allow the introduction of the laser light deeply in the root canal.

Target chromophores of near-infrared lasers are the hemoglobin, the melanin, and the pigment of some type of bacteria (Fig. 5.2). Near-infrared lasers are mainly scattered in the target tissues; the absorption is negligible and reflection minimal. Shorter wavelengths have less deep diffusion than the longer Nd:YAG laser (1,064 nm), both in soft tissues and in radicular dentin. Near-infrared lasers of different wavelengths have slight different optical behavior, depending on the affinity of the specific wavelength with the target chromophore (see the absorption curve). Different affinities with the target correspond to different energies necessary for the clinical use.

This paragraph analyzes only the constructive characteristics and the interaction with tissues typical of these lasers. Chapter 6 will analyze diffusely the effects of these lasers in endodontics.

5.2.3.1 Semiconductor Laser: Diode Laser

The diode laser was introduced in endodontics at the end of the 1980s, initially for treatment of dentin hypersensitivity [41, 42] and to bio-modulate the inflammatory response during vital pulp therapy (pulp capping or pulpectomy) and other inflammatory pathologies of the maxillary bone [43, 44].

Today, diode lasers represent a valid alternative to Nd:YAG lasers for incision, vaporization, and coagulation of soft tissues (gingiva, mucosa, and pulp), for treatment of periodontal pockets (curettage, decontamination) and root canal decontamination.

The constructive simplicity and the contained dimensions justify the contained cost, which facilitates its diffusion.

The active medium is a semiconductor, which is, nowadays, miniaturized, made up of various

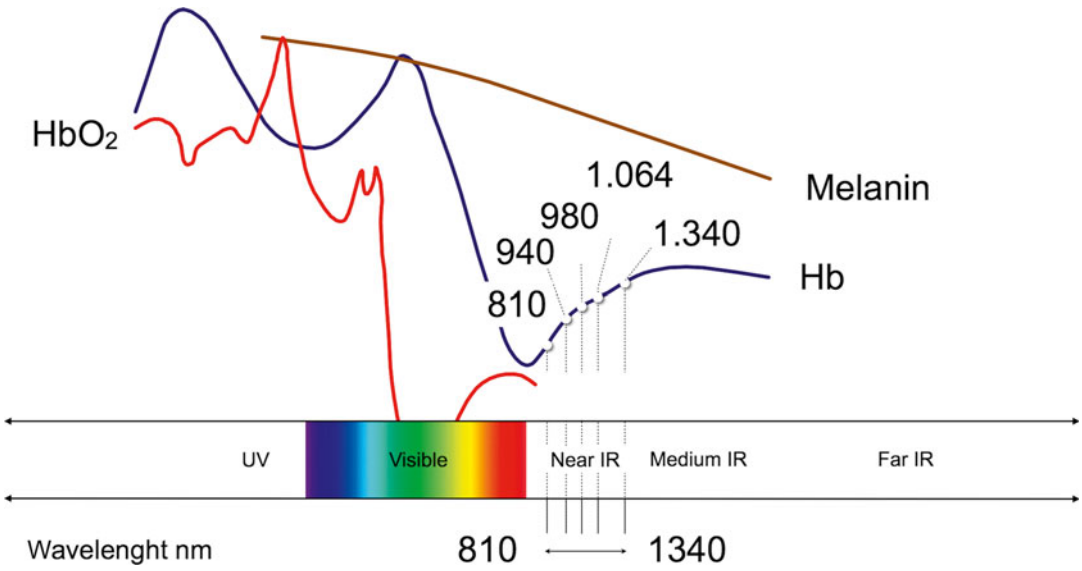

Fig. 5.2 Relative absorption in the near-infrared electromagnetic spectrum of hemoglobin (Hb), oxyhemoglobin (HbO_2), and melanin (Image courtesy of Giovanni Olivi, Rome, Italy)

layers (wafer-like construction). The gallium arsenide (GaA1As), doped with aluminum atoms, is widely used. Some lasers use the indium as doping atom (IGaAsP).

The activation of the semiconductor produces the emission of laser light in the invisible spectrum of the near infrared in different wavelengths (from 810 to 1,064 nm), depending on the type of semiconductor. In order to see and control the interaction of laser light with tissue, there is a visible aiming beam with low mW of power (1 mW), generally red at 650 nm or green at 530 nm.

Diode laser energy is emitted in continuous wave mode, and a mechanical system can interrupt the impulses (chopped or gated), dividing their exit in variable intervals (t^{on}/t^{off}). The single impulse (t^{on}) has a linear evolution without variations from the beginning to the end of the emission, and its duration is variable, from a few microseconds to many milliseconds, with variable frequency up to 20,000 Hz. The mechanical interruption of the emission (chopped or gated mode) makes it possible to choose the time interval between one pulse and another (t^{on}-t^{off}), which is important for clinical purposes because it allows cooling of the irradiated tissue. By modulating the quota of thermal energy released and its effects, it is also possible to control the patient's pain sensitivity.

The diode laser delivery system is similar to that of Nd:YAG laser and uses an optic fiber (diameter 200–300–400 μm) which ends in a terminal handpiece, going through it and coming out in a terminal curve tip. The fibers are sterilizable after cleaning and cutting of a pair of millimeters after use. Diode lasers of more recent design have fiber which ends in a handpiece where disposable tips of different diameter, angle, and length are inserted (Figs. 5.3 and 5.4). The fiber/tip must be activated before the surgical procedures. It has to be kept constantly clean using sterile dressings soaked with nonflammable disinfectant or cotton rolls. For decontamination of periodontal pockets or root canals, the activation of the tip is still a topic of debate (Fig. 5.5). It should be remembered that:

Fig. 5.3 Long and 200 μm thin disposable tip for endodontics, available for diode laser (Picasso, AMD; USA)

Fig. 5.4 Long and 200 μm thin disposable tip for endodontics, available for diode laser (BluLaser, Sirona: Germany)

Fig. 5.5 The fiber/tip activation is performed at 1 W on dark-blue articulating paper, repeating the procedure 4–5 times up to seeing the tip becomes darker

Fig. 5.6 Small hollow handpiece for Nd:YAG laser allows the passage of the fiber up to the terminal tip

The use of thin fiber (200 μm) inside a root canal permits decontamination in the endodontic system at up to 500–750 μm of distance from the main canal [45].

It should be remembered that diode lasers are also used for LLLT: the diode laser emitted at low energy and for a long time is converted into photochemical energy that bio-modulates many cellular functions. Photochemical energy is also used for the activation of (whitening) bleaching systems.

5.2.3.2 Neodymium:YAG Laser

It is one of the first lasers to be experimented with in dentistry [13, 14]. Still today it is a valid laser system for incision, vaporization, and coagulation of soft tissues (gingiva, mucosa, and pulp) and for the treatment of periodontal pockets (curettage, decontamination) and is the best system for thermal decontamination of the root canals.

Its active medium is a solid crystal of yttrium, aluminum, and garnet (YAG), doped with neodymium. Neodymium (Nd, atomic number of 60) is a metal of the group of rare heart elements. The energy of neodymium YAG laser is produced through stimulation of the active medium using a powerful flash lamp (free-running pulse mode). Each pulse has a Gaussian development, with a quick start, a peak, and an end; between one pulse and another, there is a time of latency.

The stimulated neodymium YAG emits invisible photonics radiation at 1,064 nm, and it is equipped with a coaxial aiming beam, with low power (1 mW), generally red at 650 nm or green at 530 nm.

Activation of the fiber/tip concentrates the emitted energy near the tip itself; without activation of the tip a major quota of energy can be diffused at distance.

The emitted energy is delivered through an optic fiber (diameter 200–300–400 μm) that enters in a hollow handpiece and ends in a terminal curved tip (Fig. 5.6).

The energy emitted by the laser radiation is mainly scattered in the target tissues under the form of thermal energy, while a certain quota of retrograde diffusion of energy can overlap the incident radiation, with the risk of the phenomenon of summary accumulation of thermal energy and tissue damage. For this reason, the Nd:YAG laser is only used in dentistry, in free-running pulse mode with variable frequency from 10 to 200 Hz and with a pulse duration from microseconds to milliseconds. This greatly limits the possibility of heat accumulation in irradiated tissue. The emission of short duration pulses produces elevated peak power, so to justify the elevated efficiency of Nd:YAG lasers compared to diode lasers. Only a small quota of energy is diffused for reflection.

The use of thin and flexible fibers (200 μm microns) facilitates access to the radicular canals, where the scattering and penetration in depth of this wavelength allow decontamination of the endodontic system up to a distance of 1 mm from the main canal [45–48]. The power and energy used for clinical applications produce high photothermal effect and never ablative effect on the

dentin. For this reason, the near-infrared lasers are used in endodontics only for decontamination.

5.2.3.3 Neodymium:YAP Laser

The Nd:YAP laser has been constructed with a wavelength of 1,340 nm. The active medium is solid, a crystal of yttrium, aluminum, and perovskite (YAP), doped with neodymium. The optic fiber of a reduced diameter (200 μm) permits endodontic application. The constructive characteristics of this laser are very similar to those of the Nd:YAG, with a slightly different affinity with hemoglobin, melanin, and water. It is not very diffused and the clinical indications are comparable to those of other near-infrared lasers.

5.2.4 Medium-Infrared Lasers: Erbium YAG and Erbium, Chromium YSGG Laser

At the end of the 1980s (eighties) to the beginning of the 1990s (nineties), the erbium YAG laser (2,940 nm) [49–52] first and then the erbium, chromium YSGG laser (2,780 nm) [53, 54] were introduced in dentistry with the idea of substituting the drill for caries removal.

Studies in endodontics started in 1998 for the erbium YAG laser and in 2001 for the erbium chromium YSGG laser [55, 56] for the availability of specific thin tips to access to the root canals (Fig. 5.7).

Fig. 5.7 Long and 200–300 μm thin tip and handpiece for Er,Cr:YSGG laser

The Er:YAG laser has a solid active medium, a crystal of yttrium, aluminum, or garnet, doped with erbium atoms. Erbium is a silver metal of the group of rare heart elements (Er, atomic number of 68). When stimulated, the YAG crystal emits photons of a wavelength of 2,940 nm. The laser energy is delivered to a terminal handpiece through different systems, among which the optic fiber and the articulated arm are still in use.

The Er,Cr:YSGG laser also has a solid active medium, a crystal of yttrium, scandium, gallium, and garnet (YSGG), doped with atoms of erbium and chromium. When stimulated, the crystal emits radiations in the medium-infrared spectrum at 2,780 nm. This energy is transferred to a terminal handpiece through an optic fiber.

The term erbium family lasers combines the two wavelengths and is frequently used when referring to both the wavelengths without any specific connection to one another.

Erbium lasers use a visible aiming beam, red or green, to provide good visibility and control of interaction with tissue.

These lasers can develop high power, and for this reason, the energy is emitted in free-running pulsed mode, with pulses of duration and frequency of variable repetition depending on the different equipment used.

The wavelengths of the erbium family fall on the curve of water absorption (principal target chromophore). Absorption in hydroxyapatite is also high, but it has unimportant value for clinical purposes [57–60] (Fig. 5.8).

The high absorption in water explains the effects on dentin, more pronounced in the intertubular zone, that is, more rich in water than in mineral.

The photothermal effect of erbium lasers produces vaporization of the smear layer and a certain grade of ablation and decontaminating effect that are however limited to the dentin canal surface (up to 250–300 μm in depth), where laser energy is mainly absorbed and where it produces a direct photothermal effect.

The dentin ablation happens when the energy used exceeds the threshold of dentin ablation (see Sect. 4.6.1). The ability of medium-infrared lasers to ablate radicular dentin encouraged research in

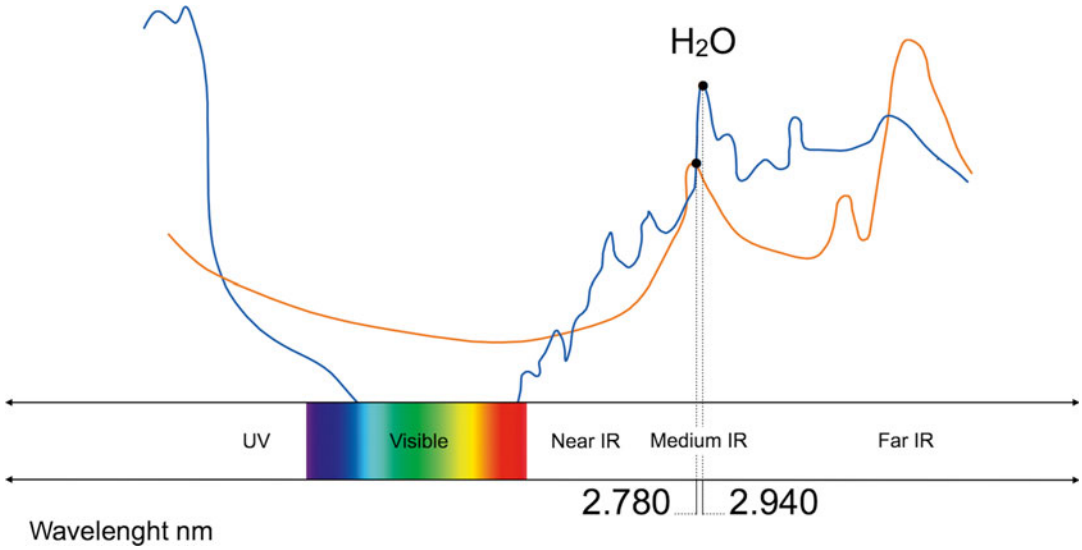

Fig. 5.8 Relative absorption in the medium-infrared electromagnetic spectrum of water (*blue line*) and hydroxyapatite (*orange line*) (Image courtesy of Giovanni Olivi, Rome, Italy)

the past years, to explore the possibility of preparing the canal with lasers, with quite poor results.

The affinity of erbium lasers with water explains the activation and agitation of the irrigant solution (NaOCl ed EDTA), their tridimensional streaming through the endodontic system (LAI and PIPS techniques), and their effect on bacteria decontamination, on debris and smear layer removal, via an indirect laser action.

The great presence of water in the oral soft tissues; in the hard dental tissue, such as the enamel and the dentin; and much more in the carious tissue explains the extensive use of erbium lasers in dentistry. Water is also present in the bone. For this reason, erbium lasers are considered "all tissue" lasers, very versatile for clinical use in dentistry, in periodontics, restorative, endodontics, and bone surgery, and also recommended for soft tissue therapy, especially on tissues with low vascularization and more evident fibrous components (fibroma removal, labial and lingual frenectomy, gingivectomy, gingivoplasty, operculectomy).

Clinically, the two wavelengths work in overlapping mode. However, the higher absorption in water tissues for the Er:YAG laser makes its tissue interaction more superficial when compared to Er,Cr:YSGG laser (Fig. 5.9). Under equal parameter used, also less energy is necessary for the Er:YAG laser, compared to the Er,Cr:YSGG, to ablate hard dental tissues (see ablation threshold, Chaps. 4 and 7) [61, 62]. However, is the different technology of construction and control (analogic or digital) of different laser units that produces variable performances of different lasers.

Different erbium lasers can have differences in terms of delivery system (optical fiber or articulated arm), handpiece (in close contact with the tip or no contact using a mirror), straight or angled, and big or small (see Figs. 4.3, 4.4, 4.5, 4.6, 4.9, and 4.10); also tips are of different shape and size, as well as the efficacy and modulability of the air-water spray. Technological characteristics include the temporal characteristic of the pulse (pulse duration) which varies from 50 to 1000 μs and the spatial characteristics of the pulse (pulse shape). Different laser systems also offer different choice of a variety of pulse frequency from 2 to 100 pps and different power output from 0.1 to 20 W, all characteristics that allow greater possibility of managing the interaction with tissues, with better clinical application and better control of pain stimulation.

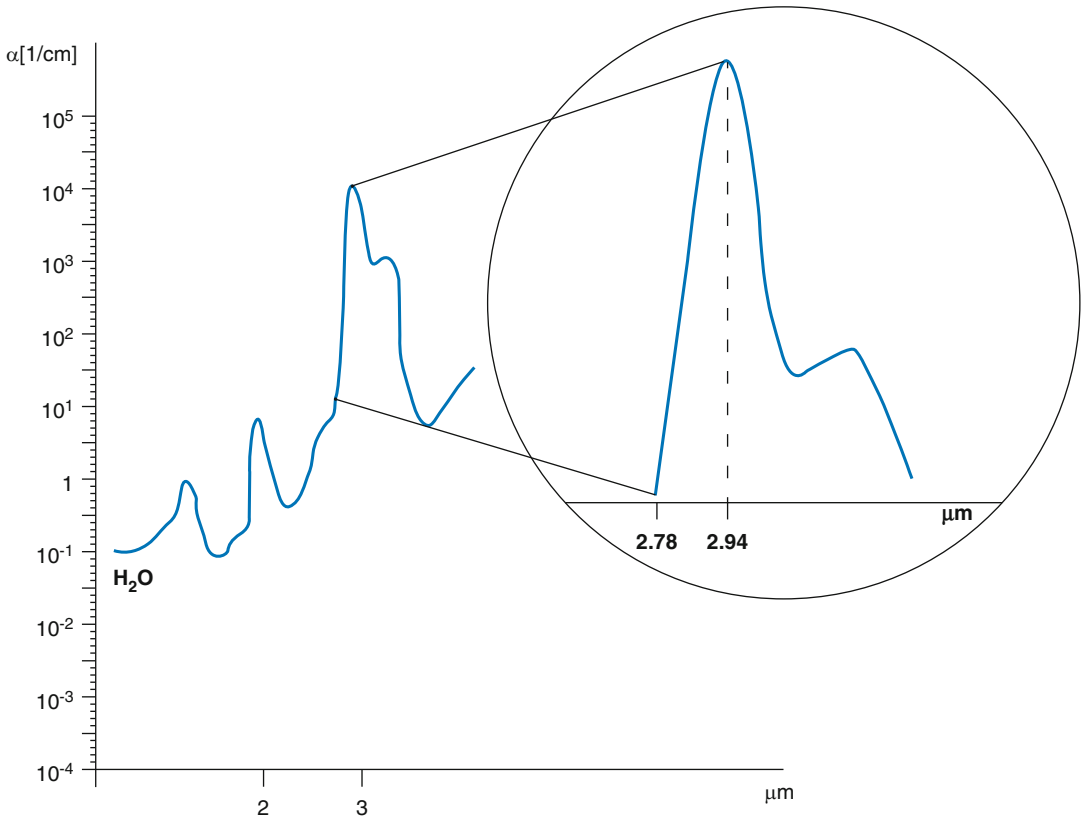

Fig. 5.9 Different water absorption coefficients in the medium electromagnetic spectrum 2780 and 2940 nm. Er:YAG at 2920 nm is three times more absorbed in water than the Er,Cr:YSGG at 2780 nm (Image courtesy of Giovanni Olivi, Rome, Italy)

5.2.5 Far-Infrared Laser: CO_2 Laser

CO_2 far-infrared lasers (9,300–10,600 nm) were the first to be studied and used in endodontics for the decontamination and fusion of the apex in endodontic surgery [7–9]. Nowadays, they are no longer used in endodontics, except for the vital pulp therapy (decontamination, vaporization, and coagulation in pulp capping and pulpotomy).

Together with KTP and near-infrared lasers, the CO_2 laser is still one of the best systems for incision, vaporization, and coagulation of soft tissues (gingiva, mucosa, and pulp) but is not very widely used because of its cost and the range of clinical applications limited to soft tissues.

The main target tissue is water that greatly absorbs the wavelengths.

The active medium is a gas, the carbon dioxide (CO_2), and the emitted laser radiation is delivered through an optic fiber or an articulated arm.

The radiation is emitted, with different wavelengths (9,300 nm, 9,600 nm, or 10,600 nm), in the invisible far-infrared spectrum. Native CO_2 laser at 10,600 nm is only useful on soft tissue. New laser technology introduced some modifications and an oxygen isotope (O_{18}) to emit a radiation at 9,300 nm, matching the peak absorption of hydroxyapatite and making also the interaction with hard tissue applicable.

Being invisible in the far-infrared spectrum, also these wavelengths are supported by a visible coaxial aiming beam (red or green, of a few mW of power).

In the past, the modality of continuous emission (CW) created problems of thermal damage, especially in the hard tissues. Today, pulsed and super-pulsed technology make this laser one of the

best systems for oral surgery, due to its elevated coagulating ability via photothermal effect. The thermal effect of CO_2 lasers is able to seal small (0.3–0.5 mm of diameter) blood or lymphatic vessels, realizing an excellent coagulating effect.

5.3 Classification of Lasers in Endodontics

Lasers are used with different techniques in endodontics (Table 5.1).

They can be used to directly irradiate the dentin walls or to irradiate/activate photoactive substances or irrigants, so performing the clinical action on the endodontic system indirectly (Table 5.1) (Fig. 5.10).

5.3.1 Conventional Laser Endodontics (Direct Laser Irradiation)

The laser technique used since the beginning involves the use of fibers or tips with end emission (end firing) positioned in the canal, conventionally at 1 mm from the apex. The activation of the laser starts during the movement of retraction of the fiber/tip, performing a helical movement, in a determined time. This technique is suitable for most of the wavelengths in the visible (445 and 532 nm), near-infrared (from 810 to 1,340 nm), and medium-infrared (2780 and 2,940 nm) zones of electromagnetic spectrum. The laser energy is delivered through fibers or tips inserted on terminal handpiece; endodontic tips have a specific diameter of 200–300 μm and a length suitable for this application, and also the optic fibers have a small diameter of 200 μm allowing the insertion within the root canal (see Figs. 5.3, 5.4, 5.6, and 5.7).

When in the canal, laser irradiation produces a direct *thermal effect* on dentin walls and bacteria that generates also undesired effects that vary depending on the wavelength used and on its interaction with the dental walls (laser-tissue interaction).

The light of the near-infrared laser (with diffusion prevalent to absorption) scatters in the dentinal tubules until it hits the pigment of the target bacteria cells, producing also thermal effects on the surface of the dentin walls.

The light of the medium infrared is mainly absorbed in the surface by the watery component of the dentin (water is the target chromophore of the erbium laser), with vaporization of the smear layer and of the debris, generating also a certain degree of dental ablation, depending on the energy used.

This technique is named by Olivi [63] "conventional laser endodontics," because it was the first to be used in endodontics and to distinguish it from the more recently introduced. This technique is extensively discussed in Chap. 6.

Table 5.1 Classification of laser techniques used in endodontics (Olivi [63])

Wavelength	Laser technique	Target chromophore	Laser tissue interaction	Laser effects
Visible Near infrared	Conventional Direct irradiation	Bacteria pigment	Diffusion	Photothermal
Medium infrared	Conventional Direct irradiation	Water content of dentin bacteria	Absorption	Photothermal
Visible Near infrared	PAD Indirect irradiation	Photosensitizers	Absorption	Photochemical
Medium infrared	LAI Indirect irradiation	Water content of irrigants	Absorption	Photothermal cavitation
Medium infrared	PIPS Indirect irradiation	Water content of irrigants	Absorption	Photothermal photo-acoustic cavitation

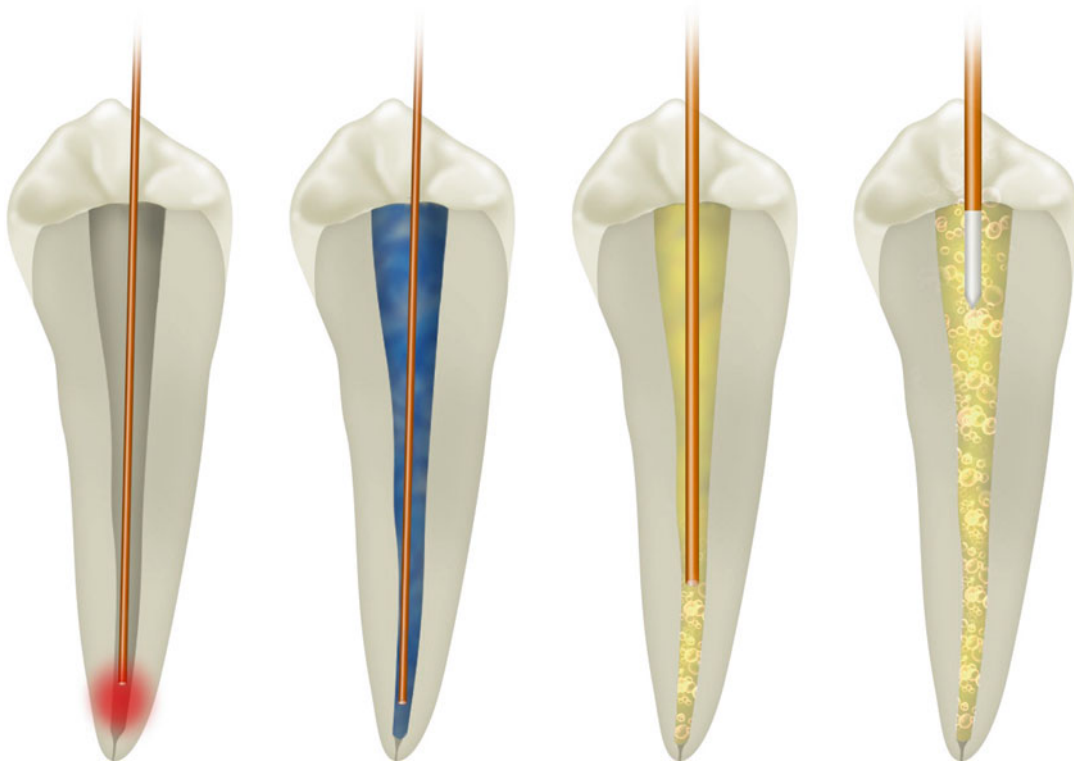

Fig. 5.10 Different laser endodontic techniques consider different positions of the tip and its movement inside the canal, or its position stationary in the chamber; also different techniques propose a dry mode or the use of different dye or irrigant solutions. From left to right: conventional laser endodontics, PAD, LAI, and PIPS (Image courtesy of Giovanni Olivi, Rome, Italy)

5.3.2 Photoactivated Disinfection (PAD)

Photoactivated disinfection (PAD) also called antibacterial photodynamic therapy (aPDT) involves the use of photosensitizers with antimicrobial activity introduced in the root canal and selectively activated by an affine wavelength: these are visible (from 635 to 675 nm) and near-infrared (810 nm) wavelengths. The laser irradiation produces a *photochemical effect* that activates the photoactive colored liquid with the release of active radicals and singlet oxygen that finally generate the bactericidal effect. There is no direct laser interaction with the dentin surface, almost eliminating any undesired collateral effect. This part is discussed in Chap. 7 (see Fig. 5.10).

5.3.3 Laser-Activated Irrigation and PIPS™

The laser-activated irrigation (LAI) involves the activation of the irrigant (watery solutions) with the use of the erbium and erbium chromium laser. The target is water that completely absorbs the radiation. Endodontic tips used are end firing and/or radial firing tips (conical and modified conical tips) (Fig. 5.11), and, in particular, the PIPS™ technique uses a radial and stripped tip (the last 3 mm), in order to increase the lateral emission of laser photons (see Chaps. 10 and 11) (Fig. 5.12). The irrigants, so activated by erbium lasers, become more reactive and can flow three-dimensionally in the canals, improving their antibacterial and cleaning effect. When the liquid is present in the canal, no direct interaction on dentin surface happens.

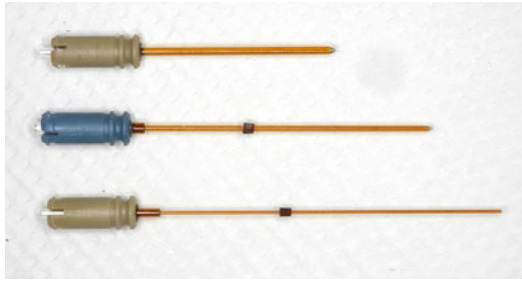

Fig. 5.11 Radial firing tips of different diameters (200–400–500 μm) and lengths for Er,Cr:YSGG laser (Waterlase MD, iPlus; Biolase; USA)

Fig. 5.12 Radial and stripped PIPS tips of 400 and 600 μm diameter, 14 and 9 mm long, respectively, for Er:YAG laser (LigthWalker, Fotona; Slovenia)

5.4 Laser-Tissue Interaction in Endodontics

The interaction between laser light and the target tissue follows the rules of physics. Laser radiation can be:

- Reflected
- Absorbed
- Diffused
- Transmitted

Reflection is an optical phenomenon due to the lack of affinity and absorption of light from the target, which, once hit, rejects the light completely. The quota reflected is about 5 % of the radiation emitted and represents the aspect of laser therapy that involves safety measures (protective glasses specific for each wavelength), because of the potential eye damage of laser radiation.

Absorption on the contrary is the expression of high affinity between light and the target which retains light in the point of irradiation. The portion of laser energy absorbed is responsible for the majority of therapeutic effects, and it is locally converted into *photochemical energy*, *photomechanical energy*, *and photo-acoustic energy* depending on the type of laser used, the modality of emission, and the parameters used.

Diffusion depends on the capacity of the light to spread irregularly deeper into the target. The portion of laser energy which diffuses into the tissues is responsible for the therapeutic effects of some wavelengths (visible red and near infrared), which allows decontamination at a distance from the irradiation point.

Transmission is the passage of light through a body or tissue, in the absence of interaction with it and, in consequence, without producing physical or biological effects.

Besides intrinsic optical properties of different wavelengths, the interaction depends also on the optical characteristics of the target and, in particular, on the absorption coefficient of the specific chromophore of the target tissue for a specific wavelength (optical affinity). Accordingly, different interactions happen with the target tissues: dentin, smear layer, debris, organic remnants, bacteria, and irrigant fluids.

In summary, three groups of laser-tissue interaction can be identified:

- Laser radiation emitted in the visible blue-green spectrum of light, such as KTP laser (or neodymium duplicate at 532 nm) and argon lasers (488–514 nm), that produces effects of *absorption* and *diffusion (scattering)* of overlapping entities, with penetration in tissue at intermediate depth
- Radiation emitted in the visible red spectrum (600–700 nm) and in the near infrared (from

810 to 1,340 nm), which renders *scattering* highly predominant over *absorption*, with deeper penetration in tissues
- Radiation emitted in the medium- or far-infrared spectrum (2,780–2,940–10,600 nm) that mainly produces *absorption* in tissue and in water, superficially with unimportant phenomena of diffusion

When the laser light interacts with the target tissue, for diffusion or absorption, it generates on it the biological effects responsible for the desired therapeutical results and for the unwanted collateral effects.

5.5 Laser Effects in Endodontics

The laser light, absorbed and/or diffused in the target, generates different effects:

(a) A photothermal effect results from the direct laser irradiation on the dentinal walls, when the lasers are used with the conventional technique for the decontamination and removal of the smear layer, positioning the fiber inside the canal; all the wavelengths produce thermal effect.

(b) A photochemical effect produces the activation of photosensitive substances (photosensitizers) inoculated in the canal and responsible for the antibacterial effects of the photoactivated disinfection (PAD), without direct irradiation (and interaction) on the dentin; this effect is characteristic of visible (635–675 nm) and near-infrared (810 nm) lasers.

(c) Photothermal effect primarily and photomechanical-acoustic effect successively activate the commonly used irrigants in endodontics during the laser-activated irrigation and PIPS, without any direct irradiation (and interaction) on the radicular dentin, when the irrigant liquids are present and remain in the canal. These effects are typical and exclusive of medium-infrared lasers.

Depending on the wavelength and on the technique used, the laser interaction will target with different modalities different substances:

- Bacteria (in their different forms of aggregation, planktonic or biofilm)
- Photosensitizer contained in the dye solutions
- Dentin, with the smear layer, debris, and pulp remnants
- Free water (of the irrigant solutions)
- (Figs. 5.13, 5.14, 5.15, and 5.16)

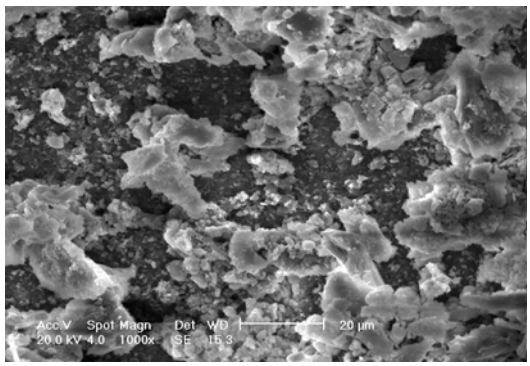

Fig. 5.13 SEM image (1000×) of dentin walls 4 mm shorter of the radicular apex after conventional chemo-mechanical rotary instrumentation (not lased). Note the presence of debris and heavy smear layer that completely occlude the dentin tubules orifices. Chemo-mechanical preparation resulted ineffective to completely shape and clean the root canal

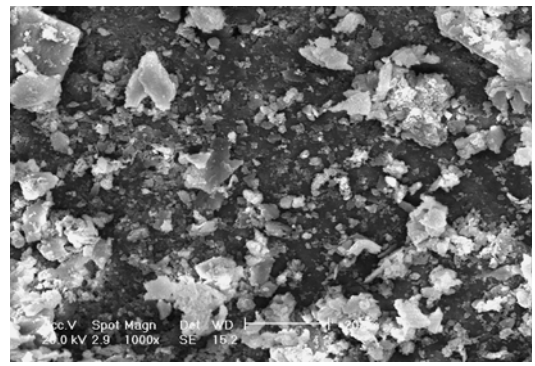

Fig. 5.14 SEM image (1000×) of dentin walls 8 mm shorter of the radicular apex after conventional chemo-mechanical rotary instrumentation (not lased). Note the presence of micro and macro debris (from few microns up to 10 µm) completely covering the dentin surface. Chemo-mechanical preparation resulted ineffective to completely shape and clean the root canal

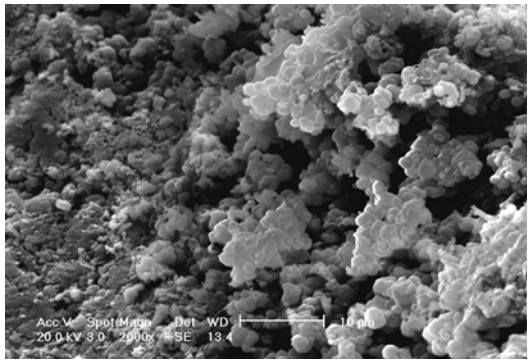

Fig. 5.15 SEM image (2000×) of *E. faecalis*-infected dentin walls 3 mm shorter of the radicular apex after conventional chemo-mechanical rotary instrumentation (not lased). Heavy smear layer and organized biofilm remain on some areas of dentin surface after instrumentation. Chemo-mechanical preparation resulted ineffective to completely shape, clean, and disinfect the root canal

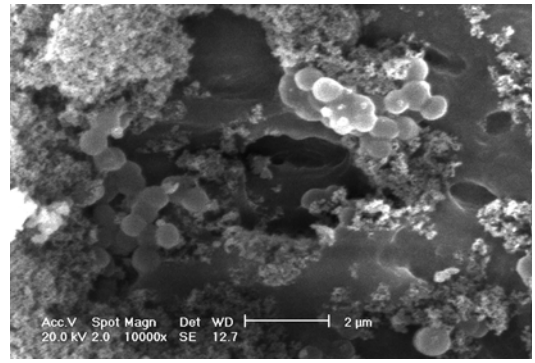

Fig. 5.16 SEM image (10,000×) of *E. faecalis*-infected dentin walls 7 mm shorter of the radicular apex after conventional chemo-mechanical rotary instrumentation (not lased). Dentin mud and planktonic bacteria colonies cover the access to dentin tubules. Chemo-mechanical preparation resulted ineffective to completely shape, clean, and disinfect the root canal

5.5.1 Effect of Laser Light on Bacteria

All of the wavelengths have different direct lytic effects on bacterial cell walls via a photothermal effect. Depending on structural characteristic of cellular wall, the gram$^-$ bacteria are easily destroyed, with less energy and less time compared to gram$^+$ [46] (see Chap. 6).

The effects of PAD and LAI techniques on bacteria are not directly performed by laser light and are discussed in the following paragraphs.

5.5.2 Effects of Laser Light on Photosensitizers

Laser wavelengths in the red and near-infrared (810 nm) window of the spectrum act as photoactivator of a chemical reaction for the specific compound that releases toxic elements to the target.

Photosensitizer substances, such as methylene blue (MB), toluidine blue (TB), tolonium chloride (TC), and green indocyanine (IG), increase the bacteria sensitivity when activated by these diode laser lights, due to the production of singlet oxygen throughout a photochemical reaction [35–40] (see Chap. 7). The reactive oxygen species (ROS), in the presence of oxygen, mediate cellular toxicity to each tissue that has affinity for the photosensitizer.

5.5.3 Effects of Laser Light on Dentinal Walls

The thermal effect of the laser, used for antibacterial effect, must be controlled to avoid damages on the dental walls. All the laser radiations, used in dry canal with the conventional techniques, can produce morphological alterations of the dental surface [64] due to the thermal effect typical for every wavelength. Heating of the substrate contributes to the (indirect) lytic effect on bacterial cells.

5.5.3.1 Near-Infrared Laser

These lasers kill bacteria but do not remove the smear layer. The heat deposited during the diffusion of thermal energy provokes the partial closure of the dental tubules through a process of fusion of the organic and inorganic dental structure (Figs. 5.17, 5.18, 5.19, 5.20, 5.21, and 5.22). Furthermore, when the terminal part of the tip/fiber comes in contact with the dental wall during the laser emission, this can provoke (produce) thermal damages such as hot spots, bubbles, and cracks [65–68] (Fig. 5.23).

When near-infrared laser is used in a wet root canal, filled with water or irrigant solutions, the water-based liquid limits the direct interaction of the laser radiation on the dentin walls, reducing the undesired side effects but also limiting its decontamination effect. The water, in this case, is

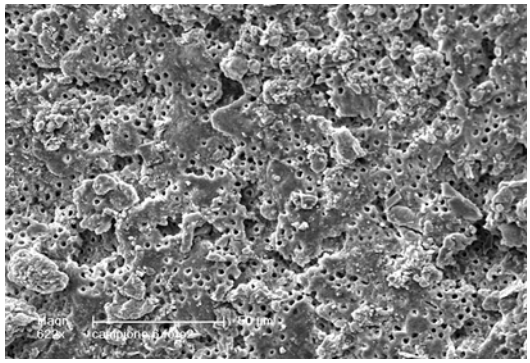

Fig. 5.17 SEM image (622×) 7 mm shorter of the apex after conventional chemo-mechanical rotary instrumentation and irradiation with an 810 nm diode laser in dry mode at 2.5 W, 20 ms ton/20 mstoff, four times ×5 s. The smear layer is partially removed by a process of fusion of the organic and inorganic dental structures; presence of superficial thermal damage with flakes, microcracks, and detached particles including debris and smear layer

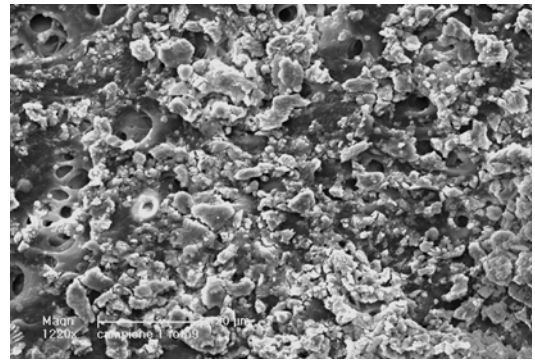

Fig. 5.18 SEM image (1222×) 7 mm shorter of the apex after conventional chemo-mechanical rotary instrumentation and irradiation with an 810 nm diode laser in dry mode at 2.5 W, 20 ms ton/20 mstoff, four times ×5 s. The smear layer is not removed and mainly occludes the dentin surface; presence of superficial thermal damage with flakes and detached particles including debris and smear layer

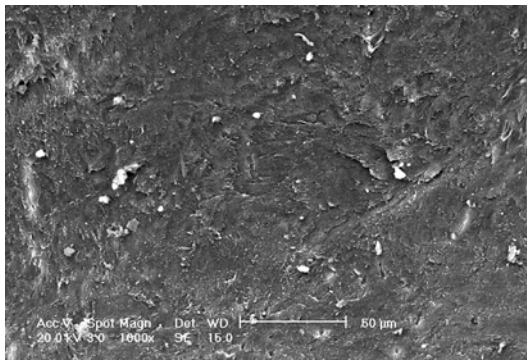

Fig. 5.19 SEM image (1000×) of the root canal surface after conventional chemo-mechanical rotary instrumentation and Nd:YAG laser irradiation in dry mode, 1.5 W, 15 Hz, 100 mJ, four times ×5 s. The canal surface presents some debris and obliterated dentin tubules

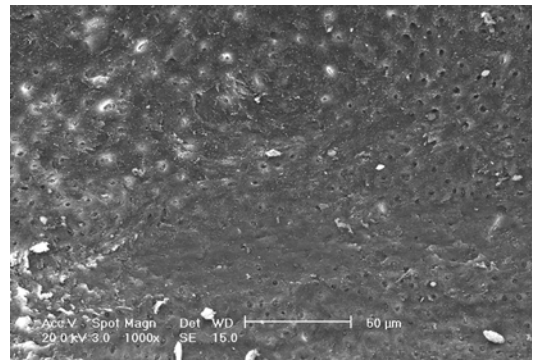

Fig. 5.20 SEM image (1000×) of the root canal surface after conventional chemo-mechanical rotary instrumentation and Nd:YAG laser irradiation in dry mode, 1.5 W, 15 Hz, 100 mJ, four times ×5 s. The canal surface presents some debris and obliterated dentin tubules

not an absorbent chromophore for these wavelengths that can be transmitted through the fluid without giving interaction (just heating it) [32] but only an intermediate medium.

In this case, the near-infrared lasers activate the irrigant solutions via heating (warming), and this procedure increases the efficacy of the irrigation [69]. The irradiation with near-infrared laser, diode laser (2.5 W, gated mode), and Nd:YAG laser (1.5 W, pulsed mode at 15 Hz), performed after irrigation in a fluid filled canal, produces a dentin pattern, more similar to the one obtained with just the irrigation alone than with dry laser irradiation. The canal irradiation associated with sodium hypochlorite irrigant produces a dentin morphology with some remaining smear layer and debris but less areas of fusion and thermal damage compared to the dry irradiation. When the irradiation follows the irrigations with EDTA, it results in cleaner surfaces with less smear layer, open dentinal tubules, and less thermal damages than with dry laser irradiation [70–74] (Figs. 5.24, 5.25, 5.26, 5.27, 5.28, and 5.29).

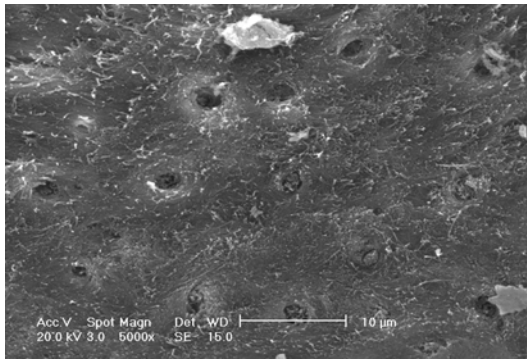

Fig. 5.21 SEM image (5000×) of the root canal surface after conventional chemo-mechanical rotary instrumentation and Nd:YAG laser irradiation in dry mode, 1.5 W, 15 Hz, 100 mJ, four times ×5 s. The canal surface presents some debris and incomplete dentin tubules obliteration

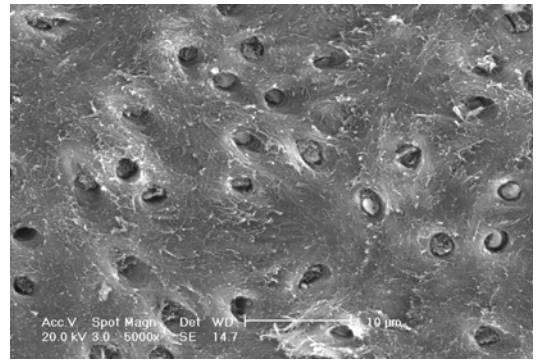

Fig. 5.22 SEM image (5000×) of the root canal surface after conventional chemo-mechanical rotary instrumentation and Nd:YAG laser irradiation in dry mode, 1.5 W, 15 Hz, 100 mJ, four times ×5 s. The canal surface presents some debris and partially obliterated dentin tubules

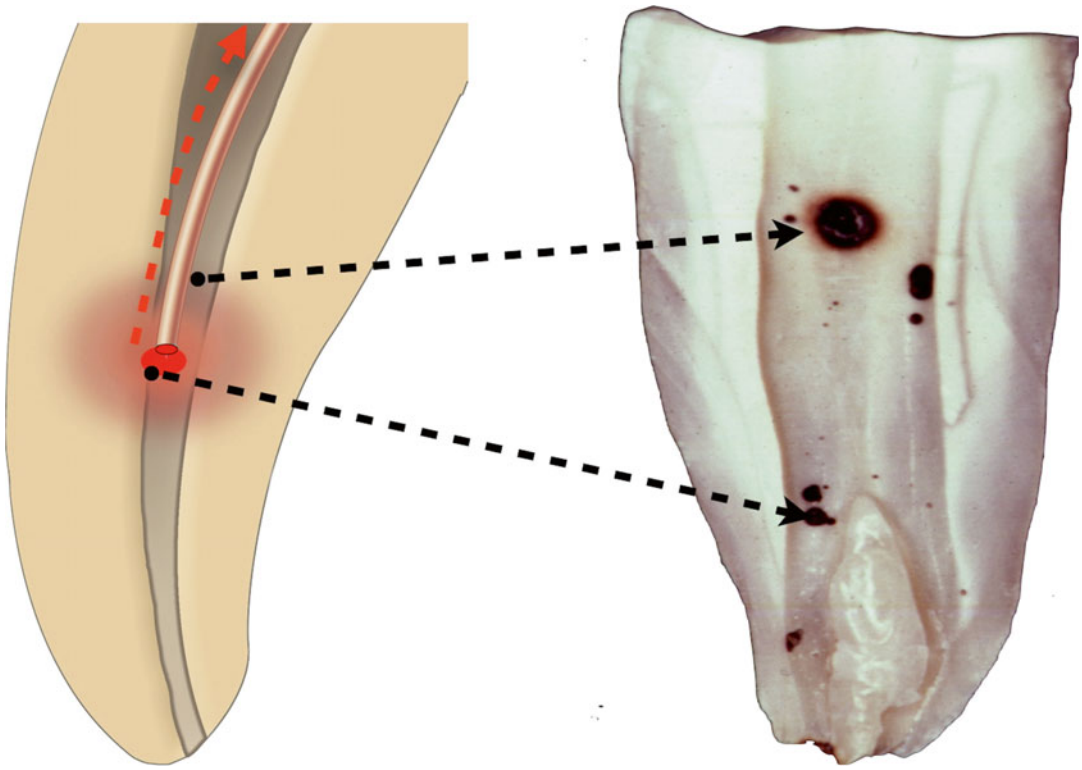

Fig. 5.23 Drawing representation and image of split root show the thermal effects produced by the contact of the fiber with dentin walls during the conventional laser irradiation performed with helical retracting movement in dry mode. Hot spots are visible on the canal surface (Image courtesy of Giovanni Olivi and Vasilios Kaitsas, Rome, Italy)

5.5.3.2 Medium-Infrared Laser

The dentin morphologic pattern after irradiation with medium-infrared laser is different than that with the near-infrared lasers. Erbium lasers vaporize the smear layer, leaving the dentinal tubules mainly clean and well open. Moreover, erbium lasers are generally used at a level of energy higher than the ablation threshold of the dentin (see Chap. 4), so that a certain degree of dentin ablation is produced, more evi-

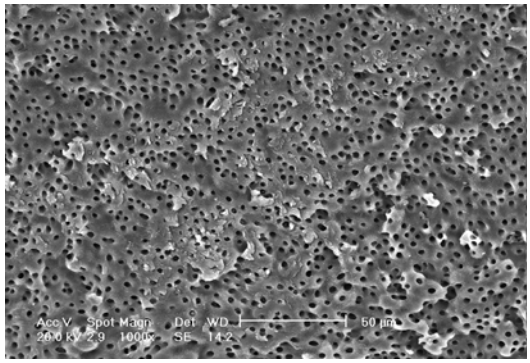

Fig. 5.24 SEM image (1000×) of dentin walls 8 mm shorter of the radicular apex after conventional chemo-mechanical rotary instrumentation and 810 nm diode laser irradiation in wet canal (2.5 W, 20 ms ton/20 mstoff), four times ×5 s after 20 s irrigation with 5 % NaOCl and followed by a final 20 s NaOCl irrigation. The use of NaOCl irrigation before and after laser irradiation reproduces more of its typical morphologic pattern than that of the laser irradiation; dentin tubules are mostly open, some debris are still present, and no thermal damage is visible

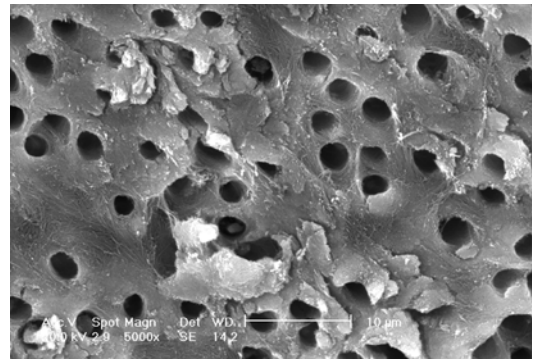

Fig. 5.25 SEM image (5000×) of dentin walls 8 mm shorter of the radicular apex after conventional chemo-mechanical rotary instrumentation and 810 nm diode laser irradiation in wet canal (2.5 W, 20 ms ton/20 mstoff), two times ×5 s after 20 s irrigation with 5 % NaOCl and irradiated again two times ×5 s after 20 s irrigation with 17 % EDTA, followed by a final washing with 20 s EDTA. Dentin surface presents some debris and smear layer; dentin tubules are mainly open; the final EDTA washing partially exposed the organic collagen structure and cleaned the surface from the debris and smear layer; laser thermal damage is absent

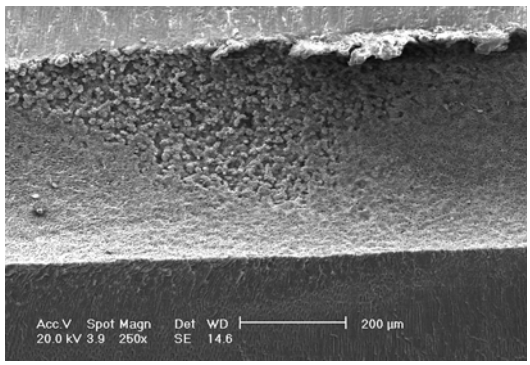

Fig. 5.26 SEM image (250×) of dentin walls 8 mm shorter of the radicular apex after conventional chemo-mechanical rotary instrumentation and 810 nm diode laser irradiation in wet canal (2.5 W, 20 ms ton/20 mstoff), two times ×5 s after 20 s irrigation with 5 % NaOCl and irradiated again two times ×5 s after 20 s irrigation with 17 % EDTA, followed by a final washing with 20 s EDTA. The main canal and the dentin walls appear clean. A central area of predentin shows the typical calcospherules or calcoglobulins: the presence of these structures clearly indicates that the mechanical preparation did not work on this area that remained untouched. However, chemical irrigation was able to clean this part of the root canal surface

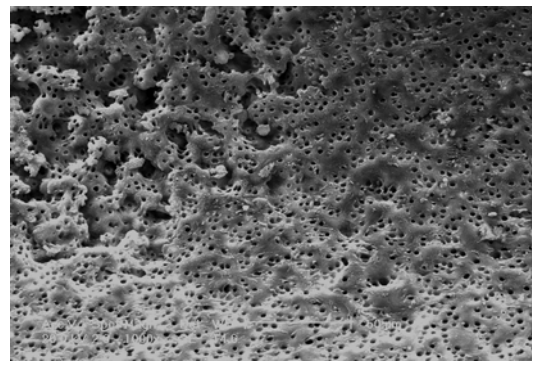

Fig. 5.27 SEM image at higher magnification (1000×) of the predentin area with calcospherules or calcoglobulins: the dentin surface shows presence of few debris from canal instrumentation and opened dentin tubules from EDTA irrigation

dent at the intertubular level, because richer in water, with a typical morphological aspect (chimney-like pattern); also superficial thermal damage is present (Figs. 5.30, 5.31, 5.32, and 5.33).

When used in curved or narrow canals and the terminal part of the tip comes in contact with the dentin wall during the laser emission, the laser energy produces typical aspects of ablation and thermal damage, depending on the power used (hot spots, ledging, cracks, superficial areas of melting), and, in some case, apical transpositions and root perforations are possible [56, 75, 76] (Figs. 5.34, 5.35, 5.36, and 5.37). Many studies agree on the need of the presence of water (from the spray or from irrigants via

Fig. 5.28 SEM image (100×) of the root canal surface after conventional chemo-mechanical rotary instrumentation and Nd:YAG laser irradiation in wet canal (1.5 W, 15 Hz, 100 mJ), two times ×5 s after 20 s irrigation with 5 % NaOCl and irradiated again two times ×5 s after 20 s irrigation with 17 % EDTA, followed by a final washing with 20 s EDTA. It is evident that rotary instruments did not work on all of the canal surface that in part remained untouched by mechanical instrumentation: in the middle area, calcospherules or calcoglobulins in the predentin are still visible

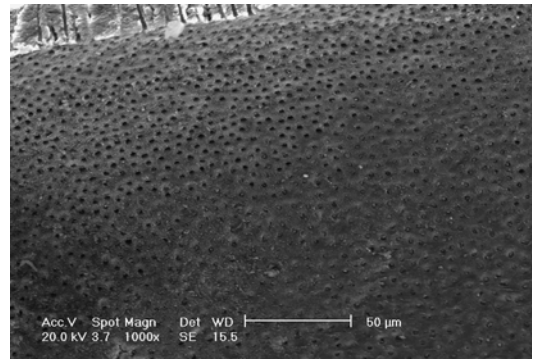

Fig. 5.29 SEM image (1000×) of the root canal surface after conventional chemo-mechanical rotary instrumentation and Nd:YAG laser irradiation in wet canal (1.5 W, 15 Hz, 100 mJ), two times ×5 s after 20 s irrigation with 5 % NaOCl and irradiated again two times ×5 s after 20 s 17 % EDTA, followed by a final washing with 20 s EDTA. The surface is quite clean but a large part of dentin tubules is obliterated by dentin-smear layer fusion

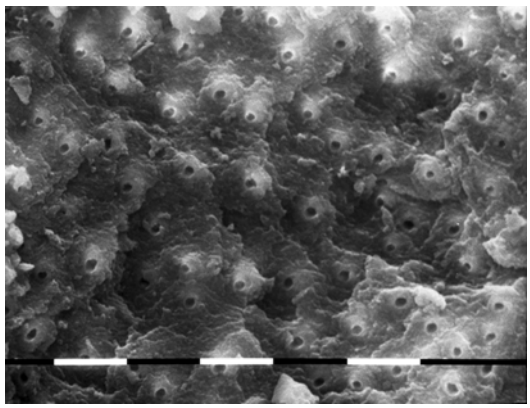

Fig. 5.30 SEM image (1300×) of the root canal surface at 1 mm from the apex, after conventional chemo-mechanical rotary instrumentation and conventional Er,Cr:YAG laser irradiation at 1.0 W, 20 Hz, 50 mJ, 140 µs pulse duration; 300 µm tip inserted into the canal and moved up and down, irrigated with distilled water. Chimney-like pattern, with ablation more pronounced at intertubular dentin, is evident (Image courtesy of Prof. V. Kaitsas (Rome, Italy))

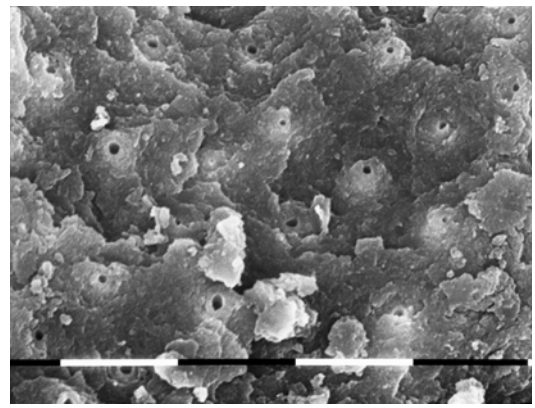

Fig. 5.31 SEM image (1500×) of the root canal surface 1 mm to the apex, after conventional chemo-mechanical rotary instrumentation and conventional Er,Cr:YAG laser irradiation at 1.5 W, 20 Hz, 75 mJ, 140 µs pulse duration; 300 µm tip inserted into the canal and moved up and down, laser air-water spray 35–25 %. Waves of laser ablation evident on the surface

syringe) during the irradiation of the canal with erbium laser to avoid the undesired thermal effect, strongly present when the irradiation is performed in dry mode [56, 76, 77], as confirmed by several studies [25, 55, 78–82].

5.5.4 Effects of Laser Light on Free Water

The use of erbium laser tips in the root canals (LAI) or in the pulp chamber (PIPS) for the acti-

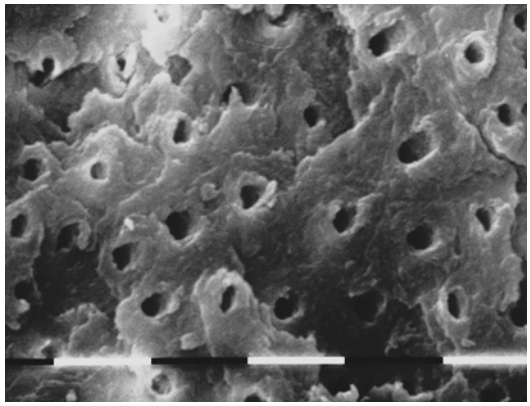

Fig. 5.32 SEM image (2000×) of the root canal surface at 1 mm from the apex, after conventional chemo-mechanical rotary instrumentation and conventional Er,Cr:YAG laser irradiation at 2.5 W, 20 Hz, 140 μs pulse duration; 300 μm tip inserted into the canal and moved up and down, laser air-water spray 35–25 %. The intertubular dentin, richer in water, is more ablated at 125 mJ than the peritubular

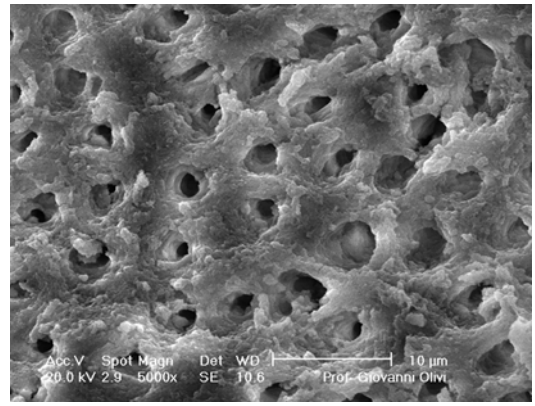

Fig. 5.33 SEM image (5000×) of the root canal surface at 4 mm from the apex, after conventional chemo-mechanical rotary instrumentation and conventional Er,Cr:YAG laser irradiation at 1.0 W, 20 Hz, 50 mJ, 140 μs pulse duration; 300 μm tip inserted into the canal and withdrawn back in 5 s. Irrigation from laser water spray (air 35 %, water 25 %). Tubules are open; few debris are present together to superficial thermal effects

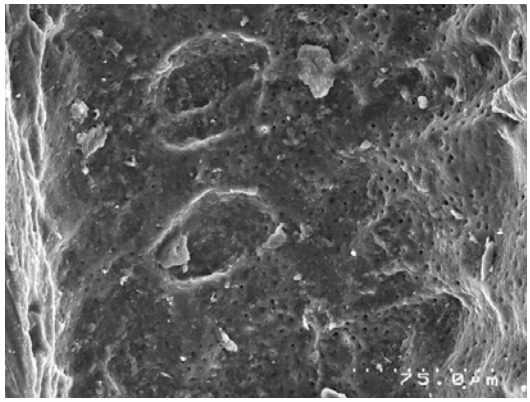

Fig. 5.34 SEM image of the middle one-third of the canal showing thermal damage seen after Er,Cr:YAG laser irradiation, with single overlapped pulses "pot marks" as tip was retracted out of canal per conventional protocol advise. Note the area of untouched mechanically prepared dentin wall (Courtesy of Dr. Graeme Milicich Hamilton, New Zealand and Dr. Enrico DiVito, Scottsdale, Arizona USA)

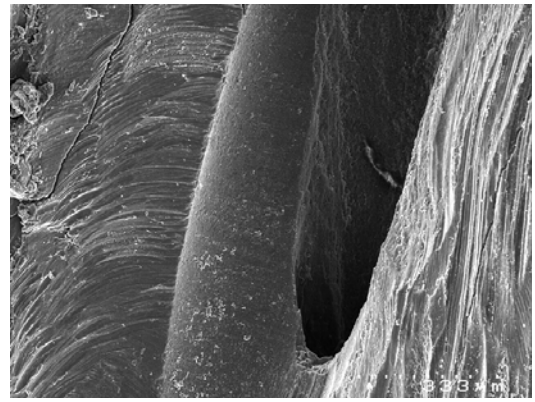

Fig. 5.35 SEM image showing ledging after Er,Cr:YSGG laser tip placed into the canal. Note the area of untouched mechanically prepared dentin wall (Courtesy of Dr. Graeme Milicich, Hamilton, New Zealand and Dr.Enrico DiVito, Scottsdale, Arizona USA)

vation of the irrigants produces absorption in water and an instantaneous superheating up to the boiling point of water (100 °C). Consequently, a vapor bubble expands at the tip of the fiber (explosion) and consecutively collapses (implosion) following immediately after the expansion; the shrinkage creates a cavitation that generates pressure wave within the water fluid (shock waves and jets) [83–85].

The shock wave provokes a direct bacteria lysis and detachment of the biofilm due to tangential shear stress action of the fluids on the dentinal walls [86]; this effect is typical when sodium hypochlorite is activated by lasers [87].

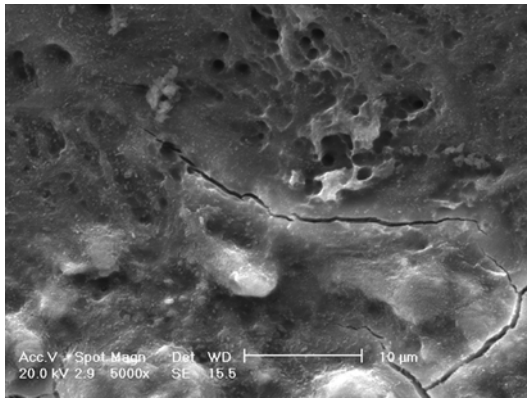

Fig. 5.36 SEM image (5000×) of the apical area after chemo-mechanical preparation and Er:YAG laser irradiation performed in a conventional way at 1 W, 15 Hz. Visible thermal damage with melting of dentin in the apical area

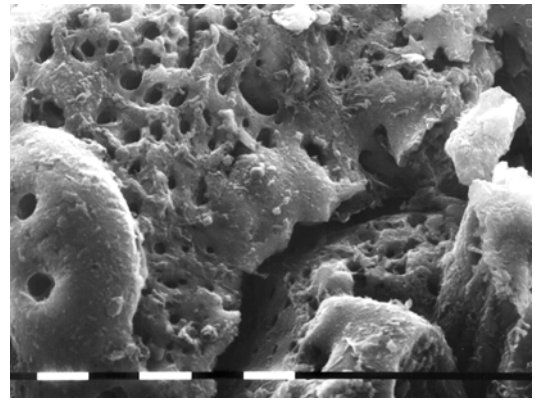

Fig. 5.37 SEM image of the middle one-third area after chemo-mechanical preparation and Er,Cr:YSGG laser irradiation performed in a conventional way at 1.5 W, 15 Hz. Visible thermal damage with bubble and recrystallization of dentin in the touched area

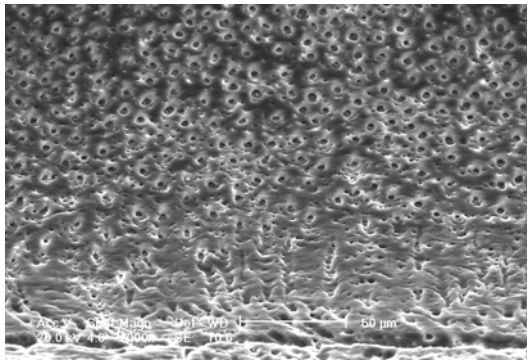

Fig. 5.38 SEM image (1000×) of the middle one-third of the canal after irrigation with 17 % EDTA activated by PIPS technique at 20 mJ, 15 Hz, 50 µs pulse duration; PIPS tip 600 µm positioned stationary in pulp chamber. PIPS irrigation resulted in very clean surface with the absence of smear layer and debris and of sign of thermal ablation

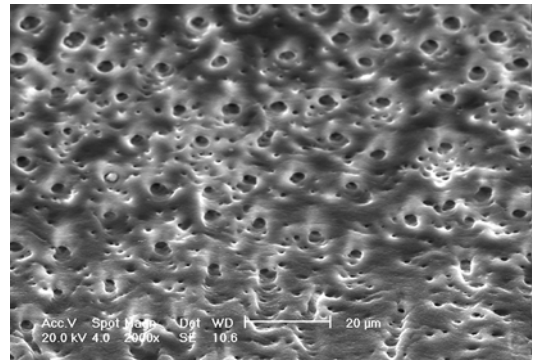

Fig. 5.39 SEM image (2000×) of the middle one-third of the canal after irrigation with 17 % EDTA activated by PIPS technique at 20 mJ, 15 Hz, 50 µs pulse duration; PIPS tip 600 µm positioned stationary in pulp chamber. Dentin tubules are open, and smear layer and debris are absent

When the fluid is the EDTA, the effect is the cleaning of dentin walls from debris and smear layer (Figs. 5.38, 5.39, and 5.40) [88–90].

Usually a direct effect of laser irradiation on dentin walls is absent, considering the massive absorption of the erbium radiation by the water present in the wet canal; anyway, depending on the amount of energy applied, the different positions of the tip in the canal or in the pulp chamber, and the continuous or interrupted irrigation using different techniques, complete vaporization of the irrigant fluid may occur with possible direct thermal damage to dentin walls

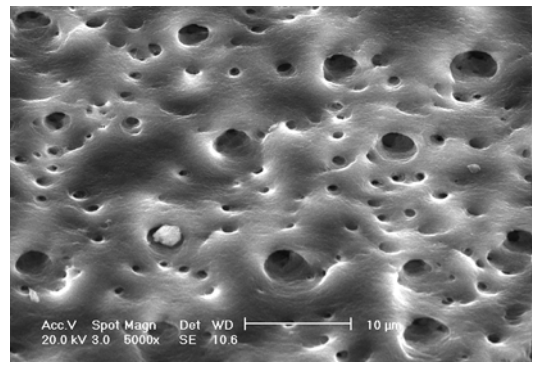

Fig. 5.40 SEM (5000×) magnification of the previous image. PIPS resulted in a very clean surface. Absence of any sign of ablation or thermal damage, with EDTA exposing the collagen matrix

[91]. Later in the text, these points will be largely debated (Chaps. 10 and 11).

5.6 Parameters that Influence the Laser Effects

The laser energy is emitted with different modalities and parameters, depending on the peculiarity of construction of different devices and operator choice, influencing the quantity and quality of tissue irradiation, and foreseeing the biological effects of the result.

5.6.1 Continuous Wave Mode

Diode lasers emit the energy in continuous wave (cw). However, at power higher than 1.5 W, the continuous emission in the root canal is inadvisable because of the excessive thermal damage released on the canal's walls. It is possible and advisable to use the mechanically interrupted (chopped or gated) modality of energy emission, in order to have a better control of the thermal effect. When diode laser continuous wave emission is "chopped" (or gated), with duration of short time (milliseconds or microseconds), it produces more or less thermal effect. Short duration of t^{on}, of 10–20 ms, is correctly and effectively used in endodontics with diode lasers at a power ranging from 2 to 3 W (see Chap. 6).

5.6.2 Pulsed Mode and Pulse Duration

Nd:YAG lasers and erbium family lasers emit laser energy in pulsed mode (defined also "free-running pulsed"), so that every pulse has a beginning, a progressive increment up to a peak, and an end in the unit time (second). Between one pulse and the other, the tissue has the time to cool down allowing a better control of the thermal effect. Short duration of pulse permits to control the side effects of thermal emission; when the energy is concentrated in a short time (high-peak power, PP) produces less thermal effect and a more powerful interaction (PP = energy ÷ duration of the single pulse).

5.6.3 Pulse Repetition Rate

Also the frequency of pulse repetition for second (expressed in Hz o pps) conditions the thermal effect of free-running pulsed laser. The more frequent the repetition is, the shorter the time for thermal release is and the greater the thermal effect on the tissue is. The time for thermal release is necessary for the tissue to dissipate thermal energy accumulated to 50 % of the initial temperature (also called thermal relaxation time).

The pulsed mode makes it possible to emit a variable succession of pulses in the unit time (second), defined in Hz or pps (generally between 2 and 100 pulses in 1 s). Low repetitions of pulse (5–10 Hz/pps) allow a longer time for thermal relaxation and more control of tissue irradiation. In endodontics, the Nd:YAG and erbium lasers are normally used at 10–20 pulses for second (Hz o pps).

5.6.4 Fluence and Power Density

The power of density (power density W/cm^2) and of energy (fluence J/cm^2) depends on the diameter of the tip used and of the irradiated square surface; for the same amount of energy and power emitted, larger is the diameter of the fiber or the irradiated surface, and lower is the density of power and energy. The higher the fluence, the more pronounced the effect is.

5.6.5 Distance Between Target and Fiber

Distance from the target influences energy density and power density. When the distance between the target and fiber/tip of the laser increases, the density of emitted energy decreases, enlarging the size of the spot due to the effect of a certain grade of emission divergence and increasing the necessary amount of energy for the interaction. If we imagine how the diameter of the canal varies from the apical part to the cervical one, we can imagine how the density of energy applied will produce different results in different areas of the canal, when applied at the same power. This condition affects the result that

varies from excessive thermal damage to decontamination or to ineffective irradiation, depending on the position of the fiber within the canal.

References

1. Weichman JA, Johnson FM. Laser use in endodontics. A preliminary investigation. Oral Surg Oral Med Oral Pathol. 1971;31(3):416–20.
2. Weichman JA, Johnson FM, Nitta LK. Laser use in endodontics. II. Oral Surg Oral Med Oral Pathol. 1972;34(5):828–30.
3. Lenz P. The use of laser beams in dentistry. Zahnarztl Mitt. 1974;64(3):112–7. German.
4. Hooks TW, Adrian JC, Gross A, Bernier WE. Use of the carbon dioxide laser in sterilization of endodontic reamers. Oral Surg Oral Med Oral Pathol. 1980;49(3):263–5.
5. Shoji S, Nakamura M, Horiuchi H. Histopathological changes in dental pulps irradiated by CO_2 laser: a preliminary report on laser pulpotomy. J Endod. 1985;11(9):379–84.
6. Paschoud Y, Holz J. Effect of the soft laser on the neoformation of a dentin bridge following direct pulp capping of human teeth with calcium hydroxide. I. Histological study with the scanning electron microscope. Schweiz Monatsschr Zahnmed. 1988;98(4):345–56. French.
7. Miserendino LJ. The laser apicoectomy: endodontic application of the CO_2 laser for periapical surgery. Oral Surg Oral Med Oral Pathol. 1988;66(5):615–9.
8. Neiburger EJ. Tooth apex welding using the CO_2 laser. Ill Dent J. 1989;58(2):108–10.
9. Neiburger EJ. Evaluation of the CO_2 laser for endodontic root apex welding. J Mass Dent Soc. 1992; 41(2):77–9.
10. Pini R, Salimbeni R, Vannini M, Barone R, Clauser C. Laser dentistry: a new application of excimer laser in root canal therapy. Lasers Surg Med. 1989;9(4): 352–7.
11. Liesenhoff T, Lenz H, Seiler T. Root canal preparation using Excimer laser beams. ZWR. 1989;98(12):1034, 1037–9.
12. Frentzen M, Koort HJ, Nolden R. Root canal preparation using Excimer lasers. Dtsch Zahnarztl Z. 1991;46(4):288–9. German.
13. Myers TD. Lasers in dentistry. CDS Rev. 1991; 84(8):26–9.
14. Gutknecht N, Behrens VG. Instrumentation of root canal walls with Nd-YAG laser. ZWR. 1991;100(10): 748–50, 752, 755.
15. Levy G. Cleaning and shaping the root canal with a Nd:YAG laser beam: a comparative study. J Endod. 1992;18(3):123–7.
16. Bahcall JK, Miserendino L, Walia H, Belardi DW. Scanning electron microscopic comparison of canal preparation with Nd:YAG laser and hand instrumentation: a preliminary study. Gen Dent. 1993;41(1):45–7.
17. Goodis HE, White JM, Marshall SJ, Marshall Jr GW. Scanning electron microscopic examination of intracanal wall dentin: hand versus laser treatment. Scanning Microsc. 1993;7(3):979–87.
18. Hardee MW, Miserendino LJ, Kos W, Walia H. Evaluation of the antibacterial effects of intracanal Nd:YAG laser irradiation. J Endod. 1994;20(8): 377–80.
19. Saunders WP, Whitters CJ, Strang R, Moseley H, Payne AP, McGadey J. The effect of an Nd-YAG pulsed laser on the cleaning of the root canal and the formation of a fused apical plug. Int Endod J. 1995; 28(4):213–20.
20. Fegan SE, Steiman HR. Comparative evaluation of the antibacterial effects of intracanal Nd:YAG laser irradiation: an in vitro study. J Endod. 1995; 21(8):415–7.
21. Moshonov J, Orstavik D, Yamauchi S, Pettiette M, Trope M. Nd:YAG laser irradiation in root canal disinfection. Endod Dent Traumatol. 1995;11(5):220–4.
22. Mor C, Stabholz A, Neev J, Rotstein I. Efficacy of XeCl-308 excimer laser in fusing hydroxyapatite to seal the root apex. Endod Dent Traumatol. 1995;11(4): 169–71.
23. Stabholz A, Neev J, Liaw LH, Stabholz A, Khayat A, Torabinejad M. Sealing of human dentinal tubules by XeCl 308-nm excimer laser. J Endod. 1993; 19(6):267–71.
24. Harashima T, Takeda FH, Zhang C, Kimura Y, Matsumoto K. Effect of argon laser irradiation on instrumented root canal walls. Endod Dent Traumatol. 1998;14(1):26–30.
25. Takeda FH, Harashima T, Kimura Y, Matsumoto K. Comparative study about the removal of smear layer by three types of laser devices. J Clin Laser Med Surg. 1998;16(2):117–22.
26. Yamazaki R, Goya C, Tomita Y, Kimura Y, Matsumoto K. Study on apical leakage of the teeth after argon laser treatment and obturation. J Clin Laser Med Surg. 1999;17(3):121–5.
27. Tewfik HM, Pashley DH, Horner JA, Sharawy MM. Structural and functional changes in root dentin following exposure to KTP/532 laser. J Endod. 1993;19(10):492–7.
28. Machida T, Wilder-Smith P, Arrastia AM, Liaw LH, Berns MW. Root canal preparation using the second harmonic KTP:YAG laser: a thermographic and scanning electron microscopic study. J Endod. 1995;21(2): 88–91.
29. Nammour S, Kowaly K, Powell GL, Van Reck J, Rocca JP. External temperature during KTP-Nd:YAG laser irradiation in root canals: an in vitro study. Lasers Med Sci. 2004;19(1):27–32. Epub 2004 Jul 16.
30. Schoop U, Kluger W, Dervisbegovic S, Goharkhay K, Wernisch J, Georgopoulos A, Sperr W, Moritz A. Innovative wavelengths in endodontic treatment. Lasers Surg Med. 2006;38(6):624–30.

31. Kuştarci A, Sümer Z, Altunbaş D, Koşum S. Bactericidal effect of KTP laser irradiation against Enterococcus faecalis compared with gaseous ozone: an ex vivo study. Oral Surg Oral Med Oral Pathol Oral Radiol Endod. 2009;107(5):e73–9.
32. Meire MA, De Prijck K, Coenye T, Nelis HJ, De Moor RJ. Effectiveness of different laser systems to kill Enterococcus faecalis in aqueous suspension and in an infected tooth model. Int Endod J. 2009; 42(4):351–9. Epub 2009 Feb 7.
33. Zan R, Hubbezoglu I, Sümer Z, Tunç T, Tanalp J. Antibacterial effects of two different types of laser and aqueous ozone against Enterococcus faecalis in root canals. Photomed Laser Surg. 2013;31(4):150–4. doi:10.1089/pho.2012.3417. Epub 2013 Mar 13.
34. Sadık B, Arıkan S, Beldüz N, Yaşa Y, Karasoy D, Cehreli M. Effects of laser treatment on endodontic pathogen Enterococcus faecalis: a systematic review. Photomed Laser Surg. 2013;31(5):192–200. Epub 2013 Apr 15.
35. Lee MT, Bird PS, Walsh LJ. Photo-activated disinfection of the root canal: a new role for lasers in endodontics. Aust Endod J. 2004;30(3):93–8.
36. Bonsor SJ, Nichol R, Reid TM, Pearson GJ. Microbiological evaluation of photo-activated disinfection in endodontics (an in vivo study). Br Dent J. 2006;200(6):337–41; discussion 329.
37. Garcez AS, Ribeiro MS, Tegos GP, Núñez SC, Jorge AO, Hamblin MR. Antimicrobial photodynamic therapy combined with conventional endodontic treatment to eliminate root canal biofilm infection. Lasers Surg Med. 2007;39(1):59–66.
38. Fonseca MB, Júnior PO, Pallota RC, Filho HF, Denardin OV, Rapoport A, Dedivitis RA, Veronezi JF, Genovese WJ, Ricardo AL. Photodynamic therapy for root canals infected with Enterococcus faecalis. Photomed Laser Surg. 2008;26(3):209–13.
39. Lim Z, Cheng JL, Lim TW, Teo EG, Wong J, George S, Kishen A. Light activated disinfection: an alternative endodontic disinfection strategy. Aust Dent J. 2009;54(2):108–14.
40. Garcez AS, Nuñez SC, Hamblim MR, Suzuki H, Ribeiro MS. Photodynamic therapy associated with conventional endodontic treatment in patients with antibiotic-resistant microflora: a preliminary report. J Endod. 2010;36(9):1463–6.
41. Furuoka M, Yokoi T, Fukuda S, Usuki M, Matsuo S, Taniguchi K, Kitamura K. Effects of GaAlAs laser diode in treatment of hypersensitive dentine. Fukuoka Shika Daigaku Gakkai Zasshi. 1988;15(1):42–8. Japanese.
42. Yamaguchi M, Ito M, Miwata T, Horiba N, Matsumoto T, Nakamura H, Fukaya M. Clinical study on the treatment of hypersensitive dentin by GaAlAs laser diode using the double blind test. Aichi Gakuin Daigaku Shigakkai Shi. 1990;28(2):703–7. Japanese.
43. Kireev AK, Evstigneev AR, Voroshnin PA, Aleksandrov MT. The use of the Uzor laser apparatus for treating inflammatory diseases of the maxillofacial area. Stomatologiia (Mosk). 1989;68(5):42–5. Russian.
44. Kurumada F. A study on the application of Ga-As semiconductor laser to endodontics. The effects of laser irradiation on the activation of inflammatory cells and the vital pulpotomy. Ou Daigaku Shigakushi. 1990;17(3):233–44. Japanese.
45. Schoop U, Kluger W, Moritz A, Nedjelik N, Georgopoulos A, Sperr W. Bactericidal effect of different laser systems in the deep layers of dentin. Lasers Surg Med. 2004;35(2):111–6.
46. Moritz A. Oral laser application. Berlin: Quintessence Verlags-GmbH; 2006. p. 258–77.
47. Moritz A, Schoop U, Jiru E, Goharkhay K, Wernisch J, Sperr W. Morphological changes of *E. Coli* and *E. faecalis* after Er:YAG and Nd:YAG laser irradiation through different layers of dentin. Abstract 2nd congress of the European Society for oral laser applications, Florence, 15–18 May 2003.
48. Franzen R, Gutknecht N, Falken S, Heussen N, Meister J. Bactericidal effect of a Nd:YAG laser on Enterococcus faecalis at pulse durations of 15 and 25 ms in dentine depths of 500 and 1,000 µm. Lasers Med Sci. 2011;26(1):95–101. doi:10.1007/s10103-010-0826-5. Epub 2010 Aug 31.
49. Hibst R, Keller U. Experimental studies of the application of the Er:YAG laser on dental hard substances: I. Measurement of the ablation rate. Lasers Surg Med. 1989;9(4):338–44.
50. Keller U, Hibst R. Experimental studies of the application of the Er:YAG laser on dental hard substances: II. Light microscopic and SEM investigations. Lasers Surg Med. 1989;9(4):345–51.
51. Keller U, Hibst R. Ablative effect of an Er:YAG laser on enamel and dentin. Dtsch Zahnarztl Z. 1989;44(8):600–2. German.
52. Keller U, Hibts R. Ultrastructural changes of enamel and dentin following Er:YAG laser on teeth laser surgery: advanced characterization. Therapeutics and systems. Proc SPIE. 1990;1200:408–15.
53. Hossain M, Nakamura Y, Yamada Y, Kimura Y, Matsumoto N, Matsumoto K. Effects of Er, Cr:YSGG laser irradiation in human enamel and dentin: ablation and morphological studies. J Clin Laser Med Surg. 1999;17(4):155–9.
54. Yu DG, Kimura Y, Kinoshita J, Matsumoto K. Morphological and atomic analytical studies on enamel and dentin irradiated by an erbium, chromium:YSGG laser. J Clin Laser Med Surg. 2000;18(3):139–43.
55. Takeda FH, Harashima T, Kimura Y, Matsumoto K. Efficacy of Er:YAG laser irradiation in removing debris and smear layer on root canal walls. J Endod. 1998;24(8):548–51.
56. Yamazaki R, Goya C, Yu DG, Kimura Y, Matsumoto K. Effects of erbium, chromium:YSGG laser irradiation on root canal walls: a scanning electron microscopic and thermographic study. J Endod. 2001;27(1):9–12.
57. Zuerlein MJ, Fried D, Featherestone JDB, Seka W. Optical properties of dental enamel in the mid-IR determined by pulsed photothermal radiometry. IEEE J Sel Top Quantum Electron. 1999;5(4):1083–9.

58. Featherestone JDB, Nelson DGA. Laser effects on dental hard tissues. Adv Dent Res. 1987;1(1):21–6.
59. Featherestone JDB, Fried D. Fundamental interactions of lasers with dental hard tissues. Med Laser Appl. 2001;16(3):181–94.
60. Moshonov J, Stabholz A, Leopold Y, Rosenberg I, Stabholz A. Laser in dentistry. Part B-interaction with biological tissues and the effect on the soft tissues of the oral cavity, the hard tissues of the tooth and the dental pulp. Refuat Hapeh Vehashinayim. 2001;18(3–4):21–8, 107–8.
61. Majaron B, Lukac M, Sustercic D, Funduk N, Skaleric U. Threshold and efficiency analysis in Er:YAG laser ablation of hard dental tissue. Laser applications in medicine and dentistry. Proc SPIE. 1996;2922:233–42.
62. Lin S, Liu Q, Peng Q, Lin M, Zhan Z, Zhang X. The ablation threshold of Er:YAG laser and Er, Cr:YSGG laser in dental dentin. Sci Res Essays. 2010; 5(16):2128–35.
63. Olivi G. Laser use in endodontics: evolution from direct laser irradiation to laser-activated irrigation. J Laser Dent. 2013;21(2):58–71.
64. Watanabe S, Saegusa H, Anjo T, Ebihara A, Kobayashi C, Suda H. Dentin strain induced by laser irradiation. Aust Endod J. 2010;36(2):74–8.
65. Kaitsas V, Signore A, Fonzi L, Benedicenti S, Barone M. Effects of Nd: YAG laser irradiation on the root canal wall dentin of human teeth: a SEM study. Bull Group Int Rech Sci Stomatol Odontol. 2001;43(3):87–92.
66. da Costa RA, Nogueira GE, Antoniazzi JH, Moritz A, Zezell DM. Effects of diode laser (810 nm) irradiation on root canal walls: thermographic and morphological studies. J Endod. 2007;33(3):252–5. Epub 2006 Dec 13.
67. Alfredo E, Marchesan MA, Sousa-Neto MD, Brugnera-Júnior A, Silva-Sousa YT. Temperature variation at the external root surface during 980-nm diode laser irradiation in the root canal. J Dent. 2008;36(7):529–34. Epub 2008 May 6.
68. He H, Yu J, Song Y, Lu S, Liu H, Liu L. Thermal and morphological effects of the pulsed Nd:YAG laser on root canal surfaces. Photomed Laser Surg. 2009;27(2):235–40.
69. Benedicenti S, Cassanelli C, Signore A, Ravera G, Angiero F. Decontamination of root canals with the gallium-aluminum-arsenide laser: an in vitro study. Photomed Laser Surg. 2008;26(4):367–70.
70. Gurbuz T, Ozdemir Y, Kara N, Zehir C, Kurudirek M. Evaluation of root canal dentin after Nd:YAG laser irradiation and treatment with five different irrigation solutions: a preliminary study. J Endod. 2008;34(3): 318–21.
71. de Moura-Netto C, de Moura AA, Davidowicz H, Aun CE, Antonio MP. Morphologic changes and removal of debris on apical dentin surfaces after Nd:YAG laser and diode laser irradiation. Photomed Laser Surg. 2008;26(3):263–6.
72. Faria MI, Souza-Gabriel AE, Marchesan MA, Sousa-Neto MD, Silva-Sousa YT. Ultrastructural evaluation of radicular dentin after Nd:YAG laser irradiation combined with different chemical substances. Gen Dent. 2008;56(7):641–6.
73. Alfredo E, Souza-Gabriel AE, Silva SR, Sousa-Neto MD, Brugnera-Junior A, Silva-Sousa YT. Morphological alterations of radicular dentine pretreated with different irrigating solutions and irradiated with 980-nm diode laser. Microsc Res Tech. 2009;72(1):22–7.
74. Olivi G, Olivi M, Kaitsas V, Benedicenti S. Morphological changes after 810 nm diode laser irradiation of prepared, wet root canals: SEM investigations. Dentista Moderno. 2013;31(10):122–8.
75. Minas NH, Gutknecht N, Lampert F. In vitro investigation of intra-canal dentine-laser beam interaction aspects: II. Evaluation of ablation zone extent and morphology. Lasers Med Sci. 2010;25(6):867–72. doi:10.1007/s10103-009-0722-z. Epub 2009 Aug 29.
76. Ebihara A, Majaron B, Liaw LH, Krasieva TB, Wilder-Smith P. Er:YAG laser modification of root canal dentine: influence of pulse duration, repetitive irradiation and water spray. Lasers Med Sci. 2002;17(3):198–207.
77. Kimura Y, Yonaga K, Yokoyama K, Kinoshita J, Ogata Y, Matsumoto K. Root surface temperature increase during Er:YAG laser irradiation of root canals. J Endod. 2002;28(2):76–8.
78. Matsuoka E, Kimura Y, Matsumoto K. Studies on the removal of debris near the apical seats by Er:YAG laser and assessment with a fiberscope. J Clin Laser Med Surg. 1998;16(5):255–61.
79. Takeda FH, Harashima T, Eto JN, Kimura Y, Matsumoto K. Effect of Er:YAG laser treatment on the root canal walls of human teeth: an SEM study. Endod Dent Traumatol. 1998;14(6):270–3.
80. Takeda FH, Harashima T, Kimura Y, Matsumoto K. A comparative study of the removal of smear layer by three endodontic irrigants and two types of laser. Int Endod J. 1999;32(1):32–9.
81. Altundasar E, Ozçelik B, Cehreli ZC, Matsumoto K. Ultramorphological and histochemical changes after Er,Cr:YSGG laser irradiation and two different irrigation regimes. J Endod. 2006;32(5):465–8.
82. Varella CH, Pileggi R. Obturation of root canal system treated by Cr, Er: YSGG laser irradiation. J Endod. 2007;33(9):1091–3. Epub 2007 Jul 5.
83. George R, Meyers IA, Walsh LJ. Laser activation of endodontic irrigants with improved conical laser fiber tips for removing smear layer in the apical third of the root canal. J Endod. 2008;34(12):1524–7. Epub 2008 Oct 2.
84. De Moor RJ, Meire M, Goharkhay K, Moritz A, Vanobbergen J. Efficacy of ultrasonic versus laser-activated irrigation to remove artificially placed dentin debris plugs. J Endod. 2010;36(9):1580–3.
85. de Groot SD, Verhaagen B, Versluis M, Wu MK, Wesselink PR, van der Sluis LW. Laser-activated irrigation within root canals: cleaning efficacy and flow visualization. Int Endod J. 2009;42(12):1077–83.

86. Pedullà E, Genovese C, Campagna E, Tempera G, Rapisarda E. Decontamination efficacy of photon-initiated photoacoustic streaming (PIPS) of irrigants using low-energy laser settings: an ex vivo study. Int Endod J. 2012;45(9):865–70. Epub 2012 Apr 5.
87. Macedo RG, Wesselink PR, Zaccheo F, Fanali D, Van Der Sluis LW. Reaction rate of NaOCl in contact with bovine dentine: effect of activation, exposure time, concentration and pH. Int Endod J. 2010;43(12):1108–15. doi:10.1111/j.1365-2591.2010.01785.x. Epub 2010 Aug 31.
88. DiVito E, Peters OA, Olivi G. Effectiveness of the erbium:YAG laser and new design radial and stripped tips in removing the smear layer after root canal instrumentation. Lasers Med Sci. 2012;27(2):273–80. Epub 2010 Dec 1.
89. Peeters HH, Suardita K. Efficacy of smear layer removal at the root tip by using ethylenediaminetetraacetic acid and erbium, chromium: yttrium, scandium, gallium garnet laser. J Endod. 2011;37(11):1585–9. doi:10.1016/j.joen.2011.08.022. Epub 2011 Sep 28.
90. Guidotti R, Merigo E, Fornaini C, Rocca JP, Medioni E, Vescovi P. Er:YAG 2,940-nm laser fiber in endodontic treatment: a help in removing smear layer. Lasers Med Sci. 2014;29:69–75.
91. Deleu E, Meire MA, De Moor RJ. Efficacy of laser-based irrigant activation methods in removing debris from simulated root canal irregularities. Lasers Med Sci. 2015;30:831–5.

Part III

Clinical Applications of Laser in Endodontics

Conventional Laser Endodontics

6

Giovanni Olivi and Matteo Olivi

Abstract

Laser irradiation of root canals is performed with the conventional fibers or tips inserted into the canal up to the working length and successively activated during the retraction. This technique is suitable for most wavelengths used in dentistry. Medium-infrared wavelengths are well absorbed by water in the dentin and spread their energy superficially over the canal surface; they produce some thermal and ablative effect, clean the canal walls very well, vaporizing the smear layer, exposing the dentinal tubules, and increasing dentinal permeability. Near-infrared wavelengths are not well absorbed by the dentin chromophore and are more penetrating in depth; they produce evident thermal effects with areas of recrystallization of the dentin surface where the smear layer is mainly fused, occluding the dentinal tubules. All wavelengths have an efficient decontaminating action on the main canal surface, with different capacity of penetration in dentin tubules. However, a precise and unambiguous determination of the real bactericidal effect in depth of different lasers has not been reached and also many results are contradictory. When the diode lasers are used in conjunction with conventional irrigation techniques, significant elimination of bacteria is reported, and the morphological pattern produced remained similar to the pattern produced by the use of irrigant alone, limiting the undesired thermal effects correlated with near-infrared laser irradiation. However, the anatomic and operative problems of the introduction of a fiber in narrow and curved canals are still not solved, with the probable impossibility or inefficiency of the procedure in teeth with complicated root canal anatomy, not completely satisfying the needs of modern endodontics.

G. Olivi, MD, DDS (✉)
InLaser Rome – Advanced Center for Esthetic and Laser Dentistry, Rome, Italy
e-mail: olivilaser@gmail.com

M. Olivi, DDS
InLaser Rome – Advanced Center for Esthetic and Laser Dentistry, Rome, Italy
e-mail: olivimatt@gmail.com

G. Olivi et al. (eds.), *Lasers in Endodontics: Scientific Background and Clinical Applications*,
DOI 10.1007/978-3-319-19327-4_6

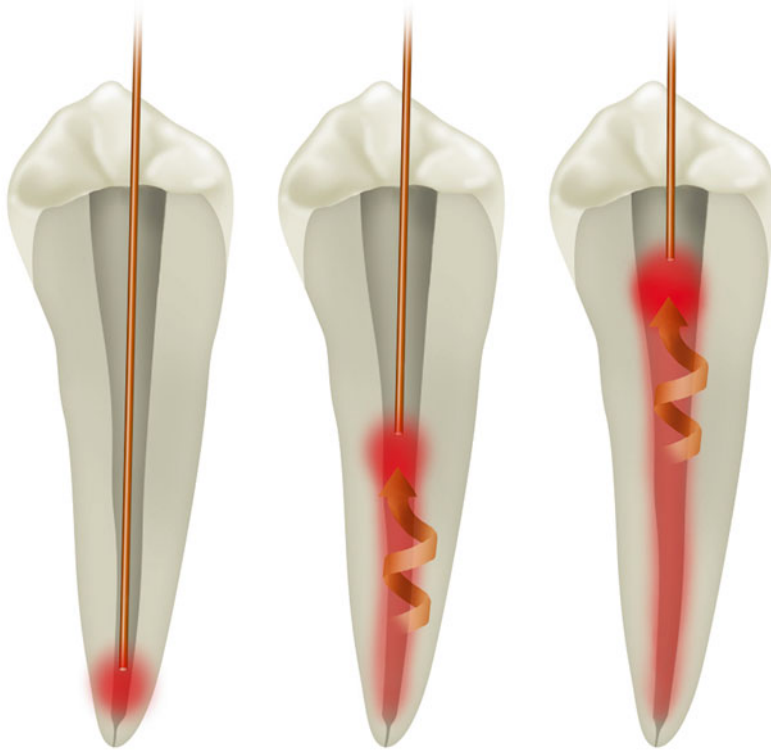

Fig. 6.1 Draft representing the typical irradiation proposed for conventional laser endodontics; the fiber is positioned in a dry canal 1 mm shorter from the apex and is retracted with helical motion in an established time (2 mm/s) (Image courtesy of Giovanni Olivi, Rome, Italy)

The first experimentations with lasers in endodontics were focused on the use of thermal energy for decontamination of endodontic bacterial flora.

Delivering the laser light to the radicular apex, conventionally one millimeter from the anatomic apex, requires the use of fibers or tips with a thin (narrow) diameter (generally 200–300 microns) that are flexible and resistant to negotiate (follow or overtake) the anatomical curvatures of dental roots with minimal risk of breakage.

Laser activation happens during fiber/tip retraction, in an established amount of time (usually 2 mm/s), in the attempt to supply a density of energy for an irradiated surface (fluence) that is uniform in different areas of the canal (Fig. 6.1).

The technique requires helical (circular) movement of the fiber, in order to increase the irradiation angle between laser fiber and dentin surface, trying to improve the angle (directionality) and energy diffusion.

This technique is suitable for most wavelengths used in dentistry, in the visible (532 nm), in the near-infrared (from 810 to 1340 nm), and medium-infrared (2780 and 2940 nm) electromagnetic spectrum and utilizes fibers or tips (flat or end firing), which permit the direct irradiation of the canal surface.

Olivi (2013) called this technique "conventional laser endodontics" (see Table 5.1) [1], in order to distinguish it from the more recent PAD (or aPDT) and LAI, which involve the irradiation and the activation of different antibacterial solutions and irrigants.

6.1 Mechanism of Conventional Laser Endodontics

When a laser fiber/tip is inserted into the canal and laser irradiation starts, it interacts with the canal surface following the optical characteristic of every wavelength (see Sect. 5.4).

The presence and concentration of specific chromophores on the canal surface and inside the

dentinal tubules determine absorption, diffusion, or transmission of laser light. Depending on the wavelength, there are different effects and different depths of penetration (see Sect. 5.4).

Under the same conditions, the medium-infrared wavelengths, which are well absorbed by the dentin water (chromophore), spread their energy superficially over the canal surface, while the near-infrared wavelengths, which are not well absorbed by the dentin chromophore, are more penetrating in depth.

If the objective is removal of tissue (ablation-preparation of the canal), correct management of the wavelength and parameters (energy, power, and pulse duration) allows superficial absorption, reducing heat diffusion which is inefficient for ablative purposes. On the contrary, if the objective is not ablation but decontamination, the ability for penetration through the target tissue of the selected wavelength can constitute a desirable and valued advantage.

The medium-infrared laser radiation is mainly absorbed at the canal surface by the watery component of dentin, with vaporization of debris and smear layer, leaving the dentinal tubules open and also producing surface decontamination and minimal dental ablation.

The near-infrared laser radiation mainly diffuses in the dentinal tubules and dentin walls, to target the pigment of bacterial cells performing a deep decontaminating effect and also a thermal effect on the surface during the diffusion of light; the thermal effect results in inorganic melting of the smear layer producing occlusion of dentin tubules, more or less evident depending on the wavelength and the parameters used (fluence, peak power, and modality of emission).

When the energy applied is high, many undesired thermal effects on the dentin walls are present, varying on the wavelength used.

Laser technology has been proposed for different phases of endodontic treatment for:

- Access cavity preparation
- Root canal preparation
- Root canal cleaning
- Root canal decontamination

Research and clinical use, after initial interest in all possible therapeutic uses of lasers in endodontics, are today limited to cleaning and decontamination of the root canal system.

6.2 Access Cavity

Beyond the conventional use of rotative instruments, the access to the pulp chamber can be performed with erbium lasers, able to remove all the hard and soft dental tissues: enamel, dentin, carious tissue, and pulp without contact. These lasers can be used both with a handpiece with terminal tip and with a tipless handpiece. When using a handpiece with a tip, the choice of diameters ranging from 600 to 1000 microns is preferable. Larger diameters give rise to more elevated energy and power during ablation of the enamel with a larger irradiated surface. Preparing the access cavity, the energy is progressively reduced in depth, from the dentin to the pulp. The high affinity with carious tissue and pulp (richer in water) helps to remove carious dentin and to selectively uncover the pulp horns with less energy, reducing the risk of a false path. The following are the suggested energy setting to progressively use on enamel, dentin, carious tissue, and pulp:

Enamel	Dentin caries	Pulp tissue	Canal orifices
250 mJ>	200 mJ >150 mJ	150 mJ	120 >80 mJ

The importance of the laser approach for access cavity preparation should not be underestimated. Erbium lasers, due to their selectivity of action, allow an access to the endodontic system after a consistent abatement of bacterial load, therefore reducing contamination with bacteria, toxins, and debris in the apical direction during subsequent instrumentation. A study by Hibst et al. (1996) demonstrated that bacteria are killed during cavity preparation up to a depth of 300–400 microns, under the irradiated surface [2].

Erbium lasers are also useful in the removal of pulp stones and in the search for calcified canals.

6.3 Lasers for Root Canal Preparation

Root canal preparation with steel and nickel-titanium instruments is today considered the gold standard in Endodontics. This section is presented with the sole aim to give information on the development of laser technology in Endodontics.

6.3.1 Excimer Laser

Among the first experiments with lasers in endodontics, root canal preparation was studied in vitro by Liesenhoff et al. (1989), which used an excimer laser (308 nm) and concluded that the laser can prepare a root canal safely and efficiently and produce a canal surface without a smear layer, with open dentinal tubules and a lack of over-instrumentation and false path (via falsa) [3].

In another in vitro study, Frentzen et al. (1991) reported opposite results, concluding that the energy density of excimer laser was not high enough for the ablation of dentin and pulp tissues [4].

The value of excimer laser technology in endodontics was limited. The latter also accounts for their use in dentistry in general.

6.3.2 Nd:YAG Laser

At the beginning of the 1990s, the first investigations with Nd:YAG laser with optical fiber in the root canals were started.

Gutknecht et al. (1991), in an in vitro preliminary study with SEM observation, showed the modifications of the root canal surface following irradiation at 1.5 W (100 mJ, 15 Hz); the smear layer was removed through superficial inorganic melting with closure of dentin tubules, and these modifications were considered useful for endodontic treatment [5].

Levy (1992) as well, in a SEM study, concluded that Nd:YAG laser preparation was possible and that it allowed better cleaning of canal surface than conventional instrumentation [6].

Goodis et al. (1993) confirmed the Nd:YAG laser's ability to interact with dentin walls with smear layer removal and, only occasionally, surface alterations were seen [7].

Some years later, Moogi and Nageshwar (2010) reported the same results. SEM observations showed the presence of areas of fusion and recrystallization, especially in the apical one-third; these dentin surface alterations were positively considered by the authors, as a possible seal to bacterial recolonization [8].

Research on the use of Nd:YAG technology for root canal preparation was soon abandoned and the technology is today used in endodontics only for the final decontamination at the end of conventional chemomechanical instrumentation.

6.3.3 Nd:YAP Laser

Blum and Abadie (1997) compared different systems of root canal preparation, using sodium hypochlorite as irrigant. Manual preparation and combined manual/laser-assisted techniques ended in similar results, differing just in size of remaining debris, that were smaller in case of laser-assisted preparation. Preparation executed with just laser irradiation produces an enhanced diameter in the prepared canals with the presence of debris. Different conventional manual preparations, associated with both laser irradiation and subsonic irrigation, showed no statistically significant differences. The combined use of subsonic and laser systems, associated with manual preparation, demonstrated better cleaning after preparation, with very small debris remnants. The study concluded by referring to the potential capacity of Nd:YAP laser to complete manual preparation of the canal with better cleaning [9].

Also for Nd:YAP laser, studies on this specific use were not continued.

6.3.4 Erbium Lasers

The recognized ablative capacity on hard tissues of erbium lasers (2780 and 2940 nm), and their FDA approval (according to the US FDA Marketing Clearance by Wavelength) for shaping,

enlarging, and cleaning of the canals, guided the following research toward medium-infrared lasers.

Many studies analyzed the erbium lasers' potential for root canal preparation in different operative conditions, evaluating the efficacy, possible morphological damage, and possible thermal damage to the periodontal tissues.

The initial studies reported positive results using Er:YAG laser with different experimental radial emission tips, encouraging future research.

Shoji et al. (2000) used a Er:YAG laser system with a conical tip with 80 % lateral emission and 20 % end emission, for the enlargement and cleansing of the canals.

Using 0.3 W (30 mJ and 10 pps), they obtained canal enlargement of about 13 % with a cleaner dentinal surface compared to the samples treated without laser [10].

Kesler et al. (2002), in a preliminary study on the effects of Er:YAG laser, equipped with microprobes with radial emission, used 140 and 90 mJ with 400 and 200 micron tips, respectively, and reported, in the study's conditions, good capacity for enlargement and shaping, quickly and better than the traditional system. The SEM observations demonstrated a dentin surface equally clean from the apex to the coronal portion, without pulp remnants and clean open dentinal tubules [11].

Stabholz et al. (2003 and 2004) also presented positive results regarding treatment executed with the same Er:YAG laser and lateral emitting endodontic microprobes [12, 13].

A study by Inamoto et al. (2009) investigated in vitro the cutting capacity and morphological effects of Er:YAG laser irradiation, using 0.3 and 0.75 W (30 mJ at 10 Hz and 25 Hz), withdrawing a fiber at a speed of 1 mm/sec and 2 mm/sec, reporting positive results [14].

Recently, Kokuzawa et al. (2012) evaluated the shaping capacity of the root canal using Er:YAG laser equipped with conical fibers of 185 and 280 micron diameter; the conical fibers diffused 80 % of the energy laterally. Irradiation was executed at 0.4 W (20 mJ, 20 pps), with water spray (5 ml/min), 3 times for 10 s. SEM observations showed clean dentin surface, with open tubule orifices. The authors underlined that for efficient ablation, a shorter distance between the fiber and the walls of the canal is necessary, in order to avoid natural dispersion of energy due to the distance between source and target [15]. This observation emphasizes the difficulty to apply the concept of fluence in endodontics that will be debated in the discussion session. Also, the difference of energy settings used in these studies underlines the different technologies of the laser systems used and the impossibility to establish a common protocol.

Studies on radial firing tips were resumed again by other investigators [16, 17] as a prelude to techniques of laser activation of the irrigants (LAI). The latter will be addressed later.

Other studies instead investigated Er, Cr:YSGG and Er:YAG lasers, equipped with plane end-firing tips.

Chen (2002 and 2003) presented case studies with root canals entirely prepared using the Er,Cr:YSGG laser (the first to obtain the FDA license for the entire endodontic procedure) with positive results. Chen used endodontic end-firing tips of different lengths, with diameters of 400, 320, and 200 microns, and used with a crown-down technique at 1.5 W (75 mJ and 20 Hz) with 35–25 % water spray [18, 19].

A study by Minas et al. (2010) showed positive results using Er,Cr:YSGG laser at 20 Hz and different power settings of 1.5, 1.75, and 2,0 W and higher water spray (65 % water, 35 % air). The study concluded that the laser's ablative capacity proved to be strongly influenced by the power and the diameter of the fiber used [20].

On the contrary, other studies reported less positive results regarding the use of the erbium lasers for root canal preparation of teeth with curved roots. The efficacy of laser was not comparable with the endodontic standard preparation with stainless steel manual and nickel-titanium rotary instruments.

The group at the Showa University School of Dentistry, Tokyo, Japan, performed a great body of research on the use of Er:YAG and Er,Cr:YSGG lasers, evaluating the thermal variations at periodontal level, the cleaning ability of dentin surface, and the ablative efficacy in straight and curved canals.

Kimura et al. (2002) measured temperature rise during root canal preparation with the Er:YAG laser for one minute, with a water spray at 2 Hz, 136 mJ, and 230 mJ. The temperature, measured with thermocouples, rose more at apical level (6 °C), demonstrating the safety of the procedure for the periodontal tissues at the tested parameters [21].

Ali et al. (2005), Matsuoka et al. (2005_1), and Jahan et al. (2006) later used a Er,Cr:YSGG laser with a power of 2 W (200 mJ and 10 Hz), with 200 and 320 micron end-firing tips. Irradiation resulted in clean dentin surfaces, with less smear layer and better cleaned surfaces as compared to conventional manual preparation. The studies concluded that the preparation of canals with curves inferior to 10 degrees can be well performed, while the preparation of canals with curves of more than 15 degrees produces ledges, perforation, and over-instrumentation [22–24].

Matsuoka et al. (2005_2), in another study, used the Er,Cr:YSGG laser for canal preparation with fibers of 200 and 320 micron diameter, at 2 W and 3 W and 20 Hz (100 mJ e 150 mJ, respectively), obtaining clean but irregular surfaces [25].

In 2010, Roper et al. (2010) compared conventional root canal preparation techniques with rotative instruments and laser-assisted techniques, measuring the quantity of dentin removed in the various sections of the radicular canals and the cleaning. Both techniques were equivalent in the coronal and the middle third, while the conventional technique was more efficient in the apical one-third [26].

In conclusion, the dentin surface prepared with erbium lasers is always well cleaned and without smear layer. However, as a result of laser ablation, the surface is irregular; some ledging can be present, often there are signs of superficial thermal damage, and there is a risk of root perforation or apical transposition (see Figs. 5.34, 5.35, 5.36 and 5.37). Canal shaping, realized with the erbium laser, is nowadays quite a complicated procedure, suitable only for straight and wide canals but without adding particular advantages to conventional techniques.

6.4 Morphological and Cleaning Effects of Lasers on Root Dentin Surface

Many thermographic and morphological preliminary studies were performed for identifying safe parameters of use and described the collateral effects of laser irradiation on the radicular walls. Medium-infrared lasers, even if they produce some thermal and ablative effects, clean the canal walls very well, vaporizing the smear layer, exposing the dentinal tubules, and increasing dentinal permeability [27–29].

Near-infrared lasers, on the other hand, produce more evident thermal effects without removal of dentin, with areas of recrystallization of the dentin surface where the smear layer is mainly fused, occluding the dentinal tubules [29–33].

When used dry, both near- and medium-infrared lasers produce peculiar thermal effects [30–32].

Irradiation with KTP 532 nm laser, in the spectrum of visible light, used in dry mode at 1 W per 1 s and 5 W per 0.5 s, also led to modifications of the dentin surface and of the smear layer without modifying dentinal permeability [34].

6.4.1 Near-Infrared Laser

Many studies evaluated the thermal rise produced by near-infrared lasers and the consequent morphological alterations of the dentin walls. The smear layer is only partially removed, dentinal tubules are mainly closed as result of superficial fusion of dentin structures, and smear layer and phenomena of recrystallization and cracks are present [33, 35–38].

The effects produced by diode lasers, with different wavelengths, Nd:YAG and Nd:YAP lasers are similar but not equal at the same parameters of use, so that laser settings must be adjusted to the wavelength used. Nd:YAG laser was among the first to be studied in endodontics.

6.4.1.1 Nd:YAG Laser

Saunders et al. (1995) studied in vitro the effects of different laser power settings at 15 pps (from 0.75 to 1.7 W), with the aim of obtaining an

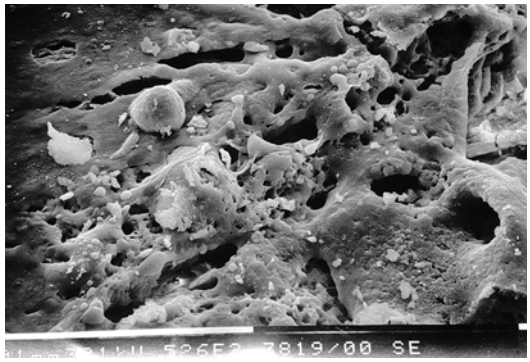

Fig. 6.2 SEM image of radicular dentin irradiated with Nd:YAG laser at 1.5 W, 100 mJ, 300 μs pulse duration, with a 200 micron fiber (2 mm/s speed). Inappropriate time of irradiation, or long pulse duration, or the contact of the fiber on dentin walls creates hot spots. The high magnification shows the dentin surface covered of melted smear layer with obliteration of dentin tubules (Imagine courtesy of Prof. V. Kaitsas Rome (Italy))

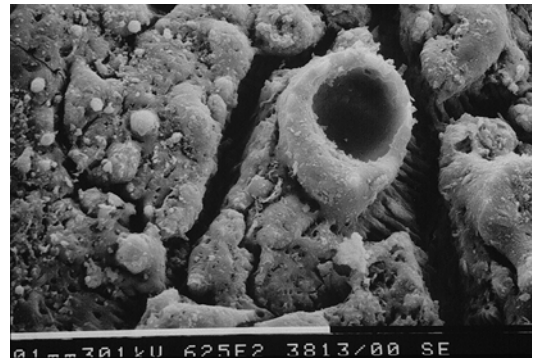

Fig. 6.3 SEM image of radicular dentin irradiated with Nd:YAG laser at 1.5 W, 100 mJ, 300 μs pulse duration, with a 200 micron fiber (2 mm/s speed). Evident melted surface with cracks and recrystallization structures resulted from laser thermal damage (Imagine courtesy of Prof. V. Kaitsas Rome (Italy))

Fig. 6.4 SEM image of radicular dentin irradiated with Nd:YAG laser at 1.5 W, 100 mJ, 300 μs pulse duration, with a 200 micron fiber (2 mm/s speed). Bubbles of recrystallization and cracks resulted from laser thermal damage (Imagine courtesy of Prof. V. Kaitsas Rome (Italy))

apical seal. The study showed the removal of pulp tissue from the non-prepared canals, but there was no creation of complete dentinal fusion [39].

Harashima et al. (1997), in an in vitro study on mono-radicular teeth treated with conventional instruments, irradiated the canals with Nd:YAG laser at 1 W (50 mJ and 20 pps) and 2 W (100 mJ and 20 pps). SEM observation of the non-lased group and the irradiated group at 1 W showed canal surfaces with debris and a smear layer that covered the dentin tubule orifices. Otherwise, the group irradiated at 2 W showed cleaner canal surfaces; debris and smear layer were partially vaporized but areas of fusion and recrystallization were present [40].

Koba et al. (1998), also in vitro, investigated the effects of Nd:YAG laser irradiation, at apical and periapical level. In the majority of cases, there was a good removal of debris, correlated with the energy used. Carbonization was visible on the canal surface at 2 W, 15 pps for 2 s and at 1 W, 15 pps for 3 and 4 s, but not at 1 W, 2 s [41].

Barbakow et al. (1999) observed in vitro areas of recrystallization in the apical area at every energy setting and at 6 and 10 mm from the apex only in the group irradiated with 318 J/cm^2. Areas of carbonization were also observed at 2 mm from the apex [42].

Kaitsas et al. (2001), in an in vitro study on mono-radicular teeth irradiated with Nd:YAG laser after conventional chemomechanical preparation, concluded that irradiation executed at 1.5 W (100 mJ, 15 Hz), with a fiber of 320 microns inserted at 1 mm from the apex and then withdrawn in 5 s with rotatory movement, produced a partial reduction in debris and smear layer together with the production of collateral thermal effects, such as melting, cracks, phenomena of recrystallization with bubbles, and partial obliteration of the dentin tubules [33] (Figs. 6.2, 6.3, and 6.4).

Santos et al. (2005) evaluated with SEM observations the effect of different parameters and angles of irradiation of Nd:YAG laser on the morphology of radicular dentin. Laser irradiation was executed at 1 W (10 Hz, 100 mJ and 20 Hz, 50 mJ) and at 3 W (10 Hz, 300 mJ and 20 Hz, 150 mJ), with a 250 micron fiber, with a retraction speed of 2 mm/s, for 1 min using a clockwise movement. More elevated parameters produced more morphological alterations of the dentin surface, with melting, glazing, recrystallization and bubbles, and superior removal of smear layer with cleaner surface. Two teeth from every group were sectioned perpendicularly and received an irradiation with perpendicular incidence. A sample received, before irradiation, a treatment with 17 % of EDTA for 5 min. The samples which received the perpendicular irradiation showed typical morphological alterations with fusion, melting, and recrystallization with bubbles. The smear layer was not removed from the dentin surface which presented a few visible tubules. The samples which received the irrigation with 17 % EDTA before irradiation showed dentinal tubules more opened and a variegated morphological pattern, depending on the energy used [43].

He et al. (2009) studied the rise in temperature at the coronal and apical levels at different power settings of a Nd:YAG laser, revealing the production of morphological thermal damage. Every sample, mono-radicular tooth, was irradiated four times for 5 s with a pause of 5 s, moving a fiber 330 micron diameter with a helicoidal movement. The most significant rise in temperature was verified at the apical level, with relevant correlation with the power and frequency of repetition used. Better results (removal of the smear layer, open dentinal tubules, rise of temperature in the acceptable limits) were obtained at 2 W (20 Hz, 100 mJ) [38].

Hasheminia et al. (2012) also confirmed the incomplete removal of the smear layer in the samples irradiated with the Nd:YAG laser and the superior efficacy of irrigants such as sodium hypochlorite and maleic acid [44].

6.4.1.2 Nd:YAP

Nd:YAP laser has a physical behavior which is slightly different from that of other near-infrared lasers, due to its major coefficient of water absorption.

Blum and Abadie (1997) underlined the usefulness of this laser in root canal cleaning [9].

Moshonov et al. (2003) also studied the capacity of the Nd:YAP laser for root canal cleaning and its influence on the mineral content of the dentin, confirming the capacity of the laser to provide cleaning statistically superior than the non-lased group, without alteration of the relationship Ca/P at dentinal level [45].

Also here, studies on this specific use were not continued.

6.4.1.3 Diode Laser

In the spectrum of the near-infrared light, diode lasers are built with different wavelengths (from 810 to 1064 nm). Their different positions on the hemoglobin absorption curve condition the adjustment of laser setting to use, but it is the lack of absorption in water that makes the interaction on the radicular dentin different.

Diode Laser 810 nm

Da Costa Ribeiro et al. (2007) studied the increase in temperature during 810 nm diode laser irradiation; at 2.5 W, the thermal rise in the apical third varied from 1.6 to 8.6 °C, while at 1.25 W, 10 Hz proved to be less, from 1.2 °C to 3.3 °C. The SEM morphological study demonstrated canal surfaces with dentinal tubules closed, especially in the apical third [36].

De Moura-Netto et al. (2005) in a study in vitro compared the effect of Nd:YAG laser (1.5 W, 100 mJ, 15 Hz) and of diode laser 810 nm (2.5 W in cw) using a fiber extraction speed of 2 mm/s, for 20 s. Both lasers proved to be able to partially remove debris and smear layer, showing also some morphological alteration (fusion and recrystallization) which was more evident with the Nd:YAG laser [46] (Figs. 6.5, 6.6, and 6.7).

Parirokh et al. (2007), in their in vitro study, concluded that 808 nm diode laser produced closure of the dentinal tubules of the irradiated surface in every condition of use and especially at the level of the apical third [47].

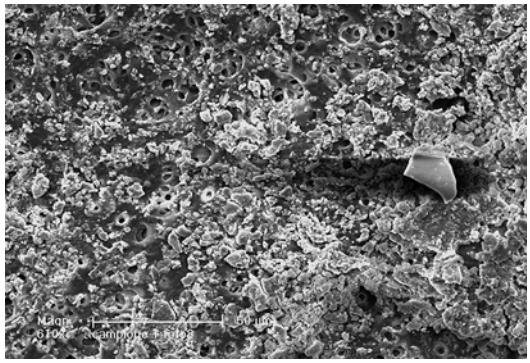

Fig. 6.5 SEM image (610×) of radicular dentin irradiated with 810 nm diode laser in dry mode at 2.5 W, 50 % duty cycle, 10 ms t^{on}, and 200 micron fiber (2 mm/s speed). Dentin surface showing debris, melted smear layer, and few open orifices

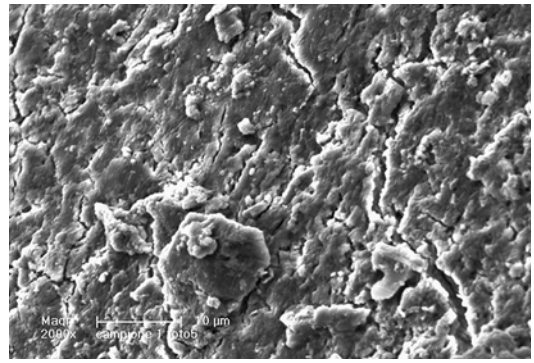

Fig. 6.7 SEM image (2000×) of radicular dentin irradiated with 810 nm diode laser in dry mode at 2.5 W, 50 % duty cycle, 10 ms t^{on}, and 200 micron fiber (2 mm/s speed). Heavy smear layer heated by laser irradiation covering dentin surface

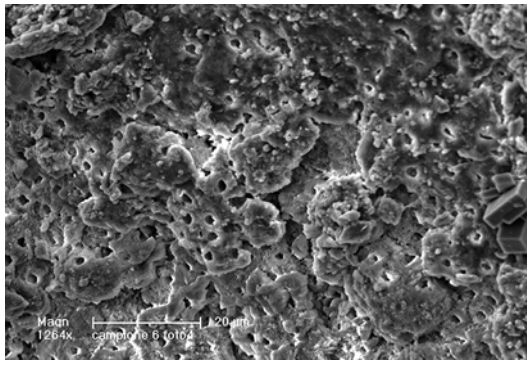

Fig. 6.6 SEM image (1264×) of dentin irradiated with 810 nm diode laser, at 1.5 W CW, 200 micron fiber, in dry mode (2 mm/s speed). Clear signs of thermal effect are visible: surface melting with detachment of dentinal substance and partial obliteration of the dentinal tubules. The smear layer is only partially removed (Reprinted with permission from Olivi et al. [70]) (Fig. 2))

Da Fonseca Alvarez et al. (2012) studied with thermocouple the variation of temperature on the external root surface of inferior incisors in order to evaluate possible periodontal damage. Samples were irradiated with a continuous circular retrograde movement at different parameters (1.5, 2.0, 2.5, 3.0, and 3.5 W). Thermal variations, measured on both buccal and lingual sides, at the apical level and at the middle third of the root were considered acceptable and safe within 7 °C, only the use of 3.5 W exceeded the 7 °C borderline [48].

Diode Laser 980 nm

Diode laser 980 nm was studied in vitro by Wang et al. (2005), who irradiated mono-radicular teeth for 7 s with different diameter fibers (550 and 365 micron) at 5 W power. The maximum rise in temperature was 8.1 °C. Laser irradiation produced good removal of smear layer, with cleaning statistically superior to the nonirradiated control group. Apical leakage, after the filling, also proved inferior in the laser group than in the control group [49].

The Brazilian group in the Endodontics Department of the University of Ribeirão Preto (SP, Brasile) carried out a series of in vitro studies on the 980 nm diode laser, investigating the morphological and thermal variations at radicular level with parameters from 1.5 to 5 W, in CW and gated at 100 and 1000 Hz, both dry and distilled water wet canals.

Marchesan et al. (2008_1) evaluated the effect on the dentinal permeability of the diode laser 980 nm after final irrigation with different solutions: distilled water, 1 % NaOCl, and 17 % EDTAC. Irradiation was performed at 1.5 and 3.0 W both in a continuous wave and gated mode (100 Hz). The laser irradiation associated with water produced an increase in dentin permeability, while a reduction in permeability was found with laser irradiation after the use of EDTAC, the conclusion being that the dentinal permeability is strictly dependent on the final irrigation solution [50].

Marchesan et al. (2008_2) evaluated also the morphological effect produced on the dentinal wall with the same parameters. Irradiation was executed using a helicoidal movement in exit for 20 s with different emission modes (1.5 W in CW and at 100 Hz, 3 W in CW and at 100 Hz), producing variable results from removal of the smear layer to fusion [51].

Alfredo et al. (2008) also evaluated the temperature variation using thermocouples localized at radicular and apical level, after irradiation with 980 nm diode laser at the studied parameters: 1.5, 3.0, and 5.0 W in CW and gated mode at 100 and 1000 Hz, both dry and irrigated with distilled water. The radicular portion with the major increase of temperature was the cervical third (+9.68 ± 5.80 °C), followed by the middle third (+7.66 ± 4.87 °C) and apical (+6.70 ± 4.23 °C), with a significant statistical difference between them. The continuous mode of irradiation, dry and with more power (3 W e 5 W), produced disadvantageous thermal variations (respectively +12.15 ± 5.14 °C and +7.88 ± 3.92 °C), which definitively contraindicate the use of those parameters and conditions of use. Continuous irradiation produced a more elevated thermal variation (+11.82 ± 5.78 °C), whether the canal was wet or dry. Gated mode irradiation produced less thermal rise, without statistically significant differences, at 100 Hz (+6.22 ± 3.64 °C) and 1000 Hz (+6.00 ± 3.36 °C). The authors concluded that canal irradiation with the 980 nm diode laser at 1.5 W, in every operational mode and at 3.0 W at 100 Hz, and 1000 Hz, for 20 s, can be used safely in endodontics in both dry and wet canals [37].

In a successive study, Alfredo et al. (2009) evaluated the alteration of the canal dentin irradiated with the 980 nm diode laser at different parameters, i.e., 1.5 and 3 W in CW and gated mode at 100 Hz after irrigation with NaOCl and EDTA. It was concluded that the laser produced morphological alterations depending on the chemical pre-treatment. Pre-treatment with NaOCI showed surfaces with typical morphological alterations induced by lasers with some cracks; smear layer and closed dentinal tubules were present; those pretreated with EDTA and then irradiated presented melting areas but instead no smear layer and partially open tubules and [52]. This combined treatment is explored ahead in Sect. 6.4.6.

6.4.2 Medium-Infrared Laser

Erbium:YAG and erbium,chromium:YSGG lasers interact with the watery component of the dentin. Consequently, laser settings above the dentin threshold of ablation, the presence or not of air-water spray or of irrigants during irradiation, are all conditions that affect the morphological effects on the dentinal surface. The latter may vary from the removal of smear layer and superficial ablation to thermal damage with areas of superficial melting and creation of ledges and perforations.

Takeda et al. (1999) compared, in vitro, the effects of laser irradiation with 17 % EDTA, with that of 6 % orthophosphoric acid and that of 6 % citric acid. The effects of the CO_2 and Er:YAG lasers lead to the removal of the smear layer. The study concluded that the irrigant solutions produced excessive intertubular demineralization with notable enlargement of dentin tubules. CO_2 lasers on the other hand, produced fusion of the smear layer with superficial melting, while Er:YAG lasers proved to be the most efficient system for removal of the smear layer [53].

The Japanese school of the Department of Endodontics, Showa University School of Dentistry (Tokyo, Japan), conducted a great deal of research on the use of erbium:YAG and erbium,chromium:YSGG lasers.

Yamazaki et al. (2001) concluded their studies on erbium,chromium:YSGG laser, stating that the presence of water was essential to avoid undesired morphological aspects, strongly present when the irradiation was performed in dry mode. The erbium,chromium:YSGG laser, used in dry mode, besides the researched vaporization of the smear layer, produced undesired signs of ablation and thermal damage, proportionally to the power used. SEM investigation of the irradiated surface showed the presence of ledges, cracks, and melting [54].

Kimura et al. (2002) investigated the thermal rise using thermocouples located on the radicular

surface after irradiation with Er:YAG lasers at 2 Hz, 136–184 mJ and 170–230 mJ for 1 minute with air-water spray. Teeth were then observed using stereo microscope and SEM. The thermal rise found at the apical level was less than 6 °C in the apical area and less than 3 °C in the radicular one-third. Morphological observations revealed the absence of carbonization or melting, using 230 mJ/pulse for 1 min [21].

When using air-water spray or in the presence of irrigant solutions, a typical pattern of dentin irradiated with the erbium laser is visible. Thermal damage is reduced; vaporization of intertubular dentin is greater than of peritubular dentine, showing a protrusion of the dentinal tubules with a cuff-like appearance; dentinal tubules are open at the peak of these peritubular areas (with more calcified dentin then for intertubular dentin and therefore less ablated). The smear layer is vaporized by irradiation with the erbium laser and mainly absent [27, 28].

Later on, Ishizaki et al. (2004) also investigated thermal rise on the periodontal surface and the morphological alterations on the dentin walls after irradiation with Er,Cr:YSGG lasers, used for smear layer removal after manual instrumentation. The Er,Cr:YSGG laser was used at 2 W (100 mJ, 20 Hz), 3 W (150 mJ, 20 Hz), and 5 W (250 mJ, 20 Hz), for 7 s with fibers of different diameters (200, 320, and 400 microns). The thermographic study showed an average thermal rise inferior to 8 °C. Observations with optical microscope showed aspects of dentin ablation at the apical terminus, while SEM indicated that the use of 5 W (250 mJ, 20 Hz), with a fiber of 400 microns, proved to be efficient in removing debris and smear layer without carbonization or melting [55].

Silva et al. (2010) investigated canal morphology and dentin permeability after Er,Cr:YSGG laser irradiation, in comparison with conventional preparation associated with EDTA-T irrigation and with conventional preparation associated with EDTA-T and irradiation with the Er,Cr:YSGG laser at different power settings: 0.75, 1.5, 2.5 W, always at 20 Hz. SEM investigation revealed irregular surfaces with morphological alterations that increased dentinal permeability, when using the laser at 1.5 W and 2.5 W [56].

Kimura et al. (2011) conducted histological examinations of the radicular surface in order to evaluate possible thermal damage after 30 s of Er:YAG laser irradiation of root canal at 2 Hz with energy of 34, 68, and 102 mJ/pulse. Irradiation with 34 mJ did not produce any thermal damage at the periodontal level, proving to be a safe parameter for irradiation. Irradiation with 68 and 102 mJ produced, in some cases, inflammation, from medium to high, with external resorption of the root surface. The difference between the control group and the laser group was not significant, with the conclusion of minimal thermal influence on the periodontal tissues, if appropriate parameters are used [57].

A study of Ebihara et al. (2012) evaluated the effects of Er:YAG laser irradiation at different parameters. The investigated fluence was 10–30 J/cm^2, using a 400 micron fiber, at 30 Hz; different pulse durations (80–280 microns) with and without cooling with air-water spray were applied. The morphological observation, performed with CLSM (confocal laser scanning microscopy) and with SEM (scanning electron microscopy), showed root canal dentin surface ablation and absence of debris in most of the irradiation conditions. Three-dimensional images revealed no smooth dentin walls. Strong melting and recrystallization, or unusually flat surfaces with open dentinal tubules, were obtained with sequences of three pulses without water cooling. This study demonstrated that varying the irradiation conditions affected the modifications of root canal surfaces [58] (Figs. 6.8, 6.9, 6.10, and 6.11).

6.4.3 Comparative Studies on Different Laser Wavelengths

A number of studies also compared the differing effects of several wavelengths on the canal surface. The real differences between wavelengths became clear, as well as the influence of some settings and modalities of use on the dentinal morphological changes after laser irradiation.

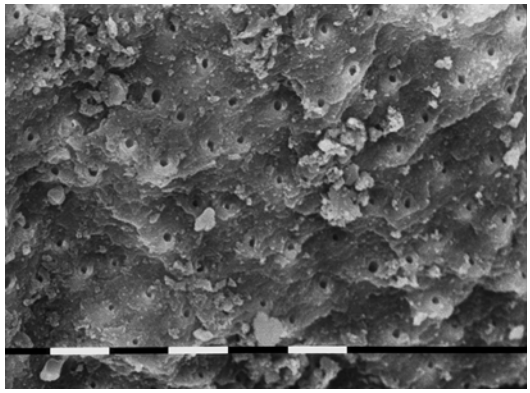

Fig. 6.8 SEM image of radicular dentin irradiated with Er,Cr:YSGG at 1.5 W, 20 Hz, air-water laser spray 35–25 %, 200 micron end-firing tip (2 mm/s speed). Signs of ablation, open dentinal tubules, and few debris are present

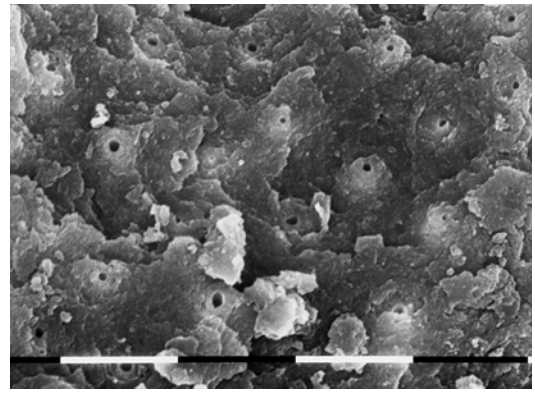

Fig. 6.10 SEM image of radicular dentin irradiated with Er,Cr:YSGG at 1.5 W, 20 Hz, air-water laser spray 35–25 %, 200 micron end-firing tip (2 mm/s speed). Dentin surface shows superficial laser thermal damage. Dentin tubules are open with few debris

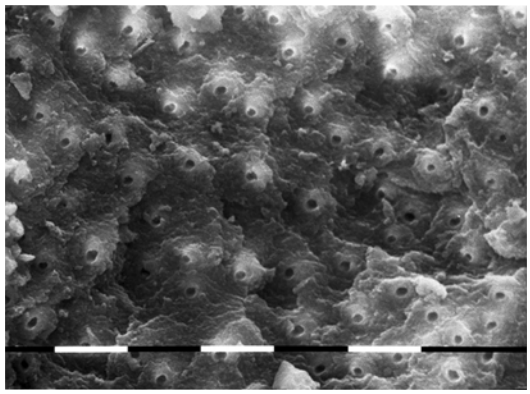

Fig. 6.9 SEM image of radicular dentin irradiated with Er,Cr:YSGG at 1.5 W, 20 Hz, air-water laser spray 35–25 %, 200 micron end-firing tip (2 mm/s speed). Typical signs of laser ablation, with typical chimneylike aspect, open dentinal tubules, and debris mainly absent in this area

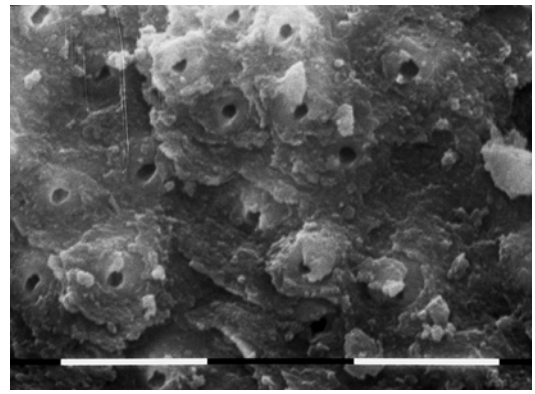

Fig. 6.11 SEM image of radicular dentin irradiated with Er,Cr:YSGG at 1.5 W, 20 Hz, air-water laser spray 35–25 %, 200 micron end-firing tip (2 mm/s speed). Dentin surface with open orifices and typical flaky surface related to laser-ablative thermal effect

Takeda et al. (1998) compared the smear layer removal efficacy of three lasers: argon, Nd:YAG, and Er:YAG versus a control group irrigated with 17 % EDTA, after conventional instrumentation, in vitro. Statistical analysis showed significant differences between the control and the laser groups. Er:YAG laser irradiation (1 W, 100 mJ at 10 Hz) resulted in absence of smear layer and the presence of open dentinal tubules in the middle and apical one-third. The Nd:YAG laser (2 W, 200 mJ at 20 Hz) showed vaporization of the smear layer but also areas of fusion and recrystallization in the middle or apical one-third. The argon laser (1 W, 50 mJ at 5 Hz) showed the presence of pulp remnants in the middle one-third [27].

Kivanc et al. (2008), at the end of their comparative SEM studies on the effects of Nd:YAG and Er:YAG laser irradiation on radicular dentin, concluded that neither wavelength was efficient in removing the smear layer and debris from the canal walls [59].

Watanabe et al. (2010) evaluated thermal variations and dentin stress induced by laser irradiation, with or without air-water spray cooling. The canal was irradiated with Er:YAG and Nd:YAG lasers at a power of 1 W (100 mJ, 10 pps) per 5 s. The fiber was positioned 2 mm short from the apex. Using water cooling, the mean maximum strain induced by the Er:YAG laser was significantly lower than that of the Nd:YAG laser. However, without cooling, there were no significant differences between the two laser systems. The results suggested that the modifications induced by irradiation with water cooling were minimal and that the risk of microfractures remained in the case of insufficient cooling [31].

Esteves-Olveira et al. (2010) conducted a comparative study on morphological alterations and dentinal permeability variations after irradiation with three lasers of different wavelengths: 808 nm diode, Nd:YAG, and Er:YAG. Root-filled teeth were colored blue with 2 % methylene blue after irradiation, divided into two halves and photographed. The percentage of penetration of the colorant in the cervical, middle, and apical third was calculated by software for statistical analysis. The group irradiated with the Nd:YAG laser showed reduced penetration of colorant in all canal areas and melted surfaces and the presence of partially obliterated dentinal tubules. The diode and Er:YAG laser group showed more permeability, with values statistically superior to the control group and Nd:YAG. SEM analysis confirmed the variation of the observed canal permeability, showing canal surfaces with diffuse obliteration of dentinal tubules and areas of melting in the Nd:YAG group; the diode laser group showed surfaces with dentinal tubules mainly obliterated, while the Er:YAG group showed clean surfaces, without smear layer and with dentinal tubules open [60].

In investigations of the group of Ghent (Ghent Dental Laser Centre) by Michiels et al. (2010) and Vergauwen et al. (2014), the previously described effects of Nd:YAG and Er,Cr:YSGG on the root canal walls were confirmed [61, 62]. Michiels et al. (2010) demonstrated that the classic melting and glazing effects were absent root canals that were rinsed with EDTA (smear layer removed) [61]. When these effects occurred, these were seen in areas where the fiber had touched the root canal wall.

6.4.4 Laser and Irrigation for Root Canal Cleaning

Many studies reported that the combined action of both canal irrigation and laser irradiation led to better cleaned surfaces as compared to the action of just one solely. These studies, even if they were not always univocal, were an introduction to those of the laser activation of the irrigants (LAI) (see Chaps. 10 and 11).

The first lasers to be used in wet canals with water or irrigants were the Er:YAG laser [63–69] and the Er,Cr:YSGG laser [18, 19] and later the near-infrared laser [32, 43, 50, 52, 70].

Pecora et al. (2000) investigated in vitro the increase in dentinal permeability produced by the irradiation of Er:YAG lasers after endodontic instrumentation and irrigation with sodium hypochlorite. The study investigated different combinations of irrigation associated or not with laser irradiation, using deionized water or 1 % NaOCl. Erbium YAG lasers, used at 2.1 W (140 mJ, 15 Hz) for 20 s in distilled water, produced a major permeability increase. The use of laser with 1 % NaOCl after endodontic instrumentation, followed by a final rinsing with 1 % NaOCl, produced intermediate results, while irrigation alone, without the use of laser, resulted in the lowest permeability [63].

Brugnera et al. (2003) evaluated in vitro the effects of Er:YAG and Nd:YAG lasers on the permeability of canal dentin using distilled or deionized water or 1%NaOCl as irrigants after manual endodontic instrumentation. The results of the study were similar to those of Pecora et al. with Er:YAG laser irradiation with water producing higher dentin permeability. The use of 1 % NaOCl, with or without Er:YAG laser irradiation, showed intermediate results, while the use of 1 % NaClO and distilled or deionized water associated with the Nd:YAG laser showed a lower increment in permeability [64].

Biedma et al. (2005) compared the cleaning effects of EDTA and sodium hypochlorite irrigation

alone or associated with Er:YAG laser irradiation at 1 W (100 mJ, 10 Hz), performed with a 285 micron fiber withdrawn with an apical-coronal movement at a speed of 2 m/s. The combination of irrigation-laser irradiation produced better cleaning. However, there were areas not perfectly cleaned with obliterated dentinal tubules [65].

Similar results were obtained by Altusandar et al. (2006) using the Er,Cr:YSGG laser, sodium hypochlorite, and a urea peroxide gel (RC-Prep). SEM observation revealed insufficient removal of the smear layer from the group irrigated solely with 5.25 % NaOCl; the group treated with a combination of RC-Prep and 5.25 % NaOCl showed a moderate presence of smear layer but also clear areas of exposed collagen. The group treated with a combination of 5.25 % NaOCl irrigation and Er,Cr:YSGG laser irradiated, followed again by NaOCl irrigation, showed the major removal of the smear layer, even if some areas of thermal damage, with carbonization and melting were observed [66].

Radatti et al. (2006) compared the efficacy of the Er,Cr:YSGG laser associated with two irrigation protocols and conventional irrigation protocols alone for the removal of debris after endodontic instrumentation, using 0.5 ml distilled water or 5.25 % NaOCl. Laser irradiation with just distilled water leaves more smear layer compared with conventional irrigation. Laser irradiation with 5.25 % NaOCl did not result in statistically significant differences with conventional irrigation [67].

Varella et al. (2007) evaluated numbers of lateral canals and isthmus obturated after different treatments: 17% EDTA for 3 minutes, Er,Cr:YSGG laser for 40 s, and control group. The laser-irradiated group showed a statistically superior number of obturated canals/isthmus [68].

Watanabe et al. (2010) evaluated thermal variations or dentinal stress induced by laser irradiation with water cooling and concluded that these were minimal and that the risk of microfractures remained in case of insufficient cooling [31].

Kalyoncuoğlu and Demiryürek (2013) analyzed with SEM the canal surface of monoradicular teeth after chemomechanical preparation followed by different methods of final irrigation: 5.25 % NaOCl, 17 % EDTA, BioPure MTDA, Er:YAG laser irradiation at 1.8 W (120 mJ, 15 Hz), or irradiation with Nd:YAG laser at 1 W (100 mJ, 15 Hz). Irrigation with EDTA and NaOCl brought about superior cleaning in every canal area, without statistically relevant differences. All the techniques produced an efficient cleaning action [69].

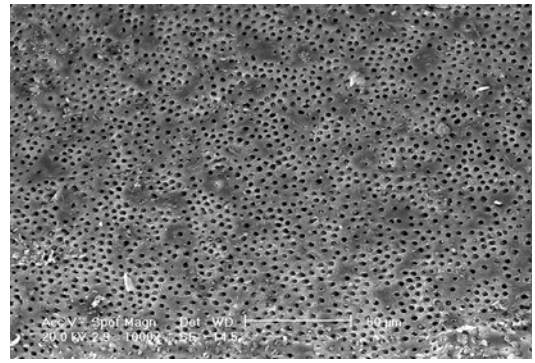

Fig. 6.12 SEM image (1000×) of radicular dentin irradiated with 810 nm diode laser at 2.5 W in gated mode (20 ms t^{on} and 20 ms t^{off}) with 200 micron tip, in root canal irrigated with 17 % EDTA (2 mm/s speed). Dentin surface with dentin tubules mainly opens with few debris and smear layer (Reprinted with permission from Olivi et al. [70] (Fig. 3))

In the near-infrared spectrum of light, both the 810 nm laser, the 940 and 980 nm lasers, as well as the 1064 Nd:YAG laser were studied in association with different irrigants as the final step, for cleaning and decontamination at the end of endodontic treatment. Several studies (Santos et al. 2005; Gurbuz et al. 2008; Faria et al. 2008; Marchesan et al. 2008_1; Alfredo et al. 2009 and Olivi et al. 2013) reported that when the canal is irradiated after or together with different irrigants (distilled water, EDTAC, chlorhexidine, sodium hypochlorite), the morphological pattern is better or similar to that produced by just the irrigation alone [32, 43, 50, 52, 70, 71] (Figs. 6.12, 6.13, 6.14, 6.15, 6.16, and 6.17).

Gurbuz et al. (2008) evaluated the effect of five different irrigant solutions combined with Nd:YAG laser irradiation on the morphology of root canal dentin surface. The use of 15 % EDTA, followed by irradiation with Nd:YAG laser, produced the best canal cleaning [71] (Figs. 6.18, 6.19, 6.20, and 6.21).

Faria et al. (2008) demonstrated that the increase in temperature was not dangerous, at a

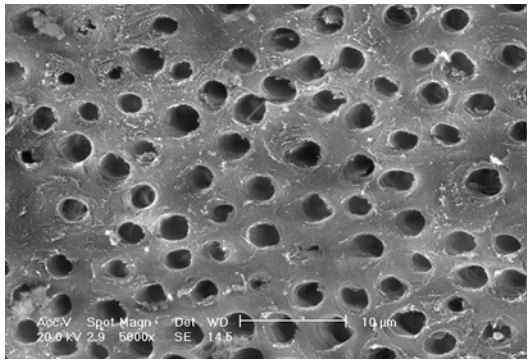

Fig. 6.13 SEM image (5000×) of radicular dentin irradiated with 810 nm diode laser at 2.5 W in gated mode (20 ms t^{on} and 20 ms t^{off}) with 200 micron tip, in root canal irrigated with 17 % EDTA (2 mm/s speed). Dentin surface with dentin tubules mainly opens with some debris and smear layer. The EDTA action produces partial exposure of intertubular and peritubular collagenic fibers. No thermal damage visible (Reprinted with permission from Olivi et al. [70] (Fig. 4))

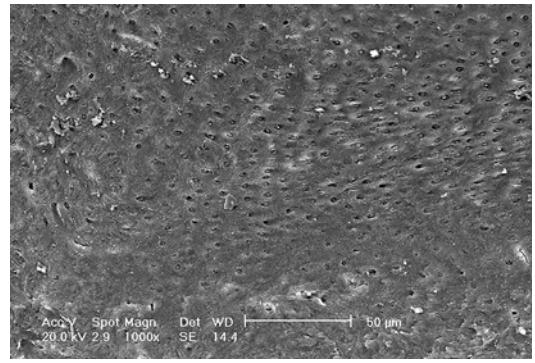

Fig. 6.15 SEM image (1000×) of radicular dentin irradiated with 810 nm diode laser at 2.5 W in gated mode (20 ms on and 20 ms off) with 200 micron tip, in root canal irrigated with 5 % NaOCl (2 mm/s speed). Dentin surface is quite clean, but orifices of dentin tubules are mainly plugged from debris and dentin tubules. Laser thermal damage is not visible (Reprinted with permission from Olivi et al. [70] (Fig. 6))

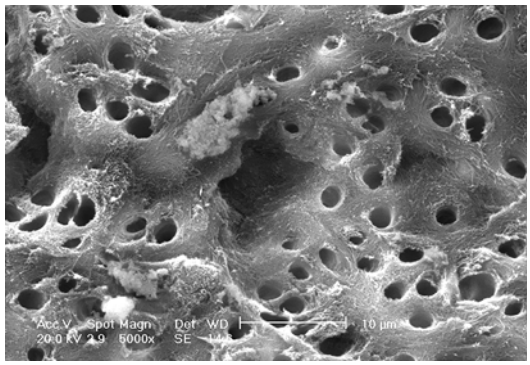

Fig. 6.14 SEM image (5000×) of radicular dentin irradiated with 810 nm diode laser at 2.5 W in gated mode (20 ms on and 20 ms off) with 200 micron tip, in root canal irrigated with 17 % EDTA (2 mm/s speed). Dentin surface with dentin tubules mainly opens with some debris and smear layer. The EDTA action produces partial exposure of intertubular and peritubular collagenic fibers. No thermal damage visible (Reprinted with permission from Olivi et al. [70] (Fig. 5))

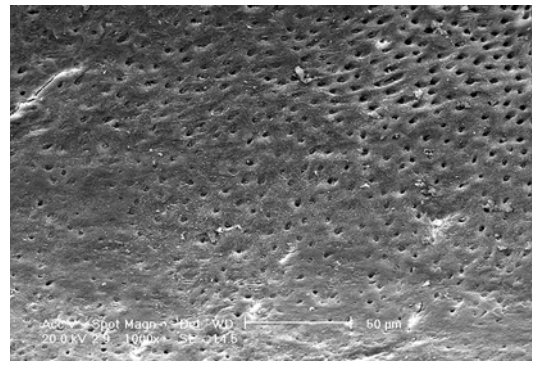

Fig. 6.16 SEM image (1000×) of radicular dentin irradiated with 810 nm diode laser at 2.5 W in gated mode (20 ms on and 20 ms off) with 200 micron tip, in root canal irrigated with 5 % NaOCl (2 mm/s speed). Dentin surface is quite clean, but orifices of dentin tubules are mainly plugged from debris and dentin tubules. Laser thermal damage is not visible (Reprinted with permission from Olivi et al. [70] (Fig. 7))

power ranging from 1.5 W up to 3 W (100–1000 Hz). The use of 5 W brought about elevated increases in temperature, independent of the continuous or gated modality of emission. However, the samples irradiated in dry mode confirmed the production of areas of fusions, craters, and carbonization, with partially open dentin tubules. When the irradiated canal was treated with different irrigants (distilled water, EDTAC, chlorhexidine, sodium hypochlorite), the morphological situation became better. The irradiated samples, irrigated with just distilled water, showed surfaces modified by the action of the laser and incorporated the smear layer. The best results were observed in the samples treated with EDTAC that showed absence of smear layer. The samples irrigated with NaOCl and chlorhexidine showed intermediate morphological results, with

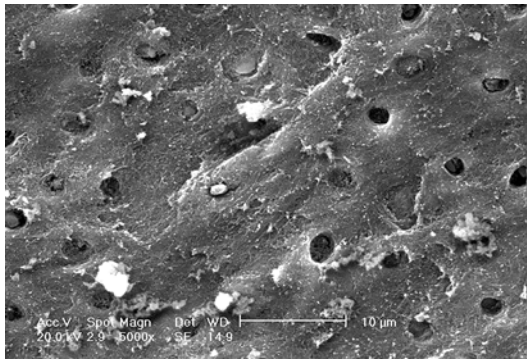

Fig. 6.17 SEM image (5000×) of radicular dentin irradiated with 810 nm diode laser at 2.5 W in gated mode (20 ms on and 20 ms off) with 200 micron tip, in root canal irrigated with 5 % NaOCl (2 mm/s speed). Orifices of dentin tubules are mainly obliterated by debris and smear layer; thermal damage is not visible (Reprinted with permission from Olivi et al. [70] (Fig. 8))

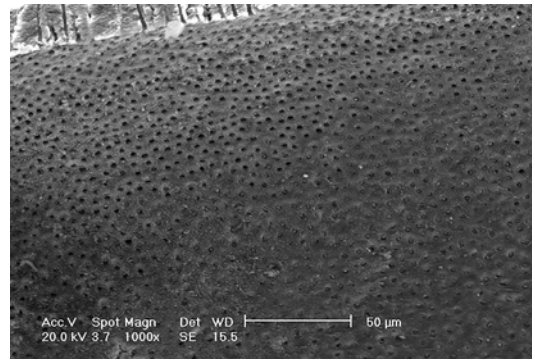

Fig. 6.18 SEM image (1000×) of radicular dentin irradiated by Nd:YAG laser at 1.5 W, 15 Hz, 100 mJ, and 100 µs pulse duration, with a 200 micron fiber (speed retraction 2 mm/s) used for two cycles of 5s after 20s NaOCl irrigation; this protocol is followed by irrigation with EDTA and again by Nd:YAG irradiation (2×5 s) in wet canal. The canal surface is mainly clean from smear layer with dentin plugs occluding the orifices of dentin tubules

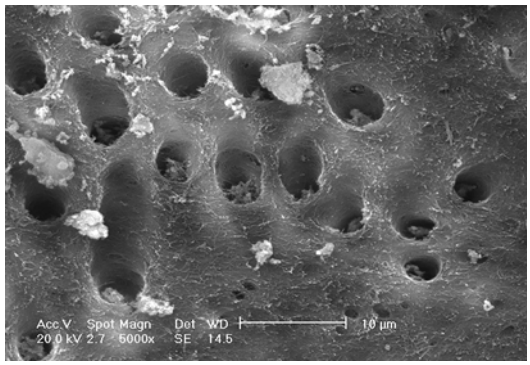

Fig. 6.19 SEM image (5000×) of radicular dentin irradiated by Nd:YAG laser at 1.5 W, 15 Hz, 100 mJ, and 100 µs pulse duration, with a 200 micron fiber (speed retraction 2 mm/s) used for two cycles of 5s after 20s NaOCl irrigation; this protocol is followed by irrigation with EDTA and again by Nd:YAG irradiation (2×5 s) in EDTA wet canal. The use of the irrigants prevents thermal damage of the surface with a pattern more similar to that of the irrigant than of the laser used. The EDTA exposed the collagen fibers and cleaned the surface: few residual debris are present

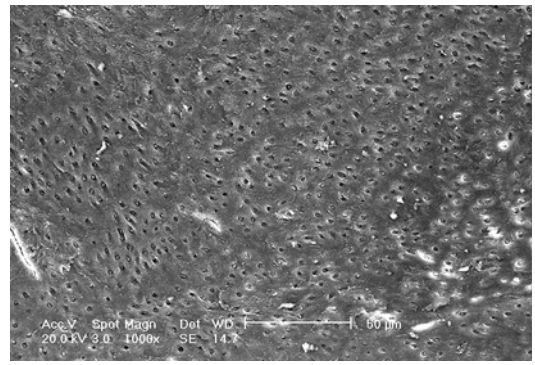

Fig. 6.20 SEM image (1000×) of radicular dentin irradiated by Nd:YAG laser at 1.5 W, 15 Hz, 100 mJ, and 100 µs pulse duration, with a 200 micron fiber (speed retraction 2 mm/s) used for 2 cycles of 5 s after 20s EDTA irrigation; this protocol is followed by final dry Nd:YAG irradiation (2×5 s). The surface is cleaned by EDTA, dentin tubules orifices present some dentin plugs partially obliterating the entrance; laser thermal damage is not visible

some areas of fusion and partially closed dentinal tubules [32].

Hmud et al. (2010_1) observed with the microscope the formation of cavitation in the tested solutions in microvial, using a diode 940 nm laser at 2.5 W/25 Hz and a diode 980 nm laser at 4 W/10 Hz, equipped with a 200 micron endodontic fiber. More cavitation was observed using 3 % hydrogen peroxide instead of distilled water [72].

Completing the preceding study, Hmud et al. (2010_2) determined the rise of temperature both inside the canal solution and at radicular level, during 5 s of irrigation with the tested solutions.

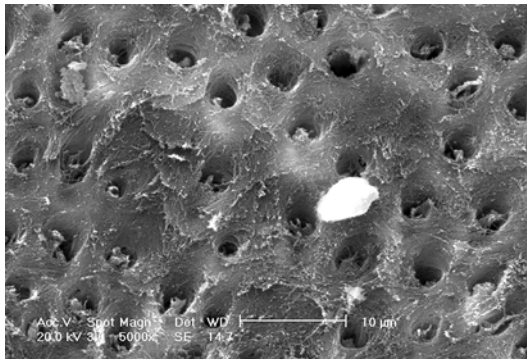

Fig. 6.21 SEM image (5000×) of radicular dentin irradiated by Nd:YAG laser at 1.5 W, 15 Hz, 100 mJ, and 100 µs pulse duration with a 200 micron fiber (speed retraction 2 mm/s) used for two cycles of 5s after 20s EDTA irrigation; this protocol is followed by final dry Nd:YAG irradiation (2×5s). The EDTA cleaned the surface, exposed the collagen fibers, and improved the dentin permeability. The EDTA morphologic pattern is produced and is not altered by the last dry irradiation

The increase in temperature in the watery solution reached 30 °C, while the maximum thermal rise on the radicular surface was 4 °C only [73].

Besides, Deleu et al. (2013), in a preliminary study, defined a minimum power of 7.5 W at 25 Hz, used for 18 s with a 200 micron fiber with 2.5 % NaOCl, in order to produce cavitation with the diodes 980 nm laser [74].

An unpublished study by the author used 810, 940, and 980 nm lasers, at power of 2.5 W/25 Hz and 4 W/10 Hz, respectively, with 5 % NaOCl irrigant, in order to evaluate the type of activation produced; irradiation for 15 s produced only minimal effervescence, to be correlated with the thermal rise (warming) produced by the laser more than by the cavitation.

The combined action of the irrigants with infrared laser irradiation was investigated by other authors for decontamination of the radicular canals and is presented in Sect. 6.5.2 [75, 76].

6.5 Laser Root Canal Decontamination

Reducing the residual bacterial load at the end of root canal treatment is the main goal for achieving a successful therapy. Full decontamination and hermetic root canal sealing reduce the possibility of recolonization of the root canal system, which causes the maintenance of periapical pathology. The gold standard in endodontics is still today, to use chemical irrigants, in particular sodium hypochlorite [77]. However, the conventional manual technique of irrigation demonstrated limited penetration depth, and Berutti et al. (1997) reported the limited decontaminating efficacy of sodium hypochlorite beyond 130 microns in dentin wall [78], while bacterial colonies have been found up to 1.15 mm from the main canal into the dentinal tubules [79].

Besides the research on different systems of activation of the irrigants, discussed in Chaps. 3, 8, and 9, extensive research was focused on the use of laser light to achieve better results in root canal decontamination.

Each laser wavelength can, through direct or indirect thermal effect, generate morphological alterations on the bacterial cell wall, leading to the death of the bacterial cells.

A first possible mechanism suggests that laser light is absorbed by the bacteria and is therefore responsible for direct damage to the bacterial cell; the most likely reason for this is the presence of black pigments (protoporphyrin IX) in some bacteria, which can absorb a limited portion of the wavelength spectrum, specifically within the near-infrared spectrum [80]. Damage takes place at the level of the cellular membrane and induces osmotic alteration that leads to cellular death [81, 82].

However, *Escherichia coli* and *Enterococcus faecalis* (nonpigmented bacteria), bacteria mostly used in decontamination studies, appear to be almost completely transparent to the 810 and 1064 nm wavelengths, and both these wavelengths have negligible direct bactericidal effects. Gram + bacteria such as *E. faecalis* are more resistant to desiccation due to the structure of their cell wall when compared to Gram − bacteria such as *E. coli* (84). In this case, the bactericidal mechanism of near-infrared lasers seems to require the presence of oxygen in the bacterial microenvironment [83, 84].

The second hypothesized mechanism suggests that the laser light is strongly absorbed in the dentin substrate onto which the bacteria adhere;

the resultant heating of the substrate causes a local rise in temperature, high enough to result in the death of the attached microorganisms [80, 85].

However, some studies reported no significant relation between temperature increase and bactericidal effect [86]; in this case, the bactericidal effect was supposed to be related to an unidentified photodamage effect [83, 84]. This appears contradictory in comparison to most of the studies that reported a bactericidal effect related to the power applied and to the thermal effect of lasers, leaving confusion on the real laser mechanism in canal decontamination.

The thermographic and morphological studies, already discussed in this chapter, represented a preliminary passage to identify safe parameters for laser decontamination of root canals.

All wavelengths have an efficient decontaminating action on the main canal surface; however, near- and medium-infrared lasers have a different capacity of penetration in dentin tubules.

Efficient decontamination depends on the interaction (absorption or diffusion) between wavelengths, energy, and parameters of use with tissues and bacteria in their variants: Gram+ or Gram−, pigmented or not. Moreover, the bacteria are also present in planktonic form or aggregated in biofilm, depending on the stadium of the periradicular lesion [87, 88]. Bacteria like *E. faecalis* usually form intraradicular biofilms, which complicate complete eradication; consequently, *E. faecalis* and other bacteria are often found to be responsible for those resistant cases and can cause long-term failures after accomplished root canal treatment.

6.5.1 Visible and Near-Infrared Laser Decontamination

Hardee et al. (1994), among the first, studied and compared Nd:YAG laser decontamination with 0.5 % sodium hypochlorite (NaOCI) irrigation or the combination. None of the samples showed complete decontamination of the root canal, and no statistically significant differences between the groups were found [89].

Fegan and Steiman (1995) evaluated different techniques of instrumentation and compared the decontaminating effectiveness of Nd:YAG laser and NaOCl, concluding that every technique that used sodium hypochlorite led to an efficient inhibition of bacterial growth [90].

Moshonov et al. (1995) investigated in vitro the efficacy of the Nd:YAG laser for canal disinfection of *Enterococcus faecalis.* Laser irradiation brought about a significant bacterial reduction, but the irrigation with NaOCI led to the most efficient canal disinfection [91].

Gutknecht et al. (1996) presented a first, positive clinical follow-up evaluating root canal therapy on teeth with apical lesions treated with Nd:YAG laser [92].

Ramsköld et al. (1997) investigated the parameters of safety and efficacy for canal decontamination with the Nd:YAG laser. The use of four cycles of irradiation at 3 W (150 mJ, 20 Hz) for 15 s, with a 15 s break between cycles, proved to be safe, without any risk of thermal damage and efficient in decontaminating seven out of the eight treated canals [93].

Also Blum et al. (1997) compared the efficacy of Nd:YAP laser disinfection, at 1,3 W (5 Hz, 260 mJ), at 2,6 W (10 Hz, 260 mJ), and at 9 W (30 Hz, 300 mJ), with conventional irrigation with 5.25 % NaOCl, in canals infected with *Streptococcus mitis*. Irrigation with NaOCl proved more efficient in inhibiting bacterial growth, while the Nd:YAP laser was efficient only at the elevated energy of 300 mJ at 30 Hz [94].

Klinke et al. (1997) evaluated in vitro the depth of the bactericidal effect of Nd:YAG laser irradiation, using an experimental model based on longitudinal sections of dentin slices, varying in thickness (100–1000 microns). The specimens were inoculated on one side with *Streptococcus mutans* suspension and irradiated on the opposite side at a different distance (100–1000 microns). The Nd:YAG laser was used four times for 10–20 s, at 1.5 W (15 Hz, 100 mJ) with a 200 micron fiber, with an irradiation angle on dentin slices of about 5° and obtained significant elimination of bacteria up to 1000 microns [95].

The School of Vienna made various bacteriological studies on different wavelengths. Moritz et al. (1997) began studies on canal decontamination with diode laser 810 nm, using teeth infected by *E. coli* and *E. faecalis*, irradiated with five cycles of 5 s at 4 W in gated mode with 10 ms t_{on} and t_{off}, reporting complete bacterial eradication after irradiation. The infrared spectroscopic examination revealed a thermal rise of 6 °C on the radicular surface, while the dye penetration study and the SEM examination showed the complete closure of the dentin tubules of irradiated canal surfaces [96].

A microbiological study in vitro on 30 patients (1997), treated with Nd:YAG laser irradiation, led to a reduction in the *Streptococcus* bacterial load in 19 canals and a minimum *Staphylococcus* growth in ten canals [97]. Again the Vienna School (1999 and 2000) examined in depth the decontaminating effects of Nd:YAG, Ho:YAG, and Er:YAG lasers [82, 98], also evaluating in 2004, in addition to the 810 nm diode laser, the Er,Cr:YSGG laser [86] and, later, the 980 nm diode laser and KTP laser [99]. Using a setting of 1 W, the KTP laser showed complete eradication of *E. coli* in 75 % of samples; at 1.5 W, significant reductions of *E. coli* were observed with all the laser systems. However, the eradication of *E. faecalis* was not achieved with any laser [82, 97–99].

Franzen et al. (2011) repeated the study by Klinke et al. (1997) on deep dentin penetration and the bactericidal effect of Nd:YAG laser irradiation [95], using the same wavelength but longer pulse duration of 15 and 25 ms, at 1,75 W [100]. Laser irradiation with a pulse duration of 15 ms eliminated an average of 49 and 29 % of *E. faecalis* at dentin depths of 500 microns and 1000 microns, respectively. Irradiation with a longer pulse duration of 25 ms eliminated 70 % (at 500 microns) and 50 % (at 1000 microns) of *E. faecalis*. However, these values resulted lower than those achieved with the established microsecond pulse protocol [100].

The bacteria killing ability of two different diode laser wavelengths (810 and 940 nm) was compared in vitro by Beer et al. (2012); the diode lasers achieved an average bacterial reduction of *E. coli* of 76.06 % (810 nm) and 68.15 % (940 nm). The study concluded that an additional irradiation at the access cavity produces significantly better bactericidal results: average *E. coli* reduction of 97.84 % (810 nm) and 98.83 % (940 nm) and average *E. faecalis* reduction of 98.8 % (810 nm) and 98.66 % (940 nm) [101].

However, a precise and unambiguous determination of the real bactericidal effect in depth of different lasers has not been reached, and also many results are contradictory.

Meire et al. (2012) evaluated the ability of Nd:YAG (2 W, 15 Hz, 40s) and Er:YAG (150 mJ or 100 mJ, 15 Hz, 40 s) used with conventional laser irradiation, of PDT antibacterial photodynamic therapy (Denfotex and Helbo system), and of conventional sodium hypochlorite (immersion in 2.5 % NaOCl for 1, 5, 10, and 30 min) to eliminate *E. faecalis* biofilms. The study concluded that NaOCl was the most effective in *E. faecalis* biofilm elimination and that the Er:YAG laser treatment also resulted in high reductions in viable counts. The use of both aPDT systems and Nd:YAG irradiation resulted in a weak reduction in the number of bacterial cells [102].

Bago et al. (2013) evaluated by SEM visualization the antimicrobial effect on *E. faecalis* of conventional diode laser irradiation (2 W, 3×20s), photoactivated disinfection (PAD at 100 mW, 60 s with and without endoProbe), and conventional (syringe and endoProbe) and sonic activated irrigation with 2.5 % NaOCl (EndoActivator system for 60 s). The PAD, using both laser systems, and the sonic activated NaOCl irrigation proved significantly more effective than diode irradiation and NaOCl irrigation alone in reducing CFUs ($P<0.05$). High-power diode laser and NaOCl irrigation alone had an equal antibacterial effect ($P>0.05$) [103].

In a recent meta-analysis considering 163 articles on the effect of different laser treatments on the *E. faecalis*, Sadik et al. (2013) only included just 12 studies of which all reported a significant reduction of the count of *E. faecalis* after irradiation with Er,Cr:YSGG, Nd:YAG, and KTP lasers at 1 and 1.5 W [104].

On the basis of these studies, the use of sodium hypochlorite remains the gold standard in achieving adequate root canal decontamination.

6.5.2 Irrigation and Visible and Near-Infrared Laser Irradiation for Root Canal Decontamination

The essential role of irrigation with sodium hypochlorite, in order to achieve efficient decontamination, was confirmed by some initial comparative studies [88, 89, 92] and by some more recent ones [102, 103]. A line of research considered the fundamental role of chemical irrigation with NaOCI and EDTA, in order to propose a technique of laser-assisted decontamination that foresees the association of conventional irrigation with laser irradiation, to reach results that could considerably increase success rates [75, 105–107].

De Souza et al. (2008) compared the conventional chemomechanical technique using 0.5 % NaOCl and 17 % EDTA-T as irrigants to the same protocol assisted by a 830 nm diode laser at 3 W. Diode laser irradiation provided an increased disinfection of the deep radicular dentin, achieving 100 % bacterial eradication in laser-assisted treatment and 98.39 % in the conventional irrigation group [105].

Benedicenti et al. (2008), in an in vitro study, utilized an 810 nm diode laser at 2.5 W (10 ms t_{on} and 10 ms t^{off}) with a 200 micron fiber combined with commonly used irrigants. Irrigation with 5.5 % NaOCl was followed by laser irradiation for 5 s, after which the canals were flushed again with 10 % citric acid and once more irradiated. Finally, irrigation with NaOCl was performed and again canals were irradiated. The combined irrigation-laser group led to *E. faecalis* bacterial reduction of 7.178 log mean CFU, with a significantly superior reduction to the conventional irrigation protocol (3.381 log mean CFU) or laser irradiation alone (1.459 log mean CFU). The study suggested the synergistic effect of laser irradiation and chemical irrigation in improving the effectiveness of the decontamination of infected root canals [75].

Later, Mehrvarzfar et al. (2011) also investigated the role of 810 nm diode laser irradiation combined with MTAD® irrigation and recommended the protocol as an effective treatment option for complete elimination of *E. faecalis* out of the root canal system. Laser irradiation was performed five times for 5 s, with a 15 s interval between irradiations; laser setting was 2 W in gated mode, using a pulse duration of 20 ms and a pulse interval of 40 ms. Laser irradiation was delivered into the canal up to 1 mm short of the working length with a 400 μm fiber; irradiation was performed with circular movements from the apical to the coronal part (step-back technique). Complete eradication of *E. faecalis* was observed only when MTAD irrigation was combined with diode laser irradiation [106].

Preethee et al. (2012) also evaluated the bactericidal effect of 908 nm diode laser combined with several irrigation protocols. A laser setting of 2.5 W was used with a 200 μm fiber introduced 1 mm short of the apex and withdrawn in a helicoidal motion at a speed of approximately 2 mm/s for 5 s. Canal irradiation was performed six times, with intervals of 10 s after a final irrigation that included the use of 5 ml 17 % EDTA followed by 5 ml 5.25 % NaOCl, for a total irrigation time of 2 min. When the 908 nm diode laser was used in conjunction with conventional irrigation techniques, significant elimination of *E. faecalis* in the apical third of root dentin was demonstrated [107].

Romeo et al. (2014) evaluated and compared the antibacterial action on *E. faecalis* biofilms, of the KTP laser (532 nm), and of the 980 nm diode laser, associated with conventional root canal procedures. The laser parameters used were 2.5 W, 35 ms t^{on}, 50 ms t^{off} for the KTP laser and 2.5 W, 30 ms t^{on}, 30 ms t^{off} for the 980 nm diode laser. The combination of chemomechanical irrigation and laser irradiation (KTP and 980 nm diode lasers) resulted in a considerable reduction in bacterial load (higher than 96 and 93 %, respectively), while conventional endodontic procedures resulted in a statistically significantly lower reduction rate of about 67 %, confirming the role of laser

systems as an additional aid in endodontic disinfection [108].

Neelakantan et al. (2014) also investigated the impact of three irrigation protocols (NaOCl + etidronic acid and NaOCl-EDTA-NaOCl and saline as a control), activated by three different methods (ultrasound, diode, and erbium lasers) on mature biofilms of *E. faecalis* in vitro. Both diode and Er:YAG lasers proved more effective than ultrasonic activation and conventional syringe irrigation in reducing *E. faecalis* biofilms. The study concluded that the use of NaOCl after or in combination with a chelating agent caused the greatest reduction in *E. faecalis* [109].

All these studies demonstrated the superior bactericidal efficacy of the association of chemical irrigation with laser irradiation, when compared to nonirradiated canals disinfected with use of the irrigants alone or to irradiated canals only.

The rationale for the combined use of chemical irrigation and diode laser irradiation is the synergistic effect of a chelating agent such as EDTA (used to dissolve the inorganic smear layer and to increase the permeability of dentinal tubules) and antibacterial agents such as sodium hypochlorite and laser irradiation. Following the removal of debris and smear layer using EDTA, both sodium hypochlorite and diode lasers have greater accessibility to the unreachable parts of the tubular network resulting in superior bactericidal effect in the root canal system [75, 105–109].

Moreover, the morphological pattern produced by these combined protocols, as described before (Sect. 6.4.6), remained identical to the pattern produced by the use of irrigant alone, limiting the undesired thermal effects correlated with near-infrared laser irradiation [50, 52, 70].

However, a study from Meire et al. (2009) reported that both Nd:YAG (at 1.5 W, 15 Hz) and KTP lasers (at 1 W, 10 Hz) used with 200 micron fibers, five times with 20 s intervals, when activated in aqueous suspension, resulted less effective than NaOCl in reducing *E. faecalis* both in vitro and in the infected tooth model, due to poor absorption of these wavelengths in water-based solutions; Meire et al. explained the survival of bacteria as the result of transmission of laser beams through bacterial suspensions, rather than by absorption [76].

6.5.3 Medium- and Far-Infrared Laser Decontamination

The laser energy emitted by erbium lasers is primarily absorbed in the root canal surface (high affinity with dentinal tissue rich in water), where they produce the highest bactericidal effect on bacteria [98, 110].

Studies on CO_2 lasers, also absorbed from water in dentin walls, did not prove to be very successful in endodontics. Kesler et al. (1998) designed a microprobe that allowed irradiation of the root canal with CO_2 laser; this type of irradiation brought about complete decontamination of the root canal [111].

Another study, published a year later by Le Goff et al. (1999), evaluated the efficacy of laser decontamination with CO_2, at 5 W for 10 s, three times with an interval of 10 s, on canals infected by *Actinomyces odontolyticus*, in comparison with 3 % NaOCl irrigation. The latter resulted in statistically superior contamination than CO_2 laser treatment [112].

In the same year, Kesler et al. (1999) reported the results of a clinical study conducted on 900 teeth with a periapical lesion, treated with conventional endodontic instrumentation and then irradiated with the microprobe of the CO_2 laser. Laser treatment was successful in 90 % of cases, with a reduction in periapical radiolucency at radiological examination and with clinical resolution of the pathology [113].

Research on CO_2 lasers was anyway soon abandoned.

Gutknecht et al. (1997) determined in vitro the bactericidal effect of a Ho:YAG laser in infected root canals. At a setting of 2 W, 5 Hz, the laser eliminated 99.98 % of *S. faecalis* [114].

Moritz et al. (1999) achieved almost a total eradication of 99.64 % of *E. coli* and *E. faecalis* using the Er:YAG laser at 1.5 W power, followed by the Nd:YAG laser (99.16 %) and the Ho:YAG laser (99.05 %) at the same average power [96]. However, Moritz et al. (2004) also underlined

that erbium lasers do not have bactericidal effects in depth, in the dentinal tubules, reaching only 300 microns of penetration depth in the root canal wall [110].

Perin et al. (2004) evaluated the antimicrobial effect of Er:YAG laser irradiation versus 1 % NaOCl irrigation in root canals inoculated with different bacterial species: *Bacillus subtilis*, *Enterococcus faecalis*, *Pseudomonas aeruginosa*, and *Staphylococcus aureus*, together with *Candida albicans*. The teeth were irradiated with Er:YAG laser at 100 mJ, 7 Hz, for 80 pulses/canal, 11 s with two different modalities: at working length or similarly 3 mm shorter. The study resulted in 1 % NaOCl solution and the Er:YAG laser irradiation at working length to be effective against all five microorganisms, while the irradiation 3 mm shorter than the working length, showed that 70 % of the specimens remained infected [115].

Schoop et al. (2004) in the already reported study compared the 810 nm diode, the Nd:YAG, the Er:YAG, and the Er,Cr:YSGG lasers and reported significant reductions in *E. coli* with the Er:YAG laser at 1 W and at the higher setting of 1.5 W; only the diode and the Er: YAG laser were capable of complete eradication of *E. faecalis* to a significant extent [86].

However, it must be considered from a microbiological point of view that the reported disinfection efficacy cannot be considered effective not having achieved the minimum of 5-log reduction.

Vezzani et al. (2006) evaluated in vitro the disinfecting effect of the Er:YAG laser in root canals contaminated with multispecies bacteria incubated for 28 days: *Bacillus subtilis*, *Staphylococcus aureus*, *Enterococcus faecalis*, *Pseudomonas aeruginosa*, *and Candida albicans*. The treatment included three Er:YAG laser irradiation groups, at 100 mJ, varying the frequency (at 7, 10, and 16 Hz) and two irrigation groups, with 1 and 2.5 % NaOCl solutions. No method totally eliminated microorganisms with no statistically significant difference within the five groups, with Er:YAG laser at 100 mJ/16 Hz showing the highest bacterial reduction (89.5 %) in comparison to the 1 and 2.5 % NaOCl solution with a 83.15 and a 84.46 % reduction [116].

Wang et al. (2007) have investigated the ability of the Er,Cr:YSGG laser in the decontamination of traditionally prepared canals. Complete eradication of bacteria was not obtained (77 % reduction) using low power (0.5 W, 10 Hz, 50 mJ, with 20 % air-water spray), while better results were obtained at higher power of 1.5 W (96 % reduction) [117].

Eldeniz et al. (2007) compared the efficacy of a 3 % NaOCl irrigation procedure (for 15 min) with that of Er,Cr:YSGG laser irradiation at 0.5 W, with water spray, to decontaminate *E. faecalis* infected root canals and confirmed that Er,Cr:YSGG laser reduced the viable microbial population in root canals but did not eradicate all bacteria. Complete sterilization was achieved only in the 3 % NaOCl group [118].

Research focused on the ability of the erbium lasers to remove bacterial biofilm from the apical third, [119] and a recent in vitro study had further validated the capacity of the Er:YAG laser to remove endodontic biofilm, with numerous bacterial species (*Actinomyces naeslundii*, *Enterococcus faecalis*, *Lactobacillus casei*, *Propionibacterium acnes*, *Fusobacterium nucleatum*, *Porphyromonas gingivalis*, *or Prevotella nigrescens*). Considerable reduction of bacterial cells and disintegration of the biofilm was found. The exception, however, was the biofilm formed by *L. casei* [120].

Schoop et al. (2007) used an Er,Cr:YSGG laser equipped with a flat 300 micron tip with two different emission parameters, 1 W (20 Hz, 50 mJ) and 1.5 W (20 Hz, 75 mJ) irradiating five times for 5 s with a cooling time of 20 s between each cycle. The level of decontamination obtained was significantly high with important differences between 1 and 1.5 W, with thermal increase contained between 2.7 and 3.2 °C [121].

Dewsnup et al. (2010) compared the reduction of *E. faecalis* in straight and curved canals using

an Er,Cr:YSGG laser and irrigation with 6.15 % NaOCl. Conventional irrigation techniques using 6.15 % NaOCl effectively eliminated all bacteria in straight and curved canals; Er,Cr:YSGG laser also effectively removed all bacteria from straight canals. However, in three curved canals, even though there were significant bacterial reductions, they failed to render canals completely free of bacteria [122].

Arnabat et al. (2010) determined in vitro the optimal irradiation conditions for the Er,Cr:YSGG laser to achieve maximal bactericidal effect. The antimicrobial effect of the laser was compared with that of 0.5 and 5 % NaOCl. The use of 5 % NaOCl to be proved the most effective procedure, however, Er,Cr:YSGG laser treatment, was as effective as NaOCl 5 % when applied at 2 W for 60 s [123].

Yavari et al. (2010) investigated the eradication of *E. faecalis* with Er,Cr:YSGG laser irradiation at 2 and 3 W for 16 s, compared to irrigation with 1 % NaOCl for 20 min. The study resulted in high bacterial reduction (2.4 and 1.53 %) for the Er,Cr:YSGG laser groups; however, the effect was less remarkable than that of NaOCl solution that resulted in no bacterial growth [124].

Yasuda et al. (2010) investigated the ability of Er:YAG and Nd:YAG lasers to decontaminate both straight and curved root canals. Two laser settings were used at 0.5 (50 mJ, 10 pps) and 1 W (100 mJ, 10 pps); the bactericidal effect of the Er:YAG laser was higher than that of Nd:YAG, but this effect was significantly lower in curved canals than in straight root canals. The results suggested further development in the endodontic laser tip and technique to ensure higher success in curved root canal sterilization [125].

Meire et al. (2012) in the already reported study confirmed the antimicrobial efficacy of Er:YAG laser at 100 mJ, but also the superior effectiveness of NaOCl in *E. faecalis* biofilm elimination [102].

Dos Santos et al. (2012) used two Er:YAG laser energy settings: 0.9 W (60 mJ, 15 Hz), and 1 W (100 mJ, 10 Hz). The remaining bacteria were counted immediately and 48 h after laser irradiation. The results showed a high bacterial reduction at both time points. With 0.9 W, there was an immediate reduction of 99.73 % and the reduction was 77.02 % after 48 h; with 1 W, there was an immediate reduction of 99.95 % and the reduction was 84.52 % after 48 h. The count performed 48 h after irradiation showed that *E. faecalis* were able to survive and can grow even from small numbers [126]. The method of double bacterial count, immediately and after 48 h, is very important to understand the possible cause of therapy failure and is discussed again in Sect. 11.11.2.

Cheng et al. (2012) evaluated the bactericidal effect of Nd:YAG, Er:YAG, Er,Cr:YSGG laser radiation, and antimicrobial photodynamic therapy (aPDT) in experimentally infected root canals compared with standard endodontic treatment of 5.25 % NaClO irrigation. The Er:YAG laser was also used with 5.25 % NaClO+0.9 % saline solution+distilled water, while the Nd:YAG, the Er,Cr:YSGG, and the aPDT were not. Only the Er:YAG/NaClO/normal saline+distilled water group showed no bacterial growth (the bacterial reduction reached up to 100 %) on the surface of root canal walls or at 100/200 μm inside the dentinal tubules. The combination of Er:YAG laser and NaOCl seemed to be an ideal protocol for root canal disinfection during endodontic therapy [127].

The determination of the most efficient and safe parameters was partially met. The problem of a uniform distribution of energy inside the canal remains unresolved; the energy is randomly concentrated in peaks of intensity that, on the one side, lead to thermal damage and, on the other side, to inefficient decontamination. The canal diameter varies progressively from the apical area to the coronal third, and in consequence of its shaping, the relationship of closeness [15] or the contact between the fiber and the canal wall and the angle of irradiation [43] modify uncontrollably the fluence supplied. Accordingly, complex anatomy, curved and narrow canals, remains in any case a difficult obstacle to negotiate for laser fibers/tips inserted deeply into the canal [22–24, 122, 125].

To avoid this problem, from 2006, new studies on erbium lasers have been conducted on tips with modified design, in order to obtain an improved and better lateral distribution of energy. These studies took into consideration both the decontaminating effect, the variations in temperature, and the morphological alterations of the canal surface and were developed for different irrigant activation techniques (LAI and PIPS).

6.5.4 Radial Firing Tips

Conventional tips of erbium lasers have a frontal emission of energy at the end of the tip and are also called "end-firing" tips; they allow limited lateral penetration into the dentinal walls, due to the disadvantageous irradiation angle and the lack of scattering of erbium laser wavelengths. After the first investigations by Shoji et al. (2000) and [10] Kesler et al. (2002) [11], a new generation of radial emitting tips has been proposed in 2007 for the Er,Cr:YSGG and studied by Gordon et al. [16] and Schoop et al. [17], who investigated the morphological and decontaminating effects of this new laser tip. Despite the innovative tip design, the following protocols were implemented in the conventional way, introducing the tip into the canal before starting the irradiation while withdrawing the tip.

Gordon et al. (2007) used an Er,Cr:YSGG laser with a 200 micron tip with radial emission, at 0.2 W (10 mJ, 20 Hz), and at 0.4 W (20 mJ, 20 Hz), both with spray a/w 34–28 % or in dry mode. The tip was positioned in the apical part and withdrawn at a speed of 1 mm/s; the radiation times varied from 15 s up to 2 min. Maximum bacterial eradication of 99.71 % was performed using the higher power (0.4 W) and the longer exposure time of 120 s, without air-water spray (in dry mode). The lower power (0.2 W) and shorter time of irradiation of 15 s, with water spray, produced a 94.7 % bacterial reduction [16].

Schoop et al. (2007) studied other parameters 0.6 and 0.9 W for the Er,Cr:YSGG that produced a very limited thermal rise, respectively, of 1.3 °C and 1.6 °C, showing a high bactericidal effect on *E. coli* and *E. faecalis* [17].

Recently, Martins et al. (2012), published the outcome of a randomized clinical trial with evaluation after 6 months, using Er,Cr:YSGG and radial firing tips versus the concomitant use of 3 % NaOCl and ad interim calcium hydroxide paste in necrotic teeth with chronic apical periodontitis. Laser irradiation was performed using a radial firing tip 200 microns in diameter, at 0.75 W (37.5 mJ, 20 Hz) and 140 μs pulse duration and a 300 micron tip at 1.25 W (62.5 mJ, 20 Hz) in the first and second appointment, respectively, per four times each, withdrawing at 2 mm/s, starting 1 mm short from the apex. Both groups resulted in similar outcomes exhibiting statistically significant decreases of periapical index (PAI) at radiographic evaluation [128].

6.6 Discussion

The laser irradiation of root canals, performed with the conventional technique through the insertion of a fiber or a tip up to the working length and successive activation of the laser during the retraction, is not completely satisfying for modern endodontics.

Current techniques of irrigation with chelating (EDTA) or antibacterial agents (NaOCI) proved to be superior or equally effective when compared to different laser protocols proposed for root canal decontamination [87–89, 92, 100, 101, 113, 116, 120–122]. Moreover, despite of the flexibility of modern fibers/tips, reaching the working length in curved and/or narrow canals, reaching all areas of bacterial contamination, remains difficult due to the complexity of the root canal anatomy [22–24, 122, 125] (Figs. 6.22, 6.23, 6.24 and 6.25).

In order to facilitate the introduction and extraction of the fiber/tip, the root canal needs to be enlarged and shaped adequately to a diameter superior to those of the fiber/tip (200–300 microns) and so up to ISO 30–35, with a conicity of .06. This preparation produces radicular dentin reduction that could be dangerous in "difficult"

Fig. 6.22 Section of lower molar with merged mesial and distal roots. Representation of the master file ISO 30 positioned 0.5 mm shorter from anatomical apex; the canal was prepared up to a size of 30/06. Note the steel instruments following the curvature of the anatomy and the correct glide path performed to facilitate the negotiation of the middle one-third of the canal

Fig. 6.23 A 300 micron fiber is positioned 1.5–2 mm shorter than anatomical length: note how the flexibility of the fiber is not able to follow the curvature of root, despite a correct shaping of the canal. Interferences of the dentin walls force the instrument toward the convexity of the canal curvature with contact of the fiber during the laser emission and production of hot spots

canals (typically the mesial roots of upper and lower molars, curved or bayonet premolars, and the lower incisors), with higher risk of root canal stripping (Figs. 6.26, 6.27, and 6.29).

Moreover, the proposed helical movement during the retraction of the fiber from the apical portion of the canal does not produce an efficient increase of lateral diffusion of the energy. Effectively, the increase of the angle of irradiation obtained is minimal, and on the opposite, the helical movement can force the fiber/tip to a close contact with the dentin, possibly producing morphological alteration (hot spots) on the canal surface [42]. Alterations vary from a minimal superficial thermal effect, with partial closure of the dentin tubules, to the production of areas of carbonization (near-infrared laser), or ablative effects (medium-infrared laser) that can produce perforation in the apical portion or ledges in the dentinal walls.

The use of lasers, near and medium infrared, after irrigation, or in any case when the canal is wet, reduces these undesirable morphological effects effectively. SEM analysis has shown

Fig. 6.24 Section of lower molar: the distal canal is enlarged up to 2 mm from the apex with 30/06: the last "S" of the apical one-third was prepared with ISO 20/02 hand file. Note the ISO 30 hand steel file unable to negotiate this part and consequently wedged at the apical one-third

Fig. 6.25 Section of lower molar: also the 200 micron fiber cannot follow the "S" of the apical one-third, with ineffective decontamination of the apex. It is important to know to not use longer time of irradiation in this area, to avoid thermal damage (see Figs. 6.30 and 6.31)

morphological modifications related more to the irrigant than to the wavelength used [70].

Also, the decontaminating efficacy proved to be the same or superior to just the irrigation or laser irradiation alone [75, 105–109, 127].

However, the anatomic and operative problems of the introduction of a fiber in narrow and curved canals are still not solved, with the probable impossibility or inefficiency of the procedure in the teeth with complicated root canal anatomy (Figs. 6.28, 6.29, and 6.30 and 6.31).

The laser activation techniques of the irrigants (LAI), and in particular the PIPS™ technique, will solve the problems of conventional laser endodontics. The agitation of the irrigant with

Fig. 6.26 Section of lower molar with moderate curvature of mesial root. Straight line access to the middle one-third and canal shaping of 25/04: the master file ISO 25 is positioned 1 mm shorter from the apex following the curvature of the root

Fig. 6.27 Section of lower molar: a 200 micron fiber arrived 4 mm shorter from the apex: during the activation of the fiber, the curvature of the canal forced the fiber to touch the canal with evident hot spots (brownish spots) (Nd:YAG laser 1.5 W, 100 mJ)

tips not necessarily positioned in the root canal lumen does not involve direct irradiation of the canal dentin and its undesirable thermal effect. While increasing the activation and tubular penetration of antibacterial irrigants, LAI will facilitate deep tridimensional decontamination, up to the areas which are less reachable by conventional irrigation or conventional laser endodontics.

In particular, the PIPS™ technique foresees positioning of the tip in the pulp chamber solving also the problem of access and insertion of the tip in the canals.

The following chapters are dedicated to laser activation of antibacterial photoactive solutions (Chap. 7) and of commonly used irrigants (Chaps. 8 and 9), for cleaning and decontamination of the root canal system.

Fig. 6.28 Section of lower molar: to overpass the interference, a 200 micron fiber touches the mesial wall of the distal canal, or changing inclination of the distal wall of the same canal. In both the case, it will create hot spots and thermal damage to dentin surface

Fig. 6.29 Section of lower molar: the 200 micron fiber is unable to reach the working length of the mesial canal

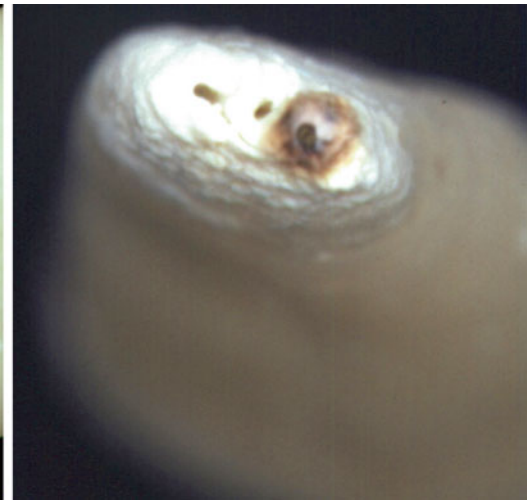

Figs. 6.30 and 6.31 Due to a longer time of irradiation stationary at the working length and higher energy setting used (Nd:YAG 2.5 W, 100 mJ, 200 micron fiber, 3 s), thermal damage on the periodontal aspect of the root occurred: the apical view shows the carbonization of several apical foramina

References

1. Olivi G. Laser use in endodontics: evolution from direct laser irradiation to laser-activated irrigation. J Laser Dent. 2013;21(2):58–71.
2. Hibst R, Stock K, Gall R, Keller U. Controlled tooth surface heating and sterilization by Er:YAG laser radiation. Proc SPIE. 1996;2922:119–1261.
3. Liesenhoff T, Lenz H, Seiler T. Root canal preparation using excimer laser beams. ZWR. 1989;98(12):1034. 1037–9.
4. Frentzen M, Koort HJ, Nolden R. Root canal preparation using Excimer lasers. Dtsch Zahnarztl Z. 1991;46(4):288–9. German.
5. Gutknecht N, Behrens VG. Instrumentation of root canal walls with Nd-YAG laser. ZWR. 1991;100(10): 748–50, 752, 755. German.
6. Levy G. Cleaning and shaping the root canal with a Nd:YAG laser beam: a comparative study. J Endod. 1992;18(3):123–7.
7. Goodis HE, White JM, Marshall SJ, Marshall Jr GW. Scanning electron microscopic examination of intracanal wall dentin: hand versus laser treatment. Scanning Microsc. 1993;7(3):979–87.
8. Moogi P, Nageshwar R. Cleaning and shaping the root canal with an Nd: YAG laser beam: a comparative study. J Conserv Dent. 2010;13(2):84–8.
9. Blum JY, Abadie MJ. Study of the Nd:YAP laser. Effect on canal cleanliness. J Endod. 1997;23(11):669–75.
10. Shoji S, Hariu H, Horiuchi H. Canal enlargement by Er:YAG laser using a cone-shaped irradiation tip. J Endod. 2000;26(8):454–8.
11. Kesler G, Gal R, Kesler A, Koren R. Histological and scanning electron microscope examination of root canal after preparation with Er:YAG laser microprobe: a preliminary in vitro study. J Clin Laser Med Surg. 2002;20(5):269–77.
12. Stabholz A, Zeltser R, Sela M, Peretz B, Moshonov J, Ziskind D, Stabholz A. The use of lasers in dentistry: principles of operation and clinical applications. Compend Contin Educ Dent. 2003;24(12): 935–48.
13. Stabholz A, Sahar-Helft S, Moshonov J. Lasers in endodontics. Dent Clin N Am. 2004;48(4):809–32.
14. Inamoto K, Horiba N, Senda S, Naitoh M, Ariji E, Senda A, Nakamura H. Possibility of root canal preparation by Er:YAG laser. Oral Surg Oral Med Oral Pathol Oral Radiol Endod. 2009;107(1): e47–55.
15. Kokuzawa C, Ebihara A, Watanabe S, Anjo T, Bolortuya G, Saegusa H, Suda H. Shaping of the root canal using Er:YAG laser irradiation. Photomed Laser Surg. 2012;30(7):367–73.
16. Gordon W, Atabakhsh VA, Meza F, Doms A, Nissan R, Rizoiu I, Stevens RH. The antimicrobial efficacy of the erbium, chromium:yttrium-scandium-gallium-garnet laser with radial emitting tips on root canal dentin walls infected with Enterococcus faecalis. J Am Dent Assoc. 2007;138(7):992–1002.
17. Schoop U, Barylyak A, Goharkhay K, Beer F, Wernisch J, Georgopoulos A, Sperr W, Moritz A. The impact of an erbium, chromium:yttrium-scandium-gallium-garnet laser with radial-firing tips on endodontic treatment. Lasers Med Sci. 2009;24(1):59–65. Epub 2007 Nov 20.
18. Chen WH. YSGG laser root canal therapy. Dent Today. 2002;21(5):74–7.
19. Chen WH. Laser root canal therapy. J Indiana Dent Assoc. 2002–2003;81(4):20–3.
20. Minas NH, Meister J, Franzen R, Gutknecht N, Lampert F. In vitro investigation of intra-canal dentine-laser beam interaction aspects: I. Evaluation of ablation capability (ablation rate and efficiency). Lasers Med Sci. 2010;25(6):835–40. Epub 2009 Jul 28.
21. Kimura Y, Yonaga K, Yokoyama K, Kinoshita J, Ogata Y, Matsumoto K. Root Surface Temperature Increase during Er:YAG laser irradiation of root canals. J Endod. 2002;28(2):76–8.
22. Ali MN, Hossain M, Nakamura Y, Matsuoka E, Kinoshita J, Matsumoto K. Efficacy of root canal preparation by Er, Cr:YSGG laser irradiation with crown-down technique in vitro. Photomed Laser Surg. 2005;23(2):196–201.
23. Matsuoka E, Jayawardena JA, Matsumoto K. Morphological study of the Er, Cr:YSGG laser for root canal preparation in mandibular incisors with curved root canals. Photomed Laser Surg. 2005;23(5):480–4.
24. Jahan KM, Hossain M, Nakamura Y, Yoshishige Y, Kinoshita J, Matsumoto K. An assessment following root canal preparation by Er, Cr:YSGG laser irradiation in straight and curved roots, in vitro. Lasers Med Sci. 2006;21(4):229–34. Epub 2006 Oct 28.
25. Matsuoka E, Jayawardena JA, Matsumoto K. Morphological study on root canal preparation using erbium, chromium:YSGG laser. J Oral Laser Appl. 2005;5(1):17–22.
26. Roper MJ, White JM, Goodi SE, Gekelman D. Two-dimensional changes and surface characteristics from an erbium laser used for root canal preparation. Lasers Surg Med. 2010;42:379–83.
27. Takeda FH, Harashima T, Kimura Y, Matsumoto K. Comparative study about the removal of smear layer by three types of laser devices. J Clin Laser Med Surg. 1998;16:117–22.
28. Takeda FH, Harashima T, Kimura Y, et al. Efficacy of Er:YAG laser irradiation in removing debris and smear layer on root canal walls. J Endod. 1998;24: 548–51.
29. Cecchini SCM, Zezell DM, Bachmann L, et al. Evaluation of two laser systems for intracanal irradiation. SPIE. 1999;3593:31–5.
30. Theodoro LH, Haypek P, Bachmann L, Garcia VG, Sampaio JE, Zezell DM, Eduardo Cde P. Effect of ER:YAG and diode laser irradiation on the root surface: morphological and thermal analysis. J Periodontol. 2003;74(6):838–43.
31. Watanabe S, Saegusa H, Anjo T, Ebihara A, Kobayashi C, Suda H. Dentin strain induced by laser irradiation. Aust Endod J. 2010;36(2):74–8.
32. Faria MI, Souza-Gabriel AE, Marchesan MA, Sousa-Neto MD, Silva-Sousa YT. Ultrastructural evaluation of radicular dentin after Nd:YAG laser

irradiation combined with different chemical substances. Gen Dent. 2008;56(7):641–6.
33. Kaitsas V, Signore A, Fonzi L, Benedicenti S, Barone M. Effects of Nd: YAG laser irradiation on the root canal wall dentin of human teeth: a SEM study. Bull Group Int Rech Sci Stomatol Odontol. 2001;43(3): 87–92.
34. Tewfik HM, Pashley DH, Horner JA, Sharawy MM. Structural and functional changes in root dentin following exposure to KTP/532 laser. J Endod. 1993;19(10):492–7.
35. Gutknecht N, Franzen R, Meister J, Vanweersch L, Mir M. Temperature evolution on human teeth root surface after diode laser assisted endodontic treatment. Lasers Med Sci. 2005;20(2):99–103. Rech Sci Stomatol Odontol. 2001;43(3):87–92. Epub 2005 Jul 9.
36. da Costa RA, Nogueira GE, Antoniazzi JH, Moritz A, Zezell DM. Effects of diode laser (810 nm) irradiation on root canal walls: thermographic and morphological studies. J Endod. 2007;33(3):252–5. Epub 2006 Dec 13.
37. Alfredo E, Marchesan MA, Sousa-Neto MD, Brugnera-Júnior A, Silva-Sousa YT. Temperature variation at the external root surface during 980-nm diode laser irradiation in the root canal. J Dent. 2008;36(7):529–34. Epub 2008 May 6.
38. He H, Yu J, Song Y, Lu S, Liu H, Liu L. Thermal and morphological effects of the pulsed Nd:YAG laser on root canal surfaces. Photomed Laser Surg. 2009;27(2):235–40.
39. Saunders WP, Whitters CJ, Strang R, Moseley H, Payne AP, McGadey J. The effect of an Nd-YAG pulsed laser on the cleaning of the root canal and the formation of a fused apical plug. Int Endod J. 1995;28(4):213–20.
40. Harashima T, Takeda FH, Kimura Y, Matsumoto K. Effect of Nd:YAG laser irradiation for removal of intracanal debris and smear layer in extracted human teeth. J Clin Laser Med Surg. 1997;15(3):131–5.
41. Koba K, Kimura Y, Matsumoto K, Takeuchi T, Ikarugi T, Shimizu T. A histopathological study of the morphological changes at the apical seat and in the periapical region after irradiation with a pulsed Nd:YAG laser. Int Endod J. 1998;31(6):415–20.
42. Barbakow F, Peters O, Havranek L. Effects of Nd:YAG lasers on root canal walls: a light and scanning electron microscopic study. Quintessence Int. 1999;30(12):837–45.
43. Santos C, Sousa-Neto MD, Alfredo E, Guerisoli DM, Pecora JD, Comelli Lia RF. Morphologic evaluation of the radicular dentine irradiated with Nd:YAG laser under different parameters and angles of incidence. Photomed Laser Surg. 2005;23(6): 590–5.
44. Hasheminia SM, Birang R, Feizianfard M, Nasouri MA. Comparative study of the removal of smear layer by two endodontic irrigants and Nd:YAG laser: a scanning electron microscopic study. ISRN Dent. 2012;2012:620951. Epub 2012 Jul 16.
45. Moshonov J, Peretz B, Brown T, Rotstein I. Cleaning of the root canal using Nd:YAP laser and its effect on the mineral content of the dentin. J Clin Laser Med Surg. 2003;21(5):279–82.
46. de Moura-Netto C, de Moura AA, Davidowicz H, Aun CE, Antonio MP. Morphologic changes and removal of debris on apical dentin surfaces after Nd:YAG laser and diode laser irradiation. Photomed Laser Surg. 2008;26(3):263–6.
47. Parirokh M, Eghbal MJ, Asgary S, Ghoddusi J, Stowe S, Forghani F, Shahravan A. Effect of 808 nm diode laser irradiation on root canal walls after smear layer removal: a scanning electron microscope study. Iran Endod J. 2007;2(2):37–42. Epub 2007 Jul 5.
48. da Fonseca Alvarez A, Moura-Netto C, Daliberto Frugoli A, Fernando C, Correa Aranha AC, Davidowicz H. Temperature changes on the root surfaces of mandibular incisors after an 810-nm high-intensity intracanal diode laser irradiation. J Biomed Opt. 2012;17(1):015006.
49. Wang X, Sun Y, Kimura Y, Kinoshita J, Ishizaki NT, Matsumoto K. Effects of diode laser irradiation on smear layer removal from root canal walls and apical leakage after obturation. Lasers Med Sci. 2005; 20(2):99–103.
50. Marchesan MA, Brugnera-Junior A, Ozorio JE, Pécora JD, Sousa-Neto MD. Effect of 980-nanometer diode laser on root canal permeability after dentin treatment with different chemical solutions. J Endod. 2008;34(6):721–4.
51. Marchesan MA, Brugnera-Junior A, Souza-Gabriel AE, Correa-Silva SR, Sousa-Neto MD. Ultrastructural analysis of root canal dentine irradiated with 980-nm diode laser energy at different parameters. Photomed Laser Surg. 2008;26(3):235–40.
52. Alfredo E, Souza-Gabriel AE, Silva SR, Sousa-Neto MD, Brugnera-Junior A, Silva-Sousa YT. Morphological alterations of radicular dentine pretreated with different irrigating solutions and irradiated with 980-nm diode laser. Microsc Res Tech. 2009;72(1):22–7.
53. Takeda FH, Harashima T, Kimura Y, Matsumoto K. A comparative study of the removal of smear layer by three endodontic irrigants and two types of laser. Int Endod J. 1999;32(1):32–9.
54. Yamazaki R, Goya C, Yu DG, Kimura Y, Matsumoto K. Effects of erbium, chromium:YSGG laser irradiation on root canal walls: a scanning electron microscopic and thermographic study. J Endod. 2001;27(1):9–12.
55. Ishizaki NT, Matsumoto K, Kimura Y, Wang X, Kinoshita J, Okano SM, Jayawardena JA. Thermographical and morphological studies of Er, Cr:YSGG laser irradiation on root canal walls. Photomed Laser Surg. 2004;22(4):291–7.
56. Silva AC, Guglielmi C, Meneguzzo DT, Aranha AC, Bombana AC, de Paula EC. Analysis of permeability and morphology of root canal dentin after Er, Cr:YSGG laser irradiation. Photomed Laser Surg. 2010;28(1):103–8.

57. Kimura Y, Tanabe M, Imai H, Amano Y, Masuda Y, Yamada Y. Histological examination of experimentally infected root canals after preparation by Er:YAG laser irradiation. Lasers Med Sci. 2011; 26(6):749–54. Epub 2010 Jun 24.
58. Ebihara A, Majaron B, Liaw LH, Krasieva TB, Wilder-Smith P. Er:YAG laser modification of root canal dentine: influence of pulse duration, repetitive irradiation and water spray. Lasers Med Sci. 2002;17(3):198–207.
59. Kivanç BH, Ulusoy OI, Görgül G. Effects of Er:YAG laser and Nd:YAG laser treatment on the root canal dentin of human teeth: a SEM study. Lasers Med Sci. 2008;23(3):247–52. Epub 2007 Jul 21.
60. Esteves-Oliveira M, de Guglielmi CA, Ramalho KM, Arana-Chavez VE, de Eduardo CP. Comparison of dentin root canal permeability and morphology after irradiation with Nd:YAG, Er:YAG, and diode lasers. Lasers Med Sci. 2010;25(5):755–60. Epub 2010 Apr 27.
61. Michiels R, Vergauwen TE, Mavridou A, Meire M, De Bruyne M, De Moor RJ. Investigation of coronal leakage of root fillings after smear-layer removal with EDTA or Nd:YAG lasing through capillary-flow porometry. Photomed Laser Surg. 2010;28 Suppl 2:S43–50.
62. Vergauwen TE, Michiels R, Torbeyns D, Meire M, De Bruyne M, De Moor RJ. Investigation of coronal leakage of root fillings after smear layer removal with EDTA or Er, Cr:YSGG laser through capillary flow porometry. Int J Dent. 2014;2014:593160.
63. Pecora JD, Brugnera-Júnior A, Cussioli AL, Zanin F, Silva R. Evaluation of dentin root canal permeability after instrumentation and Er:YAG laser application. Lasers Surg Med. 2000;26(3):277–81.
64. Brugnera Jr A, Zanin F, Barbin EL, Spanó JC, Santana R, Pécora JD. Effects of Er:YAG and Nd:YAG laser irradiation on radicular dentine permeability using different irrigating solutions. Lasers Surg Med. 2003;33(4):256–9.
65. Biedma BM, Varela Patiño P, Park SA, Barciela Castro N, Magán Muñoz F, González Bahillo JD, Cantatore G. Comparative study of root canals instrumented manually and mechanically, with and without Er:YAG laser. Photomed Laser Surg. 2005;23(5):465–9.
66. Altundasar E, Ozçelik B, Cehreli ZC, Matsumoto K. Ultramorphological and histochemical changes after ER, CR:YSGG laser irradiation and two different irrigation regimes. J Endod. 2006;32(5): 465–8.
67. Radatti DA, Baumgartner JC, Marshall JG. A comparison of the efficacy of Er, Cr:YSGG laser and rotary instrumention in root canal debridement. J Am Dent Assoc. 2006;137(9):1261–6.
68. Varella CH, Pileggi R. Obturation of root canal system treated by Er, Cr:YSGG laser irradiation. J Endod. 2007;33(9):1091–3. Epub 2007 Jul 5.
69. Kalyoncuoğlu E, Demiryürek EÖ. A comparative scanning electron microscopy evaluation of smear layer removal from teeth with different irrigation solutions and lasers. Microsc Microanal. 2013;19(6): 1465–9.
70. Olivi G, Olivi M, Kaitsas V, Benedicenti S. Utilizzo del laser a diodi 810 nm in endodonzia: indagine morfologica al SEM. Dentista Moderno. Ottobre. 2013;31(10):122–128. (article in italian).
71. Gurbuz T, Ozdemir Y, Kara N, Zehir C, Kurudirek M. Evaluation of root canal dentin after Nd:YAG laser irradiation and treatment with five different irrigation solutions: a preliminary study. J Endod. 2008;34(3):318–21.
72. Hmud R, Kahler WA, George R, Walsh LJ. Cavitational effects in aqueous endodontic irrigants generated by near-infrared lasers. J Endod. 2010; 36(2):275–8.
73. Hmud R, Kahler WA, Walsh LJ. Temperature changes accompanying near infrared diode laser endodontic treatment of wet canals. J Endod. 2010;36(5):908–11. Epub 2010 Mar 7.
74. Deleu E, Meire MA, De Moor RJ. Efficacy of laser-based irrigant activation methods in removing debris from simulated root canal irregularities. Lasers Med Sci. 2015;30(2):831–5.
75. Benedicenti S, Cassanelli C, Signore A, Ravera G, Angiero F. Decontamination of root canals with the gallium-aluminum-arsenide laser: an in vitro study. Photomed Laser Surg. 2008;26(4):367–70.
76. Meire MA, De Prijck K, Coenye T, Nelis HJ, De Moor RJ. Effectiveness of different laser systems to kill Enterococcus faecalis in aqueous suspension and in an infected tooth model. Int Endod J. 2009;42(4):351–9. Epub 2009 Feb 7.
77. Mohammadi Z, Shalavi S. Antimicrobial activity of sodium hypochlorite in endodontics. J Mass Dent Soc. 2013;62(1):28–31.
78. Berutti E, Marini R, Angeretti A. Penetration ability of different irrigants into dentinal tubules. J Endod. 1997;23(12):725–7.
79. Kouchi Y, Ninomiya J, Yasuda H, Fukui K, Moriyama T, Okamoto H. Location of Streptococcus mutans in the dentinal tubules of open infected root canals. J Dent Res. 1980;59(12):2038–46.
80. Pirnat S, Lukac M, Ihan A. Study of the direct bactericidal effect of Nd:YAG and diode laser parameters used in endodontics on pigmented and nonpigmented bacteria. Lasers Med Sci. 2011;26(6):755–61. Epub 2010 Jun 27.
81. Moritz A. Oral laser application. Berlin: Quintessence Verlags-GmbH; 2006. p. 258–77.
82. Moritz A, Jakolitsch S, Goharkhay K, Schoop U, Kluger W, Mallinger R, Sperr W, Georgopoulos A. Morphologic changes correlating to different sensitivities of Escherichia coli and enterococcus faecalis to Nd:YAG laser irradiation through dentin. Lasers Surg Med. 2000;26(3):250–61.
83. Neuman KC, Chadd EH, Liou GF, Bergman K, Block SM. Characterization of photodamage to Escherichia coli in optical traps. Biophys J. 1999; 77:2856–63.

84. Mirsaidov U, Timp W, Timp K, Mir M, Matsudaira P, Timp G. Optimal optical trap for bacterial viability. Phys Rev E Stat Nonlin Soft Matter Phys. 2008;78(2 Pt 1):021910.
85. Murray BE. The life and times of the Enterococcus. Clin Microbiol Rev. 1990;3:46–65.
86. Schoop U, Kluger W, Moritz A, Nedjelik N, Georgopoulos A, Sperr W. Bactericidal effect of different laser systems in the deep layers of dentin. Lasers Surg Med. 2004;35:111–6.
87. de Paz LE C, Bergenholtz G, Svensäter G. The effects of antimicrobials on endodontic biofilm bacteria. J Endod. 2010;36(1):70–7. doi:10.1016/j.joen.2009.09.017.
88. Mohammadi Z, Palazzi F, Giardino L, Shalavi S. Microbial biofilms in endodontic infections: an update review. Biomed J. 2013;36(2):59–70. doi:10.4103/2319-4170.110400.
89. Hardee MW, Miserendino LJ, Kos W, Walia H. Evaluation of the antibacterial effects of intracanal Nd:YAG laser irradiation. J Endod. 1994;20(8): 377–80.
90. Fegan SE, Steiman HR. Comparative evaluation of the antibacterial effects of intracanal Nd:YAG laser irradiation: an in vitro study. J Endod. 1995;21(8): 415–7.
91. Moshonov J, Orstavik D, Yamauchi S, Pettiette M, Trope M. Nd:YAG laser irradiation in root canal disinfection. Endod Dent Traumatol. 1995;11(5):220–4.
92. Gutknecht N, Kaiser F, Hassan A, Lampert F. Long-term clinical evaluation of endodontically treated teeth by Nd:YAG lasers. J Clin Laser Med Surg. 1996;14(1):7–11.
93. Ramsköld LO, Fong CD, Strömberg T. Thermal effects and antibacterial properties of energy levels required to sterilize stained root canals with an Nd:YAG laser. J Endod. 1997;23(2):96–100.
94. Blum JY, Michailesco P, Abadie MJ. An evaluation of the bactericidal effect of the Nd:YAP laser. J Endod. 1997;23(9):583–5.
95. Klinke T, Klimm W, Gutknecht N. Antibacterial effects of Nd:YAG laser irradiation within root canal dentine. J Clin Laser Med Surg. 1997;15:29–31.
96. Moritz A, Gutknecht N, Goharkhay K, Schoop U, Wernisch J, Sperr W. In vitro irradiation of infected root canals with a diode laser: results of microbiologic, infrared spectrometric, and stain penetration examinations. Quintessence Int. 1997;28(3):205–9.
97. Moritz A, Doertbudak O, Gutknecht N, Goharkhay K, Schoop U, Sperr W. Nd:YAG laser irradiation of infected root canals in combination with microbiological examinations. J Am Dent Assoc. 1997;128(11):1525–30.
98. Moritz A, Schoop U, Goharkhay K, Jakolitsch S, Kluger W, Wernisch J, Sperr W. The bactericidal effect of Nd:YAG, Ho:YAG, and Er:YAG laser irradiation in the root canal: an in vitro comparison. J Clin Laser Med Surg. 1999;17(4):161–4.
99. Schoop U, Kluger W, Dervisbegovic S, Goharkhay K, Wernisch J, Georgopoulos A, Sperr W, Moritz A. Innovative wavelengths in endodontic treatment. Lasers Surg Med. 2006;38(6):624–30.
100. Franzen R, Gutknecht N, Falken S, Heussen N, Meister J. Bactericidal effect of a Nd:YAG laser on Enterococcus faecalis at pulse durations of 15 and 25 ms in dentine depths of 500 and 1,000 µm. Lasers Med Sci. 2011;26(1):95–101. Epub 2010 Aug 31.
101. Beer F, Buchmair A, Wernisch J, Georgopoulos A, Moritz A. Comparison of two diode lasers on bactericidity in root canals-an in vitro study. Lasers Med Sci. 2012;27(2):361–4. Epub 2011 Feb 2.
102. Meire MA, Coenye T, Nelis HJ, De Moor RJ. Evaluation of Nd:YAG and Er:YAG irradiation, antibacterial photodynamic therapy and sodium hypochlorite treatment on Enterococcus faecalis biofilms. Int Endod J. 2012;45(5):482–91. Epub 2012 Jan 14.
103. Bago I, Plečko V, Gabrić Pandurić D, Schauperl Z, Baraba A, Anić I. Antimicrobial efficacy of a high-power diode laser, photo-activated disinfection, conventional and sonic activated irrigation during root canal treatment. Int Endod J. 2013;46(4):339–47. Epub 2012 Sep 13.
104. Sadık B, Arıkan S, Beldüz N, Yaşa Y, Karasoy D, Cehreli M. Effects of laser treatment on endodontic pathogen Enterococcus faecalis: a systematic review. Photomed Laser Surg. 2013;31(5):192–200. Epub 2013 Apr 15.
105. de Souza EB, Cai S, Simionato MR, Lage-Marques JL. High-power diode laser in the disinfection in depth of the root canal dentin. Oral Surg Oral Med Oral Pathol Oral Radiol Endod. 2008;106(1):e68–72.
106. Mehrvarzfar P, Saghiri MA, Asatourian A, Fekrazad R, Karamifar K, Eslami G, Dadresanfar B. Additive effect of a diode laser on the antibacterial activity of 2.5% NaOCl, 2% CHX and MTAD against Enterococcus faecalis contaminating root canals: an in vitro study. J Oral Sci. 2011;53(3):355–60.
107. Preethee T, Kandaswamy D, Arathi G, Hannah R. Bactericidal effect of the 908 nm diode laser on Enterococcus faecalis in infected root canals. J Conserv Dent. 2012;15(1):46–50.
108. Romeo U, Palaia G, Nardo A, Tenore G, Telesca V, Kornblit R, Del Vecchio A, Frioni A, Valenti P, Berlutti F. Effectiveness of KTP laser versus 980 nm diode laser to kill Enterococcus faecalis in biofilms developed in experimentally infected root canals. Aust Endod J. 2015;41(1):17–23. doi:10.1111/aej.12057. [Epub 2014 Mar 3].
109. Neelakantan P, Cheng CQ, Mohanraj R, Sriraman P, Subbarao C, Sharma S. Antibiofilm activity of three irrigation protocols activated by ultrasonic, diode laser or Er:YAG laser in vitro. Int Endod J. 2015;48(6):602–10.
110. Moritz A. Oral laser application. Berlin: Quintessence Verlags-GmbH; 2006. p. 265–6.
111. Kesler G, Koren R, Kesler A, Hay N, Gal R. Histological changes induced by CO_2 laser microprobe specially

designed for root canal sterilization: in vivo study. J Clin Laser Med Surg. 1998;16(5):263–7.
112. Le Goff A, Dautel-Morazin A, Guigand M, Vulcain JM, Bonnaure-Mallet M. An evaluation of the CO_2 laser for endodontic disinfection. J Endod. 1999; 25(2):105–8.
113. Kesler G, Koren R, Kesler A, Hay N, Gal R. Three years of clinical evaluation of endodontically treated teeth by 15 F CO_2 laser microprobe: in vivo study. J Clin Laser Med Surg. 1999;17(3):111–4.
114. Gutknecht N, Nuebler-Moritz M, Burghardt SF, Lampert F. The efficiency of root canal disinfection using a holmium:yttrium-aluminum-garnet laser in vitro. J Clin Laser Med Surg. 1997;15(2): 75–8.
115. Perin FM, França SC, Silva-Sousa YT, Alfredo E, Saquy PC, Estrela C, Sousa-Neto MD. Evaluation of the antimicrobial effect of Er:YAG laser irradiation versus 1% sodium hypochlorite irrigation for root canal disinfection. Aust Endod J. 2004;30(1): 20–2.
116. Vezzani MS, Pietro R, Silva-Sousa YT, Brugnera-Junior A, Sousa-Neto MD. Disinfection of root canals using Er:YAG laser at different frequencies. Photomed Laser Surg. 2006;24(4):499–502.
117. Wang QQ, Zhang CF, Yin XZ. Evaluation of the bactericidal effect of Er, Cr:YSGG, and Nd:YAG lasers in experimentally infected root canals. J Endod. 2007;33(7):830–2. Epub 2007 May 7.
118. Eldeniz AU, Ozer F, Hadimli HH, Erganis O. Bactericidal efficacy of Er, Cr:YSGG laser irradiation against Enterococcus faecalis compared with NaOCl irrigation: an ex vivo pilot study. Int Endod J. 2007;40(2):112–9.
119. Araki AT, Ibraki Y, Kawakami T, Lage-Marques JL. Er:Yag laser irradiation of the microbiological apical biofilm. Braz Dent J. 2006;17(4):296–9.
120. Noiri Y, Katsumoto T, Azakami H, Ebisu S. Effects of Er:YAG laser irradiation on biofilm-forming bacteria associated with endodontic pathogens in vitro. J Endod. 2008;34(7):826–9. Epub 2008 May 22.
121. Schoop U, Goharkhay K, Klimscha J, Zagler M, Wernisch J, Georgopoulos A, Sperr W, Moritz A. The use of the erbium, chromium:yttrium-scandium-gallium-garnet laser in endodontic treatment: the results of an in vitro study. J Am Dent Assoc. 2007;138(7):949–55.
122. Dewsnup N, Pileggi R, Haddix J, Nair U, Walker C, Varella CH. Comparison of bacterial reduction in straight and curved canals using erbium, chromium:yttrium-scandium-gallium-garnet laser treatment versus a traditional irrigation technique with sodium hypochlorite. J Endod. 2010;36(4):725–8. Epub 2010 Feb 6.
123. Arnabat J, Escribano C, Fenosa A, Vinuesa T, Gay-Escoda C, Berini L, Viñas M. Bactericidal activity of erbium, chromium:yttrium-scandium-gallium-garnet laser in root canals. Lasers Med Sci. 2010;25(6):805–10. Epub 2009 Jun 23.
124. Yavari HR, Rahimi S, Shahi S, Lotfi M, Barhaghi MH, Fatemi A, Abdolrahimi M. Effect of Er, Cr: YSGG laser irradiation on Enterococcus faecalis in infected root canals. Photomed Laser Surg. 2010;28 Suppl 1:S91–6.
125. Yasuda Y, Kawamorita T, Yamaguchi H, Saito T. Bactericidal effect of Nd:YAG and Er:YAG lasers in experimentally infected curved root canals. Photomed Laser Surg. 2010;28 Suppl 2:S75–8. doi:10.1089/pho.2009.2554. Epub 2010 Aug 25.
126. Dos Santos Antonio MP, Moura-Netto C, Camargo SE, Davidowicz H, Marques MM, Maranhão de Moura AA. Bactericidal effects of two parameters of Er:YAG laser intracanal irradiation: ex-vivo study. Lasers Med Sci. 2012;27(6):1165–8. Epub 2011 Nov 23.
127. Cheng X, Guan S, Lu H, Zhao C, Chen X, Li N, Bai Q, Tian Y, Yu Q. Evaluation of the bactericidal effect of Nd:YAG, Er:YAG, Er, Cr:YSGG laser radiation, and antimicrobial photodynamic therapy (aPDT) in experimentally infected root canals. Lasers Surg Med. 2012;44(10):824–31. doi:10.1002/lsm.22092. Epub 2012 Nov 20.
128. Martins MR, Carvalho MF, Vaz IP, Capelas JA, Martins MA, Gutknecht N. Efficacy of Er, Cr:YSGG laser with endodontical radial firing tips on the outcome of endodontic treatment: blind randomized controlled clinical trial with six-month evaluation. Lasers Med Sci. 2013;28(4):1049–55.

Photoactivated Disinfection

7

Giovanni Olivi and Maarten Meire

Abstract

Photoactivated disinfection (PAD), also named antimicrobial photodynamic therapy (aPDT), involves the use of dyes (photosensitizers) that are introduced into the root canal system and activated by light with a wavelength corresponding to the absorption maximum of the dye. These wavelengths are typically within the visible (from 635 to 675 nm) and near-infrared (810 nm) spectrum. Besides the presence of photosensitizer and a specific light source in the target area, this application also requires the presence of sufficient oxygen in the tissue. When all these conditions are satisfied, the exposure of the dye to the light drives a photochemical reaction producing free radicals and singlet oxygen that finally generate the bactericidal effect. Light doses required for this reaction are very low, thereby, virtually eliminating any undesired collateral effect.

Photodynamic therapy (PDT) is a treatment modality that uses a dye (photosensitizer) in combination with (laser) light to selectively kill cells. These cells can either be diseased cells, malignant or pathogenic cells or microorganisms.

When microorganisms are the targeted cells, PDT is referred to as photodynamic antimicrobial chemotherapy (PACT). Synonyms include antimicrobial photodynamic therapy (aPDT), photodynamic inactivation (PDI), lethal photosensitization, light-activated disinfection (LAD) and photoactivated disinfection (PAD). The latter term, photoactivated disinfection (PAD), most clearly describes this concept of disinfection by light-activated substances and will be used throughout this text.

G. Olivi (✉)
InLaser Rome – Advanced Center for Esthetic and Laser Dentistry, Rome, Italy
e-mail: olivilaser@gmail.com

M. Meire, DDS, MSc, PhD
Department of Restorative Dentistry and Endodontology, Ghent University,
De Pintelaan 185/P8, Ghent 9000, Belgium
e-mail: Maarten.Meire@UGent.be

G. Olivi et al. (eds.), *Lasers in Endodontics: Scientific Background and Clinical Applications*,
DOI 10.1007/978-3-319-19327-4_7

7.1 Historical Background

The earliest recorded treatment discussing the use of chemical substances and light (sunlight in this case) for medical application dates back to 3000 years ago. In the ancient Egyptian and Indian populations, vegetable substances were topically applied on the skin. Irradiation with sunlight induced photoreactions, producing repigmentation of skin lesions. From that time on, a lot of similar applications have taken place.

At the beginning of the twentieth century, modern medicine started to study the effects of light on different substances and tissues [1].

Research conducted in Germany showed that oxygen was essential for the chemical reaction of different substances [2], and von Tappeiner (1904) first coined the term "photodynamic action" [3].

The use of dyes in combination with light to kill cells was first clinically applied in the field of cancer therapy. In the seventies and eighties, cancer surgeons started to use porphyrin derivatives in conjunction with laser light as an alternative treatment of tumours [4]. Cancer photochemotherapy, or photodynamic therapy (PDT), as it was called, is a two-step procedure, involving the topical or systemic administration of a photosensitizer (PS) which is selectively taken up by the tumour cells, followed by selective illumination of the target lesion with the appropriate (laser) light, which triggers the oxidative photodamage and subsequent cell death within the target area through formation of toxic oxygen species such as singlet oxygen and free radicals. The light or drug alone is non-toxic; only cells that contain the photosensitizer and receive light are affected by the treatment. PDT has the advantage over other therapies of dual selectivity: not only is the PS targeted to the tumour or other lesion, but the light can also be accurately delivered to the affected tissue.

Results from preclinical and clinical studies conducted worldwide have established photodynamic therapy as a useful treatment approach for selective cancers of the lung, bladder, oesophagus, head and neck, digestive and genitourinary tract. PDT is also routinely used in dermatology, for the treatment of skin tumours and selective inflammatory and infective diseases. HpD, a porphyrin species derived from hematoporphyrin, was the first agent approved for clinical use in 1993 to treat a form of bladder cancer in Canada. Over later decades, research and clinical studies grew leading PDT treatments to receive US Food and Drug Administration (FDA) approval for the treatment of different types of cancer [5, 6]. Other non-oncological applications of PDT exist in ophthalmology and other fields of medicine, for example, the inactivation of viruses in human blood plasma, to reduce the risk of blood transfusion-transmitted diseases as HCV and HIV [7].

The emergence of antibiotic resistance amongst pathogenic bacteria has led to a major research effort to find alternative antibacterial therapeutics to which bacteria will not easily develop resistance. A number of studies have demonstrated that not only mammalian cells but also microbes (bacteria, fungi and viruses) can be killed by various combinations of photosensitizer and light [8, 9].

In the field of dentistry, PAD was introduced as a new disinfection method providing a powerful antibacterial action and thus improved results in a wide range of applications. PAD has been applied to treat periodontal and endodontic infections as well as other oral pathology [10–16].

7.2 Mechanism of Action of PAD

The mechanism of PAD is different from other light- or laser-based therapies such as low-level laser therapy (LLLT) and high-power laser therapy in the sense that the latter does not require a photosensitizer. The laser light source in PAD does not have a direct effect on the tissue or bacteria but photoactivates a specific compound that releases toxic elements to the target.

PAD application requires three fundamental elements [17]:

- A photosensitizer
- A light source
- Tissue oxygen

Photosensitizers are usually aromatic molecules which are efficient in the formation of long-lived triplet excited states when excited (lifted to a higher energy state) by light of a specific wavelength.

Activation of the photosensitizer upon absorption of the light transforms the drug from its ground state into an excited singlet state. This excited state may then undergo intersystem crossing (the spontaneous change of a system from one spin quantum number to another) to the slightly lower energy, but longer lived, triplet state, which may then react further by one or both of the two pathways known as the Type I and Type II photo processes, both of which require oxygen [18] (Fig. 7.1) (Fig. 7.2).

The Type I pathway involves electron transfer reactions from the PS triplet state with the participation of a substrate to produce radical ions (free radicals) that can then react with oxygen to produce cytotoxic species, such as superoxide, hydroxyl and lipid-derived radicals.

The Type II pathway involves energy transfer from the PS triplet state to ground-state molecular oxygen (triplet) to produce excited-state singlet oxygen ($^1O2$), which can oxidize many biological molecules, such as proteins, nucleic acids and lipids, and lead to cytotoxicity [19].

The reactive oxygen species (ROS) resulting from both pathways mediate cellular damage. Amongst the ROS, singlet oxygen plays a central role for cytotoxicity in PAD, and the greater the amount of singlet oxygen the target is exposed to, the more effectively cancer cells or bacteria are killed [20, 21].

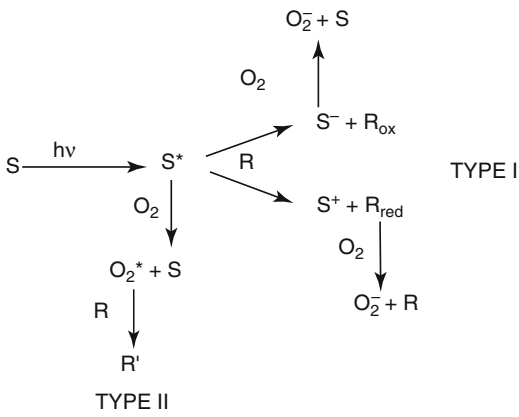

Fig. 7.1 Activation of a photosensitizer (S) by light (hν) to triplet state (*S) and reaction with oxygen (O_2) or other substrate (R) in Type I and II photo processes

Many of the target chromophores are cell components that are located close to or are part of the oxidative metabolism (mitochondria) which is essential for the cell vitality. Reactive oxygen species can damage proteins, lipids and other cellular components.

Initially, most studies investigating PAD used photosensitizers developed for use in the treatment of tumours, e.g. the hematoporphyrins, which are reportedly ineffective against gram-negative bacteria [22]. However, Macmillan et al. have shown that other dyes such as toluidine blue can sensitize many bacteria to killing by monochromatic light from a laser [23]. A wide range of PS have been used against pathogenic organisms. They include phenothiazine dyes (methylene blue (MB), toluidine blue O (TBO)), phthalocyanines, chlorins, porphyrins, xanthenes and monoterpene.

Physicochemical parameters such as lipophilicity (log P) and ionization (pKa) are obviously of importance, but other more specialized factors such as light absorption characteristics (the maximum wavelength of absorption λmax, the intensity of the absorption εmax) and the efficiency of singlet oxygen production ΦΔ must be included in a putative photoantimicrobial profile.

Toluidine blue, methylene blue, chlorin e6 conjugates, porphyrin and its derivatives are commonly used photosensitizers in PAD. These photosensitizers can be excited by light sources that fall in the range of red-visible spectrum (usually from 635 to 675 nm) [24].

Indocyanine green is another photosensitizer, activated by wavelengths in the near-infrared spectrum, with a high absorption around 800 nm [25].

Riboflavin and pheophorbide-a polylysine (pheophorbide-a-PLL) are photoactivated by light sources that fall in the range of the visible blue light (380–500 nm) [26].

As of November 2014, few studies have been published on the use of these photosensitizers

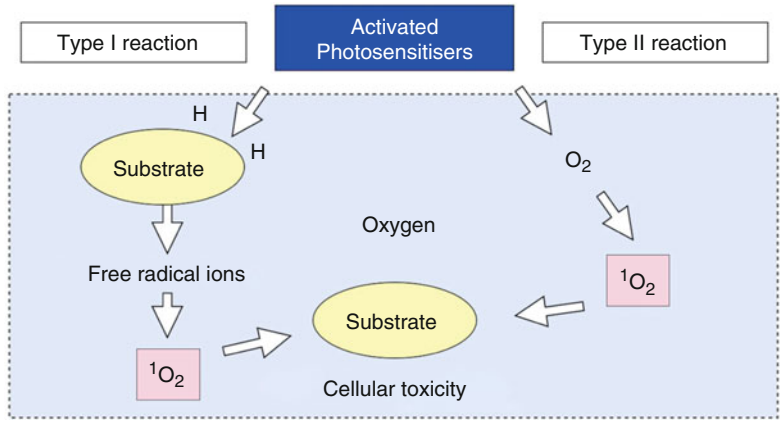

Fig. 7.2 Diagrammatic representation of the different PAD mechanisms (Image courtesy of Giovanni Olivi, Rome, Italy)

and laser sources in endodontics (MEDLINE®/PubMed® Resources Guide).

Fundamental to the PAD procedure is the match between photosensitizer and light source. The light source has to emit in the area of the electromagnetic spectrum that coincides with the absorption maximum of the photosensitizer, in order to lift the sensitizer to its triplet state.

In addition, in order to reach the photosensitizer in situ, the penetration depth of the light is also important. Therefore, the wavelengths have to fall within the so called "*therapeutic window*" of the electromagnetic spectrum between 635 and 1000 nm, the area with the maximum penetration of light into the tissues [24].

Penetration depth in biological tissue for the wavelengths from 635 to 675 nm is about 3–3.5 mm. Wavelengths in the near-infrared spectrum (from 800 to 1000 nm) can penetrate biological tissue deeper, up to 4–5 mm [25].

PAD has also been described as a new therapeutic approach in the management of oral biofilms, with the ability to disrupt the biofilm integrity and affect the biofilm homeostasis [10].

The fact that the active substances are preferentially targeted to the external cell membranes or, when inside, on other intracellular structures virtually eliminates the risk of development of resistance to PAD or inducing gene mutation on the target or surrounding cells. The safety of the procedure makes PAD a treatment strategy which is minimally toxic. The desired/undesired side effect ratio of this treatment is usually high when compared to traditional antimicrobials [27].

High-power lasers, such as the Nd:YAG, have also been reported to be useful for destroying microorganisms, presumably by a thermal effect. Thermal side effect and damage are of concern. PAD in contrast uses low-power light: microbial killing is attained with milliwatts rather than tens or hundreds of watts, without the risk of thermal damage to surrounding structures.

Regarding the effectiveness of the PAD technique, several factors must be considered:

(a) The fundamental condition for the PAD microbial killing to take place is contact between the photosensitizer and the microorganisms, since the toxic photosensitizer reaction products are short lived and do not act over a great distance. The extent of disinfection thus depends on the extent to which the chemical spreads into the root canal system and dentinal tubules. In this respect, there are no indications that the photosensitizer solution has superior spreading properties than, for example, those of sodium hypochlorite. The advantageous properties of photodynamic disinfection are then limited.
(b) Type I and II reactions require sufficient oxygenation of the target area. This might not be the case in the anaerobic environment found in primary root canal infections.

(c) Absorption of energy by the dental tissues could result in an insufficient energy density at the target site, thereby reducing the disinfecting action.
(d) The wavelengths used must sufficiently penetrate the dental tissues and have adequate differential affinity from the surrounding tissue to avoid energy loss and possible side effects.
(e) Protocols to remove photosensitizing dyes should be applied after PAD in order to minimize tooth discoloration.

7.3 PAD in Endodontics

In vitro studies on PAD have demonstrated its ability to kill photosensitized oral bacteria such as *E. faecalis*. More recent in vivo studies demonstrated the microbicidal effect of PAD in the root canal system and also its potential to eradicate persistent endodontic infections for which conventional methods have been unsuccessful [28].

Many studies have investigated the role of photoactivated disinfection as an adjunct to conventional irrigation for root canal disinfection.

Bonsor et al. (2006) published two clinical studies on PAD. The first aimed to assess the efficacy of PAD as an adjunct therapy to conventional root canal disinfection. This in vivo study was performed on teeth with symptoms of irreversible pulpitis or periradicular periodontitis. Microbiological samples were taken from the canals after accessing the canal, after conventional disinfection procedures and after the PAD process. Samples were plated onto anaerobic culture media and incubated for 5 days. Sixteen out of twenty infected canals were negative to culture after conventional endodontic therapy. Three of the four which had remained infected cultured negative after the PAD process. The last sample treated with a fibre was positive for bacteria, but upon inspection the fibre was broken reducing the effective light output by 90 %. The authors concluded that PAD offers potential to eliminate bacteria from the root canals especially where conventional techniques have failed to do so [29].

In a second study, performed in vivo on 64 teeth, Bonsor et al. (2006) compared the use of 20 % citric acid in association with PAD to the use of 20 % citric acid and 2.25 % sodium hypochlorite on the intracanal bacterial load. Samples taken before and after the disinfection therapy were anaerobically cultured. Results indicated that the combination of a chelating agent (citric acid), acting as a cleaner, with the photoactivated disinfection was an effective alternative to the use of sodium hypochlorite for the root canal cleaning and disinfection [30].

Garces et al. (2007) performed an in vitro study on extracted human teeth mechanically prepared and infected with two bioluminescent gram-negative species (*Proteus mirabilis* and *Pseudomonas aeruginosa*). The samples were cultured for 3 days to create intracanal biofilms. Conventional endodontic irrigation was compared to PAD using a conjugate between polyethylenimine and chlorin (e6) as photosensitizer activated by a 660-nm diode laser, delivered in the canals through a 200-μm fibre. The conventional therapy alone led to a reduction of bacterial bioluminescence of 90 %, whilst the PDT alone resulted in a reduction of 95 %. The combination of the two therapies resulted in a reduction of more than 98 %. Bacterial regrowth observed 24 h after treatment was much lower for the combined therapy samples compared to the single treatments ($P < 0.0005$) [31].

Foschi et al. (2007) tested aPDT in root canals of extracted teeth experimentally infected with *E. faecalis* for 3 days. Methylene blue (6.25 μg/mL) was left in the canal for 5 min, then irradiated with 665-nm laser light (60 J/cm^2) transmitted through an optical fibre of 500 μm. They observed only a 77.5 % (i.e., <1 log unit) reduction in viable counts and concluded that the photosensitizer concentration and light parameters require optimization to maximize bacterial killing in root canals [32].

Garcez et al. (2008) in another study analysed in vivo the antimicrobial effect of PAD in association with conventional endodontic treatment. They collected microbiological samples after accessing the canal, following conventional instrumentation irrigation and after photoactivated disinfection.

Conventional chemomechanical root canal cleaning resulted in a mean reduction of the bacterial load of 1.08 log units. Combination with PDT significantly enhanced the reduction to 1.83 log units. Also a second PDT session in a second visit was significantly more effective than the first. The authors concluded that the use of PDT added to endodontic treatment leads to an increased bacterial reduction [33].

Lim et al. (2009) investigated the efficacy of light-activated disinfection on 4-day-old (immature) and 4-week-old (mature) *Enterococcus faecalis* biofilms grown within root canals of extracted teeth. Different treatment protocols were investigated: chemical (NaOCl) disinfection, conventional PAD, improved PAD (photosensitizer in a specific solvent system followed by illumination in the presence of an irradiation medium) and chemomechanical disinfection (alone and in combination with improved PAD). In the 4-day-old group, inactivation of bacteria from deeper dentine was higher using improved PAD than using sodium hypochlorite alone. In 4-week-old biofilms, the combination of chemomechanical disinfection and improved PAD produced superior bacterial killing compared to either chemomechanical disinfection or improved PAD alone, highlighting the potential of improved PAD to kill bacteria within dentinal tubules [34].

Garcez et al. (2010) studied in vivo the antimicrobial effect of PAD in combination with conventional endodontic treatment on patients with necrotic pulps and resistant antibiotic microflora. They selected 30 anterior teeth with apical lesions from 21 patients that were previously treated with conventional endodontic treatment and antibiotic therapy. Microbiological samples were taken after accessing the root canal, after conventional endodontic therapy and finally after PAD. Polyethylenimine-chlorin was used as photosensitizer, and a diode laser was used as a light source (40 mW for 4 min, 9.6 J). Conventional endodontic therapy alone produced a significant reduction in numbers of microbial species but only three teeth were free of bacteria. The combination of PAD and conventional endodontic treatment significantly increased the number of bacteria-free teeth and eliminated all drug-resistant species [35].

Rios et al. (2011) evaluated the antimicrobial effect of PAD using toluidine blue O (TBO) in combination with a LED light source after a conventional disinfection protocol with 6 % NaOCl on extracted teeth infected for 2 weeks with *Enterococcus faecalis*. The bacterial survival rate of the NaOCl/TBO/light group (0.1 %) was found to be significantly lower ($P < .005$) than the NaOCl (0.66 %) and TBO/light groups (2.9 %), suggesting the potential use of PAD as an adjunctive antimicrobial procedure in conventional endodontic therapy [36].

Poggio et al. (2011) compared the antimicrobial effect of photoactivated disinfection, conventional 5.25 % NaOCl irrigation and a combination of both on *Enterococcus faecalis*-, *Streptococcus mutans*- and *Streptococcus sanguis-infected* teeth. They reported that PAD applied for a longer time or PAD associated with 5 % NaOCl showed significantly higher antibacterial effects [37].

Silva et al. (2012) studied in vivo the response of periapical tissues of dog's teeth with apical periodontitis after one-session endodontic treatment with and without antimicrobial photodynamic therapy (PAD). Phenothiazine chloride at 10 mg/mL was inoculated for 3 min as a photosensitizer and then photoactivated by a diode laser (660 nm, 60 mW/cm^2) for 1 min. After 90 days, sections from the maxillas and mandibles were histologically investigated. Qualitatively and quantitatively, the PAD-treated groups showed periapical region moderately/severely enlarged, with no inflammatory cells, moderate neoangiogenesis and fibrogenesis and the smallest periapical lesions suggesting PAD as a promising adjunct therapy to cleaning and shaping procedures in teeth with apical periodontitis undergoing one-session endodontic treatment [38].

The studies cited so far describe the use of PAD in combination with traditional chemomechanical root canal cleaning. The photoactivated disinfection has also been studied as an alternative method for root canal disinfection.

Fonseca et al. (2008) studied the effects of PAD on root canals of extracted teeth infected with *Enterococcus faecalis* and incubated for 48 h. A solution of 0.0125 % toluidine blue was used for 5 min followed by irradiation using a

diode laser (Ga-Al-As, 660 nm) at 50 mW. The mean decrease in CFU was 99.9 % in the test group, whereas in the untreated control group, an increase of 2.6 % was observed [39].

Fimple et al. (2008) investigated the effects PAD on root canal systems incubated with a combination of *Actinomyces israelii*, *Fusobacterium nucleatum* subspecies nucleatum, *Porphyromonas gingivalis* and *Prevotella intermedia*. Scanning electron microscopy analysis showed the presence of biofilms in the root canals before therapy. Methylene blue (25 μg/mL) was inoculated into the canals and left for 10 min followed by exposure to red light at 665 nm with a fluence of 30 J/cm^2 delivered with a 250-μm fibre. The PAD achieved up to 80 % reduction of colony-forming unit counts [40].

An in vitro apical lesion model was used by Nagayoshi et al. (2011) to study the direct effects of irradiation with a diode laser as well as heat produced by irradiation on the viability of microorganisms in periapical lesions. The combination of a photosensitizer and laser irradiation significantly reduced the viability of *E. faecalis*. The study also demonstrated that the rise in temperature caused by irradiation was not responsible of the cytotoxic effects on *E. faecalis* [41].

Stojicic et al. (2013) compared the efficacy of conventional and modified photoactivated disinfection (PAD) against *Enterococcus faecalis* and mixed plaque bacteria in suspension and biofilms. Conventional PAD, used for 3 min, killed from 90.76 to 100 % *E. faecalis* but failed to kill all plaque bacteria even after 5 min of laser irradiation. In modified PAD, up to 100 % of suspended *E. faecalis* and mixed plaque bacteria were killed after 1 min and 30 s of irradiation. Up to twenty times, more biofilm bacteria were killed by modified PAD than by conventional PAD with 15 μmolL MB and up to eight times more than 2 % CHX and 1 % sodium hypochlorite [42].

Bago et al. (2013) evaluated the antimicrobial effect of a diode laser irradiation (2 W, 3 × 20 s), photoactivated disinfection (PAD) (100 mW, 60 s), conventional syringe irrigation (30 gauge with 2.5 % NaOCl, 60s) and sonic activated irrigation (EndoActivator system with 2.5 % NaOCl, 60 s) on *Enterococcus faecalis*. The PAD and EndoActivator system were more successful in reducing the root canal infection than the diode laser and NaOCl syringe irrigation alone [43].

All these studies reported that the use of PAD alone or in association to conventional endodontic treatment produces an enhanced reduction of bacterial load suggesting a new approach for the treatment of oral infections.

However, other studies found that photoactivated disinfection in addition to chemomechanical preparation, using NaOCl as irrigant, did not significantly enhance the disinfection process.

Souza et al. (2010) used both methylene blue and toluidine blue (both at 15 microg/mL) as a supplement to chemomechanical instrumentation of root canals experimentally contaminated with *Enterococcus faecalis* for 7 days. The photosensitizer remained in the canal for 2 min before being exposed to red light emitted from a diode laser for 4 min. Samples taken before and after conventional instrumentation/irrigation and following the specific PAD procedure for each group demonstrated no significant PAD effect ($p>0.05$). Also no significant difference was observed between the two photosensitizers ($p > 0.05$) [44].

Furthermore, other studies reported controversial results on the effectiveness of use of PAD as an alternative to conventional use of irrigants in the endodontic.

Nunes et al. (2011) evaluated the role of the intracanal or extracanal position of the optical fibre during the PAD process and compared the decontamination efficacy of this method to conventional 1 % NaOCl irrigation. The greatest reduction of *E. faecalis* (99.99 %) was achieved with irrigation with 1 % NaOCl. PDT also significantly reduced *E. faecalis*, but the result was not significantly better than the conventional method. The different time of application (90 or 180 s) influenced the results more than the fibre position [45].

Meire et al. (2012) compared, on in vitro grown *Enterococcus faecalis* biofilms on dentine discs, the antimicrobial efficacy of two high-power lasers (Nd:YAG 2 W, 15 Hz, 40 s and Er:YAG 50 mJ or 100 mJ, 15 Hz, 40 s) and two commercially available PAD systems (Denfotex and Helbo) with that of sodium hypochlorite for 1-, 5-, 10- and 30-min intervals. NaOCl was the most effective in *E. faecalis* biofilm elimination.

The Er:YAG laser treatment using 100 mJ pulses also resulted in high reduction in viable counts. On the other hand, the use of both PAD systems resulted in a weak reduction in the number of *E. faecalis* cells. Nd:YAG irradiation was the least effective [46].

Cheng et al. (2012) compared the bactericidal effect of high-power Nd:YAG, Er:YAG and Er,Cr:YSGG laser in combination with 5.25 % sodium hypochlorite, PAD and standard endodontic irrigation with 5.25 % sodium hypochlorite on root canals infected with *Enterococcus faecalis* for 4 weeks. PAD resulted in an average reduction of 98 %, which was better than the reductions with Nd:YAG or Er,Cr:YSGG treatment. However, highest reductions (100 %) on the surface of root canal walls or at 100/200 μm inside the dentinal tubules were observed in the Er:YAG + NaOCl + saline solution group [47].

Lately, a systematic review based on PubMed/Medline and Google-Scholar databases search from 1985 up to August 2013 was carried out by Siddiqui et al. (2013). The study included sixteen ex vivo and one in vivo study investigating the bactericidal effects of PAD against *E. faecalis* in infected root canals. In these studies, diode lasers with wavelengths ranging between 625 and 805 nm were used with fibres with diameters ranging from 200 μm to 4 mm and power outputs from 40 mW to 5 W, respectively. In most of the studies, toluidine blue and methylene blue were used as photosensitizers. Twelve studies reported PAD to be effective in eliminating *E. faecalis* from infected root canals. Four studies reported conventional irrigation and instrumentation to be more efficient in killing *E. faecalis* than PAD. One study reported PAD and conventional endodontic regimes to be equally effective. The study concluded that the efficacy of PAD in eliminating *E. faecalis* from infected root canals remains questionable [48] (Fig. 7.3).

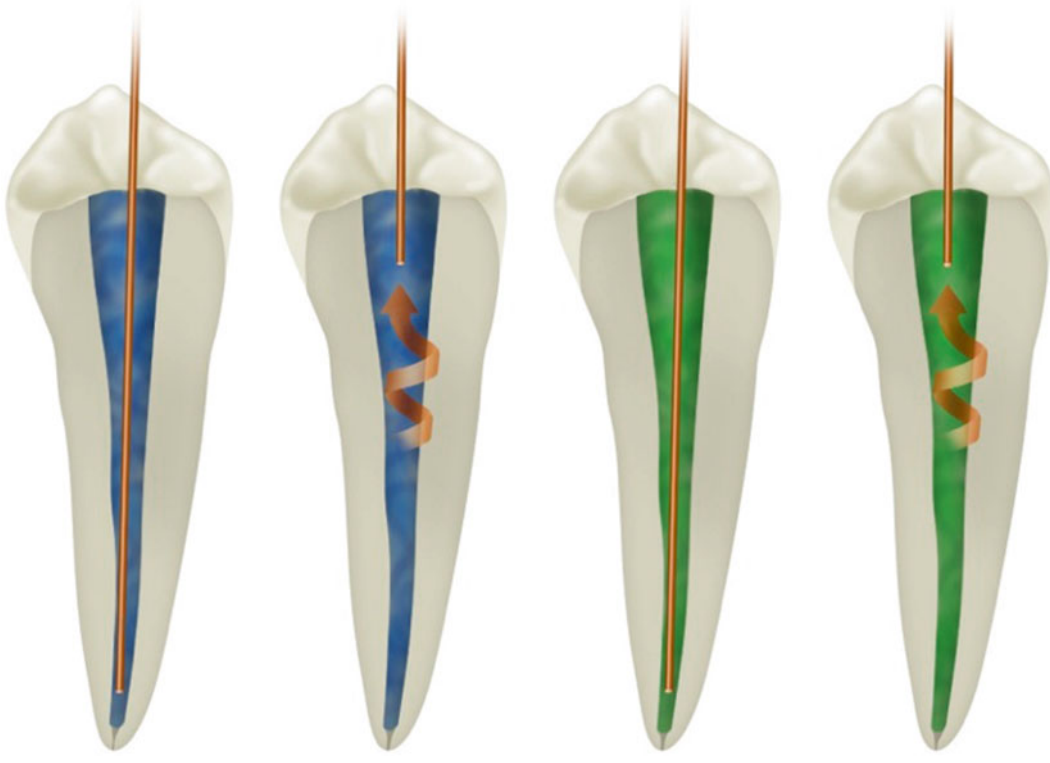

Fig. 7.3 Diagrammatic representation of the different photosensitizers used in endodontics for PAD (Image courtesy of Giovanni Olivi, Rome, Italy)

7.4 Discussion

Considering the controversial results reported in the literature, some of the previously mentioned factors remain a concern for the success of PAD.

Bacteria colonize the root canal system where they form complex biofilms on the canal walls and invade the underlying dentinal tubules. For the PAD procedure to be effective, it is essential that the photosensitizer physically reaches these microorganisms. To date, it is well known that most currently employed irrigation methods fail to adequately deliver and spread the irrigant solution within the complex three-dimensional microstructure of the canal system. Especially the apical part of the canal system and lateral extensions and isthmuses seem to be difficult to reach. There is no reason to assume that photosensitizer solutions perform better than traditional root canal irrigants in their action. Hence, the photosensitizer may not be evenly distributed across the root canal system. Also, penetration of photosensitizers into the dentinal tubules has not been investigated. As a consequence, certain areas of infection will escape the photoactivated disinfection.

Another issue with PAD is the oxygen concentration within the target area. In many cases, especially in primary root canal infections, the root canal microbiota is predominantly anaerobic, which means that all oxygen within the microbial environment has been consumed. Therefore, the oxygen required for effective PAD therapy might be lacking, rendering PAD therapy less effective.

The various light sources that are being applied in PAD therapy have different penetration in the tooth structure. In the majority of studies, visible red light is being used, whilst the investigation of green photosensitizers and more deeply penetrating near-infrared lasers is, at this time, more developed in periodontal PDT.

Accordingly, the necessity of using an intracanal or external optical fibre when performing antimicrobial photo therapy (PAD) was studied, and Garcez et al. (2013) confirmed the results of Nunes et al. (2011) concluding that the intracanal irradiation is more effective than external irradiation in reducing the endodontic bacterial load [45, 49].

When considering all the literature on PAD, the variation in irradiation parameters (irradiation time, output power, emitter tip) is striking. It seems that the ideal combination of photosensitizer and light source with the ideal irradiation parameters is yet to be found. Up to now, univocal experimental protocols with predictable results are lacking.

A study from Komine et al. (2013) concluded that 0.001–0.01 % of methylene blue (MB) resulted the most effective range for generating $^1O_2$ during the application of antimicrobial photodynamic therapy and that at least 35.2 μmol/L generated $^1O_2$ is necessary to achieve the sterilization of *E. faecalis*. This study utilized a 660-nm diode laser as activator (at 200 mW) [50].

Carvalho et al. [2011] reported that the use of 2.5 % NaOCl was effective in avoiding tooth staining caused by MB during PAD in endodontics [51], but more studies regarding other photosensitizer dyes used are required to avoid such a problem.

Adjustments in the PAD protocol are required to enhance the predictability in bacterial elimination before clinical use is recommended. Concentration, distribution and penetration depth of the photosensitizer, oxygen concentration in the target tissue and tooth staining all remain unresolved problems.

References

1. Moan J, Peng Q. An outline of the hundred-year history of PDT. Anticancer Res. 2003;23(5A):3591–600.
2. Raab O. Ueber die wirkung fluorescierenden stoffe auf infusorien. Z Biol. 1904;39:524–46.
3. von Tappeiner H, Jodlbauer A. Uber die wirkung der photodynamischen (fluorescierenden) stoffe auf protozoen und enzyme. Dtsch Arch Klin Med. 1904;80:427–87.
4. Dougherty TJ, Kaufman JE, Goldfarb A, Weishaupt KR, Boyle D, Mittleman A. Photoradiation therapy for the treatment of malignant tumors. Cancer Res. 1978;38:2628–35.
5. Dolmans DE, Fukumura D, Jain RK. Photodynamic therapy for cancer. Nat Rev Cancer. 2003;3:380–7.
6. Juarranz A, Jaen P, Sanz-Rodriguez F, Cuevas J, Gonzalez S. Photodynamic therapy of cancer .Basic principles and applications. Clin Transl Oncol. 2008;10:148–54.
7. Muller-Breitkreutz K, Mohr H. Hepatitis C and human immunodeficiency virus RNA degradation by

methylene blue/light treatment of human plasma. J Med Virol. 1998;56:239–45.
8. Kharkwal GB, Sharma SK, Huang YY, Dai T, Hamblin MR. Photodynamic therapy for infections: clinical applications. Lasers Surg Med. 2011;43:755–67.
9. Vera DM, Haynes MH, Ball AR, Dai DT, Astrakas C, et al. Strategies to potentiate antimicrobial photoinactivation by overcoming resistant phenotypes. Photochem Photobiol. 2012;88:499–511.
10. Konopka K, Goslinski T. Photodynamic therapy in dentistry. J Dent Res. 2007;86(8):694–707.
11. Herrera D. Photodynamic therapy for chronic periodontitis. Evid Based Dent. 2011;12:78–9.
12. Soukos NS, Goodson JM. Photodynamic therapy in the control of oral biofilms. Periodontol 2000. 2011;55:143–66.
13. Marsh PD, Moter A, Devine DA. Dental plaque biofilms: communities, conflict and control. Periodontol 2000. 2011;55:16–35.
14. Soukos NS, Chen PS, Morris JT, Ruggiero K, Abernethy AD, et al. Photodynamic therapy for endodontic disinfection. J Endod. 2006;32:979–84.
15. Garcia VG, Fernandes LA, Macarini VC, de Almeida JM, Martins TM, et al. Treatment of experimental periodontal disease with antimicrobial photodynamic therapy in nicotine-modified rats. J Clin Periodontol. 2011;38:1106–14.
16. Pereira Gonzales F, Maisch T. Photodynamic inactivation for controlling Candida albicans infections. Fungal Biol. 2012;116:1–10.
17. Wang SS, Chen J, Keltner L, Christophersen J, Zheng F, Krouse M, Singhal A. New technology for deep light distribution in tissue for phototherapy. Cancer J. 2002;8(2):154–63.
18. Ochsner M. Photophysical and photobiological processes in the photodynamic therapy of tumours. J Photochem Photobio. 1997;39:1–18.
19. Foote CS. Definition of type I and type II photosensitized oxidation. Photochem Photobiol. 1991;54:659.
20. Bhatti M, MacRobert A, Meghji S, Henderson B, Wilson M. A study of the uptake of toluidine blue O by Porphyromonas gingivalis and the mechanism of lethal photosensitization. Photochem Photobiol. 1998;68:370–6.
21. Yamamoto J, Yamamoto S, Hirano T, Li S, Koide M, et al. Monitoring of singlet oxygen is useful for predicting the photodynamic effects in the treatment for experimental glioma. Clin Cancer Res. 2006;12:7132–9.
22. Malik Z, Hanania J, Nitzan Y. Bactericidal effects of photoactivated porphyrins–an alternative approach to antimicrobial drugs. J Photochem Photobio. 1990;5:281–93.
23. Macmillan JD, Maxwell WA, Chichester CO. Lethal photosensitization of microorganisms with light from a continuous-wave gas laser. Photochem Photobiol. 1966;5:555–65.
24. Huang Y-Y, Chen AC, Carroll JD, Hamblin M. Biphasic dose response in low level light therapy. Dose–response. 2009;7:358–83.
25. Bashkatov AN, Genina EA, Kochubey VI, Tuchin VV. Optical properties of human skin, subcutaneous and mucous tissues in the wavelength range from 400 to 2000 nm. J Phys D Appl Phys. 2005;38:2543–55.
26. Bouillaguet S, Wataha JC, Zapata O, Campo M, Lange N, Schrenzel J. Production of reactive oxygen species from photosensitizers activated with visible light sources available in dental offices. Photomed Laser Surg. 2010;28(4):519–25.
27. Winckler KD. Editorial Special section: Focus on anti-microbial photodynamic therapy (PDT). J of Photochem Photobiol B. 2007;86:43–4. Biology.
28. Lee MT, Bird PS, Walsh LJ. Photo-activated disinfection of the root canal: a new role for lasers in endodontics. Aust Endod J. 2004;30(3):93–8.
29. Bonsor SJ, Nichol R, Reid TM, Pearson GJ. Microbiological evaluation of photo-activated disinfection in endodontics (an in vivo study). Br Dent J. 2006;200(6):337–41; discussion 329.
30. Bonsor SJ, Nichol R, Reid TM, Pearson GJ. An alternative regimen for root canal disinfection. Br Dent J. 2006;201(2):101–5.
31. Garcez AS, Ribeiro MS, Tegos GP, Núñez SC, Jorge AO, Hamblin MR. Antimicrobial photodynamic therapy combined with conventional endodontic treatment to eliminate root canal biofilm infection. Lasers Surg Med. 2007;39(1):59–66.
32. Foschi F, Fontana CR, Ruggiero K, Riahi R, Vera A, Doukas AG, Pagonis TC, Kent R, Stashenko PP, Soukos NS. Photodynamic inactivation of Enterococcus faecalis in dental root canals in vitro. Lasers Surg Med. 2007;39(10):782–7.
33. Garcez AS, Nuñez SC, Hamblin MR, Ribeiro MS. Antimicrobial effects of photodynamic therapy on patients with necrotic pulps and periapical lesion. J Endod. 2008;34(2):138–42. doi:10.1016/j.joen.2007.10.020. Epub 2007 Dec 21.
34. Lim Z, Cheng JL, Lim TW, Teo EG, Wong J, George S, Kishen A. Light activated disinfection: an alternative endodontic disinfection strategy. Aust Dent J. 2009;54(2):108–14.
35. Garcez AS, Nuñez SC, Hamblim MR, Suzuki H, Ribeiro MS. Photodynamic therapy associated with conventional endodontic treatment in patients with antibiotic-resistant microflora: a preliminary report. J Endod. 2010;36(9):1463–6.
36. Rios A, He J, Glickman GN, Spears R, Schneiderman ED, Honeyman AL. Evaluation of photodynamic therapy using a light-emitting diode lamp against Enterococcus faecalis in extracted human teeth. J Endod. 2011;37(6):856–9.
37. Poggio C, Arciola CR, Dagna A, Florindi F, Chiesa M, Saino E, Imbriani M, Visai L. Photoactivated disinfection (PAD) in endodontics: an in vitro microbiological evaluation. Int J Artif Organs. 2011;34(9):889–97.
38. Silva LA, Novaes Jr AB, de Oliveira RR, Nelson-Filho P, Santamaria Jr M, Silva RA. Antimicrobial photodynamic therapy for the treatment of teeth with

apical periodontitis: a histopathological evaluation. J Endod. 2012;38(3):360–6.
39. Fonseca MB, Júnior PO, Pallota RC, Filho HF, Denardin OV, Rapoport A, Dedivitis RA, Veronezi JF, Genovese WJ, Ricardo AL. Photodynamic therapy for root canals infected with Enterococcus faecalis. Photomed Laser Surg. 2008;26(3):209–13.
40. Fimple JL, Fontana CR, Foschi F, Ruggiero K, Song X, Pagonis TC, Tanner AC, Kent R, Doukas AG, Stashenko PP, Soukos NS. Photodynamic treatment of endodontic polymicrobial infection in vitro. J Endod. 2008;34(6):728–34.
41. Nagayoshi M, Nishihara T, Nakashima K, Iwaki S, Chen KK, Terashita M, Kitamura C. Bactericidal effects of diode laser irradiation on Enterococcus faecalis using periapical lesion defect model. ISRN Dent. 2011;870364.
42. Stojicic S, Amorim H, Shen Y, Haapasalo M. Ex vivo killing of Enterococcus faecalis and mixed plaque bacteria in planktonic and biofilm culture by modified photoactivated disinfection. Int Endod J. 2013;46(7):649–59. doi:10.1111/iej.12041. Epub 2013 Jan 4.
43. Bago I, Plečko V, Gabrić Pandurić D, Schauperl Z, Baraba A, Anić I. Antimicrobial efficacy of a high-power diode laser, photo-activated disinfection, conventional and sonic activated irrigation during root canal treatment. Int Endod J. 2013;46(4):339–47.
44. Souza LC, Brito PR, de Oliveira JC, Alves FR, Moreira EJ, Sampaio-Filho HR, Rôças IN, Siqueira Jr JF. Photodynamic therapy with two different photosensitizers as a supplement to instrumentation/irrigation procedures in promoting intracanal reduction of Enterococcus faecalis. J Endod. 2010;36(2):292–6. doi:10.1016/j.joen.2009.09.041. Epub 2009 Dec 6.
45. Nunes MR, Mello I, Franco GC, de Medeiros JM, Dos Santos SS, Habitante SM, Lage-Marques JL, Raldi DP. Effectiveness of photodynamic therapy against Enterococcus faecalis, with and without the use of an intracanal optical fiber: an in vitro study. Photomed Laser Surg. 2011;29(12):803–8.
46. Meire MA, Coenye T, Nelis HJ, De Moor RJ. Evaluation of Nd:YAG and Er:YAG irradiation, antibacterial photodynamic therapy and sodium hypochlorite treatment on Enterococcus faecalis biofilms. Int Endod J. 2012;45(5):482–91.
47. Cheng X, Guan S, Lu H, Zhao C, Chen X, Li N, Bai Q, Tian Y, Yu Q. Evaluation of the bactericidal effect of Nd:YAG, Er:YAG, Er, Cr:YSGG laser radiation, and antimicrobial photodynamic therapy (aPDT) in experimentally infected root canals. Lasers Surg Med. 2012;44(10):824–31. doi:10.1002/lsm.22092. Epub 2012 Nov 20.
48. Siddiqui SH, Awan KH, Javed F. Bactericidal efficacy of photodynamic therapy against Enterococcus faecalis in infected root canals: a systematic literature review. Photodiagnosis Photodyn Ther. 2013;10(4):632–43.
49. Garcez AS, Fregnani ER, Rodriguez HM, Nunez SC, Sabino CP, Suzuki H, Ribeiro MS. The use of optical fiber in endodontic photodynamic therapy. Is it really relevant? Lasers Med Sci. 2013;28(1):79–85.
50. Komine C, Tsujimoto Y. A small amount of singlet oxygen generated via excited methylene blue by photodynamic therapy induces the sterilization of Enterococcus faecalis. J Endod. 2013;39(3):411–4.
51. Carvalho Edos S, Mello I, Albergaria SJ, Habitante SM, Lage-Marques JL, Raldi DP. Effect of chemical substances in removing methylene blue after photodynamic therapy in root canal treatment. Photomed Laser Surg. 2011;29(8):559–63. doi:10.1089/pho.2010.2922. Epub 2011 Jun 1.

Pulp Therapy for Primary Teeth

8

Lawrence Kotlow

Abstract

The primary objective when treating the non-vital or exposed pulp in the primary dentition is to maintain the tooth until it would normally exfoliate and preserve the developing dental arches. A pulpotomy involves the removal of the coronal pulp tissue, and the remaining tissue has been treated with a variety of different medications or procedures. Treatments that have been used for primary teeth pulps include medications formocresol, glutaraldehyde, calcium hydroxide, ferric sulfate, and mineral trioxide aggregate (MTA) and electrosurgery. This chapter will discuss the use of lasers as an alternative to both chemically prepared pulpotomies and electrosurgery. There have been significant advances in the prevention of dental caries and conservative treatment of caries in the primary dentition; however, there still remains the necessity to treat the pulp of primary teeth when the pulp tissue is compromised due to mechanical exposures and when there is reversible pulpitis due to caries, pulpal death due to caries, and trauma to avoid the development of malocclusions from loss of space for the erupting permanent tooth.

8.1 Introduction

The Academy of Pediatric Dentistry's guidelines on pulp therapy for primary teeth state that "the primary objective of pulp therapy is to maintain the integrity and health of the teeth and their supporting tissues" [1].

L. Kotlow, DDS
Private Solo Specialty Practice, 340 Fuller Road, Albany, NY 12203, USA
e-mail: kiddsteeth@aol.com

When treating the pulp in the primary dentition, the main goal is to maintain the tooth with reversible pulpitis until the tooth would normally exfoliate and thus preserve the developing dental arches. Historically, a pulpotomy involves the removal of the coronal pulp tissue, and the remaining tissue can be treated with a variety of different medications or procedures. The different treatments that have been used include medications formocresol, glutaraldehyde, calcium hydroxide, ferric sulfate, and mineral trioxide aggregate (MTA) and electrosurgery [2–6]. There

G. Olivi et al. (eds.), *Lasers in Endodontics: Scientific Background and Clinical Applications*,
DOI 10.1007/978-3-319-19327-4_8

also continues to be a significant difference of opinion on whether to consider indirect or direct pulp capping procedures in the primary tooth. This chapter will discuss the use of lasers as an alternative to both chemically induced pulpotomies and electrosurgery.

Although there have been significant advances in the prevention of dental caries and conservative treatment of caries in the primary dentition, there still remains the need to treat the pulp of primary teeth when the pulp tissue is compromised due to mechanical exposures and when there is reversible pulpitis due to caries, trauma, and pulpal death due to caries and trauma. The premature loss of a primary tooth may lead to malocclusions from loss of space for the erupting permanent tooth, esthetic and psychological effect on the child, and nutritional and speech problems [7]. Concerns about leaving any diseased dentin to protect the pulp from exposure or removing all affected dentin, even its exposure is probable, still remain controversial [8].

Evaluating and diagnosing the status of the pulp tissue in primary teeth involves not only a clinical oral examination and diagnostic radiographs when the patient is cooperative but also a thorough review of the patient's health. The dental examination should include questions on history of pain or discomfort: Has the pain been spontaneous or created from cold or sweet items? A distinction needs to be made from pain related to external stimuli or pain which occurs spontaneously and is throbbing relentlessly. This type of pain may prevent sleeping and eating, and it may eventually display redness and swelling around the tooth and jaw. In the primary dentition, radiographic evidence of internal or external root resorption or bone loss in the trifurcation or bifurcation in molars, not the molar root apices and at the apices of anterior teeth, indicates irreversible pulpal death and suggests that a pulpotomy is not the treatment of choice. The usual methods of evaluating permanent teeth through evaluating tooth response to extreme temperature changes and electric pulp testing devices are not a reliable indicator of pulpal condition in the primary teeth.

8.2 Conventional Methods of Treating the Pulp in the Deciduous Dentition

The treatment approach varies depending on the status and contamination of the pulp tissue. The interventions can be summarized in:

Vital Pulp Therapy
- Indirect pulp capping procedure
- Direct pulp capping procedure
- Pulpotomy
- Non-vital pulp therapy
- Pulpectomy
- Extraction

8.3 Vital Pulp Therapy

8.3.1 Indirect Pulp Capping in Primary Teeth

At the completion of a traditional restorative intervention, the treatment of deep dentinal caries is accomplished by using either a detergent or disinfectant (sodium hypochlorite and/or peroxide rubbed on the dentin with a cotton pellet) and by applying a radiopaque protective liner [7]: conventional treatment involves either the use of calcium hydroxide, zinc oxide, and eugenol paste or placement of a glass ionomer over the dentin [9]. The removal of vital pulp tissue was first suggested in the eighteenth century by Pierre Fauchard (1728), and the first documented instance of vital pulpotomy was by Phillip Pfaff (1756), who used gold foil with the idea that it might promote pulpal healing. The application of a protective base has the purpose of maintaining pulp vitality and also promoting the formation of tertiary dentin [9–13]. When using restorative materials, there is a tendency to skip this step, thus leaving the function of the dentinal adhesive to create a dentinal seal. Several studies, however, are questioning this practice due to the toxic effect that these materials may have on the pulp [14, 15].

8.3.2 Direct Pulp Capping in Primary Teeth

Direct pulp capping procedures should be limited to teeth where the pulp has been exposed during mechanical removal of dentin or immediately after trauma and there has been no history of pulpitis or pain in the tooth [8, 10]. The exposure should be extremely small and the area has not been contaminated [16]. There should be no history of spontaneous pain, excessive bleeding at the exposure site, or signs of necrotic material which may indicate pulpal death [16]. It is recommended to achieve optimal results that the pulp capping procedure be completed when the tooth or teeth have been properly isolated to reduce contamination of the exposed area. This can include the use of rubber dam or the Isolite system [17]. The use of formocresol and glutaraldehyde is not recommended and has also raised concerns in general for its use in pulp therapy over potential toxicity and carcinogenicity. Formocresol and glutaraldehyde are therefore no longer used in pulpotomy treatment in many countries [18–21].

Conventional treatment for direct pulp capping involves placement of either calcium hydroxide or MTA over the exposed site [22].

The guidelines of the American Academy of Pediatric Dentistry state that "Direct pulp capping of carious exposures in primary is not recommended," remembering that partial or coronal pulpotomy remains the most appropriate technique for primary teeth with exposed vital pulp [1].

8.3.2.1 Laser Therapy

Cavity preparation and carious removal using the erbium and erbium chromium lasers offer many advantages as follows [23, 24]:

- Anesthesia is usually unnecessary.
- The amount of heat generated in pulp chamber is not harmful for the pulp tissue.
- Laser preparation is selective for the carious tissues with the highest content of water (chromophore for erbium laser), and unlikely, it will result in overtreatment or mechanical exposure of the pulp.
- The irradiated dentinal surface becomes highly decontaminated and cleansed, with no smear layer.

The effectiveness of laser treatment and clinical success/outcome are dependent on the therapy executed with proper parameters and techniques.

Laser-assisted pulp capping procedures are effective in pulpal exposures due to mechanical exposure since lasers have the ability to stimulate reparative dentin, decontaminate the exposure site, and produce an analgesic effect reducing pain and discomfort [25, 26].

Laser-assisted pulp capping has considerable advantages compared to traditional methods (Moritz et al. 1998a, b; Santucci 1999; Jayawardena et al. 2001; Olivi and Genovese 2006; Olivi et al. 2007; Todea et al. 2008a, b) [25–32] which can be summarized as:

- Decontaminating effect
- Hemostatic and coagulant effect
- Biostimulating effect

The American Academy of Pediatric Dentistry (AAPD) with a policy document adopted in 2013 intended to inform and educate dental professionals on the fundamentals, types, diagnostic and clinical applications, benefits, and limitations of laser use in pediatric dentistry and recognizes the judicious use of lasers as a beneficial instrument in providing dental restorative and soft tissue procedures for infants, children, and adolescents, including those with special healthcare needs [33].

8.3.2.2 Laser Direct/Indirect Pulp Capping Procedure

The Er:YAG laser is used for caries removal at settings of 100 mJ, 12 Hz, 1.2 W, at 100 μs, using a 600 μm tip and air 6/10, water 5/10. After carious removal intervention, the decontamination of deep dentinal caries is completed by using the

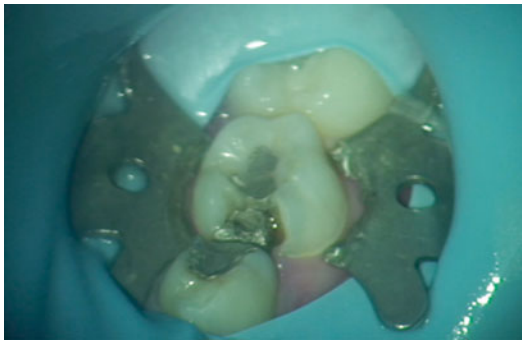

Fig. 8.1 Deep recurrent decay

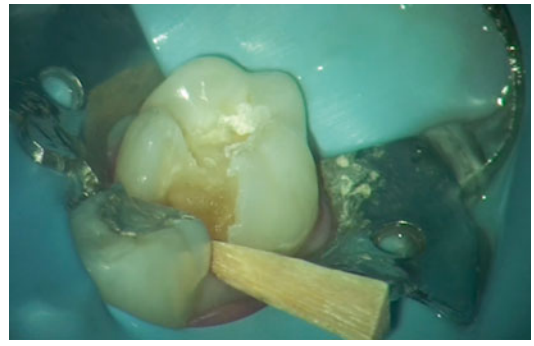

Fig. 8.2 Caries removal using the Er:YAG laser

laser. As of today, both erbium family lasers and CO_2 lasers can be used to perform an indirect pulp capping:

Er:YAG (2940 nm) is used at settings of 12 Hz and 50 mJ, 0.6 W, at 100 μs pulse duration, with air 5/10, water 4/10 for 30 s.

Alternatively, a new CO_2 laser (9300 nm) is used at settings of 51 μs pulse duration, water 40 %, and 250 μm spot size.

In case of a small or accidental exposure, the exposed pulp can be coagulated at settings of 15 Hz, 10 mJ, 600 microseconds for few seconds; handpiece water feature is used at no water and 3/10 air. The pulpal area is covered using a light-cured, resin-modified calcium silicate liner (TheraCal LC manufactured by Bisco, Inc.) (Figs. 8.1, 8.2, and 8.3). Alternatively, other pulp capping materials, such as MTA, Biodentine, or calcium hydroxide, can be used for this purpose.

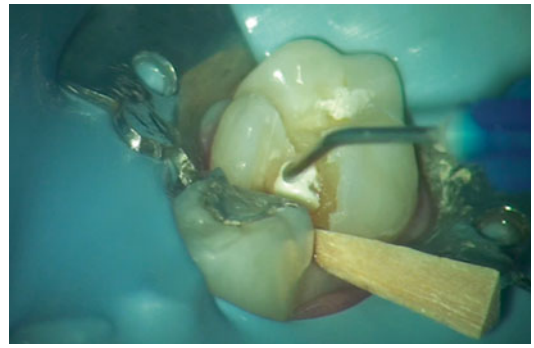

Fig. 8.3 Placement of liner

8.3.3 Pulpotomy

The American Academy of Pediatric Dentistry defines this procedure as the amputation of the pulp chamber while preserving the vitality of the radicular pulp which will be later treated with a medicinal product [34].

Pulpotomies in primary teeth are the most commonly used treatment when the pulp is cariously exposed, and the tooth appears both clinically and radiographically not infected. The rationale for completing a pulpotomy on a primary tooth is based upon the premise that by removing all or partial areas of the affected coronal pulp tissue, there continues to remain vital tissue in the remaining areas of the root canal. The goal is to maintain tooth vitality and normal pulpal activity. The material used to cover the remaining tissue should be bactericidal, compatible with the pulp and surrounding tissues; promote repair and healing of the pulp tissue; and allow the tooth to resorb without interference.

Using conventional vital pulpotomy methods, the tooth should usually be anesthetized prior to treatment. Presently, conventional treatment has seen less use of formocresol due to concerns about its safety and more emphasis on the use of mineral trioxide aggregate [35, 36]. MTA is composed of tricalcium silicate, bismuth oxide, dicalcium silicate, tricalcium aluminate, tetracalcium

aluminoferrite, and calcium sulfate dihydrate. Nonchemical pulpotomy procedures were recommended by Dean et al. (2001) using electrosurgery and pulp therapy [6].

8.4 Pulpectomy

When the pulp of the primary tooth is determined to be non-vital, a pulpectomy may be an option when it is desirable to save a restorable primary tooth. Pulpectomy should be limited to teeth where there are no signs of systemic infection, bone loss, swelling, or chronic fistulas both clinically and radiographically. The goal is to remove all infected tissue in both the coronal and root portion of the primary tooth.

The anatomic morphology of primary molar root canals makes complete conventional root canals difficult to complete. If the primary tooth's root canal shows signs of resorption and apical, bifurcation, or trifurcation bone loss and cannot be properly cleansed of all infected tissue, then endodontic (pulpectomy) treatment will most likely be unsuccessful.

8.5 Lasers in Primary Teeth Requiring Pulpal Treatments

- Laser light is able to vaporize the soft pulp tissue when appropriate wavelengths interact with it.
- Laser light is able to produce good hemostasis when it interacts with the chromophores to prevent any excessive bleeding.
- Lasers are an excellent treatment modality to decontaminate the irradiated site since lasers are bactericidal.
- Lasers produce less postsurgical discomfort and swelling at the surgical sites.

Lasers and dentistry, the idea that light energy could be harnessed and brought into the oral cavity, first became available for dentists in 1989 with the introduction of the first laser approved for dentistry by the US FDA (United States Food and Drug Administration); this was a 3 W Nd:YAG (neodymium:yttrium-aluminum-garnet) laser developed by Meyers [37]. Since the introduction of the Nd:YAG laser (1064 nm), other lasers are now used to treat a variety of soft tissue procedures such as KTP 523 nm and in the past argon 514 nm; various diode lasers (from 810 nm to 1064 nm), erbium, chromium:YSGG (2780 nm) and erbium:YAG lasers (2940 nm), and CO_2 lasers (9300 and 10,600 nm) have been used for the treatment of soft tissue dental problems.

The use of light energy creates a new potential for treating the pulp in primary teeth. Studies have investigated the possibility of using lasers for the pulpotomy procedure on primary teeth [38–41].

In 1996, Wilkerson reported in their study that after 60 days, the use of the argon laser for pulpotomies in swine showed that all pulps appeared to have normal vitality and pulpal healing [42].

The use of the Nd:YAG laser in pulpotomy procedures in primary teeth was reported to be successful in 1999 by Liu JF et al. [43].

In another study, Liu et al. (2006) compared the effect of Nd:YAG laser at 2 W (100 mJ, 20 Hz) for pulpotomy to formocresol (1:5), reporting a significantly superior clinical success of the laser group (97 %) in comparison with the formocresol (1:5) group (85.5 %) [44].

Odabas et al. (2007), using the same parameters, reported no statistically significant difference between the two groups: 85.71 % for the laser group compared to 90.47 % for the formocresol group at 12 months [45].

The use of CO_2 for pulpotomy procedures was investigated by Shoji et al. (1985) which reported clinical success for pulp therapy [46].

Elliot et al. (1999), comparing the effects of the CO_2 laser technique to formocresol therapy, found all samples similarly asymptomatic at both clinical follow-ups and histological evaluations, with a significant inverse correlation between the laser energy applied to the pulp and the degree of inflammation at 28 days [47].

Pescheck et al. (2002) reported favorable results using the CO_2 laser for primary pulpotomy with clinical survival rate of 98 % [48].

Fitzpatrick et al. (1994) had already highlighted how the superpulsed mode was more successful than the continuous mode [49].

The Er:YAG laser has demonstrated a successful alternative to conventional pulp therapy. Kimura et al. (2003) reported success using the Er:YAG laser for pulpotomy [50].

Huth et al. (2005) compared four pulpotomy techniques: diluted formocresol, ferric sulfate, Er:YAG laser, and calcium hydroxide. Calcium hydroxide (87 %) showed a much lower success than the other groups, making the laser group (93 %) a valid system for pulpotomy [51].

Research completed in 2007 by Henson reported that the clinical and radiographic findings in an unpublished study at the University of Texas, San Antonio, Dental School suggested that therapy using the 2940 nm erbium laser was as effective as formocresol in treating pulpotomies in primary teeth [52].

In 2008, Kotlow published the results of over 5 years of using Er: YAG laser for pulpotomies with radiographic evidence of successful treatments [53].

In 2010, Mareddy et al. performed a histological evaluation of laser pulpotomies using the 810 nm diode laser and concluded that lasers appear to be an acceptable alternative for pulpotomies [54].

8.5.1 Laser Pulpotomy and Pulpectomies Using the Erbium YAG Laser

The following examples represent a selection of successful pulpotomies completed by the author using the Er:YAG dental laser. All the teeth treated in this study report were of children whose medical histories were completed by the parents and indicated they were health children. Pulpotomies selected were chosen from approximately 5000 different teeth as examples for laser pulpotomies which required vital pulp therapy due to mechanical or carious exposures, trauma, or teeth considered non-vital due to either previous traumatic injury or severe caries resulting in pulpal death.

All procedures were completed using a dental microscope (Global Technologies) and under rubber dam or using the Isolite ™ system of tooth isolation. Local anesthetics were used when needed (Septocaine 1:100,000) (Fig. 8.4). All patients, staff, and dentists wore appropriate laser glasses, and high-volume suction was used during the procedure. Once it was determined that the tooth required a pulpotomy, the chamber was opened to provide proper access to the anal orifices using conventional high-speed and slow-speed handpieces. Alternative method for opening non-vital pulp chamber would include using the Er:YAG laser (2940 nm, Fotona – PowerLase AT and LightWalker) at 12–15 Hz, 250–350 mJ, depending on the energy needed to ablate the enamel and/or dentin, with air and water spray on (20–22 cc/min), using a tipless handpiece (R02-H02).

Fig. 8.4 Isolite isolation

Pulpotomies and pulpectomies were then treated irradiating each canal for approximately 20 s with a 400 μm tip (Preciso tip) at 12–15 Hz and 50 mJ up to 80 mJ, with air-water spray on. The laser energy was directed at the opening of the canals for approximately 20 s per canal, repeated three times or until adequate hemostasis was achieved. A final filling includes the use of a resorbable material such as zinc oxide and eugenol in the canal and glass-ionomeric cement-composite material in the chamber for crown reconstruction. Patients were evaluated at 1 month and 6 months for clinical signs of any failure of pulpotomy. Failure rates appeared to be similar to conventional formocresol rates (Fig. 8.5a–d). The following cases were treated using an Er:YAG laser (Figs. 8.6, 8.7, 8.8, 8.9, 8.10, and 8.11.)

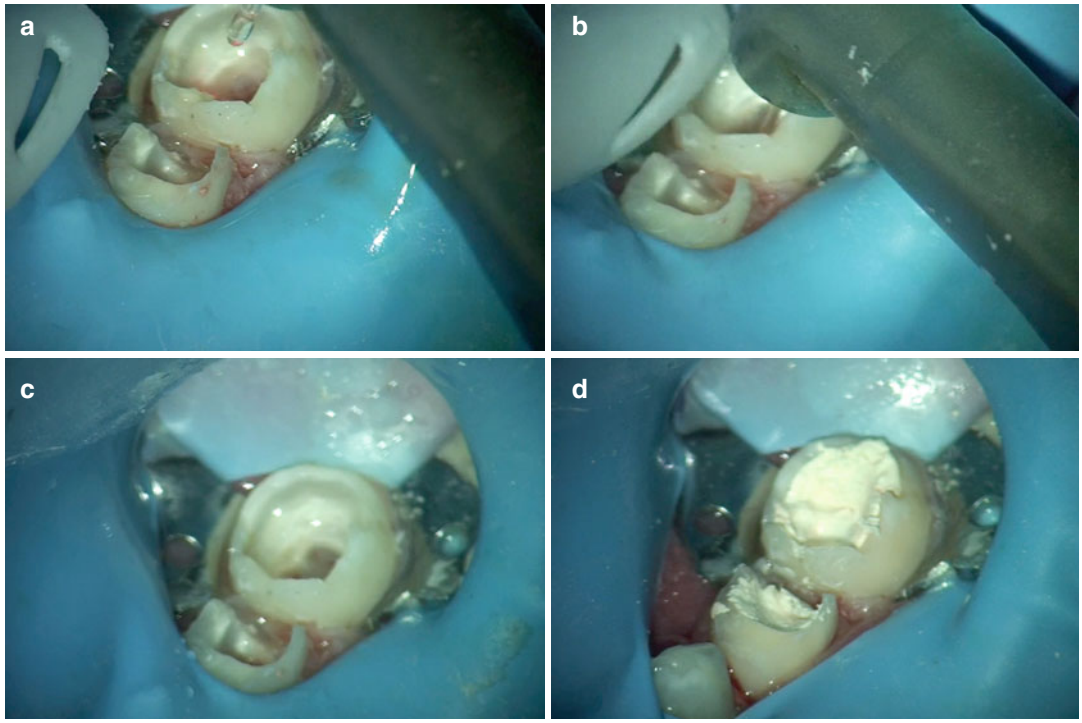

Fig. 8.5 (**a**–**d**) Laser pulpotomy using Er:YAG 2940 nm and 800 μm cylindrical tip (LightWalker by Fotona). (**a**, **b**) Cylindrical tip inside the pulp chamber performing pulpotomy on second primary molar; (**c**) pulpotomies completed on both primary molars; (**d**) final filling performed with a resorbable material (zinc oxide and eugenol)

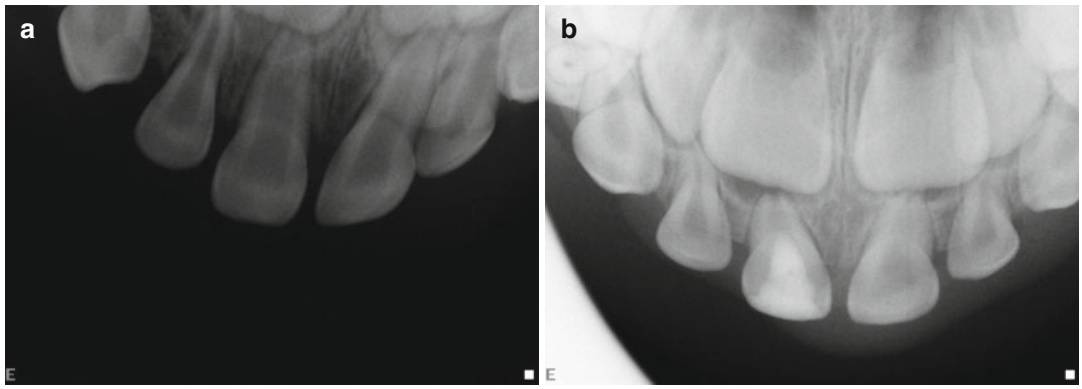

Fig. 8.6 (**a**, **b**) Traumatic injury to the right primary central incisor at age three. (**a**) Pre-treatment x-ray 1/2/2003; (**b**) post-treatment x-ray 5/12/2006

8.5.2 PIPS Protocol for Pulpotomy and Pulpectomy of Primary Deciduous Teeth

A new technology, photon-induced photoacoustic streaming (PIPS), was developed by DiVito to effectively remove canal debris and pulp remains from all the endodontic areas utilizing a stripped radial firing tip with a specific Er:YAG laser. The radial and stripped tip is placed into the upper chamber of the primary tooth. The laser is set to a subablative mode with settings of 50 μs pulse and lower and safer

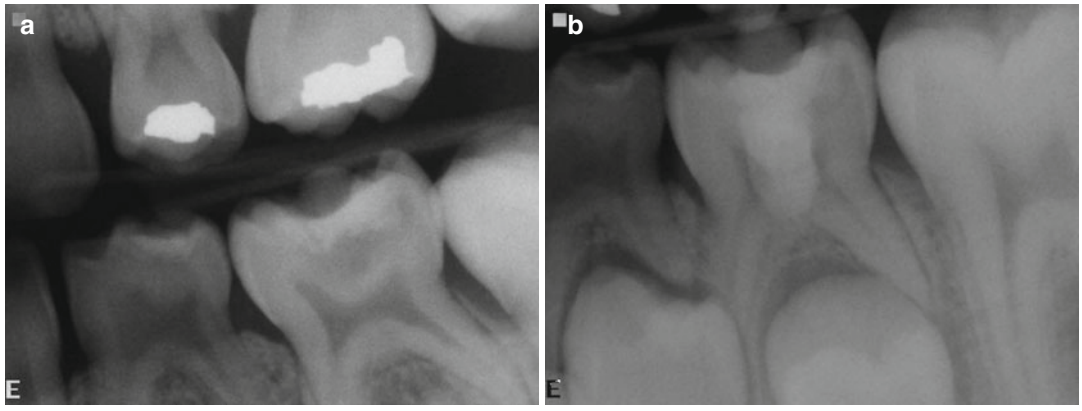

Fig. 8.7 (**a**, **b**) Dental caries, mechanical exposure of the lower left second primary molar at age five. (**a**) Pre-treatment x-ray 12/30/2003; (**b**) post-treatment x-ray 7/5/2006

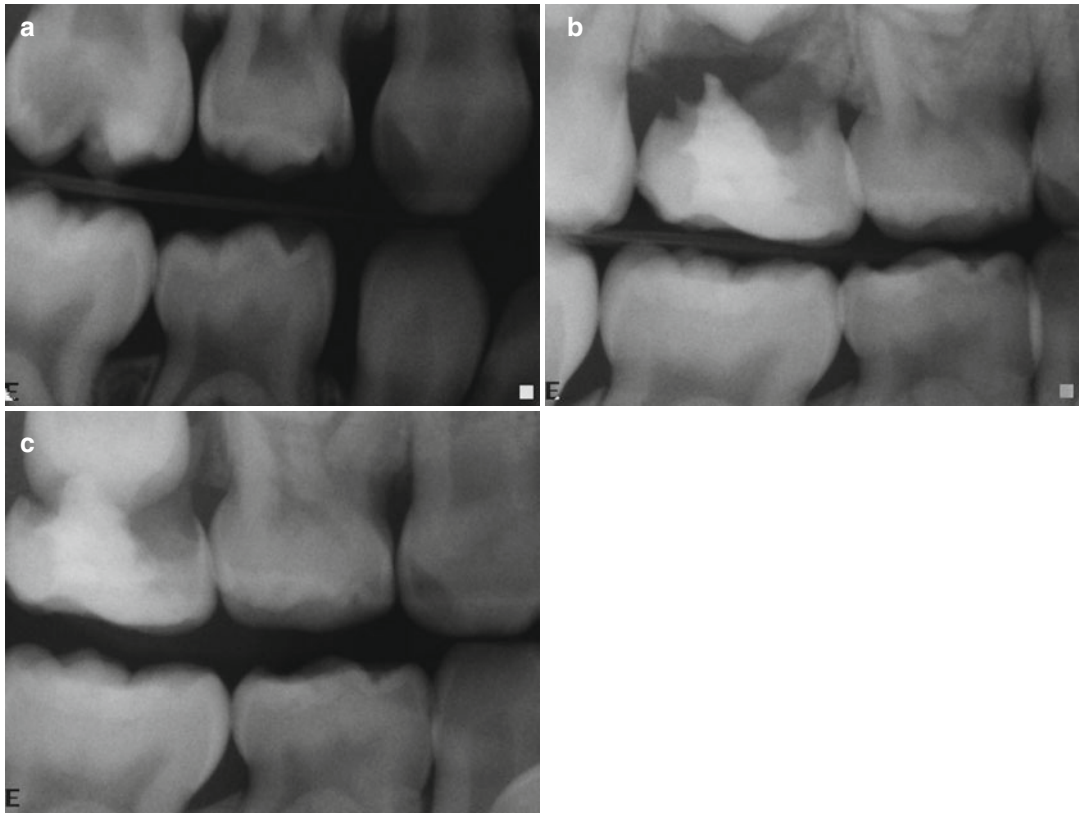

Fig. 8.8 (**a**–**c**) Dental caries, mechanical exposure of the upper right second primary molar at age four. (**a**) Pre-treatment x-ray 1/9/2003; 1st post-treatment x-ray 8/24/2006; 2nd post-treatment x-ray 6/11/2007

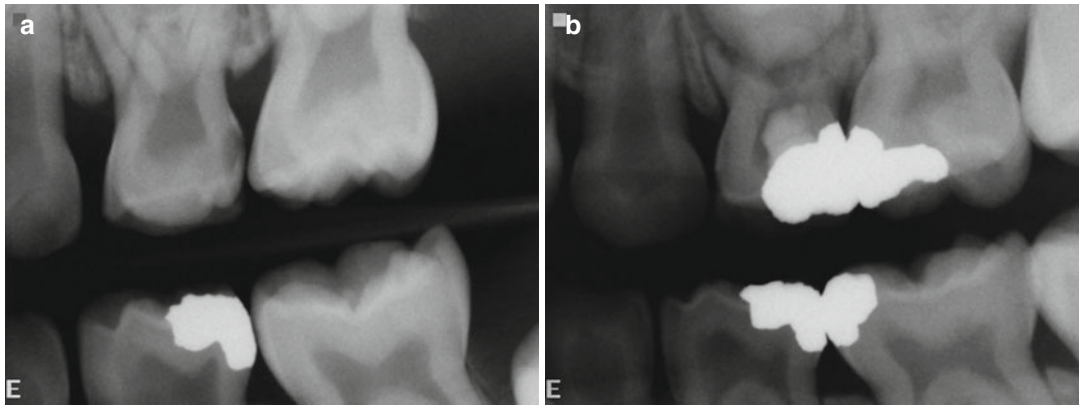

Fig. 8.9 (**a**, **b**) Dental caries, mechanical exposure of the upper left first primary molar at age 4 years and 6 months. (**a**) Pre-treatment x-ray 10/30/2002; (**b**) post-treatment x-ray 6/1/2006

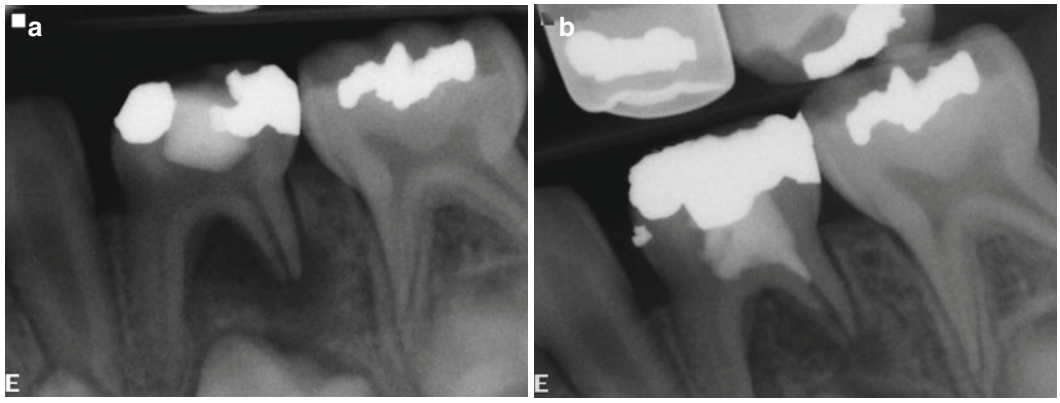

Fig. 8.10 (**a**, **b**) Non-vital caries involvement of the pulpal tissue with bifurcation radiolucency at age four. (**a**) Pre-treatment x-ray 5/21/2007; (**b**) the patient was treated with laser 20 s to each canal, placed on amoxicillin 250 mg per teaspoon for 10 days. New bone growth at 2 months' checkup; the tooth was stable and asymptomatic as depicted on the post-treatment x-ray 7/30/2007

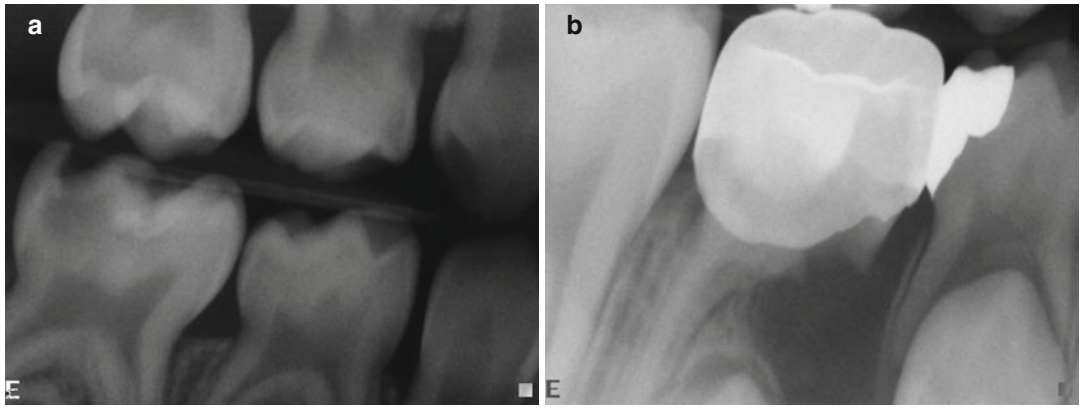

Fig. 8.11 (**a**, **b**) Carious exposure of the lower right second primary molar at age 4 years and 6 months. (**a**) Pre-treatment x-ray 1/9/2003; (**b**) tooth appears stable and asymptomatic during the following period. Post-treatment radiograph (6/11/2007) shows mesial root resorption. Tooth was not extracted but allowed to exfoliate naturally

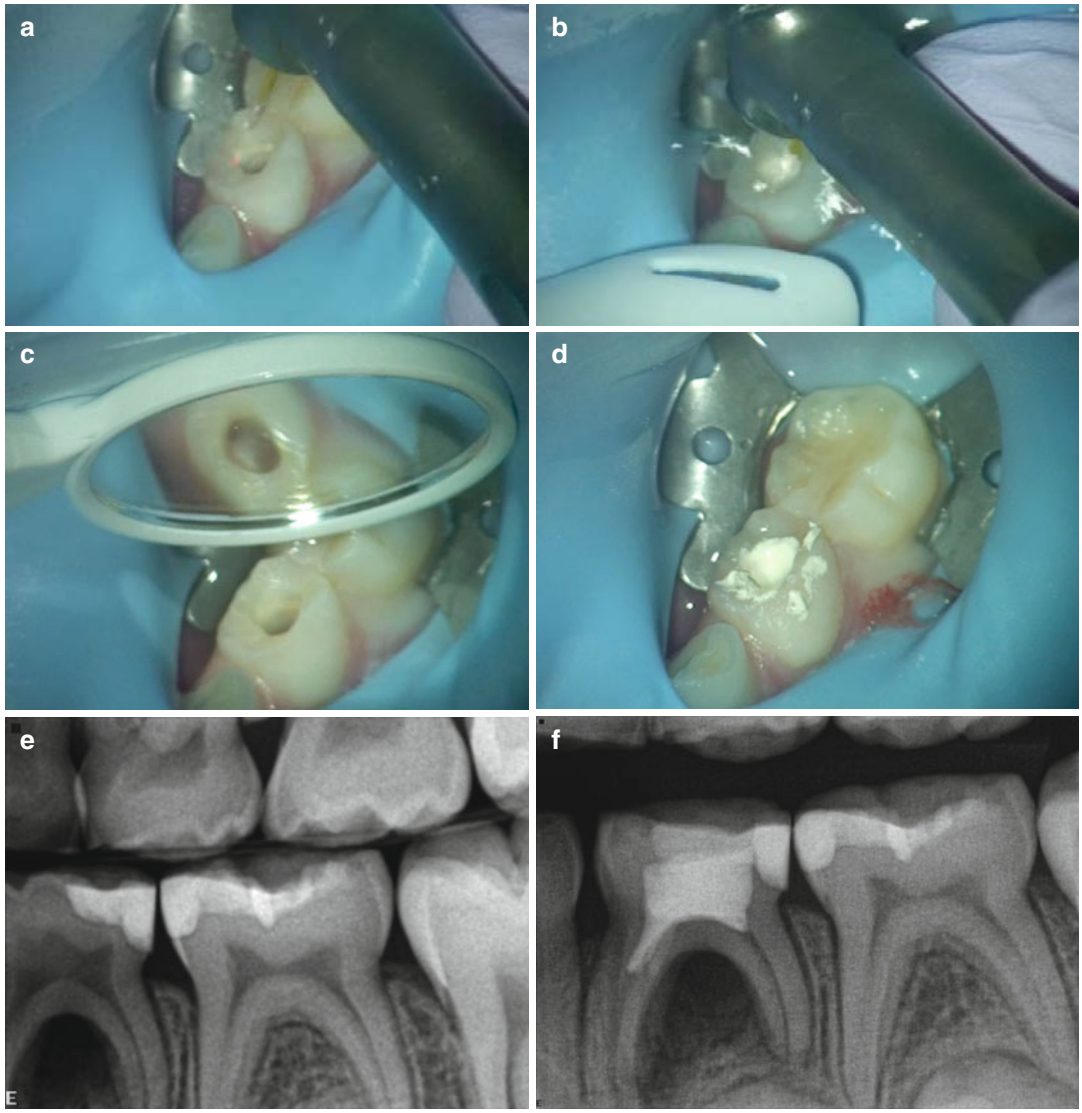

Fig. 8.12 (**a**–**f**) Non-vital primary lower left first molar. (**a**, **b**) PIPS tip placed into the pulp chamber of lower deciduous molar; (**c**) chamber cavity cleaned using PIPS and Er:YAG laser; (**d**) zinc oxide and eugenol (*ZOE*) placed into canal and chamber; (**e**) pre-treatment radiograph; (**f**) 1-month post-treatment radiograph shows new bone formation in the bifurcation

energy (5–10 mJ), at 15 Hz; the handpiece water feature is used at 2 water and no air. The procedure is repeated three times for approximately 30 s, and then the canal is filled with a resorbable material such as zinc oxide and eugenol (Figs. 8.12 and 8.13). PIPS technology is extensively debated in Chap. 11.

Because of the smaller size, length, and typically immature apexes, the settings are reduced, and only sterile distilled water is used during activation of PIPS.

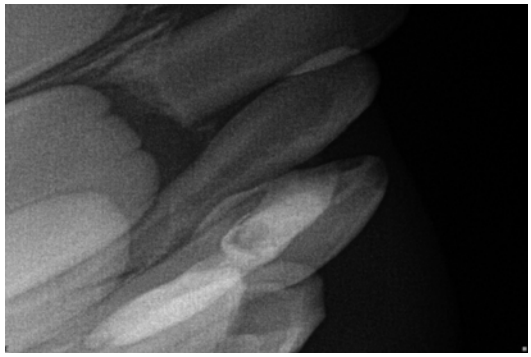

Fig. 8.13 Primary upper right cuspid (toothC) with abscess. The tooth was opened without using any local anesthesia, lasered using the PIPS technique for 30 s, 15 Hz, 15 mJ, for three times. Patient placed on amoxicillin 250 mg for 10 days returned in 1 month. Tooth was stable and no signs of infection. The tooth was re-lasered and filled with ZOE

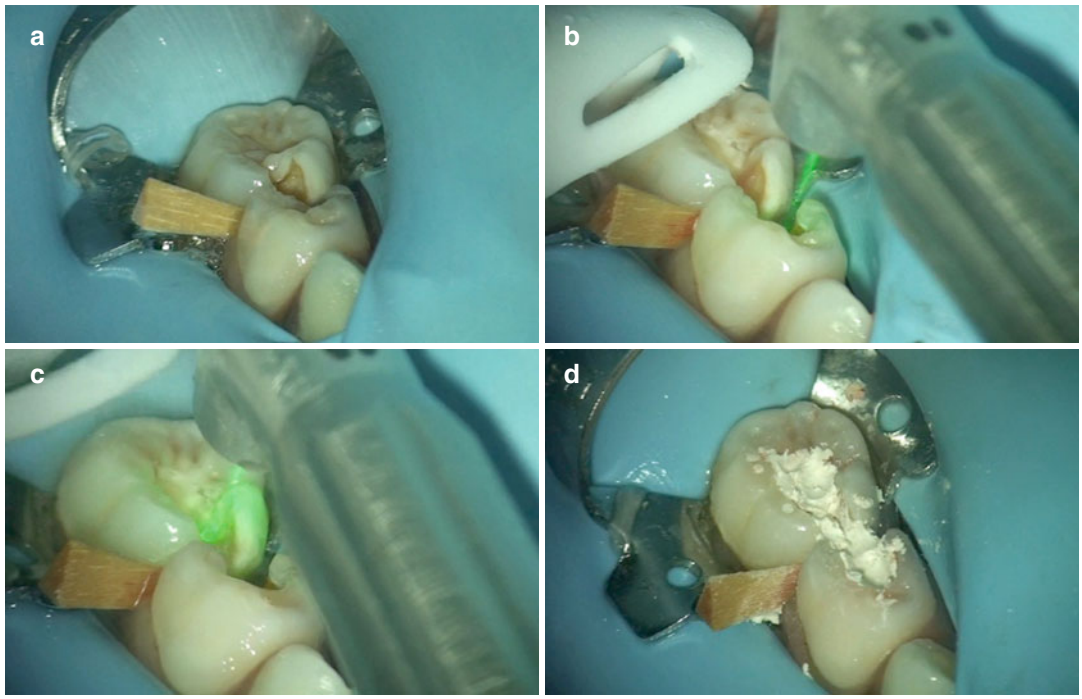

Fig. 8.14 (**a**–**d**) Alternative method for opening vital pulp chamber would include using the CO_2 laser (9300 nm, Solea by Convergent Dental, Natick, MA) at 50 pulse duration, at power modulated using a variable power foot pedal from 1 to 50 % for approximately 20 s per canal in the coronal portion (water at 100 %), using a spot size of 0.25 mm. (**a**) Pretreatment image shows rubber dam; (**b**) *green* aiming beam accessing the first primary molar; (**c**) green aiming beam performing pulpotomy on the second primary molar; (**d**) final filling performed with a resorbable material (zinc oxide and eugenol)

8.5.3 Laser Pulpotomy Using the CO_2 Laser

Recently, a CO_2 laser with a new wavelength (9300 nm) has been introduced in the market. This particular laser allows for both soft and hard tissue therapy, due to the possibility to control the thermal interaction with a water spray and to modulate the pulse duration. This CO_2 laser at 9300 nm (Solea by Convergent Dental, Natick, MA) can be used for pulpotomy and coagulation in vital primary teeth at the following settings: 50 pulse duration, at power modulated using a variable power foot pedal from 1 to 50 % for approximately 20 s per canal in the coronal portion (water at 100 %), using a spot size of 0.25 mm. Tooth can be then filled with ZOE (Fig. 8.14a–d).

Conclusions

Premature loss of primary teeth may contribute to the development of malocclusions, esthetic concerns, phonetic problems, or functional problems [7]. The goals in treating primary teeth are to prevent or eliminate pain and discomfort and maintain the integrity of the oral structures. Dental lasers provide a safe and effective alternative to conventional chemical or electrosurgical method of pulp therapy [23, 25, 26, 33].

References

1. Pediatr Dent. Guideline on Pulp Therapy for Primary and Immature Permanent Teeth. Reference Manual. 34(6) 12/13:222–9.
2. Buckley JP. The chemistry of pulp decomposition with rational treatment for this condition and its sequelae. J Am Dent Assoc. 1904;3:764.
3. Sweet CA. Procedure for the treatment of exposed and pulpless deciduous teeth. J Am Dent Assoc. 1930;17:1150–3.
4. Ibricevic H. Al-Jame Qumasha: Ferric Sulfate as pulpotomy agent in primary teeth: twenty month clinical follow-up. J Clin Pediatr Dent. 2000;24(4): 269–72.
5. Eldeman E, Holan G, Fuks AB. Mineral trioxide aggregate vs formocresol in pulpotomized primary molars: a preliminary report. Pediatr Dent. 2001; 23(1):15–8.
6. Dean JA, Mack RB, Fulkerson BT, Sanders BJ. Comparison of electrical and formocresol pulpotomy procedures in children. Int J Paediatr Dent. 2002;12(3):177–82.
7. Fuks A. Pulp therapy for the primary and young permanent dentitions. Dent Clin North Am. 2000; 44(3):571–96, vii.
8. Qudeimat MA, Al-Saieh FA, AL-Oari Q, Omar R. Restorative decisions for deep proximal carious lesions in primary molars. Eur Arch Paediatr Dent. 2007;8:37–42.
9. Cioll JA. Indirect pulp capping and primary teeth: is the primary tooth pulpotomy out of date? Pediatr Dent. 2008;30:192–6.
10. Fuks A. Vital pulp therapy with new materials for primary teeth: new directions and treatment perspectives. J Endod. 2008;34(7 Suppl):S18–24. doi:10.1016/j.joen.2008.02.031. Review.
11. Farooq CA, Coll J, Kuwabara A, Sheldon P. Success rates of formocresol pulpotomy and indirect pulp treatment of deep dentinal caries in primary teeth. Pediatr Dent. 2000;22:278–86.
12. Straffon LH, Loos P. The indirect pulp cap: a review and commentary. Isr J Dent Sci. 2000;17:7–14.
13. Marchi JJ, de Araujo FB, Froner AM, Straffon LH, Nor JE. Indirect pulp capping in the primary dentition: a 4-year follow-up study. J Clin Pediatr Dent. 2006;31:68–71.
14. Cox CF, Kim KM, Stevenson 3rd RG, Hafez AA. Histological evaluation of a self-priming etchant adhesive system. Compend Contin Educ Dent. 2003;8 Suppl:17–20; quiz 61.
15. Teixeira HM, Do Nascimento AB, Hebling J, De Souza Costa CA. In vivo evaluation of the biocompatibility of three current bonding agents. J Oral Rehabil. 2006;33(7):542–50.
16. Fuks AB. Pulp therapy for the primary dentition. In: Pediatric dentistry: infancy through adolescence. St. Louis. Mo: Elsevier; 2005. 11830.
17. Wahl P, Andrews T. Isolation: a look at the differences and benefits of rubber dam and isolite. Endo Pract. 2010;3(2):52–5.
18. Pashley EL, Myers DR, Pashley DH, Whithford GM. Systemic distribution of 14C-formaldehyde from formocresol-treated pulpotomy sites. J Dent Res. 1980;59:602–8.
19. Lewis B, Chestner SB. Formaldehyde in dentistry: a review of mutagenic and carcinogenic potential. J Am Dent Assoc. 1981;103:429–31.
20. Goldmacher VS, Thilley WG. Formaldehyde is mutagenic for cultured human cells. Mutat Res. 1983; 116:417–22.
21. Judd PL, Kenny DJ. Formocresol concerns: a review. J Can Dent Assoc. 1987;53:401–4.
22. Olivi G, Margolis F, Genovese MD. Laser pediatric dentistry: a user's guide. Chicago, IL: Quintessence Publishing; 2011. p. 93–7. ch.8.
23. Olivi G, Genovese MD. Laser restorative dentistry in children and adolescents. Eur Arch Paediatr Dent. 2011;12(2):68–78.

24. Olivi G, Caprioglio C, Genovese MD. Lasers in dental traumatology. Eur J Paediatr Dent. 2010;11(2):71–6.
25. Olivi G, Genovese MD. Erbium chromium laser in pulp capping treatment. J Oral Laser Appl. 2006;6(4): 291–9.
26. Olivi G, Genovese MD, Maturo P, Docimo R. Pulp capping: advantages of using laser technology. Eur J Paediatr Dent. 2007;8(2):89–95.
27. Moritz A, Schoop U, Goharkhay K, Sperr W. Advantages of a pulsed CO2 laser in direct pulp capping: long term in vivo study. Lasers Surg Med. 1998;22:288–93.
28. Moritz A, Schoop U, Goharkhay K, Sperr W. The CO2 laser as an aid in direct pulp capping. J Endod. 1998;24(4):248–51.
29. Santucci PJ. Dycal versus Nd:YAG laser and Vitrebond for direct pulp capping in permanent teeth. J Clin Laser Med Surg. 1999;17:69–75.
30. Jayawardena JA, Kato J, Moriya K, Takagi Y. Pulpal response to exposure with Er:YAG laser. Oral Surg Oral Med Oral Pathos Oral Radiol Endod. 2001;91: 222–9.
31. Todea C, Kerezsi C, Balabuc C, Calniceanu M, Filip L. Pulp capping-from conventional to laser-assisted therapy (I). J Oral Laser Appl. 2008;8:71–82.
32. Todea C, Kerezsi C, Balabuc C, Calniceanu M, Filip L. Pulp capping-from conventional to laser-assisted therapy (II). J Oral Laser Appl. 2008;8:147–55.
33. American Academy of Pediatric Dentistry, Reference Manual 2013. Policy on the use of lasers for pediatric dental patients V 35/NO 6 13/14:75–7.
34. American Academy of Pediatric Dentistry, Reference Manual 2005–2006, Clinical Guidelines. 130–4.
35. Holan D, Eidelman E, Fuks A. Long term evaluation of pulpotomy in primary molars using mineral trioxide aggregate or formocresol. Pediatr Dent. 2005;27:2.
36. Malekafzali B, Shekarchi F, Asgary S. Treatment outcomes of pulpotomy in primary molars using two endodontic biomaterials. A 2-year randomized clinical trial. Eur J Paediatr Dent. 2001;12(3):189–93.
37. Myers TD, Myers WD, Stone RM. First soft tissue study utilizing a pulsed Nd:YAG dental laser. Northwest Dent. 1989;68(2):14–7.
38. Jukić S, Anić I, Koba K, Najzar-Fleger D, Matsumoto K. The effect of pulpotomy using CO2 and Nd:YAG lasers on dental pulp tissue. Int Endod J. 1997; 30(3):175–80.
39. Liu H, Yan MM, Zhao EY, Chen L, Liu HW. Preliminary report on the effect of Nd: YAG laser irradiation on canine tooth pulps. Chin J Dent Res. 2000;3(4):63–5.
40. Kimura Y, Yonaga K, Yokoyama K, Watanabe H, Wang X, Matsumoto K. Histopathological changes in dental pulp irradiated by Er:YAG laser: a preliminary report on laser pulpotomy. J Clin Laser Med Surg. 2003;21(6):345–50.
41. Furze H, Furze M. Pulpotomy with laser in primary and young permanent teeth. J Oral Laser Appl. 2006; 6(1):53–8.
42. Wilkerson MK, Hill SD, Arcoria CJ. Effects of the argon laser on primary tooth pulpotomies in swine. J Clin Laser Med Surg. 1996;14:37–42.
43. Liu JF, Chen LR, Chao SY. Laser pulpotomy of primary teeth. Pediatr Dent. 1999;21(2):128–9.
44. Liu JF. Effects of Nd:YAG laser pulpotomy on human primary molars. J Endod. 2006;32(5):404–7.
45. Odabas ME, Bodur H, Bari E, Demir C. Clinical, radiographic, and histopathologic evaluation of Nd:YAG laser pulpotomy on human primary teeth. J Endod. 2007;33:415–21.
46. Shoji S, Nakamura M, Horiuchi H. Histopathological changes in dental pulp irradiated by CO2 laser: a preliminary report on laser pulpotomy. J Endod. 1985; 11:379–84.
47. Elliott RD, Roberts MW, Burkes J, Phillips C. Evaluation of the carbon dioxide laser on vital human primary pulp tissue. Pediatr Dent. 1999;21: 327–31.
48. Pescheck A, Pescheck B, Moritz A. Pulpotomy of primary molars with the use of a carbon dioxide laser: results of a long-term in vivo study. J Oral Laser Appl. 2002;2:165–9.
49. Fitzpatrick RE, Goldman MP, Ruiz-Esparza J. Clinical advantages of the CO2 laser superpulsed mode. Treatment of verruca vulgaris, seborrheic keratoses, lentigines, and actinic cheilitis. J Dermatol Surg Oncol. 1994;20:449–56.
50. Kimura Y, Yonaga K, Yokoyama K, Watanabe H, Wang X, Matsumoto K. Histological changes in the dental pulp irradiated by Er:YAG laser: a preliminary report on laser pulpotomy. J Clin Laser Med Surg. 2003;21:345–50.
51. Huth KC, Paschos E, Hajek-Al-Khatar N, et al. Effectiveness of 4 pulpotomy techniques—randomized controlled trial. J Dent Res. 2005;84:1144–8.
52. Henson T, Church A. Recall evaluation of primary pulp therapy using a dental laser. Personal communications of unpublished paper. 29 May 2008.
53. Kotlow L. Use of an Er:YAG laser fro pulpotomies in vital and nonvital primary teeth. J Laser Dent. 2008;16(2):75–9.
54. Mareddy A, Mallikarjun Shanthala B, Shetty P, Narasimha V, Chandru T. Histological evaluation of diode laser pulpotomy in dogs. J Oral Laser Appl. 2010;10(1):7–16.

Laser Doppler Flowmetry

9

Herman J.J. Roeykens and Roeland J.G. De Moor

Abstract

An early determination of pulpal vitality is crucial with respect to a correct differential diagnosis of revascularisation or necrosis and its treatment. The use of sensibility tests (cold, heat, electric pulp test) in combination with X-ray is commonly promoted. However, these tests are arbitrary, based on sensations, and therefore not always reliable. In such situation, registration of pulpal blood flow will be more than an added value. The most studied and well-documented method for registration of pulpal blood flow is laser Doppler flowmetry (LDF), a non-invasive technique with direct and objective registrations. In this chapter, we describe pulpal blood flow, LDF and its characteristics, this method's advantages and disadvantages and recent developments regarding LDF. Despite a low implementation of LDF in dentistry, this technique has proven to be an indisputable, basic asset of a dental clinic.

9.1 Introduction

Blood is a specialised bodily fluid that delivers necessary substances to the body's cells, such as nutrients and oxygen, and transports waste products, such as carbon dioxide and metabolites, away from those same cells [1]. Blood is circulated around the body through a closed system of blood vessels: arteries, arterioles, capillaries, venules and veins. In this system, blood will be transported by the pumping action of the heart and will be mechanically driven from the heart with a normal maximal pressure of 120 mmHg. The contraction of the heart muscle starts in the two atria, which push the blood into the ventricles.

H.J.J. Roeykens, DDS, MSc (✉)
Department of Restorative Dentistry and Endodontology, Ghent Dental Laser Centre, Ghent Dental Photonics Research Clustre, Dental School, Ghent University, Ghent, Belgium
e-mail: herman.roeykens@ugent.be

R.J.G. De Moor, DDS, MSc, PhD
Department of Restorative Dentistry and Endodontology, Ghent Dental Laser Centre, Ghent Dental Photonics Research Clustre, BIOMAD, Dental School, Ghent University Hospital, Ghent University, Ghent, Belgium

G. Olivi et al. (eds.), *Lasers in Endodontics: Scientific Background and Clinical Applications*,
DOI 10.1007/978-3-319-19327-4_9

Then the walls of the ventricles squeeze together and force the blood out into the arteries: the aorta to the body and the pulmonary artery to the lungs. Afterwards, the heart muscle relaxes, allowing blood to flow in from the veins and fill the atria again. In healthy people, the normal (resting) heart rate is about 72 beats per minute. So blood flows from the left heart chamber with high speed through the aorta and the arteries into the organs and tissues. Here, the arterioles will set the blood flow by drawing together and relaxing. Furthermore, there are also the capillaries (very thin blood vessels) where blood flows through very slowly with functions of delivering oxygen and nutrients and transporting waste [2].

In species with lungs, arterial blood carries oxygen from inhaled air to the tissues of the body, and venous blood carries carbon dioxide, a waste product of metabolism produced by cells, from the tissues to the lungs to be exhaled [3].

In vertebrates, blood consists of a protein-rich fluid known as plasma, with suspended cellular elements: red blood cells, white blood cells and platelets. The normal total circulating blood volume is about 8 % of the body weight (5600 mL in a 70 kg man). About 55 % of this volume is plasma, which consists mostly of water (90 % by volume). The most abundant cells in vertebrate blood are red blood cells (34 g/dL blood) [2]. The ingress of arterial blood is followed by a drain via the capillaries into short collecting venules and then via the venules into the heart. It is on the level of the arterioles, capillaries and venules that laser Doppler finds its application.

There are several ways to register the vascularity of the pulp. The evaluation of the circulatory status, in fact, is the only way to assess the pulp's vitality. The following non-invasive methods have been proposed for this purpose: photoplethysmography, pulse oximetry [4], ultrasound Doppler imaging [5] and laser Doppler flowmetry [6, 7]. A plethysmograph is an instrument for measuring changes in volume within an organ or whole body (usually resulting from fluctuations in the amount of blood or air it contains). A photoplethysmogram (PPG) is an optically obtained plethysmogram. A PPG is often obtained by illuminating the skin (peripheral microcirculation) with a pulse oximeter, which measures changes in light absorption based on the movement of red blood cells. So in photoplethysmography, the signal is proportional to the quantity of red blood cells. In pulse oximetry, light is passed from a photoelectric diode across the tooth structure into a receptor. Changes in absorption in both red and infrared light caused by alteration in tissue volume (tissue perfusion) during the cardiac cycle are detected. Hence, photoplethysmography helps to detect blood volume changes in the microvascular bed of tissue [8, 9]. Most of the supplying vessels in the pulp are arterioles. The presence of these arterioles, rather than arteries, and the insulation of the pulp, by surrounding hard tissues, are obstacles to pulse detection [4]. At present, there are also no adaptable sensors for the teeth.

Ultrasound Doppler imaging was already used successfully in dentistry to measure the blood flow of tissues surrounding the teeth [10–12]. There were several problems with ultrasound Doppler imaging when measuring the pulpal blood flow. These include a difficulty in transmitting sufficient ultrasonic energy into the pulp cavity and detecting small Doppler frequency shifts produced by the slow-moving pulpal blood. These limitations have been overcome partially by the recent development of high-frequency (20–100 MHz) ultrasonic devices [5].

LDF monitors blood perfusion, and photoplethysmography monitors blood volume changes. LDF will be preferred in view of its ease of use, low running cost (after initial purchase) and accessible technology. Furthermore, LDF is a non-invasive, objective, continuous technique with the possibility of recording and analysing blood flow in teeth. The latter also surpasses PPG due to an enhanced specificity and sensitivity for micro-capillary tubes [13]. Laser Doppler flowmetry (LDF) was originally developed to measure the blood flow in microvascular systems such as the retina [14], cortex of the kidney [15] and skin tissue [16]. Gazelius et al. demonstrated the dental usefulness of LDF in 1986 [17]. Later on, multiple technology-related publications [18–41] with a number of very specific applications, such as the use in dental traumatology [42],

periodontology [43] and orthodontic surgery [44, 45], followed. Since the actual beginning of laser Doppler blood flow measurements in dentistry, we count so far 255 (April 2015) publications (search terms: laser Doppler flowmetry and dentistry).

9.2 Working Mechanism

Light from a laser diode (red or, more frequently, near-infrared laser) is brought by optical fibre, through a blunt needle probe, onto the surface of tissue (Fig. 9.1). When tooth and pulpal tissue is involved, enamel prisms and dentine tubules will lead up this beam to the capillaries of the pulp where the light is diffused and scattered by static tissue as well as by moving blood cells. Red blood cells are the largest and most numerous cells within blood. According to the Doppler principle, light rays are scattered by the moving red blood cells and thereby subjected to a frequency shift; light is also scattered by static tissue without Doppler frequency shift. The shifted and non-frequency-shifted light is transferred from the surface of the tooth via a second optical fibre, in the same probe, and is brought to mix on a photodetector. The spectrum of 'beat' frequencies of the detected light is processed to give a signal that is proportional to the product of average blood speed and the concentration of moving blood cells; this is referred to as LD flux (optical beating occurs when two waves mix; the resulting waveforms have a 'beat frequency' that is equal to the difference between the two original wave frequencies).

$$Flux = \left(v_{rbc}\right).\left(conc\right)$$

with

$$Flux = k_i \int_{w_1}^{w_2} \frac{w.p\left(w\right).dw}{dc^2} - noise$$

$$Conc = k_{ii} . \int_{w_1}^{w_2} \frac{p\left(w\right) \cdot dw}{dc^2} - noise$$

$$Velocity = k_{iii} .Flux / Conc$$

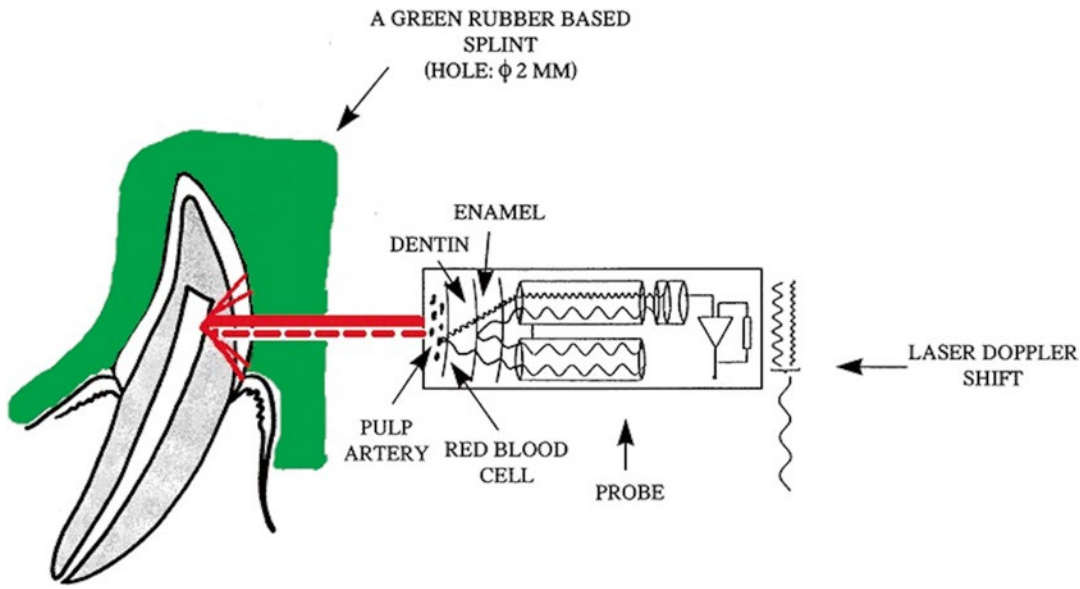

Fig. 9.1 Schematic representation of the area of positioning of a probe of a laser Doppler flowmetry monitor. The probe is fixed in contact with the buccal surface of the tooth in a rubber split. A schematic representation is given of the technique with a laser beam penetrating through the enamel and the dentine into the pulp, registering the laser Doppler shift

with w_1 = lower bandwidth limit (20 Hz)
dc = light intensity
w_2 = upper bandwidth limit (3,15,22 kHz)
dc^2 = normalisation
w = frequency = weighting factor
k_i,k_{ii} = scaling constants used for calibration
P = power of frequency w
noise = dark and shot noise components

Furthermore, pulsations in the blood circulation of teeth are registered in vital elements through the heart-driven blood. The wider the frequency bandwidth, the better another sign of tooth pulp vitality is detected, i.e. the pulse due to the cardiac cycle.

Different wavelengths are used for LDF registrations. Kolkman [45] calculated that the LDF measurement depth is related to the wavelength of the used light. The penetration depth is 2.81 mm in skin tissue with green light (543 nm), 3.14 mm with red light (632.8 nm) and 4.3 mm with almost infrared light (780 nm). These differences in measurement depth as a result of the wavelength used were also confirmed by others, e.g. Fredriksson et al. [46]. When using a 0.5 mm laser beam diameter, the measurement depth for muscle was 0.29 mm (543 nm), 0.62 mm (633 nm) and 0.73 mm (780 nm) and for liver 0.14 mm (543 nm), 0.40 mm (633 nm) and 0.52 mm (780 nm). It is clear that the tissue type is also of importance. Examples of measurement depths shown in the same study [46] were as follows (values are given for a probe-based system with 0.25 mm source-detector separation and an imaging system with a 0.5 mm beam diameter, respectively, both operating at 780 nm): muscle, 0.55/0.79 mm; liver, 0.40/0.53 mm; grey matter, 0.48/0.68 mm; white matter, 0.20/0.20 mm; index finger pulp, 0.41/0.53 mm; forearm skin, 0.53/0.56 mm; and heat-provoked forearm skin, 0.66/0.67 mm. Vongsavan and Matthews [21] found the LDF technique to be capable of making measurements in skin and mucosa up to an approximate depth of 1–2 mm and passing over the 2–3.5 mm-thick enamel and dentine of teeth to measure blood flow to dental tissues, which are more transparent and tubular than dentine and act as light guides. They speculated that the periodontium and other adjacent tissues could contribute to the signal. The penetration depth of LDF beam in teeth for contact and noncontact probe tip was determined by Polat S. et al. [38]. The root was illuminated with a probe in contact to the tooth to 4.28 ± 0.14 mm depth with high density and 13.27 ± 0.27 mm with low density. A noncontact probe illuminated 4.36 ± 0.16 mm of the root with high density and 13.28 ± 0.30 mm of the root with low density. The latter suggests contamination from periodontal tissue blood flow even with adequate precautions.

Gush and King [47] assessed skin blood flow at green and near-infrared wavelengths by spectral analysis; it was concluded that green light was more significantly influenced by capillary blood flow than by larger elements of the microvasculature, due to its much greater absorption in blood, and that the lower frequency components were derived more from capillaries.

9.3 Arbitrary Units

There was also criticism on the laser Doppler technique. Vongsaven and Matthews [21] complained about the nonlinearity of the LDF signal when blood volume fractions in tissue are greater than 1 %, a consequence of the analysis by Bonner and Nossal [48], i.e. for a LDF signal that increases with 100 %, the assumption cannot be made that the blood flow has increased with 100 %. The nonlinearity is explained by the significant number of multiple scattering events of a photon from different red blood cells prior to detection.

A second reason for criticism was the absence of an absolute medium of calibration. The current clinical active calibration is performed with an aqueous suspension of polystyrene microspheres with the probe detecting a reproducible Brownian motion; the calibration fluid is called a ‘motility standard’, and it enables comparisons between measurement over time and between individuals. At present, a representative biological zero for dental pulp blood flow registration is not on the market. A biological zero, in fact, is also not zero, but an every time calibration background reading.

Therefore, the latter calibration reference has to take into account the blood flow, the size of the red blood cells and the optical properties of enamel and dentine. This is also the reason for the use of nonstandard 'perfusion units' (PU) for LDF and not absolute quantitative measurements in mL/min/100 g.

A third criticism consists of environmental factors. Given that a part of the LDF signal for a dental measurement is of non-pulpal origin, multiple factors will have a significant impact on the LDF readings: the optical properties of the surrounding dentine and enamel (e.g. tooth discoloration), blood circulation of the gingival tissue and every movement of the patient or the probe; patient stress level and the use of medication will also affect pulpal blood flow.

To avoid movement effects, a silicone (dentist) or resin splint (lab) should be made before LDF measurements. The latter is needed for fixation of the LDF probe and should be cleaned with a mild alcohol disinfectant (isopropanol 70 %) in cases of multiple measurements; the splint will also block the ambient light and should help to reduce any influence of gingival blood flow (a green-coloured splint is ideal to block external light). Furthermore, the test area on the tooth (2 mm from the enamel-cement border) [28], the distance (500 μm) between efferent and afferent optic fibres [36], the diameter (200 μm) of each fibre in the probe and the measuring depth in the tissue will affect the obtained values.

9.4 LDF: The Diagnostic Unit

Laser Doppler flowmetry (LDF) provides a non-invasive, objective means of recording blood flow within the teeth, periodontal or bone tissue. LDF measurements are performed using one or more probes, simultaneously [32, 35].

An LDF device with a He-Ne (red, 632.8 nm) or a diode (NIR, 780 nm) laser can be used. The diode laser scores slightly better in specificity and sensitivity [21, 32], probably due to deeper penetration through discoloured teeth. The power of the device is below 2.5 mW with power at the end of the probe typically about1.0 mW (probe diameter = 1.5 mm). For each patient, an opaque splint is used to hold the probe (Fig. 9.1), with measurements made after the acclimatisation period (>10 min). For measurements of tooth vitality, a 3 kHz bandwidth (broad-spectrum, low blood volume) and, for measurements at the gums, a 14.3 kHz bandwidth are proposed. Values are displayed at 40 Hz but can be recorded every 0.1 s over a minimum interval of 2 times 30 s [37].

The location of the probe is determined by the position of the hole made for the probe in the splint, inspected from the inside. The splint is placed in the mouth together with the probe. Each measurement takes at least 30 s, in order to diagnose vasomotor changes, and is repeated two times. A control tooth will always be monitored, if we can measure simultaneously.

To keep additional pulpal components in the readings as low as possible, a rigorous protocol has to be followed. The patient will be seated in a semi-supine position on a dental chair with, for each assessment, the same ambient light. The best diagnostic results will be obtained from healthy, drug-free and relaxed patients. The use of a silicone resin or light-blocking holder, possibly in combination with a rubber dam and at least 2 × 30 s measurement time for each measurement, is highly recommended but time-consuming and therefore not evident. Moreover, there is evidence for diurnal variations. Special attention should be given to testing at the same time of the day when multiple measurements are compared [49].

Finally, the registered data can be processed in a spreadsheet (Excel, Microsoft Corp.) and statistically analysed (SPSS/PC + statistical package, SPSS Inc.).

9.5 Properties

The outgoing flux signal (perfusion units: PU) for a necrotic pulp is on average 42.7 % lower than for a vital pulp [24]. The reason why this is not 100 % relates to the impact of blood circulation in tissues surrounding the measured tooth. This external blood component should be kept as low as possible during registration. Therefore,

the position of the probe on the tooth's surface is of utmost importance.

Measuring simultaneously two contralateral teeth with both LDF probes and equal time variables is highly reliable and recommended [35]. With a ratio of 6:1, the gingival tissue (V_{rbc}=0.9 m/s) was much better perfused than pulpal tissue (V_{rbc}=0.16 m/s) [44, 49]. The latter also has an impact on the bandwidth that will be used to measure. Where normal pulp values are measured with a bandwidth of 3 kHz, it is appropriate for gingival tissue to measure at 14.3 kHz. Gingival tissue has an increased flow of red blood cells.

Yet one must also make the objection that 80 % of the LDF signal of an intact tooth, measured without rubber dam, does not originate from the pulp. This non-pulpal component drops to 43 % with rubber dam. Soo-ampon et al. therefore suggest that 43 % corresponds to the mathematical noise and environmental impact [37]. According to Wannfors and Gazelius, even 5 % of this non-pulpal component originates from circulation of the bone [50]. Studies conducted by the group around Polat already give a reason for the extra-large pulpal influence [38]. They found reflections well beyond the dental tissues and attributed this to the high intensity of the laser light and its penetration through dental tissues [38, 40].

9.6 LDF: A Benefit?

Dental pulp testing is an essential aid in endodontics. At present, most dentists rely on thermal tests and to a lesser extent on electric pulp testing to evaluate the 'pulp vitality'. These tests, however, are sensibility tests and do not provide information about pulp vitality (blood supply) and/or not decisive enough to determine whether a tooth is necrotic [51, 52]. False responses may occur for both. Especially, thermal tests are used to diagnose the diseased tooth and to reproduce the disease state [51]. The result is that misdiagnosis may lead to incorrect, inappropriate or unneeded treatment [53].

LDF has been shown to be more reliable than thermal testing, electric pulp testing and the use of pulse oximetry [54–56]. Compared with normal 'sensitivity testing', LDF is more reliable. When LDF scores 1.0 for sensitivity and 1.0 for specificity regarding vital or non-vital pulp tissue, a cold test with ethyl chloride scores 0.92 and 0.89 and an electric pulp test 0.87 and 0.96 [33]. The evaluation of heat versus cold test and electric test as a measure for pulp vitality gave a negative result in the case of pulp necrosis for the cold test in 89 %, with the heat test in 48 % and with the electric pulp test in 88 % [53]. In the same investigation, a positive cold response was given in 90 % of all cases for a 'vital pulp', 83 % with heat and 84 % with the electric pulp test [57]. For LDF, in both cases, this was 100 %. It will take traumatised pulps at least 6 weeks for a sufficient recovery of sensation [58, 59]. Therefore, standard sensitivity tests will provide 'reliable' information at the very best 6 weeks after traumatic impact, whereas one can determine the state of tooth vitality immediately after trauma with LDF.

Moreover, it was confirmed with LDF in an orthodontic surgery study that a tooth without normal innervations may have an intact blood supply despite negative response to the classic tests [45]. LDF registrations have been shown to follow the pattern of wound healing in both a non-induced trauma (Luxation) and a well-induced trauma (Le Fort I osteotomy) [35, 44].

As previously shown, there was already abundant proof in the 1980s and the 1990s that LDF could be used to evaluate and follow-up the restoration of 'vitality' in traumatised elements [17, 18, 20, 24, 25, 33].

LDF is therefore a technique that allows the practitioner to establish an early reliable diagnosis enabling correct, appropriate and not too early treatment taking into account the limitations of thermal and electric tests [41–43]. A two-probe assessment is advisable for giving instant information when comparing two teeth with LDF (Fig. 9.2) [32, 41].

9.7 Restoration of Tooth Vitality (Blood Flow) and Revascularisation

Multiple articles comment on recovery, rehabilitation or restoration of the blood circulation/blood flow and also on revascularisation after traumatic injury in different areas of medicine. All authors

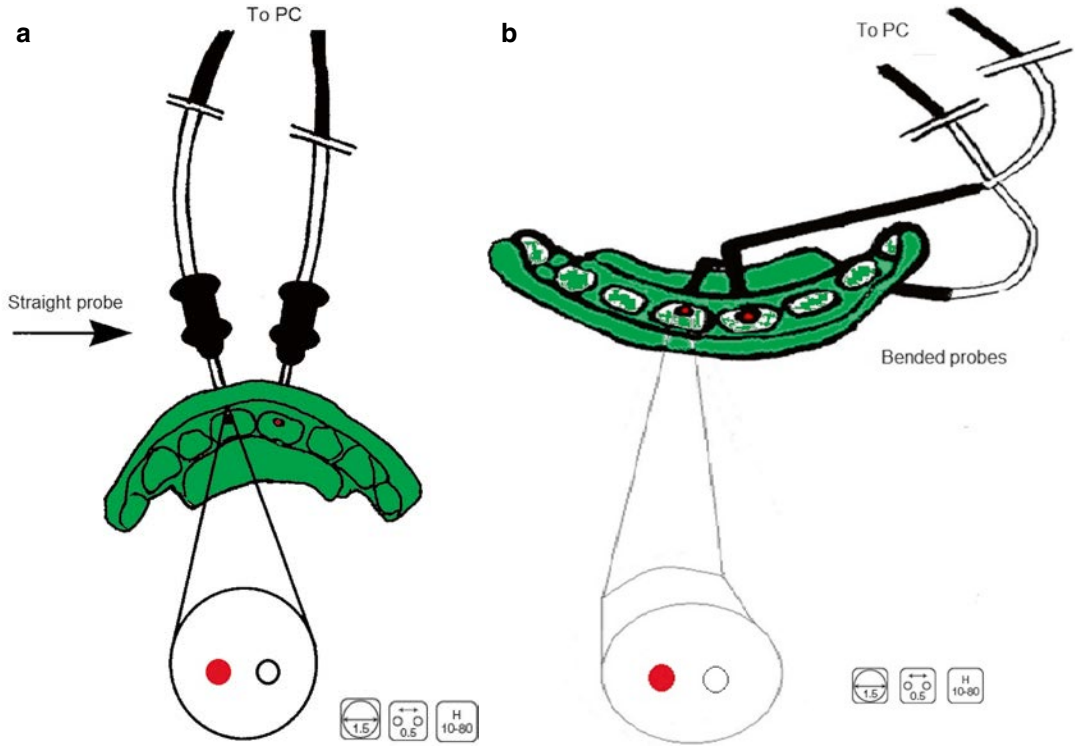

Fig. 9.2 Schematic presentation of a two-probe laser Doppler flowmetry assessment with straight and angulated probes. The latter are used when it is impossible to position straight probes. With this set-up, it is possible to register the blow flow in two teeth simultaneously, e.g. the traumatised tooth and its antimere. (**a**) straight probes positioned at the buccal side; (**b**) bended probes positioned at the palatal side

report on three major periods in the recovery of the blood flow: (1) the period immediately after trauma and an initial, brief period of hyperaemia; (2) a consecutive period of ischaemia; and (3) the restoration of the vascularisation. These periods vary according to the function of the respective tissue and the extent or severity of the tissue damage.

The evaluation of wound healing and revascularisation especially of burns turns out to be a major field of use for LDF. Here, the recovery pattern is extended to even 1 year. In this respect, LDF is the perfect example of a non-invasive evaluation technique without any need of injection of contrast agents to visualise the vessels.

Likewise, as in clinical medicine, evaluation of revascularisation is needed in a number of dental situations. In the situation of dental trauma and pulp injury, LDF is essential for the assessment of blood perfusion and will be used besides sensibility tests. Slightly different outcomes have been registered for non-induced and induced traumata with varying recovery periods [7, 41]

Three trauma cases where LDF was used to monitor the pulp vitality are now described.

9.7.1 A Complicated Trauma Case

One of the first cases that we monitored with LDF was published in 1999 [35]. It reported on a 24-year-old Caucasian female being hit by a moped driver on a footpath. The victim was treated at the emergency department of the Ghent University Hospital (Belgium) after the accident. Both central incisors (I) and the right canine (C) of the upper jaw were luxated and involved alveolar bone fracture situated above both central incisors and the left lateral incisor (detected clinically and radiographically). Moreover, the left central incisor was intruded over ±7 mm. After the repositioning of the alveolar bone segment

and the maxillary left central incisor, a rigid splint was fixed for 3 weeks (a therapy that is no longer performed nowadays). The patient was then referred to the department of endodontology for further systematic clinical follow-up.

All maxillary front teeth were screened on six successive occasions over 30 weeks with current sensitivity tests, i.e. CO_2 ice (Miracold Plus®, Hager & Werken, Duisburg, Germany), heat (gutta-percha), electric pulp test on the buccal surface of each tooth (Dentotest®, Malek, Switzerland) and LDF as test of vascularisation. Four years later, a similar assessment was repeated. The patient was in good health on each occasion and did not take any form of medication. The teeth were examined by the same investigator under standardised environmental conditions. On each occasion, two registrations were taken with an interval of 5 min. The colour of all teeth remained normal and the incisors remained untreated. Radiographs were made in order to distinguish intra-pulp and peri-radicular pathology as a part of the systematic follow-up. No periodontal disease was found.

According to the method described by Roeykens et al. [35], LDF evaluation was performed using a DRT 4 LDF monitor (Moor Instruments Ltd., Axminster, Devon, England) with a laser diode at 780 nm, and a probe output of 1.0 mW was used. The manufacturer ensured an output between 0.1 and 0.5 PU from a static reflector. The DRT 4 recorded tooth signals at a bandwidth of 3 kHz and with a time constant of 0.1 s. The display rate was set on 40 Hz with a time span of 65 s. Each probe (∅ = 1.5 mm, two optical fibres with diameter = 0.2 mm at 0.5 mm separation of centres) was labelled and calibrated following the manufacturer's instructions. An LDF signal was simultaneously obtained from both comparable teeth using two identical probes allowing for instant comparison.

The probes were fixed in a green rubber base reposition splint (Exaflex® GC) to the buccal enamel surface 2 mm from the gingival margin. The reposition splint was removed from the mouth between all measurements, disinfected with an alcohol solution and slightly adapted with Exaflex® on the second occasion after debonding of the rigid splint. This caused no significant alterations in the recorded signal.

The values obtained with the sensibility tests (CO_2 ice and gutta-percha) were negative for all teeth involved in the trauma until the ninth week (Tables 9.1 and 9.2); electric pulp testing showed significant values from the seventh week (Table 9.3). All parameters, except the electric pulp test for tooth 11 (value 6 on a scale of 10 after 4 years), returned to a normal status at the end of this follow-up. The hand temperature remained constant 35.9 °C (±0.1) (Tables 9.4 and 9.5).

The LDF measurements showed a pattern of hyperaemia, ischaemia and restored vitality. On the basis of the evaluation of the LDF blood perfusion, scored by means of the flux [13], *early hyperaemia* [flux I mean 8.05 (±0.55), flux C mean 4.5 (±0.15)] was registered within a period of 2 weeks; *ischaemia* [flux I mean 2.8 (±0.15), flux C mean 1.8 (±0.24)] was seen after 3 weeks. Nine weeks after trauma, a *restored vitality* [flux I mean 4.5 (±1.27), flux C mean 3.2 (±0.09)] was observed (Fig. 9.3). A 2-week, 6-month and 4-year control radiograph gave evidence of good peri-radicular conditions.

A good reproducibility was found for each probe and between both probes ($P < 0.001$). The blood concentration (Fig. 9.5) was also registered. From the data of Figs. 9.3 and 9.4, it is clear that flux and concentration are not systematically correlated.

9.7.2 Autotransplantation of Wisdom Teeth and Luxation of an Autotransplanted Second Upper Premolar

In a 17-year-old Caucasian girl with congenital aplasia of 4 s premolars, autotransplantations of both wisdom teeth to selected premolar sites in the lower jaw were carried out after orthodontic consultation. These transplants were performed on a 1/2 root formation stage with a follow-up period of 4 months to 4 years and a control. The condition 2 months before transplantation (Fig. 9.5) and 1 year (Fig. 9.6) and 4 years (Fig. 9.7) after transplantation shows a good integration without further endodontic treatment.

Autotransplantation of teeth is generally accepted as a reliable procedure in cases such as

Table 9.1 Registration of the sensibility of the maxillary front teeth after exposure to heat

	Heat							
Tooth/week	1 week	2 weeks	3 weeks	7 weeks	9 weeks	20 weeks	30 weeks	228 weeks
Left canine	(–)	Late	Late	±	±	nl	nl	nl
Left lateral incisor	(–)	(–)	(–)	(–)	(–)	nl	nl	nl
Left central incisor	(–)	(–)	(–)	±	±	Late	nl	nl
Right central incisor	(–)	(–)	(–)	±	±	Late	Late	nl
Right lateral incisor	nl	nl	nl	nl	nl	nl	nl	nl
Right canine	(–)	(–)	(–)	(–)	(–)	Late	Late	nl

	Morning	Noon	Afternoon	Night
Control	18.88	14.25	14.18	9.57
±	1.47	1.23	1.2	1.42
30 dentists	18.79	15.09	14.98	
±	1.54	1.3	1.4	

Table 9.2 Registration of the sensibility of the maxillary front teeth after exposure to cold

	Cold							
Tooth/week	1 week	2 weeks	3 weeks	7 weeks	9 weeks	20 weeks	30 weeks	228 weeks
Left canine	(–)	Late	(–)	±	±	nl	nl	nl
Left lateral incisor	(–)	(–)	(–)	(–)	(–)	Late	nl	nl
Left central incisor	(–)	(–)	(–)	±	±	Late	nl	nl
Right central incisor	(–)	(–)	(–)	±	±	Late	Late	nl
Right lateral incisor	nl	nl	nl	nl	nl	nl	nl	nl
Right canine	(–)	(–)	(–)	(–)	(–)	Late	Late	nl

Table 9.3 Registration of the effect of electric pulp testing on the sensibility of the maxillary front teeth

	Electric pulp test (mean value 3 measurements, SD) scale 1–10							
Tooth/week	1 week	2 weeks	3 weeks	7 weeks	9 weeks	20 weeks	30 weeks	228 weeks
Left canine	8.0 (0)	6.3 (1)	4.0 (1)	5.3 (1)	5.0 (0)	4.6 (1)	4.0 (0)	2.6 (1)
Left lateral incisor	6.0 (1)			8.0 (0)	8.0 (0)	8.0 (0)	8.0 (0)	2.0 (0)
Left central incisor				8.0 (0)	8.0 (0)	6.6 (1)	6.0 (0)	2.3 (1)
Right central incisor				7.3 (1)	7.6 (1)	8.0 (0)	8.0 (0)	6.0 (0)
Right lateral incisor		6.0 (1)	2.3 (1)	4.0 (0)	4.3 (0)	4.0 (0)	4.3 (0)	2.0 (0)
Right canine	8.0 (0)	8.0 (0)	6.0 (0)	6.3 (1)	6.0 (0)	6.3 (1)	6.0 (0)	2.3 (0)

Table 9.4 Evaluation of the colour change of the maxillary front teeth

	Colour							
Tooth/week	1 week	2 weeks	3 weeks	7 weeks	9 weeks	20 weeks	30 weeks	228 weeks
Left canine	b3	b3	b3	b3	b3	b3	b3	b3
Left lateral incisor	c2	c2	c2	c2	c2	c2	c2	c2
Left central incisor	c2	c2	c2	c2	c2	c2	c2	c2
Right central incisor	c2	c2	c2	c2	c2	c2	c2	c2
Right lateral incisor	c2	c2	c2	c2	c2	c2	c2	c2
Right canine	b3	b3	b3	b3	b3	b3	b3	b3

Table 9.5 Evaluation of the mobility of the maxillary front teeth

	Mobility							
Tooth/week	1 week	2 weeks	3 weeks	7 weeks	9 weeks	20 weeks	30 weeks	228 weeks
Left canine	Splint	Splint	Splint	nl	nl	nl	nl	nl
Left lateral incisor	Splint	Splint	Splint	nl	nl	nl	nl	nl
Left central incisor	Splint	Splint	Splint	nl	nl	nl	nl	nl
Right central incisor	Splint	Splint	Splint	nl	nl	nl	nl	nl
Right lateral incisor	Splint	Splint	Splint	nl	nl	nl	nl	nl
Right canine	Splint	Splint	Splint	nl	nl	nl	nl	nl

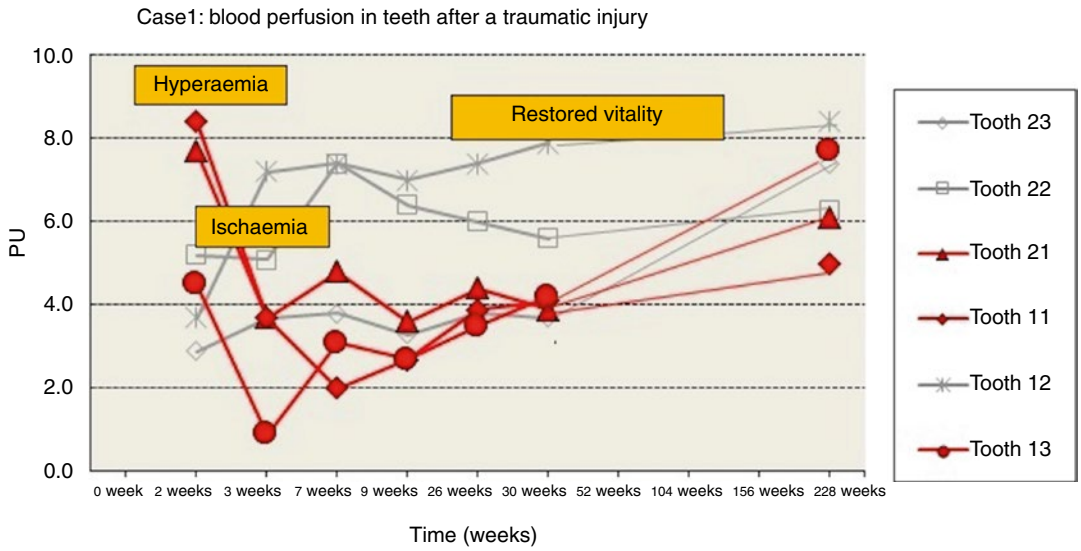

Fig. 9.3 Blood perfusion in the front teeth from 13 to 23. A pattern with hyperaemia followed by ischaemia and restored pulp vitality is found for each traumatised tooth

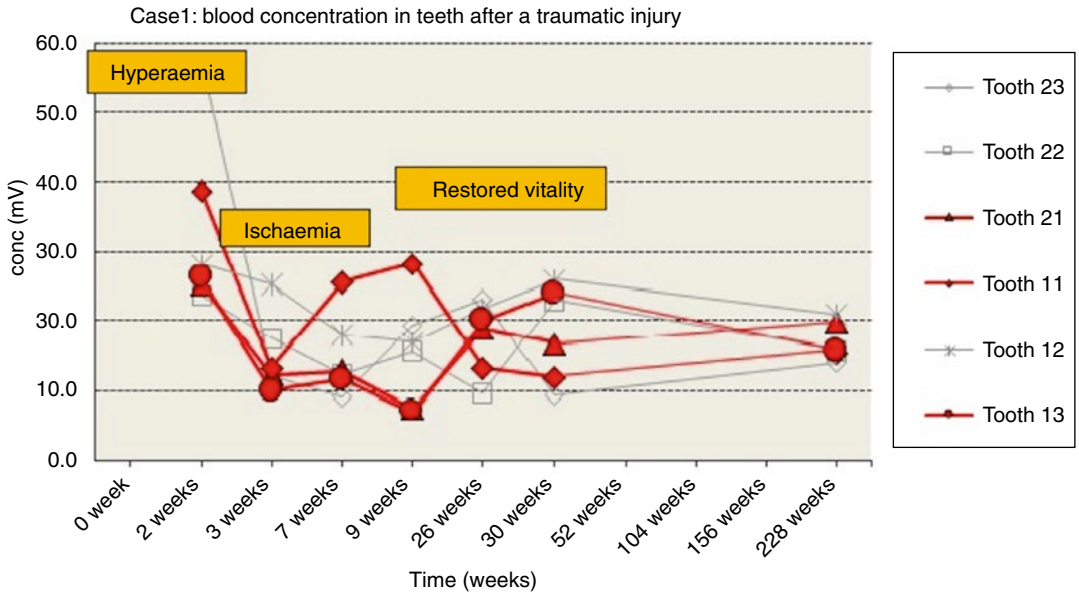

Fig. 9.4 Blood perfusion in the front teeth from 13 to 23. A pattern with hyperaemia followed by ischaemia and restored pulp vitality is found for each traumatised tooth. Intra-oral X-ray of the maxillary front teeth after 2 weeks

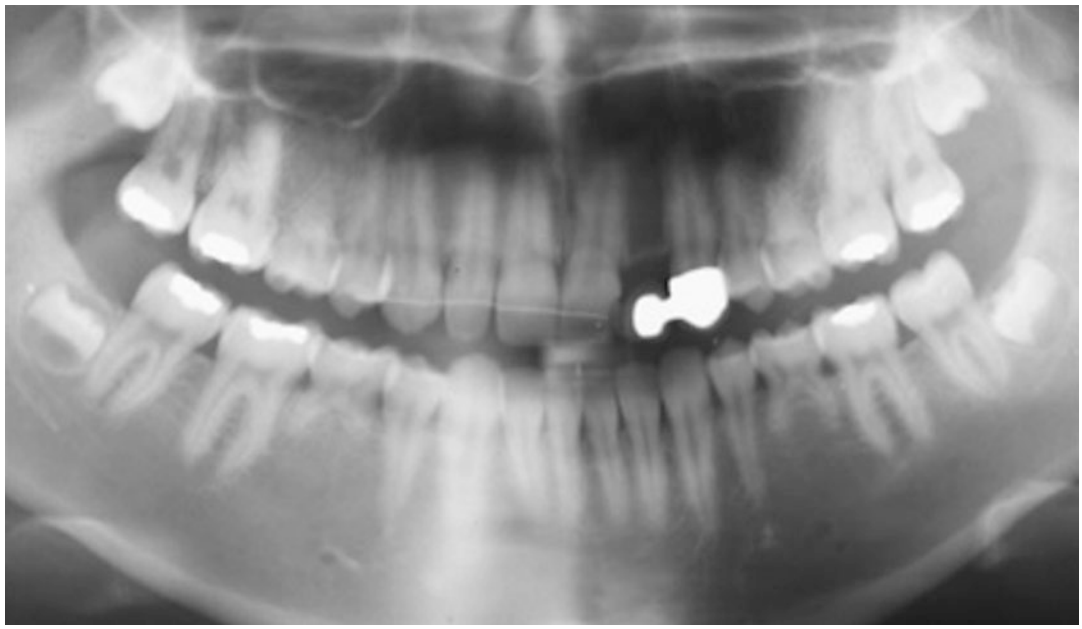

Fig. 9.5 Situation 2 months before autotransplantation of the maxillary third molars to the mandibular premolar sites (case 1)

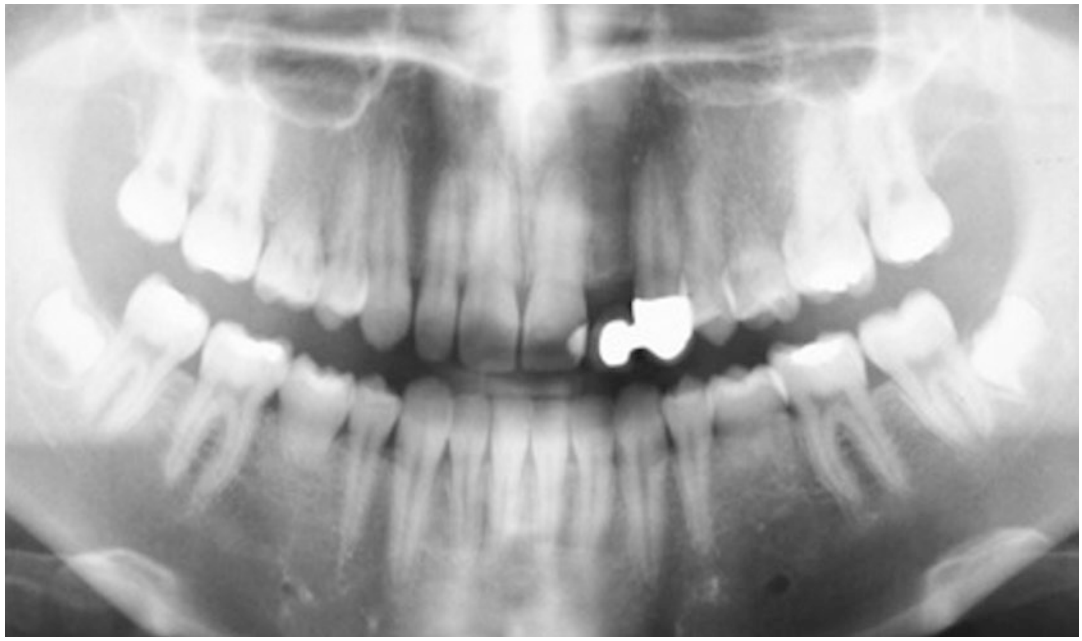

Fig. 9.6 One year after autotransplantations (case 1)

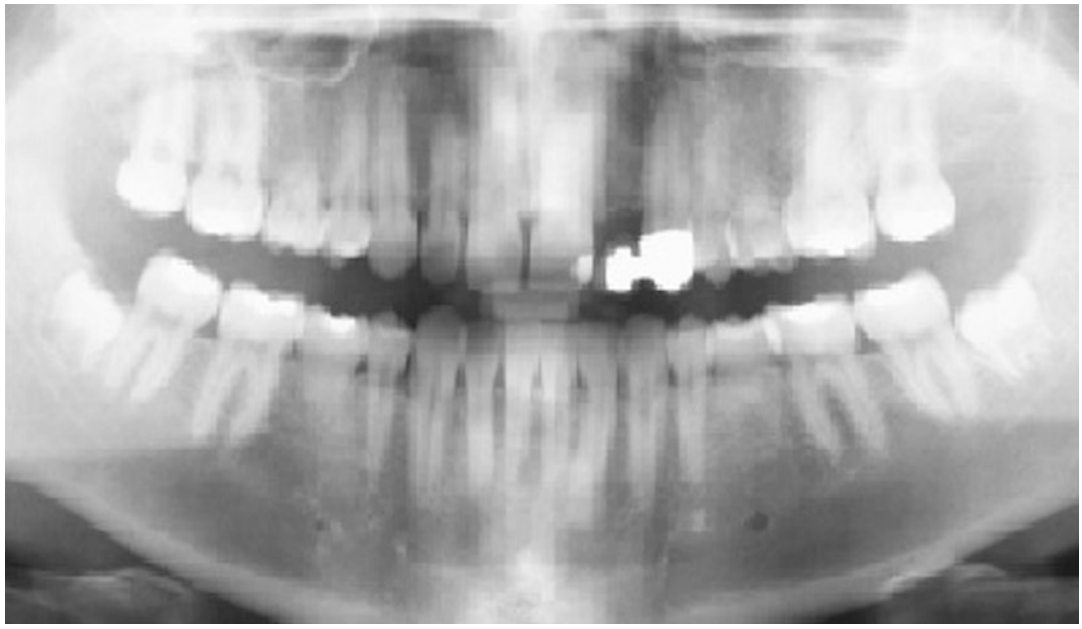

Fig. 9.7 Four years after autotransplantations (case 1)

trauma [58], early loss and congenital aplasia; these affect mainly the youngsters [59]. The vitality of these elements is almost always diagnosed by means of sensitivity and X-rays. Here, Andreasen [59] provides us with some numbers, i.e. 5-year survival for an open apex at transplantation with a 2/3 root formation = 98 % and 10-year survival for the same teeth of at least 80 %, though complications such as primary or secondary pulp necrosis in 10 % and root resorption in 10–20 % of cases are possible.

9.7.3 Luxation of an Autotransplanted Second Upper Premolar

In an 11-year-old Caucasian girl, a first premolar was transplanted to the area of the central upper incisor. This transplantation was performed to replace a reimplanted, avulsed central incisor where root canal treatment failed. The transplanted tooth was luxated at the age of 13. The luxated transplanted premolar was splinted for a period of 10 days and followed-up during 6 months with a control session after 4 years.

Here, also, a similar pattern of sensitivity values as described in the first case was registered. In this case, tooth vitality was preserved by LDF (Figs. 9.8 and 9.9). Once again, a pattern of hyperaemia, ischaemia and restored vitality could be determined.

9.7.4 Discussion

LDF is an objective, non-invasive and immediately readable recording method for blood flow from teeth with a vascularisation problem. This technique can reduce the use of subjective and unreliable sensibility tests to a minimum. An early and accurate assessment of blood flow is a significant asset to appropriate treatment, given that the impact of trauma on the survival of the pulp usually starts at the time of the accident.

A postponed root canal treatment based on inaccurate clinical information or the absence of an apical radiolucency can thus be avoided. As described by Andreasen et al. [60], we have to take into account that there is a high pulp survival for teeth with closed root tips which were involved in an alveolar bone fracture.

An assessment with simultaneous recordings using two LDF measuring probes was already proposed by Mesaros et al. (1997) [32]. They followed a total avulsion and reimplantation of upper incisors with open apices. The use of CO_2 ice was compared with LDF, LDF being the most effective and early indicator (3 weeks) for revascularisation of the pulp. Roeykens et al. confirmed and extended this observation to an electric pulp test where reproducible values were obtained for both after 7 weeks [41].

In these long-term studies, the evolution of hyperaemia followed by ischaemia and recovering vitality, starting around the ninth week, was demonstrated (Fig. 9.10). These recordings may help to give an insight in the evolution of the recovery of the pulp with impact on treatment planning of similar cases.

9.8 Is There a Need for the Use of a Splint?

Recent research from Roeykens and De Moor (2015) demonstrated that measuring with a hand-held probe, without a splint, will result in false judgements [61]. A 25–50 % increase in flux was registered as compared to the use of a splint in an identical situation (e.g. 18.8 PU versus 24.9 PU or 9.8 PU). Therefore, the use of a splint is advised enabling far more accurate LDF assessments.

9.9 Reliability/Accuracy of LDF and Diurnal Variations

9.9.1 Accuracy and Reliability

An initial accuracy of 96.3 % for LDF was obtained by Chen and Abbott [56]. In a long-term follow-up of 45 severe trauma cases with a mean of 3.5 years of monitoring, the pulpal situation with LDF was helpful in preserving tooth vitality.

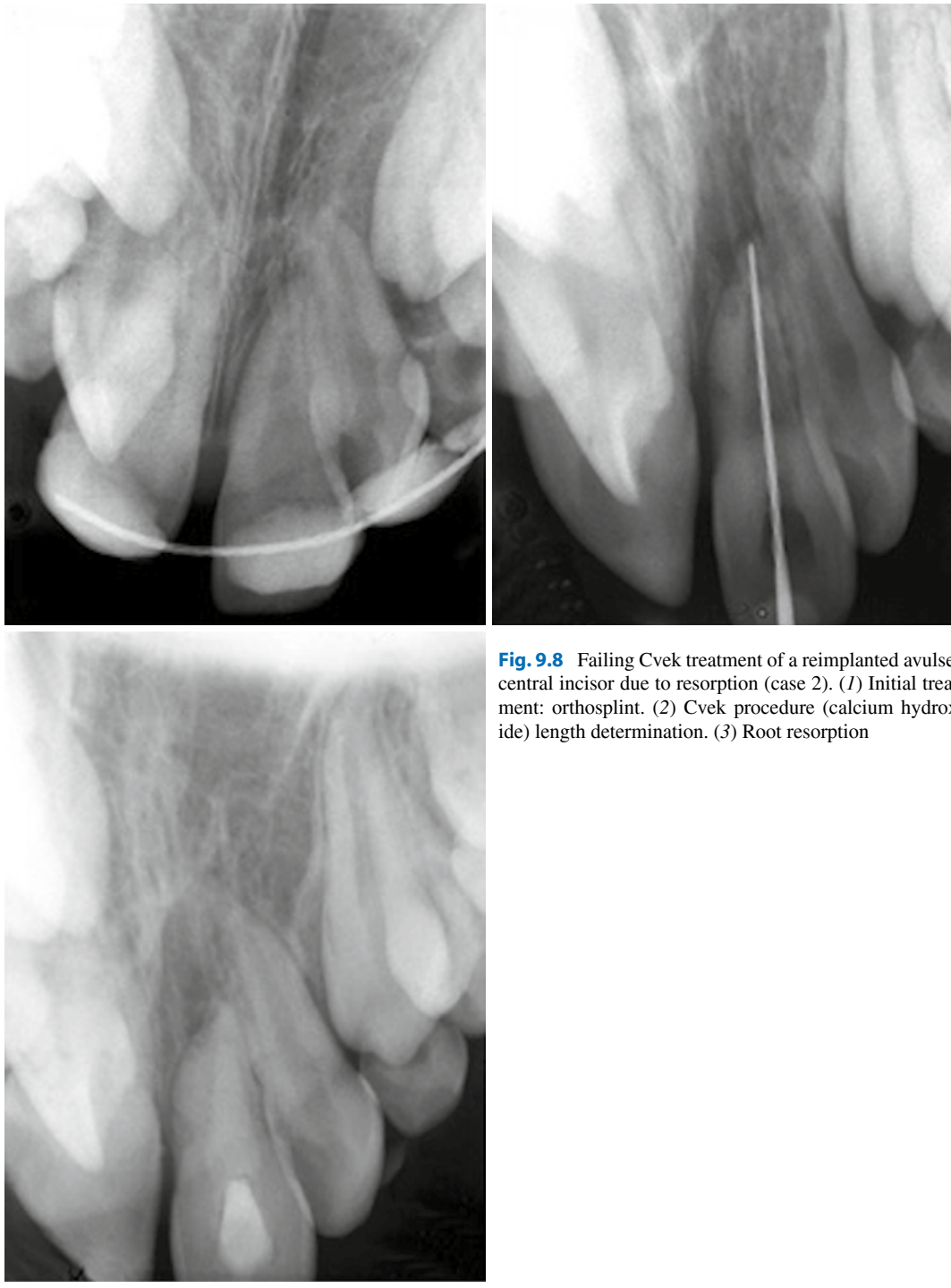

Fig. 9.8 Failing Cvek treatment of a reimplanted avulsed central incisor due to resorption (case 2). (*1*) Initial treatment: orthosplint. (*2*) Cvek procedure (calcium hydroxide) length determination. (*3*) Root resorption

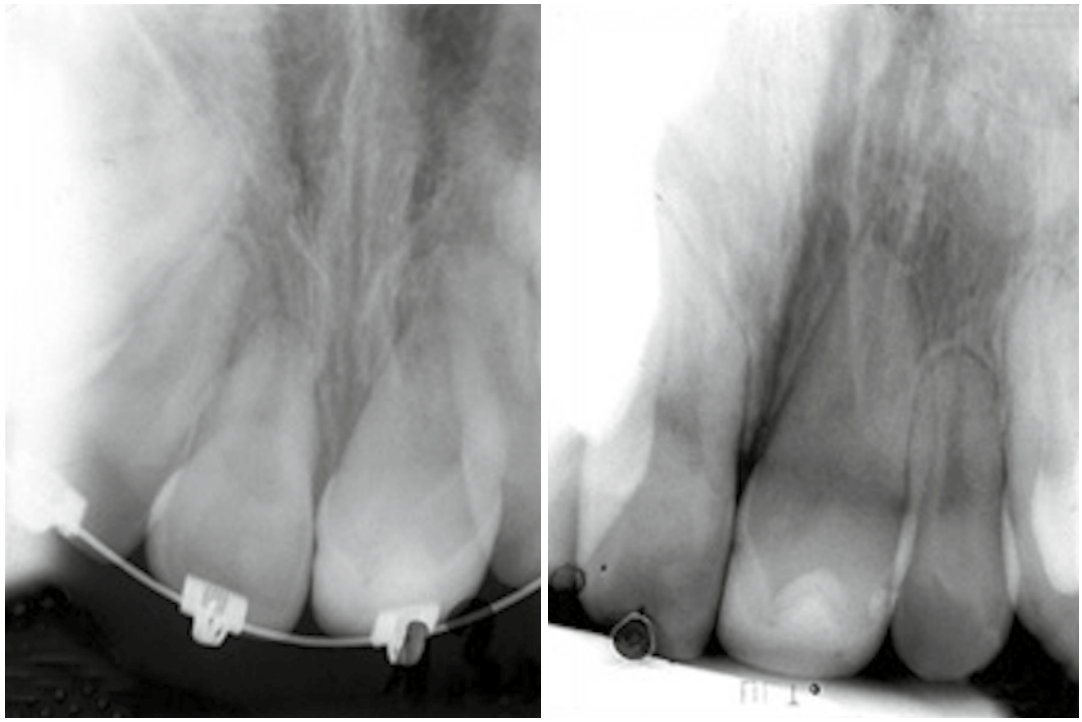

Fig. 9.9 The central incisor is replaced by an autotransplanted premolar and was subject to a luxation (case 2). (*1*) 1-year survival. (*2*) 4-year survival transplant

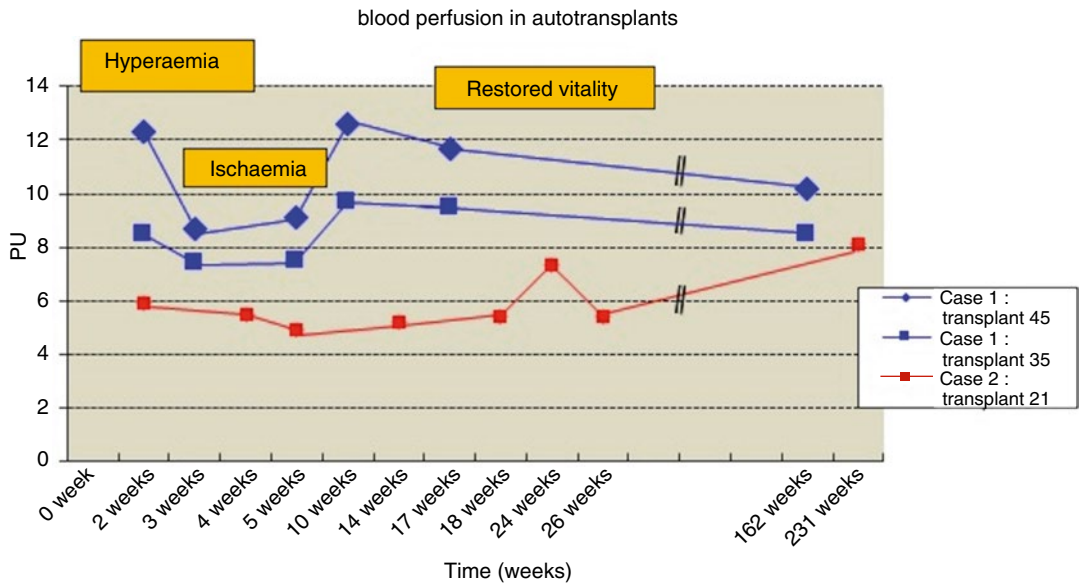

Fig. 9.10 Blood perfusion assessed in the autotransplanted teeth of case 1 and 2

In only 3 cases, root canal treatment was necessary. The maintenance of pulp vitality in trauma cases is never predictable, and even after several months, an 'initially good response' may end up with loss of vitality. As mentioned by J.O. Andreasen et al. [62], resorption may occur after luxation with the highest probability for surface resorption (26 %) in combination with lateral luxation and inflammatory resorption (38 %) with intrusive luxation. Cone beam computer tomography (CBCT) or 3D radiographical diagnosis is in these trauma cases very helpful, as described by Anderson et al. [63]. An example to emphasise the responsibility as dentist to our patients regarding the consolidation of a trauma, e.g. as part of an insurance file, is given by a case out of our clinic with 2 years of follow-up and registration of maintenance of pulp vitality with LDF (Fig. 9.11).

Fig. 9.11 Lateral resorption in the root of tooth 41, 2 years after trauma, documented with CBCT

As a result of a bike accident of a 14-year-old youngster, the negative outcome of surface and inflammatory resorption was confirmed by CBCT, despite positive readings with LDF.

It can be stated that LDF is reliable, though a combination of diagnostic tests and imaging will always result in value-added information.

9.9.2 Diurnal Variations

As already mentioned, pulpal blood flow (V_{rbc} = 0.16 mm/s) is rather slow in comparison to gingival blood flow (V_{rbc} = 0.90 mm/s) or the blood flow in the heart (V_{rbc} = 87 ± 1.5 mm/s systolic or 121 ± 2.6 mm/s diastolic annular myocardial blood velocity) [64]. As a result of diurnal/circadian variations for human blood pressure and blood velocity, there is a low blood pressure and perfusion in the morning [65]. It is therefore interesting to verify if these phenomena can be registered in human teeth. Roeykens et al. [61] used LDF on four different day-time moments, i.e. morning, noon, afternoon and night, and found the following data (perfusion units): morning (9–10 a.m.), 18.9 ± 1.5; midday, 14.3 ± 1.2; afternoon, 14.2 ± 1.2; and midnight, 9.6 ± 1.4. It is clear that it is best to register pulpal blood flow with LDF during follow-up sessions at identical day-time moments.

9.10 Does LDF Have a Future?

The use of LDF is of great value for treatment plans in traumatology, periodontology and orthodontic surgery including the evaluation of revascularisation in transplanted teeth [66] or the control of perfusion in various sites after a tissue graft.

Furthermore, LDF has already innovations [67] with LDPI (laser Doppler perfusion imaging) and LDPM (laser Doppler perfusion monitoring).

LDPI maps the perfusion of a larger surface. This is achieved by a noncontact tissue scan. A mean perfusion value is obtained from heterogeneous tissue with this approach. Well-known suppliers of these devices are Perimed AB and Moor Instruments. For this technique, Perimed uses, with its latest device (PIM3), a step scan method with the laser beam either at 670 or 690 nm with 1 mm diameter. A full scan of 5 cm by 5 cm (ability to scan 50 cm by 50 cm) with a resolution of 265 pixels by 265 pixels lasts 4–5 min. A similar technique is offered by the moorLDI-2 which uses either a 632 or 785 nm (NIR) laser. NIR has the advantage of better penetration through discoloured tissue. This new technique could be useful for imaging gingival blood flow. The zero 'probe separation' for LDI makes it unlikely to be of any use for the teeth.

LDPM or laser Doppler perfusion monitor is like a one-point LDF method which measures continuously perfusion. The measurement depth and the volume of the blood sample depend on the wavelength and the fibre separation. In normal circumstances and with a fibre separation of 250 μm and a laser output of 1 mW at 780 nm, the measuring depth will be ±0.5–1.0 mm and the volume to be measured approximately 1 mm^3. The innovation lies in the automatic search of the most favourable bandwidth (632.8 red light or 543.5 nm green light) [67]

Direct applications in dentistry of these new LDF technologies are restricted to jaw surgery with measurement of blood flow in association with osteomyelitis and in implant surgery [50, 68], to periodontology and gingival blood flow (smokers) [69] and to orthodontics with blood flow registration in the teeth after orthognathic surgery [70, 71] evaluation of the impact of conservative dentistry and the materials used (toxicity) and trauma on the pulp's vitality [71, 72].

Conclusion

The value of LDF in dentistry today lies in enabling early and accurate treatment decisions. Early recognition of a pulp problem is beneficial for the tooth's survival and prognosis. The simultaneous use of two measurement probes allows two adjacent or contralateral teeth to be compared, instantly. Moreover, this objective technique convinces both on the short and on the long term as shown by the evolution of 'troubled or irritated pulp' to 'restored pulp perfusion or vital-

ity', which has been demonstrated in different case studies. The use of LDF will also be advantageous during the evaluation of blood flow in other tissues such as tissue grafts, in bone with osteomyelitis and in the evaluation of the bone quality during monitoring of the condition of the tissues surrounding implants. Despite the limited implementation of LDF in dental practice, this technique belongs to the basic instruments of the dental clinic.

References

1. http://www.merriam-webster.com/dictionary : Blood. Last Accessed 14 Apr 2015.
2. Barrett KE, Barman S, Boitano S, Brooks HL. Ganong's review of medical physiology. 23rd ed. New York: McGraw-Hill Medical; 2010.
3. http://en.wikipedia.org/wiki : Blood. Last Accessed 14 Apr 2015.
4. Jafarzadeh H, Rosenberg PA. Pulse oximetry: review of a potential aid in endodontic diagnosis. J Endod. 2009;35:329–33.
5. Yoon M-J, Kim E, Lee S-J, Bae Y-M, Kim S, Park S-H. Pulpal blood flow measurement with ultrasound doppler imaging. J Endod. 2010;36:419–22.
6. Jafarzadeh H. Laser Doppler flowmetry in endodontics: a review. Int Endod J. 2009;42:476–90.
7. Roeykens H, De Moor R. The use of laser Doppler flowmetry in paediatric dentistry. Eur Arch Paediatr Dent. 2011;12:85–9.
8. Allen J. Photoplethysmography and its application in clinical physiological measurement. Physiol Meas. 2007;28:R1–39.
9. Tamura T, Maeda Y, Sekine M, Yoshida M. Wearable photoplethysmographic sensors – past and present. Electronics. 2014;3:282–302.
10. Cotti E, Campisi G, Ambu R, Dettori C. Ultrasound real-time imaging in the differential diagnosis of periapical lesions. Int Endod J. 2003;36:556–63.
11. Rajendran N, Sundaresan B. Efficacy of ultrasound and color power Doppler as a monitoring tool in the healing of endodontic periapical lesions. J Endod. 2007;33:181–6.
12. Lustig JP, London D, Dor BL, Yanko R. Ultrasound identification and quantitative measurement of blood supply to the anterior part of the mandible. Oral Surg Oral Med Oral Pathol Oral Radiol Endod. 2003;96:625–9.
13. Kim SW, Kim SC, Nam KC, Kang ES, Im JJ, Kim DW. A new method of screening for diabetic neuropathy using laser Doppler and photoplethysmography. Med Biol Eng Comput. 2008;46:61–7.
14. Riva C, Ross B, Bendek GB. Laser Doppler measurements of blood flow in capillary tubes and retinal arteries. Invest Ophthalmol. 1972;11:936–44.
15. Stern MD. In vivo evaluation of microcirculation by coherent light scattering. Nature. 1975;254:56–8.
16. Holloway GA, Watkins DW. Laser Doppler measurements of cutaneous blood flow. J Invest Dermatol. 1977;69:306–12.
17. Gazelius OB, Edwall BL, Edwall L. Non-invasive recording of blood flow in human dental pulp. Endod Dent Traumatol. 1986;2:219–21.
18. Wilder-Smith PEEB. A new method for the non-invasive measurement of pulpal blood flow. Int Endod J. 1988;21:307–12.
19. Raab WH. Die Laser-Doppler-Flußmessung: Untersuchungen zur Mikrozirkulation der Zahnpulpa. Dtsch Zahnarztl Z. 1989;44:198–200.
20. Ramsay DS, Artun J, Martinen SS. Reliability of pulpal blood-flow measurements utilizing laser Doppler flowmetry. J Dent Res. 1991;70:1427–30.
21. Vongsaven N, Matthews B. Experiments on extracted teeth into the validity of using laser doppler techniques for recording pulpal blood flow. Arch Oral Biol. 1993;38:431–9.
22. Vongsaven N, Matthews B. Some aspects of the use of laser Doppler flow meters for recording tissue blood flow. Exp Physiol. 1993;78:1–14.
23. Ingolfsson ER, Tronstad L, Hersh EV, Riva CE. Effect of probe design on the suitability of laser Doppler flowmetry in vitality testing of human teeth. Endod Dent Traumatol. 1993;9:65–70.
24. Ingolfsson ER, Tronstad L, Hersh EV, Riva CE. Efficacy of laser Doppler flowmetry in determining pulp vitality of human teeth. Endod Dent Traumatol. 1994;10:83–7.
25. Ingolfsson ER, Tronstad L, Riva CE. Reliability of laser Doppler flowmetry in testing vitality of human teeth. Endod Dent Traumatol. 1994;10:185–7.
26. Anderson KK, Vanardsall RL, Kim S. Measurements of pulpal blood flow in humans using laser Doppler flowmetry: a technique allowing stability and repeatability of pulpal blood flow measurement during surgical manipulations. Int J Adult Orthodon Orthognath Surg. 1995;10:247–54.
27. Odor TM, Pitt Ford TR, McDonald F. Effect of wavelength and bandwidth on the clinical reliability of laser Doppler recordings. Endod Dent Traumatol. 1996;12:9–15.
28. Odor TM, Watson TF, Pitt Ford TR, McDonald F. Pattern of transmission of laser light in teeth. Int Endod J. 1996;29(4):228–34.
29. Odor TM, Pitt Ford TR, McDonald F. Effect of probe design and bandwidth on laser Doppler readings from vital and root-filled teeth. Med Eng Phys. 1996;18:359–64.
30. Vongsaven N, Matthews B. Experiments in pigs on the sources of laser Doppler blood-flow signals recorded from teeth. Arch Oral Biol. 1996;41(1):97–103.

31. Hartmann A, Azérad J, Boucher Y. Environmental effects on laser Doppler pulpal blood-flow measurements in man. Arch Oral Biol. 1996;41:333–9.
32. Mesaros SV, Trope M, Maixner W, Burkes EJ. Comparison of two laser Doppler systems on the measurements of blood flow of premolar teeth under different pulpal conditions. Int Endod J. 1997;30:167–74.
33. Evans D, Reid J, Strang R, Stirrups D. A comparison of laser Doppler flowmetry with other methods of assessing the vitality of traumatised anterior teeth. Endod Dent Traumatol. 1999;15:284–90.
34. Odor TM, Chandler NP, Watson TF, Pitt Ford TR, McDonald F. Laser light transmission in teeth: a study of the patterns in different species. Int Endod J. 1999;32:296–302.
35. Roeykens H, Van Maele G, De Moor R, Martens L. Reliability of laser Doppler flowmetry in a 2-probe assessment of pulpal blood flow. Oral Surg Oral Med Oral Pathol Oral Radiol Endod. 1999;87:742–8.
36. Roebuck EM, Evans DJP, Stirrups D, Strang R. The effect of wavelength, bandwidth, and probe design and position on assessing the vitality of anterior teeth with laser Doppler flowmetry. Int J Paediatr Dent. 2000;10:213–20.
37. Soo-ampon S, Vongsavan N, Soo-ampon M, Chuckpaiwong S, Matthews B. The sources of laser Doppler blood-flow signals recorded from human teeth. Arch Oral Biol. 2003;48:353–60.
38. Polat S, Er K, Polat T. Penetration depth of laser Doppler flowmetry beam in teeth. Oral Surg Oral Med Oral Pathol Oral Radiol Endod. 2005;100:125–9.
39. Sasano T, Onodera D, Hashimoto K, Likubo M, Satoh-Kuriwada S, Shoji N, Miyahara T. Possible application of transmitted laser light for the assessment of human pulpal vitality. Part 2. Increased laser power for enhanced detection of pulpal blood flow. Dent Traumatol. 2005;21:37–41.
40. Polat S, Er K, Polat T. The lamp effect of laser Doppler flowmetry on teeth. J Oral Rehabil. 2005;32:844–8.
41. Roeykens H, Van Maele G, Martens L, De Moor R. A two-probe laser Doppler flowmetry assessment as an exclusive diagnostic device in a long-term follow-up of traumatised teeth: a case report. Dent Traumatol. 2002;18:86–91.
42. Patiño-Marín N, Martínez F, Loyola-Rodríguez JP, Tenorio-Govea E, Brito-Orta MD, Rodríguez-Martínez M. A novel procedure for evaluating gingival perfusion status using laser-Doppler flowmetry. J Clin Periodontol. 2005;32:231–7.
43. Emshoff R, Kranewitter R, Norer B. Effect of Le Fort I osteotomy on maxillary tooth-type related pulpal blood-flow characteristics. Oral Surg Oral Med Oral Pathol Oral Radiol Endod. 2000;89:88–90.
44. Justus T, Chang BJ, Bloomquist D, Ramsay DS. Human gingival and pulpal blood flow during healing after Le Fort I osteotomy. J Oral Maxillofac Surg. 2001;59:2–7.
45. Kolkman RGM. Photoacoustic and pulsed-laser Doppler monitoring of blood concentration and perfusion in tissue. PhD thesis, University of Twente; 1998.
46. Fredriksson I, Larsson M, Strömberg T. Measurement depth and volume in laser Doppler flowmetry. Microvasc Res. 2009;78:4–13.
47. Gush RJ, King TA. Discrimination of capillary and arteriovenular blood flow in skin by laser Doppler flowmetry. Med Biol Eng Comput. 1991;29:387–92.
48. Bonner RF, Nossal R. Model for laser Doppler measurements of blood flow in tissue. Appl Opt. 1981;20:2097–107.
49. Qu X, Ikawa M, Shimauchi H. Improvement of the detection of human pulpal blood flow using a laser Doppler flowmeter modified for low flow velocity. Arch Oral Biol. 2014;59(2):199–206.
50. Wannfors K, Gazelius B. Blood flow in jaw bones affected by chronic osteomyelitis. Br J Oral Maxillofac Surg. 1991;29:147–53.
51. Jafarzadeh H, Abbott PV. Review of pulp sensibility tests. Part I: general information and thermal tests. Int Endod J. 2010;43:738–62.
52. Jafarzadeh H, Abbott PV. Review of pulp sensibility tests. Part I: electric pulp tests and test cavities. Int Endod J. 2010;43:945–58.
53. Chen E, Abbott PV. Dental pulp testing: a review. Int J Dent. 2009;2009:365785, 12 pages.
54. Karayilmaz H, Kirzioglu Z. Comparison of the reliability of laser Doppler flowmetry, pulse oximetry and electric pulp tester in assessing the pulp vitality of human teeth. J Oral Rehabil. 2011;38(5):340–7.
55. Karayilmaz H, Kirzioğlu Z. Evaluation of pulpal blood flow changes in primary molars with physiological root resorption by laser Doppler flowmetry and pulse oximetry. J Clin Pediatr Dent. 2011;36:139–44.
56. Chen E, Abbott PV. Evaluation of accuracy, reliability, and repeatability of five dental pulp tests. J Endod. 2011;37:1619–23.
57. Petersson K, Sönderström C, Kiani-Anaraki M, Lévy G. Evaluation of the ability of thermal and electrical test to register pulp vitality. Endod Dent Traumatol. 1999;15:127–38.
58. Öhman A. Healing and sensitivity to pain in young replanted human teeth. An experimental, clinical, and histological study. Odontol Tidskr. 1965;73: 166–227.
59. Andreasen FM. Transient apical breakdown and its relation to color and sensibility changes after luxation injuries to teeth. Endod Dent Traumatol. 1986;2:9–19.
60. Andreasen JO, Andreasen FM, Andersson L. Text book and color atlas of traumatic injuries to teeth. 4th ed. Munksgaard: Blackwell publishing Ltd; 2007.
61. Roeykens H, Deschepper E, De Moor R. Reliability of dental laser Doppler flowmetry utilizing a silicone splint. Work in progress. 2015.
62. Andreasen FM, Vestergaard Pedersen B. Prognosis of luxated permanent teeth – the development of pulp necrosis. Endod Dent Traumatol. 1985;1:207–20.

63. Anderson PJ, Yong R, Surman TL, Rajion ZA, Ranjitkar S. Application of three-dimensional computed tomography in craniofacial clinical practice and research. Aust Dent J. 2014;59 Suppl 1:174–85.
64. Li VW, Chen RH, Wong WH, Cheung YF. Left ventricular contractile reserve in young adults long-term after repair of coarctation of the aorta. Am J Cardiol. 2015;115:348–53.
65. Al Mheid I, Corrigan F, Shirazi F, Veledar E, Li Q, Alexander WR, Taylor WR, Waller EK, Quyyumi AA. Circadian variation in vascular function and regenerative capacity in healthy humans. J Am Heart Assoc. 2014;15:e000845.
66. Claus I, Laureys W, Cornelissen R, Dermaut LR. Histologic analysis of pulpal revascularization of autotransplanted immature teeth after removal of the original pulp tissue. Am J Orthod. 2004;125:93–9.
67. Rajan V, Varghese B, van Leeuwen TG, Steenbergen W. Review of methodological developments in l Doppler flowmetry. Lasers Med Sci. 2009;24: 269–83.
68. Verdonck HW, Meijer GJ, Kessler P, Nieman FH, de Baat C, Stoelinga PJ. Assessment of bone vascularity in the anterior mandible using laser Doppler flowmetry. Br J Oral Maxillofac Surg. 1991;29(3):147–53.
69. Mavrapoulos A, Aars H, Brodin P. Hyperaemic response to cigarette smoking in healthy gingiva. J Clin Periodontol. 2001;30:214–21.
70. Kristerson L, Lagerström L. Autotransplantation of teeth in cases with agenesis or traumatic loss of maxillary incisors. Eur J Orthod. 1991;13:486–92.
71. Andreasen JO. Atlas of replantation and transplantation of teeth. Fribourg: Mediglobe; 1991.
72. Ajcharanukul O, Kraivaphan P, Wanachantarak S, Vongsavan N, Matthews B. Effects of potassium ions on dentine sensitivity in man. Arch Oral Biol. 2007;52:632–9.

Part IV

New Development of Laser for Endodontic Irrigation

Laser-Activated Irrigation (LAI)

10

Giovanni Olivi and Roeland J.G. De Moor

Abstract

The complex anatomy of the root canal system and the limited penetration depth of the commonly used irrigants into the dentine limit the ability to clean, debride and disinfect three-dimensionally and completely the root canal system. Erbium family lasers represent the cutting-edge technology for the activation of irrigants in endodontics. LAI is introduced here, emphasising all the different techniques proposed. The mechanism of LAI and all the conditions that influence LAI efficiency and safety are described including the wavelength to use, the energy, the pulse duration and pulse frequency, tip design and tip position into the canal or in the pulp chamber. Studies on applications of LAI for smear layer removal and canal decontamination are fully debated.

10.1 Introduction

Root canal therapy consists of the enlargement and shaping of the root canals with hand and rotary instruments to a size sufficient to deliver tissue-dissolving and antibacterial fluids to the apical area. One of the main problems in endodontics is the fluid dynamics of the irrigants in the confined canal space, which hinders the deep penetration of irrigant because of the absence of turbulence over much of the canal volume [1]. A constant flow of irrigants helps to dissolve inflamed and necrotic tissue, to disinfect the canal walls from bacteria/biofilm and to flush out debris and smear layer from the root canal, and hence is essential for the endodontic success. The complex anatomy of the root canal system and the limited penetration depth into the dentine and the branches of the endodontic space of the commonly used irrigants limit its ability to clean, debride and disinfect the root canal system three-dimensionally completely [2].

G. Olivi, MD, DDS (✉)
InLaser Rome – Advanced Center for Esthetic and Laser Dentistry, Rome, Italy
e-mail: olivilaser@gmail.com

R.J.G. De Moor, DDS, MSc, PhD
Department of Restorative Dentistry and Endodontology, Ghent Dental Laser Centre, Ghent Dental Photonics Research Clustre, BIOMAD, Dental School, Ghent University Hospital, Ghent University, Ghent, Belgium

G. Olivi et al. (eds.), *Lasers in Endodontics: Scientific Background and Clinical Applications*,
DOI 10.1007/978-3-319-19327-4_10

A study from Peters et al. (2001) investigated the efficacy of four different instrumentation techniques. Their findings demonstrated ineffective action of the instrumentation tested which left 35 % or more of the canal's surface area unchanged [3].

A study from Ricucci and Siqueira (2010) reported that the chemo-mechanical preparation partially removed vital and necrotic tissues from the entrance of lateral canals and apical ramifications, leaving adjacent tissue inflamed, sometimes infected, and associated with periradicular disease [4].

Sodium hypochlorite (NaOCl) is the most commonly used endodontic irrigant because of its antimicrobial and tissue-dissolving activity. As previously reported (see Chap. 3), many factors influence its effectiveness. Optimisation of surface tension, concentration, temperature, agitation and flow can improve tissue-dissolving effectiveness as much as 50-fold [5]. Stojicic et al. (2010) reported that the sodium hypochlorite with added surface active agent showed lower contact angle on dentin, resulting in more effective tissue dissolution when compared with conventional hypochlorite solutions [5].

Macedo et al. (2010) reported that the efficacy of NaOCl depended on the efficiency of its free chlorine form and its reactivity. In their experiments, activation of the irrigant resulted in a stronger modulation of the reaction rate of NaOCl. They demonstrated that 1 min of activation compensated for 3 min of nonactivated exposure time. Both agitation and higher temperatures considerably enhanced the efficacy of NaOCL. However, the effect of agitation on tissue dissolution was more efficient than that of temperature, with continuous agitation resulting in the fastest tissue dissolution [6].

De Gregorio et al. (2010) compared the efficacy of different agitation systems on the activity of NaOCl and found a limited penetration of the irrigant into lateral canals using apical negative-pressure irrigation system (ANP). ANP was most effective in reaching the working length, in comparison to the other tested groups (EndoActivator, sonic activation, passive ultrasonic activation (PUI), F file and positive-pressure irrigation). In contrast, PUI demonstrated significantly more penetration of irrigant into lateral canals but not up to the working length [7].

Present-day endodontic research is still focused on instrumentation and clinical procedures and finding agents that might improve the success rate of root canal treatment. Improving the fluid dynamics of the irrigants into the canal space appears to play an important role [2]. In the present chapter, the role of the *laser* in the activation of the commonly used irrigants in endodontics is explained and analysed (see also Chap. 11).

At present there are two ways to activate irrigants in root canals. First, the fibre can be used in the canal and is then activated in the canal and in the irrigant; the fibre is withdrawn at slow speed out of the canal or can be used stationary or in motion over a short distance in the canal. This technique is referred to as laser-activated irrigation (LAI). Second, the fibre is used outside the canal and is activated in irrigant in the pulp chamber over the orifice [8, 9]. The latter technique was first described as the PIPS (photon-induced photoacoustic streaming) technique [10–13]. In this chapter conventional LAI is addressed. The use of PIPS is addressed in Chap. 11.

10.2 Mechanism of Laser-Activated Irrigation

In recent years, research groups have investigated the possibility of using a laser device for activation of aqueous solutions.

Blanken and Verdaasdonk (2007), Blanken et al. (2009), de Groot et al. (2009), Matsumoto et al. (2011) and Gregorcic et al. (2012) described, through in vitro visualisation studies, the mechanism of the laser-activated irrigation [14–18]. George et al. (2008), De Moor et al. (2009–2010), DiVito et al. (2011–2012), Peeters and Suardita (2011) and Deleu et al. (2013) also investigated in vitro the role of laser to improve the efficiency of several endodontic solutions in cleaning and debriding the root canal walls [19–23]. Macedo et al. (2010) tested the ability of laser in improving the efficiency of NaOCl [6], and Peters et al. (2011) investigated in vitro

the role of the laser in improving the bactericidal efficiency of NaOCl [12].

To thoroughly understand the mechanism of laser activation of irrigants, the different devices and settings used and the protocols proposed over the last years, it is once again important to consider basic physics and all parameters that determine the slight differences in the interaction and mechanism of light energy with aqueous mediums. Important are:

- The laser-target interaction, i.e. wavelength specificity for the target or substrate and the target chromophore itself and their effects on the irrigation
- The settings including energy, pulse repetition rate, pulse duration and finally the fluence
- The geometry of the fibre/tip end, i.e. the design of the tip and tip end, the fibre/tip diameter and the position of the fibre/tip in the root canal
- The dimensions of the apical preparation

10.2.1 Wavelengths and Target Chromophore

The first concept to be introduced and understood is the use of the correct wavelength.

Irrigants are solutions with different percentages of different molecules in water.

The interaction of laser light with water follows the rules of optical physics. Light can be reflected, absorbed, diffused or transmitted (see Chap. 4).

An interaction between laser light and water occurs when there is optical affinity between them. The less the affinity, the more light will be reflected and transmitted. The more the affinity, the more the light will be absorbed.

Due to the specific affinity of water with medium infrared lasers, specifically the erbium laser family (Er:YAG and Er,Cr:YSGG), these two wavelengths are currently the only two capable of being extensively absorbed by different irrigant solutions, taking into account a safe use and respecting accepted clinical parameters [24, 25]. The erbium:YAG laser wavelength operates into the peak of absorption of water, at 2940 nm, while the erbium, chromium:YSGG laser wavelength is slightly less absorbed by water at 2780 nm (55–60 % less) [26, 27] Fig. 10.1.

In addition, the medium infrared lasers (2780–2940 nm) are absorbed also by water in

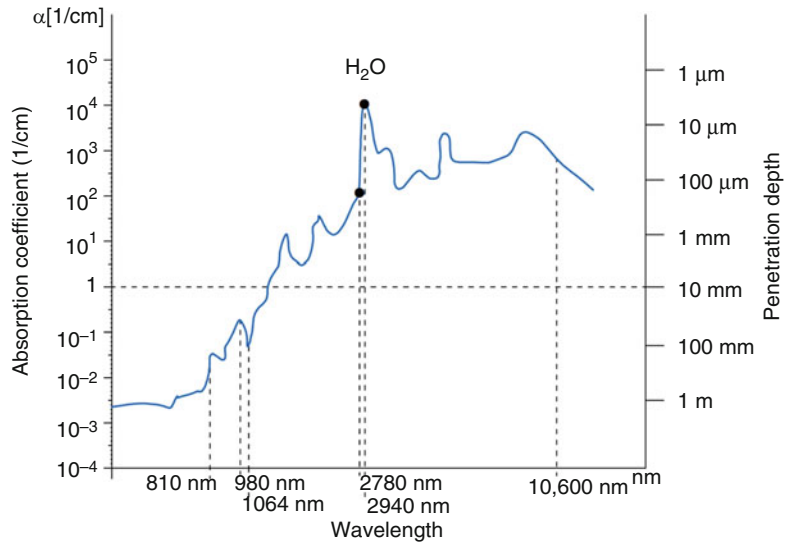

Fig. 10.1 Water absorption coefficient and penetration depth of different wavelengths

the dentinal walls [28], creating ablation in the dentin when the energy applied is appropriate (see threshold of ablation: Sect. 4.6.1). This is an important topic that differentiates conventional laser use in a dry root canal from activation of the laser in the irrigant (LAI and PIPS). The latter will be explained in more detail in Chap. 11.

Studies were also performed to investigate the ability to induce agitation of liquids using different sources such as pulsed light (optical parametric oscillator) wavelengths of 490–555 nm and Nd:YAG 1064 nm [29, 30].

Levy et al. (1996) found that Nd:YAG laser irradiation induced pressure waves when applied to water-filled root canals. The experiment was performed using the technology available at that time, with different optical fibres (200, 300, 400 and 600 μm) activated in the canal at 50 Hz with power settings of 5, 5.5 and 6.0 W, using an 800 μs pulse duration [31]. The high power used explains the extremely thermal nature of this interaction with the energy delivered by a very long pulse without any affinity of this wavelength with the substrate. In effect, the visible and near-infrared lasers are absolutely not absorbed in water. Hence, no interaction (absorption or diffusion) occurs when the water is irradiated. The laser light is only delivered through the water (transmission), transferring heat if the parameters used are very high.

This was confirmed in a study by Meire et al. (2009) who investigated the antibacterial action of irradiation with different laser wavelengths (Nd:YAG, KTP), photoactivated disinfection (PAD) and 2.5 % sodium hypochlorite (NaOCl) on *Enterococcus faecalis* bacterial suspensions (in vitro) and in infected tooth models using an aqueous suspension (ex vivo) [32]. These laser systems, at the settings used (Nd:YAG at 1.5 W, 15 Hz; KTP at 1 W, 10 Hz; both with a 200 μm fibre, activated five times during 5 s with 20 s intervals), were less effective than NaOCl in reducing *E. faecalis* both in vitro and in the infected tooth model. This might be due to poor absorption of the Nd:YAG and KTP wavelengths in water. Meire et al. explained the survival of bacteria, likely with the transmission of the laser beams through the bacterial suspension, rather than absorption. The lack of interaction with the root canal wall when Nd:YAG is activated in NaOCl was also confirmed in the study of Michiels et al. (2010) [33].

Hmud et al. (2010a) tested whether near-infrared 940 and 980 nm diode lasers could induce cavitations in aqueous media [34]. In another study they investigated the temperature variation inside a root canal and outside on the root surface during diode laser irradiation in water-filled canals [35]. At the settings used in these studies (4 W/10 Hz for the 940 nm and 2.5 W/25 Hz for the 980 nm diode lasers, both with a 200 μm optical fibre), the irradiation induced a rise in temperature as much as 30 °C within water inside the canal with only modest temperature changes of 4 °C on the external root surface reported. So, these wavelengths may be explained to act more as heaters rather than activators of the irrigants. In this respect, Deleu et al. (2013) showed that using a high-power diode laser for induction of cavitation may result in areas of carbonisation where the fibre touches the root canal wall dentine [23]. Accordingly, other studies reported more a synergistic effect of 810 and 980 nm diode lasers with NaOCl, EDTA or citric acid rather than an activation of the irrigants in root canals with these substances [36–38]. In the experience of the authors, the 810 and 940 nm diode laser or neodymium:YAG laser (1064 nm) does not induce cavitation effects using present-day advocated clinical parameters. However, using an Nd:YAG laser at 1320 nm, Moon et al. (2012) reported the induction of cavitation bubbles at 1.5 W and 15 Hz. The latter wavelength implies a higher absorption in water or aqueous solutions [39] (see Fig. 10.1).

Finally the CO_2 laser operating in the far-infrared spectrum of the light also is highly absorbed by water but is currently not used for root canal treatment because specific tips or fibres are not available.

10.2.2 Laser Target Interaction: Effects on Irrigants

Several studies investigated the fluid dynamics of laser-activated irrigation (LAI) through high-speed

visualisation both in free water and in root canal models using Er,Cr:YSGG laser [8, 9] and different Er:YAG lasers [16–18].

The high-speed imaging methods used in these studies enabled to capture images with microsecond resolution, allowing the understanding of the working mechanism of LAI in the root canal.

10.2.2.1 Photothermal Interaction: Heating of the Irrigant

Bubble Formation and Collapse: Expansion and Implosion of Vapour Bubbles in Water

The first effect of the *absorption* of erbium laser in water is a *thermal effect*. When the laser energy is absorbed in a layer of water of a few centimetres, an instantaneous superheating of the irrigant to the boiling point of water (100 °C) generates an initial vapour bubble which expands at the tip of the fibre and ends with consecutive implosion [14–18].

Blanken and Verdaasdonk (2007) first described an Er:Cr:YSGG laser generating a vapour bubble that started to expand at a high speed from an opening in front of a flat end firing fibre [14]. They observed that as the laser continued to emit energy, the light passed through the bubble, evaporating the water surface at the front of the bubble, advancing through a channel in the liquid until the pulse ends at about 130 μs (the duration of a single pulse was about 130–140 μs for the Er,Cr:YSGG laser). This mechanism had been previously referred to as "the Moses effect in the microsecond region" by van Leeuwen et al. (1991) [40].

The collapse of the laser-induced bubble follows immediately after the expansion. The shrinkage creates a cavitation-generated pressure wave that travels at supersonic speed (shock wave) in the beginning and at sonic speed (acoustic waves) later [17, 41]. Also a high-speed liquid jet is formed [42] and fluid surrounding the bubble quickly flows inside the decompressed vapour gap, inducing fluid velocities of several metres per second. It was estimated that when an Er,Cr:YSGG is used with a 400 μm flat tip within the canal, fluid movement inside the root canal occurred immediately after each pulse, with fluid speeds up to 20 m/s (72 km/h) [14]. In a following study, Blanken et al. (2009) observed a fluid velocity of 21 m/s using an Er:Cr:YSGG with a 200 μm flat tip at 75 mJ–20 Hz (velocity was calculated based on the measurement of bubble growth and collapse versus time) [15]. Research demonstrated that the dynamics of bubble growth in the root canal model was different from the free-standing water situation [15, 17]. In the root canal model, the lateral expansion is limited by the canal walls. The forward expansion is oscillated by the water in front, while the backward expansion is blocked by the fibre so that pressure inside the bubble remains high for a long time since it has to overtake the resistance of the water in such a small canal. This process delays about three times the dynamics of expansion and implosion compared to the free-water situation as described from Blanken and Verdaasdonk (2007) and Matsumoto et al. (2011) [15, 17].

10.2.2.2 Hydrodynamic Cavitation

Bubbles Cavitation and Shock Waves

Cavitation is defined as "the formation of an empty space (bubble) and fast collapse of a bubble in a liquid" [43, 44].

The process is very fast and evolves mainly in the range of 100 μs–1 ms. When a bubble collapses, primary cavitation is formed, followed by secondary cavitation bubbles that create high-speed fluid motions in the canal [15, 16]. The secondary cavitation bubbles are much smaller compared with the first vapour bubble. Also, after the collapse of secondary cavitation bubbles, even smaller bubbles are generated, later disappearing in decreasing numbers [17]. The primary and secondary cavitation bubbles create micro-jets in the fluid that generate high forces and shear stress along the dentin walls sufficient to remove smear layer and biofilm [15] (Fig. 10.2). In the previous chapter (Chap. 3), the possibility that a laser-induced plasma event through ionisation of the vapour in the induced bubble provides an additional way of cleaning the root canal walls was also reported [45].

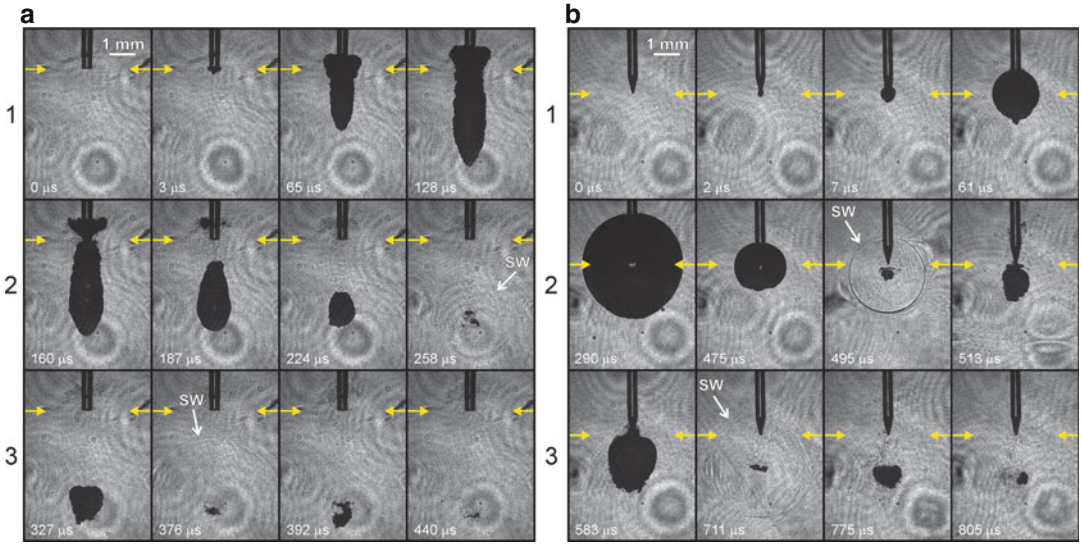

Fig. 10.2 Different bubble shape, size and cycle generated by different tips with the same laser device (**a**) 300 µm Preciso flat tip and (**b**) X-Pulse conical tip for Er:YAG laser, Fotona (Reprint with permission from Gregorcic et al. [18])

10.3 The Power of the Bubbles: Parameters That Influence Bubble Formation

10.3.1 Effect of Energy

Blanken et al. (2009) and de Groot et al. (2009) observed that the size and the life cycle of a bubble, in free-water environment, depended on the energy applied [15, 16]. These findings are also confirmed by the authors (data not published):

- The threshold of water vaporisation (the moment of bubble formation) was reached earlier when higher-pulse energy was applied and also continued longer compared to lower energies, explaining the starting time of bubble formation and different cycle time of the bubble.
- The size of the bubble was larger for higher energies.
- The dimensions of the bubble were larger for larger-diameter fibres at the same laser energy setting. This finding must be emphasised because this is opposite to the concept of fluence in laser physics.

Table 10.1 reports the energy used in the different LAI studies.

10.3.2 Effect of Pulse Duration

In addition to the energy used, the duration of the single pulse (from few microseconds to hundred microseconds) is an important parameter that influences the bubble formation and size. The lifetime (or life cycle) of a laser-induced bubble depends on the duration of the single pulse. Different pulse durations of different lasers were investigated. Pulse durations ranging from 140 µs for the Er,Cr:YSGG (Waterlase, Biolase, Irvine, CA, USA) [14, 15] to 250 µs for the Er:YAG (Erwin AdvErl, Morita, Osaka, Japan; Versawave, Hoya ConBio, Fremont, Ca, USA) influenced the start and end duration of the bubble cycle and also its size [17, 18].

Shorter pulses in the range of few microseconds are responsible for a faster start formation of the bubble. Furthermore, shorter pulses are responsible for higher peak power. Accordingly, using very short pulse duration allows for lower energy to create bubble sizes similar to a bubble induced by higher energy with longer pulse duration (data not published).

It is important to underline that the use of energy setting above the threshold of ablation of dentin can produce possible ablative and thermal effects on the dentin walls. The latter is also correlated with

Table 10.1 Studies where the laser fibre of erbium lasers (Er:YAG and Er,Cr:YSGG) is used (1) in the canal and (2) in the pulpal chamber and not referring to photon-induced photoacoustic streaming

	Wavelength	Pulse duration	Energy Pulse Frequency Power	Tip diameter and shape	Position in canal/pulp chamber	Apical preparation ISO	Temperature variation	Solution	Aim	Time
Blanken and Verdaasdonk 2007 [14]	2780 nm	130–140 µs	12.5 mJ up to 250 mJ 20 Hz	200 µm 320 µm 400 µm Flat (Z2, Z3, Z4 Waterlase, Biolase)		Glass cylinder 400 µm Taper 0.06 Length 15 mm	5–10 °C	Water	Visualisation study Cavitation bubbles	5 s
George et al. 2008 [19]	2780 nm	130–140 µs	62.5 mJ 20 Hz	400 µm Conical and flat MZ4 (Waterlase, Biolase)	Apical third 1 mm short of the working length and then activated for 5 s, withdrawing back at 1 mm/s	ProTaper F5 Maxillary anterior teeth		Distilled water, 3 % hydrogen peroxide and 15 % EDTAC	Removal of smear layer	10×5 s
	2940 nm	250 µs	200 mJ 20 Hz	400 µm Plain and conical (Kavo Key 3)						
Blanken et al. 2009 [15]	2780 nm	130–140 µs	12.5 mJ up to 125 mJ Increase per 12.5 mJ 20 Hz	200 µm Flat (Z2 Waterlase, *Biolase*)	Fibre withdrawn out of the canal in 5 s time	Glass cylinder 400 µm Taper 0.06 mm Length 15 mm		Water	Visualisation study Cavitation bubbles	5 s
			75, 125, 250 mJ 20 Hz		Fixed position in the canal 5 mm from the apex			Red dye	Visualisation study Removal of dye-coloured water	5 s (repeated until clean canal)

(continued)

Table 10.1 (continued)

	Wavelength	Pulse duration	Energy Pulse Frequency Power	Tip diameter and shape	Position in canal/pulp chamber	Apical preparation ISO	Temperature variation	Solution	Aim	Time
de Groot et al. 2009 [16]	2940 nm	250 µs	100 mJ 15 Hz 1.5 W Reduction factor of 0.36 f = 146 mJ mm^2	280 µm length 30 mm (Gr. 30×28 Kavo Key 2)	1 mm short of the working length Moved slowly up and down 4 mm in the apical half	ISO 35 Taper 0.06 Length 15 mm Decoronated Maxillary canines		2 % NaOCl	Debris removal study Mechanism study	20 s
DeMoor et al. 2009 [20]	2780 nm	130–140 µs	75 mJ 20 Hz 1.5 W	200 µm Flat (Z2 Waterlase, Biolase)	Stationary 5 mm short from the apex	ISO 40 Taper 0.06 Length 18 mm Decoronated maxillary canines		2.5 % NaOCl	Debris removal study	4×5 s
De Moor et al. 2010 [21]	2780 nm	130–140 µs	75 mJ 20 Hz 1.5 W	200 µm Flat (Z2 Waterlase, *Biolase*)	Stationary 5 mm short from the apex	ISO 40 Taper 0.06 Length 18 mm Decoronated maxillary canines		2.5 % NaOCl	Debris removal study	4×5 s
	2940 nm	250 µs		200 µm Flat (Hoya)						
Macedo et al. 2010 [6]	2940 nm	250 µs	100 mJ 15 Hz 1.5 W	280 µm length 30 mm (Gr. 30×28 Kavo Key 2)	1 mm short of the working length Moved slowly up and down 4 mm in the apical half	Apical size and taper not reported Length 24 mm Decoronated bovine maxillary central incisors		10 % NaOCl	Reaction rate of NaOCl	1 min activation phase + 3 min resting phase

	Wavelength	Pulse duration	Energy Pulse Frequency Power	Tip diameter and shape	Position in canal/pulp chamber	Apical preparation ISO	Temperature variation	Solution	Aim	Time
Matsumoto et al. 2011 [17]	2940 nm	300 µs	30, 50, 70 mJ 20 Hz Output energy: 11, 18, 26 mJ	300 µm cone shaped 18 mm (R200T Morita)	0, 2 or 5 mm short of the bottom	Artificial glass root canal model diameter 1 mm		Glass beads in water	High-speed imaging	
			50 mJ 1pps		5 mm short	Artificial model Free water ISO 40			Visualisation study	
Peeters and Suardita 2011 [22]	2780 nm	130–140 µs	28.5 mJ 35 Hz 1 W	600 µm 14 mm Flat (MZ6 Waterlase, Biolase)	In pulp chamber	ISO 20–30 taper 0.02 20 mm Mandibular premolars 20 mm		17 % EDTA	Smear layer removal study	30 and 60 s
Peeters and Mooduto 2013 [46]	2780 nm	130–140 µs	28.5 mJ 35 Hz 1 W	400 µm 14 mm Flat (MZ4 Waterlase, Biolase)	In pulp chamber	In vivo small ISO 30 Medium ISO 35–45 Large ISO 50–80 Anterior and posterior teeth		2.5 % NaOCl with contrast medium (iomeprol 0.81 g/mL)	Apical extrusion	60 s: 1 or 2 canals 120 s: 3 or 4 canals
Seet et al. 2012 [51]	2780 nm	130–140 µs	0.25 W 20 Hz	Radial firing (17 mm – 52°) Diameter n.r. (Waterlase, Biolase)	4 mm in the canal and then withdrawing	ISO 40 Taper 0.06 Preparation 1 mm through apex 15 + 1 mm Single-rooted teeth		4 % NaOCl	Disinfection study	4 × 5 s Total procedure of 60 s

(continued)

Table 10.1 (continued)

	Wavelength	Pulse duration	Energy Pulse Frequency Power	Tip diameter and shape	Position in canal/pulp chamber	Apical preparation ISO	Temperature variation	Solution	Aim	Time
Kuhn et al. 2013 [60]	2940 nm	Not mentioned	10 mJ Hz not mentioned	300 µm Flat (Key Laser 3)	From bottom to top at a speed of 1.33 mm/s	1.5 mm diameter Length 20 mm Acrylic glass plates		NaOCl (4–4.99 % available chlorine)	Soft tissue removal study	2 s (1.33 mm/s) 7×
Bolhari et al. 2014 [62]	2780 nm	140 µs	1.50 W 2.50 W 20 Hz	320 µm Radial firing (RTF3 Waterlase)	2 mm/s from apex to crown	ISO 35 Taper 0.04 14–17 mm length Single-rooted teeth		Distilled water	Smear layer removal study	3× irradiation at 2 mm/s
Guidotti et al. 2014 [52]	2940 nm	Not mentioned	50 mJ 20 Hz 1 W Fluence: 7,100 J/cm^2 in 5 s	300 µm Flat tip Preciso (Fidelis plus 3)	Inside the canal exact position not mentioned	ISO 30 ProTaper F3 WL not mentioned Single-rooted teeth	3.5 ± 0.4 °C	1/2.5 % NaOCL 2/17 %EDTA+ 2.5 % NaOCl 3/17 % EDTA	Smear layer removal study	5 s 1–2–3 cycles + Resting time 5 s each Continuous irrigant flow
Bago Juric et al. 2014 [64]	2780 nm	130-140 µs	62.5 mJ 20 Hz 1.25 W	275 µm Side firing (RFT2 Waterlase)	5 mm short of WL	ProTaper F3 Length 12 mm Mandibular incisors Maxillary second premolars		2.5 % NaOCl	Disinfection study	4×5 s
Licata et al. 2015 [53]	2780 nm	140 µs	25 mJ and 75 mJ 10 Hz	200 µm Radial firing 25 mm (RFT2 Waterlase)	Stationary at orifice entrance	ISO30 Taper 0.06 Length not mentioned Decoronated single-rooted teeth		17 % EDTA and 5.25 % NaOCl	Disinfection study	30 and 60 s

	Wavelength	Pulse duration	Energy Pulse Frequency Power	Tip diameter and shape	Position in canal/pulp chamber	Apical preparation ISO	Temperature variation	Solution	Aim	Time
Deleu et al. 2015 [23]	2940 nm	50 µs	60 mJ 20 Hz	300 µm Flat (Preciso 300/14) AT Fidelis PIPS	5 mm from WL stationary	ISO 30 Taper 0.06 WL:1 mm from apical foramen Maxillary canines		2.5 % NaOCL	Debris removal study	4×5 s
			40 mJ 20 Hz	300 µm Conical (PIPS 300/14) AT Fidelis	4 mm in the canal Stationary					4× 5 s
	980 nm		7.5 W 25 Hz	200 µm Flat	2 mm from WL Moving up and down					18 s

irrigant depletion within the canal, easily achieved when energies higher than the energy threshold (of dentin) are used. The short pulse duration of 50 μs is one of the unique features of an advanced laser activation technique, the PIPS technique, which will be presented in the next Chap. 11.

10.3.3 Effect of Pulse Frequency

The pulse frequency (or pulse repetition rate) expresses the number of pulses in 1 s.

Previously reported studies on the mechanism and the efficacy of LAI were performed isolating one single pulse and exploring cavitation through the formation and collapse of the single bubble. The succession of several pulses in 1 s generated more bubbles, and a sequence of several seconds of irradiation even more creates a strong cavitation inside the root canal. No studies were reported on the influence of different pulse frequencies on the efficiency and effectiveness of the irrigant activation. Most of the studies used 20 Hz as pulse repetition rate. In addition, it must be emphasised that the laser used in some of these studies had the pulse frequency fixed at 20 Hz and without any possibility to vary this parameter [14, 15, 20, 21]. de Groot and Macedo utilised 15 Hz [6, 16], while Peeters and Mooduto and Peeters and Suardita 35 Hz [46, 22].

In the author's experience, frequencies from 15 to 20 Hz are ideal to allow effective cavitation, while higher repetition rates create ineffective overlapping shots, resulting in a standing wave that moves irrigant only close to the end of the tip and not distant as seen with the PIPS technique.

10.3.4 Effect of Different Wavelengths

George et al. (2008) found no difference in performance between the 2780 and 2940 nm laser systems when matched for all other parameters [19].

de Groot et al. (2009) underlined that the size of the laser-generated bubble depended on the absorption by the irrigant according to the wavelength of the laser [16].

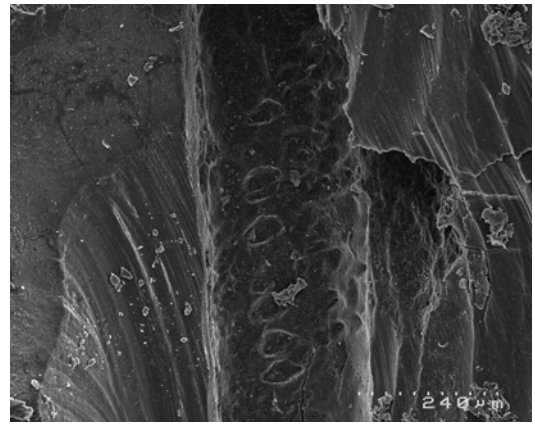

Fig. 10.3 SEM image of the root canal after LAI performed with an Er,Cr:YSGG laser (2780 nm) equipped with end-firing tip and retracting it up and down, at 1.1 W (75 mJ, 15 Hz). The irrigant vaporisation after few seconds of irradiation caused dry thermal radiation on the dentin walls and ineffective irrigation; note the overlapping hot spot expression of thermal effect (Reprint with permission from DiVito et al. [10])

De Moor et al. (2010), comparing the effects of Er:YAG and Er,Cr:YSGG wavelengths for activation of the irrigant for smear layer removal, reported similar results with both the wavelengths [21].

However, from a theoretical point of view, the difference in water absorption of the two different erbium laser wavelengths [26, 27] should suggest that the Er,Cr:YSGG laser, less absorbed in water, requires more energy to generate the same bubble size of an Er:YAG laser. This could be a problem correlated to the higher energy irradiation in the root canal as previously reported (ablative and thermal effect on dentin walls during irrigant depletion) (Figs. 10.3, 10.4 and 10.5).

10.3.5 Effect of Tip Design

The tip design also affects the shape of the laser-induced bubble and the direction of the energy emission. Conventional laser tips and fibres are flat-end firing so that no energy is directed laterally.

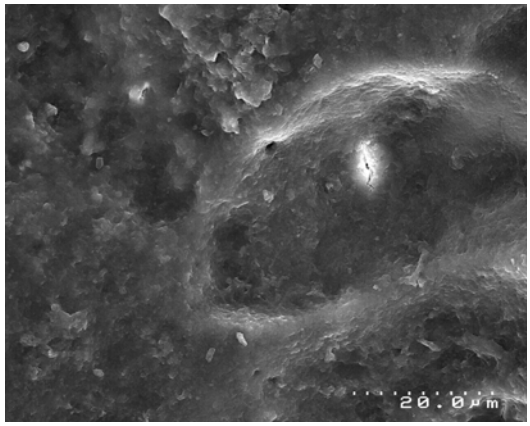

Fig. 10.4 SEM image of the root canal after LAI performed with an Er,Cr:YSGG laser (2780 nm) equipped with end-firing tip and retracting it up and down, at 1.0 W (50 mJ, 20 Hz). The irrigant depletion caused dry irradiation and successive melting of dentin surface in the apical area

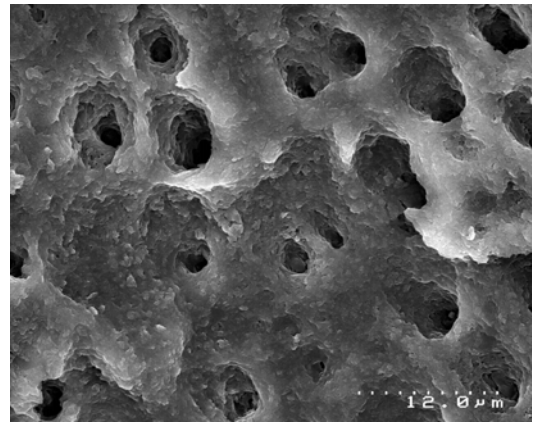

Fig. 10.5 SEM image of the root canal after LAI performed with an Er,Cr:YSGG laser (2780 nm) equipped with end-firing tip and retracting it up and down, at 1.1 W (75 mJ, 15 Hz). The irrigant depletion caused dry irradiation and successive superficial thermal damage on dentin walls (Reprint with permission from DiVito et al. [10])

Fig. 10.6 Flat end-firing tip for Er,Cr:YSGG laser (Waterlase MD and iPlus, Biolase); the tip is available in different diameters (200–300–400 µm) and length

Fig. 10.8 Conical tip for Er:YAG laser (AdvErl, Morita, Osaka, Japan); the tip is available in different diameters (200–300 µm)

Fig. 10.7 Flat end-firing and conical tips for Er:YAG laser (LightWalker, Fotona); the tips are available in different diameters (300–400 µm)

This may be problematic in some clinical procedures such as the irradiation of periodontal pockets or root canals for both the efficacy and the safety of the procedure. Today tips are available with different designs such as conical shaped, tapered and tapered and stripped (PIPS™), thereby allowing more energy to be delivered laterally and less frontally. The conical shape and the stripped part of the tip allow for lateral diffusion of the energy in the irrigant fluid, decreasing the frontal pressure and improving the safety of the procedure [17, 19, 20, 21, 47] (Fig. 10.6, 10.7 and 10.8).

This hypothesis has been confirmed by the findings of three research papers.

Blanken and Verdaasdonk (2007), Matsumoto et al. (2011) and Gregorcic et al. (2012) reported a different shape of the bubble, related to the different tip design [14, 17, 18]. The flat laser generated an oval bubble, long and almost elliptically shaped due to the frontal emission of energy [15, 18]. The use of a conically shaped tip resulted in the formation of a round bubble due to the three-dimensional (frontal and lateral) emission of the energy [17, 18] (see Fig. 10.2). Matsumoto et al. in their experiment used an Er:YAG laser (Erwin AdvErl, Morita, Osaka, Japan) equipped with a conically shaped tip (R200T; Morita), which can emit the laser energy laterally on the root canal wall [17]. The lateral emission rate was calculated at approximately 80 %. The outer diameter of the fibre was 300 μm, frontal emission rate was 37 %, top angle was 84° and the length was 18 mm. Other observations of this study confirmed also the safer use of the conically shaped tip when compared with a flat tip, avoiding apical damage or extrusion [17].

George and Walsh (2011) in one of their studies assessed the performance of four different laser systems (diode 980 nm, Nd:YAG, Er:Cr:YSGG and Er:YAG) with fibre modifications resulting in increased lateral emission. Also here, the modified design involved the tip end to reduce the irradiation directed toward the apex. The distribution of laser energy with the different tip designs was explored using a thermochromic dye used to paint the root surface of extracted teeth. The three safer-tipped ends gave reduced emissions in the forward direction (range 17–59 %) with similar lateral emission characteristics [47].

The difference in shape design of the tips and their different position into the canal, together with the size of apical preparation and the energy used, explain the conditions for the possible extrusion of the irrigants through the apex.

10.4 Other Conditions That Influence LAI Efficiency and Safety

Current studies on LAI differ in many aspects. Besides the different laser systems and settings used, the difference in enlarging and shaping of the root canal, the apical preparation size both in vitro and in experimental models and the position of the tip within the canal are all conditions closely related to the efficiency and safety of the LAI technique.

All the currently used conventional irrigation systems required that the root canal is enlarged and shaped to a size sufficient to deliver antibacterial fluids and flush out debris from the root-canal space. In order to have effective irrigation, the size of the syringe tip has to be chosen in accordance to the size of the apical preparation, and the irrigant's extrusion from the needle is limited to 1–2 mm beyond its tip [48]. Laser-activated irrigation is more efficient than conventional hand syringe and tends to be more effective than PUI [16, 19–21]. However, LAI efficacy depends on the one hand on the efficiency of the different systems used and on the other parameters previously highlighted (energy and pulse duration, tip design and diameter).

10.4.1 Apical Preparation and Root Canal Shaping

The apical constriction and the size at working length influence offset conditions for possible extrusion of irrigants.

George and Walsh (2008), with their in vitro dye study, found that there was a threefold increased extrusion in the ISO#20 apical constriction group versus the ISO#15 group when matched for the same laser system, fibre design and distance from the apex [49]. They also reported that with a considerable flaring of the canal orifice (they prepared the working length at

ISO#50), the apical direction of the fluid streaming will be enhanced, possibly resulting in greater fluid extrusion through the apex [49, 50].

Table 10.2 reports the different apical preparation dimensions used in the experimental studies on LAI.

Table 10.2 Overview of apical sizes and tapers of the root canal prepared teeth used in conventional LAI studies

Investigation	Apical sizes and taper of the preparation
George et al. 2008 [19]	ProTaper F5
De Groot et al. 2009 [16]	ISO 35 – taper 0.06
De Moor et al. 2009 [20]	ISO 40 – taper 0.06
De Moor et al. 2010 [21]	ISO 40 – taper 0.06
Peeters and Suardita [22]	ISO 20–30 – taper 0.02
Seet et al. (2012) [51]	ISO 40 – taper 0.06
Bolhari et al. (2014) [62]	ISO 35 – taper 0.04
Guidotti et al. (2014) [52]	ProTaper F3
Bago Julic (2014) [64]	ProTaper F3
Licata et al. (2015) [53]	ISO 30 – taper 0.06
Deleu et al. (2015) [23]	ISO 30 – taper 0.06

10.4.2 Tip Position

Data reported in Table 10.2 show the inconsistency in fibre/tip-end position in the root canal. In order to prevent extrusion, the laser fibre/tip should be kept away from the apex. On the other hand, efficient and safe cleaning and disinfection of the root canal have to be ensured. At present there are two approaches: the one moving or keeping the fibre tip stationary in the root canal and the other using the fibre tip stationary in the pulp chamber. The difference between the conventional approach (fibre in the root canal) and the PIPS protocol (fibre out of the root canal) will be explained in more detail in the next chapter (Fig. 10.9).

Blanken and Verdaasdonk (2007) reported the formation of the vapour bubbles up to 4.5 mm distance from the 200 μm flat tip using an Er:Cr:YSGG with a 200 μm flat tip [14] and Blanken et al. (2009) at 3.0–3.5 mm using the same wavelength and parameters [15].

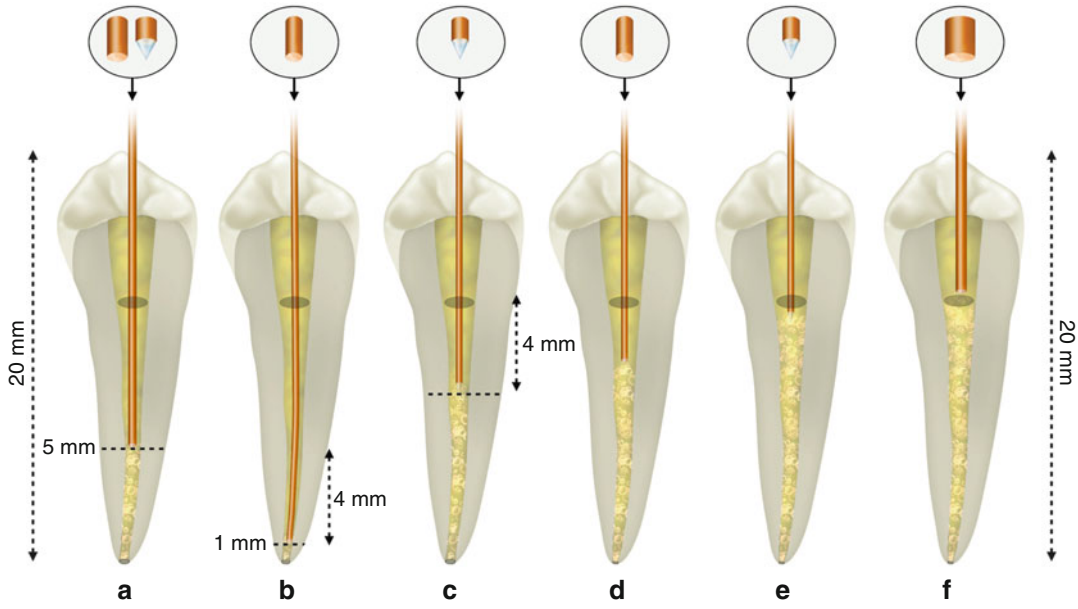

Fig. 10.9 LAI advocates positioning the tip inside the canal filled with irrigant. The graphic representation shows the different techniques proposed for laser-activated irrigation: (**a**) 200–300 μm flat and conical tips are positioned stationary 5 mm from the apex [20, 21, 23]; (**b**) 280 μm flat tip at 1 mm short of the working length and moved it slowly up and down in the final 4 mm of the apical third [16]; (**c**) conical tip inside the coronal one-third only (for 4 mm) slowly withdrawing it back to the pulp chamber [51]; (**d**) 300 μm flat tip inside the canal [52]; (**e**) 200 μm conical tip at the entrance of the orifice [53].(**f**) 600 μm flat tip in the chamber hovering over the orifice of the canal [22]

George and Walsh (2008) positioned both conical and flat 400 μm tips of both Er,Cr:YSGG and Er:YAG laser at distances of 5 mm and 10 mm from the apical stop [49].

de Groot et al. (2009) and Macedo et al. (2010) positioned the 280 μm flat tip of an Er:YAG laser 1 mm short of the working length and moved it slowly, up and down in the final 4 mm of the apical third [16, 6].

De Moor et al. (2009–2010) in their investigations on debriding efficacy used both Er,Cr:YSGG and Er:YAG laser and positioned the 200 μm flat tip of both lasers at a distance of 5 mm from the apical stop [20, 21]. In a third study (Deleu et al. 2013), this protocol was repeated with an Er:YAG laser and a 300 μm flat-ending fibre tip [23].

Matsumoto et al. (2011), in their investigation on the mechanism of LAI, inserted their 200 μm (external diameter was 300 μm) conical tip of an Er:YAG laser at 2 mm and 5 mm short of the bottom of the root canal [17].

Peeters and Suardita (2011) in their investigation on the efficacy of the Er,Cr:YSGG for smear layer removal [22] and Peeters and Mooduto (2012) in an vivo study positioned a 600 μm flat tip in the pulp chamber, hovering over the orifice of the canal [46].

Seet et al. (2012), in their bactericidal study, inserted a conical tip (diameter not reported) of an Er:Cr:YSGG laser inside the coronal one-third only (for 4 mm), slowly withdrawing it back to the pulp chamber [51].

Guidotti et al. (2012) investigated the ability of the Er:YAG laser for the debriding of the root canal, using a 300 μm flat tip, positioned inside the canal of decoronated teeth: the exact position was not specified [52].

Licata et al. (2013) in their microbiological study used an Er,Cr:YSGG laser with a 200 μm radial-firing tip positioned at the entrance of the canal orifice and kept stationary [53].

Some of the present studies agree that it is not necessary to insert the laser tip close to the apex or apical end of the preparation, but instead suggest to position the fibre tips (200–300 and 320 mm in diameter) at 5 mm from the anatomical apex [17, 20, 21, 23]. One of the reasons was to take care not to extrude the irrigant beyond the apex.

10.4.3 Apical Extrusion

George and Walsh (2008) in a dye penetration study found no significant difference in the extrusion at both the distances of 5 and 10 mm from the apical stop using both a 400 μm flat tip at 1 W and a modified 400 μm conical tip at 0.75 W for 5 s. In addition, the volume of fluid extrusion was similar to conventional 25 G needle irrigation, but it was distributed further from the apex by a factor of approximately four times [49]. They concluded that erbium lasers can create pressure waves of sufficient force to easily propel aqueous irrigant beyond the apical constriction when the apical foramen is larger and if the fibre tip is held too close to the apex inside the canal system [49].

On the other hand, De Moor et al. (2009–2010) in previously cited investigations observed under a magnification of 40× no damage on the apical structure after 4 cycles of 5 s of laser-activated irrigation [20, 21]. In their study in 2009 [12], it was demonstrated that positioning of the fibre tip at 5 mm from the apical stop resulted in total clearance of a coloured liquid. Hence, this distance of 5 mm was also chosen as a safety criterion and confirmed as safe and without damage in the studies of 2009 [20] and 2010 [21].

The difference between these two studies, performed with different settings (50 mJ and 37.5 mJ vs. 75 mJ by De Moor et al.) and laser devices, could be attributable to the different tip-design diameters used. De Moor et al. used 200 μm flat tips while George and Walsh used both the flat and conical 400 μm fibre tips with different preparation sizes at the working length: ISO#50 for George and Walsh and ISO#40 for De Moor et al. [49, 21].

Matsumoto et al. (2011) observed a second series of cavitation bubbles at the bottom of the root canal model when the conical tip of an Er:YAG laser was inserted 2 mm shorter than the bottom of the model. However, when the tip was positioned 5 mm shorter at an energy setting of 70 mJ, there were small secondary cavitation bubbles [17]. In this case the difference could also be attributable to the different pulse duration of the different laser systems used.

Peeters and Mooduto (2012) were the first to test in vivo, using radiographic interpretation, the possibility of apical extrusion of irrigant

occurring during laser-activated irrigation [46]. The study comprised 181 patients with asymptomatic anterior and posterior teeth (for a total of 300 root canals) that required endodontic therapy for pulpal necrosis, with or without radiographically visible chronic periapical lesions and without periodontal probing. The final apical preparation was performed using hand instruments ranging from ISO#30 to ISO#80, for the 56 root canals with large apices and with 12 categorised with open apices. The final irrigation was performed with a mixture of 2.5 % NaOCl and contrast medium, and LAI with an Er,Cr:YSGG laser at 1 W and 35 Hz (28.5 mJ) with a plain quartz tip of 400 μm diameter (60 s for teeth with one canal or two canals and 120 s for teeth with three or four canals). Radiography was performed to observe the presence or absence of contrast medium in the apical tissues.

Despite the finding of the in vitro study conducted by George and Walsh (2008) that showed apical extrusion following the use of Er:YAG and Er,Cr:YSGG lasers [49], this in vivo study from Peeters and Mooduto (2012) showed no evidence of apical extrusion after LAIs [46].

It must be emphasised that there is a difference in study environment between the in vitro study where there were no differences between the internal and external canal pressure and the in vivo study where the pressure of the surrounding periodontal ligament and bone or the intracystic pressure of the large lesions could create a positive pressure that inhibits the extrusion [46, 54]. Peeters and Mooduto recommended the use of the tip not introduced into the canal, but hovering above the orifice in the pulp chamber and to not exceed 2 W of power (57 mJ at 35 Hz) [46].

Peeters and De Moor (2014) showed that it is relatively easy to exceed capillary pressure (with an overall mean pressure of 88.5 (±36.2) mmHg) when 200 μm endodontic [conical (radial firing) and flat (end firing)] tips were placed 5 mm inside the orifice of a root canal [55]. The tips were used at 0.75 W and 1.75 W, at 35 Hz (21.5 mJ and 50 mJ respectively), and 140 μs pulse duration. It has been mentioned that capillary blood pressure in the human body is approximately 25 mmHg in the capillary bed [56], 30–40 mmHg at the arterial end of the capillaries and 10–15 mmHg at the venous end [56]. However, the overall mean (SD) pressure was 9.1 (±3.8) mm Hg when the conical (radial firing) and the flat (end firing) tips were placed at the orifice. In this study an apical preparation size of ISO 40 and a 6 % taper were used because apical preparation sizes of ISO 30–40 have been recommended as minimal preparation endpoints. These diameters allow for effective irrigation and facilitate the removal of debris [57]. Based on their findings, they made the following recommendations:

1. Before the procedure, all patients should be informed that if any uncomfortable feeling occurs, they should give a signal to the operator, and the operator should stop the procedure.
2. The tip of the laser should not be introduced deep into the canal, but be made to hover above the orifice or the cervical region of the tooth.
3. Because the irrigation is continuously driven, a rubber dam should be compulsory, and suction should be applied at all times.
4. No binding should occur between the tip and the canal.

Considering the different protocols presented in the various studies, not only is it not necessary to place the tip close to the apex, but it is possible to conclude that LAI is safer and similar in effectiveness for root canal wall debridement and removal of smear from the root canal walls when the tip is positioned farther from the working length [17, 20–23] and the canal is less extensively prepared during shaping. Caution, however, must always be exercised against forcing the irrigants through the apex during laser activation particularly when using NaOCl.

10.4.4 Temperature Variation

During the LAI procedure, direct irradiation of the dentin surface does not occur because the interaction is properly restricted to the irrigant fluid within the canal. Indeed, due to the high absorption in water of the erbium wavelengths, transfer of laser energy directly to the dentinal wall is negligible. Nevertheless, some problems

may occur during the procedure, such as irrigant depletion when high-energy peak power is used, requiring additional injection of irrigant during laser activation. The latter also occurs when high-energy peak powers are used in narrow canals.

Care must be taken to avoid too high an increase in temperature inside the root canal system.

George and Walsh (2010) investigated the temperature changes occurring after laser irradiation through a laterally emitting conical tip or flat tip, using both an Er:YAG and Er,Cr:YSGG laser [58]. They positioned a thermocouple located 2 mm from the apex to record temperature changes. All the combinations of lasers and fibres used caused minimal temperature increases (less than 2.5 °C) during lasing, while water irrigation attenuated completely the thermal effects of laser irradiation using an effective power of 1 W with the flat tip and 0.75 W with the conical tip at 20 Hz.

Peeters and Mooduto (2012) investigated the temperature changes, measured inside the root canal and on the outer root surface during cavitation generated by an Er,Cr:YSGG laser using 17 % EDTA and 3 % NaOCl solutions. The irrigants were activated with 2 W at 35 Hz (effective power 1.2 W) with a 600 μm flat tip for 120 s, inducing a temperature variation never exceeding 5 °C. The mean temperature was 25.2–27.1 °C. They concluded that the changes in temperature produced by laser-induced cavitation were generally acceptable [59].

Guidotti et al. (2012) tested the ability of Er:YAG laser to remove smear layer from prepared root canal walls using an intermittent activation technique (5 s of activation in fresh irrigant for at least three times) during laser treatment. Temperature variations were also analysed. An average deep temperature increase of 3.5 ± 0.4 °C was recorded by a thermocouple, while the thermal camera showed an average superficial temperature increase of 1.3 ± 0.2 °C produced by the laser tip used at 1 W with a 300 μm tip. Deep and superficial temperatures fall immediately after irradiation. No structural damage or anatomical alteration was reported by SEM investigation [52].

It can be concluded that there is no periodontal damage due to temperature increase of the irrigant during LAI.

10.5 Laser Chemical Effects on NaOCl

Blanken et al. (2009) found identical cavitation effects when an Er:Cr:YSGG laser was activated both in water and NaOCl in root canals [15]. This finding was also confirmed by Meire et al. (2013) who recently investigated the optical properties of root canal irrigants [25].

The chemical effect of LAI on sodium hypochlorite in root canals was first studied by Macedo et al. (2010), comparing different activation systems. They reported that Er:YAG laser (KeyII, KaVo, Germany) activation of NaOCl irrigant was significantly superior in increasing the reaction rate of this solution, during both the activation phase and the rest interval [6]. This finding is very important, considering that the efficacy of NaOCl depends on the availability of its free chlorine form and its reactivity. Van der Sluis suggested to use an intermittent instead of a continuous flowing technique. The inclusion of a rest phase allows NaOCl to further react. After laser activation of the irrigant and the rest phase, the consumed solution is replaced by fresh active solution. More research is needed at present to determine the duration of the rest phase after LAI. It is also seen that particles keep on moving to the surface of the irrigant solution after activation.

Lately, Kuhn et al. (2013) investigated in vitro the effect of Er:YAG laser irradiation on the ability of NaOCl to dissolve soft tissue during endodontic procedures. The study concluded that laser activation of NaOCl, using a plain-ended fibre tip at 0.2 W power leads to an effective soft tissue dissolution [60].

The aspects of the reaction rate of NaOCl are extensively discussed in Chaps. 3 and 11.

10.6 Laser-Activated Irrigation: An Appraisal of the Influencing Factors

Although there is a heterogeneity in data complicating interpretation, the amount of information available helps one to better understand the mechanism of action for LAI, its efficiency, the

different protocols being used and possible related problems. Despite some contradictory findings, a number of factors influence irrigant agitation during laser-activated irrigation:

(a) Different laser systems have been used for LAI. At present, both Er:YAG and Er,Cr:YSGG are most appropriate for agitation of irrigants. These lasers are marketed with different delivery systems (articulated arm, optical fibre or hollow fibre). It is seen that pulse duration conditions the efficiency of the irradiation and the corresponding activation. It is not possible to modify this setting for all marketed erbium lasers; the latter also accounts for the frequency. The other parameters such as energy can be more easily changed. So, comprehension of the action of the specific laser system is needed in order to modify the settings in an attempt to arrive to the same efficiency for the procedure.
(b) Different energy settings are used with the same wavelength. This includes the power setting, the pulse repetition rate and pulse duration. As explained before, the final settings are dependent on the specific laser used. Based on the good results obtained from all investigations, there is a tendency in the last several years to rely on lower energy.
(c) Different tip diameters and designs have also been investigated. Initially, only flat-end fibres were marketed. Today, since 2010 different types of conically shaped tip ends are available. The choice of use not only depends on the expected efficiency but also on the ongoing progress of the research and on the progress in technology. Not all manufacturers provide the different types of laser tips.
(d) Different fibre tip positions during activation are now proposed. From the initial use of fibre tips in the irrigant in the root canal, we have evolved to the use of fibre tips in the area of the entrance of the root canal. Next to tip design, emphasis is given to larger tip diameters responsible for superior activation.
(e) Differences in positioning of the tips inside the canal, at the orifice or in the pulp chamber, were used with different techniques. Initially the fibre tips used in the root canal demonstrated good cleaning efficiency. At present there is a tendency to no longer place the fibre in the root canal. The choice for one of these approaches has to be associated with a critical appraisal of the effects of the expected laser-target interaction. A safe use is mandatory. Therefore, it is better to rely on high peak powers (short pulse duration and low energy) with the fibre in the region of the orifice and not in the root canal, especially not in the apical third.
(f) Different time periods of irradiation were also explored to match the correct settings and protocol with each laser system. Currently a 20 s interaction (4 times 5 s) in the root canal, with energy between 50 and 80 mJ (pulse durations around 140 μs and 20 Hz) of uninterrupted activation outside the root canal is equal to the effect of ultrasonically activated irrigation. The most significant finding is that the effect of LAI is obtained in a three times shorter time period than with ultrasound.
(g) Different apical sizes of the shaped root canals were utilised in in vitro studies. There is a general tendency to limit apical preparation and avoid extensive enlargement in the apical third. This minimally invasive approach matches with the working mechanism of LAI. Investigations, however, are still needed to determine the most minimal apical preparation diameter, taper and shape.

10.7 Thoughts for the Clinical Applications of LAI

Different protocols have been investigated using different lasers to improve the fluid dynamics of the irrigants into the canal space and finally to improve the success rate of root canal treatment. Considering that in narrow curved canals, sonic and ultrasonic systems are limited by wall contact and that this limitation does not apply to cavitation [61], LAI might be an important tool to clean the root canal efficiently, improving the success rate of root canal treatment particularly in curved and narrow canals [14].

10.8 Effects of Laser-Activated Irrigation on Smear Layer and Compacted Root Canal Debris

George et al. (2008) reported a simple method to etch long conical-shaped fibres to improve the lateral emission, specifically in endodontics [49]. This method was applied to Er,Cr:YSGG (Waterlase MD, Biolase, Irvine, CA, USA) and Er:YAG tips (Key 3, KaVo Dental GmbH, Biberach, Germany) to investigate the debriding action in the root canal when used with aqueous irrigants. The panel setting was corrected according to different energy transmission losses: 1 and 0.75 W of power at 20 Hz were applied with a 400 μm flat and conical tips respectively. The laser tips were placed into EDTAC irrigant solution in the root canal to a depth 1 mm short of the working length and then withdrawn at 1 mm/s and activated for 5 s. This cycle was repeated 10 times, for a total irrigation and activation time of 50 s. The LAI groups reported an improved effectiveness of EDTAC in smear layer removal, compared to the EDTAC nonirradiated group, for the same time period.

De Groot et al. (2009) investigated three different irrigation systems to debride a standardised root canal model filled with artificially prepared dentin debris. Syringe irrigation, PUI and LAI were performed using 2 % sodium hypochlorite as irrigant [16]. An Er:YAG laser (Key 2, KaVo, Dental GmbH, Biberach, Germany) was used with a 280 μm flat tip at the energy of 100 mJ, 15 Hz, with a calibration of the optical fibre that resulted in a reduction factor of 0.36 (effective fluence of 146 mJ mm^{-2}). The tip was inserted 1 mm short of the working length and moved slowly up and down 4 mm in the apical third of the root canal. The activation time was 20 s and the total irrigation time was 50 s. Laser-activated irrigation (LAI) results were significantly more effective than passive ultrasonic irrigation (PUI) or hand irrigation (HI) in removing dentine debris from the apical part of the root canal when activated for 20 s.

De Moor et al. (2009) completed their first study comparing the efficacy of LAI for removal of debris in root canals to conventional irrigation (CI) and passive ultrasonic irrigation with an Irrisafe (Satelec, Acteon group, Mérignac, France) (PUI) for just 20 s at a frequency of 30 KHz and a displacement amplitude of ca. 30 μm. An Er,Cr:YSGG laser, equipped with a 200 μm flat tip (Z2, Endolase Tip, Biolase), was used at 75 mJ, 20 Hz, 1.5 W to activate 2.5 % NaOCl four times for 5 s, positioned stationary at 5 mm from the apical stop, prepared at ISO 40. LAI resulted in statistically significantly less debris than PUI ($P<0.005$) and CI ($P<0.0005$), both during 20 s [20].

De Moor et al. (2010) in a further study compared the cleaning efficacy of five different irrigation systems using an experimental model similar to that of de Groot et al. using 2.5 % NaOCl as irrigant. Hand irrigation for 20 s and PUI for 20 s applied three times were compared to LAI using Er:Cr:YSGG and Er:YAG laser, both with 200 μm flat tips at 1.5 W (75 mJ, 20 Hz) 4 times for 5 s. The intermittent flush technique used with PUI (3 times for 20 s) (as recommended by van der Sluis et al.) resulted as effective as both LAI protocols (4 times for 5 s) [21]. According to the visualisation study by Blanken et al. [15], the fibre tips were also placed at a distance of 5 mm from the apical stop in the latter study [21].

Peeters and Suardita (2011) investigated the smear layer removal ability of an Er,Cr:YSGG laser (Waterlase MD, Biolase, Irvine, CA, USA) equipped with a 600 μm flat tip positioned in the pulp chamber, hovering above the canal orifice at 1 W and 35 Hz [22]. Four groups were compared: one had the root canals prepared with a master apical file at ISO#30 and the other at ISO#20, and both received laser activation for 60 s. A third group had the root canals prepared at ISO#30 and was irrigated and laser activated for 30 s. The control group used 17 % ethylenediaminetetraacetic acid (EDTA) activated with PUI for 60 s. Completely clean root canals were found only in the laser group prepared at ISO#30 and activated for 60 s.

Guidotti et al. (2012) tested the Er:YAG laser's (Fidelis III, Fotona, Ljubljana, Slovenia) ability to remove the smear layer from the root

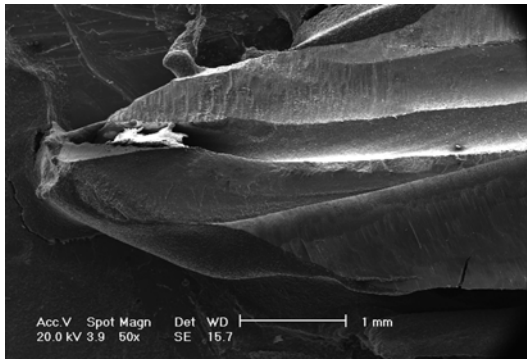

Fig. 10.10 SEM image (50×) shows dentin plugs occluding the apical foramen after mechanical instrumentation (ISO30/06) and LAI (2 cycles × 20 s) performed with an Er,Cr:YSGG laser (2780 nm) equipped with 300 μm radial-firing tip at 1.0 W (50 mJ, 20 Hz); the tip was kept stationary at a distance of 5 mm from the apex during the activation of 5 % NaOCl and 17 % EDTA

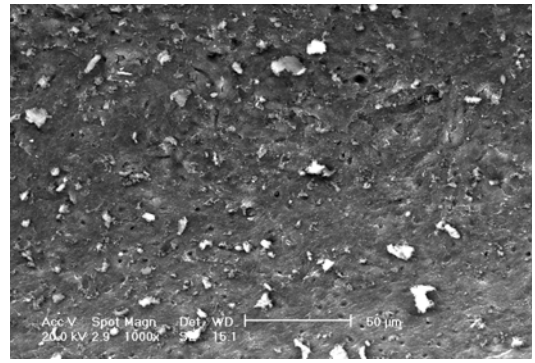

Fig. 10.12 SEM image (1000×) of the middle one-third area of the same sample 10.11. Incomplete cleaning with many debris on dentin surface

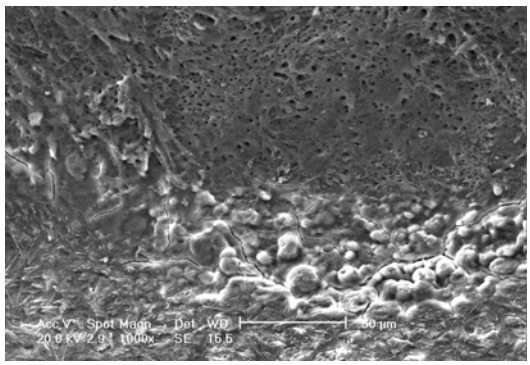

Fig. 10.11 SEM image (1000×) middle one-third area after mechanical instrumentation and LAI (2 cycles × 20 s) performed with an Er,Cr:YSGG laser (2780 nm) equipped with 300 μm radial-firing tip at 1.0 W (50 mJ, 20 Hz), kept stationary at a distance of 5 mm from the apex (5 % NaOCl and 17 % EDTA). Note the thermal damage with recrystallisation bubbles, due to water depletion and successive local heating of dentin surface; apparently this area was very close to the tip. A closer area shows cleaned surface, with some debris (*top in the figure*)

canal walls. The laser setting used was 1 W, 20 Hz and 50 mJ with very short pulse duration of 50 μs [52]. Four groups included different cycles of irradiations of 5 s each with 2.5 % NaOCl and 17 %EDTA with resting times of 5 s. The control group was only treated with a wash of 17 % EDTA solution for 2 min. Erbium laser activation of 17 % EDTA resulted in more efficient removal of smear layer than in the other groups [48].

In a study of Bolhari et al. (2014), the quality of smear layer and debris removal in the three segments of the root canal were investigated comparing an EDTA and NaOCl final rinse protocol (group 1) and Er,Cr:YSGG irradiation with a radial firing tip (320 μm) inserted in distilled water at the working length and moved continuously in a circular motion from the apex to the crown at a speed of 2 mm/s with an output of 1.5 W (group 2) and 2.5 W (group 3) [62]. The results showed no differences between groups 1 and 2 regarding the quality of smear layer removal in all areas. The irradiation at 2.5 W failed to remove the smear layer effectively. This poses a question, if increasing the power >1.5 W might not result in thermal damage with carbonisation and melted dentinal tubules as shown in this study. Regarding debris removal, the first protocol showed significantly better outcomes in all areas. In this study better cleaning efficacy was seen in the coronal and middle third. When relying on laser-activated irrigation in EDTA, however, previous studies had demonstrated better cleaning results also in the apical third [George et al. 2008 [19], Peeters and Suardita [22]] (Figs. 10.10, 10.11, 10.12, 10.13, 10.14, 10.15, 10.16, 10.17 and 10.18).

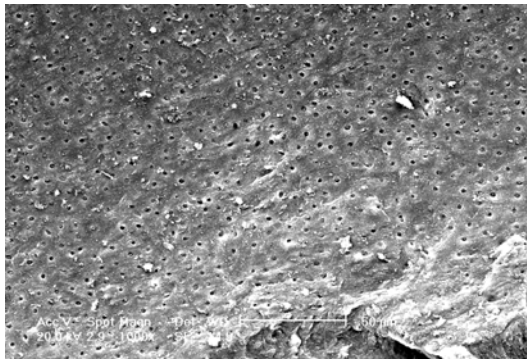

Fig. 10.13 SEM image (1000×) of the middle one-third area after mechanical instrumentation and LAI (2 cycles × 20 s) performed with an Er,Cr:YSGG laser (2780 nm) equipped with 300 μm radial-firing tip at 1.0 W (50 mJ, 20 Hz), kept stationary at a distance of 5 mm from the apex, using 5 % NaOCl and 17 % EDTA as irrigants. The irrigation resulted partially effective with presence of debris on dentin surface

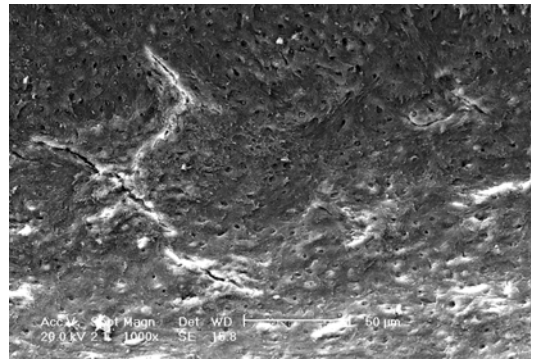

Fig. 10.15 SEM image (1000×) of the apical one-third area after mechanical instrumentation and LAI (2 cycles × 20 s) performed with an Er,Cr:YSGG laser (2780 nm) equipped with 300 μm radial-firing tip at 1.0 W (50 mJ, 20 Hz), kept stationary at a distance of 5 mm from the apex, using 5 % NaOCl and 17 % EDTA as irrigants. Incomplete cleaning of dentin surface with debris still present. Cracks are related to the dehydration process

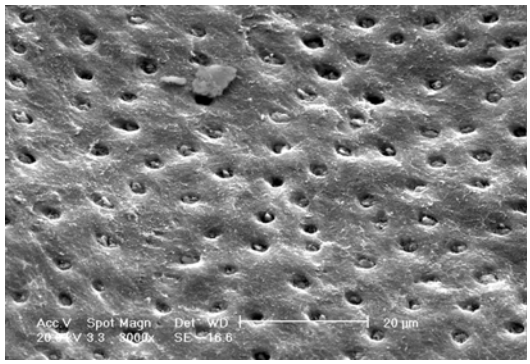

Fig. 10.14 SEM image (3000×) of the middle one-third area of the same sample of 10.12. Clean surface with presence of some debris occluding the dentin tubule orifices

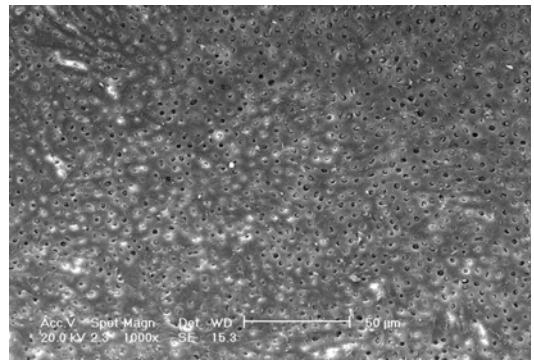

Fig. 10.16 SEM image (1000×) of the middle one-third area of the same sample 10.14. The dentin surface shows much debris occluding the dentin tubule orifices

10.9 Effects of Laser-Activated Irrigation on *Enterococcus faecalis*

Both Er:YAG and Er,Cr:YSGG have been studied for the eradication of *E. faecalis*. In their systematic review, Sadik et al. (2013) confirmed that despite the limited number of publications selected, Er,Cr:YSGG at 1 W and 1.5 W energy levels reduced *E. faecalis* count significantly [63]. In this review no studies based on LAI were taken into account. Few studies in literature investigated the bactericidal power of LAI.

Seet et al. (2012) compared the effectiveness of sonic, laser activation and syringe irrigation with 4 % NaOCl in removing 4-week-old *E. faecalis* biofilms [51]. The radial firing tip (diameter not reported) of an Er:Cr:YSGG laser was positioned inside the coronal third only (4 mm only) slowly withdrawing it back during the 5 s of activation at 0.25 W and 20 Hz after initial rinsing with NaOCl during 10 s. The procedure was repeated four times with a final exposure time to NaOCl during 60 s. Scanning electron microscopy investigation was used to determine the presence of biofilm or bacteria on the dentin

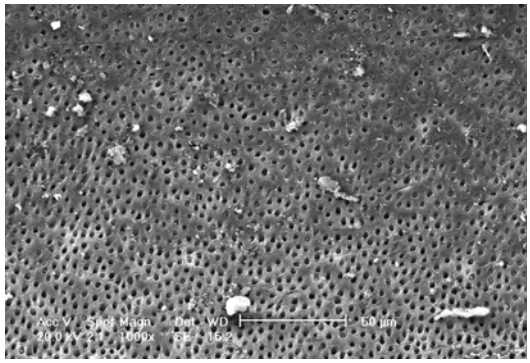

Fig. 10.17 SEM image (1000×) of the middle one-third area after mechanical instrumentation and LAI (2 cycles × 20 s) performed with an Er,Cr:YSGG laser (2780 nm) equipped with 300 µm radial-firing tip at 1.0 W (50 mJ, 20 Hz), kept stationary at a distance of 5 mm from the apex, using 5 % NaOCl and 17 % EDTA. Clean dentin surface and areas with some debris still present

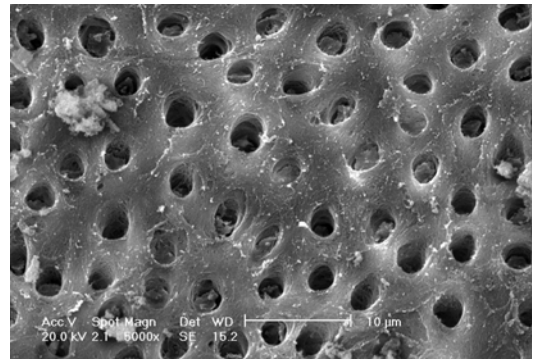

Fig. 10.18 SEM image (5000×) of the middle one-third area of the same sample of 10.16. Presence of small debris occluding the dentin tubule orifices with others well open; no thermal damage is present. The activation of NaOCl and EDTA partially removed smear layer and debris and exposed collagen fibres; insufficient shear stress from the fluids did not remove plugs from dentin orifices

surface and in the dentinal tubules. Results showed that sonic activation and syringe irrigation with NaOCl showed reduced numbers of bacterial cells on the radicular dentin, but were not effective in eliminating *E. faecalis* in the dentinal tubules. Laser activation of sodium hypochlorite resulted in clean dentine walls and undetectable levels of bacteria within dentinal tubules. Qualitatively laser activation produced the greatest overall reduction [51].

Licata et al. (2013) investigated the ability of Er,Cr:YSGG LAI with 5.25 % NaOCl and 17 % EDTA to kill *Enterococcus faecalis* in an infected tooth model. The decoronated teeth received an apical preparation of ISO#30. A 200 µm radial firing tip was positioned at the entrance of the canal orifice and kept stationary for 3 and 60 s with energy of 75 and 25 mJ. The use of laser at 75 mJ with an irradiation time of 30 and 60 s eliminated a percentage of 92.3 and 100 % of *E. faecalis* respectively. In the control group, a reduction of 92.3 % was observed, but no statistical differences, however, were observed between the four groups [53].

In the study of Bago et al. (2014), the elimination of intracanal 10-day-old *E. faecalis* biofilms was evaluated using 2.5 % NaOCl and different activation systems: LAI using Er,Cr:YSGG (1.25 W, 20 Hz, 62.5 mJ) with a 275 µm endodontic radial firing tip used during four times 5 s in a row, PUI (ISO#15 K-file, 60 s, 2 mm short of WL) and Rins-Endo (20 mL syringe and cannula (Ø: 0.45 × 12 mm), set rate 6.2 mL min^{-1}) during 60 s [64]. All three systems were equally effective, but LAI generated more negative samples.

Conclusion

At present, Er:YAG and Er,Cr:YSGG are the best suited for laser-activated irrigation. Further studies, however, are required to assess the performance of different tip shapes, i.e. flat or conical, and the influence of the tip diameter on laser activation of irrigants. In addition, due to the lack of uniformity of parameters used in the different studies (including wavelength, energy and frequency and tip diameter), confusion still remains in LAI procedures on how far the laser tip should be kept away from the apex to allow the most efficient cleaning of the root canal, taking into account the safety of the procedure. Also more studies are needed to establish the effectiveness of LAI for root canal disinfection. Nevertheless, it was demonstrated that although there was no statistically significant difference between PUI and conventional LAI, more negative samples in biofilm studies and more empty root canal grooves were seen in the majority of the LAI investigations.

References

1. Gulabivala K, Ng YL, Gilbertson M, Eames I. The fluid mechanics of root canal irrigation. Physiol Meas. 2010;31:R49–84.
2. Haapasalo M, Shen Y, Qian W, Gao Y. Irrigation in endodontics. Dent Clin North Am. 2010;54:291–312.
3. Peters OA, Schonenberger K, Laib A. Effects of four Ni-Ti preparation techniques on root canal geometry assessed by micro-computed tomography. Int Endod J. 2001;34:221–30.
4. Ricucci D, Siqueira Jr JF. Fate of the tissue in lateral canals and apical ramifications in response to pathologic conditions and treatment procedures. J Endod. 2010;36:1–15.
5. Stojicic S, Zivkovic S, Qian W, Zhang H, Haapasalo M. Tissue dissolution by sodium hypochlorite: effect of concentration, temperature, agitation, and surfactant. J Endod. 2010;36:1558–62.
6. Macedo RG, Wesselink PR, Zaccheo F, Fanali D, Van Der Sluis LW. Reaction rate of NaOCl in contact with bovine dentine: effect of activation, exposure time, concentration and pH. Int Endod J. 2010;43:1108–15.
7. de Gregorio C, Estevez R, Cisneros R, Paranjpe A, Cohenca N. Efficacy of different irrigation and activation systems on the penetration of sodium hypochlorite into simulated lateral canals and up to working length: an in vitro study. J Endod. 2010;36:1216–21.
8. De Moor R. High-power lasers in endodontics – fiber placement for laser-enhanced endodontics: in the canal or at the orifice? J LA&HA. 2014;2014:20–8.
9. De Moor R, Meire M. Laser activated irrigation. Part 2: does the position of the fiber matters? Laser. 2014;3:12. 14, 16–8.
10. DiVito EE, Colonna MP, Olivi G. The photoacoustic efficacy of an Er:YAG Laser with radial and stripped tips on root canal dentin walls: an SEM evaluation. J Laser Dent. 2011;19:156–61.
11. Peters OA, Bardsley S, Fong J, Pandher G, Divito E. Disinfection of root canals with photon-initiated photoacoustic streaming. J Endod. 2011;37:1008–12.
12. DiVito E, Peters OA, Olivi G. Effectiveness of the erbium:YAG laser and new design radial and stripped tips in removing the smear layer after root canal instrumentation. Lasers Med Sci. 2012;27:273–80.
13. DiVito E, Lloyd A. ER:YAG laser for 3-dimensional debridement of canal systems: use of photon-induced photoacoustic streaming. Dent Today. 2012;31:122,124–127.
14. Blanken JW, Verdaasdonk RM. Cavitation as a working mechanism of the Er, Cr:YSGG laser in endodontics: a visualization study. J Oral Laser Appl. 2007;7: 97–106.
15. Blanken J, De Moor RJG, Meire M, Verdaasdonk R. Laser induced explosive vapor and cavitation resulting in effective irrigation of the root canal. Part 1: a visualization study. Lasers Surg Med. 2009;41:514–9.
16. de Groot SD, Verhaagen B, Versluis M, Wu MK, Wesselink PR, van der Sluis LW. Laser-activated irrigation within root canals: cleaning efficacy and flow visualization. Int Endod J. 2009;42:1077–83.
17. Matsumoto H, Yoshimine Y, Akamine A. Visualization of irrigant flow and cavitation induced by Er:YAG laser within a root canal model. J Endod. 2011;37: 839–43.
18. Gregorcic P, Jezersek M, Mozina J. Optodynamic energy-conversion efficiency during an Er:YAG-laser-pulse delivery into a liquid through different fiber-tip geometries. J Biomed Opt. 2012;17:075006.
19. George R, Meyers IA, Walsh LJ. Laser activation of endodontic irrigants with improved conical laser fiber tips for removing smear layer in the apical third of the root canal. J Endod. 2008;34:1524–7.
20. De Moor RJ, Blanken J, Meire M, Verdaasdonk R. Laser induced explosive vapor and cavitation resulting in effective irrigation of the root canal. Part 2: evaluation of the efficacy. Lasers Surg Med. 2009;41:520–3.
21. De Moor RJ, Meire M, Goharkhay K, Moritz A, Vanobbergen J. Efficacy of ultrasonic versus laser-activated irrigation to remove artificially placed dentin debris plugs. J Endod. 2010;36:1580–3.
22. Peeters HH, Suardita K. Efficacy of smear layer removal at the root tip by using ethylenediaminetetraacetic acid and erbium, chromium: yttrium, scandium, gallium garnet laser. J Endod. 2011;37:1585–9.
23. Deleu E, Meire MA, De Moor RJ. Efficacy of laser-based irrigant activation methods in removing debris from simulated root canal irregularities. Lasers Med Sci. 2013;30:831–5.
24. Robertson CW, Williams D. Lambert absorption coefficients of water in the infrared. J Opt Soc Am. 1971; 61:1316–20.
25. Meire MA, Poelman D, De Moor RJ. Optical properties of root canal irrigants in the 300–3,000-nm wavelength region. Lasers Med Sci. 2014;29:1557–62.
26. Stock K, Hibst R, Keller U. Comparison of Er:YAG and Er:YSGG laser ablation of dental hard tissues. SPIE. 1997;3192:0277-786X/97.
27. Perhavec T, Diaci J. Comparison of Er:YAG and Er, Cr:YSGG dental lasers. J Oral Laser Appl. 2008;8: 87–94.
28. Moritz A. Oral laser application. Berlin: Quintessence Verlags-GmbH; 2006. p. 258–77.
29. Paltauf G, Schmidt-Kloiber H. Photoacoustic waves excited in liquids by fiber-transmitted laser pulses. J Acoust Soc Am. 1998;104:890–7.
30. Doukas AG, Birngruber R, Deutsch TF. Determination of the shock wave pressures generated by laser-induced breakdown in water. Laser–tissue interactions SPIE. 1990;1202:61–70.
31. Levy G, Rizoiu I, Friedman S, Lam H. Pressure waves in root canals induced by Nd: YAG laser. J Endod. 1996;22:81–4.
32. Meire MA, De Prijck K, Coenye T, Nelis HJ, De Moor RJ. Effectiveness of different laser systems to kill Enterococcus faecalis in aqueous suspension and in an infected tooth model. Int Endod J. 2009;42: 351–9.
33. Michiels R, Vergauwen TEM, Mavridou A, Meire M, De Bruyne M, De Moor RJG. Investigation of coronal

leakage of root fillings after smear layer removal with EDTA or Nd:YAG lasing through capillary flow porometry. Photomed Laser Surg. 2010;28 Suppl 2:S43–50.
34. Hmud R, Kahler WA, George R, Walsh LJ. Cavitational effects in aqueous endodontic irrigants generated by near-infrared lasers. J Endod. 2010; 36:275–8.
35. Hmud R, Kahler WA, Walsh LJ. Temperature changes accompanying near infrared diode laser endodontic treatment of wet canals. J Endod. 2010;36:908–11.
36. Benedicenti S, Cassanelli C, Signore A, Ravera G, Angiero F. Decontamination of root canals with the gallium-aluminum-arsenide laser: an in vitro study. Photomed Laser Surg. 2008;26:367–70.
37. Alfredo E, Souza-Gabriel AE, Silva SR, Sousa-Neto MD, Brugnera-Junior A, Silva-Sousa YT. Morphological alterations of radicular dentine pretreated with different irrigating solutions and irradiated with 980-nm diode laser. Microsc Res Tech. 2009;72:22–7.
38. Olivi G, Olivi M, Kaitsas V, Benedicenti S. Morphological changes after 810 nm diode laser irradiation of prepared, wet root canals: SEM investigations. Dentista Moderno. 2013:122–8.
39. Moon YM, Kim HC, Bae KS, Baek SH, Shon WJ, Lee W. Effect of laser-activated irrigation of 1320-nanometer Nd:YAG laser on sealer penetration in curved root canals. J Endod. 2012;38:531–5.
40. van Leeuwen TG, van de Veen MJ, Verdaasdonk RM, Borst C. Non contact tissue ablation by Holmium:YSGG laser pulses in blood. Lasers Surg Med. 1991;11:26–34.
41. Flotte TJ, Doukas A. Laser induced pressure effects. Laser Tissue Interactions SPIE. 1992;1646:295–300.
42. Song WD, Hong MH, Lukyanchuk B, Chong TC. Laser-induced cavitation bubbles for cleaning of solid surfaces. J Appl Phys. 2004;95:2952–6.
43. Brennen CE. Cavitation and bubble dynamics. Oxford: Oxford University Press; 1995.
44. Prosperetti A. Bubbles Phys Fluids. 2004;16: 1852–65.
45. Jiang C, Chen M-T, Gorur A, Schaudinn C, Jaramillo DE, Costerton JW, Sedghizadeh PP, Vernier PT, Gundersen MA. Nanosecond pulsed plasma dental probe. Plasma Process Polym. 2009;6:479–83.
46. Peeters HH, Mooduto L. Radiographic examination of apical extrusion of root canal irrigants during cavitation induced by Er, Cr:YSGG laser irradiation: an in vivo study. Clin Oral Investig. 2013;17:2105–12.
47. George R, Walsh LJ. Performance assessment of novel side firing safe tips for endodontic applications. J Biomed Opt. 2011;16:048004.
48. Boutsioukis C, Lambrianidis T, Kastrinakis E. Irrigant flow within a prepared root canal using various flow rates: a Computational Fluid Dynamics study. Int Endod J. 2009;42:144–55.
49. George R, Walsh LJ. Apical extrusion of root canal irrigants when using Er:YAG and Er, Cr:YSGG lasers with optical fibers: an in vitro dye study. J Endod. 2008;34:706–8.
50. George R, Walsh LJ. Laser fiber-optic modifications and their role in endodontics. J Laser Dent. 2012;20: 24–30.
51. Seet AN, Zilm PS, Gully NJ, Cathro PR. Qualitative comparison of sonic or laser energisation of 4% sodium hypochlorite on an Enterococcus faecalis biofilm grown in vitro. Aust Endod J. 2012;38:100–6.
52. Guidotti R, Merigo E, Fornaini C, Rocca JP, Medioni E, Vescovi P. Er:YAG 2,940-nm laser fiber in endodontic treatment: a help in removing smear layer. Lasers Med Sci. 2014;29:69–75.
53. Licata ME, Albanese A, Campisi G, Geraci DM, Russo R, Gallina G. Effectiveness of a new method of disinfecting the root canal, using Er, Cr:YSGG laser to kill Enterococcus faecalis in an infected tooth model. Lasers Med Sci. 2015;30:707–12.
54. Martin SA. Conventional endodontic therapy of upper central incisor combined with cyst decompression: a case report. J Endod. 2007;33:753–7.
55. Peeters HH, De Moor RJ. Measurement of pressure changes during laser-activated irrigant by an erbium, chromium: yttrium, scandium, gallium, garnet laser. Lasers Med Sci. 2015;30(5):1449–55.
56. Guyton AC, Hall JE. Guyton & Hall physiology review. Philadelphia: Elsevier Saunders; 2006.
57. Ram Z. Effectiveness of root canal irrigation. Oral Surg Oral Med Oral Pathol. 1977;44:306–12.
58. George R, Walsh LJ. Thermal effects from modified endodontic laser tips used in the apical third of root canals with erbium-doped yttrium aluminium garnet and erbium, chromium-doped yttrium scandium gallium garnet lasers. Photomed Laser Surg. 2010;28: 161–5.
59. Peeters HH, Mooduto L. Measurement of temperature changes during cavitation generated by an erbium, chromium: Yttrium, scandium, gallium garnet laser. OJST. 2012;2:286–91.
60. Kuhn K, Rudolph H, Luthardt RG, Stock K, Diebolder R, Hibst R. Er:YAG laser activation of sodium hypochlorite for root canal soft tissue dissolution. Lasers Surg Med. 2013;45:339–44.
61. Ahmad M, Pitt Ford TR, Crum LA, Walton AJ. Ultrasonic debridement of root canals: acoustic cavitation and its relevance. J Endod. 1988;14:486–93.
62. Bolhari B, Ehsani S, Etemadi A, Shafaq M, Nosrat A. Efficacy of Er, Cr:YSGG laser in removing smear layer and debris with two different output powers. Photomed Laser Surg. 2014;32:527–32.
63. Sadık B, Arıkan S, Beldüz N, Yaşa Y, Karasoy D, Cehreli M. Effects of laser treatment on endodontic pathogen Enterococcus faecalis: a systematic review. Photomed Laser Surg. 2013;31:192–200.
64. Bago Jurič I, Plečko V, Anić I. Antimicrobial efficacy of Er, Cr:YSGG laser-activated irrigation compared with passive ultrasonic irrigation and RinsEndo(®) against intracanal Enterococcus faecalis. Photomed Laser Surg. 2014;32:600–5.

11 Advanced Laser-Activated Irrigation: PIPS™ Technique and Clinical Protocols

Giovanni Olivi and Enrico E. DiVito

Abstract

PIPS™ is an advanced laser-activated irrigation process by which photons of light are emitted in very low energy levels and with short microsecond pulse duration. PIPS™ utilizes a unique tapered and stripped tip design that allows for lateral dispersion and propagation of the generated shock wave in liquids at subablative levels, via photoacoustic and photomechanical events avoiding the possibility of thermal damage and allowing for effective three-dimensional streaming of fluids when the correct specific parameters and protocols are used. By virtue of lower energy and high peak power, unique tip design, and its positioning far from the apex, PIPS™ provides safe and effective activation for exchange of irrigants. The tip is kept stationary in the coronal aspect of the access preparation only thus offering effective irrigation with a minimally invasive instrumentation optimizing the conservation of the dentin structure and thus avoiding the possibility of laser thermal damage to dentin walls. The use of NaOCl and EDTA along the correct protocol improves the cleaning and decontaminating effect for root canals when compared to conventional methods.

11.1 Introduction

PIPS is an acronym first described by Enrico DiVito (2006) and stands for photon-induced photoacoustic streaming.

It is a patented and trademarked term that covers both PIPS™ tip design and protocols.

PIPS™ is an advanced laser-activated irrigation process by which photons of light are emitted at very low energy levels and with short microsecond pulse duration. Unlike other forms

G. Olivi, MD, DDS (✉)
InLaser Rome – Advanced Center for Esthetic and Laser Dentistry, Rome, Italy
e-mail: olivilaser@gmail.com

E.E. DiVito, DDS, PC
Arizona Center for Laser Dentistry,
7900 E. Thompson Peak Parkway #101,
Scottsdale, AZ 85255, USA

G. Olivi et al. (eds.), *Lasers in Endodontics: Scientific Background and Clinical Applications*,
DOI 10.1007/978-3-319-19327-4_11

Fig. 11.1 Upper first and second premolars showing conservative shaping and obturation after PIPS

Fig. 11.2 Lower first molar showing minimal shaping of four canals and obturation post-PIPS

of laser-activated irrigation, PIPS™ utilizes a unique tapered and stripped tip design that allows for lateral dispersion and propagation of the generated shock wave in liquids at subablative levels, via photoacoustic and photomechanical events. This avoids the possibility of thermal damage and allows for effective three-dimensional streaming when the specific parameters and protocols are used.

The term PIPS is often improperly used to describe the use of generic tips to activate the intracanal fluids without using the specific PIPS™ tip, laser, and settings and also without following the science behind PIPS™: an advanced protocol of laser activation of the irrigants.

The PIPS™ protocol is validated by several in vitro studies and supported by a strong body of both published and non-published experiments and data. PIPS™ has been confirmed by thousands of clinical trials and differs from the other investigated LAI techniques in the following way:

- It uses a specific and unique tip design.
- It uses subablative or minimally ablative energy.
- It is delivered via a very short pulse duration thus producing a very high peak power.
- It requires an easy positioning of the tip in the pulp chamber only and not into the canal.
- It advocates minimal root canal and apical preparation.

By virtue of lower energy and high peak power, unique tip design, and its positioning far from the apex, PIPS™ provides safe and effective activation for exchange of irrigants when the proper protocol is followed.

Unlike other LAI techniques, PIPS™ technique is based on new “minimally invasive” or “biomimetic” concept that minimizes the use of intracanal instrumentation without compromising the ability for irrigation to effectively reach all aspects of the root canal system (Figs. 11.1 and 11.2).

This optimizes the conservation of dentin structure and avoids the possibility of laser thermal damage while creating superior cleaning and decontamination through more copious and effective exchange of irrigation activated by PIPS™. The need for enlarging and shaping of the canal system to remove infected dentin and to assure sufficient space for an appropriate flushing of irrigants, as suggested in the modern endodontics [1], is no longer necessary.

11.2 PIPS in Brief

In Chap. 10, the different LAI techniques investigated in the last 8 years were reviewed. It is evident that all the studies published in the peer-reviewed literature lack uniformity in the materials and methods used. However all the studies resulted in improved smear layer removal and bacterial reduction when compared to the other conventional irrigation techniques [2–10].

After several preliminary investigations, testing the more appropriate laser wavelength and settings, the first PIPS study on root canal cleaning dates back to 2010 (online since 2010, published in 2012) and was performed using an Er:YAG laser (Fidelis III, Fotona; Ljubljana-SLOVENIA) at 20 mJ and 15 Hz to activate the irrigant EDTA for smear layer removal [11]. Later, Peters et al. (2011) published the first PIPS study on root canal disinfection, performed with an older model of Er:YAG laser (Fidelis, Fotona; Ljubljana-SLOVENIA) at 50 mJ, 10 Hz, to activate the intracanal irrigant NaOCl [12].

In review of the published studies on PIPS, the more obvious and important values are the lower laser settings and less invasive root canal preparations required for treatment. Also of significant merit is the safe and less technique-sensitive positioning of the PIPS tip not in the canal but rather in the coronal pulp chamber only [11–15].

Photon-induced photoacoustic streaming (PIPS™) uses a cutting-edge erbium:YAG laser technology (2940 nm) at high peak power to pulse extremely low energy levels of laser light to generate photoacoustic shock waves into liquid-filled root canals. PIPS actively pumps the fluid three-dimensionally into the main canal, lateral canals, fins, anastomosis, and dentin tubules to the apex (Fig. 11.3). With the irrigant continuously delivered in the pulp chamber during PIPS activation, the resultant shock wave travels three-dimensionally in all directions and effectively debrides and removes both vital and necrotic tissue remnants (Fig. 11.4a–c). Through this laser-activated turbulent flow phenomenon, clinicians following the PIPS protocol are not required to place the tip into the canals, but the tip is held stationary in the coronal aspect of the access preparation only (Fig. 11.5). This means that the need to enlarge and remove more dentin structure normally required to deliver a standard

Fig. 11.3 Er:YAG and Nd:YAG LightWalker AT dual wavelength laser by Fotona (Ljubljana-Slovenia)

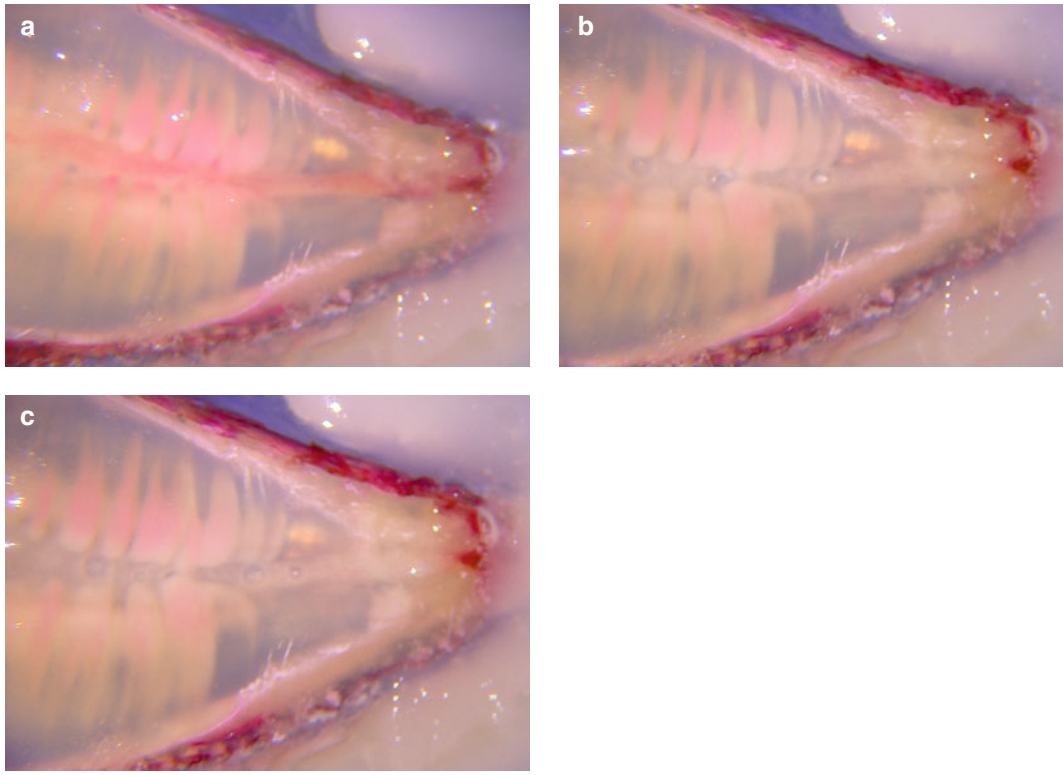

Fig. 11.4 (**a**) Cross section of single rooted, noninstrumented clarified tooth specially prepared and stained with pulp tissue in canal; (**b**) PIPS action shows streaming of irrigant in the canal and around nerve tissue; (**c**) post-PIPS application shows removal of nerve tissue from canal space with no files used (Images courtesy of Dr. Giovanni Olivi in cooperation with Drs. Augusto Malentacca and Vasilios Kaitsas, Rome, Italy)

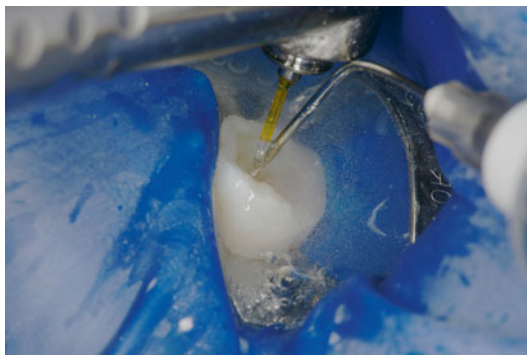

Fig. 11.5 Proper positioning of the PIPS tip held stationary in the chamber of the access opening only. Note the syringe supplying continuous replenishment of irrigation

needle, a negative pressure system, or a laser fiber is eliminated, and the smaller and more delicate anatomy commonly seen in the apical one-third is preserved (Figs. 11.6 and 11.7). Unlike other laser-activated irrigation techniques, PIPS is not a thermal event but rather a subablative one. Due to the very short pulse duration and specific PIPS design, the extremely low level of energy required to activate the irrigants is below the threshold of ablation for dentin [16, 17] (see energy threshold Sect. 4.6.1). Ledging and thermal effects that have plagued the widespread use of other conventional laser systems are completely avoided when the correct settings and PIPS™ protocol techniques are used [13, 18–20] (Figs. 11.8, 11.9, 11.10, and 11.11) (see also Figs. 5.34, 5.35, 5.36, and 5.37 in Chap. 5 and Figs. 10.3, 10.4, and 10.5 in Chap. 10).

11.3 Mechanism of PIPS

To date there are several studies investigating the fluid dynamics of laser-activated irrigation using both erbium chromium:YSGG laser [21,

Fig. 11.6 Despite the minimal instrumentation, PIPS protocol allowed the obturation of multiple portals of exit in a lower second bicuspid (Courtesy of Dr. Mark Colonna Whitefish, Montana, USA)

Fig. 11.7 Lower first molar showing minimally prepared canal shapes with adequate obturation in the apical area post-PIPS (Courtesy of Dr. Mark Colonna Whitefish, Montana, USA)

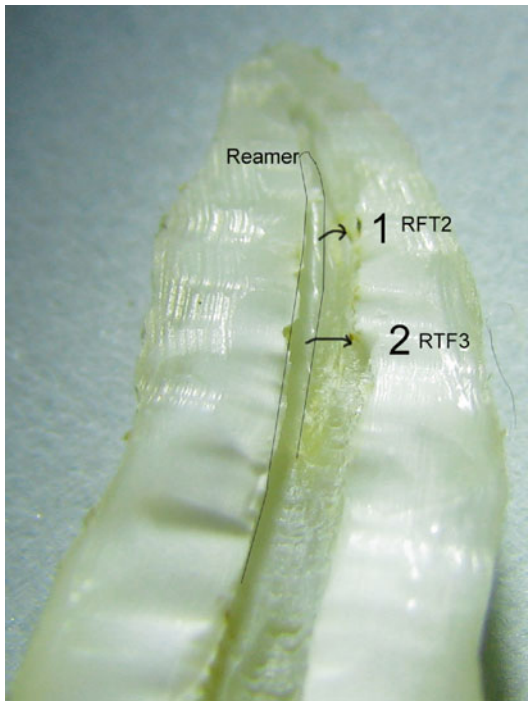

Fig. 11.8 Ledging and thermal damage on root canal surface as a result of Er,Cr:YSGG laser radial tip placed into the canal as advocated with conventional protocol (Courtesy of Dr. Graeme Milicich Hamilton, New Zealand and Dr. Enrico DiVito, Scottsdale, Arizona, USA)

Fig. 11.9 Dentin surface with thermal damage and charring seen after Er,Cr:YSGG laser radial firing tip was placed in the canal and withdrawn as per protocol (Courtesy of Dr. Graeme Milicich Hamilton, New Zealand and Dr. Enrico DiVito, Scottsdale, Arizona, USA)

Fig. 11.10 Clean canal surface seen after the correct PIPS™ protocol is used. No signs of thermal damage (Courtesy of Dr. Graeme Milicich Hamilton, New Zealand, and Dr. Enrico DiVito, Scottsdale, Arizona, USA)

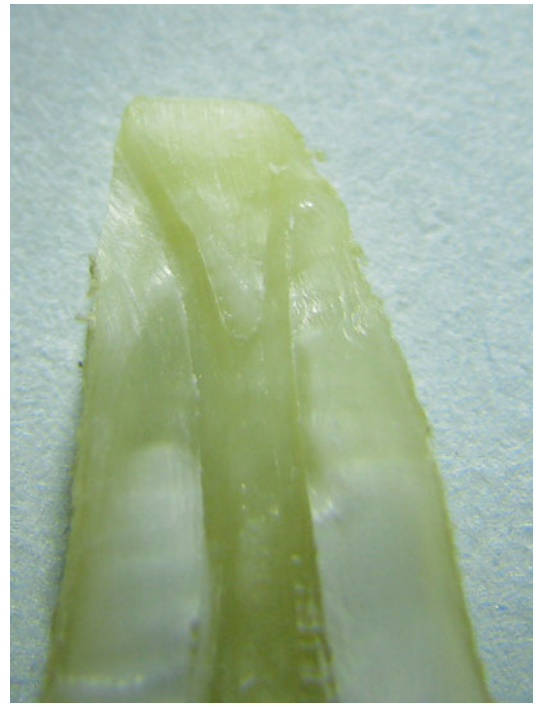

Fig. 11.11 Clean delta at the apical one-third of root canal seen after PIPS. Thermal damage is avoided because PIPS does not require that its tip be placed into the canal preparation at all but rather stationary in the coronal pulp chamber only (Courtesy of Dr. Graeme Milicich Hamilton, New Zealand and Dr. Enrico DiVito, Scottsdale, Arizona, USA)

22] and erbium:YAG lasers [4, 23]. To understand the working mechanism of PIPS, high-speed visualization methods to capture images with microsecond resolution have been performed. Also PIPS fluid dynamic studies have verified the effectiveness of PIPS (unpublished data by Drs. Peters, Jaramillo and Koch (2015), USA).

Because of the high absorption rate of the erbium laser in water, the bubble formation and its corresponding collapse create a strong pressure wave. Due to the newer and different technologies used, the shock wave is generated at lower energy levels reducing the undesirable thermal effects commonly seen with other laser systems.

11.4 Bubbles: Cavitation and Shock Wave

According to reports by other authors described in Chap. 10, when erbium:YAG laser energy is absorbed in water, an instantaneous super heating of the irrigant to the boiling point of water (100 °C) generates an initial vapor bubble expansion at the end of the tip [4, 21–24]. During expansion the bubble passes over the equilibrium state, and at its maximum volume the internal pressure is lower than the pressure in the surrounding liquid forcing the bubble to collapse. During the collapse phase a portion of energy is converted into acoustic energy with emission of acoustic shock waves [24] (Fig. 11.12).

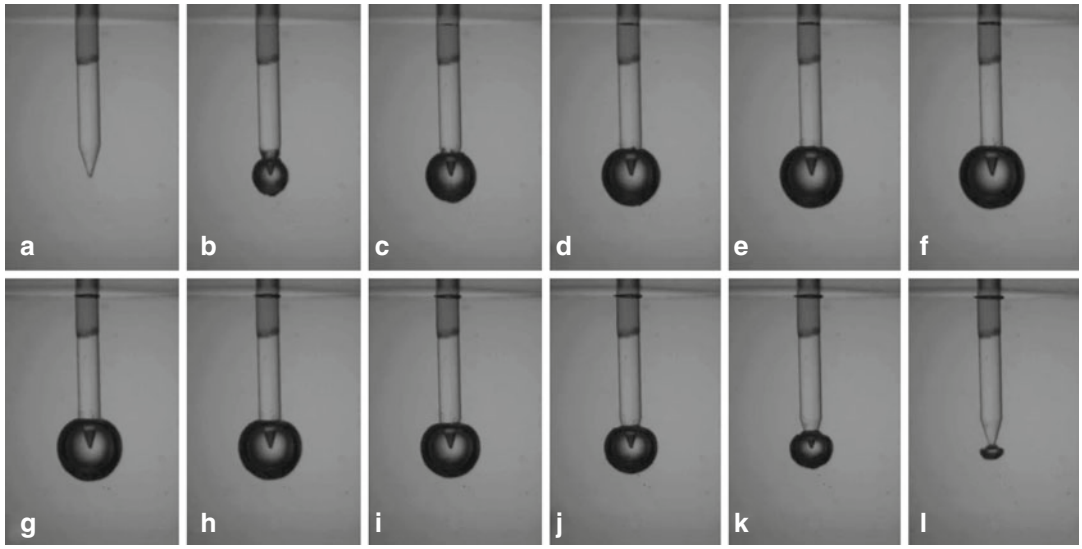

Fig. 11.12 Sequential still frame shots showing the bubble cycle with increase (**a** PIPS tip before activation, expansion from **b**–**g**) and subsequent decrease (collapse from **h**–**n**) of the bubble resulting in primary and secondary cavitation, seen from the PIPS tip during fluid activation at 20 mJ and 50 μs pulse duration (Courtesy Drs. L. van der Sluis, R. Macedo, B. Verhaaghen, M. Versluis, University of Twente, the Netherlands in cooperation with G.Olivi Rome, Italy)

11.5 Fluid Dynamics Study of PIPS

One of the main problems in endodontics is the fluid dynamics of the irrigants in the confined canal space. Vapor lock makes the deep penetration of the irrigant more difficult because of the absence of turbulence over much of the canal volume when using conventional irrigant devices. Accordingly, a preliminary study was performed in order to evaluate the fluid movement, distribution of turbulence, and the flow velocity inside experimental models comparing PIPS with passive ultrasonic (PUI) activation of fluids. Measurements were obtained using microscopic digital particle image velocimetry (micro DPIV). Under similar experimental conditions, the distribution and magnitude of the irrigant flow velocity stimulated by photon-initiated photoacoustic streaming device (PIPS; LightWalker, Fotona) and by a standard ultrasonic device (Suprasson P5 Booster with a 20 mm Irrisafe file tip) were gathered. A digital camera acquired images directly to the computer memory at 30 frames per second, throughout a 5s duration, for a total of 150 images for each experiment. A customized cylindrical Pyrex glass tube (5.8 mm diameter and 25 mm long), with a flat sealed bottom, filled with distilled water, was used to simulate a tooth model. The water was mixed with 5 mg/ml, silver-coated hollow glass spheres, 10 μm in diameter (S-HGS, Dantec Dynamics, Tonsbakken, Denmark), as tracing particles inside the liquid. The laser and the ultrasonic handpieces were supported by a micromanipulator to allow fine-tuning of the handpiece-tip-file with respect to the location of the tooth model. The PIPS tip was submerged 4 mm below the free water surface, while the ultrasonic file was submerged 8 mm below the free water surface. The measurements were performed on the plane of the central axis of the test glass tube, at four different locations under the PIPS tip. The first measurement area was located directly under the tip, with subsequent measurements being performed at 5, 10, and 15 mm below the tip. The Er:YAG laser was set to pulse at 15 Hz with 20 mJ pulses. The ultrasonic device was set at 50 % of scale. The measurements for the ultrasonic probe were performed in a similar manner to that of the PIPS with the tip of the ultrasonic file being just out of and above the measurement area. In the case of

the ultrasonic, upon descending the measurement area 5 mm from its tip, the velocity diminished fairly quickly, and for this reason additional measurements were not taken at further distance from the probe. The measurement area locations are shown in Fig. 11.13. Data acquisition commenced 2 s before the activation of the tip.

11.5.1 Qualitative Observations

After 2–3 s of PIPS activation, many particles that had settled to the bottom of the test vial were resuspended and observed to be in relatively vigorous motion globally. The ultrasonic device on the other hand was visibly less effective during the 5s of the experiment and even after 20–30 s of continuous application. No substantial global motion was observed.

In the PIPS tests, the backlit videos showed an oscillating flow with a predominantly vertical velocity component. The fluid in the entire glass tube was in motion.

In the ultrasonic tests, a decrease of the velocity fluctuations was observed. The flow did not exhibit strong temporal fluctuations, and toward the bottom of the glass tube, motion was barely perceptible.

11.5.2 Quantitative Results

Test results, using digital particle image velocimetry (DPIV), showed PIPS with a 20× magnitude of difference in flow rate when compared to ultrasonic. The amplitude of the temporal oscillation was significantly higher for the PIPS experiments, corresponding to much larger flow accelerations.

Of significant finding was the remarkable fluid movement measured distant from the PIPS tip (at 5, 10, and 15 mm) when compared to the lack or nearly no movement measured much past 1 mm from the ultrasonic tip. The clinical significance of this finding is the benefit to which clinicians can effectively irrigate, stream, and improve exchange of fluids throughout the entire canal systems without the need to create larger canal spaces and remove more tooth structure as seen with current preparation and shaping techniques described in the literature (Fig. 11.13).

Another preliminary study utilized glass models as an artificial root canal for visualization of the PIPS phenomenon. Recordings with a high-speed imaging technique allowed visualization of the explosive vapor bubbles. The sequence of frames taken of the PIPS tip activated in water represented sequential frames taken at 50,000 frames per second. Given that the width of the optical probe was 600 μm, calculations for the expansion velocity of the bubble were determined. The bubble radius initially increased quite rapidly then slowed down as the bubble grows, due to the increased volume as a function of radius. The fiber width was 40 pixels corresponding to 600 μm=>15 μm per pixel. The bubble expanded from zero to a radius of 35 pixels in between the first two frames corresponding to a velocity of 26.5 m/s.

After the initial expansion the bubble then expanded more slowly, and between the second and third frame, the expansion velocity is 9.75 m/s. The expansion slowed to zero then reversed. In the final collapse between the last two frames, the inward velocity was again 26.5 m/s (see Fig. 11.12).

11.6 Parameters that Influence the Bubble Formation

11.6.1 Effect of Energy and PIPS Tip Diameter and Design

As reported in Chap. 10, Blanken et al. (2009) [21, 22] and deGroot et al. (2009) [4] observed how the size and the life cycle of the bubble depend on the energy applied and the tip used. A spherical bubble develops when a PIPS tip is used (see Fig. 11.14). This finding is consistent from other authors that refer to conical tips [23, 24]. The authors have unpublished data showing that:

- The higher the energies used, the greater the size of the bubbles.
- Also observed was the longer life cycle of the radial and stripped PIPS tip when compared to the flat or conical tip alone.
- If energy settings are kept equal, the size of the bubbles measured is greater for the larger diameter tips (Fig. 11.14).

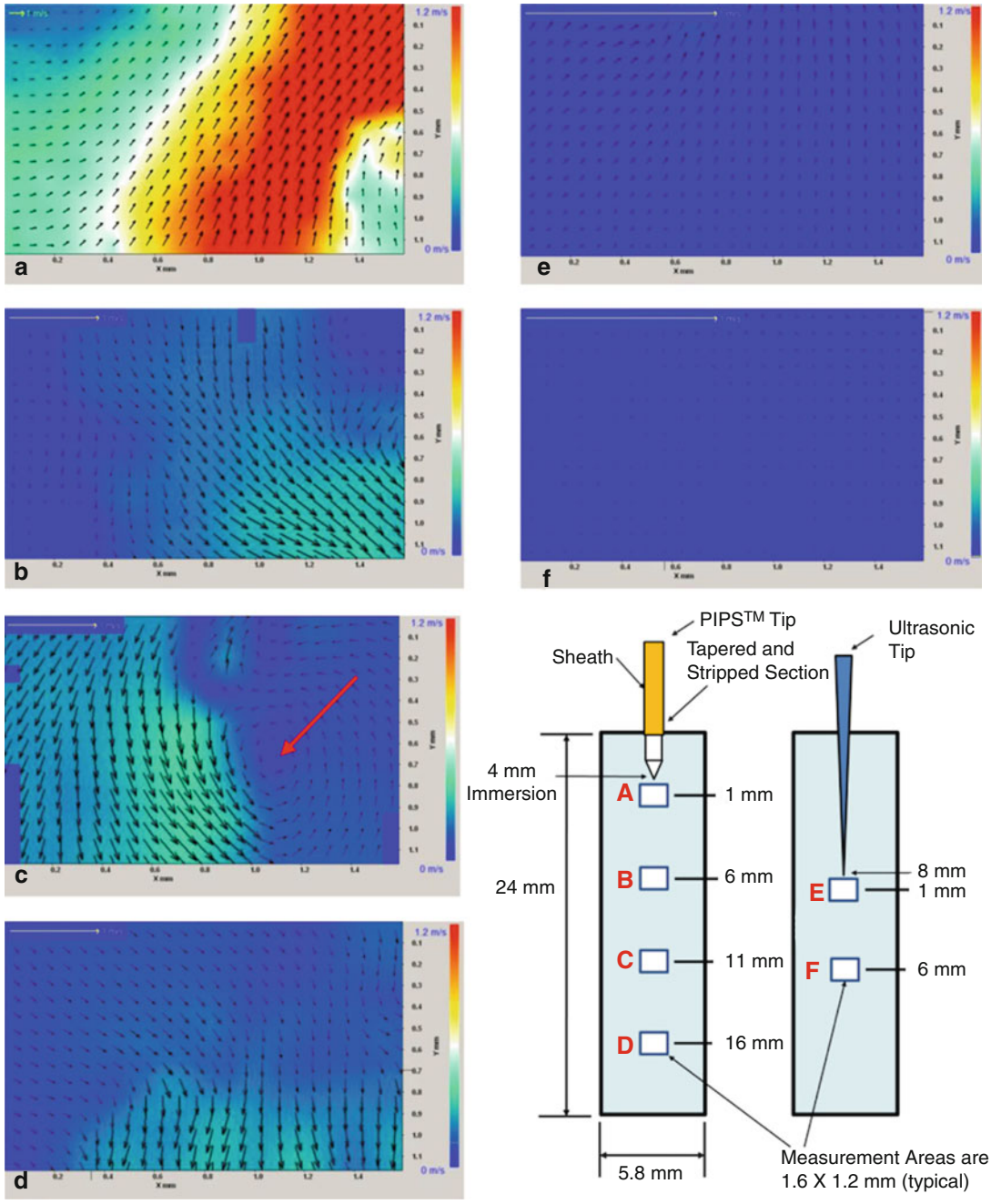

Fig. 11.13 Colored charting of fluid dynamic flow rates comparing PIPS to ultrasonics. Note the increased degree of movement with PIPS tip both near and far from the tip end position in (**a**–**d**) as compared to ultrasonic (**e**, **f**). Near tip areas of (**a**) and (**e**) show PIPS average velocities being up to 20× greater and distant areas of (**d, f**) show PIPS being about 10× greater than the average velocity of ultrasonic. Instantaneous velocity fields corresponding to the different measurement areas (**a**–**f**); the *color* represents the magnitude of the velocity vectors as indicated by the scale at *right*. Note the change of scale for the *yellow* 1 m/s reference *arrow* in the *upper left* corner of each panel. Panel **e** shows instantaneous velocity fields corresponding to the measurement directly under the ultrasonic tip and directly under the probe tip, corresponding to the initial spike in velocity that follows the activation of the device. Here the average velocity is 0.036 m/s, which is 20 times less than that measured for the PIPS data immediately under the probe tip as seen in panel **a**. Panel **f** corresponds to measurements 5.5 mm below the ultrasonic tip, the velocities are measured at less than 0.01 m/s showing significant decay from those of measurement area (**e**) (Courtesy of Dr. Ove Peters San Francisco, California, Dr. David Jaramillo USC, California in cooperation with and Dr. Enrico DiVito Scottsdale, Arizona)

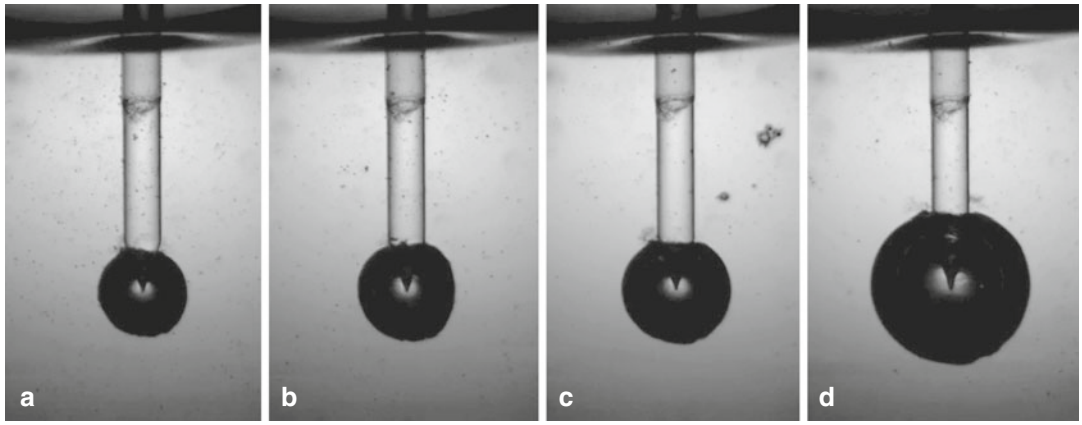

Fig. 11.14 Still frame shots showing the different bubble size resulted from different energy pulse used with PIPS at 50 µs: (**a**) 10 mJ, (**b**) 15 mJ, (**c**) 20 mJ, and (**d**) 80 mJ. The size of the bubble increases with the energy/pulse (Courtesy Drs. L. van der Sluis, R. Macedo, B. Verhaaghen, M. Versluis, University of Twente, the Netherlands in cooperation with G. Olivi Rome, Italy)

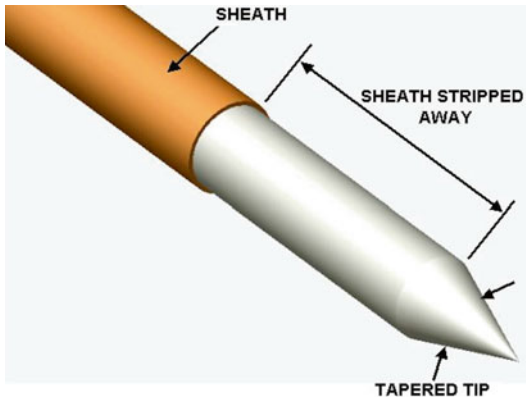

Fig. 11.15 Diagrammatic representation of the PIPS™ tapered and striped tip

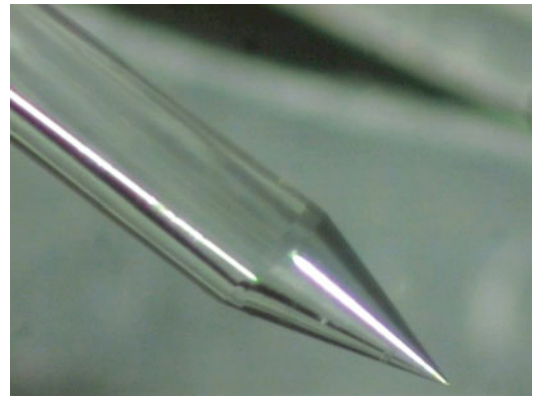

Fig. 11.16 Actual close-up magnification of the tapered and stripped tip. Look at the extreme refinement and accuracy of the manufactured tip at only 600 µm diameter

As already reported, this finding is opposite to the concept of fluence in laser physics where for the same energy the fluence increases with smaller diameter of the fiber.

Today the use of 20 mJ is considered the standard setting for the PIPS technique in endodontics together with a 600 µm, 9 mm long tip (Figs. 11.15 and 11.16). The energy can be reduced to 15, 10, or even 5 mJ for more control in activation of the irrigant such as in the case of roots with opened apices or reduced coronal access chamber size (Fig. 11.17a–d).

The radial and stripped PIPS tip emits less energy at the front of the tip, with the 4 mm stripped part improving the lateral distribution of the energy. Consecutive three-dimensional pressure waves inside the water follow the bubble implosion especially when the energy is

emitted through a very short pulse duration (50 μs). The overlapping laser impulses occurring at 15 Hz generate pressure waves that rapidly travel (shock waves) in the intracanal fluids. These shock waves create rapid fluid motion and turbulence three-dimensionally and have been demonstrated to improve both smear layer and biofilm removal [25].

The larger diameter, shorter length tip, increases the surface of interaction of the laser energy with the surrounding fluid improving the efficiency of the procedure especially for the posterior teeth given the limited intra-occlusal space (Fig. 11.18). Larger tips have also been demonstrated to be more robust and durable and as such reusable for many treatments. Thinner tips can be useful in cases of small access cavities for lower incisors and upper lateral incisors (Fig. 11.19).

11.6.2 Effect of Pulse Duration

Another fundamental parameter that modulates the efficacy of PIPS activation of intracanal fluids

Fig. 11.17 (**a**) The current recommended PIPS settings of 20 mJ, 15 Hz, in SSP mode (50 μ) results in an average power of 0.30 W (Peak Power = 400 W). The air-water spray is off; (**b**–**d**) the Fotona LightWalker model dashboard showing the energy settings to be lowered from 15 mJ, 0.2 W to 10 mJ, 0.15 W and to 5 mJ, 0.07 W, all at 50μs pulse duration (Peak Power 300 W, 200 W and 100 W respectively)

Fig. 11.18 In vivo micrograph shows the correct positioning of the PIPS tip and of the irrigation needle during PIPS: note the bubble formation around the stripped part of the tip

Fig. 11.19 PIPS™ tips: 9 mm long, 600 μm diameter tip (*left*) and 12 mm long, 400 μm diameter tip (*right*)

is the duration of each laser pulse. Experiments show that the opto-dynamic energy conversion efficiency of erbium lasers, defined as the ratio between the released acoustic energy and the energy of the laser pulse, increases rapidly with decreasing pulse duration of T_p approximately as $1/T_p^{3/2}$ [26]. Moreover the efficiency is approximately three times larger when a conical PIPS™ tip is used instead of a standard flat tip. The most current and technologically cutting-edge erbium:YAG laser available (LightWalker, Fotona, Slovenia) has the shortest laser pulse duration available for use with the PIPS tip. As a result, unlike other laser systems used for LAI, the very short pulse duration used with PIPS allows for very high peak powers at very low energy settings (see peak power Sect. 4.6.4). The rapid vapor bubble expansion results in strong acoustic transient waveforms during the subsequent bubble collapse oscillations. The possibility to modulate the peak power changing the pulse duration from 50 to 100 μs, as well as reducing the energy in millijoules, allows for another way to control the agitation and activation of the irrigants. For example, a reduction of the laser pulse duration from 100 to 50 μs results in a threefold increase in the opto-dynamic efficiency, meaning that three times less laser energy is required to achieve the same effect with the shorter pulse duration. This is very important if we consider the limited space where the laser-irrigant-dentin interaction takes place.

The triad of "tip design, low energy, and short pulse duration" is the key of the effectiveness and efficiency of the PIPS technique.

11.7 Conditions that Influence PIPS Efficiency and Safety

In addition to the factors already reported that influence the efficacy and efficiency of laser activation of the irrigants (pulse energy, tip diameter, design, and pulse duration), can also be the wavelength used, the pulse frequency, the continuous or intermittent irrigation, the location of different tip positions, as well as the size of apical preparation and the root canal shaping can also affect the efficiency and safety of the protocol used.

11.7.1 Effect of Different Wavelengths

Early investigations were started using the Er,Cr:YSGG wavelength (2780 nm). PIPS today utilizes the Er:YAG laser due to its higher efficiency and selective interaction with water. It is important to note that a laser energy threshold exists below which no acoustic transients are generated. Since the laser energy threshold depends inversely on the absorption coefficient [16, 17], laser wavelengths with high absorption coefficients in the irrigant are more suitable for laser activation.

The Er:YAG wavelength (2940 nm) has an advantage since it has the highest absorption coefficient for water and thus exhibits lowest threshold of energy for laser activation. For example, the laser energy thresholds for Er,Cr:YSGG (2780 nm), Nd:YAP (1340 nm), and Nd:YAG (1064 nm) laser wavelengths are, respectively, approximately 3×, 1000×, and 10,000× higher as compared to that of erbium:YAG (see Fig. 10.1 in Chap. 10).

Consequently wavelengths that demonstrate lower absorption properties in water require more energy to produce similar cavitation effects [27]. The longer pulse duration of the Er,Cr:YSGG laser also affects both quality and temperature rise on the dentin surface. As already reported, the use of parameters that can create good agitation in water, 50 or 75 mJ for the Er,Cr:YSGG laser, also creates thermal events to the root canal surface when the tip is positioned inside the root canal by virtue that the energy levels are in the ablative range of dentin [16, 17] and depletion of irrigant occurs (see Figs. 10.8, 10.9, 10.10, and 10.11 and also Figs. 5.34, 5.35, 5.36, and 5.37 in Chap. 5 and Figs. 10.3, 10.4 and 10.5 in Chap. 10).

11.7.2 Effect of Pulse Frequency

Studies from the authors demonstrated 15 Hz (or pps) as the preferred repetition rate to assure an efficient activation and recycling effect of the liquid in root canal model. Measurements using the standard protocol of 30 s cycling during PIPS laser activation yielded turnover of irrigants some 15×. Also noted was the effective removal of vapor lock often seen when using conventional manual and ultrasonic irrigation techniques. Lower repetition rate resulted in less efficacious exchange and greater splashing and dispersion of liquids out of the pulp chamber.

11.7.3 Effect of Continuous or Intermittent Irrigation

The presence of liquid in the canal system during the laser activation is also important. It has been suggested by several authors that intermittent irrigant flow within a limited time (5s) be used instead of the continuing flowing technique (see Chap. 3). The rest phase allows sodium hypochlorite to react and the following phase to replace the consumed solution with fresh active solution.

PIPS technique requires continuous flowing of the irrigants for 30s, not only to activate the solutions but also to promote, via the shock wave, a cleaning action of the dentin surface. After a longer agitating and activating phase, a rest time (rest phase) is necessary for the reaction rate of the solutions [28]. Effectively, if short time and intermittent irrigation (5s) does not maintain continuous presence of liquid during laser activation and if the tip is positioned incorrectly inside the canal and/or the energy applied is high, the fast consumption of the irrigant inside the apical and middle one-third of the canal produces depletion of the liquid in the apical portion. This leads to dry interaction on the dentin and consequently thermal damage from ineffective hydration, jeopardizing the results of the PIPS technique as reported in a recent study in which constant irrigant was not maintained [29]. The two steps of continuous agitation/activation and rest phase are fundamental for successful irrigation when using the PIPS technique. Following the proper PIPS protocol is critical for optimal results (Figs. 11.20, 11.21, 11.22, and 11.23).

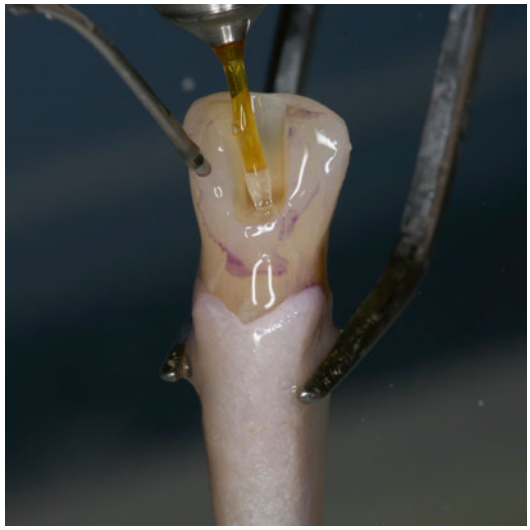

Fig. 11.20 The 600 µm PIPS tip is held stationary in the coronal access opening only and not into the canal itself

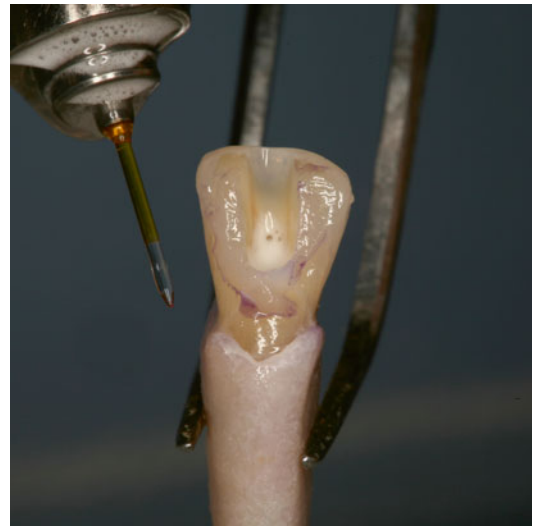

Fig. 11.21 During the required "resting phase" of 30s, a high consumption of available chlorine is seen as effervescence

Fig. 11.22 In vivo micrograph of lower first molar showing correct positioning of irrigation and PIPS tip for laser-activated irrigation: note the 27G needle resting to side of handpiece head

Fig. 11.23 Release of chlorine during the 30 s rest phase after PIPS laser activation shows foaming action

11.7.4 Effect of Tip Position in the Pulp Chamber

Comparing data from PIPS studies [11–15] with those from LAI (Table 10.2), it is evident that confusion still remains in LAI procedures on how far the laser tip should be kept away from the apex to allow efficient and safe cleaning and disinfection of the root canal.

Many disadvantages are related to the position of the tip inside the canal:

- Curved or complex anatomy may be problematic for negotiation by a laser fiber tip, as well as needle or ultrasonic files or negative pressure probes (Fig. 11.24).
- Larger and more invasive preparations are required to create space for the 300 or 400 µm fibers in the apical one-third portion of the canal (Fig. 11.25).
- When a flat or conical laser tip is positioned close to the apex (1–5 mm), keeping it stationary or moving it up and down during LAI procedures [2–8], irrigant extrusion can result at the apical terminus as described [23, 30] (Fig. 11.26).
- When a tip is positioned in the apical or middle one-third of the canal, the tip itself

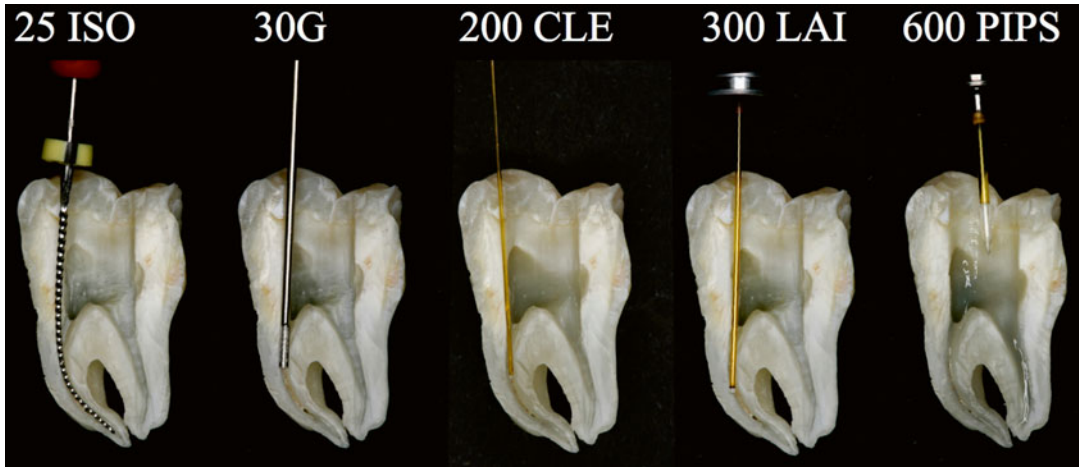

Fig. 11.24 Split section of lower molar with three canals: A steel K-file ISO#25 positioned 1 mm shorter of the apical terminus of curved mesial canal; the flexibility of the instrument follows the root canal anatomy. A 30G endodontic needle cannot reach the working length resulting in ineffective irrigation. A 200 μm near infrared laser fiber (conventional laser irradiation) is not able to follow the curvature of the shaped root canal; as a consequence the tip enters in contact with dentinal walls along the curvature, producing hot spots; also the wanted decontamination effect fails. A 300 μm tip (laser-activated irrigation) is positioned 5 mm shorter of the apical terminus: the tip itself creates an obstacle to the flow of irrigant from the tooth entrance, and a possible depletion of irrigant may occur in the apical part resulting with ineffective irrigation and thermal hot spots. PIPS is easy, safe, and effective, far from the apex, and does not require that it be placed in the canals. It allows for multiple canal irrigation at same time regardless of the shape or anatomy

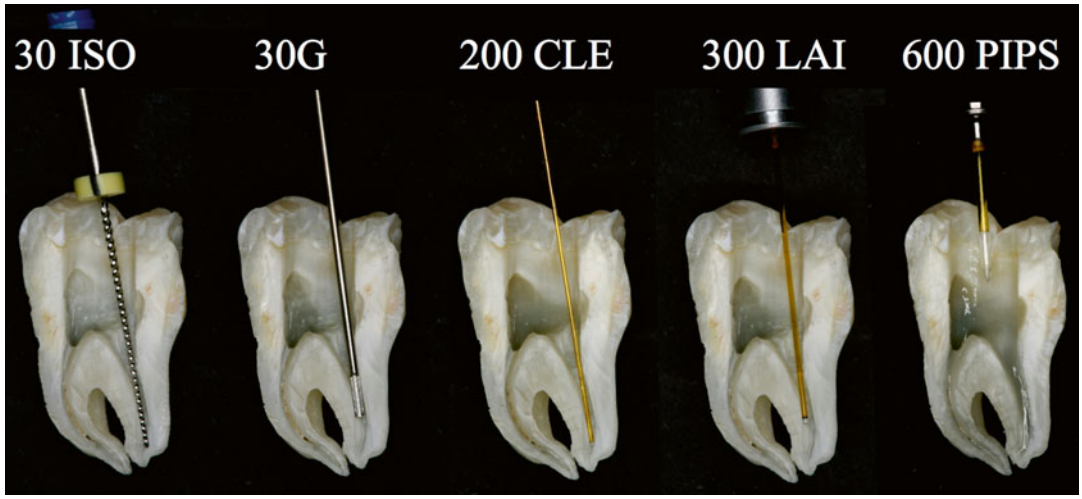

Fig. 11.25 Split section of lower molar with three canals: a steel K-file ISO#30 positioned 1 mm shorter of the apical terminus of straight distal canal. Also here the 30G endodontic needle cannot reach the working length with ineffective irrigation. Also the 200 μm near infrared laser fiber (conventional laser irradiation) is not able to follow the curvature of the root canal in the apical one-third. A 300 μm tip (laser-activated irrigation) is positioned 5 mm short of the apical terminus. PIPS is easy, safe, and effective, far from the apex, and does not require that it be placed in the canals

becomes an obstacle to the flow of irrigant from the tooth entrance, and a possible depletion of irrigant may occur in the apical part. The larger the diameter of the tip, the more it occludes the canal thus decreasing the flow of irrigant from the coronal to the apical portion.

- Moreover, it is impossible for the clinician to observe and be sure if the fluid level in the apical part is being maintained or if depletion

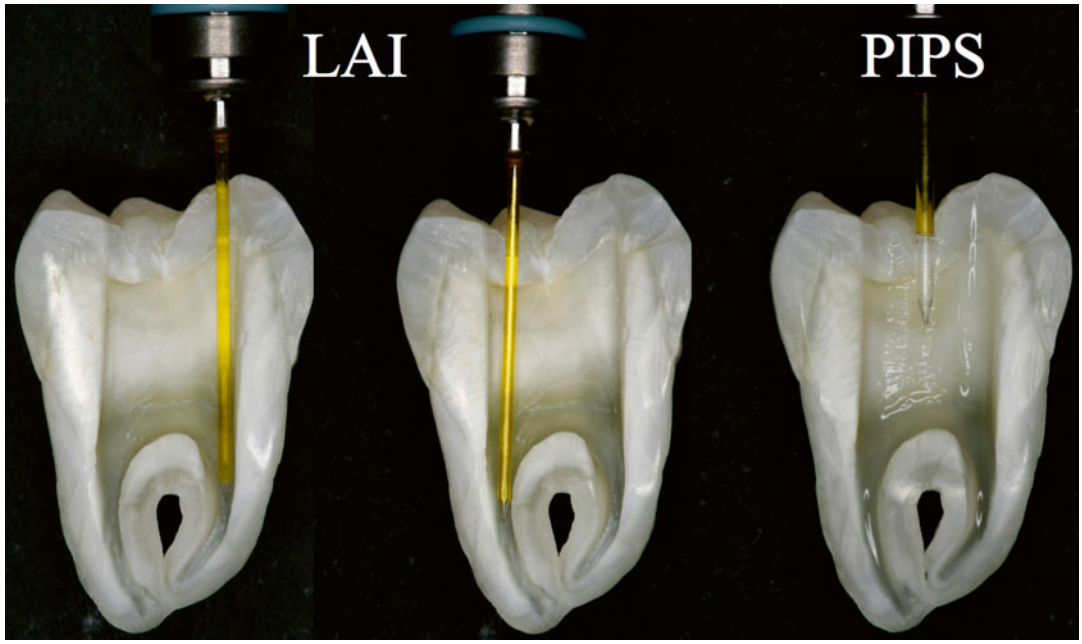

Fig. 11.26 Comparison between PIPS and LAI protocol: the tip positioned close to the apex (1–5 mm), during LAI procedures, may create irrigant extrusion and liquid depletion during laser activation of irrigants

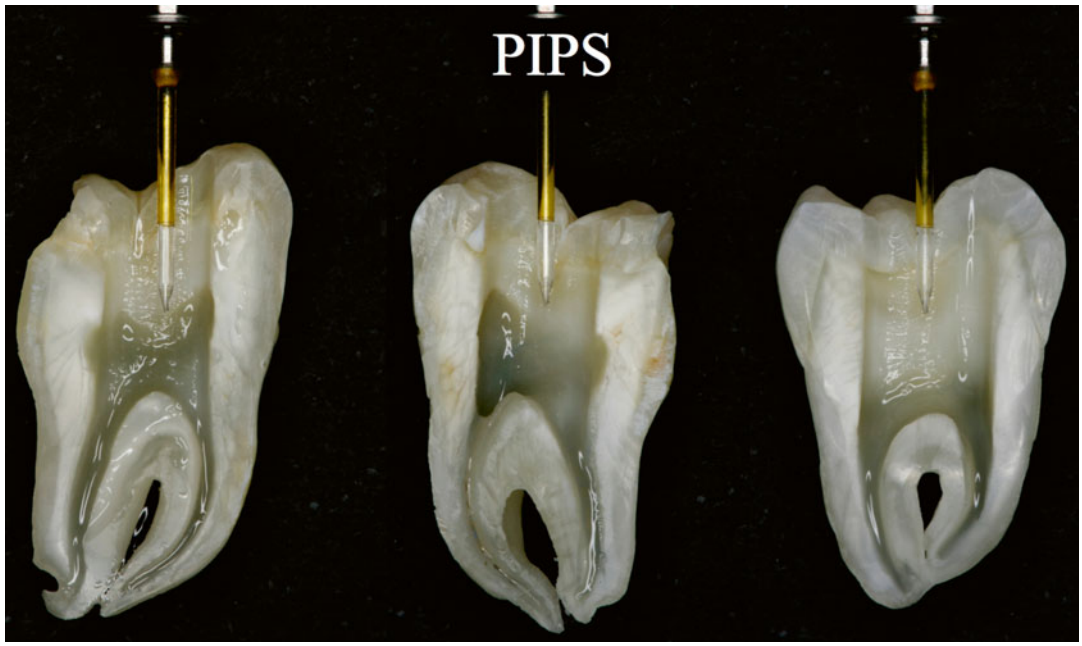

Fig. 11.27 PIPS tip correctly positioned in pulp chamber: note the border of the stripped part positioned at occlusal margin of the cavity and the tip not in contact with dentin walls: as a consequence all the canals can be irrigated both effectively and safe

occurs. Depletion of the irrigant results in thermal damage with laser spots seen on the dentin surface.

It is important to note that the use of high energy inside the canal leads to a faster vaporization and depletion of fluids and unwanted abla-

tive effects (see Figs. 11.8, 11.9, 11.10, and 11.11; see also Figs. 10.3, 10.4, and 10.5 in Chap. 10).

On the other hand, PIPS protocol does not require that the tip be placed into the canals at all, but rather in the pulp chamber only (see also Figs. 11.5, 11.18, 11.22, and 11.27).

Several advantages are related to positioning of the PIPS tip in the pulp chamber only:

- The absence of need to enlarge and remove more tooth structure as required to deliver a fiber inside the canal.
- Increased ability to efficiently irrigate all the root canal length, including the isthmus and lateral canals frequently present in the coronal and middle one-third, otherwise not irrigated when the tip is inserted into the canal.
- Increased ability to efficiently irrigate complicated anatomical systems including curved canals that would otherwise be difficult to irrigate with other techniques.
- More conservative negotiation of smaller and more delicate anatomy commonly seen in the apical one-third.
- The position of the laser tip far from the apex decreases the possibility of apical extrusion (this part will be discussed later).

The tip is kept stationary in the coronal aspect of the access preparation only thus offering a less technique-sensitive application for achieving good irrigation. The result is a canal convenience form that is more conservative, minimally invasive, and biomimetic avoiding the unnecessary removal of tooth structure (Figs. 11.28a–d and 11.29a, b).

11.7.5 Apical Preparation and Root Canal Shaping Using PIPS

This is yet another key distinguishing point of the PIPS technique.

The ability of photon-induced photoacoustic streaming to drive irrigants three-dimensionally into the root canal system by positioning the tip in the pulp chamber only where the irrigant reservoir can be maintained and visualized is complementary with the new "minimally invasive" philosophy in endodontics. Without the need to position any device (needle, ultrasonic tip, negative pressure system, or laser fiber) inside the canal, PIPS advocates minimal root canal and apical preparation while still allowing for efficacious movement and exchange of irrigants and effective cleaning and decontamination needed prior to establishing hermetic apical sealing during obturation. To maintain the natural or preexisting size of the anatomic apical constriction and to reduce the size of the preparation at a working length, PIPS technique advocates instrumenting 1 mm shorter than the measured working length from the anatomical apex. This approach maintains the natural delicate morphology often seen in the last 3 mm of the apical third while better controlling the possibility for blockage, transportation, and apical extrusion.

Zhu et al. (2013) reported that the effectiveness of PIPS may be influenced by a larger canal size, as it would reduce the superior efficacy of the PIPS, because the conventional needle or other systems can reach the apical third easier by virtue of sacrificing more tooth structure thus yielding no difference in their disinfecting ability [31].

This observation will be extensively debated ahead, in the discussion part.

11.7.6 Apical Extrusion

Apical extrusion of irrigants is a concern described in many studies [23, 30].

Different conditions, closely related one to another, can create extrusion.

11.7.6.1 Wide Apical Foramen

The apical foramen size depends on the "status quo ante" of the tooth.

Usually vital and necrotic teeth maintaining intact apical openings have a natural constriction ranging from ISO #08 to #20 [32, 33]. These clinical situations permit minimal and biomimetic approaches that limit the apical preparation to ISO #20–25. When chronic pathology leads to an apical reabsorption with a wide apical opening, or as seen in the case of immature teeth, care must be taken during the laser activation of the commonly used irrigants. PIPS protocol allows for the reduction of energy (from 15 to 5 mJ) reducing the peak power and consequently the

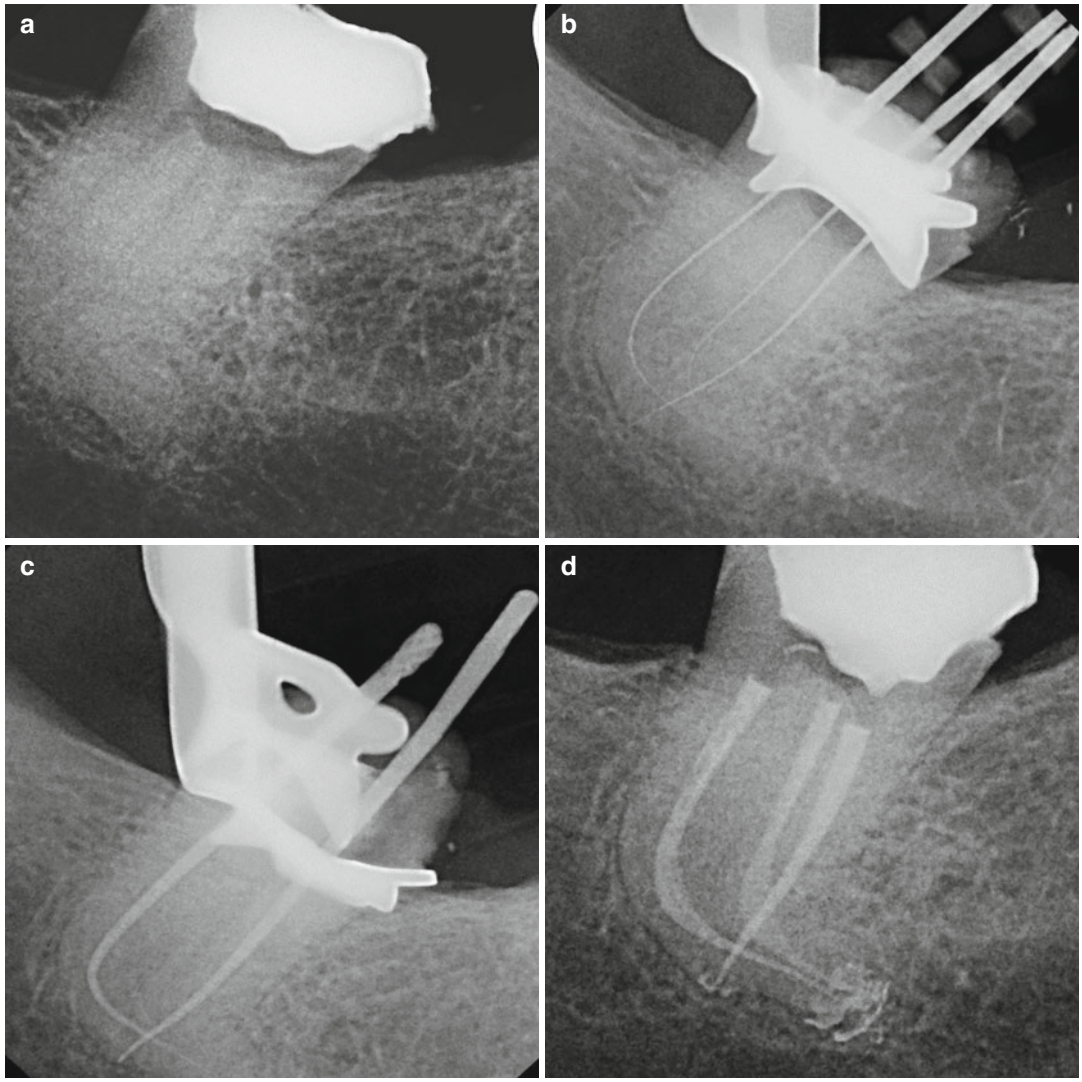

Fig. 11.28 (**a**) X-ray of the lower third molar showing accentuated curvature of distal root; (**b**) thin and flexible files to negotiate the apices; (**c**) gutta-percha master cone check; (**d**) root canal obturation with very conservative shaping of root canals (Courtesy of Dr. Enrico DiVito, Scottsdale, Arizona, USA)

photoacoustic effect limiting the force of the pressure waves in apical direction.

11.7.6.2 High Pressure Inside the Canal

Accordingly to George and Walsh (2008), high pressure inside the canal depends on the energy applied and on the position of the tip (c) [30].

11.7.6.3 Tip Position

During LAI procedures, when a flat or conical laser tip is positioned close to the apex (1 or 5 mm) either stationary or in movement, irrigant extrusion from the apical terminus was described [23, 30]. Essentially the closer the tip is to the apex, the more the pressure wave can create extrusion (see Fig. 10.9).

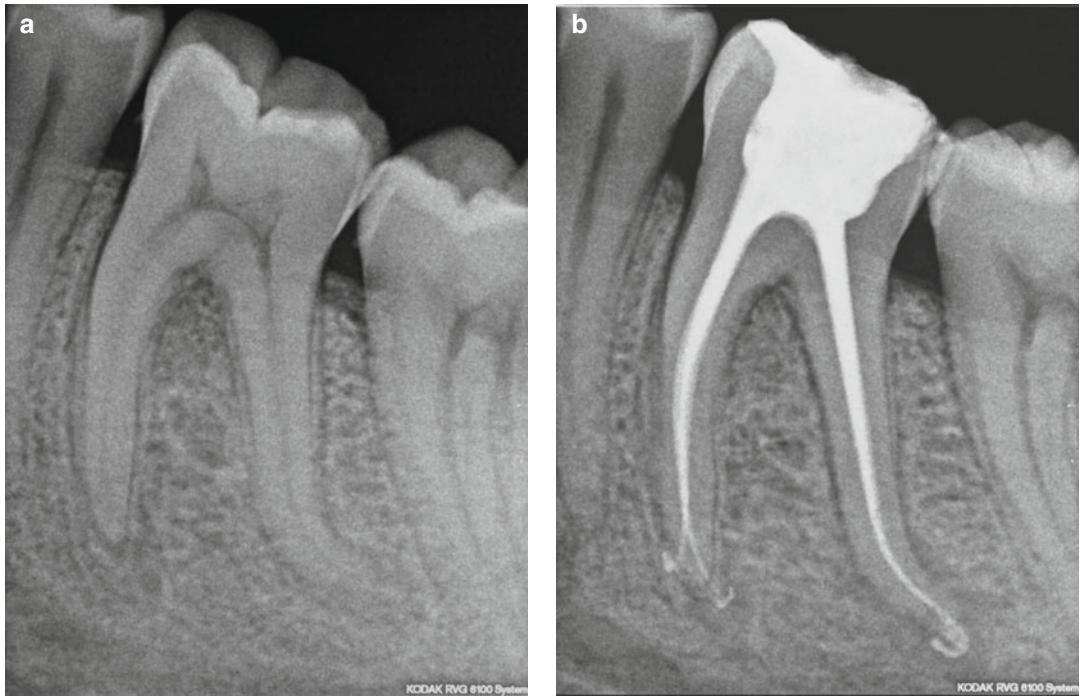

Fig. 11.29 (**a**) Pre-treatment radiograph of the lower first molar; (**b**) post-re-treatment radiograph. Note the conservative obturation (20/04) shape that can be achieved with the use of PIPS laser-activated irrigation (Courtesy of Dr. Paolo Magliano, Torino, Italy)

PIPS uses lower energy in comparison with other different LAI protocols and a safer position of the tip in the pulp chamber.

When the tip is positioned in the pulp chamber and held stationary without entering the canal orifices, no irrigant extrusion was observed by Peeters and Mooduto (2013) [34]. Possible fluid dynamic explantations include passive reflux event, surrounding periodontal ligament pressure, and intraosseous vascular pressures measured at 5.7 mm of Hg from Khan et al. (2013) creating a positive pressure that can preclude extrusion [35–38]. The capillary blood pressure in the human body is reported to be approximately 25 mmHg in the capillary bed, higher at the arterial end of the capillaries, and 10–15 mmHg at the venous end [39].

Apical extrusion of irrigants remains a controversial and debated issue, still under investigation. However the authors observed no extrusion during clinical trials when the proper PIPS protocol was used.

11.8 Temperature Variation

Because of the low energy used (20 mJ or less) and its complete absorption in water, no significant temperature rise was recorded on the root surface.

DiVito et al. (2012) [11] in an in vitro morphological study investigated the possible thermal side effects of erbium:YAG laser activation (20 mJ per pulse, 15 Hz, and 50 μs pulse duration, 400 μm PIPS tip) of 17 % EDTA, used for smear layer removal. Temperature variations on the external root surface of the teeth of the laser groups were measured by a modified thermocouple sensor of 1.5 mm diameter placed on the root surface 5 mm from the apex. Temperature variations were monitored continuously throughout all the irradiation periods. Minimal average temperature increases of 1.2 and 1.5 °C were observed at the root surface during laser irradiation for 20 s and 40 s irradiation time, respectively. SEM evaluations of 5 mm in the apical third reported no laser thermal damage on the dentin surfaces (Figs. 11.30, 11.31, 11.32 and 11.33).

11.9 PIPS Effects on Irrigants: The Activation Phase and the Resting Phase of NaOCl

Another important value of LAI and PIPS is their ability to increase not only the fluid dynamics of the irrigants but also their activation and effectiveness.

Macedo et al. (2010) [28] demonstrated that sodium hypochlorite efficacy depends on its reaction rate and on the availability of free chlorine ions, specifically the hypochlorous acid (HOCl) and the hypochlorite ion (OCl^-) (Fig. 11.34). In alkaline solutions the OCl^- prevails and brings with it a superior oxidative effect and a higher tissue-dissolving capacity than HOCl (Baker 1947). There is an activation phase occurring during agitation producing a significant portion of active chlorine ions. When activation is discontinued and the resting phase occurs, active ions produce chelates which are antibacterial and digestive in action on smear layer, bacteria, and other organic and inorganic tissues. The study reported that continuous agitation is a strong activator of sodium hypochlorite. In particular NaOCl solutions activated by laser and ultrasonics showed a higher reaction rate than nonactivated NaOCl solutions. LAI was demonstrated to be more effective than PUI after the 3 min of resting interval (Figs. 11.35a–d).

11.10 Other Effects of PIPS: Vapor Lock

Van der Sluis reported that stable bubbles, such as vapor lock occurring at the apex, can be driven and eliminated by the pressure changes from the growth and collapse of the laser-induced bubble (see

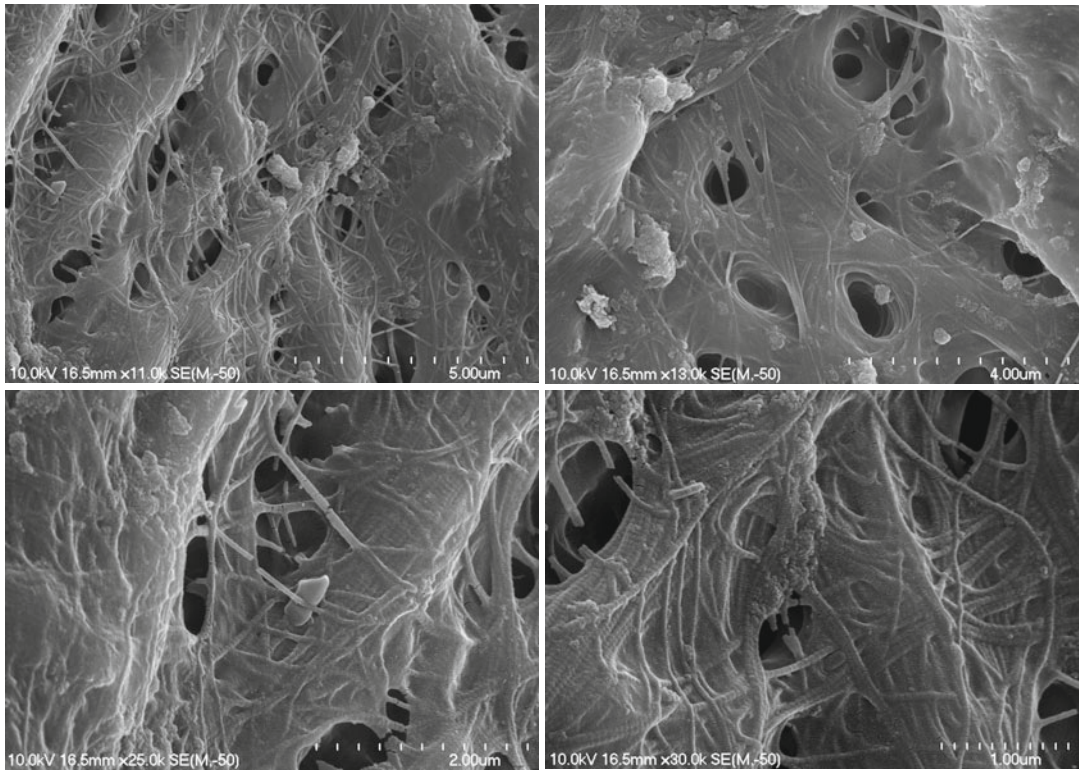

Figs. 11.30, 11.31, 11.32 and 11.33 Post-PIPS SEM images reveal extremely clean, undisturbed, and not thermally affected surfaces when correct PIPS protocol is followed (Courtesy of Dr. Graeme Milicich, Hamilton, New Zealand and Dr. Enrico DiVito, Scottsdale, Arizona, USA. Figs. 11.30, 11.32 and 11.33: Reprinted from DiVito et al. [11] with permission. Fig. 11.31: Reprinted from DiVito et al. [13] with permission)

Chap. 3) [40]. Peeters et al. (2014) in a visualization study described the disruption of the trapped air from the apical region, caused by bubble implosion produced by the use of laser-driven irrigation [41].

Also experimental records from the authors also reported the ability of PIPS pressure waves to eliminate vapor lock from inside the artificial canal model (Olivi G. and DiVito E, 2014) (Fig. 11.36a–f).

$$NaOCl \longrightarrow Na^{+} + OCl^{-}$$

$$OCl^{-} + H2O \longleftrightarrow HOCl + OH^{-}$$

Fig. 11.34 Chemical reaction of sodium hypochlorite produces free chlorine ions, specifically the hypochlorous acid (HOCl) and the hypochlorite ion (OCl^{-})

11.11 Undesired Effects: Fluid Splashing

If higher power setting (more than 20 mJ) or incorrect tip positioning is used (not completely immerged in the pulp chamber with part of the stripped portion out of the coronal opening), splashing of irrigant outside the tooth may occur. This depends on the width of the generated vapor bubble and on its consequently high pressure that pushes irrigant out of the root canal at the coronal opening causing loss of irrigant and ineffective irrigation. Unlike what was reported by van der Sluis et al. for LAI (see Chap. 3), PIPS needs continuous irrigation with an external supply to maintain constant levels of irrigant inside the canal so that the canal does not dry out thus

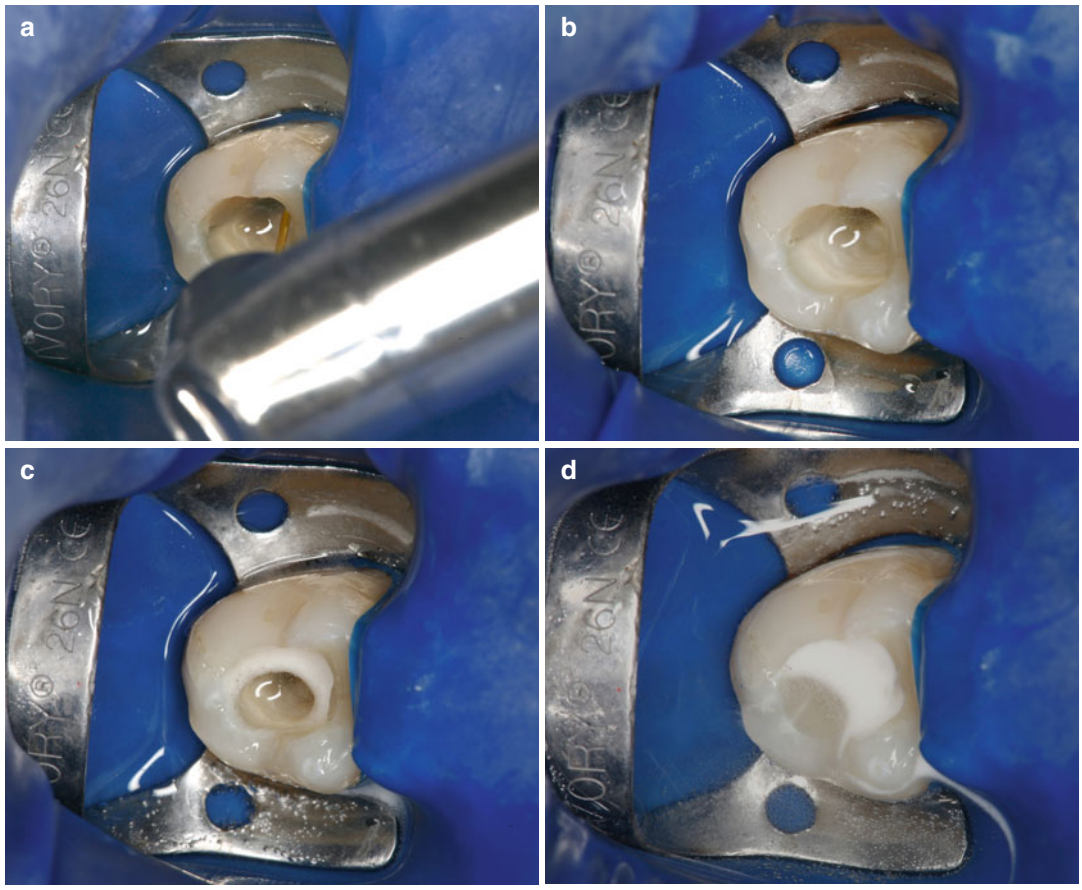

Fig. 11.35 (**a**) Intraoperative micrograph shows the correct position of PIPS tip prior to activation; (**b–d**) note the higher consumption of available chlorine with foaming after 10, 20, and 30 s of resting phase following PIPS activation

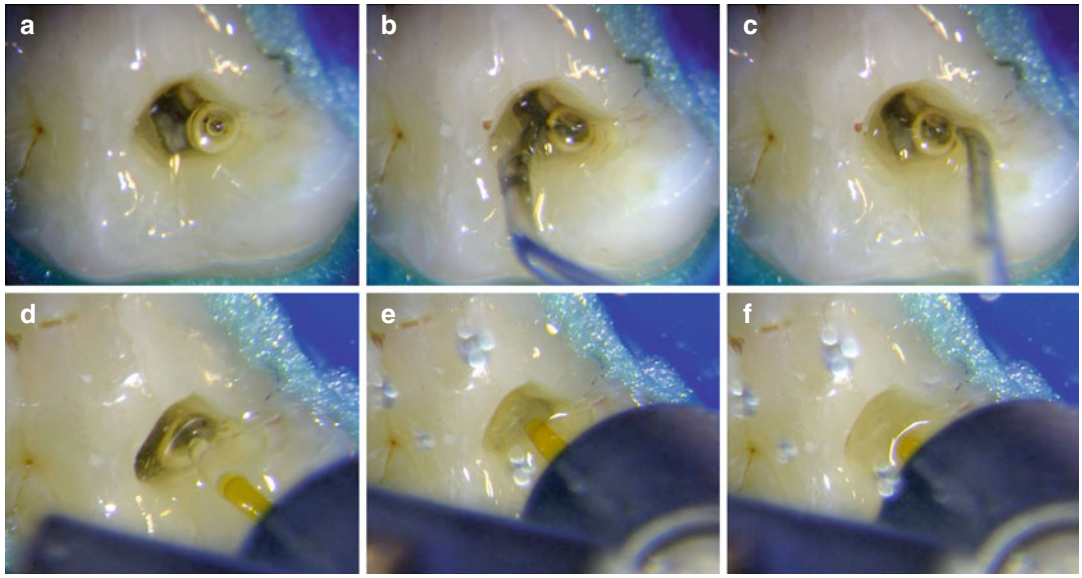

Fig. 11.36 (**a**–**c**) Ultrasonic activation not effective at removing vapor bubble; (**d**–**f**) PIPS™ laser-activated irrigation quickly removes vapor bubble

Fig. 11.37 Proper patient draping with waterproof bib to protect clothing is highly recommended to be prepared

avoiding adverse thermal effects (George and Walsh 2012) [42] or ineffective irrigation (Deleu et al. 2015) [29].

Additionally, to avoid undesired and unpleasant side effects to the patient, it is recommended that a hermetic barrier using a rubber dam be used to establish adequate isolation. Liquid dam can also be added to help achieve proper isolation. Also covering the patient with waterproof bib to protect clothing is highly recommended (Figs. 11.37 and 11.38).

11.12 Clinical Applications of PIPS

PIPS offers a variety of applications and results in cleaning and decontamination of the root canals clearly supported by the international literature. The ability of PIPS™ to remove medications from the root canal, such as double and triple antibiotic pastes or calcium hydroxide, and to remove filling materials from oval-shaped canals was investigated, suggesting the application of PIPS also in endodontic re-treatment.

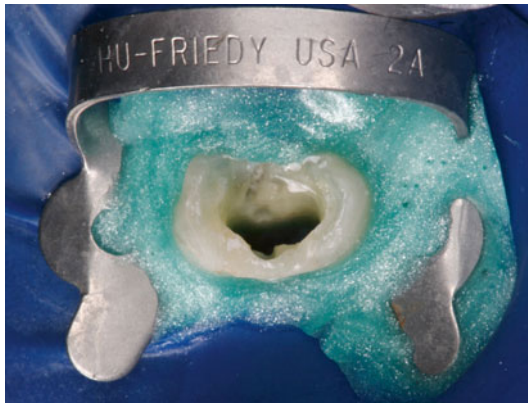

Fig. 11.38 Proper isolation for PIPS is important. Liquid dam is interlocked beneath the dam clamp

In endodontics *smear layer* (also called *dentin mud*) is defined as a film retained on the dentin surfaces after rotary instrumentation or filing. *Debris* is defined as dentin chips and generically as particles loosely attached to the root canal walls that can result from hand instrumentation or from the use rotary files and can be visualized after sectioning and splitting of the samples. Remnants of vital or necrotic pulp tissue are also present into the canal space, attached on the canal walls after instrumentation [42, 43]. Cleaning the root canal entails the removal of organic and inorganic remnants, debris, and smear layer from the canal surface after instrumentation. Decontamination is aimed to destroy planktonic bacteria and biofilm and reduce the bacterial load prior the obturation.

Among the different irrigant solutions commonly used, 17 % EDTA has been shown to be more effective and used as a worldwide irrigant for the removal of smear layer [44, 45] and hence the irrigant chosen to test PIPS efficacy in smear layer removal. Sodium hypochlorite (NaOCl) dissolves the organic tissues and kills bacteria, and it is the irrigant solution used for the antibacterial action during and at the end of the root canal therapy. Consequently it is the combination of these two solutions to produce the better results when activated by PIPS.

Clinical protocol for PIPS involves several different steps during root canal therapy:

- The continuous supply and activation of fresh NaOCl helps to dissolve the pulp tissues and to reduce the bacterial load within the endodontic system, at the beginning of and during the root canal preparation.
- The activation of continuous EDTA helps to remove debris and smear layer produced by instrumentation on the root canal walls and to open the dentinal tubules for final decontamination [11, 13].
- The continuous supply and activation of fresh NaOCl after removal of smear layer from instrumentation helps to dissolve residual organic tissue remnants and to decontaminate the endodontic system before obturation [12, 15, 46].
- The continuous irrigation with sterile distilled water prepares the endodontic system for final obturation.

There is still controversy as to if NaOCl must be used as the final step of endodontic irrigation due to the excessive peritubular erosion observed when sodium hypochlorite follows EDTA irrigation [44]. However this is a consideration based only on an observation point of view and does not take into consideration that each successive irrigation passage leads to further tissue removal and that sterile distilled water remains the final step.

11.12.1 Effects of PIPS on Intracanal Tissue, Debris, and Smear Layer

SEM imaging is typically used to evaluate the morphology and cleaning of the root canal after different instrumentation and irrigation techniques. PIPS technique also underwent SEM imaging to assess possible dentin morphologic alterations as well as the cleaning and debriding efficacy of the root canal surface. The use of 17 % EDTA activated by PIPS during the irrigation protocol after mechanical instrumentation resulted in better cleaning and smear layer removal when compared to other irrigation techniques [11, 13].

A study from DiVito et al. (2012) investigated the ability of PIPS technique to remove debris and smear layer from the root canal walls which were minimally prepared with rotary instrumentation at ISO #20 and 0.06 taper (Profile GT; Dentsply Tulsa Dental, Tulsa, OK, USA) [11]. Laser parameters were 20 mJ, 15 Hz, 0.3 W, and 50 μs pulse duration, with a 400 μm PIPS tip

delivered by an Er:YAG laser (Fidelis AT, Fotona d.d., Ljubljana, Slovenia). A scoring method for quantitative smear layer removal evaluation was used, accordingly to Hülsmann et al. [48], after observing all the sample SEM images at magnification from 1000× to 2000×.

The PIPS laser groups were tested with three different modalities and compared to sterile distilled water irrigation alone for 20s. Laser PIPS groups included sterile distilled water irrigation for 20s and 17 % EDTA for 20s and for 40s.

SEM examination demonstrated that when only water irrigation was applied, there was noticeable smear layer and debris occluding dentinal tubules on the treated surface (Figs. 11.39 and 11.40). When sterile distilled water was activated for 20s with the Er:YAG laser, the specimens showed improved cleaning compared to the control non-laser group with root canal surfaces exhibiting more open tubules, residual debris, and a smear layer still present (Fig. 11.41). The laser group treated with PIPS activation of 17 % EDTA irrigation for 20s exhibited improvement in cleaning and debridement action compared to the sterile distilled water groups (laser and no laser activation) (Figs. 11.42 and 11.43). The most effective removal of smear layer from root canal walls was achieved by the use of the Er:YAG laser plus EDTA irrigation for 40s (Figs. 11.44 and 11.45). SEM at higher magnifications (from 2040× to 10,200× mag.) showed exposed and intact collagen fibers with evidence of unaltered collagen matrix (Fig. 11.46). None of the SEM micrographs indicated signs of thermal damage to the dentin surface.

To quantify the differences in smear layer removal, the five-step scoring method was used. Results showed that all groups differed significantly from each other with PIPS and EDTA group resulting in more cleaned surfaces (Table 11.1).

Another study from DiVito et al. (2011) confirmed the Er:YAG and PIPS ability to remove debris and smear layer from the root canal walls after nickel-titanium rotatory instrumentation [13]. After root canal preparation at ISO #30/06 (Profile® GTTM, Dentsply Tulsa Dental, Tulsa, OK, USA), three different protocols of irrigation were performed activated by an Er:YAG laser (2940 nm Fidelis, Fotona d.d., Ljubljana, Slovenia) used with a 14 mm long 400 μm PIPS tip at 20 mJ, 10 Hz, 0.2 W with a 50 μs pulse duration. Laser irradiation was applied for 20 s with saline solution and then for 20 and 40s with 17 % EDTA. The irrigation was delivered via external syringe continuously to maintain fluid level in the pulp chamber. SEM examination clearly showed that when only hand irrigation with water was applied, noticeable smear layer and closed tubules were still present (Figs. 11.47 and 11.48). However, the samples treated with PIPS and EDTA showed clean dentin surface, open tubules, and essentially no smear layer or debris remaining (Figs. 11.49 and 11.50). SEM magnification at 20,000× showed that the organic and inorganic dentin matrix was intact with visible collagen fibers (Figs. 11.51 and 11.52).

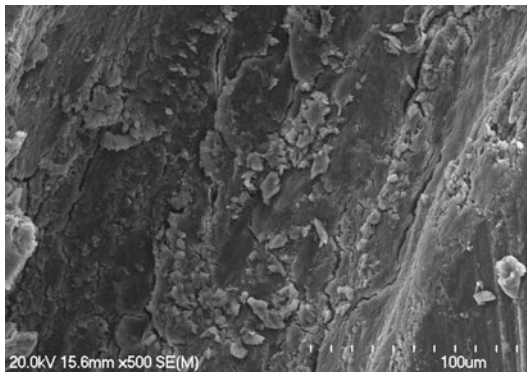

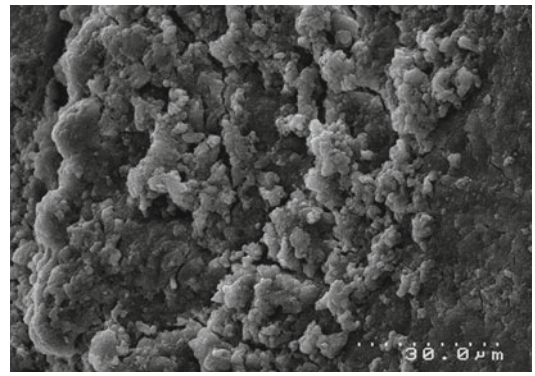

Fig. 11.39 and 11.40 SEM images show noticeable smear layer and debris occluding dentinal tubules on the treated surface when only water is used for irrigation (Courtesy of Dr. Graeme Milicich, Hamilton, New Zealand and Dr. Enrico DiVito, Scottsdale, Arizona, USA. Reprinted from DiVito et al. [11] with permission)

A study from Lloyd et al. (2013) assessed the intracanal tissue and debris elimination from canal isthmuses of extracted human mandibular molars using a high-resolution micro-computed tomography [47].

The mesial canals were prepared using a standardized instrumentation protocol up to 30/.06. Two groups ($n=7$) underwent final irrigation using either standard needle irrigation (SNI) or photon-induced photoacoustic streaming (PIPS). After instrumentation, the canal volumes were reconstructed from micro-computed tomographic scans, before and after irrigation, to assess removal of organic tissue and inorganic debris by quantitative analysis of the superimposed volumes. The total volume of sodium hypochlorite and EDTA was the same as for the SNI group. The standard needle irrigation (SNI) protocol after canal preparation involved irrigation with 17 % EDTA over a period of 60 s at a distance 1 mm short of the working length, followed by 6 % sodium hypochlorite delivered over 30 s. The PIPS protocol was performed with the standard settings of the Er:YAG laser (Fidelis; Fotona, Ljubljana, Slovenia) at 15 Hz and 20 mJ using the 600 μm PIPS tip placed into the access cavity only and activated by the following irrigating solutions: 3×30 s cycles of continuous flow sodium hypochlorite, one 30 s cycle of distilled water, one 30 s cycle of EDTA, and a final flushing with 3×30 s cycles of distilled water. Elimination of debris and organic tissue from complex canal spaces and an increase in root canal system volume were more significant ($p<.001$) for the laser-activated PIPS group than for the SNI group ($p=.04$). Irrigation using PIPS increased the canal volume and eliminated debris from the canal system 2.6 times greater than SNI (Figs. 11.53a–c and 11.54).

A recent study from Arslan et al. (2014) compared the efficacy of PIPS technique and 1 % NaOCl with conventional, sonic, and ultrasonic irrigation on the removal of apically placed dentinal debris from an artificial groove created in a root canal. PIPS resulted in significantly more effective removal of dentinal debris than conventional irrigation ($p<0.001$), sonic irrigation ($p<0.001$), or ultrasonic irrigation ($p=0.005$) [48].

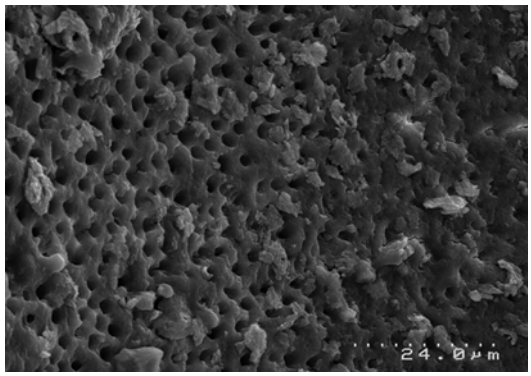

Fig. 11.41 Sterile distilled water activated for 20s with the Er:YAG laser. The SEM image shows improved cleaning compared to the control non-laser group with root canal surfaces exhibiting more open tubules. Residual debris and a smear layer still present (Courtesy of Dr. Graeme Milicich, Hamilton, New Zealand and Dr. Enrico DiVito, Scottsdale, Arizona, USA. Reprinted from DiVito et al. [11] with permission)

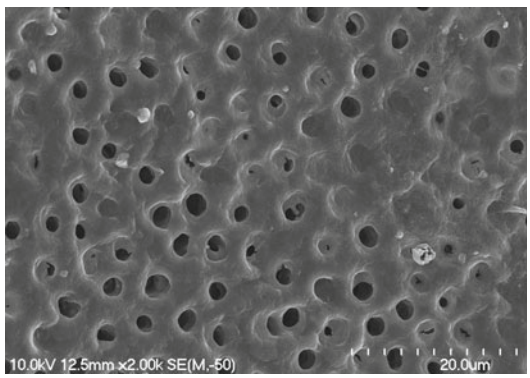

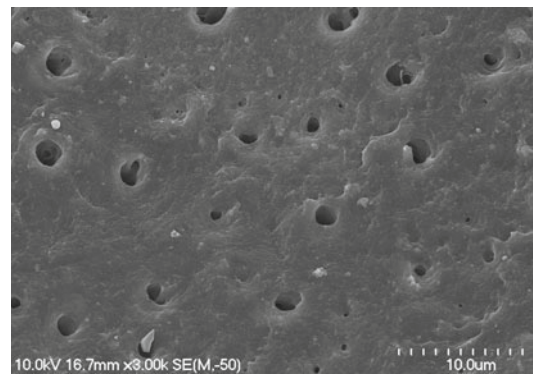

Figs. 11.42 and 11.43 SEM images of laser group samples treated with PIPS with 17 % EDTA irrigation for 20s exhibited improvement in cleaning and debridement action compared to the sterile distilled water groups (Courtesy of Dr. Graeme Milicich, Hamilton, New Zealand and Dr. Enrico DiVito, Scottsdale, Arizona, USA. Reprinted from DiVito et al. [11] with permission)

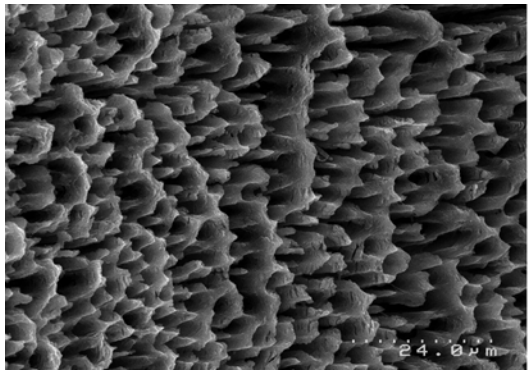

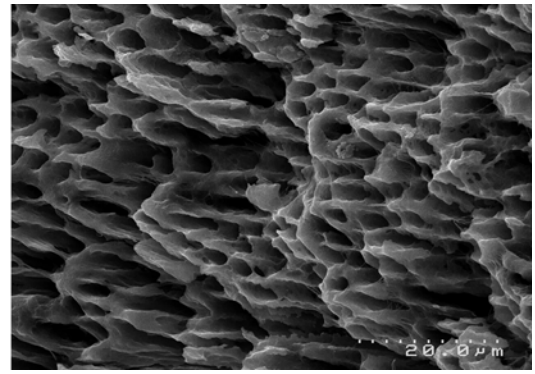

Figs. 11.44 and 11.45 SEM images of laser group samples treated using PIPS with 17 % EDTA irrigation for 40s exhibited improvement in cleaning and debridement; however, peritubular dentin was resorbed due to increase time in laser-activated irrigation (Courtesy of Dr. Graeme Milicich, Hamilton, New Zealand and Dr. Enrico DiVito, Scottsdale, Arizona, USA. Reprinted from DiVito et al. [11] with permission)

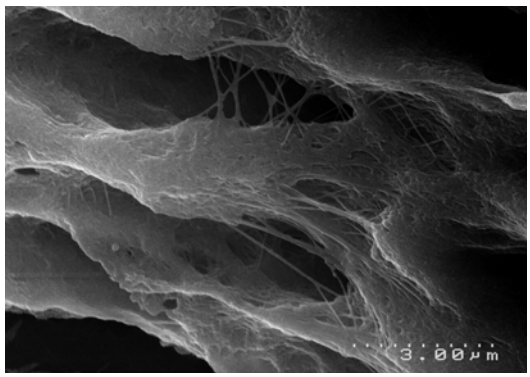

Fig. 11.46 SEM image close-up of dentin surface showing that the collagen fibers have not been disturbed after PIPS laser activation. No signs of thermal damage to the dentin surface (Courtesy of Dr. Graeme Milicich, Hamilton, New Zealand and Dr. Enrico DiVito, Scottsdale, Arizona, USA. Reprinted from DiVito et al. [11] with permission

Table 11.1 Hülsmann et al. [48] scoring method of SEM images (1000× to 2000×) for quantitative smear layer removal evaluation

Score 1: No smear layer and dental tubules open
Score 2: Small amount of smear layer, many dental tubules open
Score 3: Homogenous smear layer covering the root canals walls, only few dentinal tubules open
Score 4: Complete r oot canal wall covered by homogenous smear layer, no open tubules
Score 5: Heavy, non-homogenous smear layer covering complete root canal walls

11.12.2 Effects of PIPS on *Enterococcus faecalis* and Biofilm

Enterococcus faecalis is a commonly isolated bacterium in the teeth with failing root canals and is difficult to eradicate from the endodontic system [49]. It has been confirmed that *E. faecalis* can live in the endodontic environment as planktonic cell or biofilm. Biofilm develops after an initial attachment of planktonic bacteria to the root canal surface, and it takes several stages of development for it to mature to a structurally complex matrix that is scarcely eradicable because of its high adherence to the dentin walls (Figs. 11.55a, b, 11.56, and 11.57).

The change of biofilm bacteria from sensitive to resistant against disinfecting agents occurs between 2 and 3 weeks of biofilm maturation and is independent on the type of disinfecting agent used [50]. A 4-week incubation period enhances the bacterial penetration into dentinal tubules and promotes strong bacterial biofilm formation on the root canal surface. After the samples are vortexed (a machine that agitates the samples with a centrifugal force moving bacteria from the periphery to the main canal) and incubated for a 4-week period, a concentration of free planktonic cells is observed to correspond to a bacterial load of 10^9 bacteria [51] (Figs. 11.58 and 11.59).

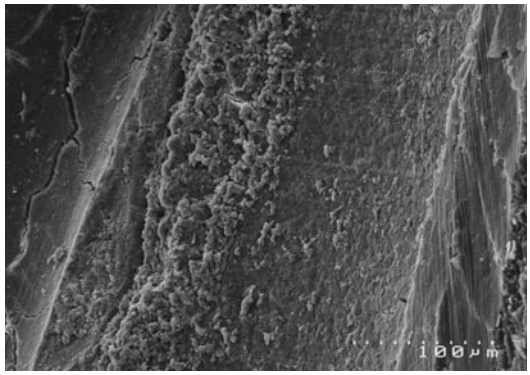
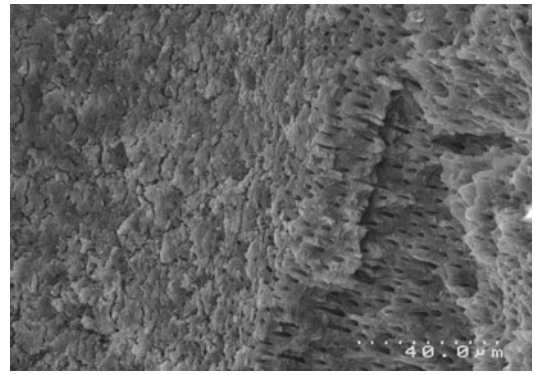

Figs. 11.47 and 11.48 SEM images of the coronal third show clean surface after laser irradiation in 17 % EDTA for 20 s and smear layer and debris removal from dentin tubules. The surface does not exhibit evidence of the application of thermal energy. Er:YAG laser at 20 mJ, 10 Hz, 0.2 W, 400 μm PIPS tip (Courtesy of Dr. Graeme Milicich, Hamilton, New Zealand and Dr. Enrico DiVito, Scottsdale, Arizona, USA. Reprinted from DiVito et al. [13] with permission)

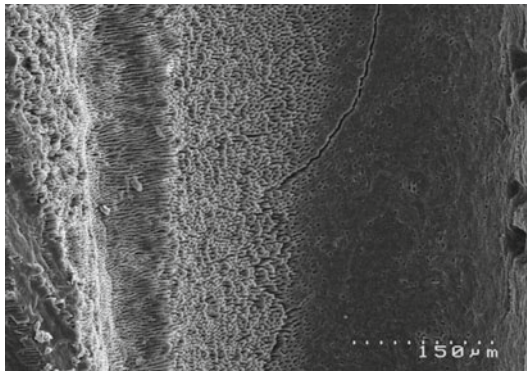
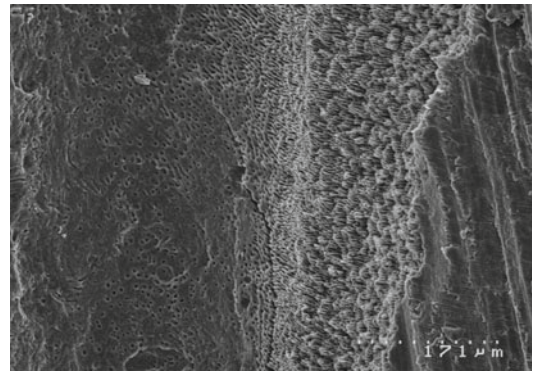

Figs.11.49 and 11.50 SEM images of samples treated with PIPS and EDTA showed clean dentin surface, open tubules, and no smear layer or debris remaining (Courtesy of Dr. Graeme Milicich, Hamilton, New Zealand and Dr. Enrico DiVito, Scottsdale, Arizona, USA. Reprinted from DiVito et al. [13] with permission)

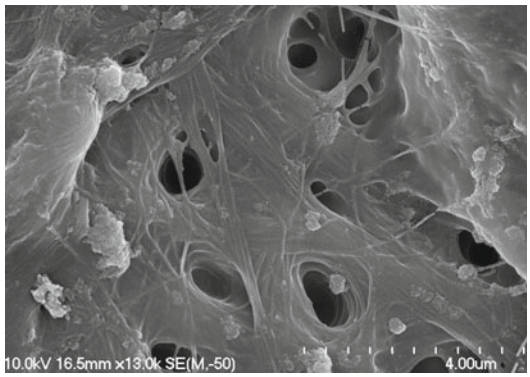

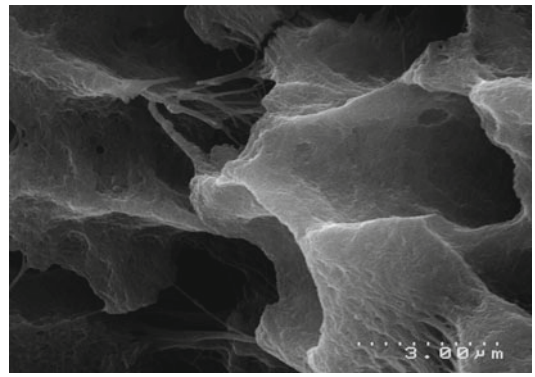

Figs. 11.51 and 11.52 SEM magnification at 20,000× showed the organic and inorganic dentin matrix intact with visible collagen fibers undisturbed (Reprinted from DiVito et al. [13] with permission)

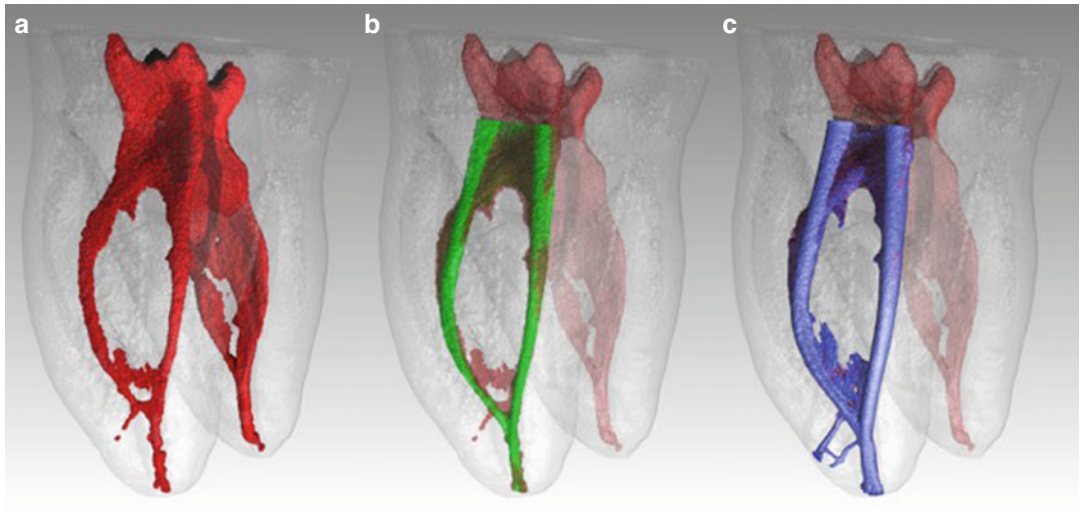

Fig. 11.53 (**a**) Micro CT scan showing canal tissue anatomy before treatment. (**b**) Micro CT after rotary preparation size 30/06 and sodium hypochlorite SNI: upon examination of the complex morphology, it is apparent that the isthmus remains untouched during canal preparation. (**c**) Micro CT after PIPS laser activation with sodium hypochlorite: note the increase in internal webs, anastomosis, and fins removed (Images courtesy of Prof. Adam Lloyd Chair Department of Endodontics, University of Tennessee Health Science Center)

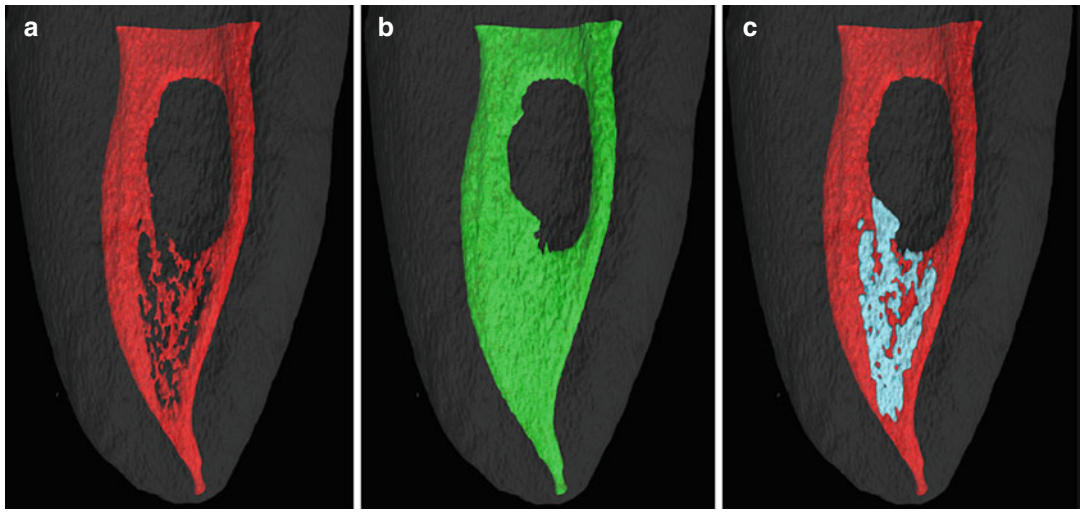

Fig. 11.54 3D volumetric reconstruction of tooth scanned with x-ray micro-focus CT showing complex non-separated canal anatomy (intracanal isthmus). (**a**) *Red* represents shaped canal system prior to PIPS. Dark voxels found as "islands" in isthmus represent soft tissue masses not removed during chemomechanical canal preparation. (**b**) *Green* represents entire complexity of isthmus cleaned following PIPS. (**c**) Composite image (*blue*) shows areas of tissue/debris removed using PIPS (Images courtesy of Prof. Adam Lloyd Chair Department of Endodontics, University of Tennessee Health Science Center. Permission received)

The bactericidal effect of PIPS is not related to direct laser irradiation and thermal effect, but rather PIPS exercises its effect via activation of the NaOCl, the most commonly used antibacterial agent in endodontics. Also noted is the lysing effect on both cells and matrix due to the complex turbulent irrigation flow demonstrated by PIPS.

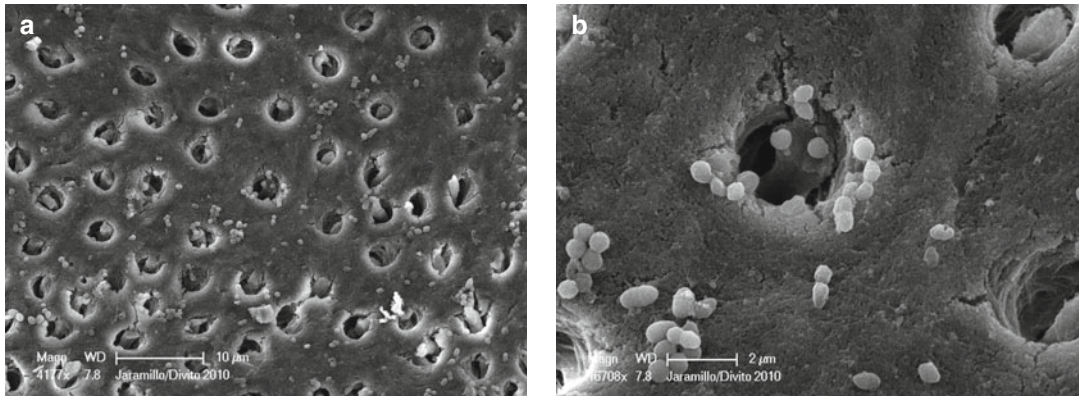

Fig. 11.55 (**a**) SEM image (4177×) of planktonic bacteria cells on root canal dentin surface; (**b**) high magnification image (16,708×) of the previous image shows initial attachment of planktonic bacteria to the root canal surface to develop bacteria conglomerated (Courtesy of Dr. David Jaramillo Loma Linda, California and Dr. Enrico DiVito, Scottsdale, Arizona, USA)

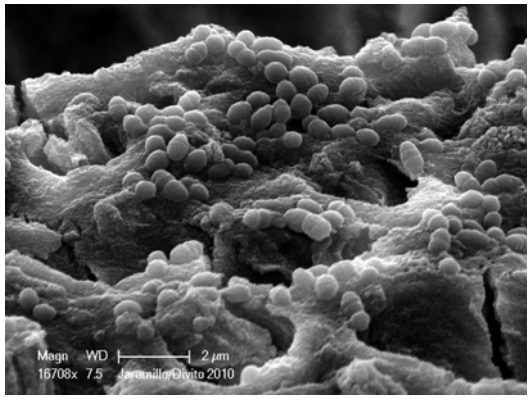

Fig. 11.56 SEM image (16,708×) shows initial attachment of planktonic bacteria to the root canal surface and the several stages of development of the biofilm to mature and form a structurally complex matrix that is scarcely eradicable because of its high adherence to the dentin walls (Courtesy of Dr. David Jaramillo Loma Linda, California and Dr. Enrico DiVito, Scottsdale, Arizona, USA)

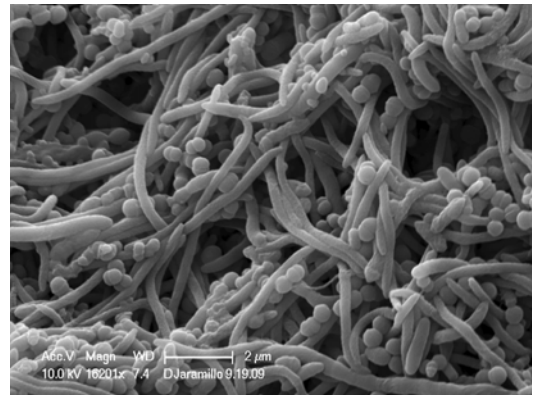

Fig. 11.57 SEM image (16,201×) shows advanced stage of development of cocci and rodlike biofilm adherent to the dentin walls (Courtesy of Dr. David Jaramillo Loma Linda, California and Dr. Enrico DiVito, Scottsdale, Arizona, USA)

The continuous activation of the sodium hypochlorite leads to three different events:

- A three-dimensional streaming of the fluids with improved penetration of the irrigant deeply in dentinal tubules [25, 46]
- An increased reaction rate of the NaOCl [28]
- A shock wave-like phenomenon that induces a direct cell lysing and mechanical breakup of the bacterial biofilm [14].

Peters et al. (2011), at the University of Pacific (San Francisco, CA, USA), first investigated the efficacy of three different techniques for root canal disinfection, specifically comparing the ability to remove bacterial biofilm formed on root canal walls of PIPS, syringe irrigation (CI), and ultrasonic activation (UI) [12].

The teeth used in this study were decoronated and trimmed to a uniform length of 14 mm. Canals were prepared at a working length (WL)

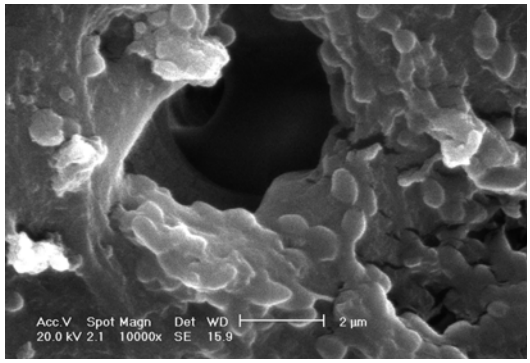

Fig. 11.58 SEM image (10,000×) of 4-week incubation period of *E. faecalis* colonizing the dentin walls: the concentration of free planktonic cells corresponds to a bacterial load of 10^9 bacteria (Image of Dr. Giovanni Olivi, Rome (Italy))

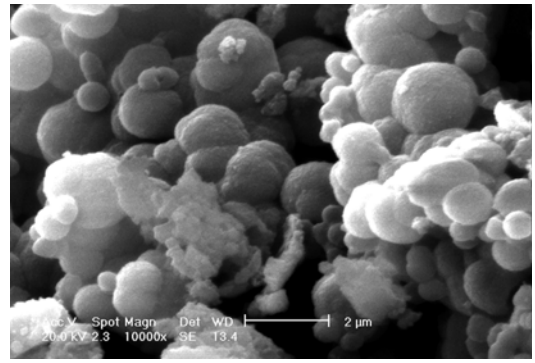

Fig. 11.59 SEM image (10,000×) of high concentration *E. faecalis* colony adherent to root dentin surface, corresponding to a bacterial load of 10^9 bacteria (Image of Dr. Giovanni Olivi, Rome (Italy))

of 0.5 mm short of the anatomical apex to a size #20 ISO and .07 taper (F1 ProTaper, Dentsply Tulsa Dental, Tulsa, OK, USA). A reservoir for irrigant placement was created in the coronal 5 mm of the canal. Conventional syringe irrigation was accomplished by placing a 30 gauge Maxiprobe needle close to WL and depositing 5 mL of 6 % NaOCl at 30 s and allowing solution to remain in the canal for an additional 30 s (reaction phase). In the PUI group, NaOCl solution was placed over 30 s and then activated for 30 s by using a non-cutting insert (EMS 600 ultrasonic unit; Endosoft ESI; EMS, Nyon, Switzerland) placed 1 mm short of WL (power was set at 5/10). In the PIPS group, the NaOCl solution was deposited continuously for 30 s with activation by a 2940 nm wavelength Er:YAG laser (Fidelis; Fotona d.d., Ljubljana, Slovenia) at 10 Hz and 50 mJs with a 400 µm PIPS tip. The continuous supply of fresh sodium hypochlorite at the beginning and during the root canal therapy helps to dissolve the pulp tissues and to reduce the bacterial load within the endodontic system. The tip was placed stationary into the coronal reservoir and not in the canals. In the laser and ultrasonic groups, additional irrigation solution was deposited in the coronal reservoir only when it was noted that the coronal reservoir was depleted.

Findings showed that syringe irrigation with NaOCl alone reduced bacterial counts by 96.6 %. However only 1 of 20 samples was negative. Passive ultrasonic activation also resulted in significant elimination of bacteria by 98.5 %, with only 2 of 20 samples negative. Finally, activation with PIPS™ led to more significant reduction in bacterial contamination by 99.5 % with 10 of 20 samples negative [12].

Pedullà et al. (2012) from the University of Catania, Italy, also investigated the ability of NaOCl and PIPS to in vitro decontaminate *Enterococcus faecalis*-infected teeth [14]. The teeth were instrumented to the anatomical apex up to #25.06, using mechanical preparation (Mtwo rotary instruments, Sweden & Martina, DueCarrare-Pd, Italy). The teeth were then infected and incubated for a period of 2 weeks leading to a median bacterial count of 10^6. Four different irrigation protocols were used, with distilled water and NaOCl, delivered through conventional syringe irrigation or laser activated. All the groups were irrigated for 30 s. In the conventional irrigation groups, the 30 G needle tip was introduced as close to the anatomical apex as possible, depositing 3 mL of irrigant solution. In the laser-activated irrigation protocol, Er:YAG laser (Fidelis AT, Fotona, Ljubljana, Slovenia), delivered at 20 mJs per pulse, 15 Hz, and 50 µs pulse duration, was using a 400 µm PIPS tip positioned and stationary in the pulp chamber. After treatment, PIPS + NaOCl protocol reduced the bacterial counts by 99.8 % rendering more negative cultures than the other groups, with 30 negative samples out of 32. Syringe irrigation with NaOCl alone reduced bacterial counts by 97.1 %, with

25 negative samples out of 32. PIPS and distilled water group resulted in an inferior two log bacterial reduction (73.0 %) not sufficient to claim the bactericidal effect of water and photon-initiated photoacoustic streaming alone and therefore confirming the role of NaOCl in the root canal decontamination. However, the production of 15 negative samples of 32 in the water + PIPS group helps explain the role of the shock wave in improving the decontamination of infected root canals by inducing direct cell lysing and mechanical breakup of the bacterial biofilm [14].

Jaramillo et al. (2012) [52], from Loma Linda University, CA, USA, performed a bacteriological study completed with confocal and SEM investigations that clearly and significantly showed the complete inhibition the growth of *Enterococcus faecalis* of the PIPS + NaOCl group when compared with the combination of Er:YAG laser and phosphate-buffered saline (PBS) [25]. Teeth samples were prepared 1 mm short of working length using ProTaper® Rotary File system (Dentsply) and minimally enlarged up to ISO #20 0.07 (F1) to keep the canal enlargement as small as possible. Er:YAG laser (Fidelis AT, Fotona d.d., Ljubljana, Slovenia) equipped with a 400 μm PIPS tip was used at 20 mJ, 15 Hz, and 0.3 W to activate for 20s a solution of 6 % NaOCl, saline solution, or phosphate-buffered saline (PBS). Statistically significant differences in colony-forming units per milliliter were found between the laser treatment groups in two of the four groups. The combination of 20s irradiation with Er:YAG laser and 6 % sodium hypochlorite completely inhibits the growth of *Enterococcus faecalis* when compared with the combination of Er:YAG laser and phosphate-buffered saline (PBS). The dental shavings of teeth treated with Er:YAG laser and sodium hypochlorite showed 100 % elimination of *Enterococcus faecalis* compared to 50 % with the combination of Er:YAG laser and phosphate-buffered saline. Pre- and post-PIPS irrigation SEM analysis, as well as the confocal microscopy analysis, further confirmed the bacteriological findings. SEM representative image clearly showed that there were no bacteria present on the canal wall of specimens treated with PIPS and sodium hypochlorite when compared to the PBS control groups (Figs. 11.60a, b and 11.61a, b). Furthermore, the confocal microscopy analysis demonstrated absence of live bacteria on the canal wall and even within the dentinal tubules in the treatment group compared to the controls [25] (Figs. 11.62a–c and 11.63a, b).

On the basis of these results, further investigations were performed with a new laser device (LightWalker AT; Fotona d.d., Ljubljana, Slovenia) and new parameters. The setting used was 15 Hz and 20 mJ, and the energy was delivered at 50 μ pulse duration with a new 600 μm, 9 mm long PIPS tip. Different studies were performed in different university centers using different investigation methods but following similar protocols: University of Genoa, Italy; University Tor Vergata, Rome, Italy; University Victor Babes, Timisoara, Romania; Boston University, MA, USA; and University of São Paulo, Bauru, Brazil.

The authors investigated the ability of PIPS to decontaminate a 4-week biofilm using laser activation for 30s with 5 or 6 % NaOCl for two times, waiting an additional 30s after each activation period to allow the reaction of the solution (reaction phase). According to Macedo and Peters, the authors believe that this step is fundamental for a superior disinfecting result using the laser-activated irrigation technique [12, 28].

A study by Olivi et al. performed at the University of Genoa, Italy, in 2011 (published in 2014) reported that when 5 % NaOCl was activated by the erbium:YAG laser two times for 30s, waiting 30s for rest time after each activation period to allow for the reaction of the solution (reaction phase), a greater reduction in bacterial infection was obtained compared with conventional hand irrigation performed with the same timing [51]. The study involved a final flushing of 30s 17 % EDTA irrigation, activated and not activated by laser, to verify the canal surface cleaning and possible morphological alteration after laser-activated irrigation. Scanning electron microscopic imaging of split root sections showed images suggestive of a qualitative reduction of bacterial presence in the two treatment groups compared to positive controls. SEM images also showed evidence of lack of smear layer, open dentin tubules, and the

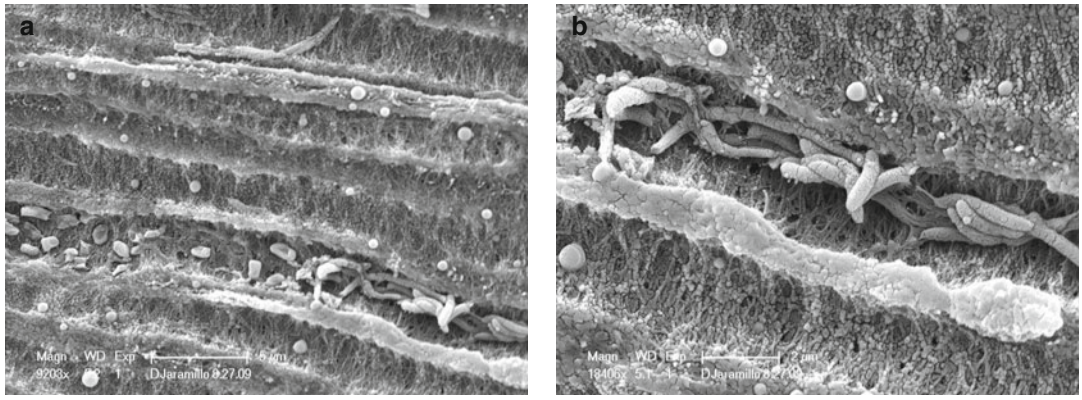

Fig. 11.60 (**a**) SEM (9203×) shows cocci and rodlike cells inside the dentin tubules; (**b**) SEM (18,406×) magnification of the previous image shows biofilm adherent to dentin tubules surface and some free planktonic cells (Courtesy of Dr. David Jaramillo, Loma Linda, California)

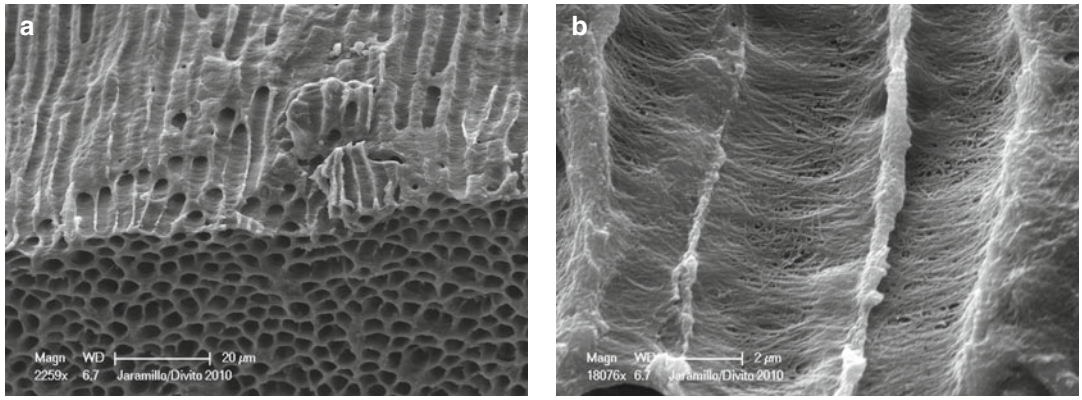

Fig. 11.61 (**a**) SEM (2259×) representative image clearly showed that there were no bacteria present on the canal walls of specimens treated with PIPS and sodium hypochlorite; (**b**) SEM (18,076×) magnification image of the previous image showing clean, bacteria-free, and no thermally damaged dentin tubules after PIPS: note the undisturbed organic dentin structure (Courtesy of Dr. David Jaramillo Loma Linda, California and Dr. Enrico DiVito, Scottsdale, Arizona, USA)

absence of laser-induced thermal damage in the PIPS group (Figs. 11.64, 11.65, 11.66, 11.67, 11.68, and 11.69).

Conventional hand irrigation (CI) showed residual smear layer with the presence of debris and partially occluded dentin tubules. Colony-forming units of bacterial suspensions were enumerated immediately after the treatment. Laser-activated irrigation group resulted in no detectable growth in all 10 samples compared to 6/10 samples with no growth in CI group. When comparing bacterial counts, this difference was statistically significant ($p < 0.05$). Furthermore, after 48 h no bacterial growth was detected in any

Fig. 11.63 (**a**) Confocal microscopic image showing the depth of live (*green*) bacteria penetration into the dentin tubules of control group and (**b**) the presence of dead (*red*) bacteria deeply into the dentin tubules (Courtesy of Dr. David Jaramillo Loma Linda, California and Dr. Enrico DiVito, Scottsdale, Arizona, USA)

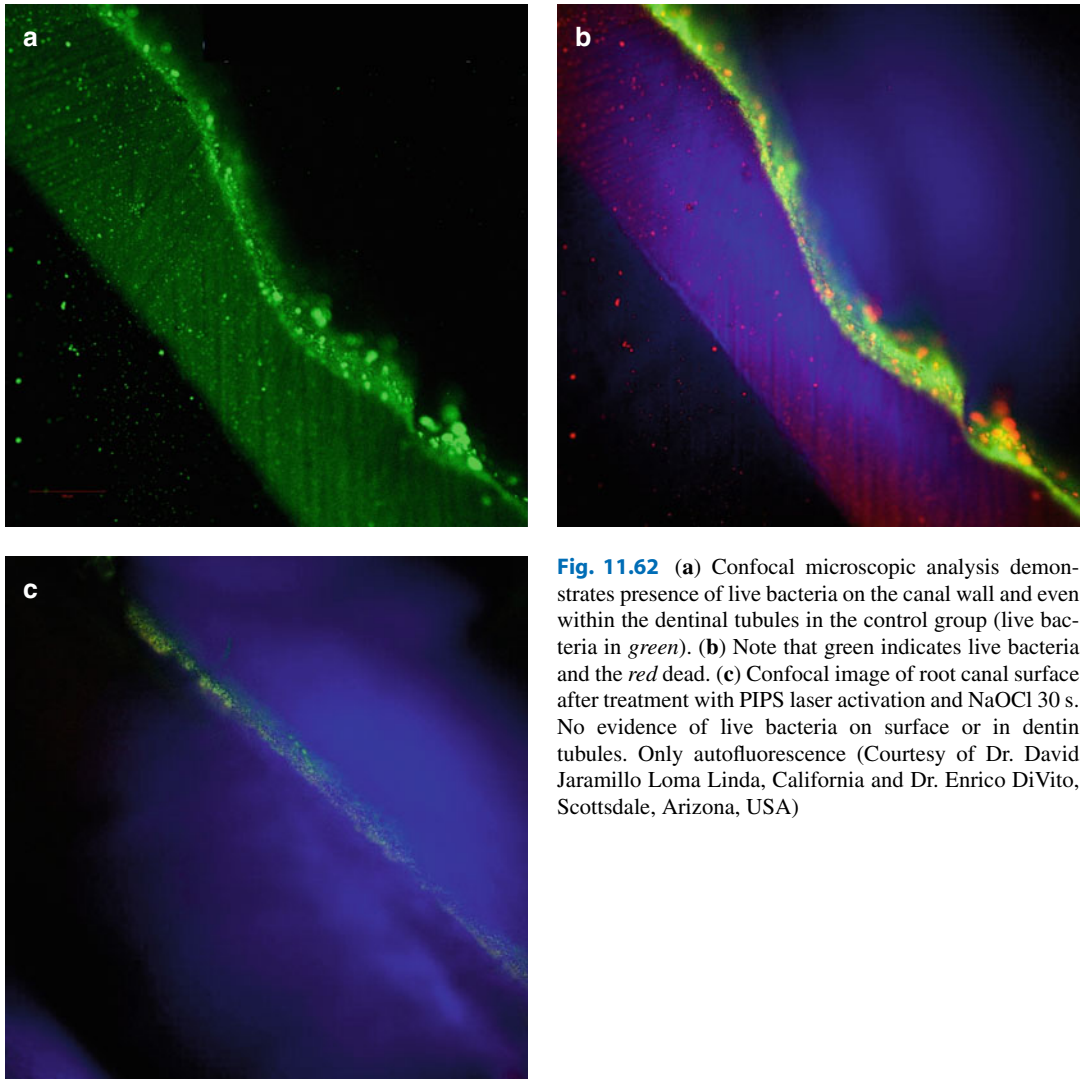

Fig. 11.62 (**a**) Confocal microscopic analysis demonstrates presence of live bacteria on the canal wall and even within the dentinal tubules in the control group (live bacteria in *green*). (**b**) Note that green indicates live bacteria and the *red* dead. (**c**) Confocal image of root canal surface after treatment with PIPS laser activation and NaOCl 30 s. No evidence of live bacteria on surface or in dentin tubules. Only autofluorescence (Courtesy of Dr. David Jaramillo Loma Linda, California and Dr. Enrico DiVito, Scottsdale, Arizona, USA)

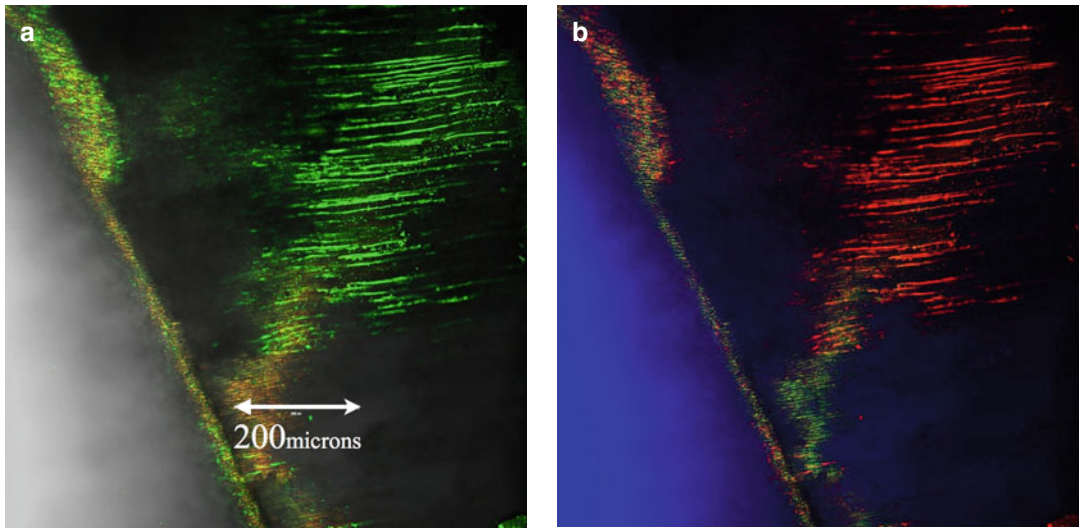

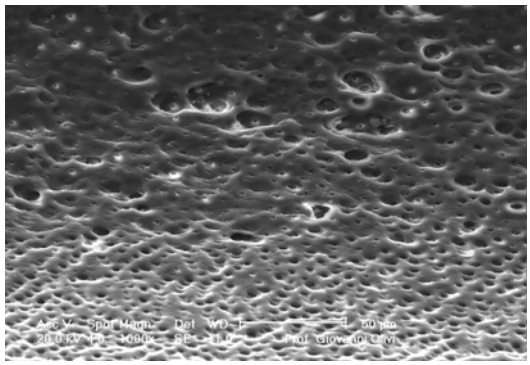

Fig. 11.64 SEM image (1000×) of *E. faecalis*-infected root canal after PIPS: two 30s cycles of sodium hypochlorite irrigation and one 30s cycle of EDTA. Note the absence of bacteria and lack of smear layer, open dentin tubules, and the absence of laser-induced thermal damage (Image of Dr. Giovanni Olivi, Rome (Italy))

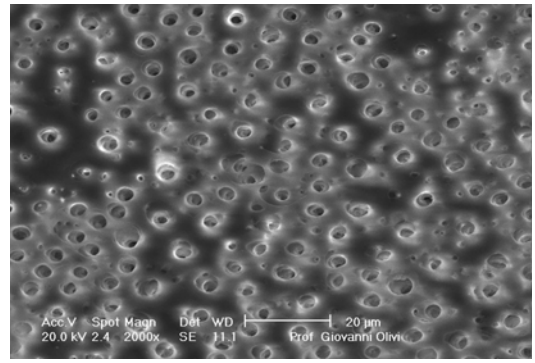

Fig. 11.65 SEM image (2000×) of middle one-third root canal (6 mm short from the apex), infected with *E. faecalis*, after PIPS, shows evidence of lack of smear layer, open dentin tubules, and the absence of laser-induced thermal damage (Image of Dr. Giovanni Olivi, Rome (Italy))

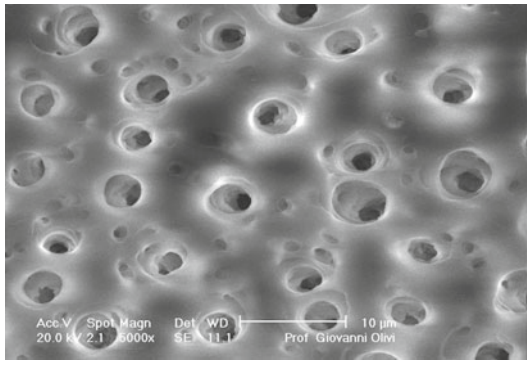

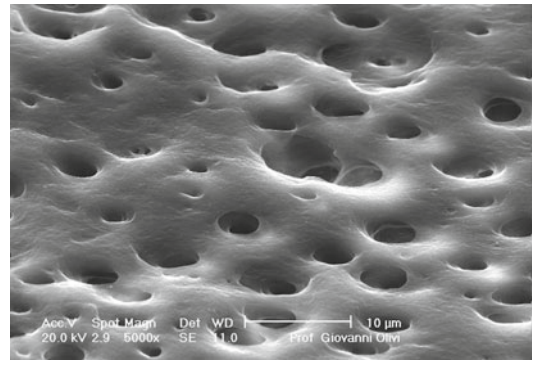

Figs. 11.66 and 11.67 SEM image (5000×) of apical one-third root canal (3 mm short from the apex), infected with *E. faecalis*, after PIPS, shows evidence of lack of smear layer, open dentin tubules, and the absence of laser-induced thermal damage (Image of Dr. Giovanni Olivi, Rome (Italy))

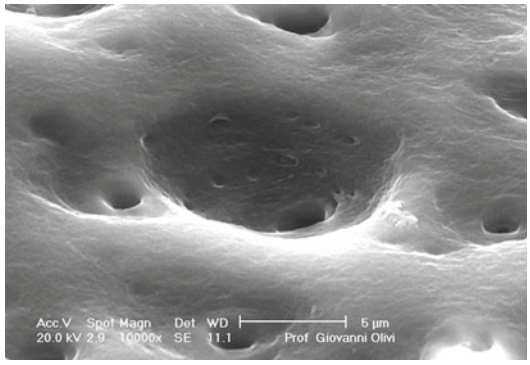

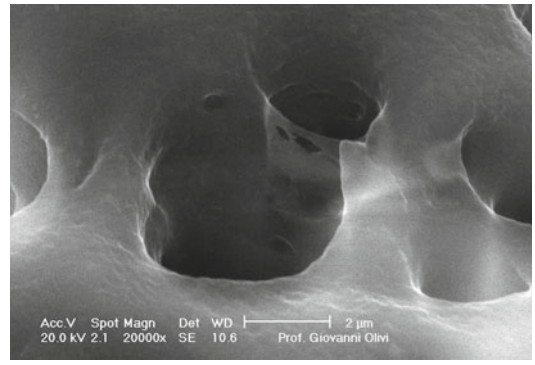

Figs. 11.68 and 11.69 Higher SEMs magnification undisturbed and preserved dentin organic structure after PIPS (two 30s cycles of sodium hypochlorite irrigation and one 30s cycle of EDTA). Lack of bacteria, debris, smear layer, and open dentin tubules (Image of Dr. Giovanni Olivi, Rome (Italy))

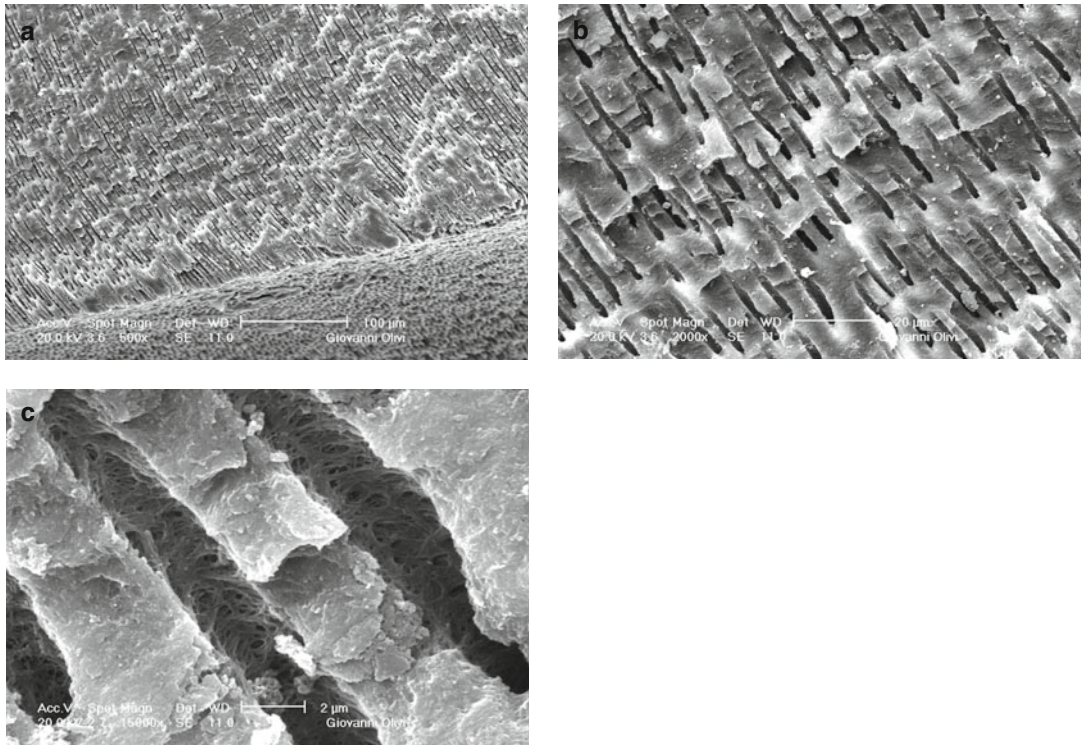

Fig. 11.70 (**a**–**c**) SEM images of split cross sections at 5 mm from the apex showed absence of debris and bacteria into dentinal tubules. (**c**) The organic structure appeared intact (Image of Dr. Giovanni Olivi, Rome (Italy))

of the incubated samples of PIPS group compared to the hand irrigation group that showed bacterial growth in 10/10 samples. SEM images of cross sections at 5 mm from the apex showed absence of debris and bacteria into dentinal tubules. The organic structures appeared intact [51] (Fig. 11.70a–c).

During the same experimental session, five samples underwent the same contamination and incubation method and were treated with the same protocol, but at lower PIPS setting of 15 mJ, 15 Hz, and 0.225 W. After treatment, preliminary test resulted in no detectable growth in all five samples, confirming the disinfecting and cleaning ability of PIPS also at a lower level setting.

Ordinola-Zapata et al. (2014) compared the removal of biofilm utilizing four irrigation techniques on a bovine root canal [15].

Plaque from human volunteer after 72 h of continuous accumulation generated oral biofilm that was collected, incubated, and used to infect 50 dentin specimens (2×2 mm) that were adapted to previously created cavities in tooth bovine model. Different treatment modalities were used for 60s (3 cycles × 20s): needle irrigation, endoactivator, passive ultrasonic irrigation, and laser-activated irrigation (PIPS), in conjunction with 6 % NaOCl, were used to clean in situ biofilm-infected bovine dentin. Subsequently, the dentin samples were separated from the model and analyzed using a scanning electron microscope (SEM). The laser-activated irrigation (PIPS) group exhibited the most favorable results in the removal of biofilm. Passive ultrasonic irrigation scores were significantly lower than both the endoactivator and needle irrigation scores. Sonic and needle irrigation were not significantly different [15].

Olivi M. et al. (2014) assessed the efficacy and effectiveness of an erbium:YAG laser-activated irrigation technique for root canal disinfection, using PIPS tip and protocol, in comparison with conventional irrigation (CI). The study resulted in very effective eradication of the *E. faecalis* from experimentally infected root canal walls, encouraging the possible application of the PIPS technique in endodontics [52].

Lately, Al Shahrani et al. (2014) reported that the use of the PIPS system along with 6 % NaOCl showed the most efficient eradication of the bacterial biofilm, greatly enhancing the disinfection of the root canal system [54].

11.13 Discussion

Despite the positive results obtained by PIPS studies that followed a standardized and controlled protocol, some study reported contradictory results or absence of significant relevant difference in the results between the PIPS group and the control groups.

Note: It is important to look into more depth with an analysis and discussion of the relative protocols used to understand why these different results occurred to thoroughly understand the mechanism of action and the protocol of this technique.

Zhu et al. (2013) investigated both the antibacterial efficacy and smear layer removal ability of PIPS in comparison with conventional syringe irrigation in vitro [31].

The results of their study reported no bacteria observed by SEM in the CI group (NaOCl, NaOCl + EDTA) and in the PIPS + NaOCl group, with no significant differences in CFU reduction between the laser and non-laser groups.

The scores of smear layer of the CI group, where NaOCl + EDTA was used, and PIPS group that used only NaOCl were significantly lower than those of the other groups in the coronal and middle-third of the root canal, but none of the methods can effectively remove smear layer in the apical third.

Two main points can explain these results:

- The canal size of the prepared teeth and
- The irrigants used

The canal size was enlarged to a size #40 K-file and 4 % taper to facilitate the placement of the irrigation needle in the apical one-third, enhancing its fluid dynamics and cleaning capacity, so that there would be less difference in their disinfecting ability. Such an aggressive preparation of the apical portion results in no difference in the disinfecting ability of the two methods. Correspondingly it also leads to reduction of the root strength and integrity making the tooth more susceptible to fracture. In the discussion session, Zhu et al. highlighted this topic, emphasizing that the canal size may play a fundamental role in the cleaning efficacy of PIPS, claiming that one of the benefits of the PIPS system is the minimal root canal preparation required. This is advantageous when treating teeth in vivo having different shapes and sizes such as the lower incisors and the mesial roots of the upper and lower molars where it is not recommended that the size of instrumentation be large at the apex (such as 40 ISO).

The second point to be made is the scientifically unacceptable comparison of two irrigation methods that use different solutions in the two groups. Hand irrigation was tested using both NaOCL and EDTA, while only NaOCL was used for laser activation only. Furthermore the use of NaOCL for smear layer removal is not appropriate.

In conclusion the investigations used in this study were not well designed and not similar to in vivo conditions resulting in misleading conclusions.

Deleu et al. (2013) investigated the efficacy of different laser-activated irrigation methods in

removing debris from simulated root canal irregularities. The results of the study were not in line with the most recent studies of PIPS technique [29].

Conventional irrigation removed significantly less debris from the groove than the three laser groups (diode 980 nm, Er:YAG with 300 μm flat, or PIPS tip), manual dynamic irrigation (MDI), and passive ultrasonic irrigation (PUI) ($p<0.001$). Erbium:YAG laser with the flat fiber tip removed significantly more debris than the diode laser ($p=0.007$), the MDI ($p=0.02$), and the erbium laser using the PIPS tip ($p=0.004$), but the amount of debris was not statistically different from that found in the PUI group. No statistically significant differences were observed between PUI, MDI, and Er:YAG-PIPS groups.

The protocol used explains the lack of evidence in the PIPS group:

- The teeth were decoronated, so the fluid reservoir needed for the photoacoustic effect was absent in the PIPS group.
- The laser was operated at too high an energy and power, 40 mJ, 20 Hz, and 0.8 W, so that the pulse length of 50 μs and the higher peak power of 800 W evaporated the intracanal irrigant causing fluid depletion. This accounted for the ineffective irrigation found as well as the thermal damage to the dry canal.
- Finally, the irrigation was not delivered continuously, but rather intermittently for 5s, with four repetition cycles. This is not the correct PIPS protocol advocated and confirmed as effective.

The study reported that when the laser was activated, small portions of NaOCl were forced out of the canal with every pulse resulting in the PIPS tip not being submerged but rather in a fluid-free canal entrance after about 4s. The authors concluded that this event evidently limited the further action of the tip.

These problems have been exhaustively explained before.

11.14 PIPS: New Concept in Cleaning and Shaping the Root Canal

Essential to the success of endodontic treatment is the elimination of microorganisms and their by-products from the root canal system.

A limiting factor in canal disinfection is the inability to adequately have the irrigant enter canal isthmuses and ramifications because they are blocked by dentin chips created during the mechanical preparation or by infected pulp tissues and their associated microbes or by residual endodontic filling material. Additionally, the blockage of canal isthmuses prevents fluid interchange regardless of the volume of irrigant.

Upon examination of the complex morphologies associated with molars and premolars, it is apparent that the isthmus remains untouched during canal preparation (Figs. 11.71 and 11.73a–e) (see also Fig. 11.53b). Enlarging canals to include isthmus preparation results in sacrificing too much tooth structure, gross enlargement, and likely root perforation while not significantly increasing the amount of contact of the instrument to dentin in the canal. Conventional endodontics claims the concept that proper shaping is a prelude to an adequate supply of irrigation and a good apical obturation [1].

Accordingly, as in the aphorism of Herbert Schilder [54], the success of endodontic therapy depends more on “what we take away” (instrumentation) than “what we put into” (obturation) the root canal system. That being said the success of endodontic therapy relies heavily on the chemomechanical preparation phase for emptying the contents of the root canal system.

PIPS has been shown to be effective in eliminating microbes, both planktonic and biofilm, in areas not effectively instrumented or prepared at all during instrumentation (Figs. 11.72a, b, 11.74a, b, and 11.75a, b). The strong body of evidence that shows PIPS action lyses bacteria and sterilizes dentin tubules, which have been reported in the previous paragraphs.

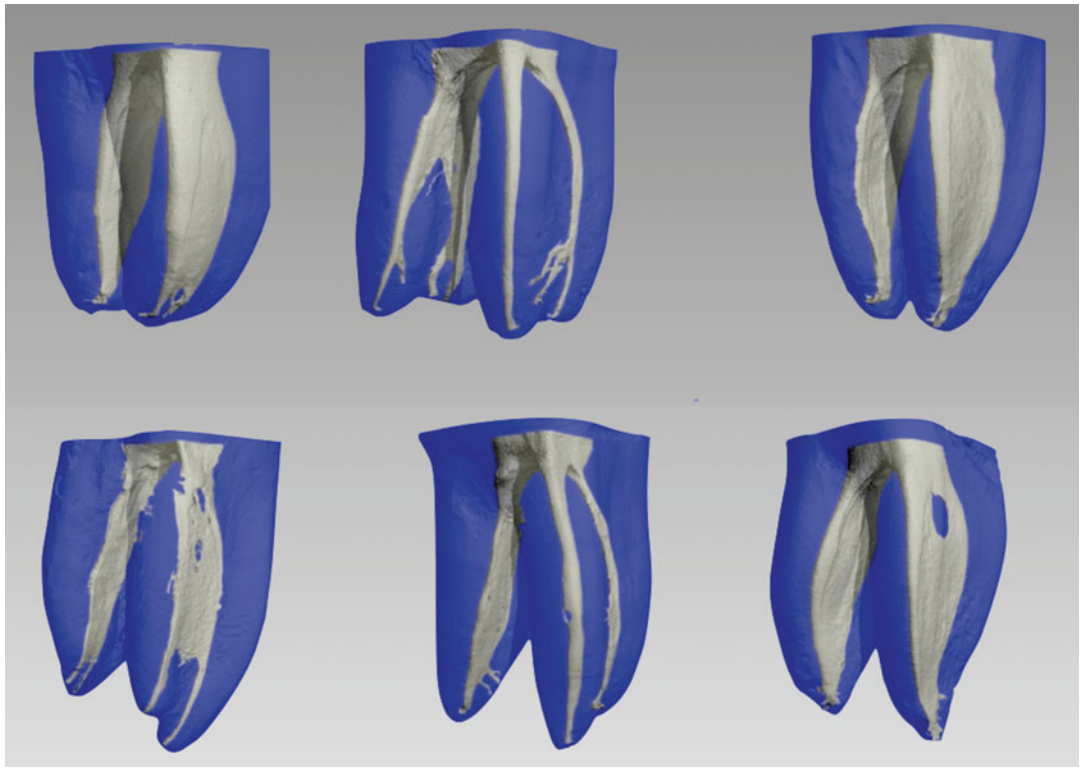

Fig. 11.71 Complex morphologies of lower molars seen with these micro CT scans (Courtesy of Dr. Ove Peters San Francisco, California and Dr. Enrico DiVito Scottsdale, Arizona)

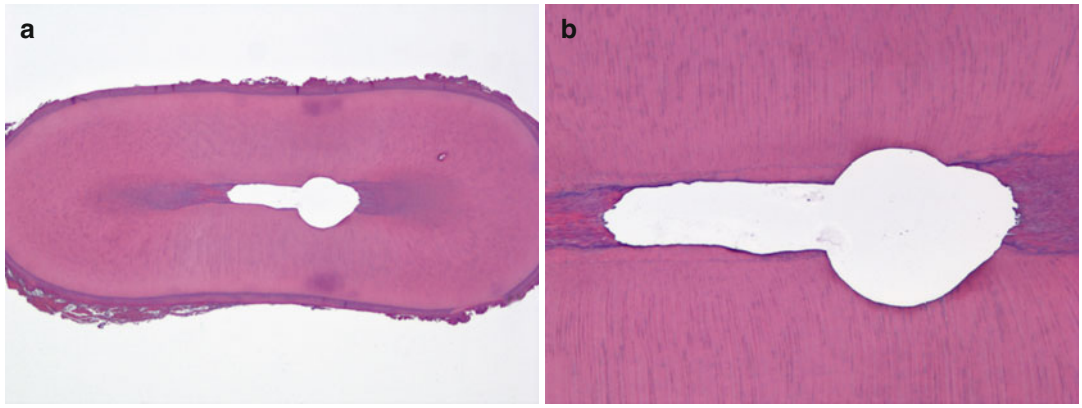

Fig. 11.72 (**a**, **b**) PIPS is effective in eliminating pulp tissue and microbes in areas not effectively instrumented or prepared at all during instrumentation. A file ISO 25/04 was used to prepare a single root lower incisor; most of the canal surface remains unchanged by the preparation but however clean (Histology images courtesy of Dr. Domenico Ricucci, in cooperation with Dr. Giovanni Olivi Rome, Italy)

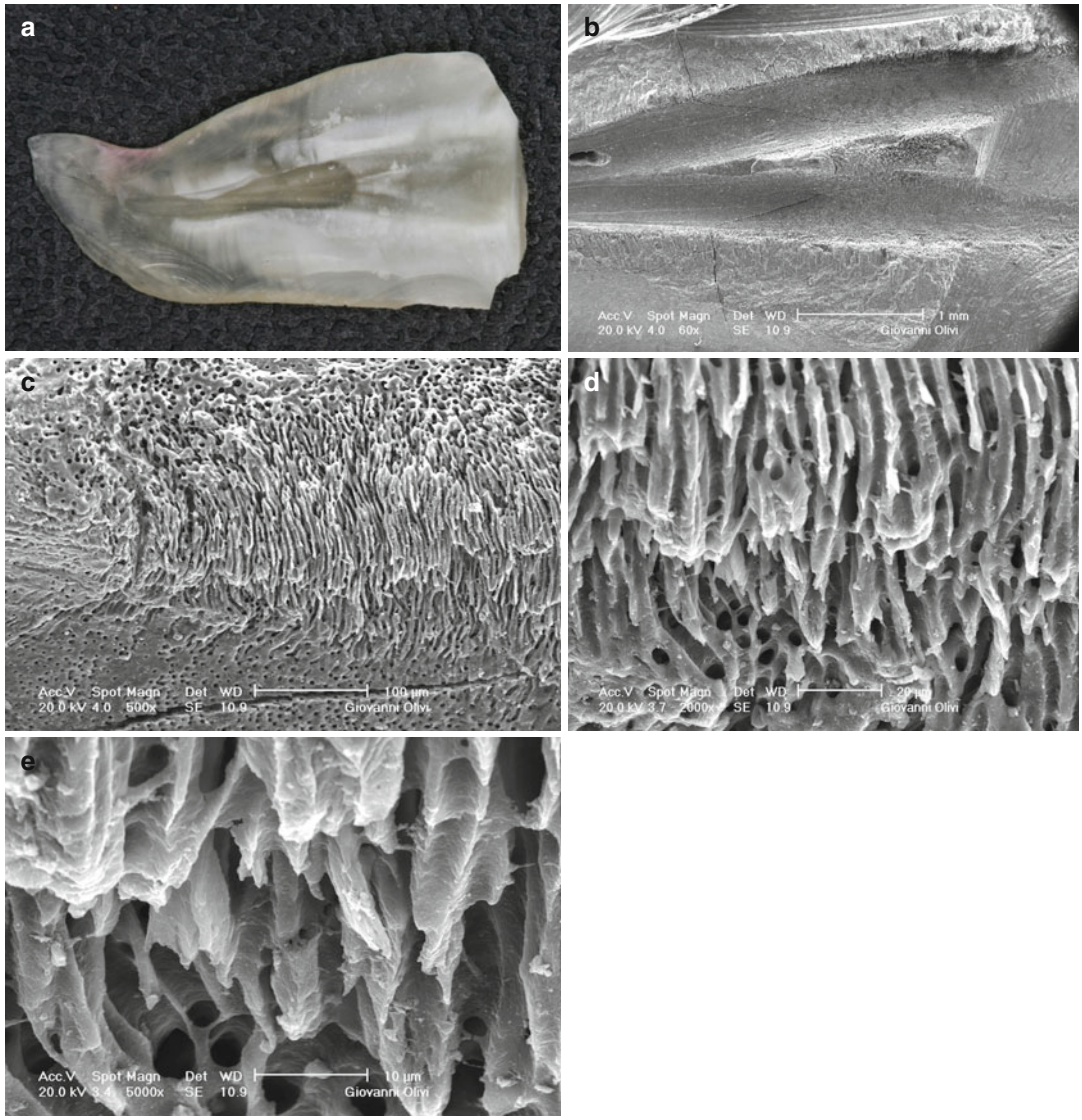

Fig. 11.73 (**a**–**e**) Upon examination of the complex morphologies associated with premolars, it is apparent that the isthmus remains untouched during canal preparation. However after two 30s cycles of sodium hypochlorite irrigation and one 30s cycle of EDTA activated by PIPS, the surfaces are clean and bacteria-free (Image of Dr. Giovanni Olivi, Rome (Italy))

It is important to know that the PIPS technique can be applied regardless of the type of shaping and instrumentation method chosen to prepare the canal system. It is very effective at removing both vital and necrotic tissue. It has also been demonstrated to be effective at opening and helping negotiate calcified canals and removing separated or fractured instruments and antibiotics and medication pastes (Figs. 11.76a, b and 11.77a, b).

The following protocols for the correct use of PIPS are described later on.

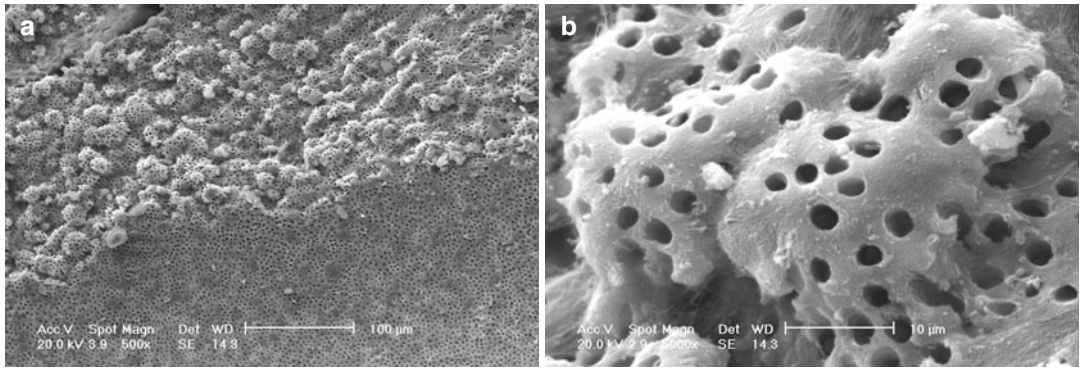

Fig. 11.74 (**a**, **b**) SEM (500× and 5000×) images of root canal surface after mechanical preparation and PIPS. The globular formation on the surface is the so-called calcospherites, the mineralization front of predentin; the presence of these structures indicates that this part of dentin wall was not shaped; however, surfaces are clean as a result of PIPS laser-activated irrigation (Image of Dr. Giovanni Olivi, Rome (Italy))

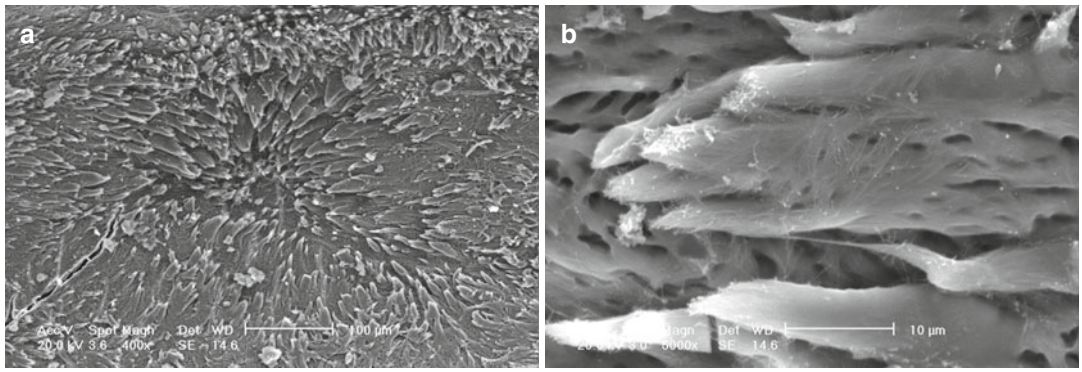

Fig. 11.75 (**a**, **b**) SEM (400× and 5000×) images of root canal surface after mechanical preparation and PIPS. Calcospherites indicate that this part of dentin wall was not shaped but was however cleaned after PIPS (Image of Dr. Giovanni Olivi, Rome (Italy))

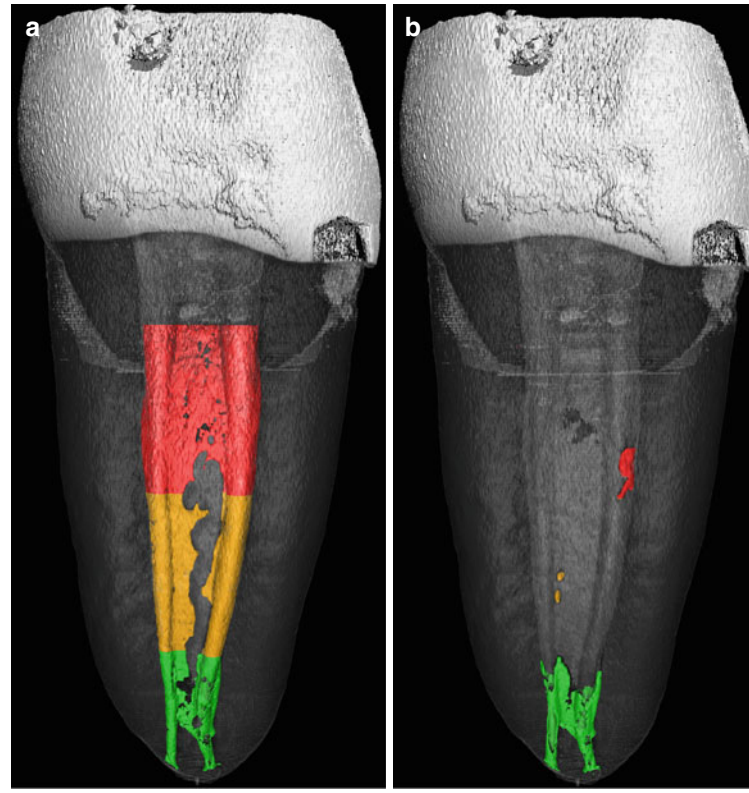

Fig. 11.76 (**a**) Sample showing distribution of Ca(OH)2 before ultrasonically activated irrigation. (**b**) *Red* and *orange* areas represent remaining Ca(OH)2 after irrigation with sodium hypochlorite energized with ultrasonics. *Green* apical third shows significant remaining Ca(OH)2 unable to be removed (Images courtesy of Prof. Adam Lloyd Chair Department of Endodontics, University of Tennessee Health Science Center)

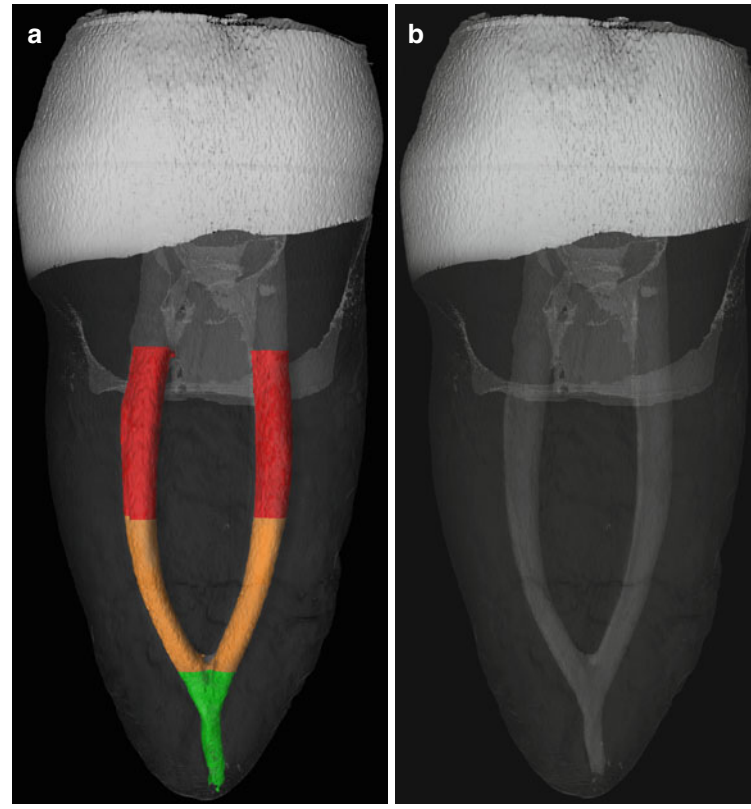

Fig. 11.77 (**a**, **b**) Weine type II canal configuration with instrumented canal filled with calcium hydroxide [Ca(OH)2] in coronal (*red*), middle (*orange*), and apical (*green*) thirds. (**b**) PIPS completely eliminated all Ca(OH)2 from complex system (Images courtesy of Prof. Adam Lloyd Chair Department of Endodontics, University of Tennessee Health Science Center)

11.15 PIPS Protocol for Primary Endodontic Treatment for Both Vital and Necrotic (Includes Acute or Chronic Pulpitis)

This paragraph describes the protocol and technique preferred by the authors that utilize a combination of hand and rotary instrumentation and PIPS irrigation.

11.15.1 Access Opening and Glide Path

Access opening is made in the usual manner using a small carbide or round diamond burr. Erbium:YAG laser can also be used to create the access to the chamber and remove the pulp tissue without a burr. Both the handpieces (with or without tip) can be utilized for this purpose. Irrigation with sodium hypochlorite helps to

Fig. 11.78 (**a**–**c**) Intraoperative micrograph of complete excavation of carious lesions and the selective removal of pulp tissue in the chamber allows remaining canal orifices to be visualized and confirmed with an endodontic explorer

remove the coronal pulp tissues. Upon complete excavation of carious lesions and the selective removal of pulp tissue in the chamber, the remaining canal orifices can be visualized and confirmed with an endodontic explorer (Fig. 11.78a–c). Creating an appropriate convenience form during access preparation (straight-line access) is always preferred and advised (Fig. 11.79a–d). For this purpose the ultrasonic instruments with a diamond tip work very well because of their long, curved, and thin stem design allowing for a very precise and controlled application while using a microscope. The cavity walls are consequently flared, rounded, and smoothed to facilitate easy and straight access into the root canal [55] (Figs. 11.80, 11.81, 11.82, 11.83, 11.84, and 11.85). The design and size of the access opening are related to the health of the remaining tissue and to the position of the canal orifices (Fig. 11.86a–c); however, in case of coronal destruction, a buildup of the crown walls is mandatory to create a coronal reservoir for adequate volume of irrigants to be activated (Fig. 11.87a, b). A preflaring of the orifice and enlarging of the coronal one-third of the canal allow for easy and direct access to the canal apex (Fig. 11.88).

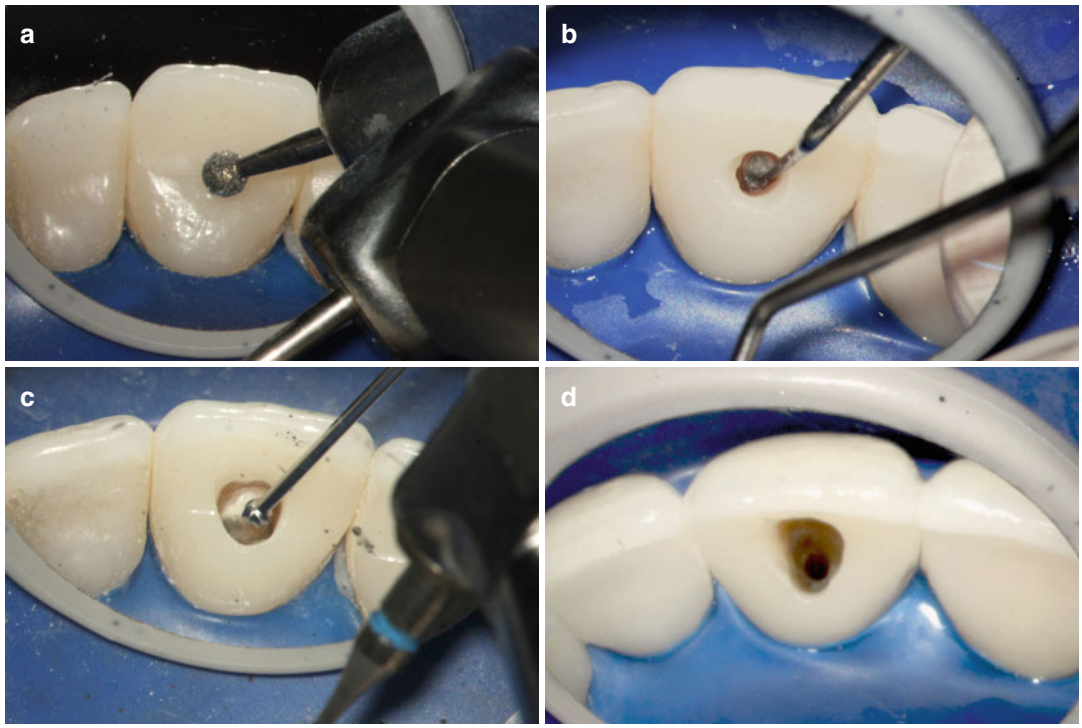

Fig. 11.79 (**a**–**d**) Creating an appropriate convenience form during access preparation (straight-line access) is always preferred and advised. (Courtesy Dr. E. DiVito, Scottsdale AZ, USA)

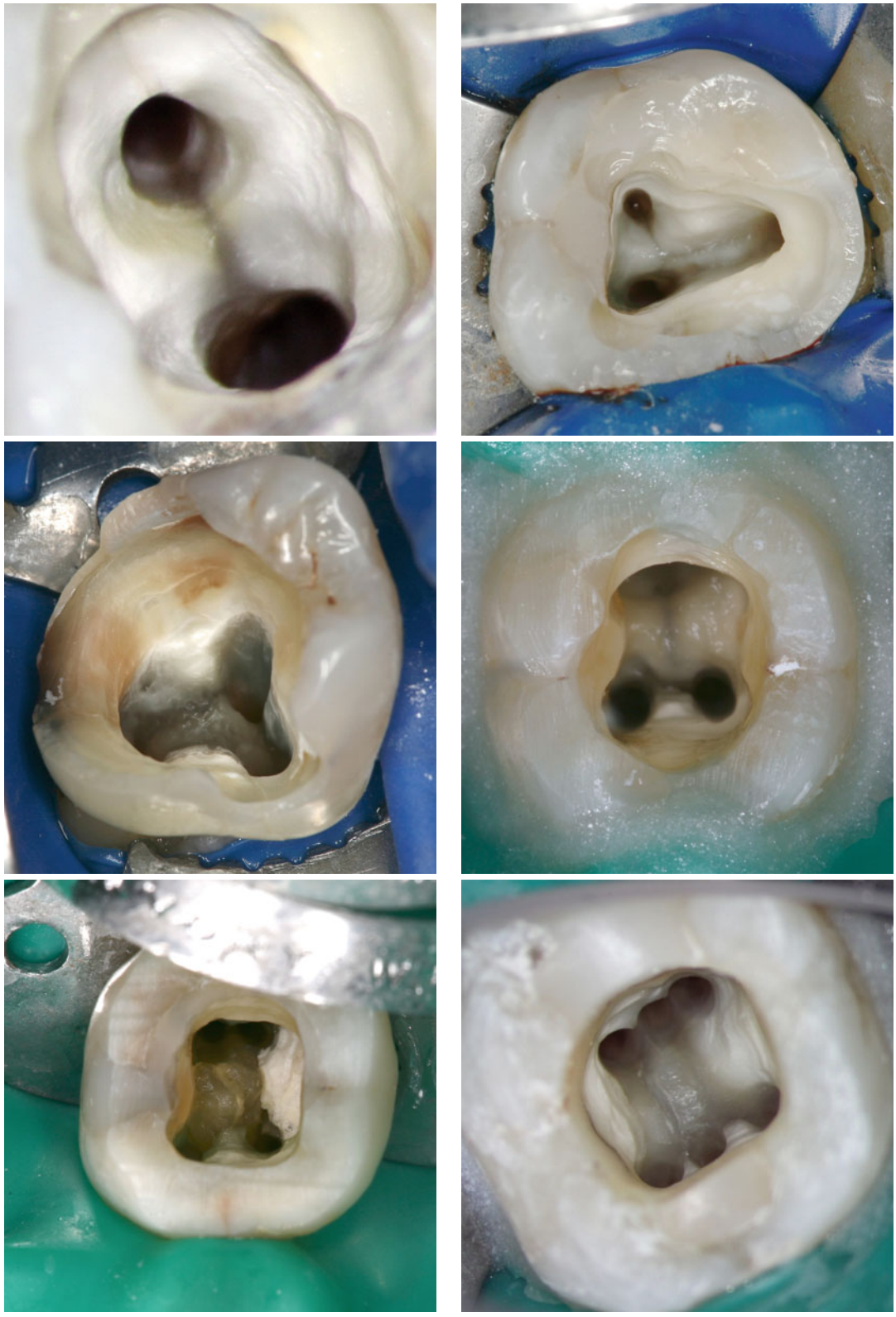

Figs. 11.80, 11.81, 11.82, 11.83, 11.84 and 11.85 Intraoperative micrographs walls are flared, rounded, and smoothed to facilitate easy straight-line access into the root canal. Note the extremely clean surface ((Figs. 11.80 and 11.85 Courtesy of Dr. Thomas McClammy Scottsdale, Arizona, USA) Permission received)

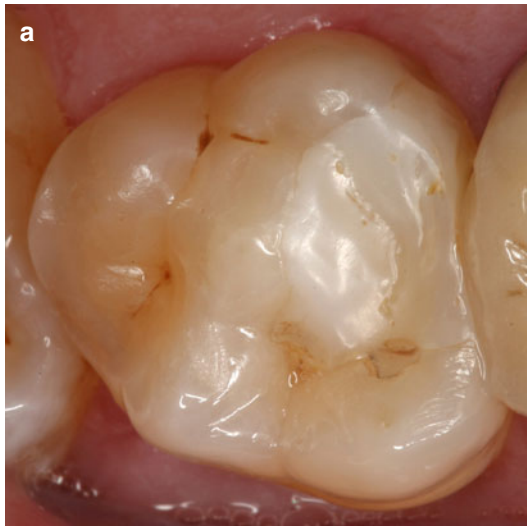

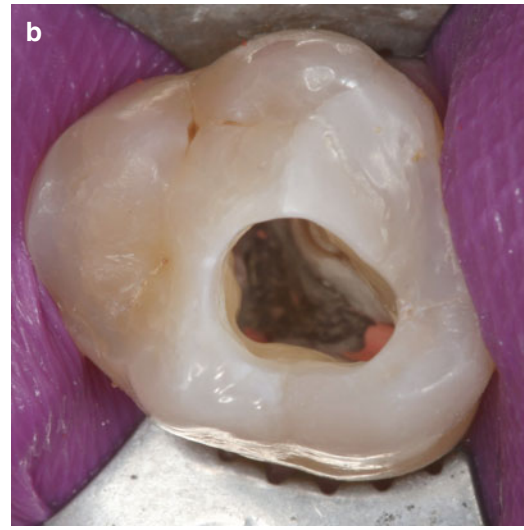

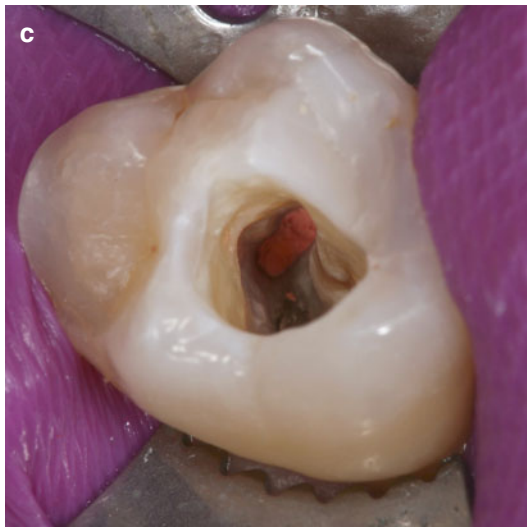

Fig. 11.86 (**a**–**c**) The design and size of the access opening are related to the health of the remaining tissue and to the position of the canal orifices

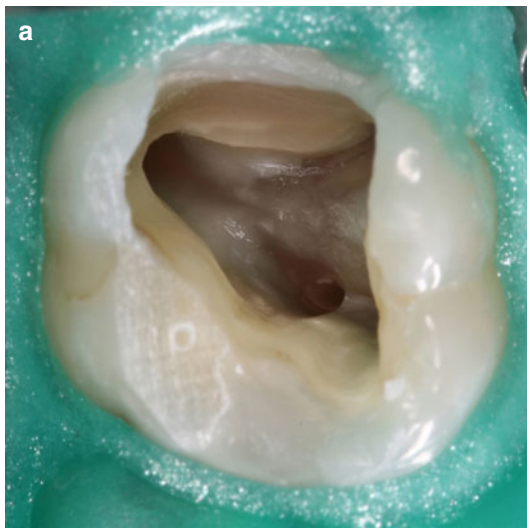

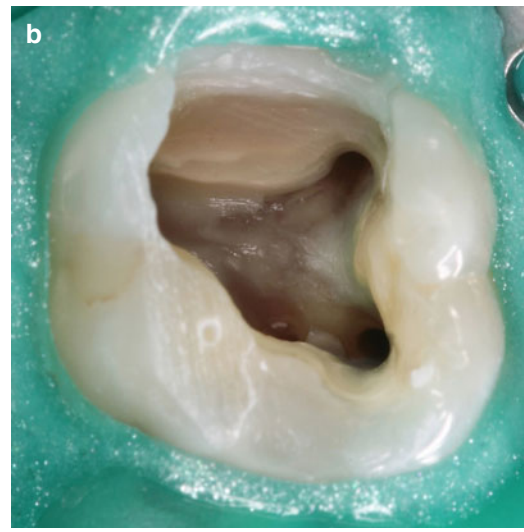

Fig. 11.87 (**a**, **b**) Buildup of the crown walls (mesial and distal walls) is mandatory to create a coronal reservoir for adequate volume of irrigants to be activated when using PIPS™

Fig. 11.88 Ultrasonic tips are used to finish and round the chamber shape. Gates Glidden drills in different sizes from 1 to 6 (corresponding to 0.50, 0.70, 0.90, 1.10, 1.30, and 1.50 mm diameter) and lengths are mainly used for enlarging the canal orifices of the coronal one-third of the root canal

11.15.2 Anatomical and Working Length of the Canal

After establishing a direct *glide path* to the apical one-third, using hand stainless steel 10 and 15 files or Ni-Ti thin and flexible rotary files in NaOCl wet canal (Fig. 11.89, 11.90, 11.91, and 11.92), a small stainless steel hand file (#.06 or #.08 ISO) is used to determine the *anatomical length* (Figs. 11.93 and 11.94). Lubricant gel containing urea peroxide (such as RC-Prep; Premier Products Co; PA-USA) is placed on the file before inserting into the canal to lubricate and avoid tissue plugging that may occur when sliding the file to the anatomic opening (Figs. 11.93 and 11.95). Use of an electronic apex locator (ROOT ZX, J Morita Co.; Kyoto, Japan or Apit-Endex, Osada Electronics) and a radiograph confirmation will provide verification of the correct working length at the apex (Figs. 11.96 and 11.97).

11.15.3 Shaping the Root Canal

Whatever the canal length is determined to be, that value is shortened by 1 mm to which all the subsequent files will be instrumented to. Irrespective of the instrumentation technique used, after each filing step, continuous laser-activated irrigation (PIPS) of 30s with sodium hypochlorite will digest the vital and/or necrotic tissue in the canal. NaOCl is left in the chamber as a lubricant, and instrumentation from here forward is always done with adequate hydration and never in a dry field. Instrumentation is always performed sequentially until reaching a size 20 or 25 ISO (Figs. 11.98, 11.99, 11.100, and 11.101). This can be done by hand, rotary, or combination. Patency is confirmed between each file using the smallest hand file possible (typically a .06–.08 ISO hand file) (Fig. 11.102).

The authors find that a combination of hand .06, .08, and .10 rotary glide path files (#13/02 and #16/02 or #10/02 to #20/02) and finally a rotary system of own choice works very well and yields a very consistent and conservative shape (Figs. 11.103, 11.104, 11.105, and 11.106).

Because the PIPS tip does not require that it be placed in the canal at all to effectively stream irrigants into the smaller and morphologically deli-

Fig. 11.89 Stainless steel 10 and 15 files and Ni-Ti rotary 0.13 and 0.16 PathFile (Dentsply; PA-USA) for the preparation of the glide path

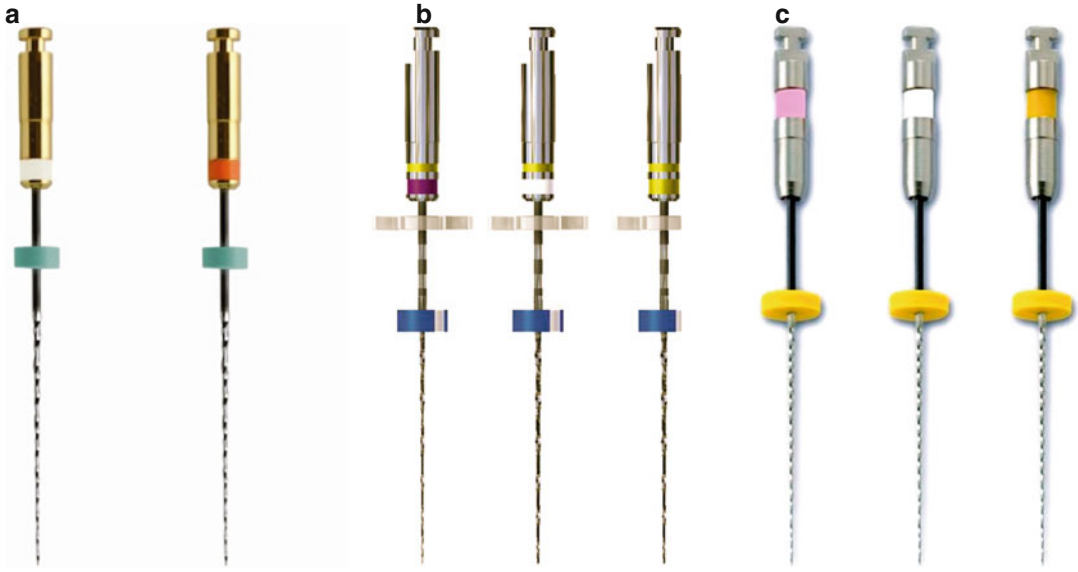

Fig. 11.90 Different Ni-Ti thin and flexible rotary files for preparation of glide path: (**a**) 0.12–0.17/03G-File MicroMega; Besancon, France; (**b**) 0.10-0.15-0.20/02 Scout Race FKG; La Chaux-de-Fonds Switzerland; (**c**) 0.10-0.15-0.20/02 Endowave MGP J Morita Co; Kyoto, Japan

cate apical areas, it is not necessary to open the canal spaces to a larger size. This results in a more conservative and biomimetic result: 25/06 is a canal shape sufficient to warrant a hermetic apical obturation. Previously reported studies have shown both dentin tubules, and biofilm removal occurred when used with the correct protocol described.

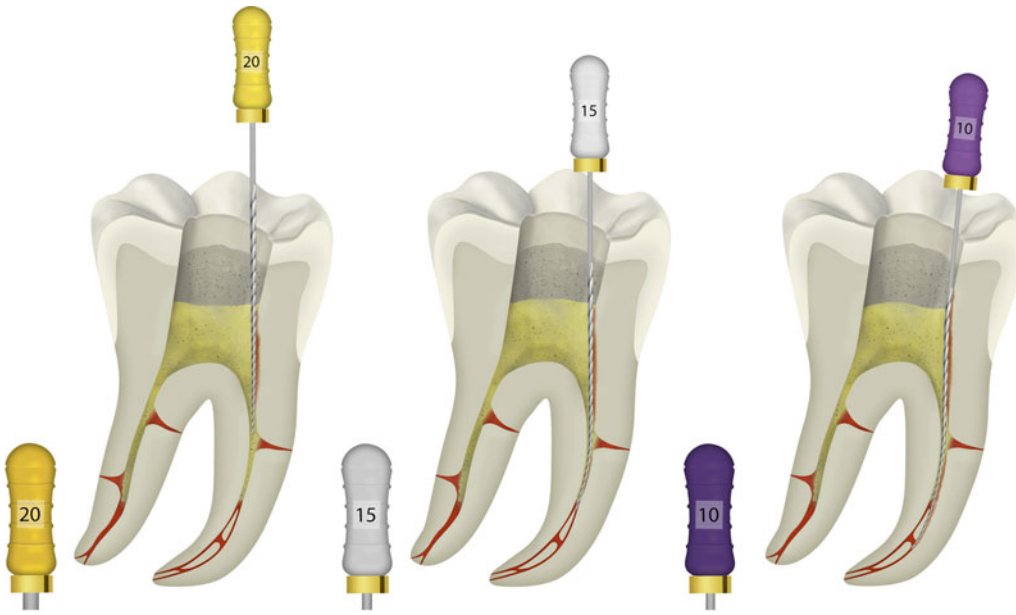

Fig. 11.91 Graphic representation of hand files progressively preparing a direct access to the apical one-third (glide path) (Courtesy of Dr. Giovanni Olivi)

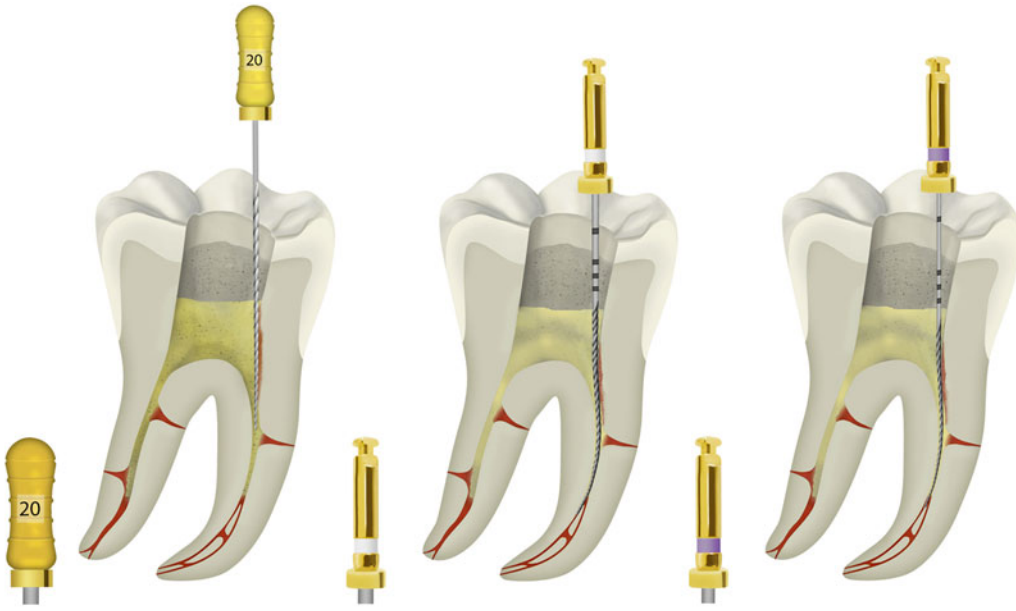

Fig. 11.92 Graphic representation of a combination of hand and rotary files for preparing the glide path (Courtesy of Dr. Giovanni Olivi)

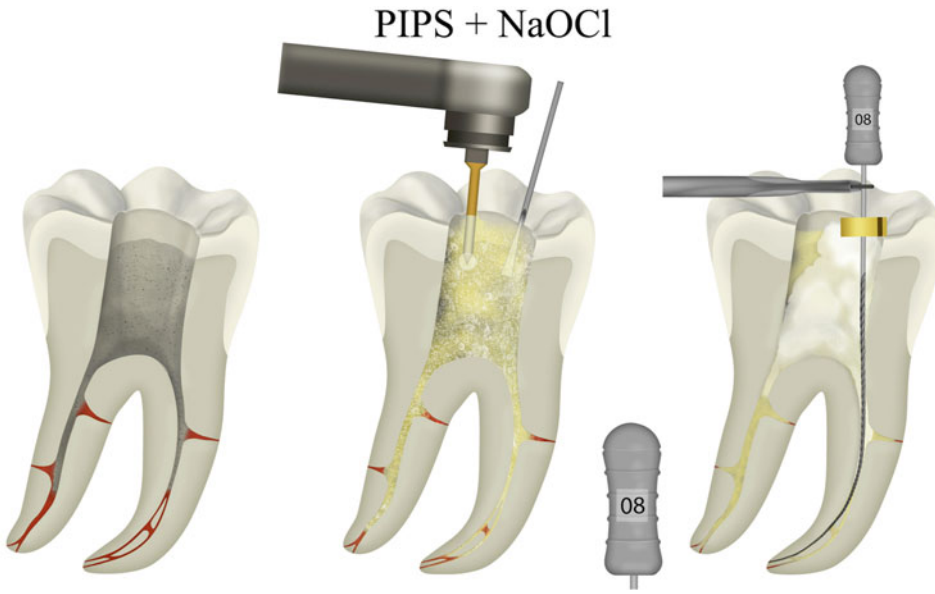

Fig. 11.93 After enlarging the coronal and middle one-third of the canal, PIPS™ and NaOCl are used before using a .06 and .08 file to determine the anatomical length. Lubricant gel containing urea peroxide is placed on the file (or in the cavity) to lubricate and avoid tissue plugging when sliding the file to the anatomic opening (Courtesy of Dr. Giovanni Olivi)

Fig. 11.94 .06 and .08 steel hand K-files are used to determine the anatomical length of the canal and to assure its patency

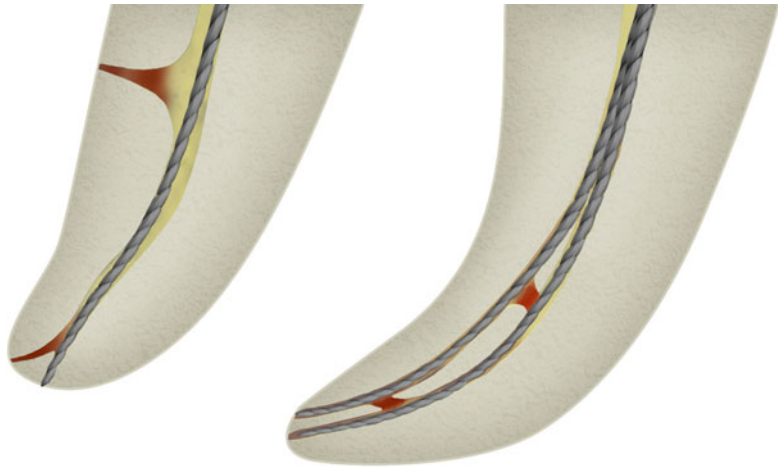

Fig. 11.95 .08 hand files to the root apex (Courtesy of Dr. Giovanni Olivi)

Fig. 11.96 Electronic apex locator (Root ZX by Morita) used to confirm anatomical length

Fig. 11.97 Electronic apex locator (OSADA by OPITA) used to confirm anatomical length

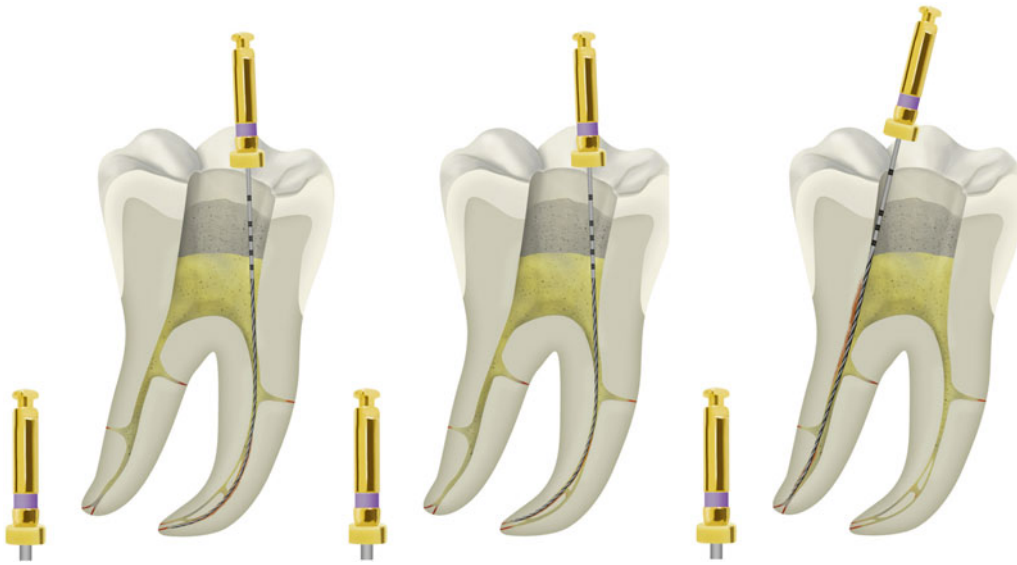

Fig. 11.98 Graphic representation of a .10/2–.13/02 glide path file at working length (anatomical length -1 mm) (Courtesy of Dr. Giovanni Olivi)

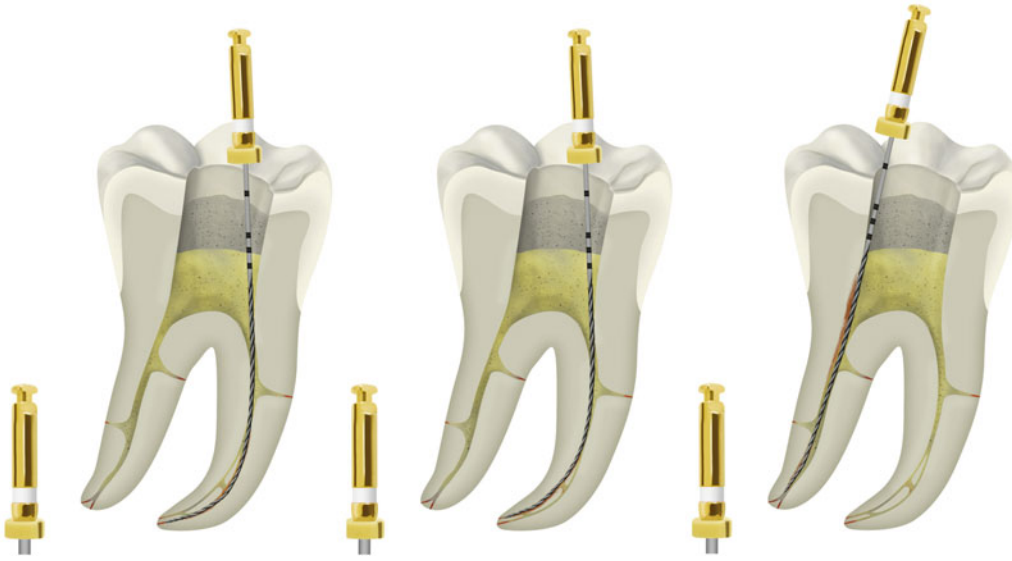

Fig. 11.99 Graphic representation of a .15/2–.16/02 glide path file at working length (anatomical length -1 mm) (Courtesy of Dr. Giovanni Olivi)

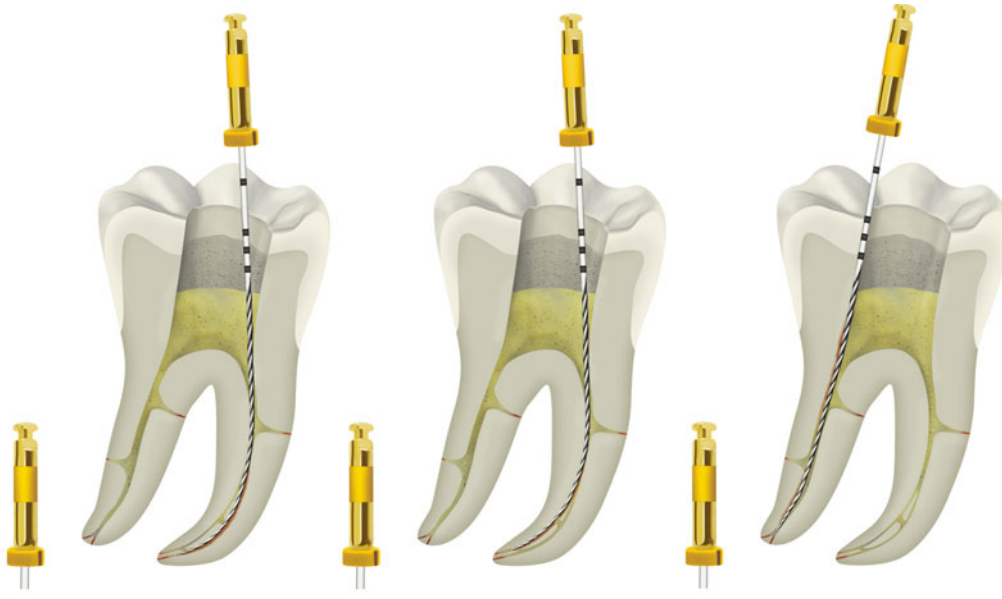

Fig. 11.100 Graphic representation of rotary .20/04 file shaping the canals at working length (Courtesy of Dr. Giovanni Olivi)

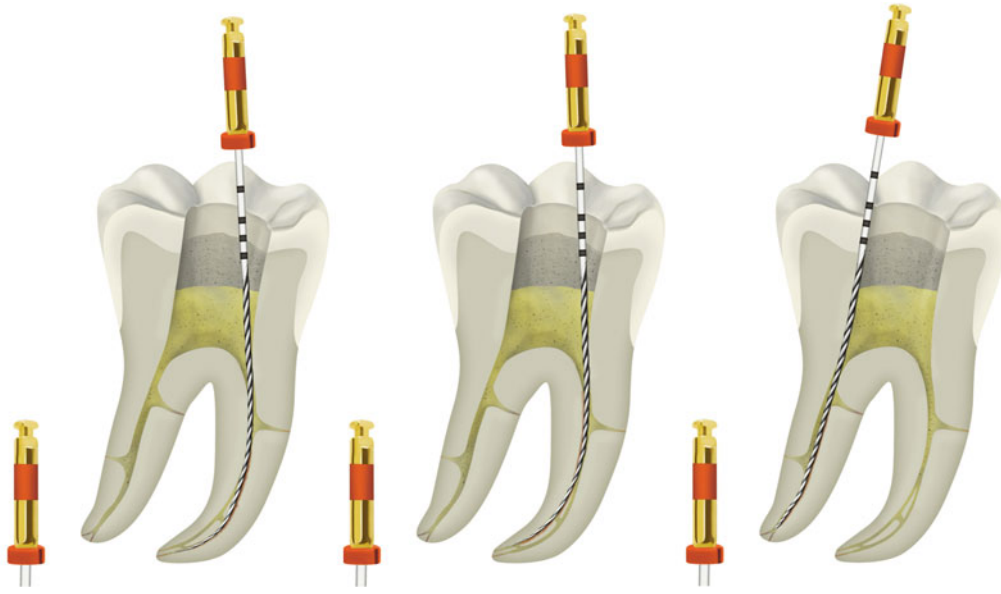

Fig. 11.101 Graphic representation of rotary 25 file enlarging the canals. A shape 04 or 06 taper is used according to anatomic and clinical needs (Courtesy of Dr. Giovanni Olivi)

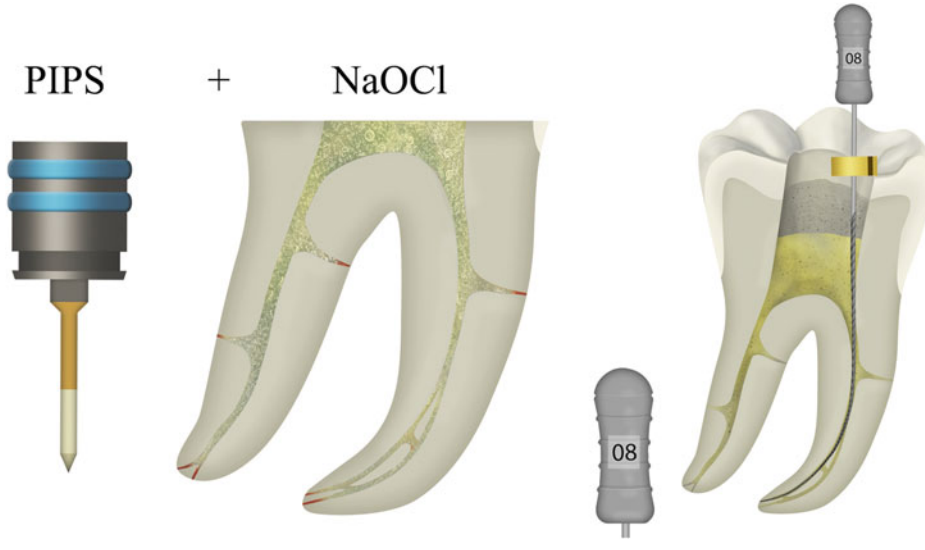

Fig. 11.102 .08 After PIPS™ and NaOCl, the recapitulation with the smaller first instrument (#ISO.06 or .08) is used at the apical anatomic constriction to ensure the apical patency and remove any vital or necrotic tissue and possible dentin plugs produced during instrumentation (Courtesy of Dr. Giovanni Olivi)

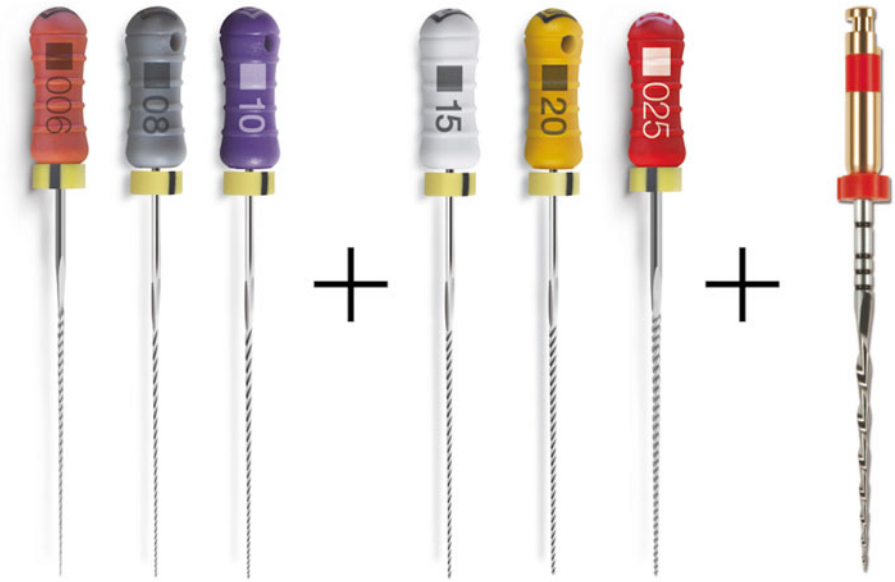

Fig. 11.103 Assortment of hand files for glide path and rotary (Reciproc, Dentsply) for shaping

Fig. 11.104 Combination of hand files and rotary pathfiles (PathFile, Dentsply) for glide path; single rotary file (Reciproc, Dentsply) is used for shaping (easy-medium canals)

Fig. 11.105 Combination of hand files and rotary pathfiles (PathFile, Dentsply) for glide path; different rotary files (WaveOne, Dentsply) are used for shaping (curved and complicated canals)

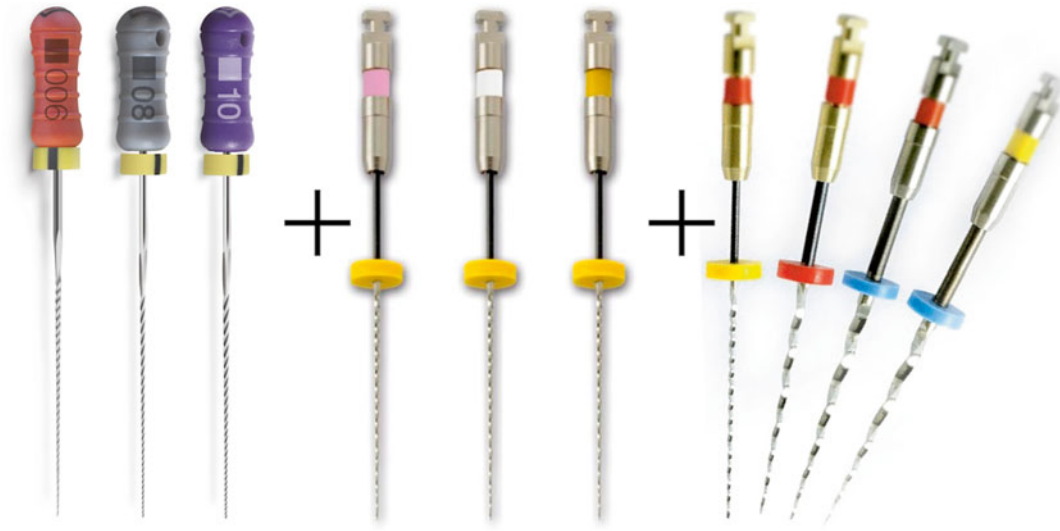

Fig. 11.106 Combination of hand files and rotary pathfiles (Endowave MGP, J Morita Co) for glide path; rotary file series (EndoWave, J Morita Co) is used for shaping curved and complicated canals

11.15.4 Ensuring Apical Patency

After instrumentation and laser-activated irrigation (PIPS) step, recapitulation with the smaller first instrument (#ISO .06 – .08) at the apical anatomic constriction will ensure the apical patency and remove any vital or necrotic tissue and possible dentin plugs produced during instrumentation (Fig. 11.107). Maintaining the natural preexisting size of the anatomic apical constriction allows for a better control of possible fluid extrusion.

Because instrumentation is done 1 mm short of measured canal length, the possibility of

transporting, blocking, or pushing debris and contaminates beyond the apex and into the sensitive periapical tissues is avoided. PIPS fluid dynamics, by virtue of its photoacoustic streaming, effectively kills and removes any remaining tissue, smear layer, and debris for the canal system including the delicate apical one-third.

An intraoral x-ray is performed to verify the correct working length and size before the final canal obturation (Figs. 11.108, 11.109, 11.110, 11.111, 11.112, and 11.113).

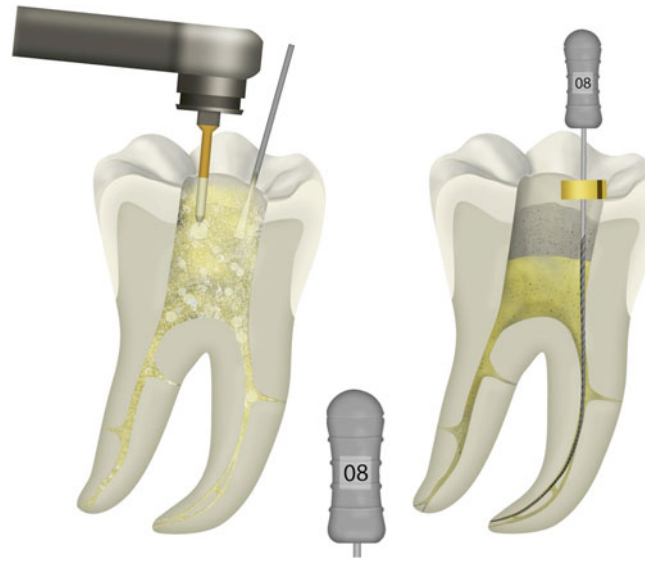

Fig. 11.107 After PIPS™ and NaOCl, the recapitulation with the smaller first instrument (#ISO .06 or .08) is used at the apical anatomic constriction after each file passage to confirm patency (Courtesy of Dr. Giovanni Olivi)

Fig. 11.108 Access cavity of lower lateral incisor allows verification of two canals

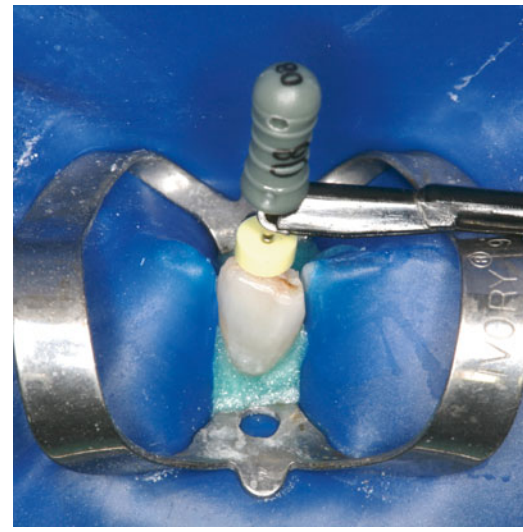

Fig. 11.109 Electronic apex finder helps to find the correct position for determination of anatomical length

Fig. 11.110 Pre-treatment radiograph lower lateral incisor

Fig. 11.111 Radiograph confirmation provides verification of the correct anatomical length at the apex (working length to be reduced 1 mm)

Fig. 11.112 Obturation (20/04) resulting in a more biomimetic conservative shape (6 m post-op)

Fig. 11.113 A 9-month post-op x-ray shows the complete healing of the periapical lesion

11.15.5 PIPS Irrigation Protocol

A laser-activated irrigation (PIPS) of 30s with continuous sodium hypochlorite is used after each filing step. Upon reaching the desired final file size, the following PIPS laser-activated irrigation protocol is performed: Use of distilled water between NaOCl and EDTA avoids any chemical reactions between the different fluids. Sterile water used as the final step in the PIPS protocol reduces the release of oxygen from the solution in the root canal system possibly modifying the polymerization of resin-based root canal sealers.

The tip is placed into the access cavity only and kept stationary and activated with each of the following irrigating solutions as they are applied into the access cavity with a 27 gauge irrigating needle (Figs. 11.114 and 11.115).

The laser parameters and settings are listed below:

PIPS 600 μm, 9 mm long tapered and stripped tip is mounted on the handpiece; pulse duration is set on SSP (50 microsecond), and pulse energy on 20 mJ, and pulse repetition rate is set on 15 Hz.
Handpiece air-water spray feature is turned off.

1. 30s of PIPS with continuous flow of 17% EDTA (3 ml)
2. 30s of PIPS with continuous flow of sterile distilled water
3. 30s of PIPS three times (3×) with continuous flow of 5 % NaOCl (3 ml) with 30s no activation between cycles (resting phase)
4. 30s of PIPS with continuous flow of distilled water as the final step before obturation

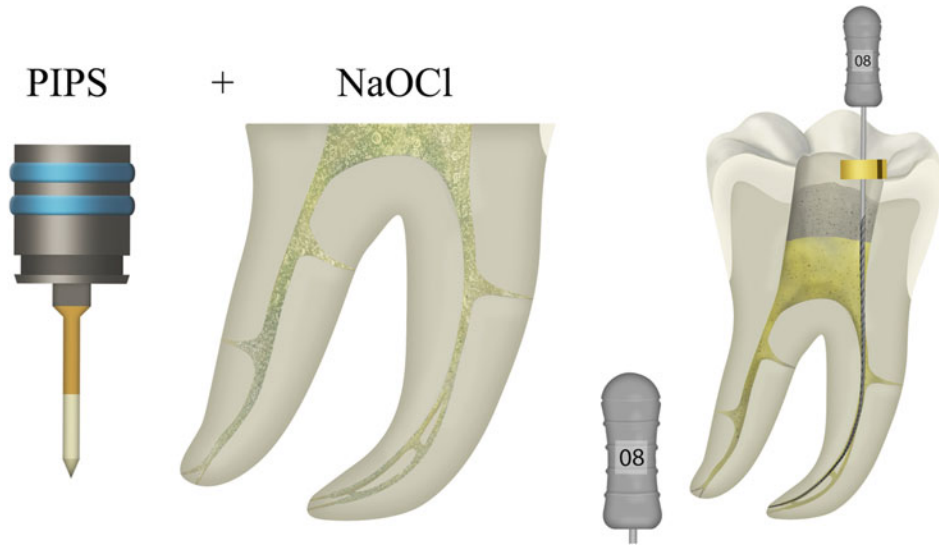

Fig. 11.114 The final step before obturation requires patency to be confirmed using .06 or .08 file after NaOCl irrigation activates by PIPS™ (Courtesy of Dr. Giovanni Olivi)

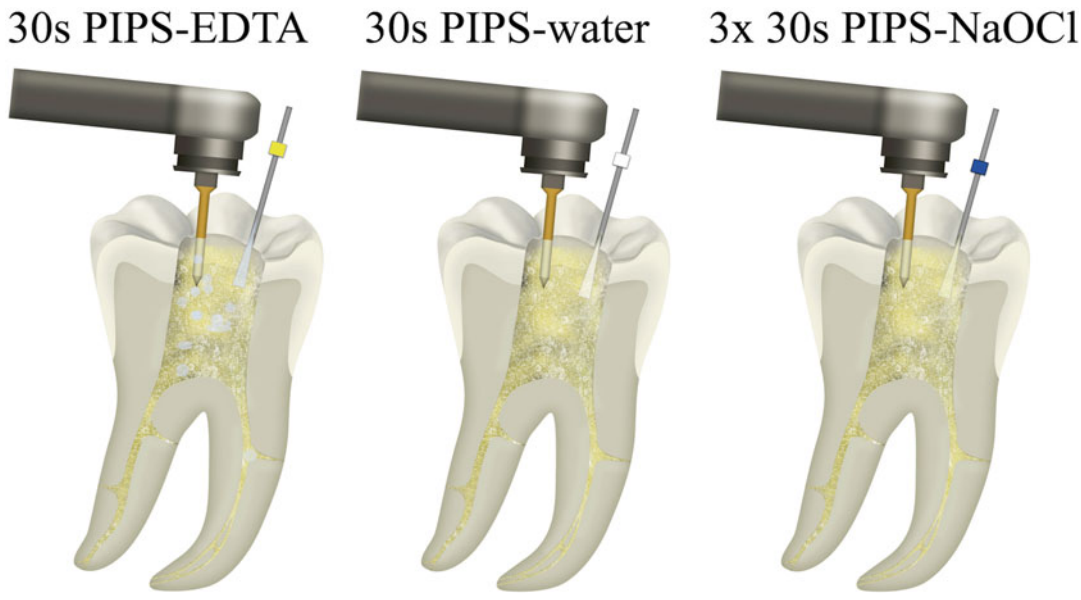

Fig. 11.115 PIPS final irrigation protocol utilizes 17% EDTA activated by PIPS™ for 30s; after 60s resting time, sterile distilled water agitated by PIPS™ is used for 30s to inactivate the EDTA; finally three cycles of 5–6 % NaOCl are activated by PIPS™ for 30s; each cycle has 30s rest phase to allow the hypochlorite to react. Again sterile distilled water agitated by PIPS™ is used for 30s to inactivate the oxygen before obturation using resin-based sealer (Courtesy of Dr. Giovanni Olivi)

11.15.6 Root Canal Obturation

Upon completion of this protocol, obturation with any system can be used. The authors use a flowable resin-based sealer (such as EndoRez by UltraDent, BC sealer by Brasseler, or AH plus from Dentsply) because of their low viscosities and higher flow rates needed to fill any remaining endodontic spaces (isthmuses, ramifications, lateral canals, apical delta) opened by PIPS. Finally resin-coated gutta-percha is placed (Figs. 11.116, 11.117, 11.118, 11.119, and 11.120).

Fig. 11.116 Post-op x-ray: A preflaring of the orifice and enlarging of the coronal one-third of the canals allow for easy and straight-line (direct) access to the canal apex; confluent canals and isthmus filling completed (Courtesy of Dr. Thomas McClammy Scottsdale, Arizona, USA)

Fig. 11.117 Post-op x-ray: straight-line direct access to the canal the middle and apical one-third of the canals improved irrigation and obturation of complicated apical anatomy

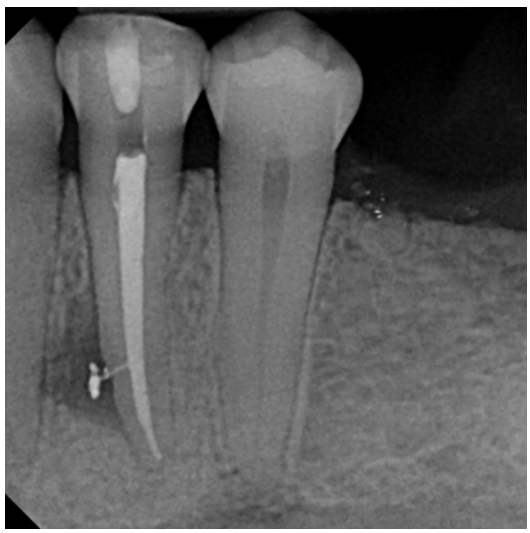

Fig. 11.118 Post-op x-ray: canal fill confirmed into lateral defect

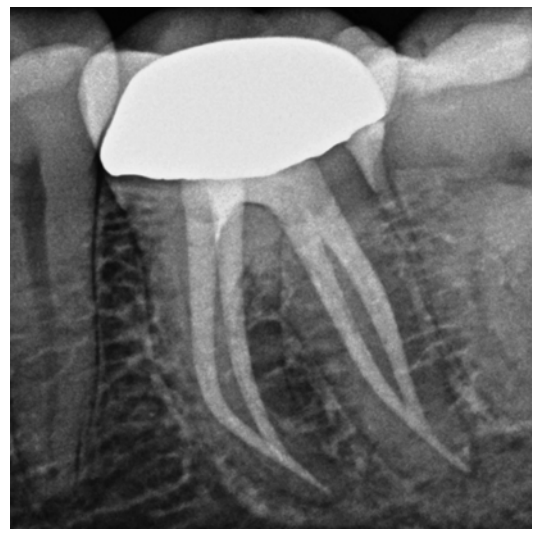

Fig. 11.119 Post-op x-ray: final obturation with continuous taper completed (Courtesy of Dr. Thomas McClammy Scottsdale, Arizona, USA)

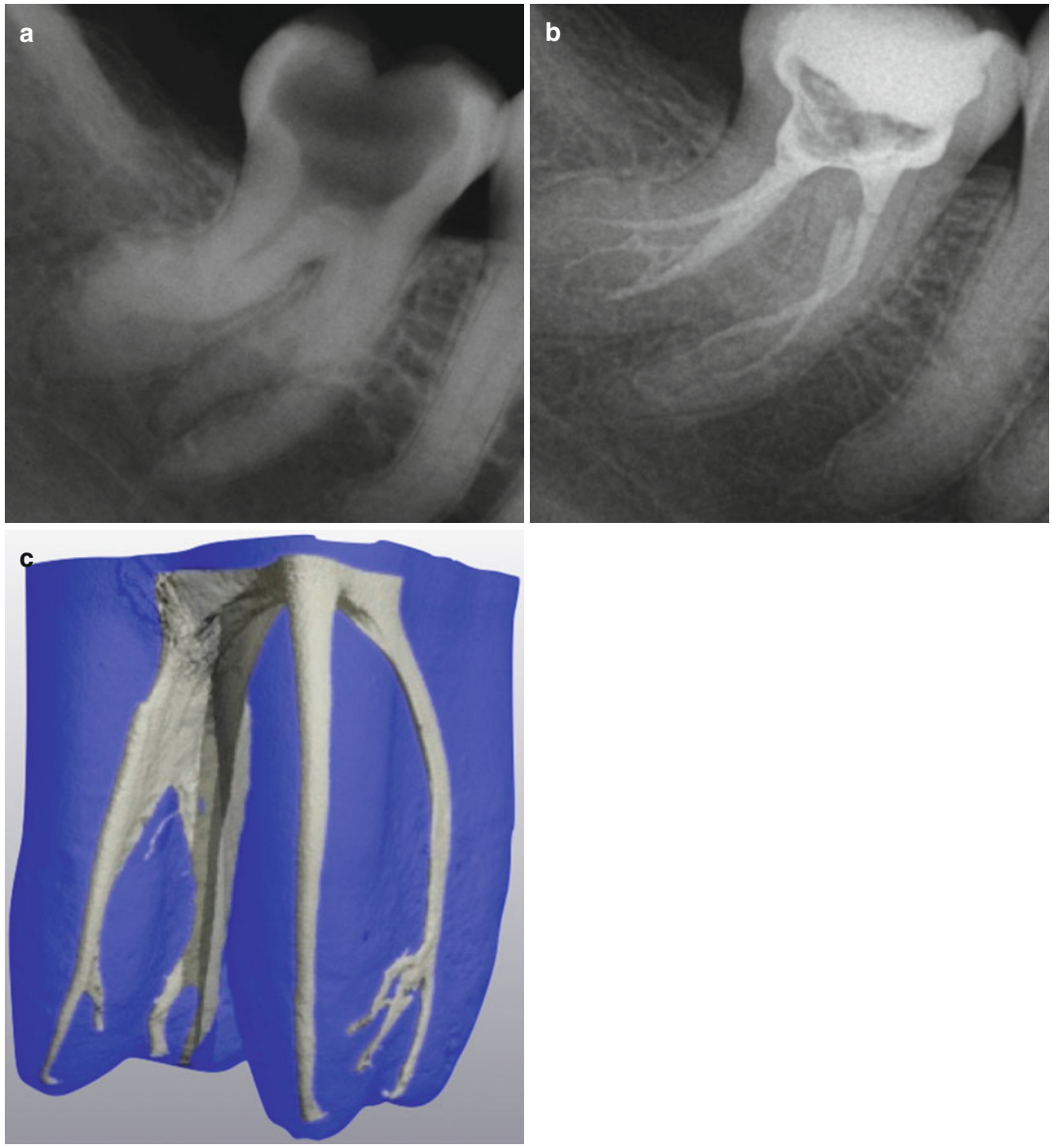

Fig. 11.120 (**a**, **b**) Pre- and post-treatment radiographs of lower first molar. Note the obturation pattern in the anastomosis area. (**c**) Complex morphologies associated with molars seen with these micro CT scans (Courtesy of Dr. Ove Peters San Francisco, California USA and Dr. Enrico DiVito Scottsdale, Arizona, USA)

Upon radiographic verification of adequate fill, it is imperative that a good coronal seal is achieved as soon as possible. This can be done by a flowable etched and bonded resin composite with or without a glass fiber post and core, together with a partial or full coverage crown. Postoperative radiographic verification of healing should be done at 1-, 3-, and 6-month intervals (Figs. 11.121, 11.122, 11.123, 11.124, 11.125, 11.126, and 11.127).

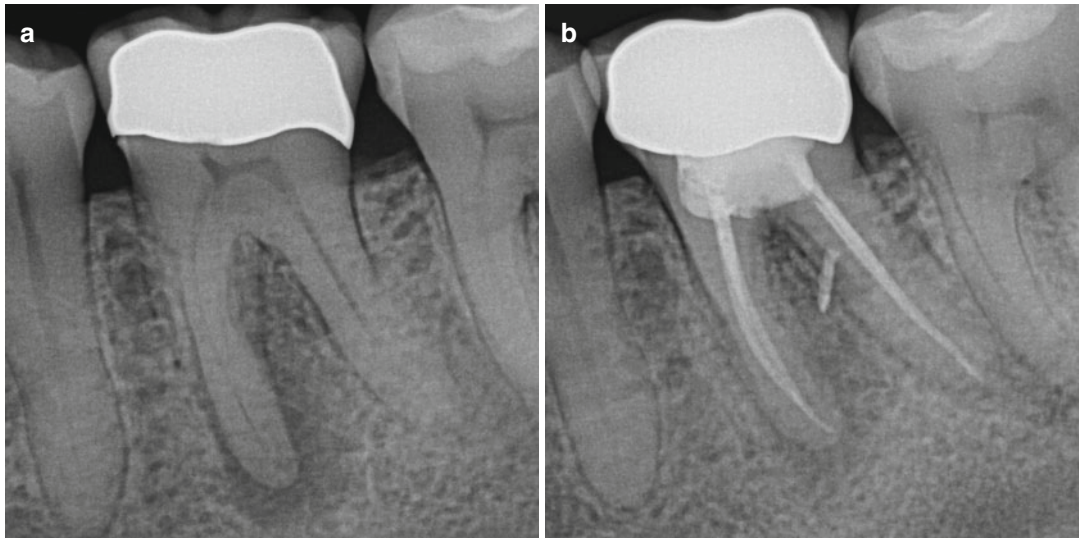

Fig. 11.121 (**a**) Pre-treatment lower first molar, with periapical lesion; (**b**) 6 months post-treatment

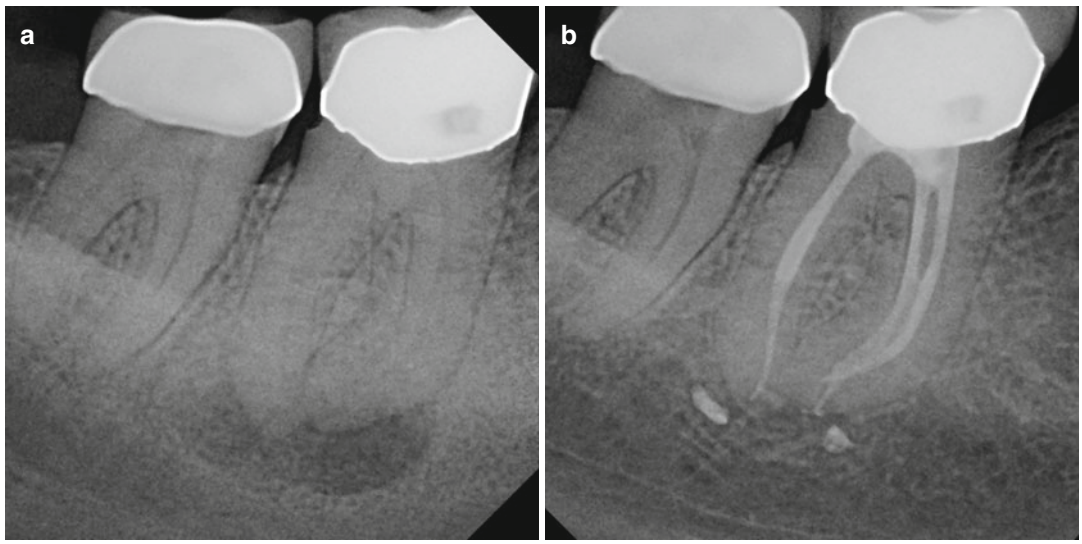

Fig. 11.122 (**a**) Pre-treatment lower first molar, with large apical lesion; (**b**) 6 months post-treatment

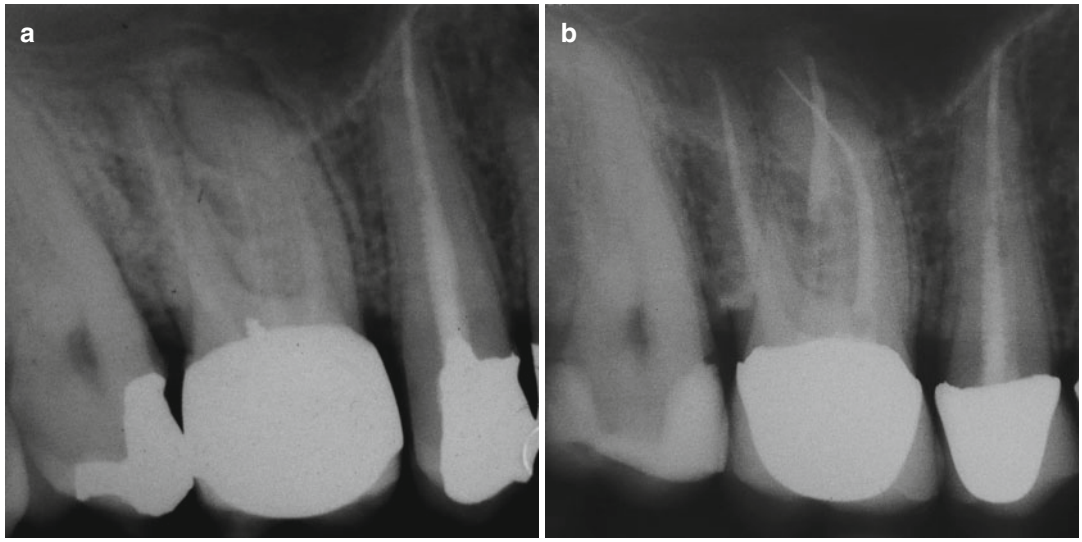

Fig. 11.123 (**a**) Pre-treatment radiograph of retreat of upper first molar showing apical lesions on mesial and palatal roots; (**b**) 1 year post-treatment

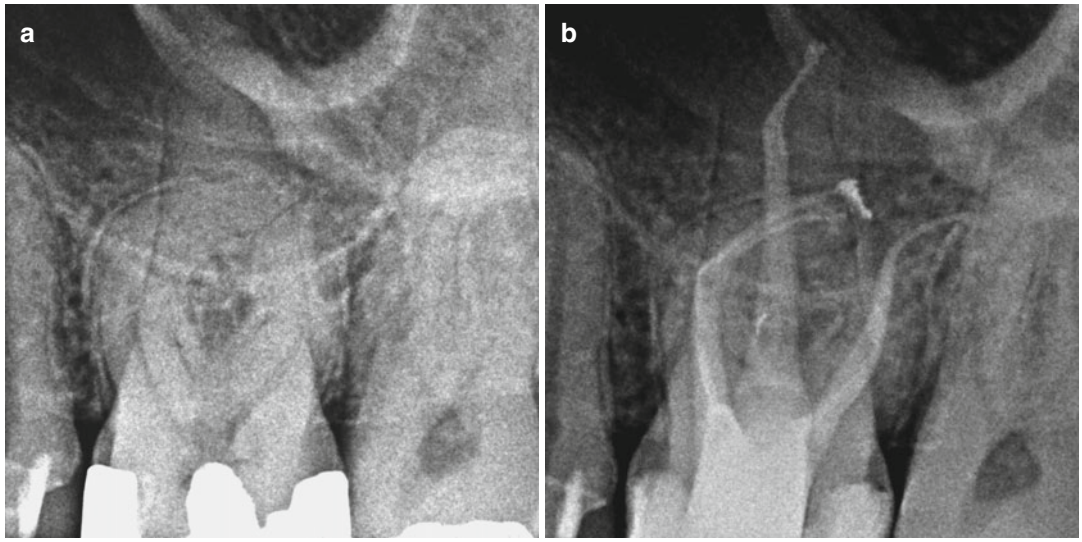

Fig. 11.124 (**a**) Pre-treatment upper first molar; (**b**) 1 year post-treatment (Courtesy Dr. Tom McClammy Scottsdale, Arizona, USA)

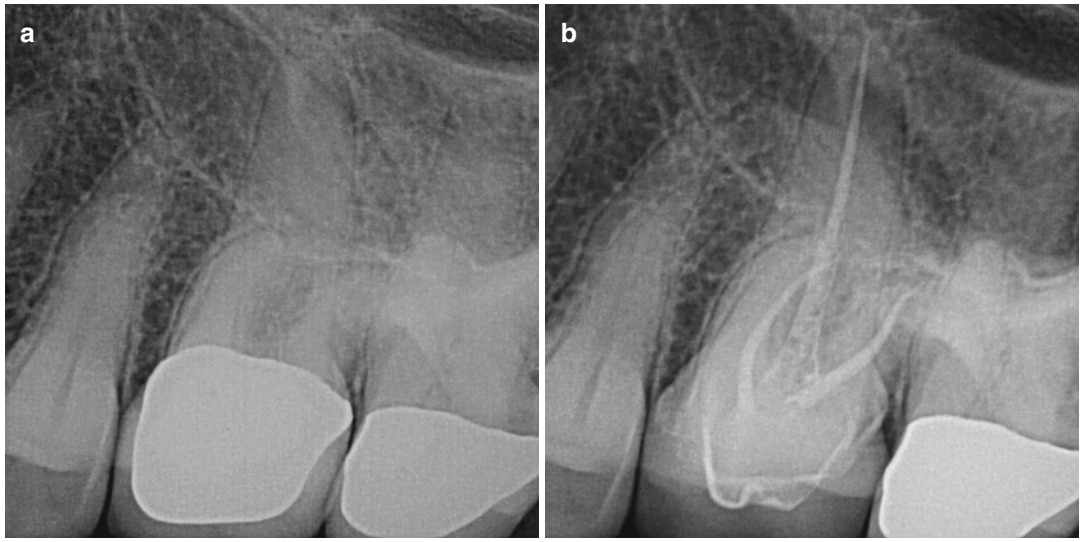

Fig. 11.125 (**a**) Pre-treatment upper first molar; (**b**) 1 year post-treatment

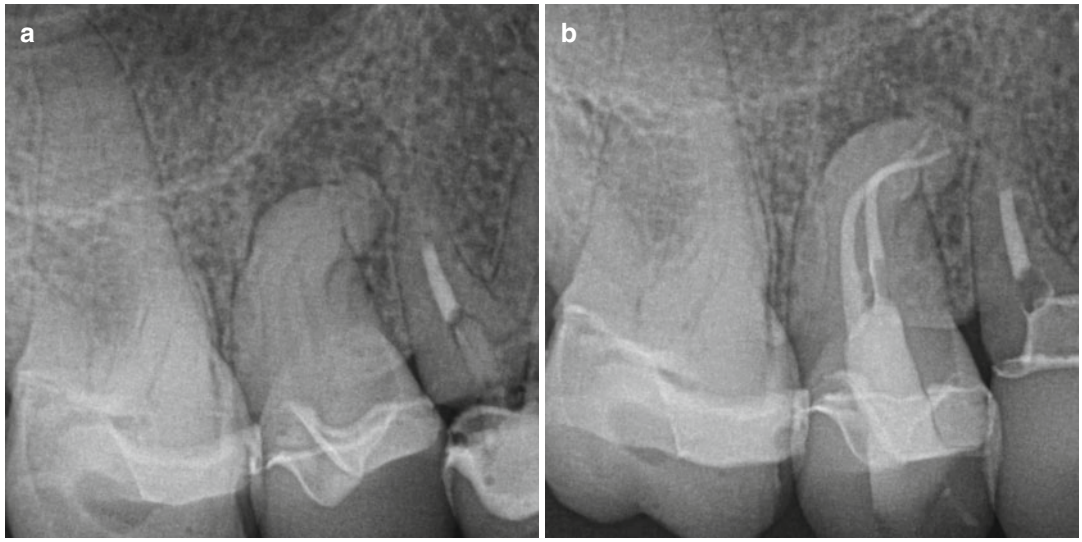

Fig. 11.126 (**a**) Pre-treatment upper second bicuspid; (**b**) 6 months post-treatment

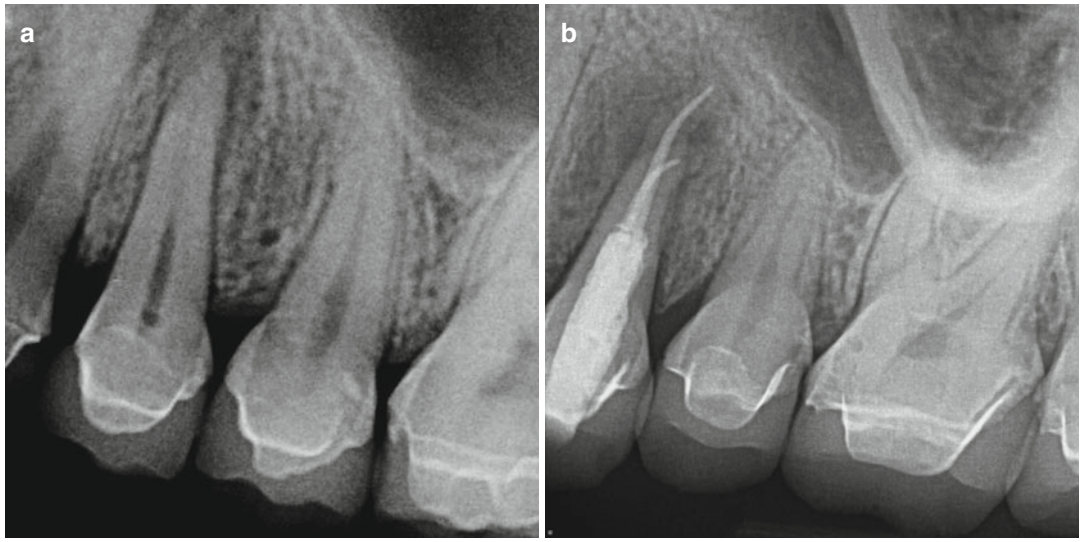

Fig. 11.127 (**a**) Pre-treatment upper first bicuspid; (**b**) 1 year post-treatment

11.16 PIPS Protocol for Endodontic Retreatment

Removing failed endodontic material from previous therapies requires the use of hand and rotary files in combination with PIPS. PIPS and continuous water between instruments are used in an alternating pattern until dislodging and cleaning of previous material occur (Figs. 11.128a–d, 11.129, 11.130, and –11.131a, b). PIPS standard settings are used with the handpiece water feature "on" at 2 water/0 air. Use of alcohol and hydrogen peroxide with PIPS aids in dissolving the previous material. For this step turn off the handpiece air/water spray feature.

The use of specific solvents for gutta-percha such as chloroform, endosolv, and other similar chemistries must be used separately from PIPS to avoid the possibility of a flammable incident due to laser activation.

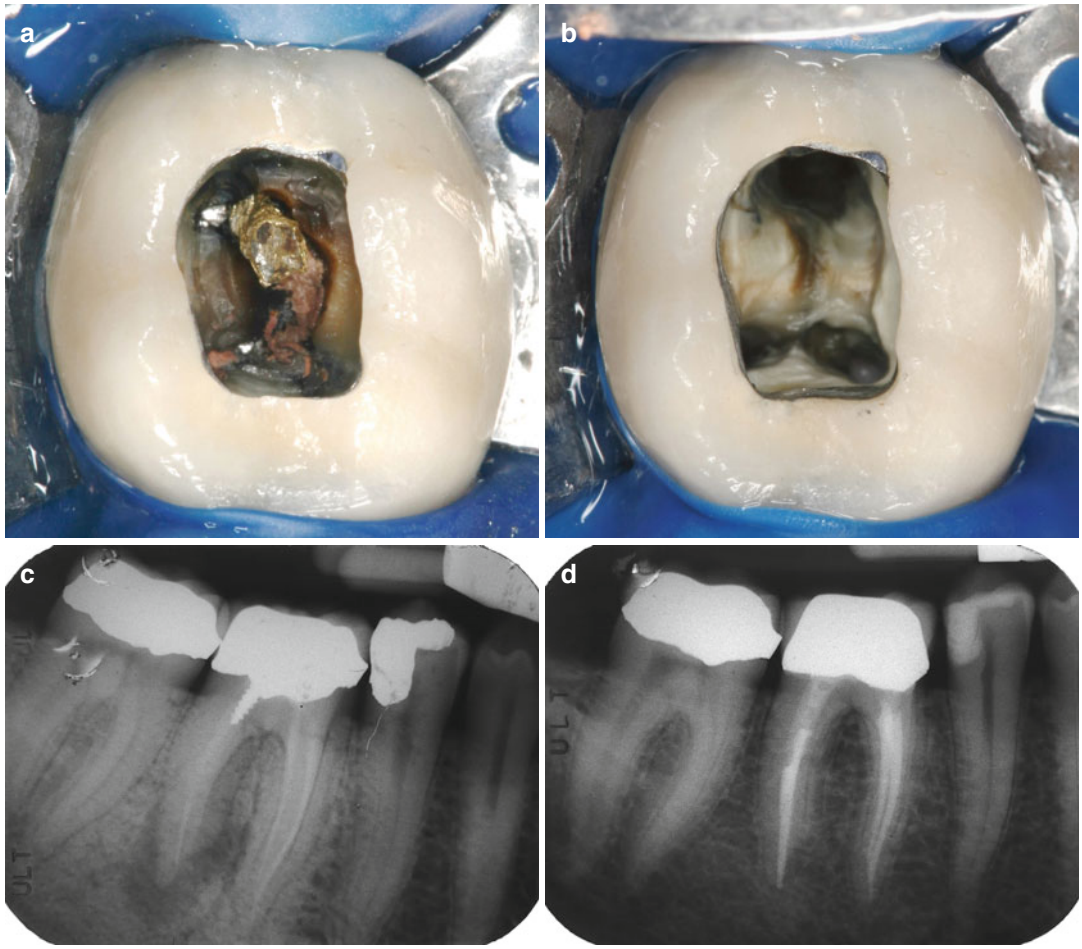

Fig. 11.128 (**a**) Pre-treatment view of treated molar. Note metal post and original gutta-percha; (**b**) post-PIPS. Note the clean walls and canal orifices; (**c**) pre-treatment radiograph of retreat; (**d**) 3-year post-treatment radiograph showing healing of the lesion

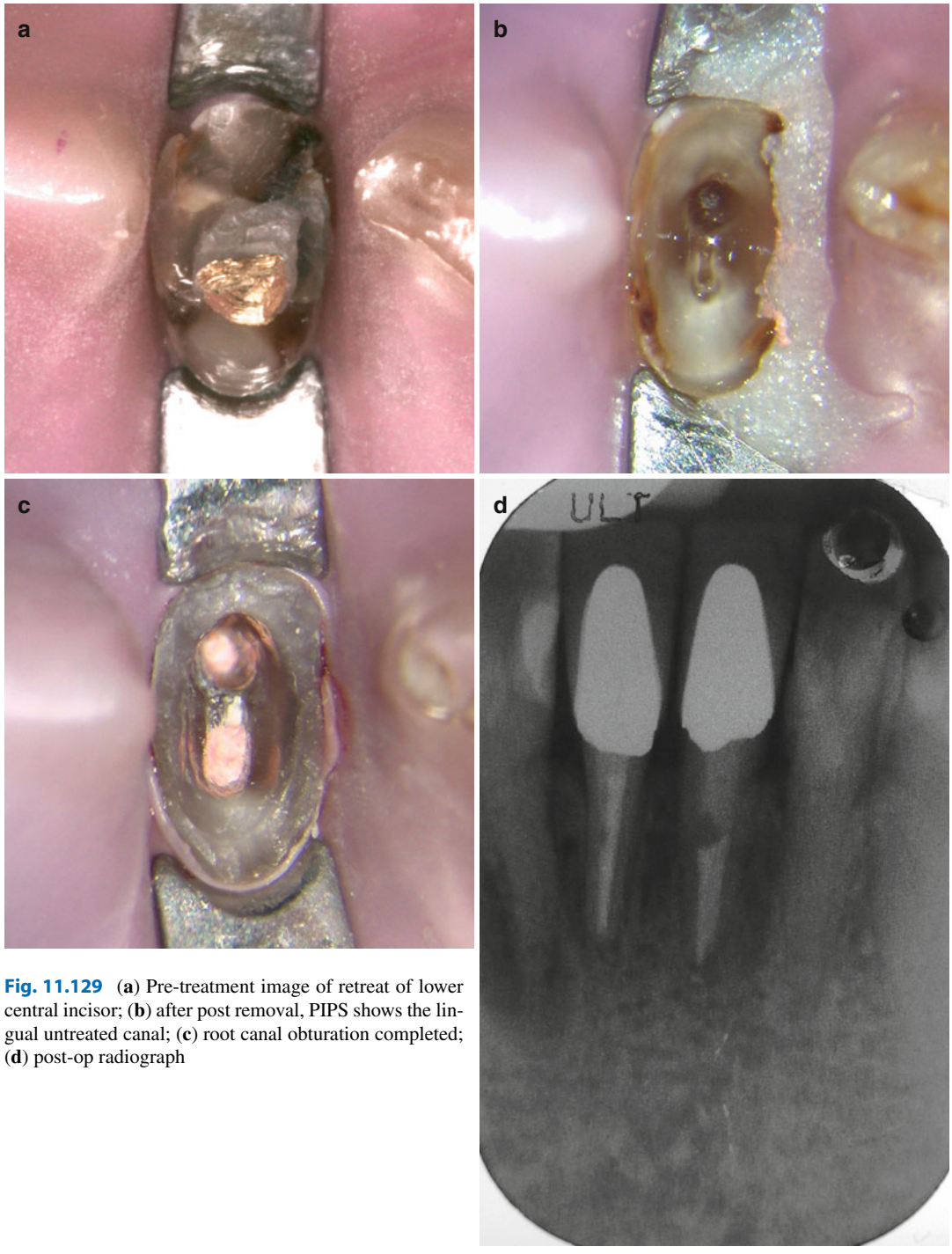

Fig. 11.129 (**a**) Pre-treatment image of retreat of lower central incisor; (**b**) after post removal, PIPS shows the lingual untreated canal; (**c**) root canal obturation completed; (**d**) post-op radiograph

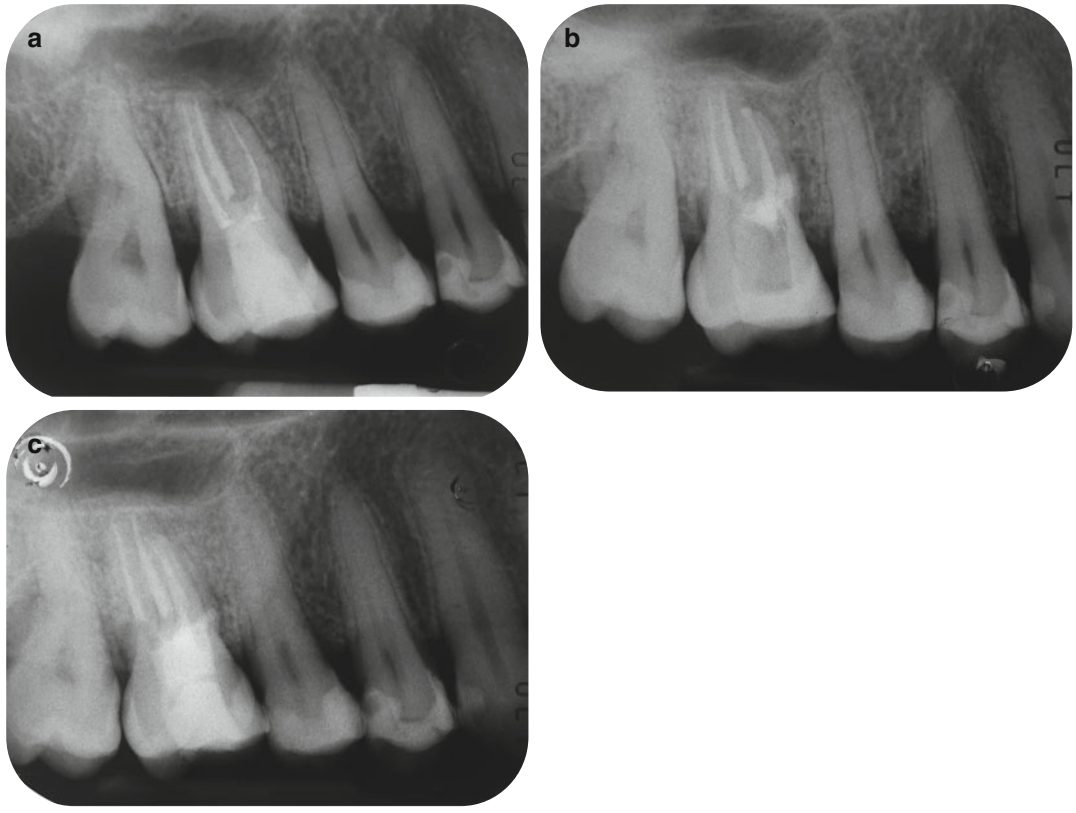

Fig. 11.130 (**a**) Pre-treatment radiograph of upper first molar retreat. Note apical lesion on mesial-buccal root; (**b**) immediate post-re-treatment radiograph; (**c**) one year post-op

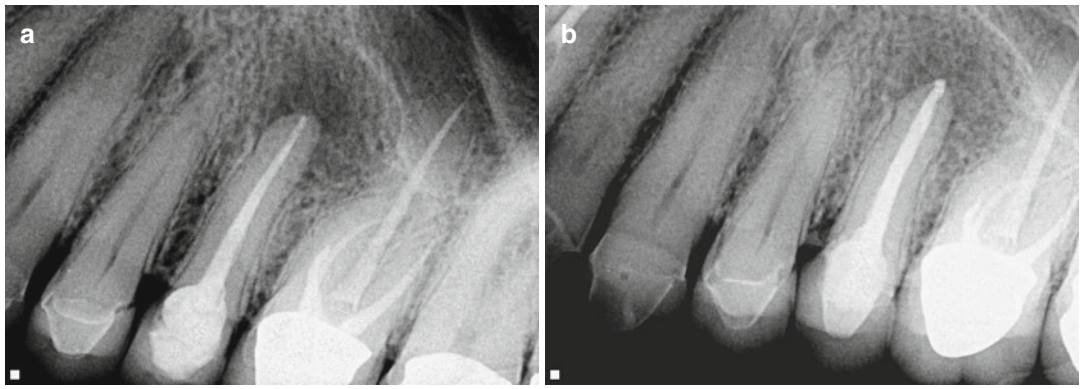

Fig. 11.131 (**a**) Pre-treatment radiograph of upper second premolar retreat; (**b**) 60-day post-op re-treatment

11.17 PIPS as an Aid for Locating and Establishing Patency in Calcified Canals

Calcified canals are one of the main problems in endodontic treatment. To help file calcified canals, chelating agents such as EDTA used with PIPS photoacoustic pressure waves help open and negotiate access to the apical part of the canal.

For calcifications and obstructions in the coronal portion of the canal or chamber, higher energy can be used for the activation (30–40 mJ); when the calcification is in the canal, the safer, standard parameter must be maintained: PIPS tip, 50 μs pulse, 20 mJ, 15 Hz, and alternating combination of continuous flow of EDTA followed by water while activating laser with the PIPS tip. Repeat until canal orifices are visualized.

11.18 PIPS as an Aid in Dislodging Fractured Instruments

During an endodontic treatment, hand or rotary instruments may accidentally separate or break in different areas of a root canal. Usually instruments in the coronal one-third can be easily removed with different devices including high-volume suction, but the breakage and wedging of a file fragment in the dentin wall of the apical or medium one-third is a challenge that many times requires the intervention of a specialist.

Different strategies can be applied for this purpose. Typically the best choice is to remove the fractured fragment. Other times if this is not possible, bypassing the instrument allows for filing, cleaning, decontaminating, and obturation of the remaining portion of root canal.

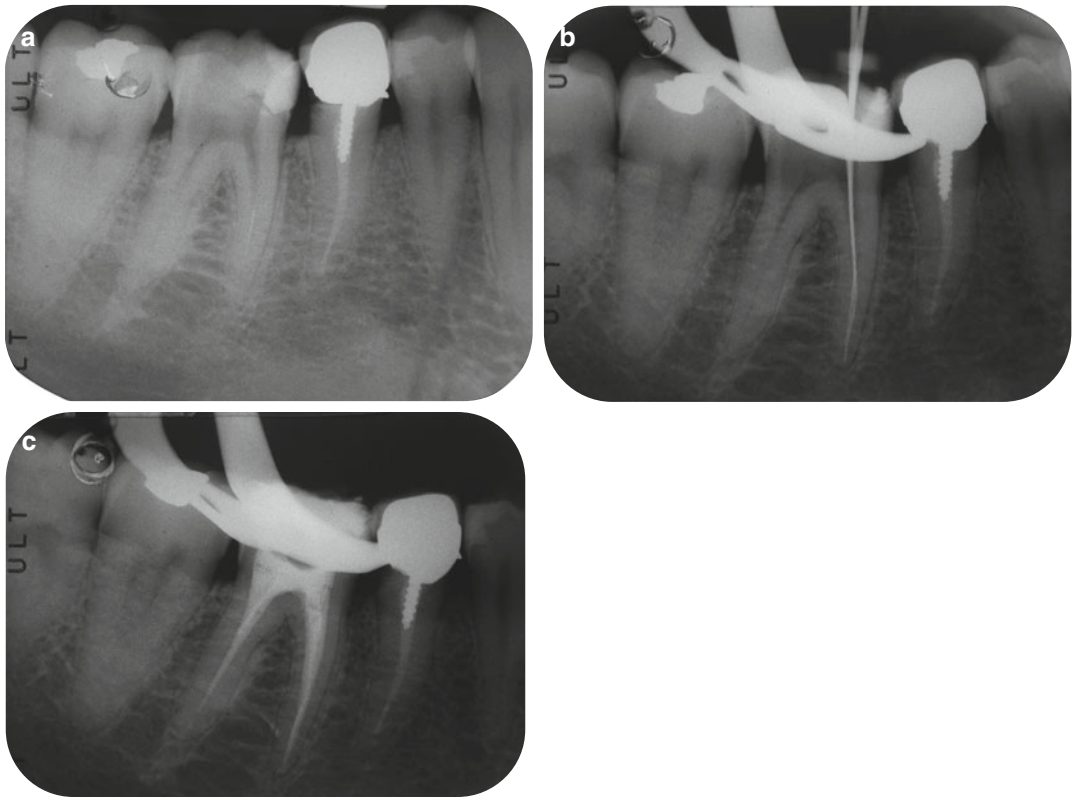

Fig. 11.132 (**a**) Pre-treatment radiograph lower first molar. Note separated file in the mesial root; (**b**) post laser-activated irrigation with PIPS creates space to allow for the passage of a hand file past the separated file. Note that this was accomplished without the need to over-instrument the canal as is often the case with conventional re-treatment. (**c**) Immediate post-op radiograph showing the final fill. Note conservative canal morphology was maintained

Accordingly different irrigant solutions are used:

- Several alternating irrigation cycles of NaOCl and EDTA (typically three to four cycles, 30 s intervals) activated by PIPS allow for decontamination and cleaning of the root canal distal to the wedged fragment. Also the use of EDTA gel (file EZE) allows for a lubrication of the canal helping smaller hand instruments (.06, .08, .10) to reach the working length, bypassing the obstacle (Figs. 11.132a–c and 11.134a–d).
- When the objective is to dislodge the fragment, the photoacoustic shock waves of the standard PIPS setting are used, with several cycles of sterile distilled water or directly with the handpiece water spray feature on (2 water/zero air), until confirmation of removal is verified radiographically (Fig. 11.133a–d).

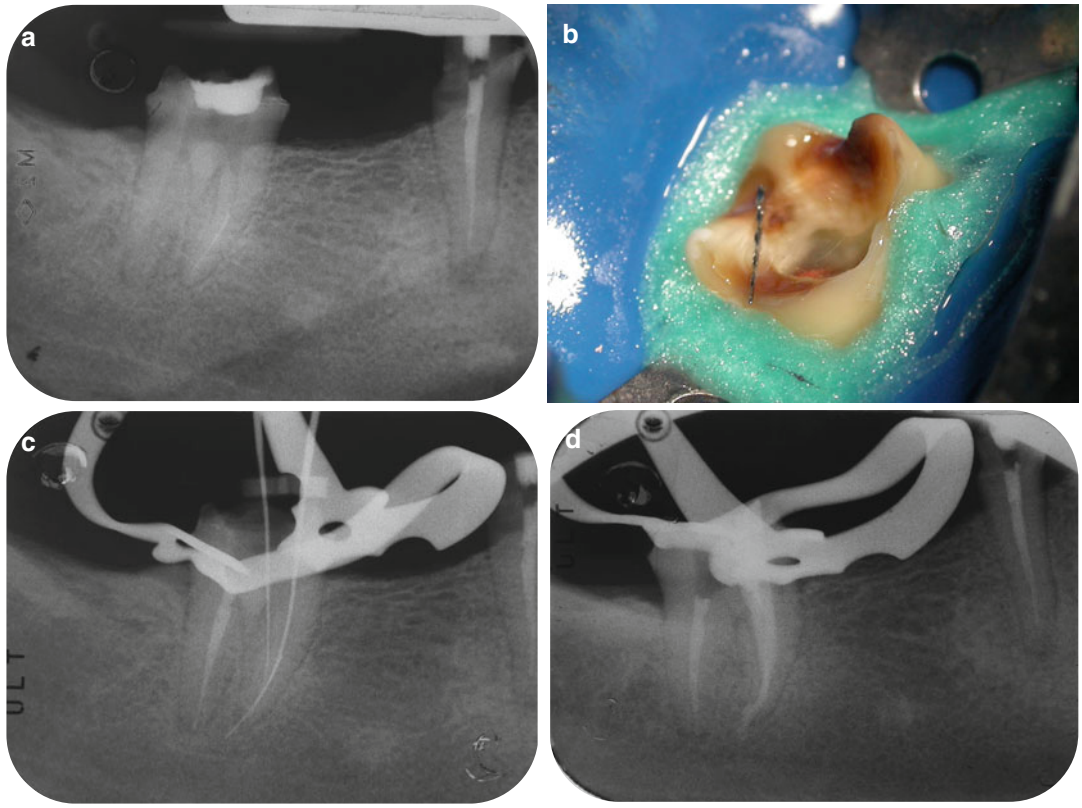

Fig. 11.133 (**a**) Lower molar showing separated instrument in the mesial canal. (**b**) Expulsion of separated instrument as a result of PIPS irrigation during preparation phase. Note the isolation of the molar using liquid dam in addition to rubber dam. PIPS laser-activated irrigation must operate with the tip continuously submerged in an adequate fluid reservoir to achieve the best photoacoustic effect. (**c**) Verification of removal of separated file and patency to working length verified. (**d**) Immediate post-op radiograph showing obturation completed

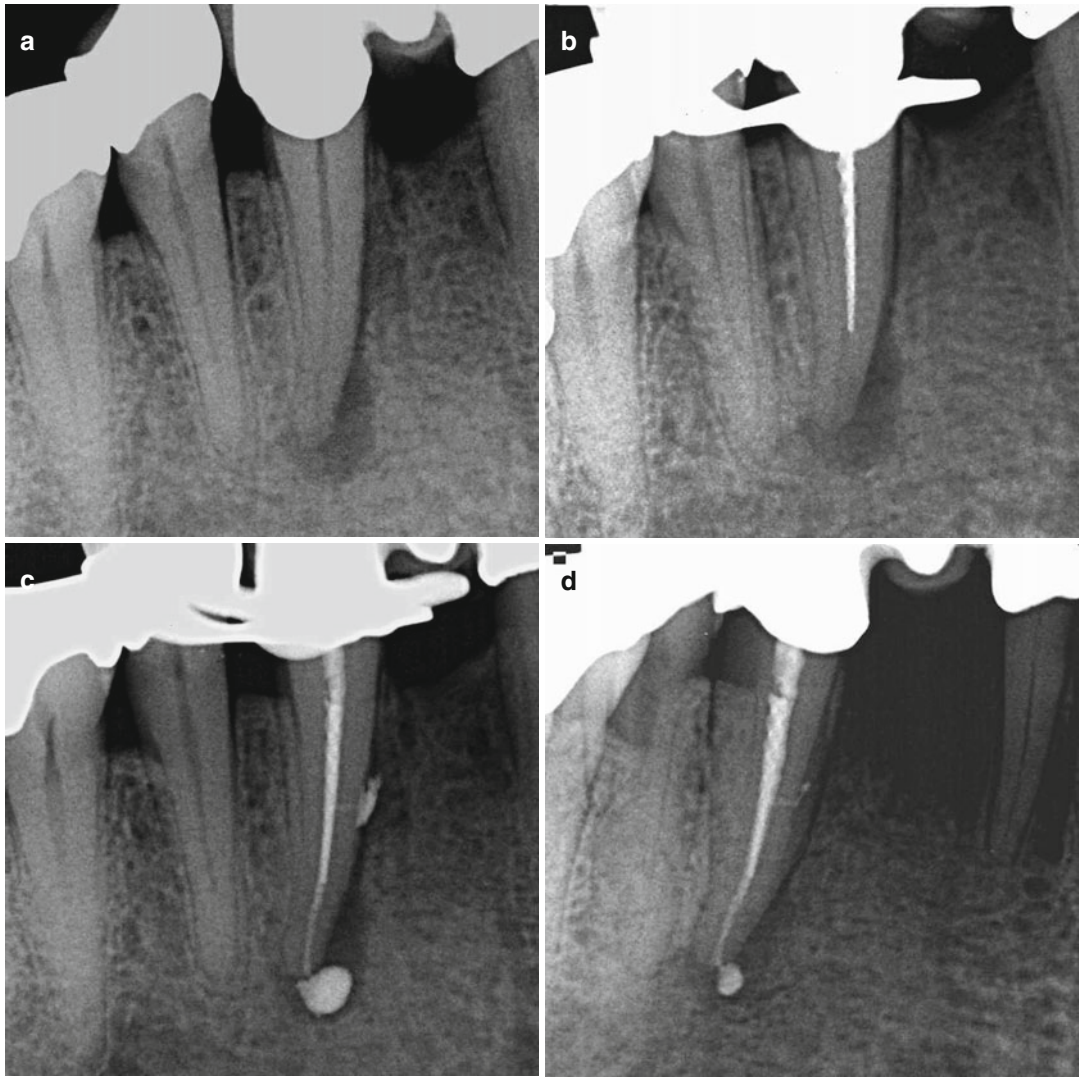

Fig. 11.134 (**a**) Pre-treat radiograph of lower cuspid. (**b**) Separated 20/06 GT rotary file. PIPS was used to continue debridement and irrigation of canal system leaving the separated instrument in the canal. (**c**) Immediate post-treatment radiograph. Cuspid was obturated using flowable sealer (EndoRez by Ultradent). Note the three-dimensional fill to the apex and the lateral mid-root canal puff. This verified the ability of PIPS to successfully remove and open portals of exit even with the separated file left in place. (**d**) 45-day post-op. Note the resorption of sealer both at the apex and lateral portal area. Apical lucency also improving confirming healing in progress

11.19 Other Application of PIPS

11.19.1 PIPS Effects on Adhesion of Resin Sealer Cement to Root Canal Dentin

Akcay et al. (2014) investigated the effects of various irrigation activation techniques on the bond strength of an epoxy resin-based sealer, used with gutta-percha to obturate root canal dentin (AH Plus-Jet sealer, Dentsply, USA). A push-out test was used to measure the bond strength between the root canal dentin and the sealer, and a statistically significant interaction between the final irrigant activation techniques used and root canal thirds resulted with PIPS and PUI providing higher bond strength of resin sealer to root dentin compared to conventional and sonic irrigation techniques. The

activation of the irrigant and effective streaming have a positive effect on the bond strength of the resin sealer to root dentin, producing more permeable dentin surface for sealing [57].

Arslan et al. (2015) also investigated the effects of various irrigation techniques (PIPS with NaOCl, PIPS with EDTA, and PIPS with distilled water at 0.3 W, 15 Hz, and 20 mJ, needle irrigation with distilled water and NaOCl, ultrasonic irrigation with NaOCl) on the bond strength of a self-adhesive resin cement and fiber post cemented to root canal dentin after 60 s irrigation. PIPS with distilled water resulted in higher push-out values than those of needle (with both distilled water and NaOCl) and ultrasonic irrigation ($p < 0.05$) [58].

11.19.2 PIPS Effect on Activation of Hydrogen Peroxide Devital Tooth Bleaching

Among the several studies on PIPS, the most recent investigated the bleaching effectiveness of photon-induced photoacoustic streaming (PIPS) on discolored teeth comparing different devital bleaching techniques: 1 week walking bleach with sodium perborate and with 35 % hydrogen peroxide gel, PIPS using 35 % hydrogen peroxide liquid for 3 min, and just 35 % hydrogen peroxide, as a liquid and as a gel for 30 min. Spectrophotometric measurements on the buccal surfaces of the crowns, at the beginning, just after the bleaching procedures and the following first, third, and seventh days [59] were performed to analyze the color variations. PIPS technique using 35 % hydrogen peroxide liquid resulted statistically superior to 35 % hydrogen peroxide liquid and gel without PIPS immediately after the procedures ($p < 0.05$). PIPS technique further bleached specimens more than all of the other techniques ($p < 0.05$) after 1, 3, and 7 days [58]. The authors concluded that further studies are needed to determine if the PIPS™-assisted bleaching technique may result in any complications, particularly cervical resorption [59].

Conclusion

The role of successful endodontics includes the process of shaping, disinfection, and obturation. When comparing different disinfection techniques, laser-activated irrigation has been proven to be more effective than conventional means.

Many peer-reviewed studies confirmed the effectiveness of PIPS™ in achieving superior bacterial decontamination, biofilm removal, dentin tubule sterilization, and root canal cleansing.

Following the proper PIPS™ protocol for laser-activated irrigation is crucial to achieve these results. PIPS™ allows the clinician to effectively stream and exchange irrigants three-dimensionally throughout the entire root canal system. Because of the unique tapered and stripped PIPS™ tip design and its high efficiency, the tip can be placed in the access chamber only, not in the canals themselves, allowing for ease of use that is of great benefit to the clinician. The higher efficiency requires only low subablative energy settings thereby avoiding completely the thermal effects associated with previous laser applications.

PIPS™ application allows the dentist to use less instrumentation and remove less dentin root structure leading to more conservative biomimetic shapes.

Regardless of the shaping or obturation technique used, PIPS™ laser-activated irrigation improves the success of endodontic therapy.

References

1. Ruddle CJ. Cleaning and shaping the root canal system. In: Cohen S, Burn RC, editors. Pathways of the pulp. 8th ed. St. Louis: The C.V. Mosby Company; 2002. p. 231.
2. George R, Meyers IA, Walsh LJ. Laser activation of endodontic irrigants with improved conical laser fiber tips for removing smear layer in the apical third of the root canal. J Endod. 2008;34(12):1524–7. Epub 2008 Oct 2.
3. De Moor RJ, Blanken J, Meire M, Verdaasdonk R. Laser induced explosive vapor and cavitation resulting in effective irrigation of the root canal. Part 2: evaluation of the efficacy. Lasers Surg Med. 2009;41(7):520–3.
4. de Groot SD, Verhaagen B, Versluis M, Wu MK, Wesselink PR, van der Sluis LW. Laser-activated irri-

gation within root canals: cleaning efficacy and flow visualization. Int Endod J. 2009;42(12):1077–83.
5. De Moor RJ, Meire M, Goharkhay K, Moritz A, Vanobbergen J. Efficacy of ultrasonic versus laser-activated irrigation to remove artificially placed dentin debris plugs. J Endod. 2010;36(9):1580–3.
6. Peeters HH, Suardita K. Efficacy of smear layer removal at the root tip by using ethylenediaminetetraacetic acid and erbium, chromium: yttrium, scandium, gallium garnet laser. J Endod. 2011;37(11):1585–9. doi:10.1016/j.joen.2011.08.022. Epub 2011 Sep 28.
7. Seet AN, Zilm PS, Gully NJ, Cathro PR. Qualitative comparison of sonic or laser energisation of 4% sodium hypochlorite on an Enterococcus faecalis biofilm grown in vitro. Aust Endod J. 2012;38(3):100–6 [Epub 2012 Jul 16].
8. Guidotti R, Merigo E, Fornaini C, Rocca JP, Medioni E, Vescovi P. Er:YAG 2,940-nm laser fiber in endodontic treatment: a help in removing smear layer. Lasers Med Sci. 2014;29(1):69–75.
9. Sahar-Helft S, Stabholtz A, Moshonov J, Gutkin V, Redenski I, Steinberg D. Effect of Er:YAG laser-activated irrigation solution on Enterococcus faecalis biofilm in an ex-vivo root canal model. Photomed Laser Surg. 2013;31(7):334–41. Epub 2013 Jun 13.
10. Licata ME, Albanese A, Campisi G, Geraci DM, Russo R, Gallina G. Effectiveness of a new method of disinfecting the root canal, using Er, Cr:YSGG laser to kill Enterococcus faecalis in an infected tooth model. Lasers Med Sci. 2015;30(2):707–12.
11. DiVito E, Peters OA, Olivi G. Effectiveness of the erbium:YAG laser and new design radial and stripped tips in removing the smear layer after root canal instrumentation. Lasers Med Sci. 2012;27(2):273–80. Epub 2010 Dec 1.
12. Peters OA, Bardsley S, Fong J, Pandher G, Divito E. Disinfection of root canals with photon-initiated photoacoustic streaming. J Endod. 2011;37(7):1008–12. Epub 2011 May 7.
13. DiVito EE, Colonna MP, Olivi G. The photoacoustic efficacy of an Er:YAG Laser with radial and stripped tips on root canal dentin walls: an SEM evaluation. J Laser Dent. 2011;19(1):156–61.
14. Pedullà E, Genovese C, Campagna E, Tempera G, Rapisarda E. Decontamination efficacy of photon-initiated photoacoustic streaming (PIPS) of irrigants using low-energy laser settings: an ex vivo study. Int Endod J. 2012;45(9):865–70. Epub 2012 Apr 5.
15. Ordinola-Zapata R, Bramante CM, Aprecio RM, Handysides R, Jaramillo DE. Biofilm removal by 6% sodium hypochlorite activated by different irrigation techniques. Int Endod J. 2014;47(7):659–66. doi:10.1111/iej.12202.
16. Majaron B, Lukac M, Sustercic D, Funduk N, Skaleric U. Threshold and efficiency analysis in Er:YAG laser ablation of hard dental tissue. Laser applications in medicine and dentistry. Proc SPIE. 1996;2922:233–42.
17. Lin S, Liu Q, Peng Q, Lin M, Zhan Z, Zhang X. The ablation threshold of Er:YAG laser and Er, Cr:YSGG laser in dental dentin. Sci Res Essays. 2010;5(16):2128–35.
18. Kaitsas V, Signore A, Fonzi L, Benedicenti S, Barone M. Effects of Nd: YAG laser irradiation on the root canal wall dentin of human teeth: a SEM study. Bull Group Int Rech Sci Stomatol Odontol. 2001;43(3):87–92.
19. Lee BS, Jeng JH, Lin CP, Shoji S, Lan WH. Thermal effect and morphological changes induced by Er:YAG laser with two kinds of fiber tips to enlarge the root canals. Photomed Laser Surg. 2004;22(3):191–7.
20. Jahan KM, Hossain M, Nakamura Y, Yoshishige Y, Kinoshita J, Matsumoto K. An assessment following root canal preparation by Er, Cr: YSGG laser irradiation in straight and curved roots, in vitro. Lasers Med Sci. 2006;21(4):229–34. Epub 2006 Oct 28.
21. Blanken JW, Verdaasdonk RM. Cavitation as a working mechanism of the Er, Cr:YSGG laser in endodontics: a visualization study. J Oral Laser Appl. 2007;7: 97–106.
22. Blanken J, De Moor RJG, Meire M, Verdaasdonk R. Laser induced explosive vapor and cavitation resulting in effective irrigation of the root canal. Part 1: a visualization study. Lasers Surg Med. 2009;41: 514–9.
23. Matsumoto H, Yoshimine Y, Akamine A. Visualization of irrigant flow and cavitation induced by Er:YAG laser within a root canal model. J Endod. 2011;37(6):839–43. Epub 2011 Apr 17.
24. Gregorčič P, Jezeršek M, Možina J. Optodynamic energy-conversion efficiency during an Er:YAG-laser-pulse delivery into a liquid through different fiber-tip geometries. J Biomed Opt. 2012;17(7): 075006.
25. Jaramillo DE, Aprecio RM, Angelov N, DiVito E, McClammy TV. Efficacy of photon induced photoacoustic streaming (PIPS) on root canals infected with Enterococcus faecalis: a pilot study. Endod Prac. 2012;5(3):28–32.
26. Jansen ED, et al. Effect of pulse duration on bubble formation and laser-induced pressure waves during holmium laser ablation. Lasers Surg Med. 1996;18(3):278–93.
27. Perhavec T, Diaci J. Comparison of Er:YAG and Er,Cr:YSGG dental lasers. J Oral Laser Appl. 2008;8:87–94.
28. Macedo RG, Wesselink PR, Zaccheo F, Fanali D, Van Der Sluis LW. Reaction rate of NaOCl in contact with bovine dentine: effect of activation, exposure time, concentration and pH. Int Endod J. 2010;43(12):1108–15. doi:10.1111/j.1365-2591.2010.01785.x. Epub 2010 Aug 31.
29. Deleu E, Meire MA, De Moor RJ. Efficacy of laser-based irrigant activation methods in removing debris from simulated root canal irregularities. Lasers Med Sci. 2015;30(2):831–5 [Epub 2013 Oct 5.].
30. George R, Walsh LJ. Apical extrusion of root canal irrigants when using Er:YAG and Er, Cr:YSGG lasers with optical fibers: an in vitro dye study. J Endod. 2008;34(6):706–8. doi:10.1016/j.joen.2008.03.003. Epub 2008 Apr 11.

31. Zhu X, Yin X, Chang JW, Wang Y, Cheung GS, Zhang C. Comparison of the antibacterial effect and smear layer removal using photon-initiated photoacoustic streaming aided irrigation versus a conventional irrigation in single-rooted canals: an in vitro study. Photomed Laser Surg. 2013;31(8):371–7. doi:10.1089/pho.2013.3515. Epub 2013 Jul 17.
32. Ingle JI. Endodontics. 3rd ed. Philadelphia: Lea & Febiger; 1985.
33. Cohen S, Burns RC. Pathways of the pulp. 4th ed. St. Louis: CV Mosby; 1987. Piccin edizione italiana.
34. Peeters HH, Mooduto L. Radiographic examination of apical extrusion of root canal irrigants during cavitation induced by Er, Cr:YSGG laser irradiation: an in vivo study. Clin Oral Investig. 2013;17(9):2105–12.
35. Khan S, Niu LN, Eid AA, Looney SW, Didato A, Roberts S, Pashley DH, Tay FR. Periapical pressures developed by nonbinding irrigation needles at various irrigation delivery rates. J Endod. 2013;39(4):529–33. Epub 2013 Feb 10.
36. Martin SA. Conventional endodontic therapy of upper central incisor combined with cyst decompression: a case report. J Endod. 2007;33(6):753–7. Epub 2007 Mar 21.
37. Lyons RH, Kennedy JA, Burwell CS. Measurement of venous pressure by direct method. Am Heart J. 1938;16:675–93.
38. Baumann UA, Marquis C, Stoupis C, et al. Estimation of central venous pressure by ultrasound. Resuscitation. 2005;64:193–9.
39. Guyton AC, Hall JE. Guyton & Hall physiology review. Philadelphia: Elsevier Saunders; 2006.
40. van der Sluis LWM et al. Chapter 3: The role of irrigation in endodontics. In: Olivi G, DiVito EE, DeMoor JR. Laser in endodontics. Springer (english edition).
41. Peeters HH, De Moor RJ, Suharto D. Visualization of removal of trapped air from the apical region in simulated root canals by laser-activated irrigation using an Er,Cr:YSGG laser. Lasers Med Sci. 2014. [Epub ahead of print].
42. George R, Walsh LJ. Laser fiber-optic modifications and their role in endodontics. J Laser Dent. 2012;20(1):24–30.
43. Peters OA, Schonenberger K, Laib A. Effects of four Ni-Ti preparation techniques on root canal geometry assessed by micro-computed tomography. Int Endod J. 2001;34:221–30.
44. Ricucci D, Siqueira Jr JF. Fate of the tissue in lateral canals and apical ramifications in response to pathologic conditions and treatment procedures. J Endod. 2010;36:1–15.
45. Niu W, Yoshioka T, Kobayashi C, Suda H. A scanning electron microscopic study of dentinal erosion by final irrigation with EDTA and NaOCl solutions. Int Endod J. 2002;35(11):934–9.
46. Zehnder M. Root canal irrigants. J Endod. 2006;32(5):389–98.
47. Lloyd A, Uhles JP, Clement DJ, Garcia-Godoy F. Elimination of intracanal tissue and debris through a novel laser-activated system assessed using high-resolution micro–computed tomography: a pilot study. J Endod. 2014;40(4):584–7. doi:10.1016/j.joen.2013.10.040. Epub 2013 Dec 12.
48. Hülsmann M, Rümmelin C, Schäfers F. Root canal cleanliness after preparation with different endodontic handpieces and hand instruments: a comparative SEM investigation. J Endod. 1997;23:301–6.
49. Arslan H, Capar ID, Saygili G, Gok T, Akcay M. Effect of photon-initiated photoacoustic streaming on removal of apically placed dentinal debris. Int Endod J. 2014;47(11):1072–7. doi:10.1111/iej.12251. Epub 2014 Apr 4.
50. Molander A, Reit C, Dahlén G, Kvist T. Microbiological status of root-filled teeth with apical periodontitis. Int Endod J. 1998;31:1–7.
51. Stojicic S, Shen Y, Haapasalo M. Effect of the source of biofilm bacteria, level of biofilm maturation, and type of disinfecting agent on the susceptibility of biofilm bacteria to antibacterial agents. J Endod. 2013;39(4):473–7. doi:10.1016/j.joen.2012.11.024. Epub 2013 Jan 17.
52. Olivi G, DiVito E, Peters O, Kaitsas V, Angiero F, Signore A, Benedicenti S. Disinfection efficacy of photon-induced photoacoustic streaming on root canals infected with Enterococcus faecalis: an ex vivo study. J Am Dent Assoc. 2014;145(8):843–8. doi:10.14219/jada.2014.46.
53. Olivi M. Stefanucci M, Todea C. Laser assisted irrigation and hand irrigation for root canal decontamination: a comparison. Proceedings of SPIE 8925, Fifth International Conference on Lasers in Medicine: Biotechnologies Integrated in Daily Medicine, 89250G 2014. doi:10.1117/12.2045494; http://dx.doi.org/10.1117/12.2045494.
54. Al Shahrani M, Divito E, Hughes CV, Nathanson D, Huang GT. Enhanced removal of Enterococcus faecalis biofilms in the root canal using sodium hypochlorite plus photon-induced photoacoustic streaming: an in vitro study. Photomed Laser Surg. 2014;32(5):260–6. doi:10.1089/pho.2014.3714. Epub 2014 Apr 9.
55. Schilder H, Yee FS. Canal debridement and disinfection. In: Cohen S, Burns RC, editors. Pathways of the pulp. 3rd ed. St. Louis: The C.V. Mosby Company; 1984. p. 175.
56. Chapter 19. In: Castellucci A. Endodontics, vol 2. Florence: Edizioni Odontoiatriche il Tridente s.r.l. Florence; 2005. p. 551.
57. Akcay M, Arslan H, Mese M, Sahin NN. The effect of photon-initiated photoacoustic streaming, ultrasonically and sonically irrigation techniques on the push-out bond strength of a resin sealer to the root dentin. Clin Oral Investig. 2015;19(5):1055–61.
58. Arslan H, Akcay M, Saygili G, Keskı A, Meşe İT, Gok A, Dalli M. Bond strength of self-adhesive resin cement to root dentin. Comparison of photon-initiated photoacoustic streaming technique with needle and ultrasonic irrigation. Acta Odontol Scand. 2015;73(5):348–52. [Epub ahead of print].
59. Arslan H, Akcay M, Yasa B, Hatirli H, Saygili G. Bleaching effect of activation of hydrogen peroxide using photon-initiated photoacoustic streaming technique. Clin Oral Investig. 2015;19(2):253–9. [Epub ahead of print].

Index

G. Olivi et al. (eds.), *Lasers in Endodontics: Scientific Background and Clinical Applications*,
DOI 10.1007/978-3-319-19327-4